FGF10 IN DEVELOPMENT, HOMEOSTASIS, DISEASE AND REPAIR AFTER INJURY

EDITED BY: Saverio Bellusci and Mohammad K. Hajihosseini
PUBLISHED IN: Frontiers in Genetics

frontiers Research Topics

Frontiers eBook Copyright Statement

The copyright in the text of individual articles in this eBook is the property of their respective authors or their respective institutions or funders. The copyright in graphics and images within each article may be subject to copyright of other parties. In both cases this is subject to a license granted to Frontiers.

The compilation of articles constituting this eBook is the property of Frontiers.

Each article within this eBook, and the eBook itself, are published under the most recent version of the Creative Commons CC-BY licence. The version current at the date of publication of this eBook is CC-BY 4.0. If the CC-BY licence is updated, the licence granted by Frontiers is automatically updated to the new version.

When exercising any right under the CC-BY licence, Frontiers must be attributed as the original publisher of the article or eBook, as applicable.

Authors have the responsibility of ensuring that any graphics or other materials which are the property of others may be included in the CC-BY licence, but this should be checked before relying on the CC-BY licence to reproduce those materials. Any copyright notices relating to those materials must be complied with.

Copyright and source acknowledgement notices may not be removed and must be displayed in any copy, derivative work or partial copy which includes the elements in question.

All copyright, and all rights therein, are protected by national and international copyright laws. The above represents a summary only. For further information please read Frontiers' Conditions for Website Use and Copyright Statement, and the applicable CC-BY licence.

ISSN 1664-8714
ISBN 978-2-88974-828-0
DOI 10.3389/978-2-88974-828-0

About Frontiers

Frontiers is more than just an open-access publisher of scholarly articles: it is a pioneering approach to the world of academia, radically improving the way scholarly research is managed. The grand vision of Frontiers is a world where all people have an equal opportunity to seek, share and generate knowledge. Frontiers provides immediate and permanent online open access to all its publications, but this alone is not enough to realize our grand goals.

Frontiers Journal Series

The Frontiers Journal Series is a multi-tier and interdisciplinary set of open-access, online journals, promising a paradigm shift from the current review, selection and dissemination processes in academic publishing. All Frontiers journals are driven by researchers for researchers; therefore, they constitute a service to the scholarly community. At the same time, the Frontiers Journal Series operates on a revolutionary invention, the tiered publishing system, initially addressing specific communities of scholars, and gradually climbing up to broader public understanding, thus serving the interests of the lay society, too.

Dedication to Quality

Each Frontiers article is a landmark of the highest quality, thanks to genuinely collaborative interactions between authors and review editors, who include some of the world's best academicians. Research must be certified by peers before entering a stream of knowledge that may eventually reach the public - and shape society; therefore, Frontiers only applies the most rigorous and unbiased reviews.
Frontiers revolutionizes research publishing by freely delivering the most outstanding research, evaluated with no bias from both the academic and social point of view. By applying the most advanced information technologies, Frontiers is catapulting scholarly publishing into a new generation.

What are Frontiers Research Topics?

Frontiers Research Topics are very popular trademarks of the Frontiers Journals Series: they are collections of at least ten articles, all centered on a particular subject. With their unique mix of varied contributions from Original Research to Review Articles, Frontiers Research Topics unify the most influential researchers, the latest key findings and historical advances in a hot research area! Find out more on how to host your own Frontiers Research Topic or contribute to one as an author by contacting the Frontiers Editorial Office: frontiersin.org/about/contact

FGF10 IN DEVELOPMENT, HOMEOSTASIS, DISEASE AND REPAIR AFTER INJURY

Topic Editors:
Saverio Bellusci, University of Giessen, Germany
Mohammad K. Hajihosseini, University of East Anglia, United Kingdom

Citation: Bellusci, S., Hajihosseini, M. K., eds. (2022). FGF10 in Development, Homeostasis, Disease and Repair After Injury. Lausanne: Frontiers Media SA. doi: 10.3389/978-2-88974-828-0

Table of Contents

frontiers in Genetics

MINI REVIEW
published: 25 September 2018
doi: 10.3389/fgene.2018.00418

Fgf10 Signaling in Lung Development, Homeostasis, Disease, and Repair After Injury

*Tingting Yuan, Thomas Volckaert, Diptiman Chanda, Victor J. Thannickal and Stijn P. De Langhe**

Division of Pulmonary, Department of Medicine, Allergy and Critical Care Medicine, University of Alabama at Birmingham, Birmingham, AL, United States

The lung is morphologically structured into a complex tree-like network with branched airways ending distally in a large number of alveoli for efficient oxygen exchange. At the cellular level, the adult lung consists of at least 40–60 different cell types which can be broadly classified into epithelial, endothelial, mesenchymal, and immune cells. Fibroblast growth factor 10 (Fgf10) located in the lung mesenchyme is essential to regulate epithelial proliferation and lineage commitment during embryonic development and post-natal life, and to drive epithelial regeneration after injury. The cells that express *Fgf10* in the mesenchyme are progenitors for mesenchymal cell lineages during embryonic development. During adult lung homeostasis, *Fgf10* is expressed in mesenchymal stromal niches, between cartilage rings in the upper conducting airways where basal cells normally reside, and in the lipofibroblasts adjacent to alveolar type 2 cells. Fgf10 protects and promotes lung epithelial regeneration after different types of lung injuries. An Fgf10-Hippo epithelial-mesenchymal crosstalk ensures maintenance of stemness and quiescence during homeostasis and basal stem cell (BSC) recruitment to further promote regeneration in response to injury. *Fgf10* signaling is dysregulated in different human lung diseases including bronchopulmonary dysplasia (BPD), idiopathic pulmonary fibrosis (IPF), and chronic obstructive pulmonary disease (COPD), suggesting that dysregulation of the FGF10 pathway is critical to the pathogenesis of several human lung diseases.

Keywords: Fgf10, regeneration, epithelium, fibrosis, injury

OPEN ACCESS

Edited by:
Saverio Bellusci, Justus Liebig Universität Gießen, Germany

Reviewed by:
Konstantinos Gkatzis, Max-Planck-Institut für Herz- und Lungenforschung, Germany
Emma Rawlins, University of Cambridge, United Kingdom

***Correspondence:**
Stijn P. De Langhe
sdelanghe@uabmc.edu

Specialty section:
This article was submitted to Stem Cell Research, a section of the journal Frontiers in Genetics

Received: *06 August 2018*
Accepted: *06 September 2018*
Published: *25 September 2018*

Citation:
Yuan T, Volckaert T, Chanda D, Thannickal VJ and De Langhe SP (2018) Fgf10 Signaling in Lung Development, Homeostasis, Disease, and Repair After Injury. Front. Genet. 9:418. doi: 10.3389/fgene.2018.00418

EPITHELIAL FGF10 SIGNALING DURING LUNG DEVELOPMENT

Fibroblast growth factor 10 (Fgf10) was first detected using whole-mount *in situ* hybridization 20 years ago in the splanchnic mesoderm surrounding the foregut around E9.5 when the primary lung buds start to emerge. Lung primordial mesoderm-specific transcription factor Tbx4 defines the *Fgf10* expression domain, at both the anterior and posterior boundaries (Sakiyama et al., 2003). The importance of Fgf10 in lung development is well illustrated by the total failure of lung formation and perinatal lethality of *Fgf10* deficient mice (Min et al., 1998; Xu et al., 1998; Sekine et al., 1999). Even though Fgf10 binds with high affinity to Fgfr2b, it has a weaker affinity for Fgfr1b (Ohuchi et al., 2000). The *Fgf10* knockout phenotype is phenocopied in mice lacking *Fgfr2b* (Arman et al., 1999; De Moerlooze et al., 2000), which is highly expressed in respiratory epithelium from the early embryonic lung bud stages through late fetal lung development (Peters et al., 1992). Intriguingly,

Fgfr2b has also been detected in the lung mesenchyme (Al Alam et al., 2015), but its mesenchymal function requires further investigation. Although Fgfr2b is a receptor for both Fgf7 and Fgf10 during lung development, *Fgf7* knockout mice do not exhibit an obvious lung defect (Guo et al., 1996), even though *Fgf7* is expressed in the developing lung mesenchyme starting at E14.5 (Mason et al., 1994). However, overexpression of *Fgf7* in mice using the human Sftpc promoter results in severe pulmonary malformations, including bronchial airway enlargement, cystic lung lesions and impaired branching morphogenesis leading to embryonic lethality (Simonet et al., 1995).

From E10.5 to E12.5, *Fgf10* expression is restricted to the distal lung mesenchyme at sites where branching occurs (Bellusci et al., 1997) and the ventral mesenchyme of the trachea (Sala et al., 2011; **Figure 1A**). For a long time, the localized pattern of *Fgf10* expression in the distal lung was thought to determine where new lung buds sprout. However, proper epithelial branching still occurs in developing $Fgf10^{-/-}$ lungs in which *Fgf10* is overexpressed in every cell. This indicates that the precise spatial organization of *Fgf10* expression is not required for the highly preserved and stereotypic branching morphogenesis. Hence, other mechanical and/or signaling pathways systems must be in place to control bud outgrowth. Instead, localized *Fgf10* expression in the distal mesenchyme is required to regulate epithelial lineage commitment (Volckaert et al., 2013) by maintaining the undifferentiated status of the distal Sox9-expressing epithelial progenitors and preventing them from differentiating into $Sox2^{pos}$ bronchial epithelium (**Figure 1A**). *Fgf10* achieves this, in part, by activating epithelial β-catenin signaling through activation of Akt, which negatively regulates Sox2 expression (Volckaert et al., 2013). Indeed, Wnt/β-catenin signaling is important for the regulation of proximal-distal differentiation in the developing airway epithelium (De Langhe et al., 2005; Hashimoto et al., 2012; Ostrin et al., 2018). As the epithelium grows out, cells which become further and further displaced from the source of Fgf10 start to differentiate into $Sox2^{pos}$ bronchial epithelium (Volckaert et al., 2013; Volckaert and De Langhe, 2014; **Figure 1A**). As a corollary, *Fgf10* hypomorphs and conditional *Fgf10* (*Dermo1-cre;Fgf10)* and *Fgfr2 (Sftpc-cre;Fgfr2)* mutants fail to maintain distal progenitors, resulting in a proximalized lung with impaired alveolar epithelial lineage formation and reduced capacity to produce surfactant proteins (Mailleux et al., 2005; Ramasamy et al., 2007; Abler et al., 2009). In addition, in lungs overexpressing *Fgf10* early on, distal epithelial progenitors fail to differentiate into bronchial epithelium (Volckaert et al., 2013). Taken together, these findings indicate that epithelial-mesenchymal interactions between Fgfr2b and its ligand Fgf10 is required for lung epithelial lineage commitment (Xu et al., 1998; Sekine et al., 1999; Ohuchi et al., 2000).

The localized expression of *Fgf10* in the trachea, on the other hand, drives submucosal gland (SMG) and basal cell development and their maintenance (Rawlins and Hogan, 2005; Volckaert et al., 2013; Volckaert et al., 2017). At the onset of lung and trachea initiation, Fgf10 is detected in the ventral mesenchyme of the trachea (Sala et al., 2011), and then becomes restricted to the intercartilage mesenchyme at later stages and into adulthood (Sala et al., 2011). Interestingly, although $Fgf10^{-/-}$ and $Fgfr2b^{-/-}$ embryos are born without lungs, they still develop a trachea (Sekine et al., 1999; De Moerlooze et al., 2000; Sala et al., 2011). SMGs are severely reduced in number and size in *Fgf10* heterozygotes (Jaskoll et al., 2005; Rawlins and Hogan, 2005). Abnormal function of SMGs of the upper respiratory tract are associated with severe/fatal asthma and cystic fibrosis later in life (Benayoun et al., 2003; Salinas et al., 2005). However, despite the significance of SMGs for human respiratory diseases, little is known about the mechanisms of Fgf10 signaling that controls their growth, differentiation, and homeostasis during early postnatal and adult life.

Overexpression of *Fgf10* at later stages of lung development, post-$Sox2^{pos}$ bronchial epithelial specification, directs the differentiation of $Sox2^{pos}$ proximal airway epithelium toward the p63/$Krt5^{pos}$ basal cell lineage while blocking $Foxj1^{pos}$ ciliated cell fate throughout the conducting airway (Volckaert et al., 2013). The cells that express *Fgf10* in the mesenchyme are themselves progenitors for airway and vascular smooth muscle cells as well as lipofibroblasts (LIFs) during embryonic development, and a subset of lung resident mesenchymal stem cells during adult life (Mailleux et al., 2005; Taniguchi et al., 2007; El Agha et al., 2014). Interestingly, Fgf10 also directly and indirectly orchestrates differentiation of these mesenchymal progenitors (El Agha and Bellusci, 2014; Chao et al., 2015). Epithelial BMP4, a target of Fgf10, controls the differentiation of cells arising from the distal mesenchymal *Fgf10*-expression domain into the airway smooth muscle cell (ASMC) lineage (Mailleux et al., 2005). In addition, *Fgf10* hypomorphs demonstrate defective formation of alveolar myofibroblasts (aMYFs) at different developmental stages (Mailleux et al., 2005; Ramasamy et al., 2007).

Starting at E16.5, $Id2^{pos}$ $Sox9^{pos}$ $Sftpc^{pos}$ $Pdpn^{pos}$ alveolar/bipotent epithelial progenitors give rise to alveolar type I and II (AT1/AT2) cells (Desai et al., 2014; Treutlein et al., 2014). Alveolar epithelial differentiation is coordinated by both mechanical forces and growth factors. In this context, it was recently shown that mechanical forces generated by fetal breathing movements stimulate AT1 cell differentiation, whereas Fgf10-mediated ERK1/2 signaling in distal progenitor cells prevents them from differentiating, thereby ensuring their AT2 fate (Li et al., 2018). In the mesenchyme, Gli^{pos} $Pdgfra^{pos}$ mesenchymal progenitor cells give rise to aMYFs and LIFs (Li et al., 2015; Chao et al., 2016). Although aMYFs and LIFs are both derived from $Gli1^{pos}$ $Pdgfr\alpha^{pos}$ mesenchymal progenitors, LIFs exhibit lower $Pdgfr\alpha^{pos}$ expression and higher levels of *Fgf10* expression in association with its receptors Fgfr1b and Fgfr2b. This suggests that different Fgfr and ligand profiles might mediate the direction of differentiation from $Pdgfr\alpha^{pos}$ mesenchymal progenitors toward LIF or aMYF (McGowan and McCoy, 2015). Interestingly, it has been shown that LIFs consist of both $Fgf10^{pos}$ and $Fgf10^{neg}$ subpopulations (Al Alam et al., 2015). *Fgf10* reduction in *Fgf10* hypomorphs as well as knockdown of *Fgfr2b* ligand *in vivo* led to significantly decreased expression of LIF marker Adrp at E18.5 in global LIF subpopulations ($Fgf10^{pos}$ and $Fgf10^{neg}$). This suggests that Fgf10 signals promote the formation of LIFs in an autocrine

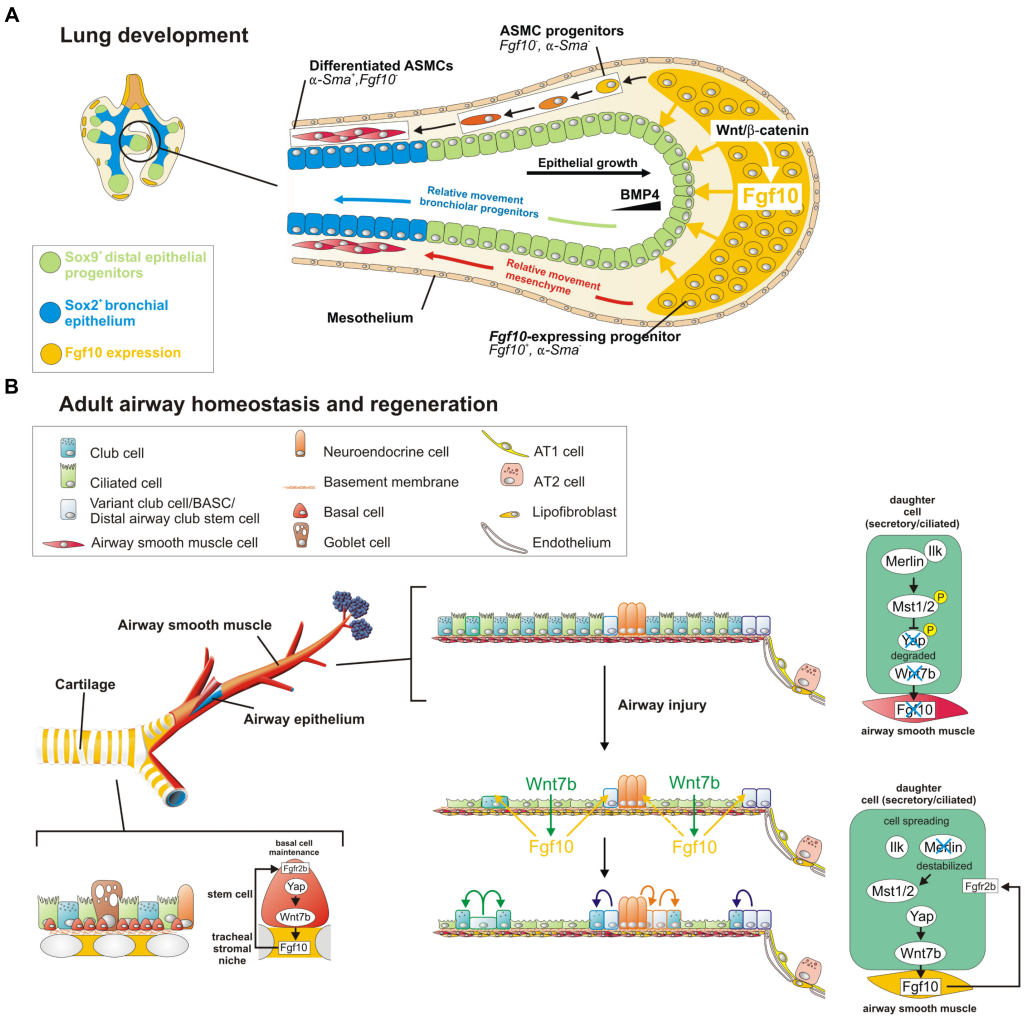

FIGURE 1 | A Wnt7b-Fgf10 epithelial-mesenchymal crosstalk maintains distal epithelial progenitors during lung development and becomes reactivated in the adult lung to regenerate injured airway epithelium. **(A)** During the branching stage of lung development, Fgf10 is expressed by mesenchymal progenitor cells, which depends on Wnt/β-catenin signaling, and acts on the distal epithelium to induce Bmp4 and Sox9 expression to keep them in an undifferentiated state. As the epithelial tube grows toward the Fgf10 source, Sox9 + progenitors acquire more proximal positions, switch on Sox2 expression and acquire bronchial epithelial fate. Simultaneously, distal Fgf10-expressing airway smooth muscle (ASMC) progenitors encounter epithelial Bmp4 and Shh (not shown) causing them to stop expressing Fgf10 and differentiate into mature ASMCs as they relocate proximally. **(B)** In the adult, basal stem cells (BSCs) generate their own Fgf10-expressing niche mediated by Yap-Wnt7b, and their maintenance is critically dependent on Fgf10-Fgfr2b signaling. The non-cartilaginous airway epithelium is kept quiescent during homeostasis, by active Integrin-linked kinase (Ilk)-Hippo signaling, which prevents Fgf10 expression in ASMCs. In response to injury, surviving epithelial cells spread out, leading to a destabilization of Merlin and inactivation (dephosphorylation) of Hippo kinases Mst1/2. This increases nuclear Yap in spreading epithelial cells causing these cells to secrete Wnt7b. Epithelial-derived Wnt7b then acts on ASMCs to induce Fgf10 expression, which is required for epithelial regeneration. Solid cell borders represent lineage labels to follow the fate of epithelial cells in response to injury.

and/or paracrine fashion (Al Alam et al., 2015). Additionally, constitutive *Fgfr1b* knockouts and conditional partial loss of *Fgfr2b* in lung mesenchyme revealed that Fgfr1b and Fgfr2b are likely to play redundant roles in LIF formation (Al Alam et al., 2015). Finally, Apert syndrome mice, which exhibit a splicing switch defect resulting in increased mesenchymal Fgfr2b expression, demonstrate increased *Fgf10* expression and signaling in the mesenchyme. These mice display reduced epithelial branching, arrested development of terminal airways and an "emphysema like" phenotype in post-natal lungs resulting from decreased canonical Wnt signaling (De Langhe et al., 2006), likely due to sequestering of the Fgf10 ligand by the misexpressed Fgfr2b receptor.

FGF10 SIGNALING DURING LUNG AND TRACHEA HOMEOSTASIS

During homeostasis, adult mouse lungs harbor three main stem cell populations that maintain the lung epithelium: basal stem/progenitor cells (BSCs) in the cartilaginous airways, club cells in the conducting airways and subsets of AT2 cells in the

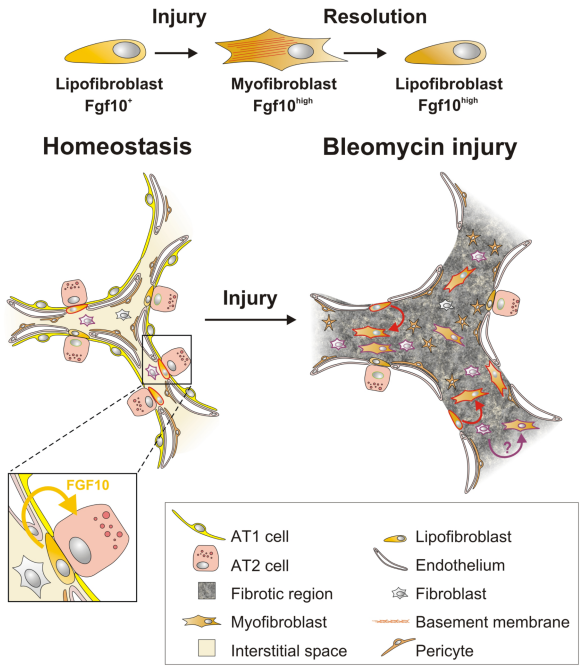

FIGURE 2 | Fgf10-expressing lipofibroblasts are a source of activated myofibroblasts, which re-acquire lipogenic fate during fibrosis resolution. During homeostasis, lipofibroblasts (LIFs) express Fgf10 and are near alveolar type II (AT2) cells. In response to bleomycin-mediated alveolar epithelial injury, LIFs undergo a lipogenic to myogenic switch in fibroblastic phenotype and upregulate Fgf10 expression. Vice versa, during fibrosis resolution, myofibroblasts re-acquire lipofibroblast fate yet retain high Fgf10 expression. Solid cell borders represent lineage labels to follow the fate of (lipo)fibroblasts.

alveoli (Rawlins et al., 2009; Rock et al., 2010; Barkauskas et al., 2013). During homeostasis *Fgf10* is expressed in mesenchymal stromal niches, between cartilage rings in the upper conducting airway where basal cells normally reside, and in the LIFs adjacent to AT2 cells in the alveoli (El Agha et al., 2014; **Figures 1B**, **2**).

BSCs are progenitors for club, Tuft1/2, neuroendocrine and ionocyte cells (Rock et al., 2009, 2010; Montoro et al., 2018). In the developing trachea, Fgf10 secreted by the inter-cartilage stromal tissue is involved in the development and maintenance of BSCs (**Figure 1B**). Overexpression of *Fgf10* in the trachea leads to BSC amplification whereas overexpressing *Fgf10* in adult club cells extends the BSC niche and induces club and BSC hyperplasia in conducting airways (Volckaert et al., 2017). Consistently, both Fgfr2b ligands Fgf7 and Fgf10 can promote basal cell colony expansion *in vitro* (Balasooriya et al., 2017). Furthermore, Fgfr2b signaling in the trachea is required for BSC maintenance during adult lung homeostasis (Volckaert et al., 2013, 2017). Even loss of one copy of *Fgfr2* in adult mouse airway BSCs is sufficient to reduce BSC self-renewal with cells quickly becoming senescent (Balasooriya et al., 2017). Interestingly, conditional deletion of *Fgfr1* or *Spry2* specifically in adult mouse tracheal BSCs using the *Krt5* promoter causes increased ERK/AKT signaling and BSC proliferation and a block in ciliated cell differentiation (Balasooriya et al., 2016), possibly due to increased Fgfr2b signaling caused by a lack of Spry2 activation by Fgfr1. This phenotype resembles that of tracheas overexpressing *Fgf10*, suggesting that this Fgfr1-SPRY2 signaling axis might function to antagonize Fgf10/Fgfr2b/ERK/AKT signaling, which is required for maintaining quiescence and restricting BSC proliferation in the steady-state airway epithelium *in vivo*.

FGF10 SIGNALING IN REPAIR OF THE INJURED LUNG

Recent studies indicate that Fgf10 prevents lung injury and promotes lung epithelial regeneration after various stresses, including bleomycin-induced alveolar epithelial lung injury (Gupte et al., 2009), influenza-induced acute respiratory distress syndrome (Quantius et al., 2016), high altitude pulmonary edema (She et al., 2012), LPS-induced lung injury (Tong et al., 2014), mechanical ventilation induced lung injury (Bi et al., 2014), ischemia-reperfusion lung injury (Fang et al., 2014), hyperoxia-induced neonatal lung injury (Chao et al., 2017), and naphthalene injury (Volckaert et al., 2011). In a post-pneumonectomy model, Fgfr2b ligands were shown to be required for aMYF formation during the regenerative response (Chen et al., 2012).

In the bleomycin model of pulmonary fibrosis, *Fgf10* overexpression in the alveolar epithelium of *Sftpc-rtTA;Tet-Fgf10* mice attenuates fibrosis through inhibition of TGF-β and improved survival of AT2 cells This indicates that Fgf10 has a protective as well as regenerative effect on epithelial progenitor cells (Gupte et al., 2009). Similarly, Fgf10 via the Grb2-SOS/Ras/Raf-1/MAPK pathway attenuates H_2O_2-induced alveolar epithelial DNA damage (Upadhyay et al., 2004). Overexpression of a dominant-negative Fgfr2 receptor (dnFgfr), specifically in the lung epithelium, inhibited retinoic acid-induced alveolar regeneration in association with increased PDGFRα^{pos} and reduced expression of SMA in interstitial myofibroblasts (Perl and Gale, 2009). Intra-tracheal administration of Fgf10 attenuates lipopolysaccharide (LPS)-induced acute lung injury with increased AT2 proliferation (Tong et al., 2014). Lung resident mesenchymal stromal cells (MSCs) isolated from Fgf10 pretreated rats are protected against LPS-induced acute lung injury (Tong et al., 2016). However, the mechanism underlying these protective effects of Fgf10 signaling during injury and regeneration in adult lung have not yet been fully elucidated.

Fgf10-expressing cells were identified as a subset of LIF progenitors during embryonic development (El Agha et al., 2014). *Fgf10*-expressing LIFs have been shown to differentiate into activated MYFs upon bleomycin injury, while simultaneously upregulating their *Fgf10* expression levels (El Agha et al., 2017). *Fgf10*-expressing MYFs dedifferentiate back into LIFs but do not downregulate their *Fgf10* expression levels during the resolution phase of lung fibrosis (El Agha et al., 2017) suggesting that they retain a memory of the injury which might protect against further injury. This supports the concept that LIFs serve as a source of activated MYFs during fibrogenesis which revert back to LIFs during fibrosis resolution (El Agha et al., 2017; **Figure 2**).

Naphthalene injury is a well-established injury model to study conducting airway epithelial regeneration by selectively ablating club cells except for a few naphthalene-resistant club stem cells located at bronchoalveolar duct junctions (BADJs) and adjacent to neuroendocrine bodies (NEBs). In the adult lung, *Fgf10* is not expressed in mature ASMCs during homeostasis (**Figure 1B**). However, upon conducting airway epithelial injury, when surviving differentiated epithelial cells spread in an attempt to maintain barrier function, they downregulate their Hippo pathway to drive Yap into the nucleus, and induce the secretion of Wnt7b. Epithelial-derived Wnt7b, in turn, induces Lgr6^{pos} ASMCs to release Fgf10 (Volckaert et al., 2011, 2017; Volckaert and De Langhe, 2014; Lee et al., 2017), which activates Notch and β-catenin signaling in surviving club cells to drive their amplification to promote regeneration (Volckaert et al., 2011; Lee et al., 2017; **Figure 1B**). Together, these findings provide strong evidence that ASMCs function as a niche for conducting airway epithelial stem cells. Besides club cell regeneration, the induction of *Fgf10* expression by the ASMC niche in non-cartilaginous airways extends the BSC niche, allowing the recruitment of tracheal BSCs and/or driving the differentiation of Sox2^{pos}p63^{pos}Krt5^{neg} progenitors along the BSC lineage (Volckaert et al., 2017; Yang et al., 2018). In summary, the Fgf10-Hippo epithelial-mesenchymal crosstalk ensures maintenance of stemness and quiescence during homeostasis and recruitment of BSCs to promote regeneration in response to injury (Volckaert et al., 2017; **Figure 1B**).

A similar tonic Hedgehog signal maintains lung airway epithelial and mesenchymal quiescence in the distal mouse airways (Peng et al., 2015). In this model, loss of Hedgehog signaling drives regeneration in response to naphthalene-induced epithelial injury via a mesenchymal feedback mechanism, and deregulation of hedgehog during naphthalene induced epithelial lung injury leads to aberrant repair and regeneration (Peng et al., 2015). These findings imply that the Wnt-Fgf10 epithelial-mesenchymal cross-talk and Shh pathway may function as an interactive signaling network in airway and alveolar remodeling responses to chronic injury in asthma, chronic obstructive pulmonary disease (COPD) and pulmonary fibrosis.

FGF10 SIGNALING IN HUMAN LUNG DISEASES

Several syndromic craniosynostoses have been associated with dominantly acting mutations of *FGFR1*, *FGFR2*, and *FGFR3* (Hajihosseini et al., 2001). *FGFR2B* is up-regulated in cultured fibroblasts of some Apert's and Pfeiffer's syndrome patients (Oldridge et al., 1999). Gain-of-Fgfr2b function mice *Fgfr2c*$^{+/\Delta}$ show phenotypic resemblance to Apert's and Pfeiffer's syndromes, including visceral and growth defects, neonatal growth retardation and death, coronal synostosis, ocular proptosis, precocious sternal fusion, and abnormalities in secondary branching in lung and kidney that undergo branching morphogenesis (Hajihosseini et al., 2001; De Langhe et al., 2006).

In humans, haploinsuffiencies for *FGF10* or *FGFR2B* result in autosomal dominant aplasia of lacrimal and salivary glands and lacrimo auriculo-dentodigital syndrome, respectively (Entesarian et al., 2005; Klar et al., 2011). In the former syndrome, patients exhibit irreversible airway obstruction, indicating that genetic variants affecting the FGF10 signaling pathway are important determinants of lung function which ultimately contribute to COPD (Klar et al., 2011). Notably, an airway branch variant with absence of the right medial-basal airway associated with polymorphisms within the *FGF10* gene is associated with COPD among smokers (Smith et al., 2018). Interestingly, increased nuclear YAP levels, along with FGFR2B and WNT7b expression, were observed in squamous metaplastic areas within the airway epithelium of COPD subjects (Volckaert et al., 2017), suggesting that the Hippo pathway is inactivated to induce FGF10 expression and BSC amplification in human COPD.

Bronchopulmonary dysplasia (BPD) is a chronic pulmonary disease of prematurely born infants characterized by arrested alveolar development (Chao et al., 2017). BPD biopsy samples show reduced *FGF10* expression (Benjamin et al., 2007), implicating that FGF10 signaling may be involved in BPD. By using hyperoxia-induced neonatal lung injury from post-natal day 0 (P0) to P8 as a mouse model of BPD, Chao et al. (2017) have shown that *Fgf10* deficiency causes lethality from P5 in *Fgf10*$^{+/-}$ pups due to impaired AT2 formation after hyperoxic injury. In this study, overexpression of a secreted dominant negative *Fgfr2b*, demonstrated that post-natal deficiency of Fgfr2b ligands in the context of hyperoxia-exposure causes decreased *Sftpc* expression and eventually leads to significant lethality. This indicates that Fgfr2b ligands are important for repair after hyperoxia exposure in neonatal lung.

Idiopathic pulmonary fibrosis (IPF) is a chronic interstitial lung disease characterized by the loss of alveolar epithelial integrity, progressive invasion of the lung parenchyma by myofibroblasts and increased extracellular matrix (ECM) deposition leading to respiratory failure, and death often within 5 years of diagnosis (Thannickal et al., 2004; King et al., 2011; Steele and Schwartz, 2013; Yang et al., 2013). Gene expression profiles of MSCs from IPF patient lungs revealed that *FGF10* expression in MSCs is suppressed in IPF subjects with progressive disease, along with upregulation of both TGF-β1 and SHH signaling. This suggests that *FGF10* deficiency is a potentially critical factor in disease progression (Chanda et al., 2016). However, recently it has been shown that FGF10 is significantly upregulated at both mRNA and protein level in IPF lungs compared to the donor lungs, especially in dense fibrotic islands where ACTA2^{pos} cells accumulate (El Agha et al., 2017).

CONCLUSION

Fgf10 signaling is essential for lung development and adult stem cell maintenance. Important questions remain regarding the mechanisms that regulate *Fgf10* expression in the niche to unleash the full therapeutic potential of Fgf10. In addition, very little is known about the importance of FGF10 signaling in human lung development and homeostasis. During homeostasis,

BSCs are restricted to the cartilaginous airway in mice as they require Fgfr2b signaling for their maintenance, whereas in humans they can be found deep in the lung. However, upon different types of injury BSCs are deployed throughout the mouse lung as ASMCs in the non-cartilaginous airways re-express *Fgf10* to regenerate the airway epithelium. It is therefore likely that the apparent restricted BSC pattern in the mouse lung is due to it being housed in a fairly sterile environment rather than constantly being exposed to environmental insults as is the case for humans.

AUTHOR CONTRIBUTIONS

TY, TV, and SDL wrote the manuscript. DC and VT edited the manuscript.

FUNDING

This study was supported by NIH R01 HL126732, HL132156 and March of Dimes Grant No. 1-FY15-463 awarded to SDL.

REFERENCES

Abler, L. L., Mansour, S. L., and Sun, X. (2009). Conditional gene inactivation reveals roles for Fgf10 and Fgfr2 in establishing a normal pattern of epithelial branching in the mouse lung. *Dev. Dyn.* 238, 1999–2013. doi: 10.1002/dvdy.22032

Al Alam, D., El Agha, E., Sakurai, R., Kheirollahi, V., Moiseenko, A., Danopoulos, S., et al. (2015). Evidence for the involvement of fibroblast growth factor 10 in lipofibroblast formation during embryonic lung development. *Development* 142, 4139–4150. doi: 10.1242/dev.109173

Arman, E., Haffner-Krausz, R., Gorivodsky, M., and Lonai, P. (1999). Fgfr2 is required for limb outgrowth and lung-branching morphogenesis. *Proc. Natl. Acad. Sci. U.S.A.* 96, 11895–11899. doi: 10.1073/pnas.96.21.11895

Balasooriya, G. I., Goschorska, M., Piddini, E., and Rawlins, E. L. (2017). FGFR2 is required for airway basal cell self-renewal and terminal differentiation. *Development* 144, 1600–1606. doi: 10.1242/dev.135681

Balasooriya, G. I., Johnson, J. A., Basson, M. A., and Rawlins, E. L. (2016). An FGFR1-SPRY2 signaling axis limits basal cell proliferation in the steady-state airway epithelium. *Dev. Cell* 37, 85–97. doi: 10.1016/j.devcel.2016.03.001

Barkauskas, C. E., Cronce, M. J., Rackley, C. R., Bowie, E. J., Keene, D. R., Stripp, B. R., et al. (2013). Type 2 alveolar cells are stem cells in adult lung. *J. Clin. Invest.* 123, 3025–3036. doi: 10.1172/JCI68782

Bellusci, S., Grindley, J., Emoto, H., Itoh, N., and Hogan, B. L. (1997). Fibroblast growth factor 10 (FGF10) and branching morphogenesis in the embryonic mouse lung. *Development* 124, 4867–4878.

Benayoun, L., Druilhe, A., Dombret, M. C., Aubier, M., and Pretolani, M. (2003). Airway structural alterations selectively associated with severe asthma. *Am. J. Respir. Crit. Care Med.* 167, 1360–1368. doi: 10.1164/rccm.200209-1030OC

Benjamin, J. T., Smith, R. J., Halloran, B. A., Day, T. J., Kelly, D. R., and Prince, L. S. (2007). FGF-10 is decreased in bronchopulmonary dysplasia and suppressed by Toll-like receptor activation. *Am. J. Physiol. Lung Cell Mol. Physiol.* 292, L550–L558. doi: 10.1152/ajplung.00329.2006

Bi, J., Tong, L., Zhu, X., Yang, D., Bai, C., Song, Y., et al. (2014). Keratinocyte growth factor-2 intratracheal instillation significantly attenuates ventilator-induced lung injury in rats. *J. Cell Mol. Med.* 18, 1226–1235. doi: 10.1111/jcmm.12269

Chanda, D., Kurundkar, A., Rangarajan, S., Locy, M., Bernard, K., Sharma, N. S., et al. (2016). Developmental reprogramming in mesenchymal stromal cells of human subjects with idiopathic pulmonary fibrosis. *Sci. Rep.* 6:37445. doi: 10.1038/srep37445

Chao, C. M., El Agha, E., Tiozzo, C., Minoo, P., and Bellusci, S. (2015). A breath of fresh air on the mesenchyme: impact of impaired mesenchymal development on the pathogenesis of bronchopulmonary dysplasia. *Front. Med.* 2:27. doi: 10.3389/fmed.2015.00027

Chao, C. M., Moiseenko, A., Zimmer, K. P., and Bellusci, S. (2016). Alveologenesis: key cellular players and fibroblast growth factor 10 signaling. *Mol. Cell Pediatr.* 3:17. doi: 10.1186/s40348-016-0045-7

Chao, C. M., Yahya, F., Moiseenko, A., Tiozzo, C., Shrestha, A., Ahmadvand, N., et al. (2017). Fgf10 deficiency is causative for lethality in a mouse model of bronchopulmonary dysplasia. *J. Pathol.* 241, 91–103. doi: 10.1002/path.4834

Chen, L., Acciani, T., Le Cras, T., Lutzko, C., and Perl, A. K. (2012). Dynamic regulation of platelet-derived growth factor receptor alpha expression in alveolar fibroblasts during realveolarization. *Am. J. Respir. Cell Mol. Biol.* 47, 517–527. doi: 10.1165/rcmb.2012-0030OC

De Langhe, S. P., Carraro, G., Warburton, D., Hajihosseini, M. K., and Bellusci, S. (2006). Levels of mesenchymal FGFR2 signaling modulate smooth muscle progenitor cell commitment in the lung. *Dev. Biol.* 299, 52–62. doi: 10.1016/j.ydbio.2006.07.001

De Langhe, S. P., Sala, F. G., Del Moral, P. M., Fairbanks, T. J., Yamada, K. M., Warburton, D., et al. (2005). Dickkopf-1 (DKK1) reveals that fibronectin is a major target of Wnt signaling in branching morphogenesis of the mouse embryonic lung. *Dev. Biol.* 277, 316–331. doi: 10.1016/j.ydbio.2004.09.023

De Moerlooze, L., Spencer-Dene, B., Revest, J. M., Hajihosseini, M., Rosewell, I., and Dickson, C. (2000). An important role for the IIIb isoform of fibroblast growth factor receptor 2 (FGFR2) in mesenchymal-epithelial signalling during mouse organogenesis. *Development* 127, 483–492.

Desai, T. J., Brownfield, D. G., and Krasnow, M. A. (2014). Alveolar progenitor and stem cells in lung development, renewal and cancer. *Nature* 507, 190–194. doi: 10.1038/nature12930

El Agha, E., and Bellusci, S. (2014). Walking along the fibroblast growth factor 10 route: a key pathway to understand the control and regulation of epithelial and mesenchymal cell-lineage formation during lung development and repair after injury. *Scientifica* 2014:538379. doi: 10.1155/2014/538379

El Agha, E., Herold, S., Al Alam, D., Quantius, J., MacKenzie, B., Carraro, G., et al. (2014). Fgf10-positive cells represent a progenitor cell population during lung development and postnatally. *Development* 141, 296–306. doi: 10.1242/dev.099747

El Agha, E., Moiseenko, A., Kheirollahi, V., De Langhe, S., Crnkovic, S., Kwapiszewska, G., et al. (2017). Two-Way conversion between lipogenic and myogenic fibroblastic phenotypes marks the progression and resolution of lung fibrosis. *Cell Stem Cell* 20, 261.e3–273.e3. doi: 10.1016/j.stem.2017.03.011

Entesarian, M., Matsson, H., Klar, J., Bergendal, B., Olson, L., Arakaki, R., et al. (2005). Mutations in the gene encoding fibroblast growth factor 10 are associated with aplasia of lacrimal and salivary glands. *Nat. Genet.* 37, 125–127. doi: 10.1038/ng1507

Fang, X., Wang, L., Shi, L., Chen, C., Wang, Q., Bai, C., et al. (2014). Protective effects of keratinocyte growth factor-2 on ischemia-reperfusion-induced lung injury in rats. *Am. J. Respir. Cell Mol. Biol.* 50, 1156–1165. doi: 10.1165/rcmb.2013-0268OC

Guo, L., Degenstein, L., and Fuchs, E. (1996). Keratinocyte growth factor is required for hair development but not for wound healing. *Genes Dev.* 10, 165–175.

Gupte, V. V., Ramasamy, S. K., Reddy, R., Lee, J., Weinreb, P. H., Violette, S. M., et al. (2009). Overexpression of fibroblast growth factor-10 during both inflammatory and fibrotic phases attenuates bleomycin-induced pulmonary fibrosis in mice. *Am. J. Respir. Crit. Care Med.* 180, 424–436. doi: 10.1164/rccm.200811-1794OC

Hajihosseini, M. K., Wilson, S., De Moerlooze, L., and Dickson, C. (2001). A splicing switch and gain-of-function mutation in FgfR2-IIIc hemizygotes causes Apert/Pfeiffer-syndrome-like phenotypes. *Proc. Natl. Acad. Sci. U.S.A.* 98, 3855–3860. doi: 10.1073/pnas.071586898

Hashimoto, S., Chen, H., Que, J., Brockway, B. L., Drake, J. A., Snyder, J. C., et al. (2012). beta-Catenin-SOX2 signaling regulates the fate of developing airway epithelium. *J. Cell Sci.* 125(Pt 4), 932–942. doi: 10.1242/jcs.092734

Jaskoll, T., Abichaker, G., Witcher, D., Sala, F. G., Bellusci, S., Hajihosseini, M. K., et al. (2005). FGF10/FGFR2b signaling plays essential roles during in vivo embryonic submandibular salivary gland morphogenesis. *BMC Dev. Biol.* 5:11. doi: 10.1186/1471-213X-5-11

King, T. E. Jr., Pardo, A., and Selman, M. (2011). Idiopathic pulmonary fibrosis. *Lancet* 378, 1949–1961. doi: 10.1016/S0140-6736(11)60052-4

Klar, J., Blomstrand, P., Brunmark, C., Badhai, J., Hakansson, H. F., Brange, C. S., et al. (2011). Fibroblast growth factor 10 haploinsufficiency causes chronic obstructive pulmonary disease. *J. Med. Genet.* 48, 705–709. doi: 10.1136/jmedgenet-2011-100166

Lee, J. H., Tammela, T., Hofree, M., Choi, J., Marjanovic, N. D., Han, S., et al. (2017). Anatomically and functionally distinct lung mesenchymal populations marked by Lgr5 and Lgr6. *Cell* 170, 1149.e12–1163.e12. doi: 10.1016/j.cell.2017.07.028

Li, C., Li, M., Li, S., Xing, Y., Yang, C. Y., Li, A., et al. (2015). Progenitors of secondary crest myofibroblasts are developmentally committed in early lung mesoderm. *Stem Cells* 33, 999–1012. doi: 10.1002/stem.1911

Li, J., Wang, Z., Chu, Q., Jiang, K., Li, J., and Tang, N. (2018). The strength of mechanical forces determines the differentiation of alveolar epithelial cells. *Dev. Cell* 44, 297.e5–312.e5. doi: 10.1016/j.devcel.2018.01.008

Mailleux, A. A., Kelly, R., Veltmaat, J. M., De Langhe, S. P., Zaffran, S., Thiery, J. P., et al. (2005). Fgf10 expression identifies parabronchial smooth muscle cell progenitors and is required for their entry into the smooth muscle cell lineage. *Development* 132, 2157–2166. doi: 10.1242/dev.01795

Mason, I. J., Fuller-Pace, F., Smith, R., and Dickson, C. (1994). FGF-7 (keratinocyte growth factor) expression during mouse development suggests roles in myogenesis, forebrain regionalisation and epithelial-mesenchymal interactions. *Mech. Dev.* 45, 15–30. doi: 10.1016/0925-4773(94)90050-7

McGowan, S. E., and McCoy, D. M. (2015). Fibroblast growth factor signaling in myofibroblasts differs from lipofibroblasts during alveolar septation in mice. *Am. J. Physiol. Lung Cell Mol. Physiol.* 309, L463–L474. doi: 10.1152/ajplung.00013.2015

Min, H., Danilenko, D. M., Scully, S. A., Bolon, B., Ring, B. D., Tarpley, J. E., et al. (1998). Fgf-10 is required for both limb and lung development and exhibits striking functional similarity to Drosophila branchless. *Genes Dev.* 12, 3156–3161. doi: 10.1101/gad.12.20.3156

Montoro, D. T., Haber, A. L., Biton, M., Vinarsky, V., Lin, B., Birket, S. E., et al. (2018). A revised airway epithelial hierarchy includes CFTR-expressing ionocytes. *Nature* 560, 319–324. doi: 10.1038/s41586-018-0393-7

Ohuchi, H., Hori, Y., Yamasaki, M., Harada, H., Sekine, K., Kato, S., et al. (2000). FGF10 acts as a major ligand for FGF receptor 2 IIIb in mouse multi-organ development. *Biochem. Biophys. Res. Commun.* 277, 643–649. doi: 10.1006/bbrc.2000.3721

Oldridge, M., Zackai, E. H., McDonald-McGinn, D. M., Iseki, S., Morriss-Kay, G. M., Twigg, S. R., et al. (1999). De novo alu-element insertions in FGFR2 identify a distinct pathological basis for Apert syndrome. *Am. J. Hum. Genet.* 64, 446–461. doi: 10.1086/302245

Ostrin, E. J., Little, D. R., Gerner-Mauro, K. N., Sumner, E. A., Rios-Corzo, R., Ambrosio, E., et al. (2018). Beta-Catenin maintains lung epithelial progenitors after lung specification. *Development* 2018:160788. doi: 10.1242/dev.160788

Peng, T., Frank, D. B., Kadzik, R. S., Morley, M. P., Rathi, K. S., Wang, T., et al. (2015). Hedgehog actively maintains adult lung quiescence and regulates repair and regeneration. *Nature* 526, 578–582. doi: 10.1038/nature14984

Perl, A. K., and Gale, E. (2009). FGF signaling is required for myofibroblast differentiation during alveolar regeneration. *Am. J. Physiol. Lung Cell Mol. Physiol.* 297, L299–L308. doi: 10.1152/ajplung.00008.2009

Peters, K. G., Werner, S., Chen, G., and Williams, L. T. (1992). Two FGF receptor genes are differentially expressed in epithelial and mesenchymal tissues during limb formation and organogenesis in the mouse. *Development* 114, 233–243.

Quantius, J., Schmoldt, C., Vazquez-Armendariz, A. I., Becker, C., El Agha, E., Wilhelm, J., et al. (2016). Influenza virus infects epithelial stem/progenitor cells of the distal lung: impact on Fgfr2b-Driven epithelial repair. *PLoS Pathog.* 12:e1005544. doi: 10.1371/journal.ppat.1005544

Ramasamy, S. K., Mailleux, A. A., Gupte, V. V., Mata, F., Sala, F. G., Veltmaat, J. M., et al. (2007). Fgf10 dosage is critical for the amplification of epithelial cell progenitors and for the formation of multiple mesenchymal lineages during lung development. *Dev. Biol.* 307, 237–247. doi: 10.1016/j.ydbio.2007.04.033

Rawlins, E. L., and Hogan, B. L. (2005). Intercellular growth factor signaling and the development of mouse tracheal submucosal glands. *Dev. Dyn.* 233, 1378–1385. doi: 10.1002/dvdy.20461

Rawlins, E. L., Okubo, T., Xue, Y., Brass, D. M., Auten, R. L., Hasegawa, H., et al. (2009). The role of Scgb1a1 + Clara cells in the long-term maintenance and repair of lung airway, but not alveolar, epithelium. *Cell Stem Cell* 4, 525–534. doi: 10.1016/j.stem.2009.04.002

Rock, J. R., Onaitis, M. W., Rawlins, E. L., Lu, Y., Clark, C. P., Xue, Y., et al. (2009). Basal cells as stem cells of the mouse trachea and human airway epithelium. *Proc. Natl. Acad. Sci. U.S.A.* 106, 12771–12775. doi: 10.1073/pnas.0906850106

Rock, J. R., Randell, S. H., and Hogan, B. L. (2010). Airway basal stem cells: a perspective on their roles in epithelial homeostasis and remodeling. *Dis. Model. Mech.* 3, 545–556. doi: 10.1242/dmm.006031

Sakiyama, J., Yamagishi, A., and Kuroiwa, A. (2003). Tbx4-Fgf10 system controls lung bud formation during chicken embryonic development. *Development* 130, 1225–1234. doi: 10.1242/dev.00345

Sala, F. G., Del Moral, P. M., Tiozzo, C., Alam, D. A., Warburton, D., Grikscheit, T., et al. (2011). FGF10 controls the patterning of the tracheal cartilage rings via Shh. *Development* 138, 273–282. doi: 10.1242/dev.051680

Salinas, D., Haggie, P. M., Thiagarajah, J. R., Song, Y., Rosbe, K., Finkbeiner, W. E., et al. (2005). Submucosal gland dysfunction as a primary defect in cystic fibrosis. *FASEB J.* 19, 431–433. doi: 10.1096/fj.04-2879fje

Sekine, K., Ohuchi, H., Fujiwara, M., Yamasaki, M., Yoshizawa, T., Sato, T., et al. (1999). Fgf10 is essential for limb and lung formation. *Nat. Genet.* 21, 138–141. doi: 10.1038/5096

She, J., Goolaerts, A., Shen, J., Bi, J., Tong, L., Gao, L., et al. (2012). KGF-2 targets alveolar epithelia and capillary endothelia to reduce high altitude pulmonary oedema in rats. *J. Cell Mol. Med.* 16, 3074–3084. doi: 10.1111/j.1582-4934.2012.01588.x

Simonet, W. S., DeRose, M. L., Bucay, N., Nguyen, H. Q., Wert, S. E., Zhou, L., et al. (1995). Pulmonary malformation in transgenic mice expressing human keratinocyte growth factor in the lung. *Proc. Natl. Acad. Sci. U.S.A.* 92, 12461–12465. doi: 10.1073/pnas.92.26.12461

Smith, B. M., Traboulsi, H., Austin, J. H. M., Manichaikul, A., Hoffman, E. A., Bleecker, E. R., et al. (2018). Human airway branch variation and chronic obstructive pulmonary disease. *Proc. Natl. Acad. Sci. U.S.A.* 115, E974–E981. doi: 10.1073/pnas.1715564115

Steele, M. P., and Schwartz, D. A. (2013). Molecular mechanisms in progressive idiopathic pulmonary fibrosis. *Annu. Rev. Med.* 64, 265–276. doi: 10.1146/annurev-med-042711-142004

Taniguchi, K., Ayada, T., Ichiyama, K., Kohno, R., Yonemitsu, Y., Minami, Y., et al. (2007). Sprouty2 and Sprouty4 are essential for embryonic morphogenesis and regulation of FGF signaling. *Biochem. Biophys. Res. Commun.* 352, 896–902. doi: 10.1016/j.bbrc.2006.11.107

Thannickal, V. J., Toews, G. B., White, E. S., Lynch, J. P. III, and Martinez, F. J. (2004). Mechanisms of pulmonary fibrosis. *Annu. Rev. Med.* 55, 395–417. doi: 10.1146/annurev.med.55.091902.103810

Tong, L., Bi, J., Zhu, X., Wang, G., Liu, J., Rong, L., et al. (2014). Keratinocyte growth factor-2 is protective in lipopolysaccharide-induced acute lung injury in rats. *Respir. Physiol. Neurobiol.* 201, 7–14. doi: 10.1016/j.resp.2014.06.011

Tong, L., Zhou, J., Rong, L., Seeley, E. J., Pan, J., Zhu, X., et al. (2016). Fibroblast growth factor-10 (FGF-10) mobilizes lung-resident mesenchymal stem cells and protects against acute lung injury. *Sci. Rep.* 6:21642. doi: 10.1038/srep21642

Treutlein, B., Brownfield, D. G., Wu, A. R., Neff, N. F., Mantalas, G. L., Espinoza, F. H., et al. (2014). Reconstructing lineage hierarchies of the distal lung epithelium using single-cell RNA-seq. *Nature* 509, 371–375. doi: 10.1038/nature13173

Upadhyay, D., Bundesmann, M., Panduri, V., Correa-Meyer, E., and Kamp, D. W. (2004). Fibroblast growth factor-10 attenuates H2O2-induced alveolar epithelial cell DNA damage: role of MAPK activation and DNA repair. *Am. J. Respir. Cell Mol. Biol.* 31, 107–113. doi: 10.1165/rcmb.2003-0064OC

Volckaert, T., Campbell, A., Dill, E., Li, C., Minoo, P., and De Langhe, S. (2013). Localized Fgf10 expression is not required for lung branching morphogenesis but prevents differentiation of epithelial progenitors. *Development* 140, 3731–3742. doi: 10.1242/dev.096560

Volckaert, T., and De Langhe, S. (2014). Lung epithelial stem cells and their niches: Fgf10 takes center stage. *Fibrogenesis Tissue Repair* 7:8. doi: 10.1186/1755-1536-7-8

Volckaert, T., Dill, E., Campbell, A., Tiozzo, C., Majka, S., Bellusci, S., et al. (2011). Parabronchial smooth muscle constitutes an airway epithelial stem cell niche in the mouse lung after injury. *J. Clin. Invest.* 121, 4409–4419. doi: 10.1172/JCI58097

Volckaert, T., Yuan, T., Chao, C. M., Bell, H., Sitaula, A., Szimmtenings, L., et al. (2017). Fgf10-hippo epithelial-mesenchymal crosstalk maintains and recruits lung basal stem cells. *Dev. Cell* 43, 48.e5–59.e5. doi: 10.1016/j.devcel.2017.09.003

Xu, X., Weinstein, M., Li, C., Naski, M., Cohen, R. I., Ornitz, D. M., et al. (1998). Fibroblast growth factor receptor 2 (FGFR2)-mediated reciprocal regulation loop between FGF8 and FGF10 is essential for limb induction. *Development* 125, 753–765.

Yang, J., Wheeler, S. E., Velikoff, M., Kleaveland, K. R., LaFemina, M. J., Frank, J. A., et al. (2013). Activated alveolar epithelial cells initiate fibrosis through secretion of mesenchymal proteins. *Am. J. Pathol.* 183, 1559–1570. doi: 10.1016/j.ajpath.2013.07.016

Yang, Y., Riccio, P., Schotsaert, M., Mori, M., Lu, J., Lee, D. K., et al. (2018). Spatial-Temporal lineage restrictions of embryonic p63(+) progenitors establish distinct stem cell pools in adult airways. *Dev. Cell* 44, 752.e4–761.e4. doi: 10.1016/j.devcel.2018.03.001

Conflict of Interest Statement: The authors declare that the research was conducted in the absence of any commercial or financial relationships that could be construed as a potential conflict of interest.

Copyright © 2018 Yuan, Volckaert, Chanda, Thannickal and De Langhe. This is an open-access article distributed under the terms of the Creative Commons Attribution License (CC BY). The use, distribution or reproduction in other forums is permitted, provided the original author(s) and the copyright owner(s) are credited and that the original publication in this journal is cited, in accordance with accepted academic practice. No use, distribution or reproduction is permitted which does not comply with these terms.

frontiers in Genetics

MINI REVIEW
published: 23 October 2018
doi: 10.3389/fgene.2018.00500

Regulation of FGF10 Signaling in Development and Disease

Joanne Watson[1,2] *and Chiara Francavilla*[1]*

[1] Division of Molecular and Cellular Function, School of Biological Sciences, Faculty of Biology Medicine and Health, The University of Manchester, Manchester, United Kingdom, [2] Division of Evolution and Genomic Sciences, School of Biological Sciences, Faculty of Biology Medicine and Health, The University of Manchester, Manchester, United Kingdom

Fibroblast Growth Factor 10 (FGF10) is a multifunctional mesenchymal-epithelial signaling growth factor, which is essential for multi-organ development and tissue homeostasis in adults. Furthermore, FGF10 deregulation has been associated with human genetic disorders and certain forms of cancer. Upon binding to FGF receptors with heparan sulfate as co-factor, FGF10 activates several intracellular signaling cascades, resulting in cell proliferation, differentiation, and invasion. FGF10 activity is modulated not only by heparan sulfate proteoglycans in the extracellular matrix, but also by hormones and other soluble factors. Despite more than 20 years of research on FGF10 functions, context-dependent regulation of FGF10 signaling specificity remains poorly understood. Emerging modes of FGF10 signaling regulation will be described, focusing on the role of FGF10 trafficking and sub-cellular localization, heparan sulfate proteoglycans, and miRNAs. Systems biology approaches based on quantitative proteomics will be considered for globally investigating FGF10 signaling specificity. Finally, current gaps in our understanding of FGF10 functions, such as the relative contribution of receptor isoforms to signaling activation, will be discussed in the context of genetic disorders and tumorigenesis.

Keywords: fibroblast growth factor 10, FGF receptor, signaling, development, cancer, genetic disorders, mass spectrometry, quantitative proteomics

OPEN ACCESS

Edited by:
Saverio Bellusci, Justus-Liebig-Universität Gießen, Germany

Reviewed by:
Jin-San Zhang, Mayo Clinic, United States
Nan Tang Tang, National Institute of Biological Sciences (NIBS), China
Elie El Agha, Justus-Liebig-Universität Gießen, Germany

***Correspondence:**
Chiara Francavilla
chiara.francavilla@manchester.ac.uk

Specialty section:
This article was submitted to Stem Cell Research, a section of the journal Frontiers in Genetics

Received: *23 August 2018*
Accepted: *05 October 2018*
Published: *23 October 2018*

Citation:
Watson J and Francavilla C (2018) Regulation of FGF10 Signaling in Development and Disease. Front. Genet. 9:500. doi: 10.3389/fgene.2018.00500

INTRODUCTION

The Fibroblast Growth Factor 10 (*Fgf10*) gene has been identified in all examined vertebrates (Emoto et al., 1997). It belongs to the FGF7 subfamily of FGFs (**Figure 1A**) which was generated from a common ancestral gene during the early evolution of vertebrates and shares amino acids sequence similarities and biochemical functions (Ornitz and Itoh, 2015; **Figure 1B**).

Fibroblast Growth Factor 10 is a paracrine signaling growth factor of 215 amino acids with a typical signal sequence for secretion and plays an essential role during development and tissue homeostasis in adults (Itoh, 2016). *Fgf10* knockout (KO) mice die at birth with defects in multiple organ development, including the limb, lung, kidney, salivary gland and adipose tissue (Ohuchi et al., 2000). *Fgf10* gene mutations have been associated with diseases, such as aplasia of lacrimal and salivary glands (ALSG) (Entesarian et al., 2007) and lacrimo-auriculo-dento-digital (LADD) syndrome (Rohmann et al., 2006); chronic obstructive pulmonary disease (Klar et al., 2011) and certain cancer types, including breast (Theodorou et al., 2004; Ghoussaini et al., 2016), pancreatic (Nomura et al., 2008), and gastric (Sun et al., 2015) cancers (**Figure 1C**).

Fibroblast Growth Factor 10 activates key intracellular signaling pathways in several cell types leading to the modulation of organ branching and cell proliferation, differentiation, and migration during development; wound healing and tissue repair; maintenance of stem cells compartment; and cancer cell invasion and proliferation (Itoh, 2016). Here, we will summarize known FGF10-dependent intracellular signaling pathways and cellular responses, before focusing on how *Fgf10* expression and activity are modulated in different cellular contexts. Mechanisms underlying FGF10-dependent control of signaling specificity will be discussed and novel technologies to study the multiple roles of FGF10 will be introduced.

FGF10-DEPENDENT REGULATORS OF INTRACELLULAR SIGNALING

Early Signaling Players

The paracrine actions of FGF10 secreted by mesenchymal cells are mediated by the activation of epithelial FGF receptors with extracellular, transmembrane, and cytoplasmic tyrosine kinase domains (Ornitz and Itoh, 2015), and by heparan sulfate proteoglycans (HSPGs) in the extracellular matrix (ECM) (Patel et al., 2008). There are four Fibroblast Growth Factor receptor *(Fgfr)* genes (*Fgfr1, 2, 3, 4*). *Fgfr1–3* are alternatively spliced into "b" and "c" isoforms, which differ in their extracellular domain and ligand binding specificity and which are expressed by epithelial or mesenchymal cells, respectively (Ornitz and Itoh, 2015). FGF10 has been shown to bind and selectively activate FGFR1b and 2b (Ornitz et al., 1996; Zhang et al., 2006).

Upon FGF10 binding, FGFRs dimerize and several intracellular tyrosine (Y) residues are trans-autophosphorylated. The sequential order of tyrosine residue phosphorylation has been reported for FGFR1 (Furdui et al., 2006). The catalytic tyrosine Y653 is phosphorylated first, followed by Y583, Y463, Y585, and Y654 phosphorylation, resulting in full receptor activation. Finally, Y677 and Y766 are phosphorylated, allowing the binding of adaptor molecules to the receptor (Furdui et al., 2006). FGF10-dependent dynamic phosphorylation of FGFR2b intracellular tyrosine residues has been studied in epithelial cells using quantitative mass spectrometry (MS)-based phosphoproteomics (Francavilla et al., 2013; **Figure 1D**, insert). This study showed that FGF10-dependent phosphorylation of Y734 on FGFR2b (or Y730 on FGFR1) specifically induced cell migration (Francavilla et al., 2013). These findings highlight the importance of the sequence surrounding phosphorylated residues on the activated receptor for ligand-dependent activation of downstream signaling pathways.

Fibroblast Growth Factor receptors engage multiple signaling pathways via adaptor proteins (**Figure 1D**). FGF-regulated substrate 2 (FRS2) binds the juxtamembrane domain of FGFRs independently of receptor activation, and is phosphorylated upon ligand binding, enabling the recruitment of other scaffold proteins, such as tyrosine-protein phosphatase non-receptor type 11 (PTPN11/SHP2) and growth factor receptor-bound protein 2 (GRB2) (Ong et al., 2000). FRS2, SHP2, and GRB2 are necessary to activate the extracellular regulated kinases (ERK1/2) pathway upon FGF10 stimulation in several examined cell types (Hadari et al., 1998; Ong et al., 2000; Upadhyay et al., 2003a) and during the growth of prostate xenografts in mice (Li et al., 2018a). Furthermore, FGF10 can induce the direct recruitment of the negative ERK1/2 signaling regulator Sprouty2 to FRS2 in lung epithelial cells (Tefft et al., 2002). Sprouty2 negatively regulates FGF10-dependent trophoblast invasion (Natanson-Yaron et al., 2007), otic placode size (Mahoney Rogers et al., 2011), and lung branching (Zhao and O'Brien, 2015). GRB2 has been shown to control basal FGFR2 activation (Lin et al., 2012) by competing with the binding of 1-phosphatidylinositol 4,5-bisphosphate phosphodiesterase gamma-1 (PLCγ) to FGFR2 (Timsah et al., 2014). PLCγ binds to Y769 of FGFR2 (or Y766 on FGFR1) in the presence of FGF10 and is phosphorylated (Marchese et al., 2001), resulting in activation of protein kinase C (PKC) and calcium release (**Figure 1D**). Finally, the regulatory subunit of phosphatidylinositol 4,5-bisphosphate 3-kinase (PI3K) p85 which is known to be indirectly recruited to FGFR via the FRS2/GRB2/GAB1 complex (Ong et al., 2001), has been shown to bind to phosphorylated Y734 on FGFR2b upon FGF10 stimulation in epithelial breast cancer cells (Francavilla et al., 2013).

These results suggest context-dependent and fine-tuned modulation of downstream signaling pathways upon FGF10 binding to its receptors. FGF10 acts as a canonical FGFR ligand in recruiting the adaptor proteins FRS2, GRB2, or PLCγ to the receptor, but it can also induce the formation of cell type-specific signaling complexes (e.g., centered on p85). Either structural rearrangements of the receptor or the presence of cell type specific co-activators may explain these two different modes of FGF10 signaling initiation.

Kinases: ERK1/2 and PI3K

Fibroblast Growth Factor receptors signal through ERK1/2 during development (Corson et al., 2003). For instance, FGF10 and ERK1/2 signaling is necessary during duct elongation of submandibular glands (Steinberg et al., 2005), epithelium tooth growth (Cho et al., 2009), and determination of vaginal epithelial cell fate in Müllerian duct epithelium (Terakawa et al., 2016). In human diseases, FGF10 is capable of stimulating the growth of endometrial carcinoma cells by activating the ERK1/2 pathway in a paracrine manner (Taniguchi et al., 2003) and is involved in the growth of ameloblastoma – an epithelial benign tumor of the odontogenic apparatus – partially signaling through ERK1/2 (Nakao et al., 2013). It has also been suggested that FGF10 has a potential therapeutic use in lung edema, as FGF10 up-regulates Na,K-ATPase activity in alveolar epithelial cells via the ERK1/2 pathway (Upadhyay et al., 2003b). Finally, the crosstalk between FGF10 and the ERK1/2 pathway has been extensively studied in cell lines, in which either manipulating the Sprouty2/FRS2 complex which controls ERK1/2 activation (Tefft et al., 2002), or inhibiting upstream activators of ERK1/2, such as MEK, resulted in decreased FGF10-induced cellular responses (Taniguchi et al., 2003; Upadhyay et al., 2003b; Francavilla et al., 2013).

The role of FGF10 in signaling regulation through PI3K and downstream kinases like protein kinase B (AKT) is less clear (**Figure 1D**). The PI3K/AKT pathway is important for

A

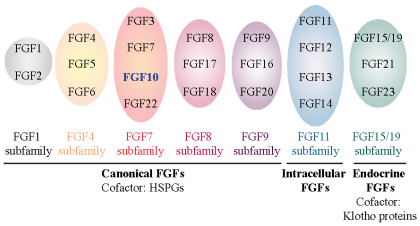

B

Organism	Chromosome location	Exon	Protein length (a.a.)	Post-translational Modifications
Human	5p12	4	208	Cleavage of signal peptide; N-linked glycosylation at position 51 and 196
Mouse	13 D2.3; 13 67.14 cM	3	209	Cleavage of signal peptide; N-linked glycosylation at position 50 and 197

C

Disease	Gene	Mutation	Reference
ALSG	*Fgf10*	R80S, G138Q, R193X, K137X	Entesarian et al., 2005; Milunsky et al., 2006; Entesarian et al., 2007
LADD	*Fgf10*	K137X, C106F, I156R	Milunsky et al., 2006; Rohmann et al., 2006
	Fgfr2	A648T, A628T, R649S Δasp650	Rohmann et al., 2006
Aperts' Syndrome	*Fgfr2*	Aberrant splicing, S252W, S252F, P253R	Wilkie et al., 1995; Oldridge et al., 1997; Oldridge et al., 1999
BBDS	*Fgfr2*	Y381D, M291R	Merrill et al., 2012
COPD	*Fgf10*	R193X	Klar et al., 2011
Autism	*Fgf10*	Gene replication	Casey et al., 2012
	Fgfr2	Gene replication	Wentz et al., 2014
Gastric cancer	*Fgfr2*	Aberrant splicing; S267P	Jang et al., 2001
Neurodevelopmental delay	*Fgfr2*	Overexpression	Coci et al., 2017
Pancreatic Cancer	*Fgf10*	Overexpression	Nomura et al., 2008
	Fgfr2	Overexpression	
Gastric cancer	*Fgf10*	Overexpression	Sun et al., 2015
	Fgfr2	Gene amplification	Su et al., 2014
Breast cancer	*Fgf10*	Overexpression	Theodorou et al., 2004; Ghoussaini et al., 2016
	Fgfr2	Overexpression, K660N	Rentjes et al., 2013

D

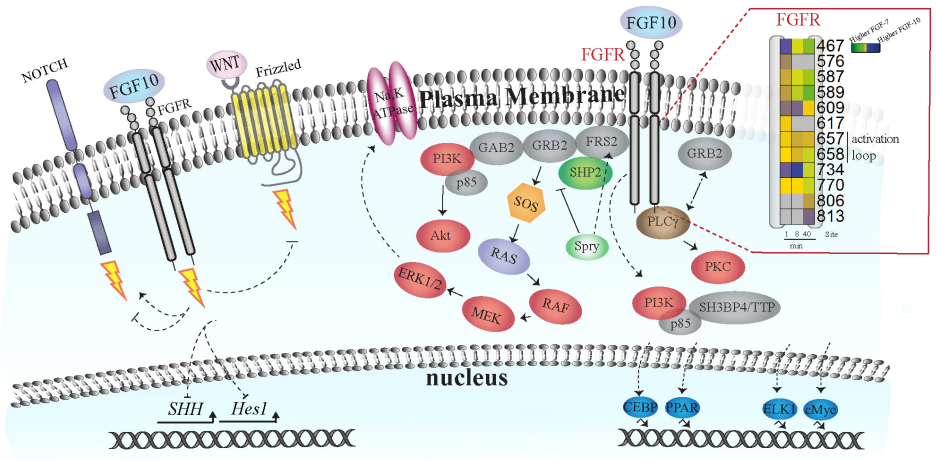

E

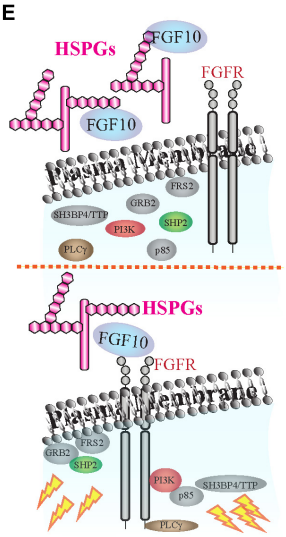

F

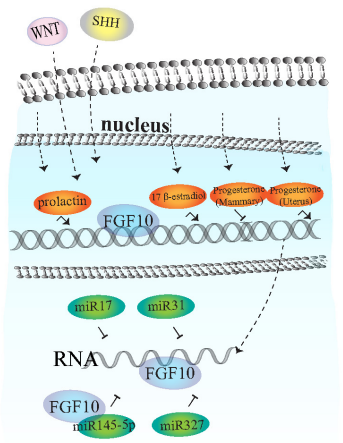

G

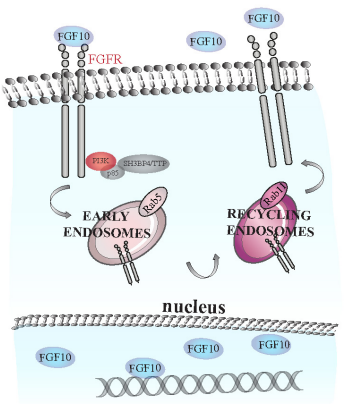

FIGURE 1 | Continued

FIGURE 1 | Fibroblast of Growth Factor (FGF) signaling activation and regulation. **(A)** Schematic of FGF subfamilies (see Ornitz and Itoh, 2015). FGF10 belongs to the FGF7 subfamily and is highlighted in blue. **(B)** Comparison of FGF10 gene/protein in human and mouse. The human FGF10 gene has an extra exon; and the protein length in the two species differs by one amino acid. FGF10 is secreted via the canonical ER-Golgi secretory pathway, as demonstrated by the cleavage of the signal peptide, and have two known glycosylation sites (Source: UniProt). **(C)** Known disease-causing mutations on Fgf10 and Fgfr2 genes. The rare developmental disorders Aplasia of Lacrimal and major Salivary Glands (ALSG), Lacrimo-Auricuo-Dentro-Digital (LADD) syndrome, Aperts' Syndrome and Bent Bone Dysplasia Syndrome (BBDS) result from either the loss of key receptor-binding sites on FGF10 or mutations in the receptor kinase (TK) domains or IgII linker regions (Wilkie et al., 1995; Oldridge et al., 1997, 1999; Entesarian et al., 2005, 2007; Milunsky et al., 2006; Rohmann et al., 2006; Merrill et al., 2012). Interestingly, cases of ALSG caused by the R193X mutation also coincide with Chronic Obstructive Pulmonary Disease (COPD) (Klar et al., 2011). More recently, chromosomal translocation and duplication events at the loci of the Fgf10 and Fgfr2 genes have been associated with neurological disorders such as developmental delay and autism (Casey et al., 2012; Wentz et al., 2014). The role of single nucleotide polymorphisms and *de novo* point mutations causing oncogenic expression of Fgf10 and Fgfr2 are also becoming clearer, particularly in pancreatic, gastric, and breast cancers (Jang et al., 2001; Theodorou et al., 2004; Nomura et al., 2008; Reintjes et al., 2013; Su et al., 2014; Sun et al., 2015; Ghoussaini et al., 2016; Coci et al., 2017). **(D)** FGF10-dependent activation of FGFR intracellular tyrosine residues (Y; insert), adaptor proteins (gray), protein kinases (red), and transcription factors (blue). Insert on the right: each square represents a phosphorylated tyrosine residue (Y); the numbers correspond to phosphorylated Y residues on FGFR2b identified by proteomics; the color blue indicates higher phosphorylation at a given time point upon FGF10 stimulation of epithelial cells; modified from Francavilla et al. (2013). Dashed arrows represent FGF10-specific activation or inhibition of signaling. The lightning bolt represents the activation of signaling cascades. **(E)** Left, FGF10 bound to heparan sulfate proteoglycans (HSPGs) in the ECM does not activate FGFR and intracellular signaling. Right, FGF10 bound to HSPGs and FGFR induces the recruitment of protein adaptors to FGFR and signaling activation (represented by lightning bolts). **(F)** Schematic representation of FGF10 regulation in response to hormones (orange), miRNAs (dark green), WNT and SHH proteins. **(G)** FGF10 induces FGFR2b internalization into early endosomes and sorting to recycling endosomes and plasma membrane. FGF10 has also been found in the nucleus of certain cell types.

FGF10-dependent survival of hepatoblasts during early stages of hepatogenesis (Mavila et al., 2012) and for lens development (Chaffee et al., 2016). A role for FGF10/FGFR2/PI3K in neuroprotection after cerebral ischemia has also recently been described (Chen et al., 2017).

Even though the role of other kinases in FGF10 signaling specification remains to be determined, FGF10 is a versatile growth factor that enables epithelial cell growth and migration via ERK1/2 and controls cell survival via PI3K/AKT signaling during development and in several pathological conditions.

Transcription Factors

Fibroblast Growth Factor 10 is known to control cellular outputs through several transcription factors (**Figure 1D**). FGF10 plays crucial roles in adipogenesis by dynamically modulating the expression of members of the CCAAT/enhancer binding protein (C/EBP) and peroxisome proliferator activated receptor (PPAR) families of transcription factors (Sakaue et al., 2002). ELK-1 and c-MYC, but surprisingly not c-FOS, are regulated by FGF10 in endometrial carcinoma (Taniguchi et al., 2003). Finally, FGF10 controls the switch between vaginal and uterine epithelial cells fate via runt-related transcription factor 1 (RUNX1) in Müllerian duct epithelium (Terakawa et al., 2016).

As FGF10 activates both ERK1/2 and PI3K all the known transcription factors that depend on these kinases (e.g., ATF2, ELK1, FOS and FOXO, NFkB, CREB, respectively) (Yang et al., 2013; Mantamadiotis, 2017) should play a role in FGF10-dependent responses. However, it is not the case for ERK1/2-regulated activation of c-FOS (Taniguchi et al., 2003), suggesting that transcriptional regulation in response to FGF10/ERK1/2 signaling is complex and requires further investigation.

FGF10 Crosstalk With Other Signaling Pathways

Among several other important players, we will focus on four families of proteins with a context-specific role in FGF10 signaling (**Figure 1D**).

Neurogenic locus notch homolog protein 1 (NOTCH1) is a receptor controlling cell signaling via several ligands and mechanisms (Bray and Gomez-Lamarca, 2018). FGF10 activates NOTCH1 signaling during pancreatic development (Hart et al., 2003; Norgaard et al., 2003) but inhibits NOTCH1-dependent regulation of the gene *Hes1* in the adult small intestine (Al Alam et al., 2015).

The functions of WNT ligands, which bind to the frizzled family of seven transmembrane receptors (Zeng et al., 2018), are modulated by FGF10 signaling during stomach (Nyeng et al., 2007) and lung (Volckaert and De Langhe, 2015) development. FGF10 also regulates Bone Morphogenetic Protein 4 (BMP4) during lung branching (Weaver et al., 2000).

The expression of *Sonic hedgehog protein (*SHH*)*, which plays crucial roles during vertebrate development (Fernandes-Silva et al., 2017), is enhanced by FGF10 during the development of limb (Yokoyama et al., 2001), prostate gland (Huang et al., 2005), and stomach (Nyeng et al., 2007).

Thus, FGF10 modulates a great variety of cellular responses during development and in pathological conditions, through both conventional and ligand-specific signaling players.

MODULATION OF *FGF10* EXPRESSION AND ACTIVITY

Besides known transcription factors (e.g., Tbx4/5, Isl1, Etv1/Ewsv1) (Cebra-Thomas et al., 2003; Yamamoto-Shiraishi et al., 2014; Ching et al., 2018), *Fgf10* expression and function are regulated by other factors, including HSPGs and soluble molecules (**Figure 1E**).

Heparan sulfate proteoglycans are a family of glycoproteins composed of a variety of heparan sulfate moieties (HS) attached to a core protein which play critical roles during organ branching and morphogenesis (Patel et al., 2017). Cleavage of HSPGs during ECM remodeling can release FGF10 from the ECM affecting epithelial cell proliferation and organ development (**Figure 1E**). FGF10 released from HS in the basement membrane

increases salivary and lacrimal gland branching morphogenesis (Patel et al., 2008; Qu et al., 2011), whereas FGF10 binding to FGFR2b regulates the extent of the response to morphogenetics gradients (Makarenkova et al., 2009). Furthermore, the HSPG gradient pattern greatly affects FGF10 functions in the developing lung (Izvolsky et al., 2003) and during stomach morphogenesis (Huang et al., 2018). At a molecular level, FGF10 has a higher affinity for heparan compared to other FGFs (Lu et al., 1999) and it has a preference for certain patterns of sulfation and oligosaccharide length (Li et al., 2016). These unique biophysical properties of FGF10 may explain the great variety of FGF10 roles depending on cellular microenvironment, and may form the basis for the therapeutic control of FGF10 activities *in vivo*.

Fibroblast Growth Factor 10 gene expression is regulated by several hormones (**Figure 1F**). In mouse mammary gland 17 beta-estradiol, but not progesterone, increased the expression of *Fgf10*, whereas prolactin significantly induced *Fgf10* gene expression during pregnancy (Cui and Li, 2008). In ovine uterus, progesterone regulates *Fgf10* gene expression resulting in improved endometrial functions (Satterfield et al., 2008). These findings might be important not only to better refine FGF10 roles during development, but also to improve hormone-dependent cancer therapies. The latter possibility requires further studies to correlate hormones and FGF10 levels in human tumors, such as prostate or breast cancers.

Other important regulators of *Fgf10* gene expression during organ branching are WNT and SHH (**Figure 1F**). For instance, members of the WNT family are crucial for FGF10-dependent signaling in lung and limb morphogenesis (Kawakami et al., 2001; Goss et al., 2011; Volckaert et al., 2013, 2017). SHH inhibits FGF10 localized expression during lung budding (Pepicelli et al., 1998). It is worth noticing that FGF10, WNT, and SHH proteins regulate each other through the establishment of feedback loops in different cells and in a spatio-temporal regulated manner during the development of branching organs (see "FGF10 Crosstalk With Other Signaling Pathways" section above and **Figure 1D**), thus confirming the importance of growth factors signaling crosstalk and dynamic regulation in human development and physiology.

Fibroblast Growth Factor 10 expression can also be controlled by micro-RNAs (miRNAs), which are crucial regulators of gene expression (Dragomir and Calin, 2018; **Figure 1F**). The mir-17 family of miRNAs is important for FGF10/FGFR2b downstream signaling during lung bud morphogenesis (Carraro et al., 2009) and miR-31 negatively regulates expression of *Fgf10* during hair follicle growth and hair fiber formation (Mardaryev et al., 2010). More recently, it has been suggested that the miR-327/FGF10/FGFR2 signaling axis may be a therapeutic target for treatment of obesity and metabolic diseases (Fischer et al., 2017) and that the crosstalk between miR-145-5p and FGF10 expression regulates vascular smooth muscle cells proliferation and migration (Shi et al., 2018).

Although a comprehensive picture of *Fgf10* expression and activity regulation has clearly emerged, a conundrum in FGF10 signaling still remains: how is FGF10 signaling specificity controlled in different cellular contexts? The importance of subcellular localization in modulating specific aspects of FGF10 responses will be discussed in the next section.

Subcellular Localization

The FGF10 receptor FGFR2b is internalized via clathrin-coated pits into intracellular vesicles (early endosomes) (**Figure 1G**), and then sorted to recycling endosomes, rather than to canonical late endosomes for degradation (Belleudi et al., 2007; Francavilla et al., 2013). Therefore, once FGFR2b is recycled back to the plasma membrane it may bind its ligands again and activate signaling in a sustained manner (Francavilla et al., 2013). Either the lack of receptor ubiquitination, which is a signal for degradation (Belleudi et al., 2007), or the recruitment of the adaptor proteins p85 and SH3BP4/TTP to phosphorylated FGFR2b (Francavilla et al., 2013) have been suggested as possible mechanisms underlying FGF10-dependent FGFR2b recycling to the plasma membrane. In either case, the sorting route of FGF10-activated receptors affects downstream signaling activation and cellular outputs, by inducing mitogenic responses in keratinocytes (Belleudi et al., 2007) or breast cancer cell migration and mouse embryonic lung branching (Francavilla et al., 2013). It would be interesting to study the endocytic route followed by FGF10 receptors in other cell types and how this affects downstream responses.

As well as in endosomes, FGF10 has been detected in the cytoplasm of cultured prostate stroma cells (Lu et al., 1999) and in the nucleus of urothelial cells (Bagai et al., 2002; **Figure 1G**). These findings suggest that different subcellular localization of FGF10 may underlie the specificity of FGF10 signaling in different cell types. The importance of FGF10 intracellular localization has been confirmed in studies about the molecular mechanisms underlying the LADD and ALSG human syndromes, which are characterized by mutations in the *Fgf10* gene (Rohmann et al., 2006; Entesarian et al., 2007; **Figure 1C**). Mutated FGF10 failed to translocate into the nucleus. This might attenuate FGF10 intracrine functions, possibly explaining the phenotype observed in LADD or ALSG patients (Mikolajczak et al., 2016).

Understanding how FGF10 regulates signaling specificity in different cell types depending on its subcellular localization and how *Fgf10* expression is modulated during organ morphogenesis and in human physiology may have therapeutic implications for cell- and growth factor-based personalized medicine.

SYSTEM BIOLOGY APPROACHES TO STUDY FGF10 SIGNALING SPECIFICITY

To improve our global understanding of FGF10 signaling specificity, 'omics approaches might be useful. MS-based quantitative proteomics has become a powerful technology for investigating proteome function, composition, and post-translational modifications (PTMs) (Aebersold and Mann, 2016). In a typical shotgun proteomic workflow, proteins from tissues or cells are digested followed by peptide separation using liquid

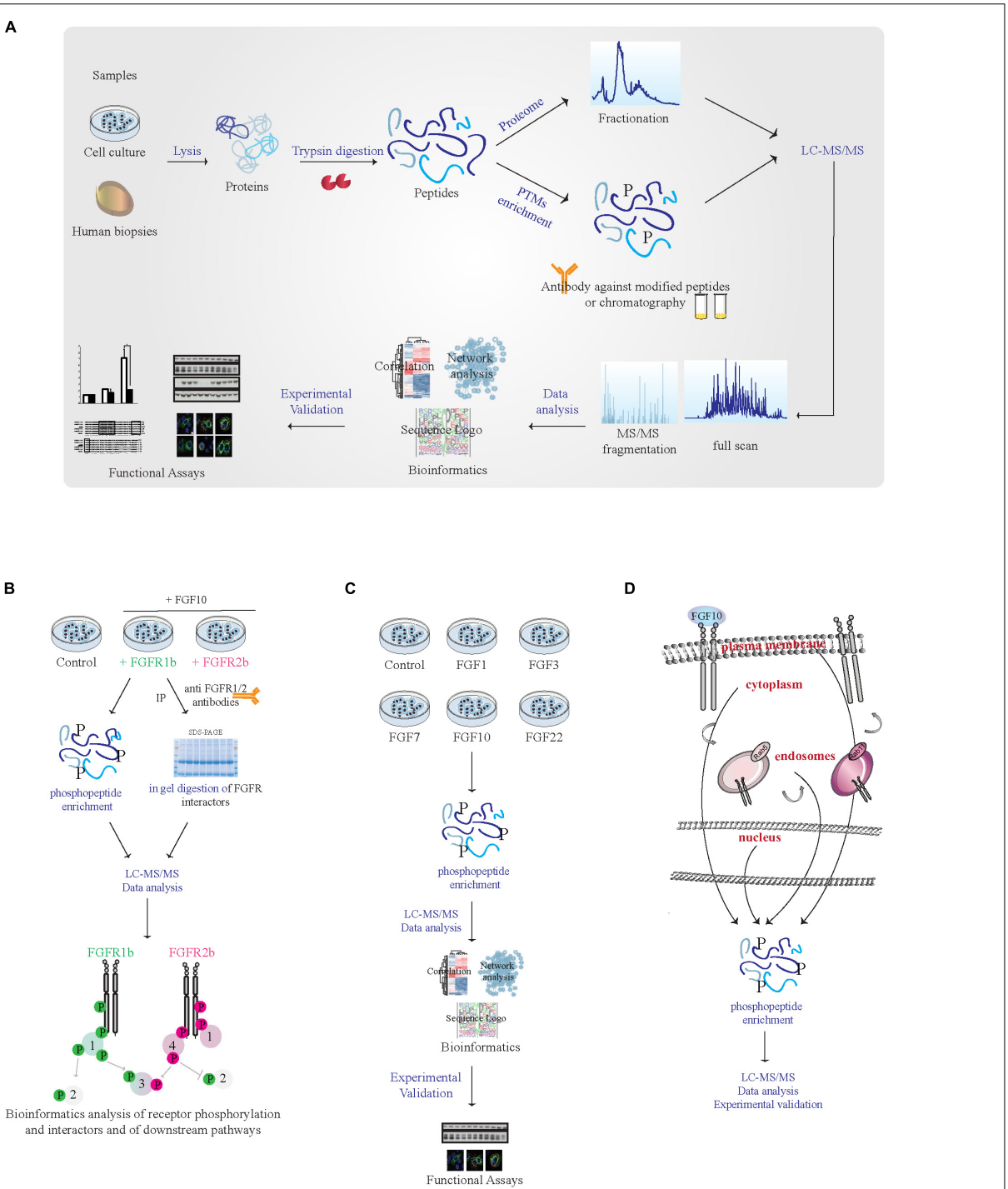

FIGURE 2 | MS-based proteomic analysis of FGF10 signaling specificity. **(A)** Workflow of a typical shotgun proteomic experiment. Samples are lysed and proteins are digested into peptides. Peptides are then either fractionated to reduce sample complexity for the analysis of the whole cellular proteome or enriched for PTMs like phosphorylation using specific antibodies and chromatographic-based methods. Peptides are then separated and analyzed in the mass spectrometer. High resolution full scan and tandem MS/MS spectra are generated. Data are then analyzed by available software and bioinformatics tools before experimental validation of the most interesting hits. **(B)** Workflow of a proteomic experiment aiming at comparing FGFR1b and FGFR2b signaling in response to FGF10 stimulation. Combining phosphorylated peptide enrichment and immunoprecipitation of FGFRs followed by SDS–PAGE separation and protein in-gel digestion may result in the identification of receptor isoform-specific PTMs, protein interactors, and downstream signaling players. **(C)** Workflow of a proteomic experiment aiming at comparing signaling activation in response to different FGFs. Phosphoproteomics followed by mass spectrometry and bioinformatics will allow uncovering ligand-specific signaling cascades. **(D)** Workflow of a proteomic experiment aiming at deciphering subcellular compartment-specific signaling activation upon FGF10 stimulation. Phosphoproteomics is followed by mass spectrometry analysis and bioinformatics.

chromatography (LC) and peptide identification using tandem mass spectrometry (LC-MS/MS) (Aebersold and Mann, 2016). To identify, quantify and localize PTMs an enrichment step is introduced at the peptide level given the low stoichiometry of PTMs, such as phosphorylation (**Figure 2A**). In combination with functional assays phosphoproteomics has been successfully employed to study changes in intracellular signaling in tissues or perturbed cells (von Stechow et al., 2015) and one "functional proteomics" study has analyzed global FGF10 signaling in epithelial cells (Francavilla et al., 2013).

We suggest a few proteomic approaches to study FGF10 signaling specificity in an unbiased manner:

(1) Given the lack of available isoform-specific antibodies, FGF10 signaling can be compared in cells or organs expressing exclusively FGFR1b or 2b, using CRISPR-Cas9-based techniques or transgenic mice, by quantitative interactomics combined with phosphoproteomics. This will (a) increase our understanding of the relative contribution of FGFR1b and 2b isoforms to FGF10 response, as the phenotype of the FGFR2b (but not FGFR1b) KO mice resembles that of FGF10 KO mice (Ornitz and Itoh, 2015); (b) dissect which signaling players depend of FGFR1-2 activation in response to FGF10, based on recent data showing receptor-specific activation of SRC in prostate cancer (Li et al., 2018b); (c) uncover the potential role of receptor heterodimerization given the reciprocal auto-phosphorylation of FGFR1 and 2 (Bellot et al., 1991; Brewer et al., 2016); and (d) allow studying ligand-dependent receptor interactors and PTMs on the receptor (**Figure 2B**).

(2) System-level analysis of cellular signaling in response to different ligands for FGFR1-2b based on quantitative phosphoproteomics would reveal whether or not cellular responses are encoded by the identity of the ligand (**Figure 2C**). Two of the FGFR2b ligands, FGF7 and FGF10, are known to induce cell proliferation and lung cyst-like growth or cell migration and lung cell branching, respectively (Bellusci et al., 1997; Francavilla et al., 2013). However, the contribution of FGF1, 3 or 22 – which also bind to FGFR2b (Ornitz and Itoh, 2015) – has never been studied in detail. Quantitative phosphoproteomics would allow dissecting ligand-specific activation of intracellular pathways in different cell-types.

(3) MS-based organelles proteomics has been recently used to map protein subcellular localization (Itzhak et al., 2017). FGF10 signaling from different sub-cellular compartments might be dissected using a similar approach at a cellular level upon organelle enrichment followed by phosphoproteomics (**Figure 2D**).

CONCLUSION

Fibroblast Growth Factor 10-dependent responses range from cell proliferation, migration, and invasion, to multi-organ development, cancer or genetic disease progression. Despite the enormous increase in our understanding of FGF10 signaling and regulation, gaps in our knowledge of FGF10 specificity depending on cellular and extracellular environment still exist. Systems biology approaches, including MS-based quantitative proteomics or high-content microscopy (not discussed here due to space limitations) will contribute to a full understanding of FGF10 signaling. Moving toward personalized treatments for human diseases, this knowledge will be fundamental to develop novel therapies. For instance, recombinant FGF10 or antibodies against FGF10 may be developed to modulate FGF10 signaling depending on cellular context.

AUTHOR CONTRIBUTIONS

All authors listed have contributed to the work and approved it for publication.

FUNDING

Research in the lab of CF is supported by Wellcome Trust Sir Henry Dale fellowship (107636/Z/15/Z) and by the Biotechnology and Biological Sciences Research Council (BBSRC, BB/R015864/1). JW is supported by the BBSRC Doctoral Training Partnership (BB/M011208/1).

ACKNOWLEDGMENTS

We thank all members of the lab and Dr. Dorey, Dr. Plusa, Dr. Kurinna, Prof. Kadler, and Prof. Sharrocks (The University of Manchester) for helpful discussion and for reading the manuscript. We also thank members of the Bio-MS facility, FBMH, The University of Manchester. We apologize to authors whose work could not be cited due to space limitations.

REFERENCES

Aebersold, R., and Mann, M. (2016). Mass-spectrometric exploration of proteome structure and function. *Nature* 537, 347–355. doi: 10.1038/nature 19949

Al Alam, D., Danopoulos, S., Schall, K., Sala, F. G., Almohazey, D., Fernandez, G. E., et al. (2015). Fibroblast growth factor 10 alters the balance between goblet and Paneth cells in the adult mouse small intestine. *Am. J. Physiol. Gastrointest. Liver Physiol.* 308, G678–G690. doi: 10.1152/ajpgi.00158.2014

Bagai, S., Rubio, E., Cheng, J. F., Sweet, R., Thomas, R., Fuchs, E., et al. (2002). Fibroblast growth factor-10 is a mitogen for urothelial cells. *J. Biol. Chem.* 277, 23828–23837. doi: 10.1074/jbc.M201658200

Belleudi, F., Leone, L., Nobili, V., Raffa, S., Francescangeli, F., Maggio, M., et al. (2007). Keratinocyte growth factor receptor ligands target the receptor to different intracellular pathways. *Traffic* 8, 1854–1872. doi: 10.1111/j.1600-0854. 2007.00651.x

Bellot, F., Crumley, G., Kaplow, J. M., Schlessinger, J., Jaye, M., and Dionne, C. A. (1991). Ligand-induced transphosphorylation between different FGF receptors. *EMBO J.* 10, 2849–2854. doi: 10.1002/j.1460-2075.1991.tb07834.x

Bellusci, S., Grindley, J., Emoto, H., Itoh, N., and Hogan, B. L. (1997). Fibroblast growth factor 10 (FGF10) and branching morphogenesis in the embryonic mouse lung. *Development* 124, 4867–4878.

Bray, S. J., and Gomez-Lamarca, M. (2018). Notch after cleavage. *Curr. Opin. Cell Biol.* 51, 103–109. doi: 10.1016/j.ceb.2017.12.008

Brewer, J. R., Mazot, P., and Soriano, P. (2016). Genetic insights into the mechanisms of Fgf signaling. *Genes Dev.* 30, 751–771. doi: 10.1101/gad.277137.115

Carraro, G., El-Hashash, A., Guidolin, D., Tiozzo, C., Turcatel, G., Young, B. M., et al. (2009). miR-17 family of microRNAs controls FGF10-mediated embryonic lung epithelial branching morphogenesis through MAPK14 and STAT3 regulation of E-Cadherin distribution. *Dev. Biol.* 333, 238–250. doi: 10.1016/j.ydbio.2009.06.020

Casey, J. P., Magalhaes, T., Conroy, J. M., Regan, R., Shah, N., Anney, R., et al. (2012). A novel approach of homozygous haplotype sharing identifies candidate genes in autism spectrum disorder. *Hum. Genet.* 131, 565–579. doi: 10.1007/s00439-011-1094-6

Cebra-Thomas, J. A., Bromer, J., Gardner, R., Lam, G. K., Sheipe, H., and Gilbert, S. F. (2003). T-box gene products are required for mesenchymal induction of epithelial branching in the embryonic mouse lung. *Dev. Dyn.* 226, 82–90. doi: 10.1002/dvdy.10208

Chaffee, B. R., Hoang, T. V., Leonard, M. R., Bruney, D. G., Wagner, B. D., Dowd, J. R., et al. (2016). FGFR and PTEN signaling interact during lens development to regulate cell survival. *Dev. Biol.* 410, 150–163. doi: 10.1016/j.ydbio.2015.12.027

Chen, J., Wang, Z., Zheng, Z., Chen, Y., Khor, S., Shi, K., et al. (2017). Neuron and microglia/macrophage-derived FGF10 activate neuronal FGFR2/PI3K/Akt signaling and inhibit microglia/macrophages TLR4/NF-kappaB-dependent neuroinflammation to improve functional recovery after spinal cord injury. *Cell Death Dis.* 8:e3090. doi: 10.1038/cddis.2017.490

Ching, S. T., Infante, C. R., Du, W., Sharir, A., Park, S., Menke, D. B., et al. (2018). Isl1 mediates mesenchymal expansion in the developing external genitalia via regulation of Bmp4, Fgf10 and Wnt5a. *Hum. Mol. Genet.* 27, 107–119. doi: 10.1093/hmg/ddx388

Cho, K. W., Cai, J., Kim, H. Y., Hosoya, A., Ohshima, H., Choi, K. Y., et al. (2009). ERK activation is involved in tooth development via FGF10 signaling. *J. Exp. Zool. B Mol. Dev. Evol.* 312, 901–911. doi: 10.1002/jez.b.21309

Coci, E. G., Auhuber, A., Langenbach, A., Mrasek, K., Riedel, J., Leenen, A., et al. (2017). Novel unbalanced translocations affecting the long arms of chromosomes 10 and 22 cause complex syndromes with very severe neurodevelopmental delay, speech impairment, autistic behavior, and epilepsy. *Cytogenet. Genome Res.* 151, 171–178. doi: 10.1159/000471501

Corson, L. B., Yamanaka, Y., Lai, K. M., and Rossant, J. (2003). Spatial and temporal patterns of ERK signaling during mouse embryogenesis. *Development* 130, 4527–4537. doi: 10.1242/dev.00669

Cui, Y., and Li, Q. (2008). Effect of mammogenic hormones on the expression of FGF7, FGF10 and their receptor in mouse mammary gland. *Sci. China C Life Sci.* 51, 711–717. doi: 10.1007/s11427-008-0092-y

Dragomir, M., and Calin, G. A. (2018). Circular RNAs in cancer - lessons learned from microRNAs. *Front. Oncol.* 8:179. doi: 10.3389/fonc.2018.00179

Emoto, H., Tagashira, S., Mattei, M. G., Yamasaki, M., Hashimoto, G., Katsumata, T., et al. (1997). Structure and expression of human fibroblast growth factor-10. *J. Biol. Chem.* 272, 23191–23194. doi: 10.1074/jbc.272.37.23191

Entesarian, M., Dahlqvist, J., Shashi, V., Stanley, C. S., Falahat, B., Reardon, W., et al. (2007). FGF10 missense mutations in aplasia of lacrimal and salivary glands (ALSG). *Eur. J. Hum. Genet.* 15, 379–382. doi: 10.1038/sj.ejhg.5201762

Entesarian, M., Matsson, H., Klar, J., Bergendal, B., Olson, L., Arakaki, R., et al. (2005). Mutations in the gene encoding fibroblast growth factor 10 are associated with aplasia of lacrimal and salivary glands. *Nat. Genet.* 37, 125–127. doi: 10.1038/ng1507

Fernandes-Silva, H., Correia-Pinto, J., and Moura, R. S. (2017). Canonical sonic hedgehog signaling in early lung development. *J. Dev. Biol.* 5:3. doi: 10.3390/jdb5010003

Fischer, C., Seki, T., Lim, S., Nakamura, M., Andersson, P., Yang, Y., et al. (2017). A miR-327-FGF10-FGFR2-mediated autocrine signaling mechanism controls white fat browning. *Nat. Commun.* 8:2079. doi: 10.1038/s41467-017-02158-z

Francavilla, C., Rigbolt, K. T., Emdal, K. B., Carraro, G., Vernet, E., Bekker-Jensen, D. B., et al. (2013). Functional proteomics defines the molecular switch underlying FGF receptor trafficking and cellular outputs. *Mol. Cell* 51, 707–722. doi: 10.1016/j.molcel.2013.08.002

Furdui, C. M., Lew, E. D., Schlessinger, J., and Anderson, K. S. (2006). Autophosphorylation of FGFR1 kinase is mediated by a sequential and precisely ordered reaction. *Mol. Cell* 21, 711–717. doi: 10.1016/j.molcel.2006.01.022

Ghoussaini, M., French, J. D., Michailidou, K., Nord, S., Beesley, J., Canisus, S., et al. (2016). Evidence that the 5p12 variant rs10941679 confers susceptibility to estrogen-receptor-positive breast cancer through FGF10 and MRPS30 regulation. *Am. J. Hum. Genet.* 99, 903–911. doi: 10.1016/j.ajhg.2016.07.017

Goss, A. M., Tian, Y., Cheng, L., Yang, J., Zhou, D., Cohen, E. D., et al. (2011). Wnt2 signaling is necessary and sufficient to activate the airway smooth muscle program in the lung by regulating myocardin/Mrtf-B and Fgf10 expression. *Dev. Biol.* 356, 541–552. doi: 10.1016/j.ydbio.2011.06.011

Hadari, Y. R., Kouhara, H., Lax, I., and Schlessinger, J. (1998). Binding of Shp2 tyrosine phosphatase to FRS2 is essential for fibroblast growth factor-induced PC12 cell differentiation. *Mol. Cell Biol.* 18, 3966–3973. doi: 10.1128/MCB.18.7.3966

Hart, A., Papadopoulou, S., and Edlund, H. (2003). Fgf10 maintains notch activation, stimulates proliferation, and blocks differentiation of pancreatic epithelial cells. *Dev. Dyn.* 228, 185–193. doi: 10.1002/dvdy.10368

Huang, L., Pu, Y., Alam, S., Birch, L., and Prins, G. S. (2005). The role of Fgf10 signaling in branching morphogenesis and gene expression of the rat prostate gland: lobe-specific suppression by neonatal estrogens. *Dev. Biol.* 278, 396–414. doi: 10.1016/j.ydbio.2004.11.020

Huang, M., He, H., Belenkaya, T., and Lin, X. (2018). Multiple roles of epithelial heparan sulfate in stomach morphogenesis. *J. Cell Sci.* 131:jcs210781. doi: 10.1242/jcs.210781

Itoh, N. (2016). FGF10: a multifunctional mesenchymal-epithelial signaling growth factor in development, health, and disease. *Cytokine Growth Factor Rev.* 28, 63–69. doi: 10.1016/j.cytogfr.2015.10.001

Itzhak, D. N., Davies, C., Tyanova, S., Mishra, A., Williamson, J., Antrobus, R., et al. (2017). A mass spectrometry-based approach for mapping protein subcellular localization reveals the spatial proteome of mouse primary neurons. *Cell Rep.* 20, 2706–2718. doi: 10.1016/j.celrep.2017.08.063

Izvolsky, K. I., Zhong, L., Wei, L., Yu, Q., Nugent, M. A., and Cardoso, W. V. (2003). Heparan sulfates expressed in the distal lung are required for Fgf10 binding to the epithelium and for airway branching. *Am. J. Physiol. Lung. Cell Mol. Physiol.* 285, L838–L846. doi: 10.1152/ajplung.00081.2003

Jang, J. H., Shin, K. H., and Park, J. G. (2001). Mutations in fibroblast growth factor receptor 2 and fibroblast growth factor receptor 3 genes associated with human gastric and colorectal cancers. *Cancer Res.* 61, 3541–3543.

Kawakami, Y., Capdevila, J., Buscher, D., Itoh, T., Rodriguez Esteban, C., and Izpisua Belmonte, J. C. (2001). WNT signals control FGF-dependent limb initiation and AER induction in the chick embryo. *Cell* 104, 891–900. doi: 10.1016/S0092-8674(01)00285-9

Klar, J., Blomstrand, P., Brunmark, C., Badhai, J., Hakansson, H. F., Brange, C. S., et al. (2011). Fibroblast growth factor 10 haploinsufficiency causes chronic obstructive pulmonary disease. *J. Med. Genet.* 48, 705–709. doi: 10.1136/jmedgenet-2011-100166

Li, Q., Alsaidan, O. A., Ma, Y., Kim, S., Liu, J., Albers, T., et al. (2018a). Pharmacologically targeting the myristoylation of the scaffold protein FRS2alpha inhibits FGF/FGFR-mediated oncogenic signaling and tumor progression. *J. Biol. Chem.* 293, 6434–6448. doi: 10.1074/jbc.RA117.000940

Li, Q., Ingram, L., Kim, S., Beharry, Z., Cooper, J. A., and Cai, H. (2018b). Paracrine fibroblast growth factor initiates oncogenic synergy with epithelial fgfr/src transformation in prostate tumor progression. *Neoplasia* 20, 233–243. doi: 10.1016/j.neo.2018.01.006

Li, Y., Sun, C., Yates, E. A., Jiang, C., Wilkinson, M. C., and Fernig, D. G. (2016). Heparin binding preference and structures in the fibroblast growth factor family parallel their evolutionary diversification. *Open Biol.* 6: 150275. doi: 10.1098/rsob.150275

Lin, C. C., Melo, F. A., Ghosh, R., Suen, K. M., Stagg, L. J., Kirkpatrick, J., et al. (2012). Inhibition of basal FGF receptor signaling by dimeric Grb2. *Cell* 149, 1514–1524. doi: 10.1016/j.cell.2012.04.033

Lu, W., Luo, Y., Kan, M., and McKeehan, W. L. (1999). Fibroblast growth factor-10. A second candidate stromal to epithelial cell andromedin in prostate. *J. Biol. Chem.* 274, 12827–12834. doi: 10.1074/jbc.274.18.12827

Mahoney Rogers, A. A., Zhang, J., and Shim, K. (2011). Sprouty1 and Sprouty2 limit both the size of the otic placode and hindbrain Wnt8a by antagonizing FGF signaling. *Dev. Biol.* 353, 94–104. doi: 10.1016/j.ydbio.2011.02.022

Makarenkova, H. P., Hoffman, M. P., Beenken, A., Eliseenkova, A. V., Meech, R., Tsau, C., et al. (2009). Differential interactions of FGFs with heparan sulfate control gradient formation and branching morphogenesis. *Sci. Signal.* 2:ra55. doi: 10.1126/scisignal.2000304

Mantamadiotis, T. (2017). Towards targeting PI3K-dependent regulation of gene expression in brain cancer. *Cancers* 9:E60. doi: 10.3390/cancers9060060

Marchese, C., Felici, A., Visco, V., Lucania, G., Igarashi, M., Picardo, M., et al. (2001). Fibroblast growth factor 10 induces proliferation and differentiation of human primary cultured keratinocytes. *J. Invest. Dermatol.* 116, 623–628. doi: 10.1046/j.0022-202x.2001.01280.x

Mardaryev, A. N., Ahmed, M. I., Vlahov, N. V., Fessing, M. Y., Gill, J. H., Sharov, A. A., et al. (2010). Micro-RNA-31 controls hair cycle-associated changes in gene expression programs of the skin and hair follicle. *FASEB J.* 24, 3869–3881. doi: 10.1096/fj.10-160663

Mavila, N., James, D., Utley, S., Cu, N., Coblens, O., Mak, K., et al. (2012). Fibroblast growth factor receptor-mediated activation of AKT-beta-catenin-CBP pathway regulates survival and proliferation of murine hepatoblasts and hepatic tumor initiating stem cells. *PLoS One* 7:e50401. doi: 10.1371/journal.pone.0050401

Merrill, A. E., Sarukhanov, A., Krejci, P., Idoni, B., Camacho, N., Estrada, K. D., et al. (2012). Bent bone dysplasia-FGFR2 type, a distinct skeletal disorder, has deficient canonical FGF signaling. *Am. J. Hum. Genet.* 90, 550–557. doi: 10.1016/j.ajhg.2012.02.005

Mikolajczak, M., Goodman, T., and Hajihosseini, M. K. (2016). Interrogation of a lacrimo-auriculo-dento-digital syndrome protein reveals novel modes of fibroblast growth factor 10 (FGF10) function. *Biochem. J.* 473, 4593–4607. doi: 10.1042/BCJ20160441

Milunsky, J. M., Zhao, G., Maher, T. A., Colby, R., and Everman, D. B. (2006). LADD syndrome is caused by FGF10 mutations. *Clin. Genet.* 69, 349–354. doi: 10.1111/j.1399-0004.2006.00597.x

Nakao, Y., Mitsuyasu, T., Kawano, S., Nakamura, N., Kanda, S., and Nakamura, S. (2013). Fibroblast growth factors 7 and 10 are involved in ameloblastoma proliferation via the mitogen-activated protein kinase pathway. *Int. J. Oncol.* 43, 1377–1384. doi: 10.3892/ijo.2013.2081

Natanson-Yaron, S., Anteby, E. Y., Greenfield, C., Goldman-Wohl, D., Hamani, Y., Hochner-Celnikier, D., et al. (2007). FGF 10 and Sprouty 2 modulate trophoblast invasion and branching morphogenesis. *Mol. Hum. Reprod.* 13, 511–519. doi: 10.1093/molehr/gam034

Nomura, S., Yoshitomi, H., Takano, S., Shida, T., Kobayashi, S., Ohtsuka, M., et al. (2008). FGF10/FGFR2 signal induces cell migration and invasion in pancreatic cancer. *Br. J. Cancer* 99, 305–313. doi: 10.1038/sj.bjc.6604473

Norgaard, G. A., Jensen, J. N., and Jensen, J. (2003). FGF10 signaling maintains the pancreatic progenitor cell state revealing a novel role of Notch in organ development. *Dev. Biol.* 264, 323–338. doi: 10.1016/j.ydbio.2003.08.013

Nyeng, P., Norgaard, G. A., Kobberup, S., and Jensen, J. (2007). FGF10 signaling controls stomach morphogenesis. *Dev. Biol.* 303, 295–310. doi: 10.1016/j.ydbio.2006.11.017

Ohuchi, H., Hori, Y., Yamasaki, M., Harada, H., Sekine, K., Kato, S., et al. (2000). FGF10 acts as a major ligand for FGF receptor 2 IIIb in mouse multi-organ development. *Biochem. Biophys. Res. Commun.* 277, 643–649. doi: 10.1006/bbrc.2000.3721

Oldridge, M., Lunt, P. W., Zackai, E. H., McDonaldMcGinn, D. M., Muenke, M., Moloney, D. M., et al. (1997). Genotype-phenotype correlation for nucleotide substitutions in the IgII-IgIII linker of FGFR2. *Hum. Mol. Genet.* 6, 137–143. doi: 10.1093/hmg/6.1.137

Oldridge, M., Zackai, E. H., McDonald-McGinn, D. M., Iseki, S., Morriss-Kay, G. M., Twigg, R. F., et al. (1999). De novo Alu-element insertions in FGFR2 identify a distinct pathological basis for Apert syndrome. *Am. J. Hum. Genet.* 64, 446–461. doi: 10.1086/302245

Ong, S. H., Guy, G. R., Hadari, Y. R., Laks, S., Gotoh, N., Schlessinger, J., et al. (2000). FRS2 proteins recruit intracellular signaling pathways by binding to diverse targets on fibroblast growth factor and nerve growth factor receptors. *Mol. Cell. Biol.* 20, 979–989. doi: 10.1128/MCB.20.3.979-989.2000

Ong, S. H., Hadari, Y. R., Gotoh, N., Guy, G. R., Schlessinger, J., and Lax, I. (2001). Stimulation of phosphatidylinositol 3-kinase by fibroblast growth factor receptors is mediated by coordinated recruitment of multiple docking proteins. *Proc. Natl. Acad. Sci. U.S.A.* 98, 6074–6079. doi: 10.1073/pnas.111114298

Ornitz, D. M., and Itoh, N. (2015). The fibroblast growth factor signaling pathway. *Wiley Interdiscip. Rev. Dev. Biol.* 4, 215–266. doi: 10.1002/wdev.176

Ornitz, D. M., Xu, J., Colvin, J. S., McEwen, D. G., MacArthur, C. A., Coulier, F., et al. (1996). Receptor specificity of the fibroblast growth factor family. *J. Biol. Chem.* 271, 15292–15297. doi: 10.1074/jbc.271.25.15292

Patel, V. N., Likar, K. M., Zisman-Rozen, S., Cowherd, S. N., Lassiter, K. S., Sher, I., et al. (2008). Specific heparan sulfate structures modulate FGF10-mediated submandibular gland epithelial morphogenesis and differentiation. *J. Biol. Chem.* 283, 9308–9317. doi: 10.1074/jbc.M709995200

Patel, V. N., Pineda, D. L., and Hoffman, M. P. (2017). The function of heparan sulfate during branching morphogenesis. *Matrix Biol.* 5, 311–323. doi: 10.1016/j.matbio.2016.09.004

Pepicelli, C. V., Lewis, P. M., and McMahon, A. P. (1998). Sonic hedgehog regulates branching morphogenesis in the mammalian lung. *Curr. Biol.* 8, 1083–1086. doi: 10.1016/S0960-9822(98)70446-4

Qu, X., Carbe, C., Tao, C., Powers, A., Lawrence, R., van Kuppevelt, T. H., et al. (2011). Lacrimal gland development and Fgf10-Fgfr2b signaling are controlled by 2-O- and 6-O-sulfated heparan sulfate. *J. Biol. Chem.* 286, 14435–14444. doi: 10.1074/jbc.M111.225003

Reintjes, N., Li, Y., Becker, A., Rohmann, E., Schmutzler, R., and Wollnik, B. (2013). Activating somatic FGFR2 mutations in breast cancer. *PLoS One* 8:e60264. doi: 10.1371/journal.pone.0060264

Rohmann, E., Brunner, H. G., Kayserili, H., Uyguner, O., Nurnberg, G., Lew, E. D., et al. (2006). Mutations in different components of FGF signaling in LADD syndrome. *Nat. Genet.* 38, 414–417. doi: 10.1038/ng1757

Sakaue, H., Konishi, M., Ogawa, W., Asaki, T., Mori, T., Yamasaki, M., et al. (2002). Requirement of fibroblast growth factor 10 in development of white adipose tissue. *Genes Dev.* 16, 908–912. doi: 10.1101/gad.983202

Satterfield, M. C., Hayashi, K., Song, G., Black, S. G., Bazer, F. W., and Spencer, T. E. (2008). Progesterone regulates FGF10, MET, IGFBP1, and IGFBP3 in the endometrium of the ovine uterus. *Biol. Reprod.* 79, 1226–1236. doi: 10.1095/biolreprod.108.071787

Shi, L., Tian, C., Sun, L., Cao, F., and Meng, Z. (2018). The lncRNA TUG1/miR-145-5p/FGF10 regulates proliferation and migration in VSMCs of hypertension. *Biochem. Biophys. Res. Commun.* 501, 688–695. doi: 10.1016/j.bbrc.2018.05.049

Steinberg, Z., Myers, C., Heim, V. M., Lathrop, C. A., Rebustini, I. T., Stewart, J. S., et al. (2005). FGFR2b signaling regulates ex vivo submandibular gland epithelial cell proliferation and branching morphogenesis. *Development* 132, 1223–1234. doi: 10.1242/dev.01690

Su, X., Zhan, P., Gavine, P. R., Morgan, S., Womack, C., Ni, X., et al. (2014). FGFR2 amplification has prognostic significance in gastric cancer: results from a large international multicentre study. *Br. J. Cancer.* 110, 967–975. doi: 10.1038/bjc.2013.802

Sun, Q., Lin, P., Zhang, J., Li, X., Yang, L., Huang, J., et al. (2015). Expression of fibroblast growth factor 10 is correlated with poor prognosis in gastric adenocarcinoma. *Tohoku J. Exp. Med.* 236, 311–318. doi: 10.1620/tjem.236.311

Taniguchi, F., Harada, T., Sakamoto, Y., Yamauchi, N., Yoshida, S., Iwabe, T., et al. (2003). Activation of mitogen-activated protein kinase pathway by keratinocyte growth factor or fibroblast growth factor-10 promotes cell proliferation in human endometrial carcinoma cells. *J. Clin. Endocrinol. Metab.* 88, 773–780. doi: 10.1210/jc.2002-021062

Tefft, D., Lee, M., Smith, S., Crowe, D. L., Bellusci, S., and Warburton, D. (2002). mSprouty2 inhibits FGF10-activated MAP kinase by differentially binding to upstream target proteins. *Am. J. Physiol. Lung. Cell Mol. Physiol.* 283, L700–L706. doi: 10.1152/ajplung.00372.2001

Terakawa, J., Rocchi, A., Serna, V. A., Bottinger, E. P., Graff, J. M., and Kurita, T. (2016). FGFR2IIIb-MAPK activity is required for epithelial cell fate decision in the lower mullerian duct. *Mol. Endocrinol.* 30, 783–795. doi: 10.1210/me.2016-1027

Theodorou, V., Boer, M., Weigelt, B., Jonkers, J., van der Valk, M., and Hilkens, J. (2004). Fgf10 is an oncogene activated by MMTV insertional mutagenesis in mouse mammary tumors and overexpressed in a subset of human breast carcinomas. *Oncogene* 23, 6047–6055. doi: 10.1038/sj.onc.1207816

Timsah, Z., Ahmed, Z., Lin, C. C., Melo, F. A., Stagg, L. J., Leonard, P. G., et al. (2014). Competition between Grb2 and Plcgamma1 for FGFR2 regulates basal phospholipase activity and invasion. *Nat. Struct. Mol. Biol.* 21, 180–188. doi: 10.1038/nsmb.2752

Upadhyay, D., Correa-Meyer, E., Sznajder, J. I., and Kamp, D. W. (2003a). FGF-10 prevents mechanical stretch-induced alveolar epithelial cell DNA damage via MAPK activation. *Am. J. Physiol. Lung Cell Mol. Physiol.* 284, L350–L359.

Upadhyay, D., Lecuona, E., Comellas, A., Kamp, D. W., and Sznajder, J. I. (2003b). Fibroblast growth factor-10 upregulates Na,K-ATPase via the MAPK pathway. *FEBS Lett.* 545, 173–176.

Volckaert, T., Campbell, A., Dill, E., Li, C., Minoo, P., and De Langhe, S. (2013). Localized Fgf10 expression is not required for lung branching morphogenesis but prevents differentiation of epithelial progenitors. *Development* 140, 3731–3742. doi: 10.1242/dev.096560

Volckaert, T., and De Langhe, S. P. (2015). Wnt and FGF mediated epithelial-mesenchymal crosstalk during lung development. *Dev. Dyn.* 244, 342–366. doi: 10.1002/dvdy.24234

Volckaert, T., Yuan, T., Chao, C. M., Bell, H., Sitaula, A., Szimmtenings, L., et al. (2017). Fgf10-hippo epithelial-mesenchymal crosstalk maintains and recruits lung basal stem cells. *Dev. Cell* 43, 48–59.e5. doi: 10.1016/j.devcel.2017.09.003

von Stechow, L., Francavilla, C., and Olsen, J. V. (2015). Recent findings and technological advances in phosphoproteomics for cells and tissues. *Expert Rev. Proteomics* 12, 469–487. doi: 10.1586/14789450.2015.1078730

Weaver, M., Dunn, N. R., and Hogan, B. L. (2000). Bmp4 and Fgf10 play opposing roles during lung bud morphogenesis. *Development* 127, 2695–2704.

Wentz, E., Vujic, M., Karrstedt, E. L., Erlandsson, A., and Gillberg, C. (2014). A case report of two male siblings with autism and duplication of Xq13-q21, a region including three genes predisposing for autism. *Eur. Child Adolesc. Psychiatry* 23, 329–336. doi: 10.1007/s00787-013-0455-1

Wilkie, A. O. M., Slaney, S. F., Oldridge, M., Poole, M. D., Ashworth, G. J., Hockley, A. D., et al. (1995). Apert syndrome results from localized mutations of Fgfr2 and is allelic with crouzon syndrome. *Nat. Genet.* 9, 165–172. doi: 10.1038/ng0295-165

Yamamoto-Shiraishi, Y., Higuchi, H., Yamamoto, S., Hirano, M., and Kuroiwa, A. (2014). Etv1 and Ewsr1 cooperatively regulate limb mesenchymal Fgf10 expression in response to apical ectodermal ridge-derived fibroblast growth factor signal. *Dev. Biol.* 394, 181–190. doi: 10.1016/j.ydbio.2014.07.022

Yang, S. H., Sharrocks, A. D., and Whitmarsh, A. J. (2013). MAP kinase signalling cascades and transcriptional regulation. *Gene* 513, 1–13. doi: 10.1016/j.gene.2012.10.033

Yokoyama, H., Ide, H., and Tamura, K. (2001). FGF-10 stimulates limb regeneration ability in Xenopus laevis. *Dev. Biol.* 233, 72–79. doi: 10.1006/dbio.2001.0180

Zeng, C. M., Chen, Z., and Fu, L. (2018). Frizzled receptors as potential therapeutic targets in human cancers. *Int. J. Mol. Sci.* 19:E1543. doi: 10.3390/ijms19051543

Zhang, X., Ibrahimi, O. A., Olsen, S. K., Umemori, H., Mohammadi, M., and Ornitz, D. M. (2006). Receptor specificity of the fibroblast growth factor family. The complete mammalian FGF family. *J. Biol. Chem.* 281, 15694–15700. doi: 10.1074/jbc.M601252200

Zhao, Y., and O'Brien, T. P. (2015). Spry2 regulates signalling dynamics and terminal bud branching behaviour during lung development. *Genet. Res.* 97:e12. doi: 10.1017/S0016672315000026

Conflict of Interest Statement: The authors declare that the research was conducted in the absence of any commercial or financial relationships that could be construed as a potential conflict of interest.

Copyright © 2018 Watson and Francavilla. This is an open-access article distributed under the terms of the Creative Commons Attribution License (CC BY). The use, distribution or reproduction in other forums is permitted, provided the original author(s) and the copyright owner(s) are credited and that the original publication in this journal is cited, in accordance with accepted academic practice. No use, distribution or reproduction is permitted which does not comply with these terms.

frontiers in Genetics

MINI REVIEW
published: 24 October 2018
doi: 10.3389/fgene.2018.00499

Emerging Roles of Fibroblast Growth Factor 10 in Cancer

*Natasha S. Clayton and Richard P. Grose**

Centre for Tumour Biology, Barts Cancer Institute, CRUK Centre of Excellence, Queen Mary University of London, London, United Kingdom

Whilst cross-talk between stroma and epithelium is critical for tissue development and homeostasis, aberrant paracrine stimulation can result in neoplastic transformation. Chronic stimulation of epithelial cells with paracrine Fibroblast Growth Factor 10 (FGF10) has been implicated in multiple cancers, including breast, prostate and pancreatic ductal adenocarcinoma. Here, we examine the mechanisms underlying FGF10-induced tumourigenesis and explore novel approaches to target FGF10 signaling in cancer.

Keywords: FGF10, FGFR2, FGFR2b, FGFR1, FGFR1b, cancer

OPEN ACCESS

Edited by:
Mohammad K. Hajihosseini, University of East Anglia, United Kingdom

Reviewed by:
Agamemnon E. Grigoriadis, King's College London, United Kingdom
Michael Grusch, Medizinische Universität Wien, Austria
Fen Wang, Texas A&M University, United States

***Correspondence:**
Richard P. Grose
r.p.grose@qmul.ac.uk

Specialty section:
This article was submitted to Stem Cell Research, a section of the journal Frontiers in Genetics

Received: *22 August 2018*
Accepted: *05 October 2018*
Published: *24 October 2018*

Citation:
Clayton NS and Grose RP (2018) Emerging Roles of Fibroblast Growth Factor 10 in Cancer. Front. Genet. 9:499. doi: 10.3389/fgene.2018.00499

INTRODUCTION

The majority of secreted FGFs signal in an autocrine or paracrine manner, by binding to FGF receptors (FGFR1-4) on the surface of target cells. Alternative splicing of the immunoglobin-like domain III in FGFR1-FGFR3 produces two variants, IIIb and IIIc, which confer different ligand binding specificities. FGF10, a member of the FGF7 subfamily, signals in a paracrine manner through activation of the IIIb splice variants of FGFR2 (FGFR2b) and FGFR1 (FGFR1b), which are predominantly expressed on the surface of cells of epithelial origin. Whilst *in vitro* assays have shown FGF10 to activate FGFR1b more weakly than FGFR2b, FGFR1b activation *in vivo* may be achieved in scenarios where extracellular FGF10 reaches high concentrations (Zhang et al., 2006; Ornitz and Itoh, 2015). It has been suggested that FGF10 may also perform intracrine roles within FGF10-producing cells, primarily through trafficking to the nucleus. Whilst the functional significance of FGF10 nuclear localization remains to be determined, disrupted nuclear localization of FGF10 has been linked to lacrimo-auriculo-denot-digital syndrome (Mikolajczak et al., 2016).

FGF10 is known to be critical for brain, lung and limb development (Sekine et al., 1999; Hajihosseini et al., 2008) and contributes to wound healing and tissue repair by promoting cell migration and proliferation (Werner et al., 1994; Volckaert et al., 2011). Given this role of FGF10 in adult tissues, it is unsurprising that aberrant signaling of FGF10 through FGFR2b, and in some instances FGFR1b, contributes to the progression of a number of human cancers.

FGF10 IN BREAST CANCER

Studies in $Fgf10^{-/-}$ and $Fgfr2b^{-/-}$ mouse embryos demonstrate that FGF10-FGFR2b signaling plays a key role in mammary gland development (Mailleux et al., 2002; Veltmaat et al., 2006). Whilst FGF10 is not expressed in the luminal epithelial cells of the normal human breast duct (Grigoriadis et al., 2006), transcription of the *FGF10* gene is elevated

10% of breast carcinomas (Theodorou et al., 2004) and genome-wide association studies have identified variants near the *FGF10* locus as a genetic risk factor for breast cancer susceptibility (Stacey et al., 2008). Similarly, SNPs affecting FGFR2b expression have been correlated with breast cancer susceptibility (Meyer et al., 2008; Fachal and Dunning, 2015) and amplification of *FGFR1,* occurring in up to 12% of breast cancer cases (Cerami et al., 2012; Gao et al., 2013; Pereira et al., 2016), is correlated with poor prognosis (Reis-Filho et al., 2006; Elbauomy Elsheikh et al., 2007). A number of *in vitro* studies have shed light on the cellular roles of FGF10-FGFR2/1 signaling in breast cancer cell behavior (**Figure 1**).

FGFR2 activation has been shown to repress the activity of the estrogen receptor (ER) regulon (Campbell T. M. et al., 2016), which has been correlated with poor prognosis in a cohort of ER^+ breast cancer patients (Castro et al., 2016). Stimulation of the ER^+ breast cancer cell line MCF-7 with FGF10 enhanced the interaction of the transcription factors NFIB and YBX1 with the ER, which inhibited its transcriptional activity and shunted the cells toward a more ER^-, basal-like cancer phenotype with reduced estrogen dependency and lower sensitivity to anti-estrogen therapy. Treatment of ER^+ breast cancer cell lines with the FGFR inhibitors AZD4547 and PD173074 sensitized the cells to the anti-estrogen tamoxifen, suggesting that targeting FGF10-FGFR2 signaling may offer a new approach to overcoming resistance to hormone-deprivation therapy in ER^+ breast cancer (Campbell et al., 2018).

Nuclear localization of receptor tyrosine kinases (RTKs) has been documented for 12 RTK families (Chen and Hung, 2015) and has been correlated with poor prognosis in various cancers (Aleksic et al., 2010; Hadžisejdić et al., 2010; Traynor et al., 2013; Coleman et al., 2014). *In vitro* studies using breast cancer cell lines showed that FGF10 stimulation lead to the nuclear translocation of a 55 kDa C-terminal fragment of FGFR1, which in turn promoted the transcription of genes that stimulate cell migration and invasion. Cleavage of FGFR1 to yield this C-terminal fragment was found to be mediated by granzyme B activity, which was itself positively regulated by FGF10 stimulation. In 3D organotypic cell culture models, FGFR1 nuclear localization was most apparent in invading cells. Importantly, increased nuclear FGFR1 staining was also detected in tissue sections of invasive breast carcinoma (Chioni and Grose, 2012).

Analysis of FGFR2b signaling networks *in vitro* revealed that stimulation of FGFR2b with FGF10 promoted receptor recycling and led to an increase in breast cancer migration, whilst stimulation of FGFR2b with FGF7 resulted in receptor degradation and led to increased cell proliferation. Using quantitative proteomics to explore the mechanism underlying this functional dichotomy, it was revealed that FGF10 binding resulted in the novel phosphorylation of FGFR2b at Y734,

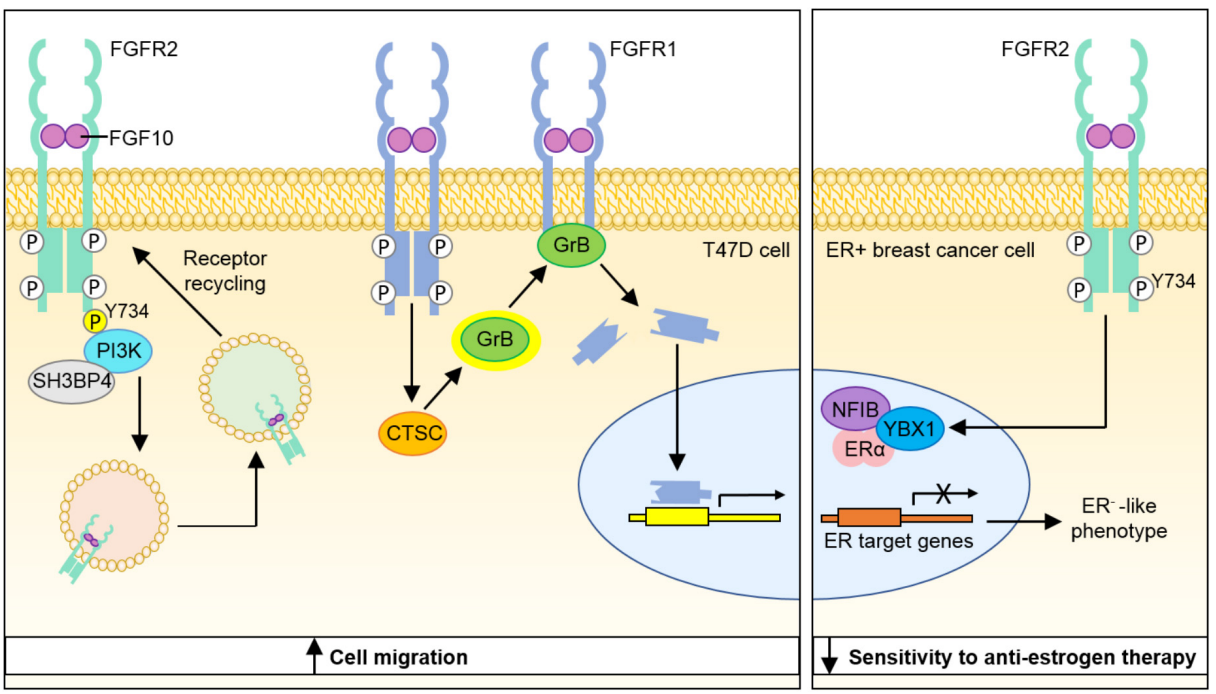

FIGURE 1 | Model depicting molecular mechanisms through which FGF10-FGFR1 and FGF10-FGFR2 signaling may contribute to breast cancer progression. Binding of FGF10 to FGFR2b leads to phosphorylation of the receptor at Y734 and recruitment of PI3K and SH3BP4, which promote receptor recycling and increased cell migration. FGF10 binding to FGFR1 leads to cleavage of the receptor by granzyme B and the translocation of a 55 kDa fragment of FGFR1 to the nucleus, leading to increased cell migration. Stimulation of ER^+ breast cancer cells with FGF10 enhances the interaction of NFIB and YBX1 with the ER and inhibits its transcriptional activity to produce a more ER^- phenotype with lower sensitivity to anti-estrogen therapy. PI3K, phosphatidylinositide 3-kinase; SH3BP4, SH3-binding protein 4; CTSC, cathepsin C; GrB, granzyme B; NFIB, nuclear factor I B; YBX1, Y-Box Binding Protein-1; ERα, estrogen receptor α.

which led to the recruitment of PI3K and SH3BP4 and targeting of the receptor to recycling endosomes. Whilst the mechanism through which FGFR2b recycling promotes cell migration is not fully understood, the role of FGFR2b-PI3K-SH3BP4 complex formation in this response to FGF10 was illustrated by experiments showing that FGF10-stimulated cell migration could be inhibited by depletion of SH3BP4 or expression of a FGFR2b-Y734F mutant (Francavilla et al., 2013).

FGF10 IN PROSTATE CANCER

In vivo models have shown that elevated paracrine FGF10 stimulation of mouse prostate epithelial cells led to the development of adenocarcinoma, predominantly via activation of epithelial FGFR1. These lesions showed heightened levels of androgen receptor (AR), caused most likely by post-translational modifications augmenting AR stability. Following host castration, a subset of FGF10-induced prostate adenocarcinoma cells showed continued survival and proliferation, suggesting that paracrine FGF10 stimulation may contribute to the development of androgen independence in this murine model of prostate cancer (Memarzadeh et al., 2007). Later work using testicular feminized mice revealed that FGF10-induced prostate neoplasia is dependent on the expression of functional AR (Memarzadeh et al., 2011), demonstrating a role for FGF10-AR cross-talk in early prostate tumourigenesis.

AR expression has also been detected in prostate cancer-associated fibroblasts (CAFs) *in vitro* and siRNA-mediated depletion of AR from these stromal cells resulted in a decrease in FGF10 expression. Thus, there may exist a positive feedback loop whereby increased stromal cell AR levels promote the expression of FGF10, which then acts in a paracrine manner to elevate AR levels in prostate epithelial cells and potentially also in an autocrine manner to further elevate levels of AR in the stroma (**Figure 2**; Yu et al., 2013).

In a model of FGF10-induced prostate tumourigenesis, enhanced phosphorylation of Src-family kinases (SFKs) was detected in the adenocarcinoma lesions. Prostate epithelium from $Src^{-/-}Fyn^{+/-}$ mice showed normal histology following exposure to elevated paracrine FGF10, suggesting that the tumourigenic effects of FGF10 on prostate epithelial cells are in part mediated by epithelial Src and Fyn kinases. Importantly, this work also established a link between FGF10, SFK signaling and AR levels by demonstrating that FGF10-stimulated $Src^{-/-}Fyn^{+/-}$ xenografts showed downregulation of AR relative to FGF10-stimulated wild type xenografts (Cai et al., 2011). Recent *in vivo* studies have provided further evidence for a role of a FGF10/FGFR/Src signaling axis in prostate cancer. Ectopic expression of FGFR1, FGFR2, or Src in mouse prostate epithelial cells growing in a normal microenvironment was not sufficient to induce prostate tumourigenesis *in vivo*. However, paracrine FGF10 was found to synergize with FGFR1/2 over-expression to induce epithelial-mesenchymal transition and FGF10 synergized with Src overexpression to induce high-grade epithelial tumors. Importantly, inhibition of Src signaling, either by pharmacological Src kinase inhibitors or by deletion of the Src myristoylation site, inhibited paracrine FGF10-induced prostate tumourigenesis (Li et al., 2018b).

Whilst these studies in mouse models of prostate cancer have revealed potential novel roles for FGF10 in androgen signaling, it is important to note that elevated FGF10 has not been detected in human prostate cancer tissue (Abate-Shen and Shen, 2007; Eiro et al., 2017) and levels of FGF10 in the normal adult prostate are extremely low, compared to those of FGF7 (Ropiquet et al., 2000). Transfection of malignant prostate tumor cells with FGFR2b cDNA has been shown to reduce the growth rate of the derived tumors (Feng et al., 1997) and restoration of FGFR2b expression in castration-resistant prostate cancer cells increased sensitivity to chemotherapeutic agents (Shoji et al., 2014). Further investigation is therefore required to fully elucidate the complex roles of FGF10-FGFR2b signaling in prostate tumourigenesis.

FGF10 IN PANCREATIC CANCER

Whilst FGF10 expression is not detected in the normal adult human pancreas (Ishiwata et al., 1998), FGF10 is required for the proliferation of pancreatic epithelial progenitor cells and $FGF10^{-/-}$ mouse embryos show pancreatic hypoplasia, arrested pancreatic epithelial branching and an absence of islet cells (Bhushan et al., 2001). Expression of FGFR2 and FGFR1 are up-regulated in approximately 25% of pancreatic adenocarcinoma (PDAC) cases and elevated stromal FGF10 expression coupled with high cancer cell FGFR2b expression has been correlated with poor prognosis (Cerami et al., 2012; Gao et al., 2013; Bailey et al., 2016). *In vitro* studies using FGFR2b-expressing pancreatic cancer cell lines revealed that FGF10 stimulation promoted cancer cell migration and invasion through the up-regulation of MT1-MMP and TGF-β1 (**Figure 2**; Nomura et al., 2008).

More recent work aiming to identify diagnostic and predictive markers for pancreatic cancer found that FGF10 levels were elevated in the sera of untreated patients with PDAC compared to healthy controls and found that in combination with a panel of 4 other cytokine markers, FGF10 could be used as a diagnostic biomarker for PDAC (Torres et al., 2014).

FGF10 IN STOMACH CANCER

During development, FGF10 signaling plays a key role in stomach morphogenesis, through regulating gastric gland formation and maintaining an epithelial progenitor cell niche (Nyeng et al., 2007). In a cohort of 961 gastric cancers from the United Kingdom, Korea and China, *FGFR2* amplification was detected in 4.2–7.4% of cases and was associated with lymph node metastasis and poor overall survival (Su et al., 2014). *FGF10* amplification has also been detected in 3% of gastric cancers (Ooi et al., 2015) and immunohistochemical analysis of 178 gastric adenocarcinoma samples revealed that FGF10 levels are correlated with poor prognosis (Sun et al., 2015). Interrogation of most recent cBioPortal data suggests this could be an underestimate, with *FGF10* amplifications reported in 5.7%

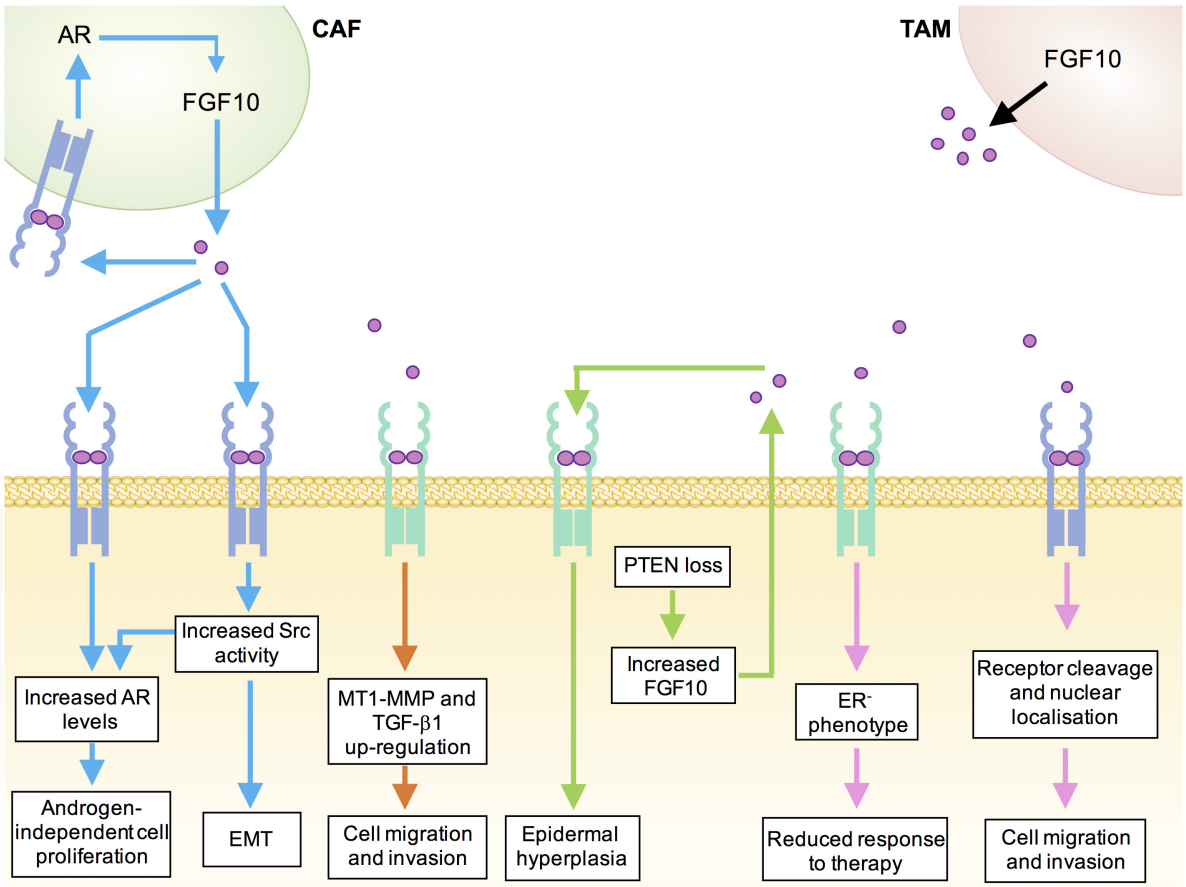

FIGURE 2 | Mechanisms underlying tumor-promoting functions of FGF10 in human cancers. Blue, prostate cancer; orange, pancreatic ductal adenocarcinoma; green, cutaneous squamous cell carcinoma; pink, breast cancer; black, lung cancer; CAF, cancer-associated fibroblast; TAM, tumor-associated macrophage.

of stomach adenocarcinoma cases (Cerami et al., 2012; Gao et al., 2013).

FGF10 IN SKIN CANCER

Whilst local elevation of FGF22, FGF7, and FGF10 are required for efficient healing of skin lesions (Braun et al., 2004), sustained elevation of FGF10 has also been implicated in cutaneous squamous cell carcinoma (SCC). Epidermal deletion of the tumor suppressor *Pten* produces a model of cutaneous squamous cell carcinoma in mice (Suzuki et al., 2003). The epidermis of these mice showed elevated keratinocyte expression of FGF10, with no change in levels of FGF7, FGF2, and FGF1. This increase in FGF10 was not accompanied by any *Fgf10* transcriptional changes and was found to be dependent on the elevated mTORC1 signaling resulting from loss of the negative regulator, PTEN. The specific contribution of FGF10 to carcinogenesis was demonstrated by induction of constitutive epidermal FGF10 expression, which produced epidermal hyperplasia and spontaneous papillomas in all mice by 3 weeks of age. Crucially, it was shown that genetic ablation of *Fgfr2* prevented hyperplasia in PTEN-deficient epidermis, suggesting that epidermal tumourigenesis induced by PTEN loss is mediated by an up-regulation of FGF10-FGFR2 autocrine signaling. Low levels of PTEN accompanied by elevated FGF10 have been observed in a panel of clinical SCC samples, highlighting the potential importance of this mechanism in the human disease (Hertzler-Schaefer et al., 2014).

In contrast to these data implicating FGF10 in skin carcinogenesis, previous work has suggested that FGF10-FGFR2b signaling may perform tumor-suppressive functions in the skin. Mice lacking epidermal Fgfr2b showed increased sensitivity to chemical carcinogens and 10% of animals surviving into adulthood developed spontaneous papillomas. Epidermal *Fgfr2b* ablation induced several changes in gene expression in the skin, including downregulation of Serpin a3b, a potential tumor suppressor (Grose et al., 2007).

FGF10 IN LUNG CANCER

Whilst FGF10 is crucial for branching morphogenesis in the developing lung (Sekine et al., 1999), induction of FGF10 over-expression in the respiratory epithelial cells of adult mice has been shown to cause multifocal pulmonary adenomas

(Clark et al., 2001). A recent study designed to identify genomic variations in cell-free DNA in small cell lung cancer patients identified *FGF10* amplification in 37.5% and of patients tested and *FGFR1* amplification in 25% of cases (Du et al., 2018). Analysis of 1144 lung cancer tumors comprising lung adenocarcinomas and lung squamous cell carcinomas revealed *FGF10* amplifications in 8.7% and FGFR1 amplifications in 9.3% of cases (Campbell J. D. et al., 2016).

The role of FGF10 in lung cancer initiation and progression remains poorly understood. However, emerging evidence suggests that FGF10 secreted from tumor-associated macrophages may play a role in promoting lung tumourigenesis (**Figure 2**). Tumour-associated macrophages (TAMs) are macrophages that have been co-opted by the tumor microenvironment to promote the growth and invasion of cancer cells (Noy and Pollard, 2014). Recent work showed that induction of FGF9 overexpression in the lungs of transgenic mice resulted in the development of adenocarcinoma-like nodules that are infiltrated with an immune response consisting mostly of macrophages. Expression analysis revealed that the TAMs from these transgenic mice expressed significantly higher levels of FGF2, FGF10, and FGFR2 than macrophages from wild-type mice. It has been suggested that activation of an FGF10-FGFR2 pathway may underlie the transition to FGF9-independent tumor growth, which has been observed in previous studies using this lung cancer model (Hegab et al., 2018). Expression profiling of TAMs in other pre-clinical cancer models will reveal the clinical significance of these early findings.

THERAPEUTIC APPROACHES TARGETING FGF10-FGFR2 SIGNALING

In light of mounting evidence supporting a role for aberrant FGF10-FGFR2b signaling in tumourigenesis, FGFR2b has become an attractive therapeutic target. Whilst a number of pan-FGFR inhibitors have entered the clinic (Clayton et al., 2017), the development FGFR2-specific inhibitors is hindered by the structural similarity of the kinase domains of FGFR1-3 (Belov and Mohammadi, 2013). For this reason, ATP-mimetic inhibitors of the FGFR2b isoform are currently unavailable. However, the development of monocloncal antibodies targeting FGFR2b may provide an opportunity to target this isoform specifically. Bemarituzumab (2018) (FPA144) is an anti-FGFR2b humanized monoclonal antibody currently in Phase I clinical trials as a monotherapy for FGFR2b-amplified gastric cancers. Bemarituzumab prevents the binding of FGF10, FGF7 and FGF22 to the FGFR2b and is reported to also promote antibody-dependent cell-mediated cytotoxicity through the recruitment of natural killer cells to the tumor (*Bemarituzumab (FPA144)* | *Gastric Cancer* | *Five Prime Therapeutics*).

FGF10 signal transduction requires recruitment of the myristoylated scaffold protein FRS2α to the activated receptor, and recent pre-clinical work has highlighted the potential of targeting FRS2α myristoylation in paracrine FGF10-induced tumourigenesis. Primary mouse prostate cells transduced with FRS2α(wt) or FRS2α(G2A), a mutant that cannot be myristolyated, were mixed with mouse urogenital sinus mesenchyme (UGSM) cells expressing either FGF10 or GFP as a control. The cells were implanted sub-renally into SCID mice. Xenografts derived from FRS2α(wt) prostate cells mixed with FGF10-UGSM showed adenocarcinoma, whilst xenografts of FRS2α(G2A) cells with FGF10-UGSM cells showed normal prostate tubules. *In vitro* work showed that FRS2α myristolylation can be targeted pharmacologically by treating with the myristoyl-coA analog B13 (Li et al., 2018a).

Recent evidence has demonstrated that a FGF10/FGFR/Src signaling axis may contribute to prostate tumourigenesis via a mechanism that is dependent on Src activity. Inhibition of Src myristoylation, and therefore membrane localization, has been suggested as a viable therapeutic strategy for these prostate cancer subtypes. *In vitro* studies showed that loss of Src myristoylaton had a significant inhibitory effect on FGF10-induced oncogenic signaling in comparison with a kinase-dead Src mutant (Li et al., 2018b). These data have prompted efforts to develop an N-myristoyltransferase inhibitor as a means to therapeutically target the FGF10/FGFR/Src signaling axis in cancer (French et al., 2004; Thinon et al., 2014; Kim et al., 2017).

CONCLUSION AND FUTURE PERSPECTIVES

The receptors for FGF10, FGFR2, and FGFR1 have been implicated in several human cancers, including pancreatic ductal adenocarcinoma and gastric cancer. However, since FGFR2 and FGFR1 are activated by a number of FGF family members, it has been difficult to attribute the tumor-promoting effects of these receptors to binding of a specific ligand. Recent data have begun to shed light on the role of FGF10 in these cancers, demonstrating that paracrine FGF10 synergizes with FGFR1/2 over-expression to induce epithelial-mesenchymal transition in a pre-clinical model of prostate cancer. The development of isoform-selective pharmacological tools will clarify the role of FGF10-FGFR2b/1b signaling in different cancer types and will allow the potential of FGF10 as a therapeutic target to be explored.

AUTHOR CONTRIBUTIONS

Both authors listed have made a substantial, direct and intellectual contribution to the work, and approved it for publication.

FUNDING

This work was supported by a Cancer Research UK Centre Grant to Barts Cancer Institute (C16420/A18066).

REFERENCES

Abate-Shen, C., and Shen, M. M. (2007). FGF signaling in prostate tumorigenesis—new insights into epithelial-stromal interactions. *Cancer Cell* 12, 495–497. doi: 10.1016/j.ccr.2007.11.021

Aleksic, T., Chitnis, M. M., Perestenko, O. V., Gao, S., Thomas, P. H., Turner, G. D., et al. (2010). Type 1 insulin-like growth factor receptor translocates to the nucleus of human tumor cells. *Cancer Res.* 70, 6412–6419. doi: 10.1158/0008-5472.CAN-1 0-0052

Bailey, P., Chang, D. K., Nones, K., Johns, A. L., Patch, A.-M., Gingras, M.-C., et al. (2016). Genomic analyses identify molecular subtypes of pancreatic cancer. *Nature* 531, 47–52. doi: 10.1038/nature16965

Belov, A. A., and Mohammadi, M. (2013). Molecular mechanisms of fibroblast growth factor signaling in physiology and pathology. *Cold Spring Harb. Perspect. Biol.* 5:a015958. doi: 10.1101/cshperspect.a015958

Bemarituzumab (2018). *(FPA144) | Gastric Cancer | Five Prime Therapeutics*. Available at: http://www.fiveprime.com/pipeline/fpa144 [accessed May 23, 2018]

Bhushan, A., Itoh, N., Kato, S., Thiery, J. P., Czernichow, P., Bellusci, S., et al. (2001). Fgf10 is essential for maintaining the proliferative capacity of epithelial progenitor cells during early pancreatic organogenesis. *Development* 128, 5109–5117.

Braun, S., auf dem Keller, U., Steiling, H., and Werner, S. (2004). Fibroblast growth factors in epithelial repair and cytoprotection. *Philos. Trans. R. Soc. Lond. B Biol. Sci.* 359, 753–757. doi: 10.1098/rstb.2004.1464

Cai, H., Smith, D. A., Memarzadeh, S., Lowell, C. A., Cooper, J. A., and Witte, O. N. (2011). Differential transformation capacity of Src family kinases during the initiation of prostate cancer. *Proc. Natl. Acad. Sci. U.S.A.* 108, 6579–6584. doi: 10.1073/pnas.1103904108

Campbell, J. D., Alexandrov, A., Kim, J., Wala, J., Berger, A. H., Pedamallu, C. S., et al. (2016). Distinct patterns of somatic genome alterations in lung adenocarcinomas and squamous cell carcinomas. *Nat. Genet.* 48, 607–616. doi: 10.1038/ng.3564

Campbell, T. M., Castro, M. A. A., de Santiago, I., Fletcher, M. N. C., Halim, S., Prathalingam, R., et al. (2016). FGFR2 risk SNPs confer breast cancer risk by augmenting oestrogen responsiveness. *Carcinogenesis* 37, 741–750. doi: 10.1093/carcin/bgw065

Campbell, T. M., Castro, M. A. A., de Oliveira, K. G., Ponder, B. A. J., and Meyer, K. B. (2018). ERα binding by transcription factors NFIB and YBX1 enables FGFR2 signaling to modulate estrogen responsiveness in breast cancer. *Cancer Res.* 78, 410–421. doi: 10.1158/0008-5472.CAN-17-1153

Castro, M. A. A., de Santiago, I., Campbell, T. M., Vaughn, C., Hickey, T. E., Ross, E., et al. (2016). Regulators of genetic risk of breast cancer identified by integrative network analysis. *Nat. Genet.* 48, 12–21. doi: 10.1038/ng.3458

Cerami, E., Gao, J., Dogrusoz, U., Gross, B. E., Sumer, S. O., Aksoy, B. A., et al. (2012). The cBio cancer genomics portal: an open platform for exploring multidimensional cancer genomics data. *Cancer Discov.* 2, 401–404. doi: 10.1158/2159-8290.CD-12-0095

Chen, M.-K., and Hung, M.-C. (2015). Proteolytic cleavage, trafficking, and functions of nuclear receptor tyrosine kinases. *FEBS J.* 282, 3693–3721. doi: 10.1111/febs.13342

Chioni, A.-M., and Grose, R. (2012). FGFR1 cleavage and nuclear translocation regulates breast cancer cell behavior. *J. Cell Biol.* 197, 801–817. doi: 10.1083/jcb.201108077

Clark, J. C., Tichelaar, J. W., Wert, S. E., Itoh, N., Perl, A.-K. T., Stahlman, M. T., et al. (2001). FGF-10 disrupts lung morphogenesis and causes pulmonary adenomas in vivo. *Am. J. Physiol. Cell. Mol. Physiol.* 280, L705–L715. doi: 10.1152/ajplung.2001.280.4.L705

Clayton, N. S., Wilson, A. S., Laurent, E. P., Grose, R. P., and Carter, E. P. (2017). Fibroblast growth factor-mediated crosstalk in cancer etiology and treatment. *Dev. Dyn.* 246, 493–501. doi: 10.1002/dvdy.24514

Coleman, S. J., Chioni, A.-M., Ghallab, M., Anderson, R. K., Lemoine, N. R., Kocher, H. M., et al. (2014). Nuclear translocation of FGFR1 and FGF2 in pancreatic stellate cells facilitates pancreatic cancer cell invasion. *EMBO Mol. Med.* 6, 467–481. doi: 10.1002/emmm.201302698

Du, M., Thompson, J., Fisher, H., Zhang, P., Huang, C.-C., and Wang, L. (2018). Genomic alterations of plasma cell-free DNAs in small cell lung cancer and their clinical relevance. *Lung Cancer* 120, 113–121. doi: 10.1016/j.lungcan.2018.04.008

Eiro, N., Fernandez-Gomez, J., Sacristán, R., Fernandez-Garcia, B., Lobo, B., Gonzalez-Suarez, J., et al. (2017). Stromal factors involved in human prostate cancer development, progression and castration resistance. *J. Cancer Res. Clin. Oncol.* 143, 351–359. doi: 10.1007/s00432-016-2284-3

Elbauomy Elsheikh, S., Green, A. R., Lambros, M. B., Turner, N. C., Grainge, M. J., Powe, D., et al. (2007). FGFR1 amplification in breast carcinomas: a chromogenic in situhybridisation analysis. *Breast Cancer Res.* 9:R23. doi: 10.1186/bcr1665

Fachal, L., and Dunning, A. M. (2015). From candidate gene studies to GWAS and post-GWAS analyses in breast cancer. *Curr. Opin. Genet. Dev.* 30, 32–41. doi: 10.1016/j.gde.2015.01.004

Feng, S., Wang, F., Matsubara, A., Kan, M., and McKeehan, W. L. (1997). Fibroblast growth factor receptor 2 limits and receptor 1 accelerates tumorigenicity of prostate epithelial cells. *Cancer Res.* 57, 5369–5378.

Francavilla, C., Rigbolt, K. T. G., Emdal, K. B., Carraro, G., Vernet, E., Bekker-Jensen, D. B., et al. (2013). Functional proteomics defines the molecular switch underlying FGF receptor trafficking and cellular outputs. *Mol. Cell* 51, 707–722. doi: 10.1016/j.molcel.2013.08.002

French, K. J., Zhuang, Y., Schrecengost, R. S., Copper, J. E., Xia, Z., and Smith, C. D. (2004). Cyclohexyl-octahydro-pyrrolo[1,2-a]pyrazine-based inhibitors of human N-myristoyltransferase-1. *J. Pharmacol. Exp. Ther.* 309, 340–347. doi: 10.1124/jpet.103.061572

Gao, J., Aksoy, B. A., Dogrusoz, U., Dresdner, G., Gross, B., Sumer, S. O., et al. (2013). Integrative analysis of complex cancer genomics and clinical profiles using the cBioportal. *Sci. Signal.* 6:pl1. doi: 10.1126/scisignal.2004088

Grigoriadis, A., Mackay, A., Reis-Filho, J. S., Steele, D., Iseli, C., Stevenson, B. J., et al. (2006). Establishment of the epithelial-specific transcriptome of normal and malignant human breast cells based on MPSS and array expression data. *Breast Cancer Res.* 8:R56. doi: 10.1186/bcr1604

Grose, R., Fantl, V., Werner, S., Chioni, A.-M., Jarosz, M., Rudling, R., et al. (2007). The role of fibroblast growth factor receptor 2b in skin homeostasis and cancer development. *EMBO J.* 26, 1268–1278. doi: 10.1038/sj.emboj.7601583

Hadžisejdić, I., Mustać, E., Jonjić, N., Petković, M., and Grahovac, B. (2010). Nuclear EGFR in ductal invasive breast cancer: correlation with cyclin-D1 and prognosis. *Mod. Pathol.* 23, 392–403. doi: 10.1038/modpathol.2009.166

Hajihosseini, M. K., De Langhe, S., Lana-Elola, E., Morrison, H., Sparshott, N., Kelly, R., et al. (2008). Localization and fate of Fgf10-expressing cells in the adult mouse brain implicate Fgf10 in control of neurogenesis. *Mol. Cell. Neurosci.* 37, 857–868. doi: 10.1016/j.mcn.2008.01.008

Hegab, A. E., Ozaki, M., Kagawa, S., Hamamoto, J., Yasuda, H., Naoki, K., et al. (2018). Tumor associated macrophages support the growth of FGF9-induced lung adenocarcinoma by multiple mechanisms. *Lung Cancer* 119, 25–35. doi: 10.1016/j.lungcan.2018.02.015

Hertzler-Schaefer, K., Mathew, G., Somani, A.-K., Tholpady, S., Kadakia, M. P., Chen, Y., et al. (2014). Pten loss induces autocrine FGF signaling to promote skin tumorigenesis. *Cell Rep.* 6, 818–826. doi: 10.1016/j.celrep.2014.01.045

Ishiwata, T., Friess, H., Büchler, M. W., Lopez, M. E., and Korc, M. (1998). Characterization of keratinocyte growth factor and receptor expression in human pancreatic cancer. *Am. J. Pathol.* 153, 213–222. doi: 10.1016/S0002-9440(10)65562-9

Kim, S., Alsaidan, O. A., Goodwin, O., Li, Q., Sulejmani, E., Han, Z., et al. (2017). Blocking myristoylation of Src inhibits its kinase activity and suppresses prostate cancer progression. *Cancer Res.* 77, 6950–6962. doi: 10.1158/0008-5472.CAN-17-0981

Li, Q., Alsaidan, O. A., Ma, Y., Kim, S., Liu, J., Albers, T., et al. (2018a). Pharmacologically targeting the myristoylation of the scaffold protein FRS2α inhibits FGF/FGFR-mediated oncogenic signaling and tumor progression. *J. Biol. Chem.* 293, 6434–6448. doi: 10.1074/jbc.RA117.000940

Li, Q., Ingram, L., Kim, S., Beharry, Z., Cooper, J. A., and Cai, H. (2018b). Paracrine fibroblast growth factor initiates oncogenic synergy with epithelial FGFR/Src transformation in prostate tumor progression. *Neoplasia* 20, 233–243. doi: 10.1016/j.neo.2018.01.006

Mailleux, A. A., Spencer-Dene, B., Dillon, C., Ndiaye, D., Savona-Baron, C., Itoh, N., et al. (2002). Role of FGF10/FGFR2b signaling during mammary gland development in the mouse embryo. *Development* 129, 53–60.

Memarzadeh, S., Cai, H., Janzen, D. M., Xin, L., Lukacs, R., Riedinger, M., et al. (2011). Role of autonomous androgen receptor signaling in prostate cancer initiation is dichotomous and depends on the oncogenic signal. *Proc. Natl. Acad. Sci. U.S.A.* 108, 7962–7967. doi: 10.1073/pnas.1105243108

Memarzadeh, S., Xin, L., Mulholland, D. J., Mansukhani, A., Wu, H., Teitell, M. A., et al. (2007). Enhanced paracrine FGF10 expression promotes formation of multifocal prostate adenocarcinoma and an increase in epithelial androgen receptor. *Cancer Cell* 12, 572–585. doi: 10.1016/j.ccr.2007.11.002

Meyer, K. B., Maia, A.-T., O'Reilly, M., Teschendorff, A. E., Chin, S.-F., Caldas, C., et al. (2008). Allele-specific up-regulation of FGFR2 increases susceptibility to breast cancer. *PLoS Biol.* 6:e108. doi: 10.1371/journal.pbio.0060108

Mikolajczak, M., Goodman, T., and Hajihosseini, M. K. (2016). Interrogation of a lacrimo-auriculo-dento-digital syndrome protein reveals novel modes of fibroblast growth factor 10 (FGF10) function. *Biochem. J.* 473, 4593–4607. doi: 10.1042/BCJ20160441

Nomura, S., Yoshitomi, H., Takano, S., Shida, T., Kobayashi, S., Ohtsuka, M., et al. (2008). FGF10/FGFR2 signal induces cell migration and invasion in pancreatic cancer. *Br. J. Cancer* 99, 305–313. doi: 10.1038/sj.bjc.6604473

Noy, R., and Pollard, J. W. (2014). Review tumor-associated macrophages: from mechanisms to therapy. *Immunity* 41, 49–61. doi: 10.1016/j.immuni.2014.06.010

Nyeng, P., Norgaard, G. A., Kobberup, S., and Jensen, J. (2007). FGF10 signaling controls stomach morphogenesis. *Dev. Biol.* 303, 295–310. doi: 10.1016/j.ydbio.2006.11.017

Ooi, A., Oyama, T., Nakamura, R., Tajiri, R., Ikeda, H., Fushida, S., et al. (2015). Semi-comprehensive analysis of gene amplification in gastric cancers using multiplex ligation-dependent probe amplification and fluorescence in situ hybridization. *Mod. Pathol.* 28, 861–871. doi: 10.1038/modpathol.2015.33

Ornitz, D. M., and Itoh, N. (2015). The fibroblast growth factor signaling pathway. *WIREs Dev. Biol.* 4, 215–266. doi: 10.1002/wdev.176

Pereira, B., Chin, S.-F., Rueda, O. M., Vollan, H.-K. M., Provenzano, E., Bardwell, H. A., et al. (2016). The somatic mutation profiles of 2,433 breast cancers refines their genomic and transcriptomic landscapes. *Nat. Commun.* 7:11479. doi: 10.1038/ncomms11479

Reis-Filho, J. S., Simpson, P. T., Turner, N. C., Lambros, M. B., Jones, C., Mackay, A., et al. (2006). FGFR1 emerges as a potential therapeutic target for lobular breast carcinomas. *Clin. Cancer Res.* 12, 6652–6662. doi: 10.1158/1078-0432.CCR-06-1164

Ropiquet, F., Giri, D., Kwabi-Addo, B., Schmidt, K., and Ittmann, M. (2000). FGF-10 is expressed at low levels in the human prostate. *Prostate* 44, 334–338. doi: 10.1002/1097-0045(20000901)44:4<334::AID-PROS11>3.0.CO;2-G

Sekine, K., Ohuchi, H., Fujiwara, M., Yamasaki, M., Yoshizawa, T., Sato, T., et al. (1999). Fgf10 is essential for limb and lung formation. *Nat. Genet.* 21, 138–141. doi: 10.1038/5096

Shoji, K., Teishima, J., Hayashi, T., Ohara, S., Mckeehan, M. L., and Matsubara, A. (2014). Restoration of fibroblast growth factor receptor 2IIIb enhances the chemosensitivity of human prostate cancer cells. *Oncol. Rep.* 32, 65–70. doi: 10.3892/or.2014.3200

Stacey, S. N., Manolescu, A., Sulem, P., Thorlacius, S., Gudjonsson, S. A., Jonsson, G. F., et al. (2008). Common variants on chromosome 5p12 confer susceptibility to estrogen receptor–positive breast cancer. *Nat. Genet.* 40, 703–706. doi: 10.1038/ng.131

Su, X., Zhan, P., Gavine, P. R., Morgan, S., Womack, C., Ni, X., et al. (2014). FGFR2 amplification has prognostic significance in gastric cancer: results from a large international multicentre study. *Br. J. Cancer* 110, 967–975. doi: 10.1038/bjc.2013.802

Sun, Q., Lin, P., Zhang, J., Li, X., Yang, L., Huang, J., et al. (2015). Expression of fibroblast growth factor 10 is correlated with poor prognosis in gastric adenocarcinoma. *Tohoku J. Exp. Med.* 236, 311–318. doi: 10.1620/tjem.236.311

Suzuki, A., Itami, S., Ohishi, M., Hamada, K., Inoue, T., Komazawa, N., et al. (2003). Keratinocyte-specific Pten deficiency results in epidermal hyperplasia, accelerated hair follicle morphogenesis and tumor formation. *Cancer Res.* 63, 674–681.

Theodorou, V., Boer, M., Weigelt, B., Jonkers, J., van der Valk, M., and Hilkens, J. (2004). Fgf10 is an oncogene activated by MMTV insertional mutagenesis in mouse mammary tumors and overexpressed in a subset of human breast carcinomas. *Oncogene* 23, 6047–6055. doi: 10.1038/sj.onc.1207816

Thinon, E., Serwa, R. A., Broncel, M., Brannigan, J. A., Brassat, U., Wright, M. H., et al. (2014). Global profiling of co- and post-translationally N-myristoylated proteomes in human cells. *Nat. Commun.* 5:4919. doi: 10.1038/ncomms5919

Torres, C., Perales, S., Alejandre, M. J., Iglesias, J., Palomino, R. J., Martin, M., et al. (2014). Serum cytokine profile in patients with pancreatic cancer. *Pancreas* 43, 1042–1049. doi: 10.1097/MPA.0000000000000155

Traynor, A. M., Weigel, T. L., Oettel, K. R., Yang, D. T., Zhang, C., Kim, K., et al. (2013). Nuclear EGFR protein expression predicts poor survival in early stage non-small cell lung cancer. *Lung Cancer* 81, 138–141. doi: 10.1016/j.lungcan.2013.03.020

Veltmaat, J. M., Relaix, F., Le, L. T., Kratochwil, K., Sala, F. G., van Veelen, W., et al. (2006). Gli3-mediated somitic Fgf10 expression gradients are required for the induction and patterning of mammary epithelium along theembryonic axes. *Development* 133, 2325–2335. doi: 10.1242/dev.02394

Volckaert, T., Dill, E., Campbell, A., Tiozzo, C., Majka, S., Bellusci, S., et al. (2011). Parabronchial smooth muscle constitutes an airway epithelial stem cell niche in the mouse lung after injury. *J. Clin. Invest.* 121, 4409–4419. doi: 10.1172/JCI58097

Werner, S., Smola, H., Liao, X., Longaker, M. T., Krieg, T., Hofschneider, P. H., et al. (1994). The function of KGF in morphogenesis of epithelium and reepithelialization of wounds. *Science* 266, 819–822. doi: 10.1126/science.7973639

Yu, S., Xia, S., Yang, D., Wang, K., Yeh, S., Gao, Z., et al. (2013). Androgen receptor in human prostate cancer-associated fibroblasts promotes prostate cancer epithelial cell growth and invasion. *Med. Oncol.* 30:674. doi: 10.1007/s12032-013-0674-9

Zhang, X., Ibrahimi, O. A., Olsen, S. K., Umemori, H., Mohammadi, M., and Ornitz, D. M. (2006). Receptor specificity of the fibroblast growth factor family. The complete mammalian FGF family. *J. Biol. Chem.* 281, 15694–15700. doi: 10.1074/jbc.M601252200

Conflict of Interest Statement: The authors declare that the research was conducted in the absence of any commercial or financial relationships that could be construed as a potential conflict of interest.

Copyright © 2018 Clayton and Grose. This is an open-access article distributed under the terms of the Creative Commons Attribution License (CC BY). The use, distribution or reproduction in other forums is permitted, provided the original author(s) and the copyright owner(s) are credited and that the original publication in this journal is cited, in accordance with accepted academic practice. No use, distribution or reproduction is permitted which does not comply with these terms.

frontiers in Genetics

MINI REVIEW
published: 29 October 2018
doi: 10.3389/fgene.2018.00482

Fibroblast Growth Factor 10 in Pancreas Development and Pancreatic Cancer

Rodrick Ndlovu[1], Lian-Cheng Deng[2], Jin Wu[1], Xiao-Kun Li[1,2] and Jin-San Zhang[1,2,3]**

[1] College of Life and Environmental Sciences, Wenzhou University, Wenzhou, China, [2] School of Pharmaceutical Sciences, Wenzhou Medical University, Wenzhou, China, [3] Centre for Precision Medicine, the First Affiliated Hospital, Wenzhou Medical University, Wenzhou, China

The tenacious prevalence of human pancreatic diseases such as diabetes mellitus and adenocarcinoma has prompted huge research interest in better understanding of pancreatic organogenesis. The plethora of signaling pathways involved in pancreas development is activated in a highly coordinated manner to assure unmitigated development and morphogenesis in vertebrates. Therefore, a complex mesenchymal–epithelial signaling network has been implicated to play a pivotal role in organogenesis through its interactions with other germ layers, specifically the endoderm. The Fibroblast Growth Factor Receptor FGFR2-IIIb splicing isoform (FGFR2b) and its high affinity ligand Fibroblast Growth Factor 10 (FGF10) are expressed in the epithelium and mesenchyme, respectively, and therefore are well positioned to transmit mesenchymal to epithelial signaling. FGF10 is a typical paracrine FGF and chiefly mediates biological responses by activating FGFR2b with heparin/heparan sulfate (HS) as cofactor. A substantial number of studies using genetically engineered mouse models have demonstrated an essential role of FGF10 in the development of many organs and tissues including the pancreas. During mouse embryonic development, FGF10 signaling is crucial for epithelial cell proliferation, maintenance of progenitor cell fate and branching morphogenesis in the pancreas. FGF10 is also implicated in pancreatic cancer, and that overexpression of FGFR2b is associated with metastatic invasion. A thorough understanding of FGF10 signaling machinery and its crosstalk with other pathways in development and pathological states may provide novel opportunities for pancreatic cancer targeted therapy and regenerative medicine.

Keywords: FGF10, FGFR2b, SOX9, pancreas development, pancreatic adenocarcinoma, mesenchyme, epithelium

OPEN ACCESS

Edited by:
Saverio Bellusci,
Justus-Liebig-Universität Gießen, Germany

Reviewed by:
Richard Grose,
Queen Mary University of London, United Kingdom
Chun-Bo Teng,
Northeast Forestry University, China

****Correspondence:***
Xiao-Kun Li
profxiaokunli@163.com
Jin-San Zhang
Zhang_JinSan@163.com;
zhang.jinsan@mayo.edu

Specialty section:
This article was submitted to Stem Cell Research, a section of the journal Frontiers in Genetics

Received: *01 September 2018*
Accepted: *28 September 2018*
Published: *29 October 2018*

Citation:
Ndlovu R, Deng L-C, Wu J, Li X-K and Zhang J-S (2018) Fibroblast Growth Factor 10 in Pancreas Development and Pancreatic Cancer. Front. Genet. 9:482. doi: 10.3389/fgene.2018.00482

INTRODUCTION

The Fibroblast Growth Factor (FGF) family of peptides and the corresponding family of receptor tyrosine kinases (RTKs) collectively constitute one of the most adaptable, complex, and diverse growth factor signaling systems that are involved in many developmental and repair processes in virtually all vertebrate and invertebrate tissues and cells (Goetz and Mohammadi, 2013). Currently, the mammalian FGF nomenclature encompasses FGF1 to FGF23, comprising of secreted signaling proteins that transduce signals via their specific FGF receptors (FGFRs), and intracellular FGFs that

serve as cofactors for voltage-gated sodium channels. These ligands are divided and grouped into seven subfamilies based on phylogenetic analysis, sequence similarities, and function (Goetz et al., 2009; Ornitz and Itoh, 2015).

FGFR family of RTKs comprises of FGFR1, FGFR2, FGFR3, and FGFR4. As the name suggests, FGFRs bind to members of secreted FGFs along with the sequential formation of complexes with heparin/heparan sulfate (HS) cofactor-proteoglycans to propagate downstream signal transduction pathways, which include activation of PLCγ, MAPK, AKT, and STAT cascades. At the cellular level, paracrine FGF-FGFR-HS signaling engages in vital roles in regulating cell proliferation, migration, survival, and differentiation during the development of the embryo (Kato and Sekine, 1999; Ornitz and Itoh, 2015).

FGF10, a FGF7 subfamily member, is a typical paracrine FGF and chiefly mediates its biological responses by activating FGFR2b. FGF10 is a potent morphogen and plays a crucial role in transmitting mesenchyme signaling to the epithelium. Genetic ablation of FGF10 in mice results in gross developmental defects characterized by agenesis and dysgenesis in a variety of organs and tissues highlighting an essential role of FGF10 signaling for the development of multiple organs including the pancreas (Bellusci et al., 1997; Bhushan et al., 2001; Itoh and Ohta, 2014). Although not as widely explored as in the development field, there is strong evidence suggesting that FGF10 is also involved in the pancreatic carcinogenesis (Nomura et al., 2008). Herein, we summarize the recent information about the involvement of FGF10 in pancreas development and diseases with a focus on pancreatic cancer.

FGF10 SIGNALING MACHINERY

Alternative splicing of the extracellular IgIII loop of FGFR1-3 generates IIIb- and IIIc-variants of the receptors. Tissue- and cell-specific expression of these isoforms and modification in binding properties for the FGF ligands confer signaling specificity and functional diversity in regulating interactions in embryonic development, tissue homeostasis, repair, and cancer (Itoh and Ohta, 2014). FGFR2 generates two isoforms via alternative splicing, FGFR2b, predominantly expressed in epithelial cells and FGFR2c, chiefly expressed in mesenchymal cells. A distinct feature of the FGF7 subfamily is the preferential binding to their cognate receptor FGFR2b in a HS dependent manner in contrast to most other FGFs predominantly interacting with FGFR2c (Givol and Yayon, 1992; Orr-Urtreger et al., 1993; Lindahl et al., 1998; Holzmann et al., 2012).

Formation of the FGF10-FGFR2b-HS (2:2:2) ternary complex results in the phosphorylation of intracellular tyrosine residues in FGFRs (**Figure 1A**). Phosphorylated FGFRs activate FGFR substrate 2α(FRS2α) and phospholipase Cγ (PLCγ1), which mediate cell motility (Zhang et al., 2006; Itoh and Ohta, 2014). FRS2α, in turn, facilitates the activation of RAS-MAPK or PI3K-AKT and PLCγ activates protein kinase C. The RAS-MAPK and PI3K-AKT pathways are predominantly involved in mitogenic cell responses or cell survival and are subjected to negative regulation by SPRY1 and SPRY2 (Tefft et al., 2002; Zhang et al., 2006). These signaling cascades mediate a diverse range of biological outcomes that define FGF10/FGFR2b dependent signaling (**Figure1A**). The spatiotemporal expression and activity of FGFs and FGFR isoforms is additionally enhanced by the diversity of HS structures, which are also involved in developmental processes, insinuating that tissue-specific HS regulates FGF signaling (Lindahl et al., 1998; Makarenkova et al., 2009).

Interestingly, although FGF7 and FGF10 share a common receptor, expression in mesenchyme and the ability to promote proliferation of embryonic pancreatic epithelial cells *in vitro* (Ye et al., 2005), the phenotypes of their knockout mice are drastically different in that FGF7 null mice are born with no obvious abnormalities (Guo et al., 1996), whereas FGF10 knockout mice die at birth with major defects in multiple organs such as lung agenesis and pancreas dysgenesis (Min et al., 1998; Sekine et al., 1999; Ohuchi et al., 2000; Itoh and Ornitz, 2011). Based on a sophisticated quantitative proteomics approach, Francavilla et al. (2013) uncovered a fascinating ligand-dependent mechanism for the control of FGFR2b turnover and signaling outputs. FGF7 stimulation leads to FGFR2b degradation and, ultimately, cell proliferation, whereas FGF10 triggers additional phosphorylation on Y734 of FGFR2b leading to its recruitment of PI3K and SH3BP4 to promote receptor recycling and sustained signaling.

Zinkle and Mohammadi recently proposed a threshold model for RTK signaling specificity and cell fate determination (Makarenkova et al., 2009; Francavilla et al., 2013; Zinkle and Mohammadi, 2018). It is suggested that the intensity and duration of signaling via FGFR2b is dependent on the phosphorylation of Y734 within the kinase domain. Higher affinity of FGF10 for binding both FGFR2b and the co-receptor HS (Makarenkova et al., 2009) generates a more robust interaction than FGF7-FGFR2b dimers, therefore propagates more sustained MAPK signal that leads to cell proliferation and migration whilst FGF7 propagates a transient MAPK signal that leads to cell proliferation. It is conceivable that the difference in ligand-induced dimer stability distinguishes FGF7 from FGF10 on the choice and durability of intracellular pathways, which may well contribute to their functional discrepancies on branching morphogenesis during embryonic development.

FGF10 IN PANCREAS DEVELOPMENT

The pancreas is an endoderm-derived glandular organ that partakes in the regulation of glucose homeostasis and nutrient uptake through the concerted functions of its endocrine and exocrine compartments, respectively (Edlund, 1999; Shih et al., 2013). Early mouse pancreas development has two characteristic periods: a primary transition (E9.5–12.5) that is characterized by rapid cell proliferation and histogenesis and a secondary transition (E12,5-birth) after rotation of the gut at E12.5 that is chiefly characterized by cytodifferentiation and formation of the significant intracellular organelles of the adult pancreatic cell (Pictet et al., 1972; Jorgensen et al., 2007; Benitez et al., 2012).

The mesenchyme is critical for the growth of all pancreatic lineages (Landsman et al., 2011). Reports indicate that FGF

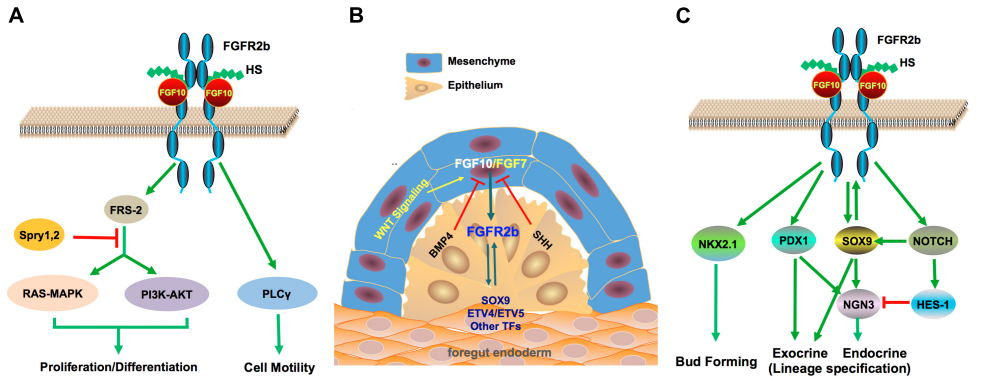

FIGURE 1 | FGF10 signaling and its key crosstalk during pancreas development. **(A)** FGF10 is a high affinity ligand for FGFR2b. FGF10 interacts with FGFR2b with HS as cofactor and induces activation of the RAS-MAPK, PI3K-AKT, and PLCγ pathways, which mediate cell differentiation, proliferation, and motility. SPRYs are negative regulators of the RAS-MAPK and PI3K-AKT pathways. **(B)** FGF10 mediates mesenchyme to epithelial signaling through crosstalk with several key developmental pathways including WNT factors, BMP and SHH, which are important in pancreatic cell fate specification and branching morphogenesis. BMP signaling is required for the normal development of the mesenchyme as well as the epithelium. **(C)** FGF10 has a crucial role in epithelial branching morphogenesis through crosstalk with several key TFs and regulators for pancreas development. The FGF10/FGFR2b/SOX9 regulatory loop promotes proliferation and maintains pancreatic fate in pancreatic progenitors.

signaling derived from the surrounding mesenchymal tissue is pivotal for the genesis of specific cellular domains (Hart et al., 2003; Zhou et al., 2007). FGF10, as a mesenchymal factor, has an indispensable role in ensuring the development of the pancreatic epithelium, which gives rise to the functional endocrine and exocrine cell types (Bhushan et al., 2001; Elghazi et al., 2002; Hart et al., 2003; Norgaard et al., 2003). To ascertain the role of FGF10 in pancreas development, Bhushan et al. (2001) demonstrated that FGF10 expressed from E9.5 until E11.5 in mice is vital for pancreas growth and differentiation of Pdx1 $^{+}$ epithelial precursor cells. The absence of this mesenchymal protein led to pancreatic hypoplasia (Bhushan et al., 2001). Furthermore, the pancreata of *Fgfr2b*$^{-/-}$ mutant mice were smaller than the wild type littermates with pancreatic duct cell proliferation notably reduced (Miralles et al., 1999; Pulkkinen et al., 2003). FGF10 signaling predominantly targets the adjacent tissue due to its paracrine nature, hence in *Fgf10* null mutant mice, the pancreatic progenitor cells are diminished even before the onset of secondary transition. The few exocrine cells present do undergo differentiation and form acinar structures (Bhushan et al., 2001). Mice deficient in FGFR2b exhibit mild phenotypes comparable to the FGF10 null mice with differentiation of both pancreas compartments and consequent reduction of organ size (Miralles et al., 1999; Pulkkinen et al., 2003).

While many literature sources substantiate the role of FGF10 in epithelial development, the expression levels of the protein decrease to almost unperceivable levels at E13.5 in mice (Bhushan et al., 2001; Elghazi et al., 2002; Kobberup et al., 2010). Explant studies in mice involving pharmacological inhibition of FGF signaling proved that FGF10 is dispensable at later stages of gestation, implying that different epithelial cell types not only depend on FGF10 signals but also on other (same or distinct) mesenchymal factors (Greggio et al., 2013). Possibly, FGF10′s primary role is vital for the initial stage of progenitor growth, then might work in concert with other mesenchymal derived factors or signaling pathways.

FGF10 CROSSTALK WITH OTHER SIGNALING PATHWAYS

The mesenchyme is a source of cell-extrinsic signals that promotes pancreatic specification, yet limits differentiation, so as to allow expansion of the pancreatic epithelium. Besides FGFs, other mesenchymal signals that promote growth of the pancreatic epithelium include WNT factors (Jonckheere et al., 2008), Retinoic Acid (RA) (Stafford et al., 2006), BMP (Ahnfelt-Ronne et al., 2010), and the TGF-β pathway (Crisera et al., 2000; **Figure 1B**).

FGFs and WNT factors are known to act in synergy to promote proliferation in a variety of developmental systems (ten Berge et al., 2008; Afelik et al., 2015). Canonical WNT signaling is a mediator of epithelial to mesenchymal signaling, several WNT ligands plus frizzled (FRZ) receptors (e.g., WNT2b, WNT7b, and FRZ2-9) are expressed by both the mesenchyme and pancreatic epithelial cells during organogenesis (Heller et al., 2002; Afelik et al., 2015). Comparable phenotypes are observed between *Pdx1/Frz8CRD* (dominant-negative frizzled 8 receptor) and *Pdx1/Fgf10* null neonates revealing pancreatic hypoplasia, as early as E14, further implying a role for both signaling pathways in pancreatic growth (Papadopoulou and Edlund, 2005; Jonckheere et al., 2008).

RA signaling is also an indispensable mediator of mesenchymal function. In the lung, mesenchyme RA signaling has been implicated in the induction of FGF10 (Desai et al., 2004). Furthermore, absence of RA signaling leads to pancreatic hypoplasia (severe in the dorsal pancreas) (Martin et al., 2005). In an effort to produce functional β cells from endoderm derived human embryonic stem (hES) cells, Mfopou et al. (2010) exposed

these hES cells to noggin and RA, followed by FGF10 during early stage of induction, and successfully generated pancreatic cells, the majority of them are *Pdx1* $^+$ that coexpressed FOXA2, HNF6, and SOX9.

Unmitigated differentiation of the mesenchyme, which further ensures proper epithelial development, is reliant on many signaling molecules except members of the Hedgehog family from the early pancreatic niche (Kawahira et al., 2005). Ectopic expression of Sonic Hedgehog (SHH) in mice driven by the *Pdx1* promoter results in differentiation of the pancreatic mesenchyme into smooth muscle and the epithelium assumes an intestinal fate with the generation of few early endocrine cell types (Apelqvist et al., 1997). SHH is also implicated in repressing expression of *Fgf10* (**Figure 1B**; Bhushan et al., 2001).

TRANSCRIPTION FACTORS IMPLICATED IN FGF10 SIGNALING

Genetic lineage tracing experiments have elucidated that cell clusters committed to adopting the pancreatic lineage express the transcription factor (TF) PDX1 (Pancreatic and duodenal homeobox 1) and PTF1a (Pancreas transcription factor 1). Ablation of either *Pdx1* or *Ptf1a* causes pancreatic agenesis or diabetes and wide gastro-duodenal deformations (Offield et al., 1996; Stoffers et al., 1997; Kawaguchi et al., 2002; Burlison et al., 2008; Fukuda et al., 2008).

After the establishment of the pancreatic anlage, a gene regulatory network is established with *Pdx1* at the focal apex in order to maintain pancreatic identity (Shih et al., 2015). PDX1 exhibits an extensive cross-regulation network between individual TFs and FGFs such as FGF10; however, sustentation of the pancreatic lineage requires high levels of PDX1 (Shih et al., 2015). Augmentation of PDX1 expression levels is supplemented by PTF1a, which binds to enhancer elements of PDX1 (Wiebe et al., 2007), whilst FGF10 is required to maintain the PDX1 $^+$ expressing progenitor cell pool (**Figure 1C**; Bhushan et al., 2001).

Genetic lineage tracing has shown that multipotent progenitor cells (MPCs) can be similarly defined by several TFs such as SOX9, HNF6, NKX2.2, HNF1β, HES1, CAP1, and NKX6.1. At this juncture, MPCs not only have the potential to self-renew, but also can differentiate to form exocrine and endocrine progenitors with PDX1 functioning as the central node (Zhou et al., 2007; Pan and Wright, 2011; Seymour, 2014).

The SOX9 interacts with the FGF signaling pathway in concert with PDX1 to maintain both expansion (in a dosage-dependent manner) and organ identity of MPCs (Shih et al., 2013). SOX9 and PDX1 co-regulate the pancreatic versus intestinal lineage choice, ablation of both genes causes MPCs to embrace an alternative hepatic fate (Seymour et al., 2012; Shih et al., 2015). In mice, SOX9, FGFR2b, and FGF10 form a feed-forward expression loop; SOX9 cell-autonomously maintains FGFR2b expression, which in turn, augments its epithelial receptivity to FGF10, whilst FGF10 maintains SOX9 expression (**Figure 1C**). Hence nullification of any component in this loop leads to pancreatic hypoplasia and loss of both SOX9 plus FGFR2b in FGF10-deficient MPCs leads to hepatic reprogramming (Seymour et al., 2012).

FGF10 MEDIATES PANCREATIC CELL FATE

Spatial and temporal regulation of gene function is vital in the modeling of specialized cell types from a field of competent cells. FGF10 is known to maintain progenitor cells in an undifferentiated state to allow subsequent proliferation, ectopic expression results in a hyperplastic pancreas. Nascent emergent patterns of budding cells are additionally controlled by conserved developmental pathways such as the NOTCH signaling via lateral inhibition/specification in order to integrate terminal differentiation in FGF10 signaling. FGF10-positive progenitor cells express NOTCH1 and NOTCH2, the NOTCH-ligand genes JAG1 and JAG2, as well as the NOTCH target gene HES1 (Murtaugh et al., 2003; Norgaard et al., 2003; Miralles et al., 2006).

During the primary transition, NOTCH and FGF10 signaling are predominantly involved in restricting premature endocrine differentiation and maintenance of the progenitor state. Ablation of Notch target genes such as *Dll1* (Hrabe de Angelis et al., 1997), *Rbp-jk* (Fujikura et al., 2006), or *Hes1* (Jensen et al., 2000) results in an increase of NGN3 $^+$ cells, leading to premature differentiation of the MPCs into glucagon $^+$-cells (Apelqvist et al., 1999) and p57-expressing progenitor cells, which undergo premature cell cycle exit evident with the expression of a hypoplastic pancreas (Georgia et al., 2006). This phenotype is comparable to *Fgf10* and *Sox9* null mutant mice. HES1 is known to repress both the transcriptional activation of *Ngn3* and the cyclin kinase inhibitor *P57* (**Figure 1C**; Georgia et al., 2006).

SOX9 is a positive regulator of NGN3 in a dosage-dependent manner, and is expressed chiefly in trunk progenitor cells and its depletion results in the reduction of NGN3 $^+$ cells. This suggests that there may exist a complicated but well-organized regulatory system involving FGF10, FGFR2b, NOTCH, HES1, SOX9, and NGN3 that controls endocrine differentiation and maintenance of progenitor cells (Miralles et al., 2006; Kobberup et al., 2010; Gouzi et al., 2011; Afelik and Jensen, 2013; Shih et al., 2015). It can be postulated that both FGF10 and NOTCH signaling pathways are critical for the establishment of two cell lineages:

(i) NGN3 $^+$ cells that form the early α-cells.
(ii) NGN3 $^+$ that will remain proliferative and available to differentiate to other endocrine cell types (Apelqvist et al., 1999; Jensen et al., 2000; Miralles et al., 2006; Kobberup et al., 2010; Afelik and Jensen, 2013).

Ectopic expression of *Fgf10* from E10.5 to E13.5 leads to nearly complete loss of endocrine and ductal differentiation (Kobberup et al., 2010). This, in turn, favors the exocrine lineage because of the lack of competence to form the endocrine cell lineage. Furthermore, exocrine (acinar) differentiation has been observed to occur in FGF10 null mutant mice implying that FGF10

does not entirely control exocrine differentiation but rather it is permissive toward exocrine lineage fate (Miralles et al., 1999; Bhushan et al., 2001; Kobberup et al., 2010). This is observed with sustained expression of PTF1A in both *Fgf10*$^{-/-}$ mutant and wild type mice though reports have indicated that downstream effectors of FGF10, such as *Etv4* and *Etv5,* influence expression of PTF1A (**Figure 1C**; Dong et al., 2007; Kobberup et al., 2007, 2010).

Cellular proliferation and differentiation are mutually exclusive events; hence overexpression of FGF10 beyond the primary transition perturbs differentiation of endocrine and ductal cell types. At this stage, progenitor cells typically co-express PDX1, NKX6.1, and PTF1A, failure of endocrine cell formation leads to diabetes in mice (Hart et al., 2003; Petri et al., 2006; Kobberup et al., 2010). FGF10 signaling via FGFR2b is at the expense of endocrine cellular differentiation (Celli et al., 1998; Miralles et al., 1999; Pulkkinen et al., 2003). By understanding the exact timing of the competence window toward endocrine fate, FGF10 could be best exploited in cell-based therapeutic strategies to combat diabetes (Madsen and Serup, 2006).

FGF10 -FGFR2B IN PANCREATIC DUCTAL ADENOCARCINOMA

Pancreatic ductal adenocarcinoma (PDAC) is the most common exocrine malignancy and represents one of the deadliest diseases with high mortality due to difficulties in its early diagnosis, metastasis and intrinsic resistance to conventional chemoradiotherapy. At a molecular level, cancer cells in PDAC are often characterized by mutations in the KRAS oncogene, SMAD4, and TP53. Several FGFs and FGFRs are expressed in stromal cells scattered around pancreatic cancer cells and their expression levels have been linked to increased cancer motility, proliferation and metastatic invasion (Kalluri and Zeisberg, 2006; Ying et al., 2016). FGF7 and 10 are both expressed in stromal cells surrounding cancer cells. Regardless of the high homology the latter induces cell migration and invasion whilst the former stimulates cell proliferation. FGF10-FGFR2b signaling induces the expression of type1-matrix metalloproteinase and *TGF-β1* genes (Nomura et al., 2008), these genes are related to cell motility (Friess et al., 1993; Seiki, 2003). Moreover, FGF10-FGFR2b signaling induced the secretion of TGF-β1, a crucial regulator of epithelial to mesenchymal transition (**Figure 2**; Moustakas and Heldin, 2007; Nomura et al., 2008).

A hallmark genetic alteration of PDAC is the high frequency mutation of KRAS. Numerous studies demonstrate that oncogenic KRAS mutations induce Acinar-to-ductal metaplasia (ADM), pancreatic intraepithelial neoplasia (PanIN), and eventually PDAC. Significantly, SOX9 is imperative for KRAS^{G12D}-mediated ADM and PanIN formation (Kopp et al., 2012). A more recent study demonstrated that KRAS can independently induce SOX9 expression and promoted its nuclear translocation and transcriptional activity, which plays a positive role in the proliferation of PDAC cells (Zhou et al., 2018).

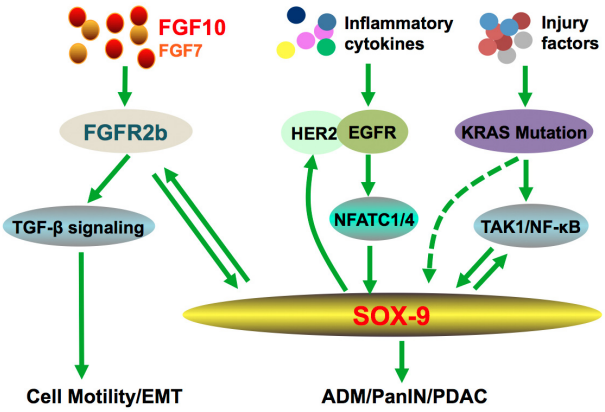

FIGURE 2 | Crosstalk of FGF10 during pancreatic cancer. Interactions of FGF10 with TGF-β pathway promote EMT and cancer cell invasion. The positive feedback loops between FGF10-SOX9, KRAS/NF-κB-SOX9, and ERBB-SOX9, respectively, are enhanced under inflammatory condition, which contributes to PDAC initiation and progression.

Our recent studies further showed that SOX9 could be induced by NFATC1 and NFATC4 in response to EGFR activation and pancreatitis, which promote ADM and PanIN (Chen et al., 2015; Hessmann et al., 2016). In a separate study, SOX9 is reported to stimulate expression of several members of the ERBB pathway, and is required for ERBB signaling activity to promote pancreatic tumorigenesis (Grimont et al., 2015). These studies further consolidate SOX9 as a central player in pancreatic adenocarcinoma via promoting ADM, particularly in the context of oncogenic KRAS and pancreatitis to accelerate development of premalignant lesions and PDAC (**Figure 2**). Therefore, three positive feedback loops have emerged from these studies (**Figure 2**): (1) FGF10/FGFR2/SOX9 inter-dependent expression is also present in a subset of PDAC patients (Seymour et al., 2012; O'Sullivan et al., 2017); (2) EGFR, via activation of NFATC1 and NFATC4, promotes SOX9 expression, whereas activated SOX9 stimulates ERBB2 protein expression (Chen et al., 2015; Grimont et al., 2015; Hessmann et al., 2016); (3) Oncogenic KRAS via TAK1/NF-κβ promotes SOX9 expression/activation, and SOX9 in turn enhances NF-κβ activity (Zhou et al., 2018). These findings open new perspectives for precision therapeutic strategies targeting specific cancer-driven signaling molecules such as ERBB2 or FGFR2.

CONCLUSION AND PERSPECTIVE

Animal models lacking each of the secreted FGFs have been developed with diverse phenotypes ranging from mild abnormality in adult physiology to early embryonic lethality. Only three FGFs (FGF9, FGF10, and FGF18) upon knockout result in early postnatal lethality due to severe developmental defects in multiple organs. While *Fgf9* and *Fgf18* are essential for the development of mesenchymal components, numerous studies highlight FGF10 as an indispensable mesenchyme to epithelium signal required for the development of epithelial components

in multiple organs. Despite the interesting observations from previous reports, research on FGF10/FGFR2b in the pancreas is lagging behind compared to some other organs such as the lung. There remain some critical questions unanswered regarding how FGF/FGFR2b signaling influence acinar and ductal specification (e.g., further proliferation and differentiation from the progenitor cells), as well as its impact on the endocrine system remain largely unexplored. More elegant and specifically targeted genetic models allowing better spatiotemporal manipulation of gene expression will be essential to better address these questions. During both embryonic development and oncogenic process, FGF10 acquires the ability for unique crosstalk with other pathways as exemplified by its inter-dependent expression with SOX9, which may represent a key knot linking oncogenic KRAS, inflammation and other growth factor signaling. Understanding of FGF10 signaling machinery and its crosstalk with other pathways may provide novel opportunities for PDAC precision therapy and regenerative medicine.

AUTHOR CONTRIBUTIONS

RN, L-CD, JW, X-KL, and J-SZ conceived the study. RN and J-SZ wrote the manuscript. RN, L-CD, JW and J-SZ designed and drew the figures. J-SZ designed and edited the manuscript. J-SZ and X-KL supervised the study and acquired funding.

FUNDING

This work is partially supported by the National Natural Science Foundation of China (Grant Nos. 81472601 and 81500519).

ACKNOWLEDGMENTS

We apologize to colleagues whose work we could not include due to space considerations.

REFERENCES

Afelik, S., and Jensen, J. (2013). Notch signaling in the pancreas: patterning and cell fate specification. *Wiley Interdiscip. Rev. Dev. Biol.* 2, 531–544. doi: 10.1002/wdev.99

Afelik, S., Pool, B., Schmerr, M., Penton, C., and Jensen, J. (2015). Wnt7b is required for epithelial progenitor growth and operates during epithelial-to-mesenchymal signaling in pancreatic development. *Dev. Biol.* 399, 204–217. doi: 10.1016/j.ydbio.2014.12.031

Ahnfelt-Ronne, J., Ravassard, P., Pardanaud-Glavieux, C., Scharfmann, R., and Serup, P. (2010). Mesenchymal bone morphogenetic protein signaling is required for normal pancreas development. *Diabetes* 59, 1948–1956. doi: 10.2337/db09-1010

Apelqvist, A., Ahlgren, U., and Edlund, H. (1997). Sonic hedgehog directs specialised mesoderm differentiation in the intestine and pancreas. *Curr. Biol.* 7, 801–804. doi: 10.1016/S0960-9822(06)00340-X

Apelqvist, A., Li, H., Sommer, L., Beatus, P., Anderson, D. J., Honjo, T., et al. (1999). Notch signalling controls pancreatic cell differentiation. *Nature* 400, 877–881. doi: 10.1038/23716

Bellusci, S., Grindley, J., Emoto, H., Itoh, N., and Hogan, B. L. (1997). Fibroblast growth factor 10 (FGF10) and branching morphogenesis in the embryonic mouse lung. *Development* 124, 4867–4878.

Benitez, C. M., Goodyer, W. R., and Kim, S. K. (2012). Deconstructing pancreas developmental biology. *Cold Spring Harb. Perspect. Biol.* 4:a012401. doi: 10.1101/cshperspect.a012401

Bhushan, A., Itoh, N., Kato, S., Thiery, J. P., Czernichow, P., Bellusci, S., et al. (2001). Fgf10 is essential for maintaining the proliferative capacity of epithelial progenitor cells during early pancreatic organogenesis. *Development* 128, 5109–5117.

Burlison, J. S., Long, Q., Fujitani, Y., Wright, C. V., and Magnuson, M. A. (2008). Pdx-1 and Ptf1a concurrently determine fate specification of pancreatic multipotent progenitor cells. *Dev. Biol.* 316, 74–86. doi: 10.1016/j.ydbio.2008.01.011

Celli, G., LaRochelle, W. J., Mackem, S., Sharp, R., and Merlino, G. (1998). Soluble dominant-negative receptor uncovers essential roles for fibroblast growth factors in multi-organ induction and patterning. *EMBO J.* 17, 1642–1655. doi: 10.1093/emboj/17.6.1642

Chen, N. M., Singh, G., Koenig, A., Liou, G. Y., Storz, P., Zhang, J. S., et al. (2015). NFATc1 Links EGFR Signaling to Induction of Sox9 Transcription and Acinar-Ductal Transdifferentiation in the Pancreas. *Gastroenterology* 148, 1024.e9–1034.e9. doi: 10.1053/j.gastro.2015.01.033

Crisera, C. A., Maldonado, T. S., Kadison, A. S., Li, M., Alkasab, S. L., Longaker, M. T., et al. (2000). Transforming growth factor-beta 1 in the developing mouse pancreas: a potential regulator of exocrine differentiation. *Differentiation* 65, 255–259. doi: 10.1046/j.1432-0436.2000.6550255.x

Desai, T. J., Malpel, S., Flentke, G. R., Smith, S. M., and Cardoso, W. V. (2004). Retinoic acid selectively regulates Fgf10 expression and maintains cell identity in the prospective lung field of the developing foregut. *Dev. Biol.* 273, 402–415. doi: 10.1016/j.ydbio.2004.04.039

Dong, P. D., Munson, C. A., Norton, W., Crosnier, C., Pan, X., Gong, Z., et al. (2007). Fgf10 regulates hepatopancreatic ductal system patterning and differentiation. *Nat. Genet.* 39, 397–402. doi: 10.1038/ng1961

Edlund, H. (1999). Pancreas: how to get there from the gut? *Curr. Opin. Cell Biol.* 11, 663–668. doi: 10.1016/S0955-0674(99)00033-2

Elghazi, L., Cras-Meneur, C., Czernichow, P., and Scharfmann, R. (2002). Role for FGFR2IIIb-mediated signals in controlling pancreatic endocrine progenitor cell proliferation. *Proc. Natl. Acad. Sci. U.S.A.* 99, 3884–3889. doi: 10.1073/pnas.062321799

Francavilla, C., Rigbolt, K. T., Emdal, K. B., Carraro, G., Vernet, E., Bekker-Jensen, D. B., et al. (2013). Functional proteomics defines the molecular switch underlying FGF receptor trafficking and cellular outputs. *Mol. Cell.* 51, 707–722. doi: 10.1016/j.molcel.2013.08.002

Friess, H., Yamanaka, Y., Buchler, M., Berger, H. G., Kobrin, M. S., Baldwin, R. L., et al. (1993). Enhanced expression of the type II transforming growth factor beta receptor in human pancreatic cancer cells without alteration of type III receptor expression. *Cancer Res.* 53, 2704–2707.

Fujikura, J., Hosoda, K., Iwakura, H., Tomita, T., Noguchi, M., Masuzaki, H., et al. (2006). Notch/Rbp-j signaling prevents premature endocrine and ductal cell differentiation in the pancreas. *Cell Metab.* 3, 59–65. doi: 10.1016/j.cmet.2005.12.005

Fukuda, A., Kawaguchi, Y., Furuyama, K., Kodama, S., Horiguchi, M., Kuhara, T., et al. (2008). Reduction of Ptf1a gene dosage causes pancreatic hypoplasia and diabetes in mice. *Diabetes Metab. Res. Rev.* 57, 2421–2431. doi: 10.2337/db07-1558

Georgia, S., Soliz, R., Li, M., Zhang, P., and Bhushan, A. (2006). p57 and Hes1 coordinate cell cycle exit with self-renewal of pancreatic progenitors. *Dev. Biol.* 298, 22–31. doi: 10.1016/j.ydbio.2006.05.036

Givol, D., and Yayon, A. (1992). Complexity of FGF receptors: genetic basis for structural diversity and functional specificity. *FASEB J.* 6, 3362–3369. doi: 10.1096/fasebj.6.15.1464370

Goetz, R., Dover, K., Laezza, F., Shtraizent, N., Huang, X., Tchetchik, D., et al. (2009). Crystal structure of a fibroblast growth factor homologous factor (FHF) defines a conserved surface on FHFs for binding and modulation of voltage-gated sodium channels. *J. Biol. Chem.* 284, 17883–17896. doi: 10.1074/jbc.M109.001842

Goetz, R., and Mohammadi, M. (2013). Exploring mechanisms of FGF signalling through the lens of structural biology. *Nat. Rev. Mol. Cell Biol.* 14, 166–180. doi: 10.1038/nrm3528

Gouzi, M., Kim, Y. H., Katsumoto, K., Johansson, K., and Grapin-Botton, A. (2011). Neurogenin3 initiates stepwise delamination of differentiating endocrine cells during pancreas development. *Dev. Dyn.* 240, 589–604. doi: 10.1002/dvdy.22544

Greggio, C., De Franceschi, F., Figueiredo-Larsen, M., Gobaa, S., Ranga, A., Semb, H., et al. (2013). Artificial three-dimensional niches deconstruct pancreas development in vitro. *Development* 140, 4452–4462. doi: 10.1242/dev.096628

Grimont, A., Pinho, A. V., Cowley, M. J., Augereau, C., Mawson, A., Giry-Laterriere, M., et al. (2015). SOX9 regulates ERBB signalling in pancreatic cancer development. *Gut* 64, 1790–1799. doi: 10.1136/gutjnl-2014-307075

Guo, L., Degenstein, L., and Fuchs, E. (1996). Keratinocyte growth factor is required for hair development but not for wound healing. *Genes Dev.* 10, 165–175. doi: 10.1101/gad.10.2.165

Hart, A., Papadopoulou, S., and Edlund, H. (2003). Fgf10 maintains notch activation, stimulates proliferation, and blocks differentiation of pancreatic epithelial cells. *Dev. Dyn.* 228, 185–193. doi: 10.1002/dvdy.10368

Heller, R. S., Dichmann, D. S., Jensen, J., Miller, C., Wong, G., Madsen, O. D., et al. (2002). Expression patterns of Wnts, Frizzleds, sFRPs, and misexpression in transgenic mice suggesting a role for Wnts in pancreas and foregut pattern formation. *Dev. Dyn.* 225, 260–270. doi: 10.1002/dvdy.10157

Hessmann, E., Zhang, J. S., Chen, N. M., Hasselluhn, M., Liou, G. Y., Storz, P., et al. (2016). NFATc4 regulates Sox9 gene expression in acinar cell plasticity and pancreatic cancer initiation. *Stem Cells Int.* 2016:5272498. doi: 10.1155/2016/5272498

Holzmann, K., Grunt, T., Heinzle, C., Sampl, S., Steinhoff, H., Reichmann, N., et al. (2012). Alternative splicing of fibroblast growth factor receptor IgIII loops in cancer. *J. Nucleic Acids* 2012:950508. doi: 10.1155/2012/950508

Hrabe de Angelis, M., McIntyre, J. II, and Gossler, A. (1997). Maintenance of somite borders in mice requires the Delta homologue DII1. *Nature* 386, 717–721. doi: 10.1038/386717a0

Itoh, N., and Ohta, H. (2014). Fgf10: a paracrine-signaling molecule in development, disease, and regenerative medicine. *Curr. Mol. Med.* 14, 504–509. doi: 10.2174/1566524014666140414204829

Itoh, N., and Ornitz, D. M. (2011). Fibroblast growth factors: from molecular evolution to roles in development, metabolism and disease. *J. Biochem.* 149, 121–130. doi: 10.1093/jb/mvq121

Jensen, J., Pedersen, E. E., Galante, P., Hald, J., Heller, R. S., Ishibashi, M., et al. (2000). Control of endodermal endocrine development by Hes-1. *Nat. Genet.* 24, 36–44. doi: 10.1038/71657

Jonckheere, N., Mayes, E., Shih, H. P., Li, B., Lioubinski, O., Dai, X., et al. (2008). Analysis of mPygo2 mutant mice suggests a requirement for mesenchymal Wnt signaling in pancreatic growth and differentiation. *Dev. Biol.* 318, 224–235. doi: 10.1016/j.ydbio.2008.03.014

Jorgensen, M. C., Ahnfelt-Ronne, J., Hald, J., Madsen, O. D., Serup, P., and Hecksher-Sorensen, J. (2007). An illustrated review of early pancreas development in the mouse. *Endocr. Rev.* 28, 685–705. doi: 10.1210/er.2007-0016

Kalluri, R., and Zeisberg, M. (2006). Fibroblasts in cancer. *Nat. Rev. Cancer* 6, 392–401. doi: 10.1038/nrc1877

Kato, S., and Sekine, K. (1999). FGF-FGFR signaling in vertebrate organogenesis. *Cell Mol. Biol.* 45, 631–638.

Kawaguchi, Y., Cooper, B., Gannon, M., Ray, M., MacDonald, R. J., and Wright, C. V. (2002). The role of the transcriptional regulator Ptf1a in converting intestinal to pancreatic progenitors. *Nat. Genet.* 32, 128–134. doi: 10.1038/ng959

Kawahira, H., Scheel, D. W., Smith, S. B., German, M. S., and Hebrok, M. (2005). Hedgehog signaling regulates expansion of pancreatic epithelial cells. *Dev. Biol.* 280, 111–121. doi: 10.1016/j.ydbio.2005.01.008

Kobberup, S., Nyeng, P., Juhl, K., Hutton, J., and Jensen, J. (2007). ETS-family genes in pancreatic development. *Dev. Dyn.* 236, 3100–3110. doi: 10.1002/dvdy.21292

Kobberup, S., Schmerr, M., Dang, M. L., Nyeng, P., Jensen, J. N., MacDonald, R. J., et al. (2010). Conditional control of the differentiation competence of pancreatic endocrine and ductal cells by Fgf10. *Mech. Dev.* 127, 220–234. doi: 10.1016/j.mod.2009.11.005

Kopp, J. L., von Figura, G., Mayes, E., Liu, F. F., Dubois, C. L., Morris, J. P., et al. (2012). Identification of Sox9-dependent acinar-to-ductal reprogramming as the principal mechanism for initiation of pancreatic ductal adenocarcinoma. *Cancer Cell* 22, 737–750. doi: 10.1016/j.ccr.2012.10.025

Landsman, L., Nijagal, A., Whitchurch, T. J., Vanderlaan, R. L., Zimmer, W. E., Mackenzie, T. C., et al. (2011). Pancreatic mesenchyme regulates epithelial organogenesis throughout development. *PLoS Biol.* 9:e1001143. doi: 10.1371/journal.pbio.1001143

Lindahl, U., Kusche-Gullberg, M., and Kjellen, L. (1998). Regulated diversity of heparan sulfate. *J. Biol. Chem.* 273, 24979–24982. doi: 10.1074/jbc.273.39.24979

Madsen, O. D., and Serup, P. (2006). Towards cell therapy for diabetes. *Nat. Biotechnol.* 24, 1481–1483. doi: 10.1038/nbt1206-1481

Makarenkova, H. P., Hoffman, M. P., Beenken, A., Eliseenkova, A. V., Meech, R., Tsau, C., et al. (2009). Differential interactions of FGFs with heparan sulfate control gradient formation and branching morphogenesis. *Sci. Signal.* 2:ra55. doi: 10.1126/scisignal.2000304

Martin, M., Gallego-Llamas, J., Ribes, V., Kedinger, M., Niederreither, K., Chambon, P., et al. (2005). Dorsal pancreas agenesis in retinoic acid-deficient Raldh2 mutant mice. *Dev. Biol.* 284, 399–411. doi: 10.1016/j.ydbio.2005.05.035

Mfopou, J. K., Chen, B., Mateizel, I., Sermon, K., and Bouwens, L. (2010). Noggin, retinoids, and fibroblast growth factor regulate hepatic or pancreatic fate of human embryonic stem cells. *Gastroenterology* 138, 2233.e14–2245.e14. doi: 10.1053/j.gastro.2010.02.056

Min, H., Danilenko, D. M., Scully, S. A., Bolon, B., Ring, B. D., Tarpley, J. E., et al. (1998). Fgf-10 is required for both limb and lung development and exhibits striking functional similarity to Drosophila branchless. *Genes Dev.* 12, 3156–3161. doi: 10.1101/gad.12.20.3156

Miralles, F., Czernichow, P., Ozaki, K., Itoh, N., and Scharfmann, R. (1999). Signaling through fibroblast growth factor receptor 2b plays a key role in the development of the exocrine pancreas. *Proc. Natl. Acad. Sci. U.S.A.* 96, 6267–6272. doi: 10.1073/pnas.96.11.6267

Miralles, F., Lamotte, L., Couton, D., and Joshi, R. L. (2006). Interplay between FGF10 and Notch signalling is required for the self-renewal of pancreatic progenitors. *Int. J. Dev. Biol.* 50, 17–26. doi: 10.1387/ijdb.052080fm

Moustakas, A., and Heldin, C. H. (2007). Signaling networks guiding epithelial-mesenchymal transitions during embryogenesis and cancer progression. *Cancer Sci.* 98, 1512–1520. doi: 10.1111/j.1349-7006.2007.00550.x

Murtaugh, L. C., Stanger, B. Z., Kwan, K. M., and Melton, D. A. (2003). Notch signaling controls multiple steps of pancreatic differentiation. *Proc. Natl. Acad. Sci. U.S.A.* 100, 14920–14925. doi: 10.1073/pnas.2436557100

Nomura, S., Yoshitomi, H., Takano, S., Shida, T., Kobayashi, S., Ohtsuka, M., et al. (2008). FGF10/FGFR2 signal induces cell migration and invasion in pancreatic cancer. *Br. J. Cancer* 99, 305–313. doi: 10.1038/sj.bjc.6604473

Norgaard, G. A., Jensen, J. N., and Jensen, J. (2003). FGF10 signaling maintains the pancreatic progenitor cell state revealing a novel role of Notch in organ development. *Dev. Biol.* 264, 323–338. doi: 10.1016/j.ydbio.2003.08.013

Offield, M. F., Jetton, T. L., Labosky, P. A., Ray, M., Stein, R. W., Magnuson, M. A., et al. (1996). PDX-1 is required for pancreatic outgrowth and differentiation of the rostral duodenum. *Development* 122, 983–995.

Ohuchi, H., Hori, Y., Yamasaki, M., Harada, H., Sekine, K., Kato, S., et al. (2000). FGF10 acts as a major ligand for FGF receptor 2 IIIb in mouse multi-organ development. *Biochem. Biophys. Res. Commun.* 277, 643–649. doi: 10.1006/bbrc.2000.3721

Ornitz, D. M., and Itoh, N. (2015). The Fibroblast Growth Factor signaling pathway. *Wiley Interdiscip. Rev. Dev. Biol.* 4, 215–266. doi: 10.1002/wdev.176

Orr-Urtreger, A., Bedford, M. T., Burakova, T., Arman, E., Zimmer, Y., Yayon, A., et al. (1993). Developmental localization of the splicing alternatives of fibroblast growth factor receptor-2 (FGFR2). *Dev. Biol.* 158, 475–486. doi: 10.1006/dbio.1993.1205

O'Sullivan, H., Kelleher, F. C., Lavelle, M., McGovern, B., Murphy, J., Swan, N., et al. (2017). Therapeutic potential for FGFR inhibitors in SOX9-FGFR2 coexpressing pancreatic cancer. *Pancreas* 46, e67–e69. doi: 10.1097/MPA.0000000000000870

Pan, F. C., and Wright, C. (2011). Pancreas organogenesis: from bud to plexus to gland. *Dev. Dyn.* 240, 530–565. doi: 10.1002/dvdy.22584

Papadopoulou, S., and Edlund, H. (2005). Attenuated Wnt signaling perturbs pancreatic growth but not pancreatic function. *Diabetes Metab. Res. Rev.* 54, 2844–2851.

Petri, A., Ahnfelt-Ronne, J., Frederiksen, K. S., Edwards, D. G., Madsen, D., Serup, P., et al. (2006). The effect of neurogenin3 deficiency on pancreatic gene

expression in embryonic mice. *J. Mol. Endocrinol.* 37, 301–316. doi: 10.1677/jme.1.02096

Pictet, R. L., Clark, W. R., Williams, R. H., and Rutter, W. J. (1972). An ultrastructural analysis of the developing embryonic pancreas. *Dev. Biol.* 29, 436–467. doi: 10.1016/0012-1606(72)90083-8

Pulkkinen, M. A., Spencer-Dene, B., Dickson, C., and Otonkoski, T. (2003). The IIIb isoform of fibroblast growth factor receptor 2 is required for proper growth and branching of pancreatic ductal epithelium but not for differentiation of exocrine or endocrine cells. *Mech. Dev.* 120, 167–175. doi: 10.1016/S0925-4773(02)00440-9

Seiki, M. (2003). Membrane-type 1 matrix metalloproteinase: a key enzyme for tumor invasion. *Cancer Lett.* 194, 1–11. doi: 10.1016/S0304-3835(02)00699-7

Sekine, K., Ohuchi, H., Fujiwara, M., Yamasaki, M., Yoshizawa, T., Sato, T., et al. (1999). Fgf10 is essential for limb and lung formation. *Nat. Genet.* 21, 138–141. doi: 10.1038/5096

Seymour, P. A. (2014). Sox9: a master regulator of the pancreatic program. *Rev. Diabetes Stud.* 11, 51–83. doi: 10.1900/RDS.2014.11.51

Seymour, P. A., Shih, H. P., Patel, N. A., Freude, K. K., Xie, R., Lim, C. J., et al. (2012). A Sox9/Fgf feed-forward loop maintains pancreatic organ identity. *Development* 139, 3363–3372. doi: 10.1242/dev.078733

Shih, H. P., Seymour, P. A., Patel, N. A., Xie, R., Wang, A., Liu, P. P., et al. (2015). A gene regulatory network cooperatively controlled by Pdx1 and Sox9 governs lineage allocation of foregut progenitor cells. *Cell Rep.* 13, 326–336. doi: 10.1016/j.celrep.2015.08.082

Shih, H. P., Wang, A., and Sander, M. (2013). Pancreas organogenesis: from lineage determination to morphogenesis. *Annu. Rev. Cell Dev. Biol.* 29, 81–105. doi: 10.1146/annurev-cellbio-101512-122405

Stafford, D., White, R. J., Kinkel, M. D., Linville, A., Schilling, T. F., and Prince, V. E. (2006). Retinoids signal directly to zebrafish endoderm to specify insulin-expressing beta-cells. *Development* 133, 949–956. doi: 10.1242/dev.02263

Stoffers, D. A., Zinkin, N. T., Stanojevic, V., Clarke, W. L., and Habener, J. F. (1997). Pancreatic agenesis attributable to a single nucleotide deletion in the human IPF1 gene coding sequence. *Nat. Genet.* 15, 106–110. doi: 10.1038/ng0197-106

Tefft, D., Lee, M., Smith, S., Crowe, D. L., Bellusci, S., and Warburton, D. (2002). mSprouty2 inhibits FGF10-activated MAP kinase by differentially binding to upstream target proteins. *Am. J. Physiol. Lung Cell Mol. Physiol.* 283, L700–L706. doi: 10.1152/ajplung.00372.2001

ten Berge, D., Brugmann, S. A., Helms, J. A., and Nusse, R. (2008). Wnt and FGF signals interact to coordinate growth with cell fate specification during limb development. *Development* 135, 3247–3257. doi: 10.1242/dev.023176

Wiebe, P. O., Kormish, J. D., Roper, V. T., Fujitani, Y., Alston, N. I., Zaret, K. S., et al. (2007). Ptf1a binds to and activates area III, a highly conserved region of the Pdx1 promoter that mediates early pancreas-wide Pdx1 expression. *Mol. Cell. Biol.* 27, 4093–4104. doi: 10.1128/MCB.01978-06

Ye, F., Duvillie, B., and Scharfmann, R. (2005). Fibroblast growth factors 7 and 10 are expressed in the human embryonic pancreatic mesenchyme and promote the proliferation of embryonic pancreatic epithelial cells. *Diabetologia* 48, 277–281. doi: 10.1007/s00125-004-1638-6

Ying, H., Dey, P., Yao, W., Kimmelman, A. C., Draetta, G. F., Maitra, A., et al. (2016). Genetics and biology of pancreatic ductal adenocarcinoma. *Genes Dev.* 30, 355–385. doi: 10.1101/gad.275776.115

Zhang, X., Ibrahimi, O. A., Olsen, S. K., Umemori, H., Mohammadi, M., and Ornitz, D. M. (2006). Receptor specificity of the fibroblast growth factor family. The complete mammalian FGF family. *J. Biol. Chem.* 281, 15694–15700. doi: 10.1074/jbc.M601252200

Zhou, Q., Law, A. C., Rajagopal, J., Anderson, W. J., Gray, P. A., and Melton, D. A. (2007). A multipotent progenitor domain guides pancreatic organogenesis. *Dev. Cell* 13, 103–114. doi: 10.1016/j.devcel.2007.06.001

Zhou, H., Qin, Y., Ji, S., Ling, J., Fu, J., Zhuang, Z., et al. (2018). SOX9 activity is induced by oncogenic Kras to affect MDC1 and MCMs expression in pancreatic cancer. *Oncogene* 37, 912–923. doi: 10.1038/onc.2017.393

Zinkle, A., and Mohammadi, M. (2018). A threshold model for receptor tyrosine kinase signaling specificity and cell fate determination. *F1000Res* 7:F1000FacultyRev–872.

Conflict of Interest Statement: The authors declare that the research was conducted in the absence of any commercial or financial relationships that could be construed as a potential conflict of interest.

Copyright © 2018 Ndlovu, Deng, Wu, Li and Zhang. This is an open-access article distributed under the terms of the Creative Commons Attribution License (CC BY). The use, distribution or reproduction in other forums is permitted, provided the original author(s) and the copyright owner(s) are credited and that the original publication in this journal is cited, in accordance with accepted academic practice. No use, distribution or reproduction is permitted which does not comply with these terms.

frontiers in Genetics

MINI REVIEW
published: 31 October 2018
doi: 10.3389/fgene.2018.00517

FGF10 and Human Lung Disease Across the Life Spectrum

*Lawrence S. Prince**

Department of Pediatrics, University of California, San Diego, Rady Children's Hospital, San Diego, CA, United States

Lung diseases impact patients across the lifespan, from infants in the first minutes of life through the aged population. Congenital abnormalities of lung structure can cause lung disease at birth or make adults more susceptible to chronic disease. Continuous inhalation of atmospheric components also requires the lung to be resilient to cellular injury. Fibroblast growth factor 10 (FGF10) regulates multiple stages of structural lung morphogenesis, cellular differentiation, and the response to injury. As a driver of lung airway branching morphogenesis, FGF10 signaling defects during development lead to neonatal lung disease. Alternatively, congenital airway abnormalities attributed to FGF10 mutations increase the risk of chronic airway disease in adulthood. FGF10 also maintains progenitor cell populations in the airway and promotes alveolar type 2 cell expansion and differentiation following injury. Here we review the cellular and molecular mechanisms linking FGF10 to multiple lung diseases, from bronchopulmonary dysplasia in extremely preterm neonates, cystic fibrosis in children, and chronic adult lung disorders. Understanding the connections between FGF10 and lung diseases may lead to exciting new therapeutic strategies.

Keywords: branching morphogenesis, alveolar epithelia, lung injury, inflammation, lung regeneration and repair

OPEN ACCESS

Edited by:
Saverio Bellusci,
Justus-Liebig-Universität Gießen, Germany

Reviewed by:
David Warburton,
Children's Hospital Los Angeles, United States
Cho-Ming Chao,
German Center for Lung Research, Germany

***Correspondence:**
Lawrence S. Prince
lprinceucsd@gmail.com

Specialty section:
This article was submitted to Stem Cell Research, a section of the journal Frontiers in Genetics

Received: *24 August 2018*
Accepted: *12 October 2018*
Published: *31 October 2018*

Citation:
Prince LS (2018) FGF10 and Human Lung Disease Across the Life Spectrum. Front. Genet. 9:517. doi: 10.3389/fgene.2018.00517

INTRODUCTION

Lung structure and physiology has remained consistent throughout mammalian evolution (Mess and Ferner, 2010). With a >100 m^2 surface area available for gas exchange (Colebatch and Ng, 1992), human lungs efficiently deliver oxygen to the circulation and expel carbon dioxide produced by aerobic cellular respiration. The lung can be separated into two distinct regions based on physiological function. Conducting airways begin just below the larynx and trachea. Stereotypical branches form 23 generations in human lungs (Weibel and Gomez, 1962) and 10 generations in mice (Kizhakke Puliyakote et al., 2016) of smaller and smaller airways. The trachea, bronchi, and bronchioles serve to warm and humidify inhaled air from the environment. In addition, airway mucous captures inhaled particulates, allowing efficient removal by mucociliary clearance (Munkholm and Mortensen, 2014). Multiciliated epithelia move aggregates of mucous and its sequestered material upon a thin layer of airway surface liquid in a cranial direction for expectoration or ingestion. The movement and filtering of inhaled gas through the conducting airways delivers clean, warm air to the alveolar structures for oxygen and carbon dioxide exchange.

The alveolar surface is lined with two types of epithelial cells (Guillot et al., 2013). Alveolar type 1 (AT1) cells are flat, thin epithelia that cover the vast majority of the alveolar surface. AT1 cells reside in intimate proximity with underlying alveolar capillary vascular endothelial cells, permitting efficient oxygen uptake and carbon dioxide removal. AT1 and endothelial cells rely

upon mechanical support from extracellular elastic fibers and a variety of mesenchymal-derived interstitial lung fibroblasts (Pierce et al., 1995; Starcher, 2000). Alveolar type 2 (AT2) cells are cuboidal epithelial cells responsible for the production of lung surfactant (Veldhuizen et al., 2000). The combination of amphipathic surfactant proteins and lipids form organized structures along the alveolar surface termed tubular myelin. As intra-alveolar pressures change with each breath, folding and unfolding of the tubular myelin maintains alveolar size by modulating surface tension (Johansson et al., 1994). In addition to the physiological roles of delivering oxygen to the systemic circulation and removing carbon dioxide, each of the cell populations in the lung play important roles in protecting against infection and repairing the lung following mechanical, chemical, or biological damage (Barkauskas et al., 2013; Chambers and Mercer, 2015; Wang et al., 2016).

FGF10 AND LUNG MORPHOGENESIS

Formation of the unique structures within the lung involves complex molecular and cellular processes. Fibroblast growth factors (FGFs) play important roles throughout lung morphogenesis. Twenty-two different FGF family members have been identified and characterized, with seven subfamilies based on protein structure similarities (Ornitz and Itoh, 2015). FGF10 (KGF2) is a member of the FGF7 subfamily and critical for lung morphogenesis, cellular differentiation, and repair following injury. Produced primarily by mesenchymal populations in the lung interstitium, secreted FGF10 tightly binds heparin sulfate proteoglycans (HSPG) in the extracellular matrix. HSPG interactions stabilize FGF10, restrict its diffusion, and facilitate binding to FGF receptors (Makarenkova et al., 2009). FGF10 binds both FGFR1 and FGFR2, with highest affinity for the alternatively spliced FGFR2IIIb isoform (Lu et al., 1999). Formation of symmetrical FGF10, HSPG, and FGFR2 dimers leads to receptor activation of downstream receptor tyrosine kinase targets (Schlessinger et al., 2000).

During the earliest stages of lung development, FGF10 is expressed in the mesenchyme surrounding the distal tips of branching airways (Bellusci et al., 1997). Retinoic acid and Wnt ligands stimulate early FGF10 expression (Desai et al., 2004; Li et al., 2005). Epithelial cells in the branching airways express the receptor FGFR2, establishing a paracrine signaling system. Knockout mice studies have demonstrated the critical importance of FGF10 in lung morphogenesis. Mice lacking FGF10 form an embryonic trachea, but only two rudimentary buds marking where the right and left mainstem bronchi should normally develop (Sekine et al., 1999). Conditional mouse models and *ex vivo* studies have illustrated how FGF10 promotes later stages of lung morphogenesis. FGF10 stimulates migration of the leading edge of newly developing airways. Elongation of these tubular, epithelial-lined structures involves specific orientation of FGF-stimulated, dividing epithelial cells (Tang et al., 2011). Unlike some other branching epithelial organs, lung airways maintain a simple epithelial orientation with nearly continuous contact with luminal lung fluid.

Along with promoting airway elongation, FGF10 induces expression of epithelial factors that negatively regulate FGF10 expression. Activated FGFR2 signals through ETS-related transcription factors Etv4 and Etv5 (Herriges et al., 2015). In the branching embryonic lung, FGF10 induces epithelial expression of Bmp4 and Shh at the leading airway edge. In a coordinated negative feedback loop, both Bmp4 and Shh reduce expression of FGF10 in the adjacent mesenchyme. As FGF10 expression distal to the leading airway falls, a branch point is established, generating a structural split of the airway and subsequent elongation toward more lateral locations where FGF10 expression has not yet been inhibited. Multiple iterations of the process generate the stereotypical pattern of conducting airways unique to each mammalian species (Miura, 2008; Celliere et al., 2012). Bmp4 also promotes mesenchymal differentiation of peribronchial smooth muscle and slows epithelial proliferation, both of which could regulate the branching process (Kim and Vu, 2006). Precise regulation of FGF10 expression is critical for normal morphogenesis, as overexpression of FGF10 during development leads to cystic adenomatoid malformations (Gonzaga et al., 2008).

After conducting airway branching completes, formation of saccular airways occurs via presumably random branching and division of distal airway structures. Saccular airways become alveolar ducts later in development and the number of terminal saccular airways likely determine the eventual number of alveolar units in the mature lung (Burri, 1984). The mechanisms of saccular branching share many attributes with conducting airway branching, including the role of FGF10 in airway elongation and branching (Benjamin et al., 2007). The branching process ceases as saccular airway epithelia begin differentiating into AT1 and AT2 cells.

FGF10 also drives formation of normal alveolar structures later in lung development. Following completion of distal airway branching at the end of the saccular stage, alveolar formation produces the mature lung structures capable of efficient gas exchange. Generation of mature alveoli involves the division of distal airspaces into smaller structures, increasing the effective surface area for gas exchange. Alveolar division or septation requires mechanical forces generated by *Acta2*-positive alveolar myofibroblasts within the lung mesenchyme (Branchfield et al., 2016). Myofibroblasts arise from *Pdgfra*-positive mesenchymal cells, which express FGF10 and often have lipofibroblast characteristics. Mice with reduced FGF10 expression have fewer *Acta2*-positive myofibroblasts at birth and fail to form normal alveolar structures (Ramasamy et al., 2007). Overexpression of a dominant negative, soluble *Fgfr* transgene also reduced alveolar formation. In a pneumonectomy model of alveolar regeneration, interfering with FGFR2 signaling prevented myofibroblast differentiation (Chen et al., 2012). These observations could involve autocrine mechanisms where FGF ligands including FGF10 directly regulate fibroblast phenotype or paracrine signaling loops involving Shh, Wnt, Bmp, or TGFβ signaling between adjacent cell populations.

In addition to driving structural morphogenesis of conducting airways and alveoli, FGF10 also regulates lung cell differentiation. Epithelia lining the trachea and large airways contain multipotent

progenitor basal cells – sometimes referred to as basal stem cells (Pardo-Saganta et al., 2015). Mesenchymal FGF10 expression in the trachea establishes a unique niche for basal cells, with FGF10 driving basal cell expansion and preventing terminal epithelial differentiation. Interestingly, FGF10 expression in the peri-tracheal mesenchyme is restricted to areas between cartilaginous rings (Sala et al., 2011). Within the tracheal epithelium, downregulation of Hippo activity in basal cells results in nuclear Yap localization and Wnt7b expression (Volckaert et al., 2017). Epithelial Wnt7b then increases or at least maintains FGF10 expression in the underlying mesenchyme. In smaller distal airways, the lack of FGF10 expression in peribronchial smooth muscle cells correlates with epithelial differentiation and reduced basal cell number. However inactivation of Hippo in smaller airways increases FGF10 expression in smooth muscle and leads to ectopic basal cell expansion. This highly regulated basal cell niche beautifully illustrates the paracrine nature of FGF10 signaling in maintaining normal lung biology throughout the lifespan.

FGF10 is also important for AT2 cell differentiation. As fetal saccular airways complete branching, elongation, and expansion, alveolar epithelial differentiation begins proximal to the airway leading edge. As the distal air saccules expand with fetal lung fluid, cuboidal cells are observed protruding from the epithelial monolayer in a basal direction (Li et al., 2018). These protruding cells differentiate into AT2 cells, while cells remaining in the epithelial monolayer are subjected to increased stretch and acquire an AT1 phenotype. Increasing airway distension promotes AT1 differentiation, while reducing stretch increases AT2 cell numbers. FGF10 drives cell protrusion by stimulating the ERK1/2 pathway and Arp2/3 based actin rearrangement. Developing AT2 cells are protected from the pro-AT1 effects of airway dilation and stretching by constricting their apical membrane via non-muscle myosin activity. Consistent with this model of FGF10-mediated AT2 cell differentiation, mice heterozygous for FGF10 or lacking FGFR2 have fewer protruding cells and subsequently reduced AT2 numbers.

ROLE OF FGF10 IN HUMAN DISEASE

COPD and Developmental Airway Abnormalities

Early events in lung morphogenesis that impact formation of the conducting airways can have lifelong consequences. Defects in the formation of the trachea, bronchi, and bronchioles lead to increased turbulent airflow, accumulation of inhaled particulates, and reduced surface area available for gas exchange. Congenital defects in airway branching could cause disease in the immediate newborn period or in adulthood as defects in airway function predispose to chronic airway infection and injury. Decades ago, investigators proposed the concept of dysanaptic lung growth, where abnormalities in airway development could impact available surface area for gas exchange in the context of normal lung volume (Green et al., 1974). These defects become clinically significant during lung injury or challenges to normal gas exchange.

Chronic obstructive pulmonary disease (COPD) is a major cause of lung related illness and death throughout the world (Terzikhan et al., 2016). With aging populations, COPD now affects over 300 million people worldwide. While tobacco smoking clearly increases COPD risk, only approximately 20% of smokers develop COPD. In addition, between 20–45% of COPD patients are non-smokers but appear to develop airway disease through other environmental and occupational exposures (Salvi and Barnes, 2009). Recent studies connected genetic variants to structural airway abnormalities in patients with COPD (Smith et al., 2018). Up to 26% of the general human population have abnormalities in airway branching patterns, increasing COPD risk. Absence of the right medial-basal lung segment is present in approximately 6% of the population. These individuals have reduced luminal airway volume and a higher risk of COPD if also smokers. Investigators identified gene variants in the FGF10 intronic region in individuals with absence of the right medial-basal segment using two independent cohorts.

Striking results were also uncovered in a smaller study of adults with aplasia of salivary and lacrimal glands (ASLG), known to result from mutations causing FGF10 haploinsufficiency (Klar et al., 2011). Compared to both predicted values and unaffected siblings, subjects with FGF10 haploinsufficiency had significant, non-reversible airway obstruction by spirometry consistent with COPD. Similar studies have not yet been reported on patients with lacrimo-auriculo-dento-digital (LADD) syndrome, another disorder resulting from either FGF10 or FGFR2 haploinsufficiency (Shams et al., 2007). The rs1448044 SNP near the *FGF10* gene has been associated with reduced pulmonary function (Jackson et al., 2018), although the connection of this SNP to *FGF10* expression remains unclear. These studies provide strong evidence that mutations and variants in a critical gene during early lung morphogenesis (FGF10) can cause structural abnormalities in humans leading to disease following years of environmental exposures.

Cystic Fibrosis, FGF10, and Airway Diameter

In addition to inherent defects in mucociliary clearance and bacterial killing, patients with cystic fibrosis (CF) have congenital abnormalities in airway shape and size (Meyerholz et al., 2010; Fischer et al., 2014). Infants with CF have smaller caliber tracheas and demonstrate airway abnormalities before developing clinical signs of respiratory infection (Sly et al., 2009). The developmental origins of these structural abnormalities have been confirmed and further investigated using the CF pig model. Newborn CF pigs have smaller diameter tracheas and bronchi compared to wild type pigs (Meyerholz et al., 2010). More recent studies measured reduced airway diameter in fetal CF pig lungs as early as the pseudoglandular stage of development during active branching morphogenesis of the conducting airways (Meyerholz et al., 2018). FGF10 treatment induced airway expansion in wild type fetal pig lung explants, but had no effect on CF explants. In the developing CF pig lung, FGF10 expression was similar to controls and could still increase epithelial proliferation in primary cultures of CF epithelia. However FGF10 could not stimulate CFTR-mediated

increases in epithelial short circuit current in CF cells. So, while FGF10 signaling in CF lungs remains intact, the inability to stimulate epithelial transport impacts airway morphogenesis. The human and experimental animal data clearly show that early defects in fluid transport impact structural lung development in CF, likely contributing to the pathogenesis of CF lung disease.

FGF10 and Connecting Inflammation to Newborn Lung Disease

Bronchopulmonary dysplasia (BPD) is the most common serious complication of extreme prematurity. Infants before 28-week gestation are still in the canalicular stage of lung development and must complete airway morphogenesis while exposed to the external environment. Infection and inflammation are the major clinical risk factors leading to BPD (Bhandari, 2014). In experimental models, fetal macrophage activation and IL-1β release inhibit saccular stage airway branching (Nold et al., 2013; Stouch et al., 2016). Reduction in saccular airway branching leads to fewer numbers of mature alveoli. In human newborn lungs, FGF10 localizes to clusters of cells within the lung interstitium. However in patients that died with BPD, fewer FGF10-positive cells could be detected throughout the lung tissue (Benjamin et al., 2007). The reduction in FGF10 could both have led to abnormal structural development and make the lung more susceptible to injury.

Inflammatory mediators that disrupt normal lung development in BPD do so at least in part by inhibiting FGF10 expression. Microbial products and inflammatory cytokines activate receptors that signal through the IKK/NF-κB pathway. Activated NF-κB translocates to the nucleus and regulates gene transcription (Dev et al., 2011). While mostly studied in the context of stimulating expression of pro-inflammatory response genes, NF-κB also inhibits expression of genes important for normal development. In the case of FGF10, NF-κB appears to interfere with the normal machinery that maintains FGF10 transcription in mesenchymal cells (Benjamin et al., 2007, 2010). Lacking a TATA sequence, the FGF10 promoter contains multiple conserved GC boxes which bind Sp family members and serve as sites of RNA polymerase recruitment (Carver et al., 2013). Sp1 binds the FGF10 promoter and stimulates transcription; Sp3 can either activate or repress FGF10 transcription. Upon nuclear translocation, NF-κB binds Sp3 and NF-κB-Sp3 complexes repress FGF10 promoter activity. Further understanding the molecular basis of FGF10 transcriptional regulation in normal and disease states could identify new treatment strategies for BPD and other clinical scenarios where maintaining FGF10 expression could provide benefit.

FGF10 is also critical for how the developing lung responds to injury. Mice heterozygous for FGF10 appear healthy with seemingly normal lung development. However haploinsufficiency for FGF10 leads to dramatic pathology in an experimental BPD model (Chao et al., 2017). Exposing newborn mice to transient hyperoxia leads to lung injury, inflammation, and reduced alveolarization. Wild type mice typically survive hyperoxia exposure with steady improvement in lung morphology. In contrast, FGF10 heterozygous mice exposed to hyperoxia following birth have more severe defects in alveolar development with 100% mortality. FGF10 heterozygous mice also have abnormal alveolar epithelial differentiation following hyperoxia with increased AT1 cells and reduced AT2 cell number. Reduction in AT2 cells could both impact surfactant production and lung compliance and prevent normal repair of alveolar structures following injury.

ROLE OF FGF10 IN AIRWAY INJURY AND REPAIR

Consistent with its role in airway morphogenesis, AT2 cell differentiation, and airway basal cell maintenance, FGF10 drives lung repair following various injuries. Pretreating adult rats with intratracheal FGF10 improves the recovery following high volume mechanical ventilation (Bi et al., 2014), altitude-associated hypoxia (She et al., 2012), bacterial endotoxin/sepsis (Tong et al., 2014), and ischemia/reperfusion (Fang et al., 2014). Most of these effects are thought due to increased AT2 expansion and/or differentiation. FGF10 also reduces bleomycin-induced lung fibrosis, potentially through its AT2 protective effects (Gupte et al., 2009). Large airway repair may involve a different mechanism. Following naphthalene treatment, activation of the basal cell niche in the trachea and large airways is required for epithelial repopulation and differentiation (Volckaert et al., 2017). Epithelial Myc and Yap activity stimulate mesenchymal FGF10 expression during the repair process, likely through Wnt ligands. Data in this study suggested overstimulation of this pathway might also lead to pathological airway changes.

RATIONALE FOR THERAPEUTIC APPROACHES

Because of its important roles in structural morphogenesis, epithelial differentiation, and protection from injury, FGF10 is an intriguing target for preventing and treating lung disease. Unfortunately, early human studies have so far failed to show a benefit of FGF10 in treating venous ulcers, mucositis, or ulcerative colitis (Sandborn et al., 2003; Plichta and Radek, 2012). As FGF10 is expressed by some cancer cell lines and can promote cell migration and proliferation, consideration of tumorigenic potential in preclinical studies will be critical (Sugimoto et al., 2014). Delivery of FGF10 into the correct biochemical HSPG containing microenvironment may represent a difficult therapeutic challenge. Compared to other FGF family members, FGF10 has unique HSPG binding characteristics with limited mobility when bound to the cell surface (Sun et al., 2016). In addition, the different relative activities of FGF10 and FGF7 may be due to their distinct HSPG interactions (Makarenkova et al., 2009). Other strategies could involve

molecular and pharmacologic approaches aimed at increasing FGF10 expression and/or release. We now have multiple experimental animal lung disease models for testing these effects across the lifespan. Because constitutive overexpression of FGF10 during development can lead to dramatically altered lung morphogenesis (Gonzaga et al., 2008), the most effective approaches will likely promote the beneficial effects of FGF10 in the diseased lung while maintaining the complex regulatory mechanisms necessary for organ homeostasis.

AUTHOR CONTRIBUTIONS

LP surveyed the literature and wrote the manuscript.

FUNDING

The author's laboratory received research support from the National Institutes of Health (HL143256 and HL126703) and the Gerber Foundation (20180324).

REFERENCES

Barkauskas, C. E., Cronce, M. J., Rackley, C. R., Bowie, E. J., Keene, D. R., Stripp, B. R., et al. (2013). Type 2 alveolar cells are stem cells in adult lung. *J. Clin. Invest.* 123, 3025–3036. doi: 10.1172/JCI68782

Bellusci, S., Grindley, J., Emoto, H., Itoh, N., and Hogan, B. L. (1997). Fibroblast growth factor 10 (FGF10) and branching morphogenesis in the embryonic mouse lung. *Development* 124, 4867–4878.

Benjamin, J. T., Carver, B. J., Plosa, E. J., Yamamoto, Y., Miller, J. D., Liu, J. H., et al. (2010). NF-kappaB activation limits airway branching through inhibition of Sp1-mediated fibroblast growth factor10 expression. *J. Immunol.* 185, 4896–4903. doi: 10.4049/jimmunol.1001857

Benjamin, J. T., Smith, R. J., Halloran, B. A., Day, T. J., Kelly, D. R., and Prince, L. S. (2007). FGF10 is decreased in bronchopulmonary dysplasia and suppressed by Toll-like receptor activation. *Am. J. Physiol. Lung. Cell Mol. Physiol.* 292, L550–L558. doi: 10.1152/ajplung.00329.2006

Bhandari, V. (2014). Postnatal inflammation in the pathogenesis of bronchopulmonary dysplasia. *Birth Defects Res. A Clin. Mol. Teratol.* 100, 189–201. doi: 10.1002/bdra.23220

Bi, J., Tong, L., Zhu, X., Yang, D., Bai, C., Song, Y., et al. (2014). Keratinocyte growth factor-2 intratracheal instillation significantly attenuates ventilator-induced lung injury in rats. *J. Cell Mol. Med.* 18, 1226–1235. doi: 10.1111/jcmm.12269

Branchfield, K., Li, R., Lungova, V., Verheyden, J. M., Mcculley, D., and Sun, X. (2016). A three-dimensional study of alveologenesis in mouse lung. *Dev. Biol.* 409, 429–441. doi: 10.1016/j.ydbio.2015.11.017

Burri, P. H. (1984). Fetal and postnatal development of the lung. *Annu. Rev. Physiol.* 46, 617–628. doi: 10.1146/annurev.ph.46.030184.003153

Carver, B. J., Plosa, E. J., Stinnett, A. M., Blackwell, T. S., and Prince, L. S. (2013). Interactions between NF-kappaB and SP3 connect inflammatory signaling with reduced FGF10 expression. *J. Biol. Chem.* 288, 15318–15325. doi: 10.1074/jbc.M112.447318

Celliere, G., Menshykau, D., and Iber, D. (2012). Simulations demonstrate a simple network to be sufficient to control branch point selection, smooth muscle and vasculature formation during lung branching morphogenesis. *Biol. Open* 1, 775–788. doi: 10.1242/bio.20121339

Chambers, R. C., and Mercer, P. F. (2015). Mechanisms of alveolar epithelial injury, repair, and fibrosis. *Ann. Am. Thorac. Soc.* 12(Suppl. 1), S16–S20. doi: 10.1513/AnnalsATS.201410-448MG

Chao, C. M., Yahya, F., Moiseenko, A., Tiozzo, C., Shrestha, A., Ahmadvand, N., et al. (2017). Fgf10 deficiency is causative for lethality in a mouse model of bronchopulmonary dysplasia. *J. Pathol.* 241, 91–103. doi: 10.1002/path.4834

Chen, L., Acciani, T., Le Cras, T., Lutzko, C., and Perl, A. K. (2012). Dynamic regulation of platelet-derived growth factor receptor alpha expression in alveolar fibroblasts during realveolarization. *Am. J. Respir. Cell Mol. Biol.* 47, 517–527. doi: 10.1165/rcmb.2012-0030OC

Colebatch, H. J., and Ng, C. K. (1992). Estimating alveolar surface area during life. *Respir. Physiol.* 88, 163–170. doi: 10.1016/0034-5687(92)90037-W

Desai, T. J., Malpel, S., Flentke, G. R., Smith, S. M., and Cardoso, W. V. (2004). Retinoic acid selectively regulates Fgf10 expression and maintains cell identity in the prospective lung field of the developing foregut. *Dev. Biol.* 273, 402–415. doi: 10.1016/j.ydbio.2004.04.039

Dev, A., Iyer, S., Razani, B., and Cheng, G. (2011). NF-kappaB and innate immunity. *Curr. Top. Microbiol. Immunol.* 349, 115–143. doi: 10.1007/82_2010_102

Fang, X., Wang, L., Shi, L., Chen, C., Wang, Q., Bai, C., et al. (2014). Protective effects of keratinocyte growth factor-2 on ischemia-reperfusion-induced lung injury in rats. *Am. J. Respir. Cell Mol. Biol.* 50, 1156–1165. doi: 10.1165/rcmb.2013-0268OC

Fischer, A. J., Singh, S. B., Adam, R. J., Stoltz, D. A., Baranano, C. F., Kao, S., et al. (2014). Tracheomalacia is associated with lower FEV1 and *Pseudomonas* acquisition in children with CF. *Pediatr. Pulmonol.* 49, 960–970. doi: 10.1002/ppul.22922

Gonzaga, S., Henriques-Coelho, T., Davey, M., Zoltick, P. W., Leite-Moreira, A. F., Correia-Pinto, J., et al. (2008). Cystic adenomatoid malformations are induced by localized FGF10 overexpression in fetal rat lung. *Am. J. Respir. Cell Mol. Biol.* 39, 346–355. doi: 10.1165/rcmb.2007-0290OC

Green, M., Mead, J., and Turner, J. M. (1974). Variability of maximum expiratory flow-volume curves. *J. Appl. Physiol.* 37, 67–74. doi: 10.1152/jappl.1974.37.1.67

Guillot, L., Nathan, N., Tabary, O., Thouvenin, G., Le Rouzic, P., Corvol, H., et al. (2013). Alveolar epithelial cells: master regulators of lung homeostasis. *Int. J. Biochem. Cell Biol.* 45, 2568–2573. doi: 10.1016/j.biocel.2013.08.009

Gupte, V. V., Ramasamy, S. K., Reddy, R., Lee, J., Weinreb, P. H., Violette, S. M., et al. (2009). Overexpression of fibroblast growth factor10 during both inflammatory and fibrotic phases attenuates bleomycin-induced pulmonary fibrosis in mice. *Am. J. Respir. Crit. Care Med.* 180, 424–436. doi: 10.1164/rccm.200811-1794OC

Herriges, J. C., Verheyden, J. M., Zhang, Z., Sui, P., Zhang, Y., Anderson, M. J., et al. (2015). FGF-regulated ETV transcription factors control FGF-SHH feedback loop in lung branching. *Dev. Cell* 35, 322–332. doi: 10.1016/j.devcel.2015.10.006

Jackson, V. E., Latourelle, J. C., Wain, L. V., Smith, A. V., Grove, M. L., Bartz, T. M., et al. (2018). Meta-analysis of exome array data identifies six novel genetic loci for lung function. *Welcome Open Res.* 3:4. doi: 10.12688/wellcomeopenres.12583.3

Johansson, J., Curstedt, T., and Robertson, B. (1994). The proteins of the surfactant system. *Eur. Respir. J.* 7, 372–391. doi: 10.1183/09031936.94.07020372

Kim, N., and Vu, T. H. (2006). Parabronchial smooth muscle cells and alveolar myofibroblasts in lung development. *Birth Defects Res. C Embryo. Today* 78, 80–89. doi: 10.1002/bdrc.20062

Kizhakke Puliyakote, A. S., Vasilescu, D. M., Sen Sharma, K., Wang, G., and Hoffman, E. A. (2016). A skeleton-tree-based approach to acinar morphometric analysis using microcomputed tomography with comparison of acini in young and old C57BL/6 mice. *J. Appl. Physiol.* 120, 1402–1409. doi: 10.1152/japplphysiol.00923.2015

Klar, J., Blomstrand, P., Brunmark, C., Badhai, J., Hakansson, H. F., Brange, C. S., et al. (2011). Fibroblast growth factor 10 haploinsufficiency causes chronic obstructive pulmonary disease. *J. Med. Genet.* 48, 705–709. doi: 10.1136/jmedgenet-2011-100166

Li, C., Hu, L., Xiao, J., Chen, H., Li, J. T., Bellusci, S., et al. (2005). Wnt5a regulates Shh and Fgf10 signaling during lung development. *Dev. Biol.* 287, 86–97. doi: 10.1016/j.ydbio.2005.08.035

Li, J., Wang, Z., Chu, Q., Jiang, K., Li, J., and Tang, N. (2018). The strength of mechanical forces determines the differentiation of alveolar epithelial cells. *Dev. Cell* 44, e295. doi: 10.1016/j.devcel.2018.01.008

Lu, W., Luo, Y., Kan, M., and Mckeehan, W. L. (1999). Fibroblast growth factor10. A second candidate stromal to epithelial cell andromedin in prostate. *J. Biol. Chem.* 274, 12827–12834. doi: 10.1074/jbc.274.18.12827

Makarenkova, H. P., Hoffman, M. P., Beenken, A., Eliseenkova, A. V., Meech, R., Tsau, C., et al. (2009). Differential interactions of FGFs with heparan sulfate control gradient formation and branching morphogenesis. *Sci. Signal.* 2:ra55. doi: 10.1126/scisignal.2000304

Mess, A. M., and Ferner, K. J. (2010). Evolution and development of gas exchange structures in Mammalia: the placenta and the lung. *Respir. Physiol. Neurobiol.* 173(Suppl.), S74–S82. doi: 10.1016/j.resp.2010.01.005

Meyerholz, D. K., Stoltz, D. A., Gansemer, N. D., Ernst, S. E., Cook, D. P., Strub, M. D., et al. (2018). Lack of cystic fibrosis transmembrane conductance regulator disrupts fetal airway development in pigs. *Lab. Invest.* 98, 825–838. doi: 10.1038/s41374-018-0026-7

Meyerholz, D. K., Stoltz, D. A., Namati, E., Ramachandran, S., Pezzulo, A. A., Smith, A. R., et al. (2010). Loss of cystic fibrosis transmembrane conductance regulator function produces abnormalities in tracheal development in neonatal pigs and young children. *Am. J. Respir. Crit. Care Med.* 182, 1251–1261. doi: 10.1164/rccm.201004-0643OC

Miura, T. (2008). Modeling lung branching morphogenesis. *Curr. Top. Dev. Biol.* 81, 291–310. doi: 10.1016/S0070-2153(07)81010-6

Munkholm, M., and Mortensen, J. (2014). Mucociliary clearance: pathophysiological aspects. *Clin. Physiol. Funct. Imaging* 34, 171–177. doi: 10.1111/cpf.12085

Nold, M. F., Mangan, N. E., Rudloff, I., Cho, S. X., Shariatian, N., Samarasinghe, T. D., et al. (2013). Interleukin-1 receptor antagonist prevents murine bronchopulmonary dysplasia induced by perinatal inflammation and hyperoxia. *Proc. Natl. Acad. Sci. U.S.A.* 110, 14384–14389. doi: 10.1073/pnas.1306859110

Ornitz, D. M., and Itoh, N. (2015). The fibroblast growth factor signaling pathway. *Wiley Interdiscip. Rev. Dev. Biol.* 4, 215–266. doi: 10.1002/wdev.176

Pardo-Saganta, A., Law, B. M., Tata, P. R., Villoria, J., Saez, B., Mou, H., et al. (2015). Injury induces direct lineage segregation of functionally distinct airway basal stem/progenitor cell subpopulations. *Cell Stem Cell* 16, 184–197. doi: 10.1016/j.stem.2015.01.002

Pierce, R. A., Mariani, T. J., and Senior, R. M. (1995). Elastin in lung development and disease. *Ciba Found Symp.* 192, 199–212;discussion212–194.

Plichta, J. K., and Radek, K. A. (2012). Sugar-coating wound repair: a review of FGF10 and dermatan sulfate in wound healing and their potential application in burn wounds. *J. Burn Care Res.* 33, 299–310. doi: 10.1097/BCR.0b013e318240540a

Ramasamy, S. K., Mailleux, A. A., Gupte, V. V., Mata, F., Sala, F. G., Veltmaat, J. M., et al. (2007). Fgf10 dosage is critical for the amplification of epithelial cell progenitors and for the formation of multiple mesenchymal lineages during lung development. *Dev. Biol.* 307, 237–247. doi: 10.1016/j.ydbio.2007.04.033

Sala, F. G., Del Moral, P. M., Tiozzo, C., Alam, D. A., Warburton, D., Grikscheit, T., et al. (2011). FGF10 controls the patterning of the tracheal cartilage rings via Shh. *Development* 138, 273–282. doi: 10.1242/dev.051680

Salvi, S. S., and Barnes, P. J. (2009). Chronic obstructive pulmonary disease in non-smokers. *Lancet* 374, 733–743. doi: 10.1016/S0140-6736(09)61303-9

Sandborn, W. J., Sands, B. E., Wolf, D. C., Valentine, J. F., Safdi, M., Katz, S., et al. (2003). Repifermin (keratinocyte growth factor-2) for the treatment of active ulcerative colitis: a randomized, double-blind, placebo-controlled, dose-escalation trial. *Aliment. Pharmacol. Ther.* 17, 1355–1364. doi: 10.1046/j.1365-2036.2003.01589.x

Schlessinger, J., Plotnikov, A. N., Ibrahimi, O. A., Eliseenkova, A. V., Yeh, B. K., Yayon, A., et al. (2000). Crystal structure of a ternary FGF-FGFR-heparin complex reveals a dual role for heparin in FGFR binding and dimerization. *Mol. Cell.* 6, 743–750. doi: 10.1016/S1097-2765(00)00073-3

Sekine, K., Ohuchi, H., Fujiwara, M., Yamasaki, M., Yoshizawa, T., Sato, T., et al. (1999). Fgf10 is essential for limb and lung formation. *Nat. Genet.* 21, 138–141. doi: 10.1038/5096

Shams, I., Rohmann, E., Eswarakumar, V. P., Lew, E. D., Yuzawa, S., Wollnik, B., et al. (2007). Lacrimo-auriculo-dento-digital syndrome is caused by reduced activity of the fibroblast growth factor 10 (FGF10)-FGF receptor 2 signaling pathway. *Mol. Cell. Biol.* 27, 6903–6912. doi: 10.1128/MCB.00544-07

She, J., Goolaerts, A., Shen, J., Bi, J., Tong, L., Gao, L., et al. (2012). KGF-2 targets alveolar epithelia and capillary endothelia to reduce high altitude pulmonary oedema in rats. *J. Cell Mol. Med.* 16, 3074–3084. doi: 10.1111/j.1582-4934.2012.01588.x

Sly, P. D., Brennan, S., Gangell, C., De Klerk, N., Murray, C., Mott, L., et al. (2009). Lung disease at diagnosis in infants with cystic fibrosis detected by newborn screening. *Am. J. Respir. Crit. Care Med.* 180, 146–152. doi: 10.1164/rccm.200901-0069OC

Smith, B. M., Traboulsi, H., Austin, J. H. M., Manichaikul, A., Hoffman, E. A., Bleecker, E. R., et al. (2018). Human airway branch variation and chronic obstructive pulmonary disease. *Proc. Natl. Acad. Sci. U.S.A.* 115, E974–E981. doi: 10.1073/pnas.1715564115

Starcher, B. C. (2000). Lung elastin and matrix. *Chest* 117, 229S–234S. doi: 10.1378/chest.117.5_suppl_1.229S-a

Stouch, A. N., Mccoy, A. M., Greer, R. M., Lakhdari, O., Yull, F. E., Blackwell, T. S., et al. (2016). IL-1beta and inflammasome activity link inflammation to abnormal fetal airway development. *J. Immunol.* 196, 3411–3420. doi: 10.4049/jimmunol.1500906

Sugimoto, K., Yoshida, S., Mashio, Y., Toyota, N., Xing, Y., Xu, H., et al. (2014). Role of FGF10 on tumorigenesis by MS-K. *Genes Cells* 19, 112–125. doi: 10.1111/gtc.12118

Sun, C., Marcello, M., Li, Y., Mason, D., Levy, R., and Fernig, D. G. (2016). Selectivity in glycosaminoglycan binding dictates the distribution and diffusion of fibroblast growth factors in the pericellular matrix. *Open Biol.* 6:150277. doi: 10.1098/rsob.150277

Tang, N., Marshall, W. F., Mcmahon, M., Metzger, R. J., and Martin, G. R. (2011). Control of mitotic spindle angle by the RAS-regulated ERK1/2 pathway determines lung tube shape. *Science* 333, 342–345. doi: 10.1126/science.1204831

Terzikhan, N., Verhamme, K. M., Hofman, A., Stricker, B. H., Brusselle, G. G., and Lahousse, L. (2016). Prevalence and incidence of COPD in smokers and non-smokers: the Rotterdam Study. *Eur. J. Epidemiol.* 31, 785–792. doi: 10.1007/s10654-016-0132-z

Tong, L., Bi, J., Zhu, X., Wang, G., Liu, J., Rong, L., et al. (2014). Keratinocyte growth factor-2 is protective in lipopolysaccharide-induced acute lung injury in rats. *Respir. Physiol. Neurobiol.* 201, 7–14. doi: 10.1016/j.resp.2014.06.011

Veldhuizen, E. J., Batenburg, J. J., Van Golde, L. M., and Haagsman, H. P. (2000). The role of surfactant proteins in DPPC enrichment of surface films. *Biophys. J.* 79, 3164–3171. doi: 10.1016/S0006-3495(00)76550-7

Volckaert, T., Yuan, T., Chao, C. M., Bell, H., Sitaula, A., Szimmtenings, L., et al. (2017). Fgf10-Hippo epithelial-mesenchymal crosstalk maintains and recruits lung basal stem cells. *Dev. Cell* 43, 48.e–59.e. doi: 10.1016/j.devcel.2017.09.003

Wang, X., Zhang, L., and Sun, B. (2016). Neonatal type II alveolar epithelial cell transplant facilitates lung reparation in piglets with acute lung injury and extracorporeal life support. *Pediatr. Crit. Care Med.* 17, e182–e192. doi: 10.1097/PCC.0000000000000667

Weibel, E. R., and Gomez, D. M. (1962). Architecture of the human lung. Use of quantitative methods establishes fundamental relations between size and number of lung structures. *Science* 137, 577–585. doi: 10.1126/science.137.3530.577

Conflict of Interest Statement: The author declares that the research was conducted in the absence of any commercial or financial relationships that could be construed as a potential conflict of interest.

Copyright © 2018 Prince. This is an open-access article distributed under the terms of the Creative Commons Attribution License (CC BY). The use, distribution or reproduction in other forums is permitted, provided the original author(s) and the copyright owner(s) are credited and that the original publication in this journal is cited, in accordance with accepted academic practice. No use, distribution or reproduction is permitted which does not comply with these terms.

frontiers in Genetics

ORIGINAL RESEARCH
published: 09 November 2018
doi: 10.3389/fgene.2018.00530

FGF10 and the Mystery of Duodenal Atresia in Humans

Warwick J. Teague[1,2,3,4], Matthew L. M. Jones[1,3,4], Leanne Hawkey[5], Ian M. Smyth[5,6,7], Angelique Catubig[1], Sebastian K. King[1,2,4,8], Gulcan Sarila[1], Ruili Li[1] and John M. Hutson[1,2,9]*

[1] F. Douglas Stephens Surgical Research Laboratory, Murdoch Children's Research Institute, Melbourne, VIC, Australia, [2] Department of Paediatrics, The University of Melbourne, Melbourne, VIC, Australia, [3] Discipline of Surgery, Sydney Medical School, The University of Sydney, Sydney, NSW, Australia, [4] Department of Paediatric Surgery, The Royal Children's Hospital, Melbourne, VIC, Australia, [5] Australian Phenomics Network, Department of Anatomy and Developmental Biology, Monash University, Melbourne, VIC, Australia, [6] Department of Anatomy and Developmental Biology, Monash Biomedicine Discovery Institute, Monash University, Melbourne, VIC, Australia, [7] Department of Biochemistry and Molecular Biology, Monash Biomedicine Discovery Institute, Monash University, Melbourne, VIC, Australia, [8] Department of Gastroenterology and Clinical Nutrition, The Royal Children's Hospital, Melbourne, VIC, Australia, [9] Department of Urology, The Royal Children's Hospital, Melbourne, VIC, Australia

Background: Duodenal atresia (DA) is a congenital obstruction of the duodenum, which affects 1 in 7000 pregnancies and requires major surgery in the 1st days of life. Three morphological DA types are described. In humans, the association between DA and Down syndrome suggests an underlying, albeit elusive, genetic etiology. In mice, interruption of fibroblast growth factor 10 (*Fgf10*) gene signaling results in DA in 30–50% of embryos, supporting a genetic etiology. This study aims to validate the spectrum of DA in two novel strains of *Fgf10* knock-out mice, in preparation for future and translational research.

Methods: Two novel CRISPR *Fgf10* knock-out mouse strains were derived and embryos generated by heterozygous plug-mating. E15.5–E19.5 embryos were genotyped with respect to *Fgf10* and micro-dissected to determine the presence and type of DA.

Results: One twenty seven embryos (32 wild-type, 34 heterozygous, 61 null) were analyzed. No wild-type or heterozygous embryos had DA. However, 74% of *Fgf10* null embryos had DA (49% type 1, 18% type 2, and 33% type 3).

Conclusion: Our CRISPR-derived strains showed higher penetrance of DA due to single-gene deletion of *Fgf10* in mice than previously reported. Further, the DA type distribution in these mice more closely reiterated that observed in humans. Future experiments will document RNA and protein expression of FGF10 and its key downstream signaling targets in normal and atretic duodenum. This includes exploitation of modern, high-fidelity developmental tools, e.g., $Fgf10^{flox/+}$–$tomato^{flox/flox}$ mice.

Keywords: duodenal obstruction, congenital intestinal atresia, fibroblast growth factor 10, morphogenesis, models, animal, CRISPR-Cas systems

OPEN ACCESS

Edited by:
Saverio Bellusci, Justus-Liebig-Universität Gießen, Germany

Reviewed by:
Denise Al Alam, University of Southern California, United States
Cho-Ming Chao, The German Center for Lung Research, Germany

****Correspondence:***
Warwick J. Teague
warwick.teague@rch.org.au

Specialty section:
This article was submitted to Genetic Disorders, a section of the journal Frontiers in Genetics

Received: *24 August 2018*
Accepted: *22 October 2018*
Published: *09 November 2018*

Citation:
Teague WJ, Jones MLM, Hawkey L, Smyth IM, Catubig A, King SK, Sarila G, Li R and Hutson JM (2018) FGF10 and the Mystery of Duodenal Atresia in Humans. Front. Genet. 9:530. doi: 10.3389/fgene.2018.00530

INTRODUCTION

Duodenal atresia (DA) is an important congenital cause of bowel obstruction in newborns. Often diagnosed prenatally on ultrasound scan or postnatally on abdominal radiograph, it requires intensive care after birth and major surgery in the 1st days of life. Three morphological types of DA are described, reflecting increasing degrees of obstruction and discontinuity; type 1: bowel

continuity but luminal obstruction or stenosis, type 2: bowel discontinuity with a connecting "bridge" of tissue, and type 3: bowel discontinuity with complete separation (Skandalakis and Gray, 1994). While modern surgical and neonatal management of DA achieves survival in more than 95% of cases (Khan et al., 2017), the embryological etiology of this condition remains an unanswered question amongst researchers, clinicians and patients' families.

In 1900, the Viennese anatomist Julius Tandler meticulously studied 11 human embryos with apparently normal gut, and theorized that the duodenum underwent a normal "solid cord" phase during development, secondary to exuberant endodermal (epithelial) growth. Further, he suggested failure of this proposed cord to re-canalize accounted for DA (Tandler, 1900). At the time, Tandler himself cautiously stated, "*It is clear to me that the opinion represented here does not exceed the status of a new hypothesis, and is not meant to exceed this*" (Nichol et al., 2011). Despite this caution, Tandler's theory was rapidly and widely adopted as dogma, and went largely unchallenged for many years. Merrot et al. (2006) were amongst the first to counter the "recanalization theory," asserting that it failed to explain the different morphological types and other variability seen in humans with DA. Furthermore, clinical reports have suggested a genetic basis for DA, with an autosomal recessive inheritance pattern reported for some cases (Berant and Kahana, 1970; Gross et al., 1996; Lambrecht and Kluth, 1998), and the well-recognized association with Down syndrome (Trisomy 21), which occurs in approximately one fifth of DA cases (Khan et al., 2017).

Fairbanks et al. (2004) were the first to report a link between DA and fibroblast growth factor (FGF) pathways in mice, specifically fibroblast growth factor 10 (FGF10) and its receptor fibroblast growth factor receptor 2b (FGFR2b). The FGF family of signaling molecules composed of at least 22 members involved in different aspects of organogenesis (Ornitz and Itoh, 2001), of which FGF10 is associated with instructive mesenchymal/epithelial interactions, occurring during budding and branching morphogenesis. The homozygous deletion of the *Fgf10* gene results in mice which are non-viable after birth due to lung agenesis, also exhibiting defects of the limbs, anterior pituitary gland, salivary glands, inner ear, teeth, skin, and skull (De Moerlooze et al., 2000; Mailleux et al., 2002). Since 2004, several reports have highlighted the importance of the FGF10-FGFR2b signaling pathway in DA as well as other congenital gut malformations such as caecal atresia (Kanard et al., 2005; Fairbanks et al., 2006; Nichol et al., 2011; Botham et al., 2012; Reeder et al., 2012).

We report here our experiences with an *Fgf10* knock-out mouse model, the strains for which were developed using novel CRISPR/Cas9 techniques. Our investigations to date have focused upon characterization of these strains, with a view toward hypothesis-driven determination of the genetic etiology of DA. Herein, we also discuss our future directions and investigations, which aim to make optimal use of modern and powerful developmental biology tools.

MATERIALS AND METHODS

Mouse Strain Derivation

Mutant animals were produced via CRISPR/Cas9 injection of C57/Bl6 oocytes by Monash University as a node of the Australian Phenomics Network (APN). In contrast to Yasue et al. (2014), who used CRISPR technique to target exon 1 of the *Fgf10* gene, our strains were derived using RNA guides targeting exon 3, designed with the aim of minimizing "off-target" events.

Thus, two novel murine strains were developed, the first with a 7 bp duplication and 140 bp deletion (B6-*Fgf10*<c.[464_470dup; 506_645del]APNMu>), and the second with a 13 bp deletion (B6-*Fgf10*<c.495_507delAPNMu>) (Eppig et al., 2006). These strains are coined here as "tm1" (464_470dup; 506_645del) and "tm2" (495_507del), respectively.

Animal Husbandry and Mating Strategies

Mice were maintained in a temperature- (24°C) and lighting- (14:10 h light-dark cycle) controlled room with free access to food and water within the accredited, institutional animal facility, and cared for in strict adherence with animal welfare and ethical requirements.

To establish breeding colonies for each strain, wild-type and heterozygous mice were mated, and liveborn pups genotyped to inform successive matings; see genotyping protocols below. *Fgf10* mutation is fatal in its homozygous (null) form due to lung agenesis (Sekine et al., 1999). Therefore, heterozygous plug-mating was reserved for experimental use only, with the aim of generating null, heterozygous, and wild-type embryos. For these experimental matings, pregnant dams were humanely culled at timed gestations to provide timed embryos ranging from E15.5 to E19.5.

Mouse Strain Genotype Characterization

Animals were genotyped by PCR analysis of DNA, extracted from tail or ear clippings. For the tm1 strain, a common forward primer was used (5′-GGAGTGTAGATCATTACATGGC-3′) with a tm1-specific reverse primer (5′-GTGAGGATACCATCTCTTTCTGTCC-3′) to produce a wild-type allele of 348 bp and mutant allele of 215 bp. For tm2, the same forward primer was used (5′-GGAGTGTAGATCATTACATGGC-3′) with the tm2-specific reverse primer (5′-GAATTCAGGGCTATGTCTTTGC-3′) producing a wild-type allele of 242 and 148 bp (390 bp before Nsi1 digestion) and mutant allele of 377 bp. The full details of DNA extraction and standard PCR protocols used are provided as **Supplementary Material**.

RNA and RT-qPCR Analysis

Total RNA was extracted using the RNeasy mini column (Qiagen, Cat: 74104), treated with DNase I (Qiagen, Cat: 79254), and the concentration was determined using NanoDrop spectrophotometer (Thermo Scientifics, 2000). Complementary DNA (cDNA) was synthesized using Bio-Rad iScript Advanced cDNA kit (Bio-Rad, Cat: 170-8842). Gene expression (2 μl of cDNA) was measured by GoTaq qPCR

(Promega, Cat: A6001) for real time quantitative polymerase chain reaction (RT-qPCR). Nucleotide sequences for *Fgf10* mRNA (*Fw* 5′-CACCTATGCATCTTTTAACTGGC-3′) (*Rv* 5′-TCTATGTTTGGATCGTCATGGGG-3′) was used and expression was normalized to *Rpl32* (*Fw* 5′-GAGG ACCAAGAAGTTCATCAGG-3′) (*Rv* 5′-CATTGTGGACCAGG AACTTGC-3′). The results were analyzed using the 7500 SDS software and relative expression was calculated to determine the fold change. Statistical analysis was performed in Prism 7.0 (GraphPad Software). Error bars on the results are presented as a standard error of the mean (SEM), and a p-value of <0.05 was considered significant. Statistical significance was evaluated using Student's unpaired t-test. The full details of RT-qPCR protocols used are provided as **Supplementary Material**.

Mouse Strain Phenotype Characterization

Embryos of gestation E15.5–E19.5 were humanely collected, culled and micro-dissected, during which key phenotypic features were recorded using bright-field microscopy. Greatest attention was shown to the morphology of the foregut, and determination made as to the presence and type of DA where applicable. Where ambiguous, duodenal morphology, and patency was further investigated using either wholemount immunostaining or paint-filling as adapted from techniques to delineate embryonic murine inner ear morphology (Morsli et al., 1998). The entirety of the duodenum from the pylorus to the duodenojejunal flexure was preserved intact, with back-light microscopy to confirm patency. Duodenal type was determined by consensus of two investigators at the time of dissection, and then representative images secondarily re-assessed independently by two or more authors blinded to the original type determination to provide internal validation.

Ethical Considerations

Ethics approval for the experiment was granted from the Murdoch Children's Research Institute (MCRI) Animal Ethics Committee (#A792), and the MCRI Institutional Biosafety Committee (#215-2014 PC1 NLRD).

RESULTS

Population

A total of 280 embryos were collected for this study (144 tm1 and 136 tm2 embryos).

Of the 144 tm1 strain embryos, genotyping determined 42 (29.2%) embryos to be wild-type, 74 (51.4%) heterozygous, and 28 (19.4%) *Fgf10* null embryos. With respect to gestation, 70 embryos were collected at E15.5, 32 at E16.5, 23 at E17.5, and 19 at E18.5. In total, 67 tm1 embryos were further micro-dissected, that being 20 wild-type, 19 heterozygous, and all 28 *Fgf10* null embryos.

Of the tm2 strain embryos, genotyping determined 35 (25.7%) embryos to be wild-type, 68 (50%) heterozygous, and 33 (24.3%) *Fgf10* null embryos. Eighteen embryos were collected at E15.5, 29 at E16.5, 25 at E17.5, 48 at E18.5, and 16 at E19.5. In total, 60 tm2 strain embryos were micro-dissected, that being 12 wild-type, 15 heterozygous, and all 33 *Fgf10* null embryos.

Genotype Characterization

The product from classic PCR genotyping confirmed expected genetics according to the tm1 and tm2 mutations (**Figure 1A**). The PCR product for each strain was formally sequenced to confirm correct action of the primers in each protocol. Semiquantitative PCR showed RNA expression for heterozygote and *Fgf10* null embryos in both tm1 and tm2 strains (**Figure 1A**). With wild-type litter mates providing controls for *Fgf10* gene expression in both strains, the heterozygous embryos expressed approximately half the *Fgf10* (tm1 = 42.29% and tm2 = 51.16%), and no expression was seen in *Fgf10* null embryos.

General Phenotype Characterization

The general phenotype of both tm1 and tm2 strain *Fgf10* null embryos was consistent with previously reported *Fgf10* knock-out mouse strains (Sekine et al., 1999; Sala et al., 2011; Teshima et al., 2016). These *Fgf10* null embryos demonstrated characteristic lack of limbs and smaller than normal body size (**Figures 1B,C**), abnormal facies (**Figure 1C**), lung agenesis (**Figures 1D–F**) anomalous tracheal rings (**Figure 1F**), and caecal atresia (**Figure 1G**). Expected (i.e., normal) changes in organ morphology during development notwithstanding, these abnormalities in general phenotype were represented at all gestational ages of *Fgf10* null embryos assessed. Further, as our experimental question and aim placed primary focus on abdominal foregut morphology, we did not undertake detailed comparisons of these general phenotypic features during *Fgf10* null embryo development, e.g., between tm1 and tm2.

The general phenotype of tm1 and tm2 *Fgf10* heterozygotes mirrored that of wild-type (i.e., normal) litter mates, including morphologically normal limb buds, bilateral and branched lungs, normal appearance of tracheal rings and no caecal atresia. Finally, whilst the morphology and ultrastructure of some organs in *Fgf10* heterozygous mice is known to be abnormal (Jaskoll et al., 2005; El Agha et al., 2012), these were not formally assessed for the tm1 and tm2 strains, with the exception of foregut morphology as detailed below.

Duodenal Phenotype Characterization

Wild-type litter mates provided controls for normal gastric, pyloric, and duodenal morphology (**Figure 2A**). Without exception, *Fgf10* heterozygous embryos also demonstrated normal gastroduodenal morphology (**Figures 2B,C**), as distinct from *Fgf10* null embryos.

Of 61 *Fgf10* null embryos, 45 (74%) demonstrated DA. With DA observed in 21 (75%) of tm1, and 24 (73%) of tm2 *Fgf10* null embryos. *Fgf10* null embryos without DA did, however, demonstrate microgastria, which was a universal phenotypic feature for the *Fgf10* null cohort (**Figures 2D,E**). Both tm1 and tm2 strains provided examples for all three DA types: tm1 with 9 (43%) type 1, 4 (19%) type 2, and 8 (38%) type 3 DA; tm2 with 13 (54%) type 1, 4 (17%) type 2, and 7 (29%) type 3 DA (**Figures 2F–K**). The small sample sizes for each strain precluded

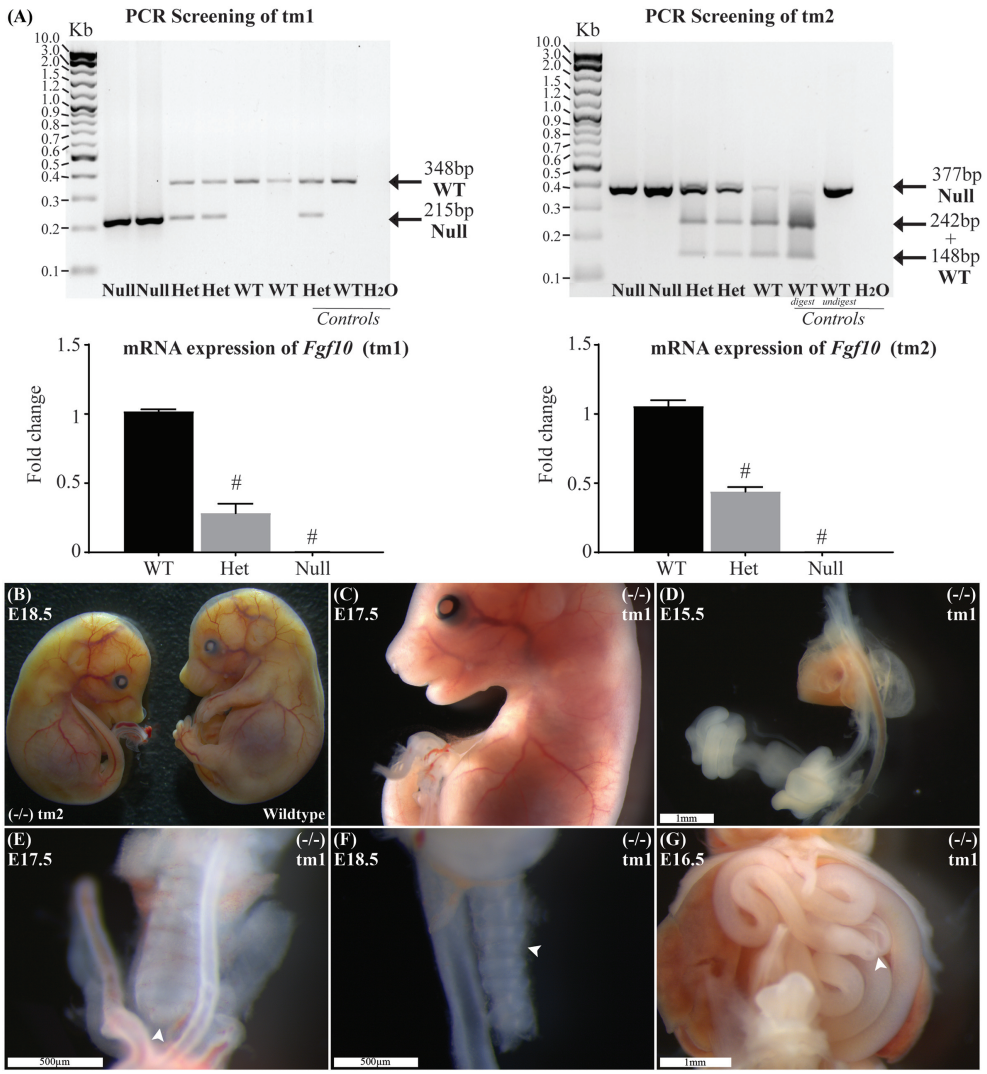

FIGURE 1 | Genotype and general phenotype characterization. **(A)** Product from standard and RT-qPCR shows genotyping and RNA expression for both tm1 and tm2 strains. **(B)** General phenotype of a representative *Fgf10* null embryo (left embryo) with the expected lack of limbs and smaller than body-size when compared with wild type litter mate (right embryo). Fgf10 null embryos also demonstrated: abnormal facies **(C)**, lung agenesis **(D–F)**, anomalous tracheal rings **(F)**, and caecal atresia **(G)**. Arrows highlight features of interest. Gestational ages for panels **B–G** are as stated. $^{\#}p$-value < 0.001, comparing either *Fgf10* heterozygous or null mice to their wild-type littermates using Student's *t*-test.

meaningful comparison of relative type frequency between the strains and gestational ages.

Duodenal atresia in *Fgf10* null embryos reiterated the type morphology of DA in humans. In each case, the morphology of DA was recognizably distinct from the physiological luminal narrowing at the junction between the stomach and duodenum, i.e., pylorus (**Figures 2A–E**). Type 1 DA is characterized in these examples (**Figures 2F,G**) by continuity of the outer (serosal) aspect of the fetal gut wall, whilst the lumen is obstructed by a web at the site of atresia. Other examples of type 1 DA (not shown in **Figure 2**) demonstrate stenosis of the gut lumen, such that the lumen is notably and abnormally narrowed, whilst epithelial continuity persists. Type 2 DA (**Figures 2H,I,M**) represents a more severe duodenal anomaly, in which the gut wall and lumen are discontinuous, albeit a bridge or span of tissue maintains a physical connection between the two ends. Finally, type 3 DA (**Figures 2J–L**) is the most severe duodenal phenotype, recognized here by complete disconnection of the atretic gut ends.

Other Intestinal Phenotype Characterization

Given the recognized association between DA and esophageal atresia in humans, DA-affected *Fgf10* null embryos were analyzed for esophageal continuity. **Figure 2L** (tm1) and **Figure 2M** (tm2) provide representative images of the universally intact esophagus for these embryos, i.e., no esophageal atresia. The 100% penetrance of caecal atresia in tm1 and tm2 *Fgf10* null embryos has been noted above.

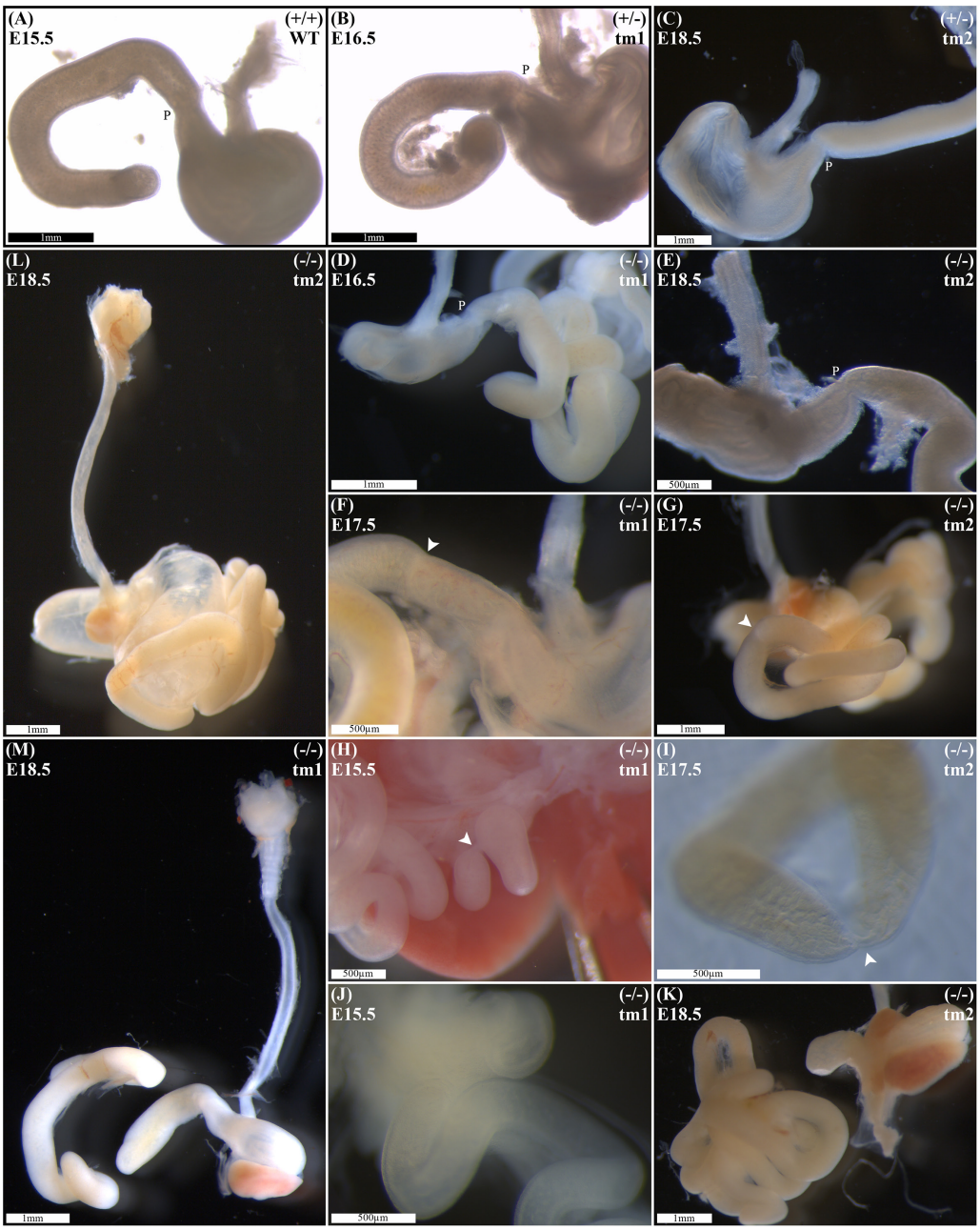

FIGURE 2 | Duodenal phenotype characterization. Normal gastric, pyloric, and duodenal morphology was demonstrated by wild type embryos **(A)**, as well as *Fgf10* heterozygous embryos for tm1 **(B)**, and tm2 **(C)** strains. Null *Fgf10* embryos universally demonstrated microgastria, but duodenal morphology varied according to presence and type of DA. Null embryos provided examples of: normal continuity and morphology of the duodenum for tm1 **(D)** and tm2 **(E)**; type 1 DA, tm1 **(F)** and tm2 **(G)**; type 2 DA, tm1 **(H)** and tm2 **(I)**; and type 3 DA, tm1 **(J)** and tm2 **(K)**. **(L)** Type 2 DA demonstrating a "double bubble" with significantly dilated proximal duodenum; tm2. **(M)** Type 3 DA demonstrating an intact esophagus, in the presence of tracheal atresia; tm1. Annotations denote genotype, scale bars, and location of pylorus, P. Arrows indicate location atresia in type 1 DA and type 2 DA examples. Gestational ages for each panel are as stated.

DISCUSSION

A Necessary Model

A limited understanding of the etiology of DA presently restricts the design and assessment of strategies to prevent or ameliorate the phenotype of DA in humans. As it is not possible to directly investigate the pathogenesis of DA in human embryos, a suitable animal model is required to advance knowledge toward such translation. Although the association between DA and Down syndrome is the best understood genetic link with DA in humans, the animal models for Down syndrome are not applicable here as they universally fail to demonstrate DA or indeed any other

Trisomy 21-associated gastrointestinal abnormalities (Delabar et al., 2006).

Like Trisomy 21 in humans, interruption of FGF10/FGFR2b signaling is the best demonstrated genetic link to DA in mice (Fairbanks et al., 2004; Kanard et al., 2005; Botham et al., 2012; Reeder et al., 2012). Despite this, mice lacking expression of either *Fgf10* or its receptor gene did not provide a promising model for future study due to relatively poor penetration of the DA phenotype with DA present in only 35–45% (Fairbanks et al., 2004; Kanard et al., 2005; Botham et al., 2012; Reeder et al., 2012). Further, these strains failed to reiterate in mice the full spectrum and distribution of DA types seen in humans within a single strain with, at times, unexplained contradiction in the distribution of DA types demonstrated (Kanard et al., 2005; Reeder et al., 2012).

An Improved and Promising Model

The DA penetrance and types evident in our novel CRISPR-derived, *Fgf10* knockout mouse strains, reported here as tm1 and tm2, represent an important and positive development in the field. In distinction to previous reports, our novel *Fgf10* null embryo strains demonstrate both a significantly higher penetrance (74%), as well as examples for all three morphological types of DA.

The basis for the differences in DA penetrance and DA type distribution between our and previously reported *Fgf10* knockout mouse strains remains unclear. The strains are of consistent background, namely C57/Bl6 (Fairbanks et al., 2004; Kanard et al., 2005), and whilst the genetics differ, each represents a nonsense mutation (Eppig et al., 2006). The exact genetics, and its interplay on downstream targets, may well be playing a role in penetration of the DA phenotype. Interestingly, Reeder et al. (2012) observed that the addition of haploinsufficiency of retinaldehyde dehydrogenase 2 (*Raldh2* ±) to *Fgfr2IIIb* homozygous null embryos resulted in a reduced penetrance of DA, accompanied by a less severe DA phenotype. Of note, type 2 DA was evident in *Fgfr2IIIb*(−/−); *Raldh2*(±) but not in *Fgfr2IIIb*(−/−) mouse embryos (Reeder et al., 2012). Reeder et al. (2012) results could be interpreted as demonstrating a relationship between DA penetrance and type distribution in the murine model. If this were so, a model demonstrating all DA types might be expectedly undermined by weak penetrance. However, our results demonstrate both improved penetrance as well as expression of all three DA types, affirming applicability of the tm1 and tm2 strains presented here as a promising model of DA.

Whilst the performance of the tm1 and tm2 strains is enhanced, neither strain demonstrated complete penetrance of DA. Incomplete penetrance of the duodenal phenotype is distinct from other phenotypic features of *Fgf10* null embryos, which demonstrate complete penetrance, e.g., absent limbs, absent lungs, and caecal atresia. Presently undefined developmental differences notwithstanding, we consider the incomplete penetrance of DA indicates redundancy in the requirements for "normal" duodenal morphogenesis. As such, tm1 and tm2 *Fgf10* null embryos without DA provide a rich population for future study, to discern signature signaling differences when compared with wild-type, heterozygote and DA-affected *Fgf10* null embryos. Understanding such differences may reveal key etiological components responsible for DA, as well as attributes for exploitation in future translations to achieve normal duodenal development in humans with a genetic predisposition to DA.

A Hypothesis-Driven and Disciplined Model

Fundamentally, we hypothesize that the etiology of DA in humans is genetic, with the causative genetic changes located downstream of the FGF10/FGFR2b signaling pathway. This downstream locus may account for the incomplete penetrance of DA in the murine model as discussed previously. Further, interruption of downstream signaling may account for both the lack of either *FGF10* or *FGFR2b* gene deletion in human DA cases previously screened for this (Tatekawa et al., 2007), as well as the absence of non-survivable associations of *FGF10* deletion in humans with DA, such as pulmonary agenesis.

However, before we may begin to scrutinize and develop this hypothesis within our *Fgf10* knockout model, our rigor must be first directed to gaining a better understanding of the temporo-spatial expression patterns relevant to the Fgf10/Fgfr2b signaling pathway in the murine fore and midgut. Existing similar expression patterns have focused on the more anterior foregut (Nyeng et al., 2007, 2008), the question of gut boundary regionalization (as reviewed in San Roman and Shivdasani, 2011), or lacked sufficient temporo-spatial resolution to adequately inform further investigation within our DA model (Fon Tacer et al., 2010). To understand the expression pattern of *Fgf10* in the developing duodenum, we plan to exploit the fidelity and imaging possibilities afforded by the *Fgf10*^{CreERT2}_tomato$^{flox/flox}$ [B6-*Fgf10*<tm1.1(cre/ERT2)Sbel> Gt(ROSA)26Sor<tm9(CAG-tdTomato)Hze>] and *Fgf10*$^{flox/+}$–tomato$^{flox/flox}$ [B6.*Fgf10*<tm1.2 Sms>] mouse strains (El Agha et al., 2012). Using these powerful developmental biology tools, we will assess stage- and tissue-specific expression of *Fgf10*, and correlate this with coincident expression patterns for *Fgfr2b* and their collective downstream targets. Expression patterns will be assessed using immunohistochemistry, as well standard and quantitative PCR methods.

Having established normal expression patterns, we will then be able to compare and contrast expression of the same signaling pathway components in tm1 and tm2 *Fgf10* heterozygote and *Fgf10* null embryos, both those with and without DA. The use of staged-gestation embryos, including embryos from earlier gestation than the previous threshold of E15.5, will allow us to determine when and how in development molecular divergence between these genetically distinct mice arises. These temporo-spatial molecular characteristics will then be correlated with concurrent normal or abnormal morphogenic changes in the developing duodenum.

A Testable and Translational Model

The ultimate aim of our DA research is to identify targets for translational therapies to prevent or ameliorate DA in humans. In humans, DA is associated with a wide range of

associated anomalies, the presence of which negatively impact prognosis (Hemming and Rankin, 2007; Choudhry et al., 2009). We have established an ethics-approved (#DB077) clinical database for all children managed with DA at The Royal Children's Hospital, Melbourne since 2000. Within this cohort of more than 100 DA patients (unpublished data), we have identified a thought-provoking subset with associated anomalies akin to Fgf10-Fgfr2b signaling-related defects, namely craniofacial, limb and lung anomalies (Sekine et al., 1999; De Moerlooze et al., 2000; Teshima et al., 2016). We consider this human subset to be at particular "risk" of an underlying genetic changes impacting the FGF10/FGFR2b signaling pathway, and plan to undertake detailed clinical genetic phenotyping and exon sequencing of phenotypically homogenous patient groups. Candidate mutations thus identified will be tested by introducing these variants into mice using CRISPR, and confirming whether this (or these) mutations do indeed generate DA in these increasingly bespoke murine models. Moreover, a putative genetic mutation (or mutations) responsible for DA would represent a landmark development in the understanding of normal gut morphogenesis and DA, opening the door to superior genetic and antenatal counseling, as well as potential future therapies for DA-affected fetuses and families.

AUTHOR CONTRIBUTIONS

WT conceived the project and prepared the study design, methodology, molecular biology techniques, performed the microsurgical tissue dissection, image capture, analyzed and interpreted the results, and wrote and finalized the manuscript. MJ assisted in study design, molecular biology techniques, microsurgical tissue dissection, image capture, results analysis and interpretation, preparation, and finalization of the manuscript. LH assisted in design and performance of mouse strain derivation using CRISPR technique. IS assisted in design and performance of mouse strain derivation using CRISPR technique and finalization of the manuscript. AC assisted in design and performance of molecular biology techniques. GS performed the molecular biology techniques. SK assisted in study design, results interpretation, and finalization of the manuscript. RL assisted in study design, establishment of methodology, molecular biology techniques, and finalization of the manuscript. JH mentored WT, assisted in study design, results interpretation, and finalization of the manuscript.

FUNDING

This work was supported by a Royal Australasian College of Surgeons (RACS) Foundation in Surgery Small Project Grant, and an Australian New Zealand Association of Paediatric Surgeons (ANZAPS) Douglas Stephens Research Grant. In addition, Associate Professor WT and Associate Professor SK are both generously supported by The Royal Children's Hospital Foundation. APN was supported by the Australian Government Department of Education through the National Collaborative Research Infrastructure Strategy (NCRIS) Program.

ACKNOWLEDGMENTS

Dr. Treve Menheniott (MCRI) is thanked for his assistance with PCR primer design. We thank Dr. Dirk Truman, Australian Phenomics Network (APN), for his assistance with CRISPR target design and injection.

SUPPLEMENTARY MATERIAL

The Supplementary Material for this article can be found online at: https://www.frontiersin.org/articles/10.3389/fgene.2018.00530/full#supplementary-material

REFERENCES

Berant, M., and Kahana, D. (1970). Familial duodenal atresia. *Arch. Dis. Child.* 45, 281–282. doi: 10.1136/adc.45.240.281

Botham, R. A., Franco, M., Reeder, A. L., Lopukhin, A., Shiota, K., Yamada, S., et al. (2012). Formation of duodenal atresias in fibroblast growth factor receptor 2IIIb-/- mouse embryos occurs in the absence of an endodermal plug. *J. Pediatr. Surg.* 47, 1369–1379. doi: 10.1016/j.jpedsurg.2012.02.001

Choudhry, M. S., Rahman, N., Boyd, P., and Lakhoo, K. (2009). Duodenal atresia: associated anomalies, prenatal diagnosis and outcome. *Pediatr. Surg. Int.* 25, 727–730. doi: 10.1007/s00383-009-2406-y

De Moerlooze, L., Spencer-Dene, B., Revest, J. M., Hajihosseini, M., Rosewell, I., and Dickson, C. (2000). An important role for the IIIb isoform of fibroblast growth factor receptor 2 (FGFR2) in mesenchymal-epithelial signalling during mouse organogenesis. *Development* 127, 483–492.

Delabar, J. M., Aflalo-Rattenbac, R., and Créau, N. (eds) (2006). Developmental defects in trisomy 21 and mouse models. *ScientificWorldJournal* 6, 1945–1964. doi: 10.1100/tsw.2006.322

El Agha, E., Al Alam, D., Carraro, G., MacKenzie, B., Goth, K., De Langhe, S. P., et al. (2012). Characterization of a novel fibroblast growth factor 10 (Fgf10) knock-in mouse line to target mesenchymal progenitors during embryonic development. *PLoS One* 7:e38452. doi: 10.1371/journal.pone.0038452

Eppig, J. J., Fox, J., Barthold, S., Davvison, M., Newcomber, C., Quimby, F., et al. (2006). Mouse strain and genetic nomenclature: an abbreviated guide. *Mouse Biomed. Res.* 1, 79–98.

Fairbanks, T. J., Kanard, R., Del Moral, P. M., Sala, F. G., De Langhe, S., Warburton, D., et al. (2004). Fibroblast growth factor receptor 2 IIIb invalidation–a potential cause of familial duodenal atresia. *J. Pediatr. Surg.* 39, 872–874. doi: 10.1016/j.jpedsurg.2004.02.026

Fairbanks, T. J., Sala, F. G., Kanard, R., Curtis, J. L., Del Moral, P. M., De Langhe, S., et al. (2006). The fibroblast growth factor pathway serves a regulatory role in proliferation and apoptosis in the pathogenesis of intestinal atresia. *J. Pediatr. Surg.* 41, 132–136; discussion 132–136. doi: 10.1016/j.jpedsurg.2005.10.054

Fon Tacer, K., Bookout, A. L., Ding, X., Kurosu, H., John, G. B., Wang, L., et al. (2010). Research resource: comprehensive expression atlas of the fibroblast growth factor system in adult mouse. *Mol. Endocrinol.* 24, 2050–2064. doi: 10.1210/me.2010-0142

Gross, E., Armon, Y., Abu-Dalu, K., Gale, R., and Schiller, M. (1996). Familial combined duodenal and jejunal atresia. *J. Pediatr. Surg.* 31:1573.

Hemming, V., and Rankin, J. (2007). Small intestinal atresia in a defined population: occurrence, prenatal diagnosis and survival. *Prenat. Diagn.* 27, 1205–1211. doi: 10.1002/pd.1886

Jaskoll, T., Abichaker, G., Witcher, D., Sala, F. G., Bellusci, S., Hajihosseini, M. K., et al. (2005). FGF10/FGFR2b signaling plays essential roles during in vivo

embryonic submandibular salivary gland morphogenesis. *BMC Dev. Biol.* 5:11. doi: 10.1186/1471-213X-5-11

Kanard, R. C., Fairbanks, T. J., De Langhe, S. P., Sala, F. G., Del Moral, P. M., Lopez, C. A., et al. (2005). Fibroblast growth factor-10 serves a regulatory role in duodenal development. *J. Pediatr. Surg.* 40, 313–316. doi: 10.1016/j.jpedsurg.2004.10.057

Khan, A., Tanny, S. T., Perkins, E. J., Hunt, R. W., Hutson, J. M., King, S. K., et al. (2017). Is selective echocardiography in duodenal atresia the future standard of care? *J. Pediatr. Surg.* 52, 1952–1955. doi: 10.1016/j.jpedsurg.2017.08.046

Lambrecht, W., and Kluth, D. (1998). Hereditary multiple atresias of the gastrointestinal tract: report of a case and review of the literature. *J. Pediatr. Surg.* 33, 794–797. doi: 10.1016/S0022-3468(98)90225-1

Mailleux, A. A., Spencer-Dene, B., Dillon, C., Ndiaye, D., Savona-Baron, C., Itoh, N., et al. (2002). Role of FGF10/FGFR2b signaling during mammary gland development in the mouse embryo. *Development* 129, 53–60.

Merrot, T., Anastasescu, R., Pankevych, T., Tercier, S., Garcia, S., Alessandrini, P., et al. (2006). Duodenal duplications. Clinical characteristics, embryological hypotheses, histological findings, treatment. *Eur. J. Pediatr. Surg.* 16, 18–23. doi: 10.1055/s-2006-923798

Morsli, H., Choo, D., Ryan, A., Johnson, R., and Wu, D. (1998). Development of the mouse inner ear and origin of its sensory organs. *J. Neurosci.* 18, 3327–3335. doi: 10.1523/JNEUROSCI.18-09-03327.1998

Nichol, P. F., Reeder, A., and Botham, R. (2011). Humans, mice, and mechanisms of intestinal atresias: a window into understanding early intestinal development. *J. Gastrointest. Surg.* 15, 694–700. doi: 10.1007/s11605-010-1400-y

Nyeng, P., Norgaard, G. A., Kobberup, S., and Jensen, J. (2007). FGF10 signaling controls stomach morphogenesis. *Dev. Biol.* 303, 295–310. doi: 10.1016/j.ydbio.2006.11.017

Nyeng, P., Norgaard, G. A., Kobberup, S., and Jensen, J. (2008). FGF10 maintains distal lung bud epithelium and excessive signaling leads to progenitor state arrest, distalization, and goblet cell metaplasia. *BMC Dev. Biol.* 8:2. doi: 10.1186/1471-213X-8-2

Ornitz, D. M., and Itoh, N. (2001). Fibroblast growth factors. *Genome Biol.* 2, reviews3005.1–reviews3005.12. doi: 10.1186/gb-2001-2-3-reviews3005

Reeder, A. L., Botham, R. A., Zaremba, K. M., and Nichol, P. F. (2012). Haploinsufficiency of retinaldehyde dehydrogenase 2 decreases the severity and incidence of duodenal atresia in the fibroblast growth factor receptor 2IIIb-/- mouse model. *Surgery* 152, 768–775; discussion 775–776. doi: 10.1016/j.surg.2012.07.022

Sala, F. G., Del Moral, P. M., Tiozzo, C., Alam, D. A., Warburton, D., Grikscheit, T., et al. (2011). FGF10 controls the patterning of the tracheal cartilage rings via *Shh*. *Development* 138, 273–282. doi: 10.1242/dev.051680

San Roman, A. K., and Shivdasani, R. A. (2011). Boundaries, junctions and transitions in the gastrointestinal tract. *Exp. Cell Res.* 317, 2711–2718. doi: 10.1016/j.yexcr.2011.07.011

Sekine, K., Ohuchi, H., Fujiwara, M., Yamasaki, M., Yoshizawa, T., Sato, T., et al. (1999). Fgf10 is essential for limb and lung formation. *Nat. Genet.* 21, 138–141. doi: 10.1038/5096

Skandalakis, J. E., and Gray, S. W. (1994). *Embryology for Surgeons : The Embryological Basis for the Treatment of Congenital Anomalies*, 2nd Edn. Baltimore, MD: Williams & Wilkins, 1101.

Tandler, J. (1900). Zur entwicklingsgeschichte des menschlichen duodenums im frühen embryonalstadium. *Morphol. Jahrb.* 29, 187–216.

Tatekawa, Y., Kanehiro, H., and Nakajima, Y. (2007). Duodenal atresia associated with "apple peel" small bowel without deletion of fibroblast growth factor-10 or fibroblast growth factor receptor 2IIIb: report of a case. *Surg. Today* 37, 430–433. doi: 10.1007/s00595-006-3415-2

Teshima, T. H., Lourenco, S. V., and Tucker, A. S. (2016). Multiple cranial organ defects after conditionally knocking out Fgf10 in the neural crest. *Front. Physiol.* 7:488. doi: 10.3389/fphys.2016.00488

Yasue, A., Mitsui, S. N., Watanabe, T., Sakuma, T., Oyadomari, S., Yamamoto, T., et al. (2014). Highly efficient targeted mutagenesis in one-cell mouse embryos mediated by the TALEN and CRISPR/Cas systems. *Sci. Rep.* 4:5705. doi: 10.1038/srep05705

Conflict of Interest Statement: The authors declare that the research was conducted in the absence of any commercial or financial relationships that could be construed as a potential conflict of interest.

Copyright © 2018 Teague, Jones, Hawkey, Smyth, Catubig, King, Sarila, Li and Hutson. This is an open-access article distributed under the terms of the Creative Commons Attribution License (CC BY). The use, distribution or reproduction in other forums is permitted, provided the original author(s) and the copyright owner(s) are credited and that the original publication in this journal is cited, in accordance with accepted academic practice. No use, distribution or reproduction is permitted which does not comply with these terms.

frontiers in Genetics

MINI REVIEW
published: 14 November 2018
doi: 10.3389/fgene.2018.00545

Role of Fibroblast Growth Factor 10 in Mesenchymal Cell Differentiation During Lung Development and Disease

Jin Wu[1†], Xuran Chu[1,2†], Chengshui Chen[3] and Saverio Bellusci[1,2,3]*

[1] Institute of Life Sciences, Wenzhou University, Wenzhou, China, [2] Excellence Cluster Cardio-Pulmonary System, Universities of Giessen and Marburg Lung Center, Member of the German Center for Lung Research, Justus-Liebig-University Giessen, Giessen, Germany, [3] Department of Pulmonary and Critical Care Medicine, The First Affiliated Hospital of Wenzhou Medical University, Wenzhou, China

OPEN ACCESS

Edited by:
Takashi Nakamura,
Tohoku University, Japan

Reviewed by:
Jangho Kim,
Chonnam National University, South Korea
Tetsuya S. Tanaka,
Elixirgen, LLC, United States
Maria Fernanda Forni,
Universidade de São Paulo, Brazil

***Correspondence:**
Saverio Bellusci
saverio.bellusci@innere.med.uni-giessen.de

[†] These authors have contributed equally to this work

Specialty section:
This article was submitted to Stem Cell Research, a section of the journal Frontiers in Genetics

Received: 24 July 2018
Accepted: 26 October 2018
Published: 14 November 2018

Citation:
Wu J, Chu X, Chen C and Bellusci S (2018) Role of Fibroblast Growth Factor 10 in Mesenchymal Cell Differentiation During Lung Development and Disease. Front. Genet. 9:545. doi: 10.3389/fgene.2018.00545

During organogenesis and pathogenesis, fibroblast growth factor 10 (Fgf10) regulates mesenchymal cell differentiation in the lung. Different cell types reside in the developing lung mesenchyme. Lineage tracing *in vivo* was used to characterize these cells during development and disease. Fgf10-positive cells in the early lung mesenchyme differentiate into multiple lineages including smooth muscle cells (SMCs), lipofibroblasts (LIFs) as well as other cells, which still remain to be characterized. Fgf10 signaling has been reported to act both in an autocrine and paracrine fashion. Autocrine Fgf10 signaling is important for the differentiation of LIF progenitors. Interestingly, autocrine Fgf10 signaling also controls the differentiation of pre-adipocytes into mature adipocytes. As the mechanism of action of Fgf10 on adipocyte differentiation via the activation of peroxisome proliferator-activated receptor gamma (Pparγ) signaling is quite well established, this knowledge could be instrumental for identifying drugs capable of sustaining LIF differentiation in the context of lung injury. We propose that enhanced LIF differentiation could be associated with improved repair. On the other hand, paracrine signaling is considered to be critical for the differentiation of alveolar epithelial progenitors during development as well as for the maintenance of the alveolar type 2 (AT2) stem cells during homeostasis. Alveolar myofibroblasts (MYFs), which are another type of mesenchymal cells critical for the process of alveologenesis (the last phase of lung development) express high levels of Fgf10 and are also dependent for their formation on Fgf signaling. The characterization of the progenitors of alveolar MYFs as well the mechanisms involved in their differentiation is paramount as these cells are considered to be critical for lung regeneration. Finally, lineage tracing in the context of lung fibrosis demonstrated a reversible differentiation from LIF to "activated" MYF

during fibrosis formation and resolution. FGF10 expression in the lungs of idiopathic pulmonary fibrosis (IPF) vs. donors as well as progressive vs. stable IPF patients supports our conclusion that FGF10 deficiency could be causative for IPF progression. The therapeutic application of recombinant human FGF10 is therefore very promising.

Keywords: Fgf10, lung, lipofibroblasts, alveolar myofibroblasts, fibrosis

INTRODUCTION

Fibroblast growth factor 10 is a member of the Fgf7 subfamily of secreted growth factors. Fgf10 is mostly secreted by the mesenchyme and acts on the epithelium via the Fgfr2b and Fgfr1b receptor (Ornitz and Itoh, 2015). *Fgf10* deletion in mice leads to aborted limb development as well as perinatal lethality due to impaired lung development. This phenotype is shared with *Fgfr2b* knockout embryos indicating that Fgf10 acts mostly via Fgfr2b during organogenesis (Sekine et al., 1999; De Moerlooze et al., 2000).

Fibroblast growth factor 10 also contributes to the formation of the white adipose tissue and the associated mammary gland as well as the heart, liver, brain, kidney, prostate, cecum, ocular and salivary glands, thymus, inner ear, tongue and trachea (Itoh and Ohta, 2014). In the developing lung, *Fgf10* expression is detected at the onset of the pseudoglandular stage (embryonic day (E) 9.5-E16.5), as early as E10, when the primary bronchi are formed. *Fgf10* expression in the distal mesenchyme between E10 and E12.5 coincides with epithelial bud formation suggesting that this growth factor plays a key role during branching morphogenesis. Interestingly, at E10, the rudiments of the two primary bronchi are clearly visible in the lungs of *Fgf10* KO embryos suggesting that Fgf10 is dispensable for the very initial step of lung development involving the formation of the two primary lung buds from the ventral foregut endoderm. At E13.5, Fgf10 expression is found ubiquitously throughout the mesenchyme and its role in guiding the branching process is not clear (Bellusci et al., 1997). Its widespread spatial expression suggests that Fgf10 plays a permissive more than an instructive role during the branching process. It is very likely that other players such as heparan sulfate proteoglycans, which have a high affinity for Fgf10 as well as other growth factors, are interacting with Fgf10 to restrict its activity distally in order to control the branching process. For details on Fgf10 signaling *per se*, we refer to other mini-reviews also published as part of this special issue (Ndlovu et al., 2018; Watson and Francavilla, 2018). During the subsequent stages of mouse development (canalicular: E16.5 to E17.5, saccular: E17.5 to postanatal day (P) 5; alveolar: P5 to P28), Fgf10 is still significantly expressed suggesting that Fgf10 could play multiple roles beyond the pseudoglandular stage not only in the epithelium, but also directly or indirectly in the mesenchyme. This last aspect in particular has been widely ignored, yet may hold the key to potential therapeutic interventions to treat human lung diseases.

Abbreviations: Adrp, Adipose differentiation-related protein; ASMC, Airway smooth muscle cell; AT1, Alveolar type 1; AT2, Alveolar type 2; Fgf10, Fibroblast growth factor 10; Fgfr2b, Fibroblast growth factor receptor 2 b; LIF, Lipofibroblast; miR, microRNA; MYF, Myofibroblast; Pdgfrα, Platelet derived growth factor receptor alpha; Pparγ, Peroxisome proliferator-activated receptor gamma; PthrP, Parathyroid hormone related protein; RA, Retinoic acid; SHF, Second heart field; Tgfβ1, Transforming growth factor beta 1; VSMC, Vascular smooth muscle cell.

DIFFERENT MESENCHYMAL CELL TYPES EXIST IN THE DEVELOPING LUNG MESENCHYME

The embryonic lung mesenchyme displays many different types of cells such as chondrocytes, airway smooth muscle cells (ASMCs), vascular smooth muscle cells (VSMCs), nerve cells, endothelial cells, lipofibroblasts (LIFs), lymphatic cells, alveolar myofibroblasts (MYFs) and cells that are uncharacterized previously. Altogether these cells play important roles during embryonic development (**Figure 1A**) as well as homeostasis in the post-natal stages (for more details on this topic please see El Agha et al., 2014).

FGF10 REGULATES MESENCHYMAL CELL DIFFERENTIATION IN THE LUNG

Ramasamy et al. (2007) demonstrated that *Fgf10* hypomorphic embryos (displaying around 20% of the normal *Fgf10* expression) exhibited major defects in different mesenchymal cell types. Those include ASMCs, endothelial cells and alveolar MYFs. As Fgf10 acts mostly on the epithelium via the fibroblast growth factor receptor 2b (Fgfr2b), some of these defects could be due to impaired epithelial to mesenchymal interactions. However, it was also reported that Fgf10 acts directly on the mesenchyme to control the differentiation of LIF progenitors (Al Alam et al., 2015). In the following sections, we will delineate what is known about the formation of the different mesenchymal cell lineages in the lung and further develop the function of Fgf10 in this context.

LINEAGE TRACING *IN VIVO* HAS BEEN USED TO CHARACTERIZE DIFFERENT MESENCHYMAL LINEAGES DURING LUNG DEVELOPMENT

The secondary heart field (SHF), a cell set contributing progressively to the poles of the elongating heart tube during

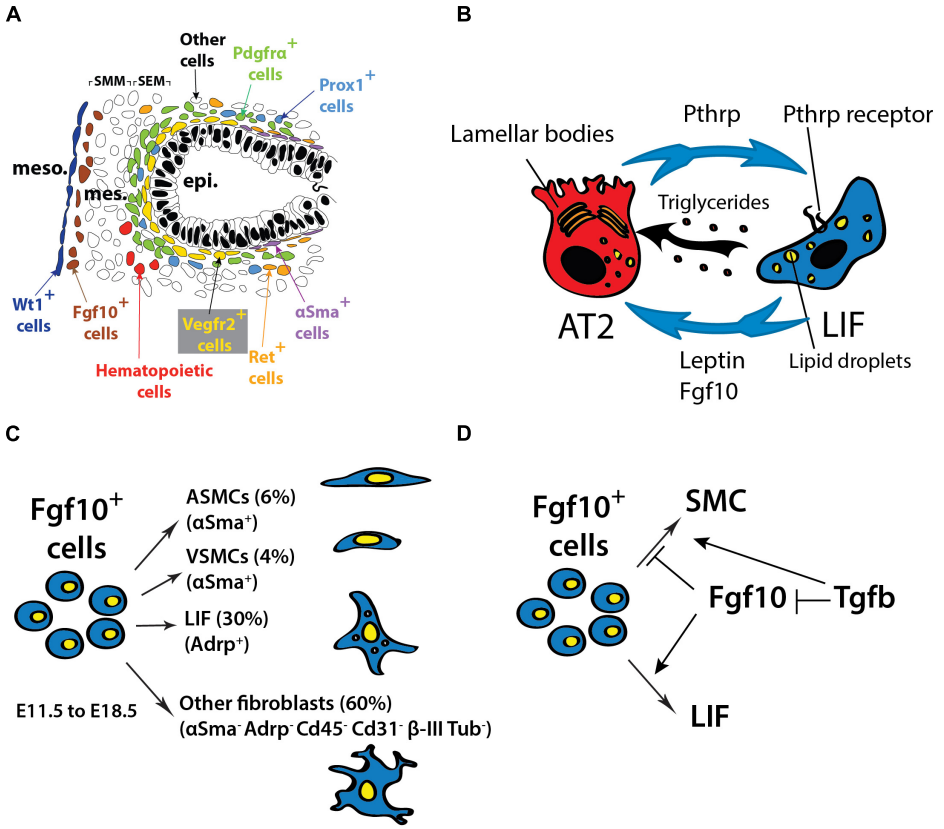

Development		Disease	
ASMC	El Agha et al, 2014 Mailleux et al, 2005	Activated MYF (IPF)	El Agha et al, 2017
VSMC	El Agha et al, 2014	VSMC (PH)	El Agha et al, 2018
Alveolar MYF	Moiseenko et al., 2017		
LIF	El Agha et al, 2014 McGowan et al., 2015		
Others	El Agha et al, 2014		

FIGURE 1 | (A) Schematic of the cells in the distal part of the lung at E13.5 showing the different lung domains including the mesothelium (meso), the submesothelial mesenchyme (SMM), the subepithelial mesenchyme (SEM), the epithelium (epi) and the position of the different mesenchymal cell progenitors located at this stage. **(B)** Interaction between AT2 and LIF. LIF produce leptin and triglycerides that are essential for surfactant production. The Pthrp/ Pparγ axis is critical for LIF formation and maintenance. **(C)** Fgf10-positive cells lineage-traced at E11.5 and analyzed at E18.5. **(D)** Fgf10 acts directly on the mesenchyme to induce the differentiation of LIF progenitors. Tgfβ1 antagonizes this differentiation (adapted from El Agha et al., 2014; Al Alam et al., 2015; Chao et al., 2015). **(E)** Table summarizing the cell types expressing *Fgf10* in the lung during development and disease. IPF, Idiopathic pulmonary fibrosis; PH, pulmonary hypertension.

looping morphogenesis, was recently described as a source of multipotent cardiopulmonary progenitors and is identified and defined by the co-expression of *Wnt2*, *Gli1* and *Isl1* (Peng et al., 2013). These cells migrate into the lung and differentiate into vascular and airway SMCs as well as other lineages. Fate-mapping of platelet derived growth factor receptor beta (Pdgfrβ)-positive cells showed that VSMCs do not arise from mesothelial but rather from mesenchymal progenitor cells (Greif et al., 2012). Two studies using animal models published contradicting results. The first study using the *Wilms tumor 1 homolog* (*Wt1*)-*Cre* transgenic line, showed that the mesothelium contains progenitors for vascular but not airway SMCs (Que et al., 2008). On the other hand, the second study showed, using the inducible $Wt1^{Cre-ERT2/+}$ knock-in mice, that the mesothelium is a source of airway and vascular SMCs as well as desmin-positive fibroblasts (Dixit et al., 2013). More work will have to be done to clarify the contribution of the mesothelium to the SMC lineages during development. Endothelial progenitors

express fetal liver kinase 1 (Flk-1 or Vegfr2) (Yamaguchi et al., 1993; Kappel et al., 1999; del Moral et al., 2006a,b) whereas lymphatic cells arise from prospero homeobox protein 1 (*Prox1*)-positive progenitor cells (Srinivasan et al., 2007). Finally, nerve cells originate from the neural crest and are marked by receptor tyrosine kinase expression (Langsdorf et al., 2011).

FGF10-POSITIVE CELLS IN THE EARLY LUNG MESENCHYME DIFFERENTIATE INTO MULTIPLE LINEAGES

Mailleux et al. (2005) previously utilized the transgenic reporter line *Mlcv1v-nLacZ-24* (or simply $Fgf10^{lacZ}$) to demonstrate that Fgf10-positive cells serve as progenitors for ASMCs in the distal lung during early development. These results were validated using an $Fgf10^{Cre-ERT2}$ knock-in line (El Agha and Bellusci, 2014). Lineage labeled Fgf10-positive cells mainly differentiates into the airway and vascular SMC and the LIF lineages (El Agha et al., 2014; **Figures 1C,E**). However, it is still unclear whether this population of Fgf10-positive mesenchymal progenitor cells contains unipotent or multipotent progenitor cells. The progeny of Fgf10-expressing cells needs to be analyzed using single-cell transcriptomic approaches as well as multi-color Cre-reporter mice to better characterize these progenitor cells. During the early pseudoglandular stage, Fgf10 itself is not acting on the ASMCs to control their differentiation. It has been proposed that bone morphogenetic protein 4 (Bmp4), which is induced by Fgf10 in the distal epithelium, is responsible for their differentiation (Mailleux et al., 2005). In addition, it has been shown that β-catenin signaling in the mesenchyme does not contribute to the differentiation of Fgf10-positive progenitors but rather to their proliferation (De Langhe et al., 2008). More recently, *miR-142-3p*, a miR that is enriched in the mesenchyme, was reported to target *adenomatous polyposis coli* (*Apc*), a gene encoding a negative regulator of β-catenin. Upregulated *Apc* expression in the lung mesenchyme upon *miR-142* knock down using morpholinos leads to the inhibition of mesenchymal proliferation and premature SMC differentiation. The corresponding loss of mesenchymal β-catenin signaling in the mesenchyme was associated with decreased *Fgfr2c* and *Fgf10* expression (Carraro et al., 2014).

LIF-DERIVED FGF10 AND AT2 STEM CELL HOMEOSTASIS

Lipofibroblasts are adipocyte-like fibroblasts located close to AT2 stem cells (O'Hare and Sheridan, 1970; Vaccaro and Brody, 1978). It has recently been suggested that LIFs represent a special niche for AT2 stem cells. LIFs are likely important for AT2 stem cell homeostasis and express high levels of *Pparg*, *Adrp* and *Pthrp receptor* (*PthrpR*) (Habiel and Hogaboam, 2017). LIFs also contribute to the maturation of alveolar epithelial cells and the formation of surfactant, a phospholipoprotein complex produced by AT2 cells involved in the reduction of surface tension (Rehan et al., 2005). The growth of AT2 stem cells in Matrigel to form alveolosphere-like structures is drastically enhanced when co-cultured with LIFs (Barkauskas et al., 2013). The role that LIFs play under these conditions remains unclear. As previously described, LIFs (or at least a subset of them) are derived from Fgf10-positive cells (El Agha and Bellusci, 2014). Interestingly, a significant proportion of the LIFs in the post-natal lungs are positive for *Fgf10* expression (Al Alam et al., 2015). It is possible that Fgf10 secreted by the LIFs is needed for the maintenance of the AT2 stem cells in the adult lung during homeostasis and/or after injury (**Figure 1B**). This function would then be similar to what is proposed for the role of Fgf10 in the developing lung, where Fgf10 maintains the sex-determining region Y-box 9 (Sox9)-positive multipotent progenitor cells at the tips of the developing lung. In the future, it will be important to characterize the role of Fgf10 in LIF formation/maintenance in the context of the adult AT2 stem cell niche. In addition, a better characterization of the molecular differences among the diverse LIF subpopulations (Fgf10-positive and -negative LIFs) will be important to identify the mesenchymal cell types that play critical roles in repair processes after lung injury.

COMMON MOLECULAR MECHANISMS CONTROLLING LIF AND ADIPOCYTE FORMATION: A CRITICAL ROLE FOR FGF10 IN CONTROLLING CELL DIFFERENTIATION

Lipofibroblasts and adipocytes require Pparγ, a master regulator of lipogenesis, for their differentiation (Torday et al., 2003). *In vitro* differentiation assays using NIH3T3-L1 pre-adipogenic cells show that insulin and cortisone, which are used to push these cells toward a mature adipocyte phenotype, induce *Fgf10* expression. In this system, use of blocking antibodies against Fgf10 inhibits pre-adipocyte differentiation (Sakaue et al., 2002). *In vivo*, *Fgf10* is detected both in pre- and mature adipocytes and is critical for white adipose tissue formation (Mailleux et al., 2002; Sakaue et al., 2002). Beyond its role on differentiation, Fgf10 has also been described to increase cell proliferation in the white adipose tissue (Konishi et al., 2006).

At the end of the pseudoglandular stage of lung development (from E15.5 to E16.5), a subpopulation of mesenchymal cells containing lipid vesicles can be detected using LipidTOX, a non-toxic fluorescent dye that has been instrumental to label LIFs for immunofluorescence studies, flow cytometry and sorting (Al Alam et al., 2015). The emergence of these cells is associated with the increase in the expression of *Fgf10*, *Adrp* and *Pparg* in the mesenchymal compartment. Even though Fgf10-positive LIFs represent only a subset of the total LIF population, the inactivation of Fgfr2b ligands as

well as decreased *Fgf10* expression decreases the overall LIF population. Our results indicate that Fgfr1b and Fgfr2b in the mesenchyme, which can both bind Fgf10, play redundant functions in controlling LIF formation. Interestingly, the LIFs found in the P8 lung display high levels of *Fgf10* and its associated receptors *Fgfr1b* and *Fgfr2b* (McGowan and McCoy, 2015) suggesting that Fgf10 may also play a role postnatally.

In the human lung, *FGF10* expression is increased between 10 and 18 weeks of gestation (corresponding to the pseudoglandular stage of lung development) while *ADRP* expression is unchanged between 10 and 21 weeks (the canalicular stage in human is from 17 to 26 weeks of gestation) (Chao et al., 2015), These results suggest that as in mice, the formation of LIFs in humans occurs mostly during the mid-canalicular stage of lung development.

The emerging picture is that Fgf10 signaling is critical for LIF formation during the late phases of lung development. Fgf10 secreted by mesenchymal progenitor cells, as well as Pthrp, a cytokine secreted by the AT2 cells are both capable of triggering Pparγ signaling on LIF progenitors, which is likely important for their differentiation along the LIF lineage, as well as for the maintenance of their differentiation. Indeed, the deletion of *Pthrp* in mice results in impaired alveoleogenesis and deficient surfactant production (Rubin et al., 2004; Torday and Rehan, 2007; Rehan and Torday, 2012). LIFs depend on Pparγ signaling to express Adrp, which is required for triglycerides trafficking from LIFs cytosol to adjacent AT2 cells. This process is essential for surfactant production (Schultz et al., 2002). Leptin, which is secreted by LIFs, also acts on AT2 to increase surfactant synthesis (Torday et al., 2002). Additionally, LIFs contain high levels of RA, which has been shown to be critical for alveolar septation (Simon and Mariani, 2007).

During lung development, Tgfβ1 signaling through Alk5 in the mesenchyme is critical to control the cell fate decision between MYFs and LIFs. *Alk5* conditional knockout (CKO) lungs displayed reduced number of Acta2-positive cells and corresponding increase in LIFs. Alk5 signaling directly or indirectly regulates the expression of *Pdgfra*, *Pparg*, *pair related homeobox 1* (*Prrx1*) and *zinc finger protein 343* (*Zfp423*) (Li et al., 2016). As Tgfβ1 and Fgf10 signaling pathways antagonize each other (McQualter et al., 2013) (**Figure 1D**), it is proposed that the loss of Tgfβ1 signaling in the mesenchyme allows enhanced Fgf10 signaling in the same cellular compartment thereby leading to increased LIF formation.

ALVEOLAR MYF AND PDGFA SIGNALING

Alveolar MYFs are Acta2-positive fibroblasts present in the lung during alveologenesis, that starts postnatally in mice. These cells secrete extracellular matrix (ECM) fibers such as elastin and collagen that are required for secondary-crest formation (Vaccaro and Brody, 1978; Noguchi et al., 1989; Yamada et al., 2005; **Figures 2A–D**). Alveolar MYFs have been suggested to originate from Pdgfrα-positive cells. Pdgfa signaling via Pdgfrα plays a critical role in the formation of the alveolar MYFs as demonstrated by the lungs in *Pdgfa*-null newborns that suffer from the absence of alveolar MYFs and consequently display arrested alveologenesis (Bostrom et al., 1996; Lindahl et al., 1997). However, lineage tracing of Pdgfrα-positive cells during lung development is lacking in the studies mentioned above. It needs to be demonstrated that Pdgfrα-positive cells labeled early during the pseudoglandular stage are progenitors for alveolar MYFs. Postnatally, Pdgfrα is expressed by multiple mesenchymal cell types including ASMCs, alveolar MYFs, and LIFs (Ntokou et al., 2015; Li et al., 2018).

ECTOPIC MESENCHYMAL FGF10-FGFR2B AUTOCRINE LOOP DURING THE EARLY PSEUDOGLANDULAR STAGE LEADS TO THE ABSENCE OF ALVEOLAR MYF FORMATION AT BIRTH

So far, the impact of fibroblast growth factor signaling on the differentiation of the lung mesenchyme has been poorly investigated. *Fgfr2c*$^{+/\Delta}$ mice were used as an *in vivo* experimental model to investigate the function of mesenchymal Fgf signaling. These mice ectopically express Fgfr2b in mesenchymal tissues from early developmental stages and therefore display an Apert syndrome-like phenotype, which is characterized by malformations of the face, skull and feet and the respiratory system (Hajihosseini et al., 2001). Former studies have proved that early establishment of autocrine Fgf10–Fgfr2b signaling in the lung mesenchyme inhibits the formation of the SMCs as well as the alveolar MYFs and results in reduced fibronectin and elastin deposition. In addition, the branching process is impaired and the level of Fgf and canonical β-catenin signaling in the epithelium is reduced. These mutant lungs display arrested development of the terminal airways and an "emphysema like" phenotype postnatally (De Langhe et al., 2006). These results indicate that Fgf signaling represses the differentiation of the early alveolar MYF progenitors. It is not clear whether this is due to a direct effect of Fgf on the mesenchyme or to an indirect effect via the epithelium. However, Fgf9, which is the natural and major Fgf ligand acting on the mesenchyme during early lung development, is capable of repressing *in vitro* the expression of Acta2 in primary cultures of lung mesenchymal cells. This suggests that *in vivo* Fgf signaling maintains the mesenchymal progenitors undifferentiated and proliferative (del Moral et al., 2006a). A counter-intuitive result was obtained by Perl and Gale. The authors took advantage of the *Tg(Sftpc-rtTA)/+; Tg(tet(O)solFgfr2b)/+* double-transgenic mice to induce in the lung, via the administration of docycyclin, the expression of soluble Fgfr2b acting as a receptor to sequester all Fgfr2b ligands. Expression of this decoy receptor in the lung from E14.5 to E18.5 disrupts alveologenesis postnatally. Secondary-septa formation with the presence of alveolar MYFs, can be partially enhanced in this model by treating the animals with RA between P35 and P48. The effect of RA can be blocked by the concomitant re-expression of the soluble form of Fgfr2b

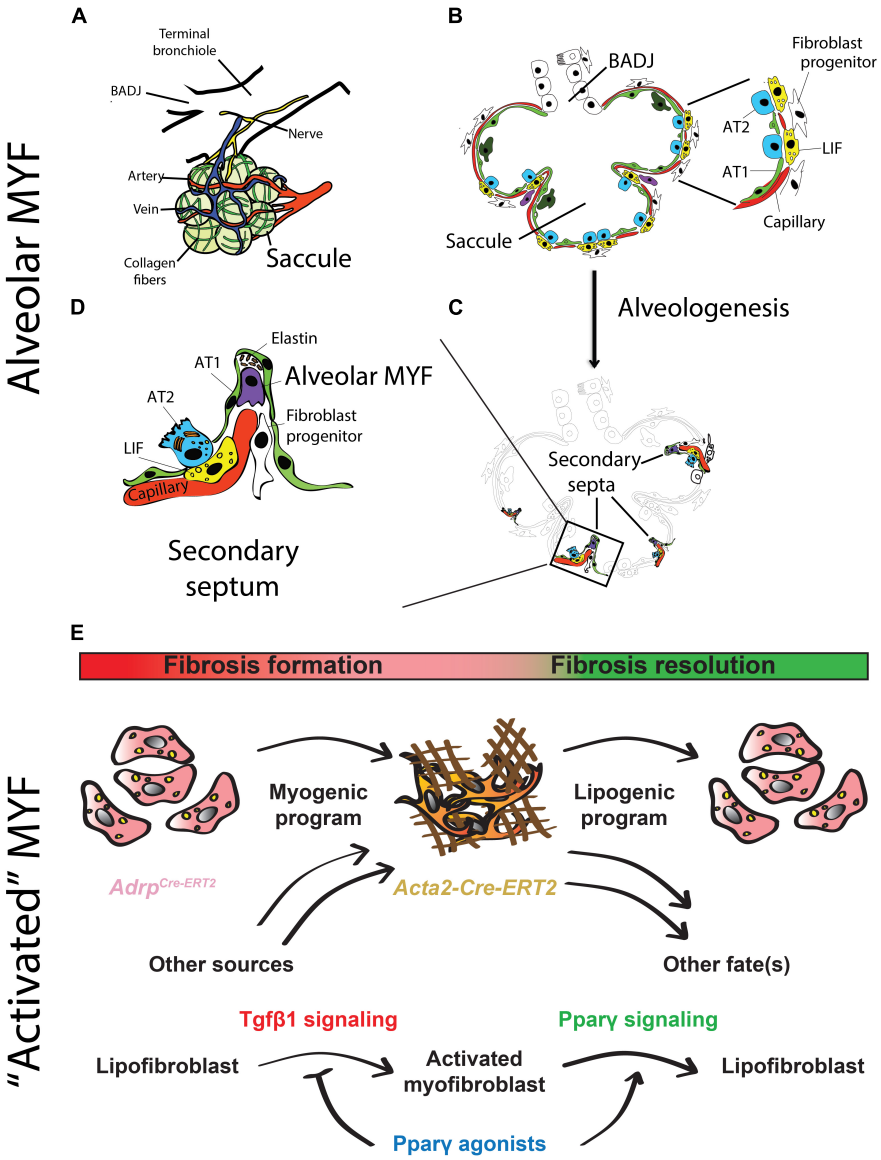

FIGURE 2 | Schematic representation of alveologenesis and cell types involved. **(A)** During the saccular stage (stage preceding the beginning of alveologenesis), the lung exhibits primitive alveoli (called saccules), which are surrounded by blood vessels, collagen fibers and nerves. **(B)** The alveolar saccule in the saccular stage is characterized by the presence of AT1/2, coating the walls of the saccule, surfactant production, production of collagen and elastin by fibroblasts as well as expansion of the capillary tree. **(C)** During the alveolar stage, the lung undergoes a subdivision of the saccules by a process called "secondary septation" that will give rise to mature alveoli. **(D)** Secondary septa start to appear at the place of elastin deposition, which is produced by alveolar MYF. The septa elongate toward the alveolar sac airspace. A double layer of capillaries become thinner giving rise to a one-layer network for more efficient gas exchange. **(E)** The origin and fate of "activated" MYFs was investigated using lineage-tracing approaches. LIFs are progenitors for "activated" MYFs in lung fibrosis. Some of the labeled "activated" MYFs dedifferentiate to LIF during fibrosis resolution. Pparγ activation blocks LIF-to-MYF transdifferentiation induced by Tgfβ1 and enhances "activated" MYF-to-LIF transdifferentiation. (adapted from Chao et al., 2016; El Agha et al., 2017).

using doxycycline. This leads to an increase in Pdgfrα-positive cells and an associated decrease in Acta2-positive cells (Perl and Gale, 2009). One possible interpretation for these results is that alveolar MYFs require Fgfr2b ligands, likely Fgf10, for their differentiation. It was also proposed that Pdgfrα-positive LIFs can transdifferentiate into alveolar MYFs but, so far, there is no lineage tracing-based evidence to support this conclusion. It was also shown that Fgfr2b ligands are required for alveolar MYFs formation during alveolar regeneration after pneumonectomy (Chen et al., 2012). However, the attenuation of all Fgfr2b ligands postnatally does not result in any lung development defect. Alveologenesis, which is characterized by the formation of secondary septa containing alveolar MYFs, occurs normally (Hokuto et al., 2003). It can therefore be concluded that normal alveologenesis does not require secreted Fgfr2b ligands.

CHARACTERIZATION OF THE ALVEOLAR MYFS IN THE DEVELOPING LUNG

The analysis of the differentiation of labeled progenitor cells (using the *Fgf10*^{CreERT2}, *Wt1*^{CreERT2}, *Gli1*^{CreERT2}, and *Axin2*^{CreERT2} driver lines crossed with a fluorescent reporter line) toward the MYF and SMC lineages showed that Fgf10-positive and Wt1-positive cells displayed a minor contribution to the SMC lineages, while Gli1-positive and Axin2-positive cells significantly contributed to both the SMC and alveolar MYF lineages, but also to other lineages (Moiseenko et al., 2017). Labeling at E11.5 of Acta2-positive cells using the *Tg (Acta2-CreERT2)* transgenic line showed that these cells did not proliferate to produce new SMCs at later stages. However, if the labeling of Acta2-positive cells occured at E15.5, the labeled cells constituted most of the SMCs (85–97%) as well as the majority of the alveolar MYF progenitors in the E18.5 lungs. Gene arrays of Acta2-positive cells isolated by fluorescence-activated cell sorting allowed establishing transcriptomic signatures for airway and VSMCs vs alveolar MYF progenitors at E18.5. Interestingly, alveolar MYF progenitors expressed very high levels of *Fgf10* compared to SMCs (Fold Change = 29.04, $p < 0.0001$). It is still unclear if Fgf10 acts in an autocrine or paracrine way on alveolar MYF progenitors to sustain their differentiation (Moiseenko et al., 2017). These results will allow defining pathways potentially important for the formation of alveolar MYF.

EVIDENCE FOR LIF TO "ACTIVATED" MYF REVERSIBLE DIFFERENTIATION DURING FIBROSIS FORMATION AND RESOLUTION

Idiopathic pulmonary fibrosis (IPF) is a form of progressive interstitial lung disease of unknown origin. As no efficient treatment is available, IPF patients exhibit a high lethality rate. In this disease, a prominent number of "activated" MYFs are present in the lung parenchyma. These cells excessively deposit extracellular matrix proteins, literally turning the lung into "a block of cement". These changes compromise the lung architecture and function, thereby leading to impaired gas exchange. The origin of "activated" MYFs as well as the molecular mechanisms governing the formation and the fate of these cells in fibrosis formation and resolution have been investigated using specific driver lines to target different mesenchymal populations (El Agha et al., 2017; **Figure 2E**). Interestingly, a reversible lipogenic-to-myogenic transdifferentiation during fibrosis formation in mice has been demonstrated. In addition, in IPF lungs, compared to the donor controls, loss of LIFs and accumulation of "activated" MYFs were observed (El Agha et al., 2017). Finally, this fate switching has been validated in primary human lung fibroblasts from IPF patients, suggesting that drugs that are capable of enhancing myogenic-to-lipogenic transdifferentiation could be instrumental in treating IPF patients (El Agha et al., 2017). Interestingly, the concept of LIF to "activated" MYF transition was already proposed but not proven using modern lineage tracing approaches by several teams including Rehan and colleagues. They showed that LIFs derived from neonatal rat lungs transdifferentiated into MYF in response to hyperoxia (Rehan and Torday, 2003) as well as to nicotine exposure (Rehan et al., 2005).

FGF10 EXPRESSION INVERSELY CORRELATES WITH DISEASE PROGRESSION IN IPF PATIENTS

The expression levels of *FGF10* in IPF vs non-IPF donor lung tissue samples were monitored by qPCR. A significant increase in *FGF10* expression in IPF lungs compared to donor's lungs was reported (El Agha et al., 2017). By immunohistochemisty, FGF10 expression in IPF lungs appears to be higher in highly remodeled parenchyma compared to the fibrotic foci (which are sites of early fibrotic response) (El Agha et al., 2018). It has been therefore proposed that FGF10 could be associated with either the fibrotic process or with the associated repair process. Suggesting that FGF10 is rather involved in the repair process, it was shown that FGF10 expression levels are inversely correlated with disease progression (El Agha et al., 2018). Supporting this result, mesenchymal stromal cells isolated from the bronchoalveolar lavage of patients with progressive IPF displayed less *FGF10* expression compared to corresponding cells isolated from patients with stable IPF suggesting that FGF10 deficiency could be indeed causative for disease progression (Chanda et al., 2016).

ACTIVATION OF PPARγ SIGNALING ANTAGONIZES TGFβ1-MEDIATED FIBROGENIC RESPONSE

Peroxisome proliferator-activated receptor gamma signaling activation by rosiglitazone has been identified to antagonize Tgfβ1 activity in IPF patients and as a result decreased fibrosis formation in bleomycin-treated mice was reported (Genovese et al., 2005; El Agha et al., 2017). One potential mechanism of action of rosiglitazone is reinforcing the lipogenic phenotype at the expense of the MYF phenotype. This hypothesis is consistent with increased LIF formation in the developing lung *in vivo* following deletion of the Tgfβ1 receptor *Alk5* in the mesenchyme (Li et al., 2016). To test this possibility, human lung fibroblasts were cultured in the presence of rosiglitazone (20 mM) and/or recombinant Tgfβ1 (1 ng/mL). When the cells were treated with TGFβ1, the expression of lipogenic markers *PPARγ* and *ADRP* were significantly inhibited while the expression of myogenic markers *ACTA2* and *COL1A1* were promoted compared to the normal cells. Rosiglitazone treatment strongly up-regulated *ADRP* expression and reduced the effect of TGFβ1. Consistent with this finding, rosiglitazone treatment significantly attenuated TGFβ1-mediated up-regulation of *ACTA2* and *COL1A1*. These results demonstrate that TGFβ1 in IPF functions

by reinforcing the myogenic phenotype. Recently, it was reported that metformin, an adenosine monophosphate-activated protein kinase (AMPK) agonist used to treat diabetes was also efficient in accelerating fibrosis resolution after bleomycin-injury in mice (Rangarajan et al., 2018). It remains to be determined if metformin is also capable of accelerating the "activated" MYFs to LIFs transdifferentiation. An important question to ask is what is the impact of metformin on the LIF-AT2 interaction and on *FGF10* expression in particular: does it re-enforce this interaction? This would suggest that metformin could be used as a powerful drug to enhance lung regeneration after injury.

FGF10 AND OTHER HUMAN LUNG DISEASES

Fibroblast growth factor 10 haploinsufficiency in human is associated with chronic obstructive pulmonary disease (COPD). COPD is a disease characterized by major remodeling of the conducting airway epithelium as well as alterations of the respiratory epithelium. Patients with *FGF10* haploinsufficiency display a nonreversible airway obstruction ultimately resulting in the development of COPD (Klar et al., 2011). Reduction in FGF10 levels in the lungs of prematurely born infants is also associated with a disease called bronchopulmonary dysplasia, where the lungs are arrested at the saccular stage, prior to the formation of the alveoli, the mature respiratory units critical for normal lung function (**Figure 1E**). For more information on this topic, we refer the readers to two excellent reviews, which are part of this special issue on FGF10 in development, homeostasis, disease and repair after injury (Prince, 2018; Yuan et al., 2018).

WHAT IS NEXT FOR FGF10?

Even though a plethora of knowledge has been gained on Fgf10's mechanisms of action, interaction with different signaling pathways, and its cellular targets, progress in the field has been delayed by the fact that early *Fgf10* deletion *in vivo* leads to organ agenesis. The rapid and complete disappearance of the organ or cells of interest following *Fgf10* deletion makes it difficult, for example, to identify its primary transcriptional targets and its biological activity. Better tools, such as inducible and reversible specific decoy Fgfr2b receptors will be very useful in this context. Despite its powerful effect in promoting lung regeneration following different types of injury, the use of FGF10 in clinical trials is lagging behind. One major obstacle for its clinical use is the relatively low level of biological activity of the corresponding recombinant protein, which associates with a high affinity with heparan sulfate proteoglycans, resulting in the trapping of the protein in the extracellular matrix. Progressive loss of activity and lack of diffusion of the protein, combined with undesired side effects (such as swelling of the tongue or the eyelid and high mucus production in the gut due to goblet cell metaplasia) following systemic FGF10 intravenous delivery, have obscured potential beneficial effects. In the future, localized administration of a stable form of FGF10 should be the new *modus operandi* for successful clinical trials.

AUTHOR CONTRIBUTIONS

JW and XC wrote the review. CC and SB edited the review.

FUNDING

SB was supported by grants from the Deutsche Forschungsgemeinschaft (DFG; BE4443/6-1, KFO309 P7, and SFB1213-projects A02 and A04), DZL, and First Affilated Hospital, Wenzhou Medical University. JW and XC were supported through a scholarship from Wenzhou University.

ACKNOWLEDGMENTS

We thank Dr. Elie El Agha and Mathew Jones for critical reading of this mini-review. We apologize to those colleagues whose references have been omitted from this review; due to space restrictions and focus we were not able to include all articles on this interesting and diverse subject matter.

REFERENCES

Al Alam, D., El Agha, E., Sakurai, R., Kheirollahi, V., Moiseenko, A., Danopoulos, S., et al. (2015). Evidence for the involvement of fibroblast growth factor 10 in lipofibroblast formation during embryonic lung development. *Development* 142, 4139–4150. doi: 10.1242/dev.109173

Barkauskas, C. E., Cronce, M. J., Rackley, C. R., Bowie, E. J., Keene, D. R., Stripp, B. R., et al. (2013). Type 2 alveolar cells are stem cells in adult lung. *J. Clin. Invest.* 123, 3025–3036. doi: 10.1172/JCI68782

Bellusci, S., Grindley, J., Emoto, H., Itoh, N., and Hogan, B. L. (1997). Fibroblast growth factor 10 (FGF10) and branching morphogenesis in the embryonic mouse lung. *Development* 124, 4867–4878.

Bostrom, H., Willetts, K., Pekny, M., Leveen, P., Lindahl, P., Hedstrand, H., et al. (1996). PDGF-A signaling is a critical event in lung alveolar myofibroblast development and alveogenesis. *Cell* 85, 863–873. doi: 10.1016/S0092-8674(00)81270-2

Carraro, G., Shrestha, A., Rostkovius, J., Contreras, A., Chao, C. M., El Agha, E., et al. (2014). miR-142-3p balances proliferation and differentiation of mesenchymal cells during lung development. *Development* 141, 1272–1281. doi: 10.1242/dev.105908

Chanda, D., Kurundkar, A., Rangarajan, S., Locy, M., Bernard, K., Sharma, N. S., et al. (2016). Developmental Reprogramming in Mesenchymal Stromal Cells of Human Subjects with Idiopathic Pulmonary Fibrosis. *Sci. Rep.* 6:37445. doi: 10.1038/srep37445

Chao, C. M., El Agha, E., Tiozzo, C., Minoo, P., and Bellusci, S. (2015). A breath of fresh air on the mesenchyme: impact of impaired mesenchymal development on the pathogenesis of bronchopulmonary dysplasia. *Front. Med.* 2:27. doi: 10.3389/fmed.2015.00027

Chao, C.-M., Moiseenko, A., Zimmer, K.-P., and Bellusci, S. (2016). Alveologenesis: key cellular players and fibroblast growth factor 10 signaling. *Mol. Cell. Pediatr.* 3:17. doi: 10.1186/s40348-016-0045-7

Chen, L., Acciani, T., Le Cras, T., Lutzko, C., and Perl, A. K. (2012). Dynamic regulation of platelet-derived growth factor receptor alpha expression in

alveolar fibroblasts during realveolarization. *Am. J. Respir. Cell Mol. Biol.* 47, 517–527. doi: 10.1165/rcmb.2012-0030OC

De Langhe, S. P., Carraro, G., Tefft, D., Li, C., Xu, X., Chai, Y., et al. (2008). Formation and differentiation of multiple mesenchymal lineages during lung development is regulated by beta-catenin signaling. *PLoS One* 3:e1516. doi: 10.1371/journal.pone.0001516

De Langhe, S. P., Carraro, G., Warburton, D., Hajihosseini, M. K., and Bellusci, S. (2006). Levels of mesenchymal FGFR2 signaling modulate smooth muscle progenitor cell commitment in the lung. *Dev. Biol.* 299, 52–62. doi: 10.1016/j.ydbio.2006.07.001

De Moerlooze, L., Spencer-Dene, B., Revest, J. M., Hajihosseini, M., Rosewell, I., and Dickson, C. (2000). An important role for the IIIb isoform of fibroblast growth factor receptor 2 (FGFR2) in mesenchymal-epithelial signalling during mouse organogenesis. *Development* 127, 483–492.

del Moral, P. M., De Langhe, S. P., Sala, F. G., Veltmaat, J. M., Tefft, D., Wang, K., et al. (2006a). Differential role of FGF9 on epithelium and mesenchyme in mouse embryonic lung. *Dev. Biol.* 293, 77–89.

del Moral, P. M., Sala, F. G., Tefft, D., Shi, W., Keshet, E., Bellusci, S., et al. (2006b). VEGF-A signaling through Flk-1 is a critical facilitator of early embryonic lung epithelial to endothelial crosstalk and branching morphogenesis. *Dev. Biol.* 290, 177–188.

Dixit, R., Ai, X., and Fine, A. (2013). Derivation of lung mesenchymal lineages from the fetal mesothelium requires hedgehog signaling for mesothelial cell entry. *Development* 140, 4398–4406. doi: 10.1242/dev.098079

El Agha, E., and Bellusci, S. (2014). Walking along the fibroblast growth factor 10 route: a key pathway to understand the control and regulation of epithelial and mesenchymal cell-lineage formation during lung development and repair after injury. *Scientifica* 2014:538379. doi: 10.1155/2014/538379

El Agha, E., Herold, S., Al Alam, D., Quantius, J., MacKenzie, B., Carraro, G., et al. (2014). Fgf10-positive cells represent a progenitor cell population during lung development and postnatally. *Development* 141, 296–306. doi: 10.1242/dev.099747

El Agha, E., Moiseenko, A., Kheirollahi, V., De Langhe, S., Crnkovic, S., Kwapiszewska, G., et al. (2017). Two-Way Conversion between Lipogenic and Myogenic Fibroblastic Phenotypes Marks the Progression and Resolution of Lung Fibrosis. *Cell Stem Cell* 20:e263. doi: 10.1016/j.stem.2016.10.004

El Agha, E., Schwind, F., Ruppert, C., Gunther, A., Bellusci, S., Schermuly, R. T., et al. (2018). Is the fibroblast growth factor signaling pathway a victim of receptor tyrosine kinase inhibition in pulmonary parenchymal and vascular remodeling? *Am. J. Physiol. Lung Cell. Mol. Physiol.* 315, L248–L252. doi: 10.1152/ajplung.00140.2018

Genovese, T., Cuzzocrea, S., Di Paola, R., Mazzon, E., Mastruzzo, C., Catalano, P., et al. (2005). Effect of rosiglitazone and 15-deoxy-Delta12,14-prostaglandin J2 on bleomycin-induced lung injury. *Eur. Respir. J.* 25, 225–234. doi: 10.1183/09031936.05.00049704

Greif, D. M., Kumar, M., Lighthouse, J. K., Hum, J., An, A., Ding, L., et al. (2012). Radial construction of an arterial wall. *Dev. Cell* 23, 482–493. doi: 10.1016/j.devcel.2012.07.009

Habiel, D. M., and Hogaboam, C. M. (2017). Heterogeneity of Fibroblasts and Myofibroblasts in Pulmonary Fibrosis. *Curr. Pathobiol. Rep.* 5, 101–110. doi: 10.1007/s40139-017-0134-x

Hajihosseini, M. K., Wilson, S., De Moerlooze, L., and Dickson, C. (2001). A splicing switch and gain-of-function mutation in FgfR2-IIIc hemizygotes causes Apert/Pfeiffer-syndrome-like phenotypes. *Proc. Natl. Acad. Sci. U.S.A.* 98, 3855–3860. doi: 10.1073/pnas.071586898

Hokuto, I., Perl, A. K., and Whitsett, J. A. (2003). prenatal, but not postnatal, inhibition of fibroblast growth factor signaling causes emphysema. *J. Biol. Chem.* 278, 415–421. doi: 10.1074/jbc.M208328200

Itoh, N., and Ohta, H. (2014). Fgf10: a paracrine-signaling molecule in development, disease, and regenerative medicine. *Curr. Mol. Med.* 14, 504–509. doi: 10.2174/1566524014666140414204829

Kappel, A., Ronicke, V., Damert, A., Flamme, I., Risau, W., and Breier, G. (1999). Identification of vascular endothelial growth factor (VEGF) receptor-2 (Flk-1) promoter/enhancer sequences sufficient for angioblast and endothelial cell-specific transcription in transgenic mice. *Blood* 93, 4284–4292.

Klar, J., Blomstrand, P., Brunmark, C., Badhai, J., Hakansson, H. F., Brange, C. S., et al. (2011). Fibroblast growth factor 10 haploinsufficiency causes chronic obstructive pulmonary disease. *J. Med. Genet.* 48, 705–709. doi: 10.1136/jmedgenet-2011-100166

Konishi, M., Asaki, T., Koike, N., Miwa, H., Miyake, A., and Itoh, N. (2006). Role of Fgf10 in cell proliferation in white adipose tissue. *Mol. Cell. Endocrinol.* 249, 71–77. doi: 10.1016/j.mce.2006.01.010

Langsdorf, A., Radzikinas, K., Kroten, A., Jain, S., and Ai, X. (2011). Neural crest cell origin and signals for intrinsic neurogenesis in the mammalian respiratory tract. *Am. J. Respir. Cell Mol. Biol.* 44, 293–301. doi: 10.1165/rcmb.2009-0462OC

Li, A., Ma, S., Smith, S. M., Lee, M. K., Fischer, A., Borok, Z., et al. (2016). Mesodermal ALK5 controls lung myofibroblast versus lipofibroblast cell fate. *BMC Biol.* 14:19. doi: 10.1186/s12915-016-0242-9

Li, R., Bernau, K., Sandbo, N., Gu, J., Preissl, S., and Sun, X. (2018). Pdgfra marks a cellular lineage with distinct contributions to myofibroblasts in lung maturation and injury response. *eLife* 7:e36865. doi: 10.7554/eLife.36865

Lindahl, P., Karlsson, L., Hellstrom, M., Gebre-Medhin, S., Willetts, K., Heath, J. K., et al. (1997). Alveogenesis failure in PDGF-A-deficient mice is coupled to lack of distal spreading of alveolar smooth muscle cell progenitors during lung development. *Development* 124, 3943–3953.

Mailleux, A. A., Kelly, R., Veltmaat, J. M., De Langhe, S. P., Zaffran, S., Thiery, J. P., et al. (2005). Fgf10 expression identifies parabronchial smooth muscle cell progenitors and is required for their entry into the smooth muscle cell lineage. *Development* 132, 2157–2166. doi: 10.1242/dev.01795

Mailleux, A. A., Spencer-Dene, B., Dillon, C., Ndiaye, D., Savona-Baron, C., Itoh, N., et al. (2002). Role of FGF10/FGFR2b signaling during mammary gland development in the mouse embryo. *Development* 129, 53–60.

McGowan, S. E., and McCoy, D. M. (2015). Fibroblast growth factor signaling in myofibroblasts differs from lipofibroblasts during alveolar septation in mice. *Am. J. Physiol. Lung Cell. Mol. Physiol.* 309, L463–L474. doi: 10.1152/ajplung.00013.2015

McQualter, J. L., McCarty, R. C., Van der Velden, J., O'Donoghue, R. J., Asselin-Labat, M. L., Bozinovski, S., et al. (2013). TGF-beta signaling in stromal cells acts upstream of FGF-10 to regulate epithelial stem cell growth in the adult lung. *Stem Cell Res.* 11, 1222–1233. doi: 10.1016/j.scr.2013.08.007

Moiseenko, A., Kheirollahi, V., Chao, C. M., Ahmadvand, N., Quantius, J., Wilhelm, J., et al. (2017). Origin and characterization of alpha smooth muscle actin-positive cells during murine lung development. *Stem Cells* 35, 1566–1578. doi: 10.1002/stem.2615

Ndlovu, R., Deng, L.-C., Wu, J., Li, X.-K., and Zhang, J.-S. (2018). Fibroblast growth factor 10 in pancreas development and pancreatic cancer. *Front. Genet.* 9:482. doi: 10.3389/fgene.2018.00482

Noguchi, A., Reddy, R., Kursar, J. D., Parks, W. C., and Mecham, R. P. (1989). Smooth muscle isoactin and elastin in fetal bovine lung. *Exp. Lung Res.* 15, 537–552. doi: 10.3109/01902148909069617

Ntokou, A., Klein, F., Dontireddy, D., Becker, S., Bellusci, S., Richardson, W. D., et al. (2015). Characterization of the platelet-derived growth factor receptor-alpha-positive cell lineage during murine late lung development. *Am. J. Physiol. Lung Cell. Mol. Physiol.* 309, L942–L958. doi: 10.1152/ajplung.00272.2014

O'Hare, K. H., and Sheridan, M. N. (1970). Electron microscopic observations on the morphogenesis of the albino rat lung, with special reference to pulmonary epithelial cells. *Am. J. Anat.* 127, 181–205. doi: 10.1002/aja.1001270205

Ornitz, D. M., and Itoh, N. (2015). The Fibroblast Growth Factor signaling pathway. *Wiley Interdiscip. Rev. Dev. Biol.* 4, 215–266. doi: 10.1002/wdev.176

Peng, T., Tian, Y., Boogerd, C. J., Lu, M. M., Kadzik, R. S., Stewart, K. M., et al. (2013). Coordination of heart and lung co-development by a multipotent cardiopulmonary progenitor. *Nature* 500, 589–592. doi: 10.1038/nature12358

Perl, A. K., and Gale, E. (2009). FGF signaling is required for myofibroblast differentiation during alveolar regeneration. *Am. J. Physiol. Lung Cell. Mol. Physiol.* 297, L299–L308. doi: 10.1152/ajplung.00008.2009

Prince, L. S. (2018). FGF10 and human lung disease across the life spectrum. *Front. Genet.* 9:517. doi: 10.3389/fgene.2018.00517

Que, J., Wilm, B., Hasegawa, H., Wang, F., Bader, D., and Hogan, B. L. (2008). Mesothelium contributes to vascular smooth muscle and mesenchyme during lung development. *Proc. Natl. Acad. Sci. U.S.A.* 105, 16626–16630. doi: 10.1073/pnas.0808649105

Ramasamy, S. K., Mailleux, A. A., Gupte, V. V., Mata, F., Sala, F. G., Veltmaat, J. M., et al. (2007). Fgf10 dosage is critical for the amplification of epithelial

cell progenitors and for the formation of multiple mesenchymal lineages during lung development. *Dev. Biol.* 307, 237–247. doi: 10.1016/j.ydbio.2007.04.033

Rangarajan, S., Bone, N. B., Zmijewska, A. A., Jiang, S., Park, D. W., Bernard, K., et al. (2018). Metformin reverses established lung fibrosis in a bleomycin model. *Nat. Med.* 8, 1121–1127. doi: 10.1038/s41591-018-0087-6

Rehan, V., and Torday, J. (2003). Hyperoxia augments pulmonary lipofibroblast-to-myofibroblast transdifferentiation. *Cell Biochem. Biophys.* 38, 239–250. doi: 10.1385/CBB:38:3:239

Rehan, V. K., and Torday, J. S. (2012). PPARgamma Signaling Mediates the Evolution, Development, Homeostasis, and Repair of the Lung. *PPAR Res.* 2012:289867. doi: 10.1155/2012/289867

Rehan, V. K., Wang, Y., Sugano, S., Romero, S., Chen, X., Santos, J., et al. (2005). Mechanism of nicotine-induced pulmonary fibroblast transdifferentiation. *Am. J. Physiol. Lung Cell. Mol. Physiol.* 289, L667–L676. doi: 10.1152/ajplung.00358.2004

Rubin, L. P., Kovacs, C. S., De Paepe, M. E., Tsai, S. W., Torday, J. S., and Kronenberg, H. M. (2004). Arrested pulmonary alveolar cytodifferentiation and defective surfactant synthesis in mice missing the gene for parathyroid hormone-related protein. *Dev. Dyn.* 230, 278–289. doi: 10.1002/dvdy.20058

Sakaue, H., Konishi, M., Ogawa, W., Asaki, T., Mori, T., Yamasaki, M., et al. (2002). Requirement of fibroblast growth factor 10 in development of white adipose tissue. *Genes Dev.* 16, 908–912. doi: 10.1101/gad.983202

Schultz, C. J., Torres, E., Londos, C., and Torday, J. S. (2002). Role of adipocyte differentiation-related protein in surfactant phospholipid synthesis by type II cells. *Am. J. Physiol. Lung Cell. Mol. Physiol.* 283, L288–L296. doi: 10.1152/ajplung.00204.2001

Sekine, K., Ohuchi, H., Fujiwara, M., Yamasaki, M., Yoshizawa, T., Sato, T., et al. (1999). Fgf10 is essential for limb and lung formation. *Nat. Genet.* 21, 138–141. doi: 10.1038/5096

Simon, D. M., and Mariani, T. J. (2007). Role of PPARs and Retinoid X Receptors in the Regulation of Lung Maturation and Development. *PPAR Res.* 2007:91240. doi: 10.1155/2007/91240

Srinivasan, R. S., Dillard, M. E., Lagutin, O. V., Lin, F. J., Tsai, S., Tsai, M. J., et al. (2007). Lineage tracing demonstrates the venous origin of the mammalian lymphatic vasculature. *Genes Dev.* 21, 2422–2432. doi: 10.1101/gad.1588407

Torday, J. S., and Rehan, V. K. (2007). The evolutionary continuum from lung development to homeostasis and repair. *Am. J. Physiol. Lung Cell. Mol. Physiol.* 292, L608–L611. doi: 10.1152/ajplung.00379.2006

Torday, J. S., Sun, H., Wang, L., Torres, E., Sunday, M. E., and Rubin, L. P. (2002). Leptin mediates the parathyroid hormone-related protein paracrine stimulation of fetal lung maturation. *Am. J. Physiol. Lung Cell. Mol. Physiol.* 282, L405–L410. doi: 10.1152/ajplung.2002.282.3.L405

Torday, J. S., Torres, E., and Rehan, V. K. (2003). The role of fibroblast transdifferentiation in lung epithelial cell proliferation, differentiation, and repair *in vitro*. *Pediatr. Pathol. Mol. Med.* 22, 189–207. doi: 10.1080/pdp.22.3.189.207

Vaccaro, C., and Brody, J. S. (1978). Ultrastructure of developing alveoli. I. The role of the interstitial fibroblast. *Anatom. Record* 192, 467–479. doi: 10.1002/ar.1091920402

Watson, J., and Francavilla, C. (2018). Regulation of FGF10 signaling in development and disease. *Front. Genet.* 9:500. doi: 10.3389/fgene.2018.00500

Yamada, M., Kurihara, H., Kinoshita, K., and Sakai, T. (2005). Temporal expression of alpha-smooth muscle actin and drebrin in septal interstitial cells during alveolar maturation. *J. Histochem. Cytochem.* 53, 735–744. doi: 10.1369/jhc.4A6483.2005

Yamaguchi, T. P., Dumont, D. J., Conlon, R. A., Breitman, M. L., and Rossant, J. (1993). flk-1, an flt-related receptor tyrosine kinase is an early marker for endothelial cell precursors. *Development* 118, 489–498.

Yuan, T., Volckaert, T., Chanda, D., Thannickal, V. J., and De Langhe, S. P. (2018). Fgf10 signaling in lung development, homeostasis, disease and repair after injury. *Frontiers*. doi: 10.3389/fgene.2018.00418

Conflict of Interest Statement: The authors declare that the research was conducted in the absence of any commercial or financial relationships that could be construed as a potential conflict of interest.

Copyright © 2018 Wu, Chu, Chen and Bellusci. This is an open-access article distributed under the terms of the Creative Commons Attribution License (CC BY). The use, distribution or reproduction in other forums is permitted, provided the original author(s) and the copyright owner(s) are credited and that the original publication in this journal is cited, in accordance with accepted academic practice. No use, distribution or reproduction is permitted which does not comply with these terms.

frontiers in Genetics

REVIEW
published: 16 November 2018
doi: 10.3389/fgene.2018.00542

Bones, Glands, Ears and More: The Multiple Roles of FGF10 in Craniofacial Development

*Michaela Prochazkova[1], Jan Prochazka[1], Pauline Marangoni[2] and Ophir D. Klein[2]**

[1] Laboratory of Transgenic Models of Diseases, Czech Centre for Phenogenomics, Institute of Molecular Genetics, Czech Academy of Sciences, Prague, Czechia, [2] Program in Craniofacial Biology, Departments of Orofacial Sciences and Pediatrics, Institute for Human Genetics, University of California, San Francisco, San Francisco, CA, United States

OPEN ACCESS

Edited by:
Saverio Bellusci, Justus-Liebig-Universität Gießen, Germany

Reviewed by:
Francesca V. Mariani, University of Southern California, United States
Abigail Saffron Tucker, King's College London, United Kingdom

***Correspondence:**
Ophir D. Klein
ophir.klein@ucsf.edu

Specialty section:
This article was submitted to Stem Cell Research, a section of the journal Frontiers in Genetics

Received: *16 August 2018*
Accepted: *26 October 2018*
Published: *16 November 2018*

Citation:
Prochazkova M, Prochazka J, Marangoni P and Klein OD (2018) Bones, Glands, Ears and More: The Multiple Roles of FGF10 in Craniofacial Development. Front. Genet. 9:542. doi: 10.3389/fgene.2018.00542

Members of the fibroblast growth factor (FGF) family have myriad functions during development of both non-vertebrate and vertebrate organisms. One of these family members, *FGF10*, is largely expressed in mesenchymal tissues and is essential for postnatal life because of its critical role in development of the craniofacial complex, as well as in lung branching. Here, we review the function of FGF10 in morphogenesis of craniofacial organs. Genetic mouse models have demonstrated that the dysregulation or absence of FGF10 function affects the process of palate closure, and FGF10 is also required for development of salivary and lacrimal glands, the inner ear, eye lids, tongue taste papillae, teeth, and skull bones. Importantly, mutations within the *FGF10* locus have been described in connection with craniofacial malformations in humans. A detailed understanding of craniofacial defects caused by dysregulation of FGF10 and the precise mechanisms that underlie them offers new opportunities for development of medical treatments for patients with birth defects and for regenerative approaches for cancer patients with damaged gland tissues.

Keywords: FGF10, craniofacial development, palate, salivary gland, lacrimal gland, inner ear, eyelid, taste papillae

INTRODUCTION

FGF10 is a member of the fibroblast growth factor (FGF) family, a highly evolutionarily conserved group of proteins that trigger signaling via receptor tyrosine kinases. The FGF signaling pathway plays central roles in developmental processes from head to toe, including formation of the brain, limbs, kidneys, hair follicles, and body axis elongation (Rosenquist and Martin, 1996; Lewandoski et al., 2000; Basson et al., 2008; Walker et al., 2016; Oginuma et al., 2017). The FGF family contains 22 ligands grouped into 7 subfamilies, and these ligands can bind to 4 receptors (FGFR1–4) (Ornitz and Itoh, 2001). The interaction of FGF ligands with their receptors is regulated by the extracellular environment, through proteoglycan cofactors and extracellular binding proteins. Activation of FGF receptors involves phosphorylation of specific tyrosine residues that mediate interaction with cytosolic adaptor proteins and the RAS-MAPK, PI3K-AKT, PLCγ, and STAT intracellular

signaling pathways (Ornitz and Itoh, 2015). FGF10 is a canonical FGF and belongs to the FGF7 subfamily, together with FGF3, FGF7, and FGF22. The common feature of these FGF ligands is their specific binding of the IIIb splice variant of FGFR 1 and 2 (Zhang et al., 2006). Moreover, during organogenesis FGF10 serves as a major ligand for the FGFR 2 IIIb isoform, which localizes to the epithelium (Ohuchi et al., 2000), and in general *Fgf10* is predominantly expressed in the mesenchyme, with the protein it encodes signaling to the epithelium.

The majority of studies on the role of FGF10 in vertebrates have been performed using mice carrying null mutations in *Fgf10*. In addition to the craniofacial complex, many other organs of the body are affected in the *Fgf10* null mutants. Among the most prominent phenotypes in the mutants are that both hindlimbs and forelimbs are completely missing (amelia), and there is lung agenesis (Ohuchi et al., 2000; **Figure 1**). Perinatal lethality in the *Fgf10* mutants results from respiratory failure. Notably, the phenotype of *Fgfr2* mutant mice almost completely overlaps with that of *Fgf10* mutants (Ohuchi et al., 2000).

Mutations in *FGF10* have been found to cause numerous developmental defects and pathologies in humans. For example, loss-of-function mutations in *FGF10* have been reported to cause LADD (Lacrimo-auriculo-dento-digital) syndrome (Milunsky et al., 2006; Shams et al., 2007), which affects multiple organs, the majority of which are in the craniofacial complex. This and other human conditions connected to craniofacial development are further discussed below.

ROLE OF FGF10 IN CRANIOFACIAL MORPHOGENESIS

Fgf10 is expressed largely in the mesenchyme of many developing structures within the craniofacial complex, including teeth, tongue and palatal shelves, and it signals to epithelia where *Fgfr2* is expressed. Mutations in *Fgf10* lead to a wide range of defects, emphasizing the central importance of FGF10 signaling in many developmental processes.

Palatogenesis

FGF10 is crucial for the process of closure of the secondary palate. Both *Fgf10* (**Figures 2C,D**) and *Fgfr2* null mouse strains exhibit cleft palate with complete penetrance (Rice et al., 2004). *Fgf10* is expressed most strongly between embryonic day (E)11 and E13 in the mesenchyme of the anterior and middle portion of the shelves (Rice et al., 2004; Alappat et al., 2005). During this developmental period, palatal shelf outgrowth occurs prior to the subsequent elevation and fusion of the shelves between E14 and E15. At later stages, the *Fgf10* mutant shelves are shorter, square in shape, and missing the finger-like projections that normally reach each other and fuse (Rice et al., 2004). This change in morphology can be explained by differences in the regulation of cell proliferation and apoptosis. While one study reported that

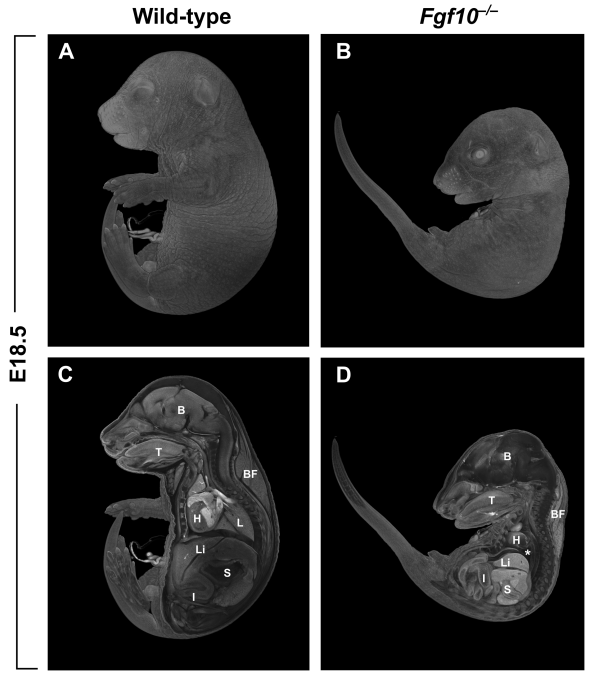

FIGURE 1 | (A,B) Whole-mount μCT images of wild-type and *Fgf10* null mouse embryos at E18.5. **(C,D)** Medial cross-sections through wild-type and mutant embryo. *Fgf10* mutant embryos show complete amelia; another pronounced phenotype is lung agenesis (asterisk). B, brain; BF, brown fat; H, heart; I, intestines; L, lungs; Li, liver; S, stomach; T, tongue.

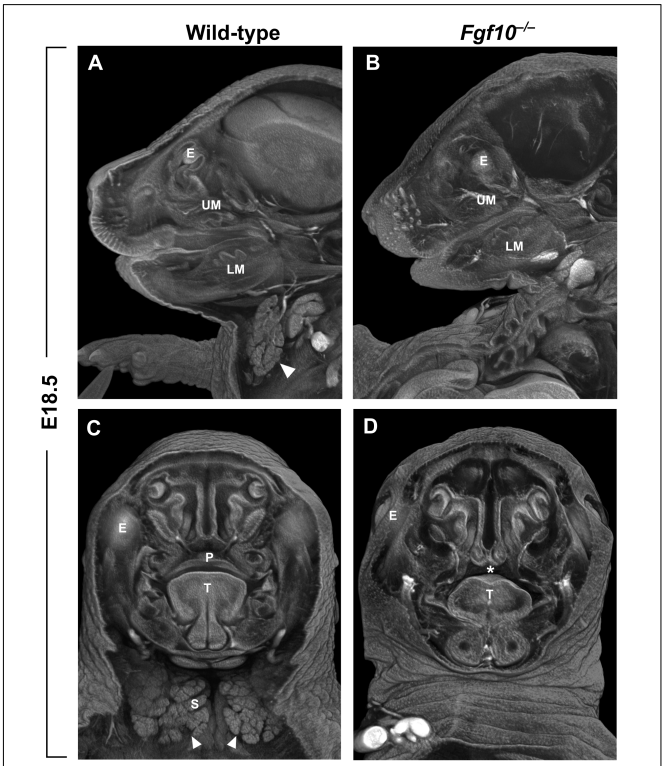

FIGURE 2 | (A–D) Sagittal **(A,B)** and frontal **(C,D)** μCT sections of wild-type and *Fgf10* null embryos at E18.5. Absence of submandibular salivary gland (structure marked by arrowhead in wild-type in panels **A,C**) and cleft palate phenotype (asterisk in panel **D**) can be observed in *Fgf10* null embryos. E, eye; LM, lower molar; P, palate; T, tongue; S, salivary gland; UM, upper molar.

there are no apparent differences in the overall proliferation of the shelves (Alappat et al., 2005), another suggested that proliferation of epithelial cells is decreased in the FGF10 deficient palatal shelves along with downregulation of the morphogen encoded by *Shh* (Rice et al., 2004). Both studies then showed a significant increase in apoptosis mainly in the medial edge epithelium of the developing shelves (Rice et al., 2004; Alappat et al., 2005). Despite the discrepancies, it appears that FGF10 signals from the palatal mesenchyme to the epithelium and affects the cell fate and subsequently the outgrowth and shape of the palatal shelves.

Besides cell proliferation and survival, another mechanism possibly contributing to the formation of cleft palate in *Fgf10* mutants is the presence of aberrant adhesions of the epithelium of the shelves with the epithelium of the tongue or with other parts of the oral epithelium (Rice et al., 2004; Alappat et al., 2005). Presence of these fusions likely prevents the horizontalization (elevation) process of the palatal shelves, so they are kept in a vertical position and cannot begin to reach each other. Of note, when the tissue explants of the palatal shelves of *Fgfr2*$^{-/-}$ mice were isolated and cultured *in vitro* in close proximity, the epithelia fused normally (Rice et al., 2004). The molecular basis behind the tendency to form aberrant epithelial fusions may be related to the regulation of Notch signaling by FGF10. Mutations in the Notch ligand *Jagged2* cause cleft palate with unelevated shelves heavily fused to the tongue epithelium (Jiang et al., 1998), and the *Fgf10* mutants exhibit severe downregulation of *Jagged2* expression within the palatal shelf epithelium at E12.5 (Alappat et al., 2005). This suggests that FGF10 is upstream of Notch signaling in the developing palatal shelves and affects the ability and correct timing of their fusion potential.

Tongue morphology is also altered in the *Fgf10* mutants. Likely due to the presence of aberrant epithelial fusions, the tongue does not descend as it should, which perturbs this necessary step in the process of shelf elevation (Rice et al., 2004). Indeed, a partial ankylosis of the tongue (adherence to the floor of mouth accompanied by immobility) is present in the *Fgf10* mutant embryos (Rice et al., 2004). Notably, overexpression of *Fgf10* also affects the tongue shape and can lead to cleft palate. This phenomenon was described in mice with neural crest-specific *Tak1* deletion, which affects TGFβ signaling, in turn leading to activation of FGF10, higher cell proliferation, and significantly increased height of the tongue that prevents the elevation of palatal shelves (Song et al., 2013). The role of TGFβ signaling upstream of FGF10 in morphogenesis of the tongue was also confirmed when *Tgfbr2* was conditionally deleted in neural crest cell progeny, as the addition of endogenous FGF10 rescued the muscle cell number in mutant tongues (Hosokawa et al., 2010). FGF10 also regulates tongue taste papillae development, which is discussed below.

In humans, genome-wide association studies (GWAS) have shown that SNPs near *FGF10* are highly associated with cleft lip and/or palate (Shi et al., 2009; Yu et al., 2017). Likely, due to their different orofacial shape with a more prominent rostral component, cleft lip does not typically occur spontaneously in mice, and it is rarely observed even with genetic or environmental challenge. Therefore, this model organism is theoretically not an ideal one to study cleft lip etiology. Nevertheless, there are certain mouse strains that are susceptible to developing cleft lip, e.g., the group of so-called A strains that exhibit smaller midface size compared to other strains (Young et al., 2007). Among the A strains, A/WySn has the highest spontaneous incidence of cleft lip, ranging between 20 and 30% (Juriloff, 1982). The high prevalence and susceptibility of these mice to cleft lip is thought to be caused by a mutation in *Wnt9b,* which is also on the list of top clefting genes from human GWAS data (Juriloff et al., 2006; Yu et al., 2017) *Wnt9b* knockout mice exhibit cleft lip and, importantly, the expression of *Fgf8*, *Fgf10*, and *Fgf17* is down-regulated in the tissue of facial processes forming the future lip in these mice. Taken together, the data from GWAS along with the data from susceptible mouse strains suggest a role for FGF10 in lip development, despite the absence of cleft lip in *Fgf10*$^{-/-}$ mice.

Notably, soft palate development is also dependent on FGF10, and this cannot be evaluated in *Fgf10* null mutants, because the wide hard cleft palate interferes with the later development of the soft palate. Loss of *Dlx5* leads to shortening of the soft palate and absence of adjacent muscles that are derived from the fourth pharyngeal arch. *Fgf10* was shown to lie downstream of DLX5, and the *Dlx5* mutant phenotype can be rescued by addition of FGF10 (Sugii et al., 2017).

Eye Lid Development

Another clefting-like pathology in the craniofacial area is the phenotype of open eyelids in *Fgf10* null mice at prenatal stages when the eye is normally covered by skin (**Figures 1B**, **3B**). The absence of *Fgf10*, which is normally expressed in the mesenchyme beneath the protruding epidermal cells of the nascent eyelid, causes a decrease in proliferation of these cells as well as changes in their shape, along with hampering their coordinated migration (Tao et al., 2005). These effects are due to downstream regulation of pathways important for these processes, including activin, TGFα, and SHH (Tao et al., 2005).

Skull Morphology

A major group of human craniosynostosis syndromes, including Apert, Crouzon, or Pfeiffer syndromes, is caused by mutations leading to overactivation of Fgf receptors. Apert and Crouzon syndromes are caused by mutations in *FGFR2* that increase affinity of the receptor for the ligand, and Pfeiffer syndrome is caused by mutations in either *FGFR2* or *FGFR1* (Schell et al., 1995; Anderson et al., 1998; Hibberd et al., 2016). The search for specific ligands involved in the process of fusion of the sutures revealed that FGF10 can play a significant role in proper formation of skull shape. *Fgf10* mRNA is present in the osteoprogenitors in the frontal bone condensation (Veistinen et al., 2009), and genetic knock-down of *Fgf10* rescues the skeletal phenotype in an Apert syndrome mouse model *FgfR2*-IIIc$^{+/\Delta}$ (Hajihosseini et al., 2009). When compared perinatally, the *Fgf10* null embryos do not exhibit pathological morphology of calvarial bones, while the *FgfR2*-IIIc$^{+/\Delta}$ mice already lack the coronal suture (Hajihosseini et al., 2009). Unfortunately, postnatal development of skull bones and sutures cannot be followed in the perinatal lethal *Fgf10* null mutants, so it is not possible to exclude that the loss of FGF10 has an impact on skull morphology.

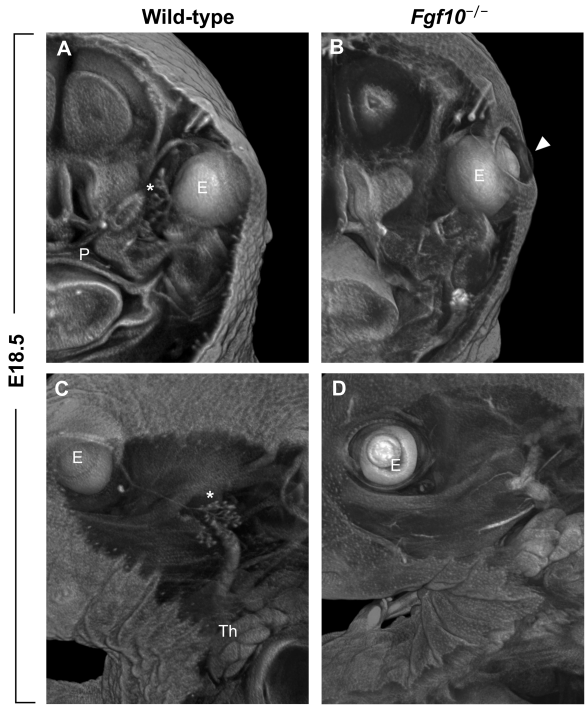

FIGURE 3 | (A–D) Frontal **(A,B)** and sagittal **(C,D)** μCT sections of wild-type and *Fgf10* null embryos at E18.5. Note absence of eyelid (arrowhead in panel **B**) and hypoplasia of ocular glands (Harderian and extraorbital lacrimal glands marked by asterisks in panels **A,C**, respectively) in *Fgf10* null embryos. E, eye; P, palate; Th, thymus.

Nevertheless, it is instructive to consider the Apert syndrome model, in which the mice are hemizygous for *Fgfr2 IIIC* and exhibit a splicing switch resulting in ectopic expression of *FGFR2 IIIb* in calvarial mesenchyme; similar mutations are only rarely found in humans (Hajihosseini et al., 2001, 2009; Bochukova et al., 2009). More than 98% of Apert syndrome patients carry either Ser252Trp or Pro253Arg missense gain-of-function mutations in the IIIa exon (common for IIIb and IIIc variants). These mutations likely predominantly cause the skull defects through aberrant function of FGFR2 IIIc, which is involved in proper bone formation (Eswarakumar et al., 2002). Taken together, these findings suggest that FGF10 may be dispensable for the properly timed fusion of sutures and skull development, but unphysiologically high and/or ectopically activated FGFR2 signaling triggered by FGF10 can cause developmental defects of these structures.

Sensory Organs

FGF10 also affects the development of organs that possess a sensory function or will sustain it postnatally, including, as mentioned above, the taste papillae of the tongue. The mammalian tongue epithelium contains three types of papillary structures that house taste cells – the foliate, fungiform, and circumvallate (CVP) papillae. The multiple fungiform papillae covering approximately two thirds of the tongue dorsum and the posteriorly situated CVP have been shown to be regulated by FGF10 (Petersen et al., 2011; Prochazkova et al., 2017). Interestingly, the effect of *Fgf10* is opposite in these two types of taste papillae. The CVP, which is normally a single structure in mouse, is absent or diminished in *Fgf10* null murine tongues, whereas the overactivation of RTK signaling in embryos carrying mutations in the RTK negative feedback regulator *Sprouty (Spry)* genes led to enlargement of the papillary field and presence of multiple CVPs (Petersen et al., 2011). In contrast, the development of fungiform papillae is negatively affected by the level of FGF10, such that the fungiform papillae of $Fgf10^{-/-}$ tongues are significantly larger, and in $Spry2^{-/-}$ tongues with increased FGF signaling they are much smaller. Notably, fungiform size is controlled by FGF10, but the overall patterning is not; at a mechanistic level, the downstream action of FGF10 is likely exerted by affecting the diffusion as opposed to the transcription of Wnt ligands (Prochazkova et al., 2017). The difference in regulation of papillary area in CVP and fungiform papillae might result from a different developmental origin of the part of the tongue covered by fungiform papillae (ectodermal) versus the posterior part near the root of the tongue housing the CVP (endodermal) (Rothova et al., 2012). Whether the level of FGF10 signaling can impact the quality of taste remains an open question.

Another sensory organ with dysregulated development in *Fgf10* mutant embryos is the inner ear. Absence of FGF10 leads to complete agenesis of the posterior semicircular canal. In addition, malformations are present in the anterior and lateral canals as well as in the positioning of the remaining sensory epithelia with respect to the utricle; defects were also observed in the cilia of hair cells (Pauley et al., 2003). Interestingly, heterozygous $Fgf10^{+/-}$ mice also exhibit reduction or even absence of the posterior canal, suggesting a strong dependence on FGF10 dosage during development of this structure (Urness et al., 2015). In addition to the motion detection part of the inner ear, the *Fgf10* mutant embryos also exhibit pathologies in morphology of cochlear non-sensory regions, including shorter and narrower duct, absence of Reissner's membrane within the cochlear epithelium, and agenesis of a large portion of the outer sulcus (Urness et al., 2015). Even though these structures belong to the non-sensory part of the cochlea, both the Reissner's membrane and the outer sulcus are important for maintenance of the endolymph homeostasis and therefore necessary for hearing. Similar defects might be present also in humans and explain a part of the phenotype LADD syndrome caused by mutations in *FGF10 or FGFR2* (Milunsky et al., 2006). More than half of the affected individuals suffer from hearing loss, and cochlear hypoplasia was also observed in some of the patients (Lemmerling et al., 1999; Milunsky et al., 2006). The severity of hearing defects might be more pronounced when a causative mutation in FGFR2 is present, as FGF10 has a redundant role with FGF3 during inner ear formation – the murine double mutants for these FGFs fail to form otic vesicles (Alvarez et al., 2003; Wright, 2003). Notably, the FGFR2 IIIb knock-out mice exhibit more severe phenotypes than single *Fgf3* and *Fgf10* mutants, but their inner ear is affected less than in the *Fgf3/Fgf10* dKOs (Pirvola et al., 2000; Alvarez et al., 2003). This discrepancy suggests that FGF3 and FGF10 in the ear region can possibly also bind other FGF receptors, such

as FGFR1, which has affinity for these two ligands (Zhang et al., 2006). The FGFR2 IIIc form may also be activated by FGF3/10, because the general FGFR2 mutant has a more pronounced phenotype than FGFR2 IIIb only (Xu et al., 1998; Alvarez et al., 2003). However, this might be explained by an additional role of FGF8 during early inner ear development (Domínguez-Frutos et al., 2009).

Fgf10 is also highly expressed in the external ear (pinna) of mouse embryos (El Agha et al., 2012) and, interestingly, one of the defects observed in the LADD patients are low-set, cup-shaped ears. Nevertheless, no external ear abnormalities have so far been described in direct connection to FGF10 (see normal pinna in *Fgf10* mutant embryos in **Figure 1**). It may be again a case of compensation by another FGF ligand and their common dysfunction in patients with *FGFR2* rather than *FGF10* mutations *per se*.

Development of Teeth and Mandible

The molar tooth germ is a widely used model for studying epithelial morphogenesis and epithelial–mesenchymal interactions. In mouse, tooth development starts at ∼E11.5 with active rearrangement of epithelial cells in the posterior area of the jaws, where FGF8 serves as a major signaling molecule (Prochazka et al., 2015). A cylindrical epithelial invagination called the dental lamina is formed at E12.5, and at E13.5, progressive budding of epithelium from the dental lamina takes place, which is supported by condensing neural crest-derived cells expressing *Fgf3* and *Fgf10* (Kettunen et al., 2000). The rapid epithelial ingrowth is accompanied by formation of a signaling center called the enamel knot. Mesenchymal *Fgf10* is expressed in the area of the mandible where future molar teeth form, and complete agenesis of molars was described in *Fgfr2* deficient mouse embryos, but with the loss of *Fgf10* only minor morphological defects are observed in molar development (Ohuchi et al., 2000); the absence of a dramatic *Fgf10* mutant tooth phenotype is likely due to compensation by *Fgf3*. The budding process of the molar primordia in $Fgf10^{-/-}$ embryos is delayed around E13, but at later stages tooth development catches up, and the final molar tooth is only slightly smaller in size compared to wild-type (Ohuchi et al., 2000; Veistinen et al., 2009; **Figure 2**).

In rodents, the incisors are evergrowing, with a population of adult stem cells present in the most proximal region called the cervical loop (Harada et al., 1999). *Fgf10* plays a major role in maintenance of the stem cell niche of the mouse incisor by regulation of Notch signaling in the dental epithelium (Harada et al., 1999). The *Fgf10* null embryo incisor is apparently smaller, mainly because of an absent cervical loop (Ohuchi et al., 2000; Harada et al., 2002). Related to this, FGF10 has been suggested as a principal morphogenetic factor driving the teeth toward an evergrowing fate, as *Fgf10* expression is maintained in continuously growing teeth (e.g., mouse incisor or vole molar) throughout life, and the *Fgf10* mutant incisors lose continuously growing features when cultured in kidney capsules (Yokohama-Tamaki et al., 2006).

One group of pathologies associated with LADD syndrome are dental defects. The patients often have underdeveloped teeth with thin enamel and peg-shaped incisors. Even though molar development does not seem to be severely affected in the absence of FGF10 when evaluated prenatally in the mouse model, the findings in LADD patients support the role of FGF10 in tooth development. Some of the LADD patients suffering from dental pathologies may carry a specific genetic alteration in *FGFR2* (Rohmann et al., 2006; Shams et al., 2007). However, there are also reports of patients with enamel hypoplasia or small teeth with disrupted caps and crown morphology that are associated with *FGF10* mutations (Milunsky et al., 2006). Moreover, increased expression of *FGF10* along with *FGF7* was found in samples from human ameloblastoma, a benign jaw tumor originating from the cells of odontogenic epithelium, and FGF10 was shown to directly support proliferation of these cells (Nakao et al., 2013). The mild phenotype and normal cell-differentiation gradient of ameloblasts and odontoblasts in *Fgf10* null embryos (Harada et al., 2002) suggest that human dental development might differ from that of mice. Because the post-eruption dentition cannot be studied in the perinatal lethal $Fgf10^{-/-}$ mice, conditional models will be needed in the future.

Similarly to tooth development, mandibular morphogenesis is not severely altered in *Fgf10* null embryos. Nevertheless, the developing jaw is apparently sensitive to the dosage of FGF10, as in the rat model, *Fgf10* overexpression was described to cause elongation of Meckel's cartilage and enhanced chondrogenic differentiation within the mandible. Notably, proliferation of mandibular cells was not affected by higher levels of FGF10, and the longer Meckel's cartilage was deformed and spiral-shaped, which affected the final shape of the jaw (Terao et al., 2011). The importance of FGF10 for proper mandibular development is also supported by association between genetic polymorphisms in *FGF10* and mandibular prognathism in humans (Cruz et al., 2017).

Salivary and Lacrimal Glands

As with its critical role during lung development, FGF10 plays an important role in morphogenesis of branching organs within the craniofacial complex, including the salivary and lacrimal glands. The expression of *Fgf10* is high in the mesenchyme surrounding the developing salivary glands. *Fgf10* null embryos display aplasia of the salivary glands (**Figure 2**) with their development arrested at the bud stage (Ohuchi et al., 2000; Jaskoll et al., 2005). FGF10 acts upstream of SOX9 to positively regulate the progenitor cell population and drive outgrowth of the glands (Chatzeli et al., 2017). Furthermore, explant cultures of salivary gland tissue can recapitulate the physiological branching morphogenesis *in vitro* only if the epithelium is cultured with the surrounding mesenchyme or if FGF10 is added to the culture of the isolated epithelial tissue (Rebustini and Hoffman, 2009; Knosp et al., 2012). Notably, regulation of binding affinity of FGF10 to heparan sulfate is a decisive feature in the balance between promoting gland morphogenesis fate toward branching versus elongation (Patel et al., 2007; Makarenkova et al., 2009). FGF10 dose-dependence during development of salivary glands is further supported by the fact that mice heterozygous for *Fgf10* have hypoplastic salivary glands and xerostomia (dry mouth) (Jaskoll et al., 2005; May et al., 2015).

The role of FGF10 in lacrimal gland development is similar to its role in salivary gland morphogenesis. *Fgf10,* which is expressed in the mesenchyme adjacent to developing lacrimal epithelial bud, induces lacrimal gland development, and *Fgf10* null murine embryos exhibit agenesis of all ocular glands – the extraorbital and intraorbital lacrimal glands as well as the Harderian gland (Govindarajan et al., 2000; Makarenkova et al., 2000; **Figure 3**). The proteoglycans at the cell surface and in the extracellular matrix also affect lacrimal gland morphogenesis – the *O*-sulfation of heparan sulfate was shown to be essential for FGF10–FGFR2 interaction on lacrimal gland cell surface (Qu et al., 2011). In addition to the large orofacial glands, FGF10 also plays an important role during development of nasal submucosal glands responsible for mucus secretion in airways (May et al., 2016).

Patients with ALSG (aplasia of the lacrimal and major salivary glands) exhibit both salivary and lacrimal phenotypes, and this rare disorder is caused by loss-of-function mutations in *FGF10* (Entesarian et al., 2007; Scheckenbach et al., 2008; Seymen et al., 2017). ALSG patients suffer from xerostomia and dental decay, eye irritation, and epiphora (excessive tearing). In contrast, LADD syndrome covers a wider spectrum of malformations, including the above mentioned dental and auditory defects and also an abnormal number of fingers or digits. Nevertheless, LADD syndrome overlaps with ALSG in terms of lacrimal and salivary defects, and thus these two autosomal dominant disorders are considered part of the same phenotypic spectrum. The data from affected families support this idea, with reports of a daughter with typical features of LADD inheriting the mutation from her mother with ALSG (Milunsky et al., 2006). Taken together, the human clinical data confirm the importance of the correct function and level of FGF10 in the development of craniofacial structures, even though the precise regulation and severity of the phenotype apparently depend on both genetic and environmental factors. A systematically generated overview of the phenotypes in *Fgf10* null embryos is available at the International Mouse Phenotype Consortium (IMPC) database: www.mousephenotype.org.

SUMMARY AND DISCUSSION

FGF10 signaling plays important roles in the development of many craniofacial structures. FGF10 is required for the branching morphogenesis of salivary and lacrimal glands, for the closure of the secondary palate, and for eyelid development; it also affects the structure of the inner ear, taste papillae on the tongue, and the shape of the teeth and skull. The craniofacial phenotypes connected to FGF10 function along with known expression data are summarized in **Supplementary Table 1**.

FGF10 is predominantly expressed in the mesenchyme of developing structures and signals to adjacent epithelium. In contrast to this classical epithelial–mesenchymal interaction, structures of the inner ear exhibit strong epithelial expression of both *Fgf10* and *Fgfr2 IIIb* during development suggesting dependence on paracrine signaling (Pirvola et al., 2000; Pauley et al., 2003). Epithelial expression of *Fgf10* within orofacial tissues was described also in early oral epithelium (Kettunen et al., 2000). Nevertheless, the conditional *Fgf10* knock-out in neural crest cells using Wnt1-Cre phenocopied the tooth as well as oral cavity glands' phenotype of the full knock-out and generally confirmed that, in orofacial structures comprised of mesenchyme originated fully from neural crest, the mesenchymal FGF10 plays the major role (Teshima et al., 2016).

FGF10 exerts its function in development via diverse and complex mechanisms. Perhaps the most widespread of these is a direct or indirect influence on epithelial cell proliferation and apoptosis, as in eyelid (Tao et al., 2005) or palate development (Rice et al., 2004). Nevertheless, multiple other actions of FGF10, such as regulation of migration or effect on adhesive behavior of the oral epithelium, have also been described in these organs. Control of proper morphogenesis and cell differentiation has also been proposed as one of the roles of FGF10 in many organs, such as salivary gland or inner ear (Alvarez et al., 2003; Makarenkova et al., 2009).

The striking overlap between phenotypes of *Fgf10* and *Fgfr2* null mice explains why FGF10 is considered as the major ligand of FGFR2 IIIb. Multiple FGFs can activate both FGFR2 IIIb (FGF3, 7, and 22 from the Fgf7 subfamily; but also FGF1) and FGFR2 IIIc (e.g., FGF1, 2, 4, 5, 6, 8, 9, or 16) (Zhang et al., 2006). Nevertheless, the *Fgf10* and *Fgfr2* null mice share the majority of defects within the orofacial area, with the exception of milder tooth and inner ear defects in *Fgf10* mutant mice (Kettunen et al., 2000; Ohuchi et al., 2000; Pirvola et al., 2000), and development of medial nasal glands, which are absent in *Fgfr2* null mutants but form normally in *Fgf10* null mice (May et al., 2016). The milder phenotypes in *Fgf10* mutants are mostly explained by compensation by FGF3 (Kettunen et al., 2000; Wright, 2003) or FGF7 (May et al., 2016). Under certain conditions, FGF10 can also likely bind to FGFR1.

Because of the perinatal lethality of *Fgf10* null mutants, some of the functions of FGF10 can be revealed only in conditional knock-outs. Even the conditional approach is complicated by the fact that many developmental events within the orofacial area overlap both in timing and also in expression of similar genes, so the choice of induction time and appropriate driver is challenging, e.g., to avoid simultaneous cleft palate formation. Other approaches such as genetic rescue by changing FGF10 dosage in particular mutants may be used and can bring valuable information, but these must be interpreted with caution, as can be seen for example in the case of the Apert syndrome model.

The impact of absence or malfunction of FGF10 is apparent not only from the animal model data but also from findings in human patients. Thus, the FGF10 pathway presents a potential pharmacological target for cure of rare diseases related to overactivated or downregulated FGFR2 signaling. Also, this knowledge lays the groundwork for potential medical treatment to harness the regenerative potential of gland tissues, after damage. A number of regenerative approaches are being developed and tested in animal models (Lombaert et al., 2011; Garg and Zhang, 2017; Emmerson et al., 2018). For example, healthy lacrimal epithelial cell progenitor cultures (ECPCs) were

isolated and cultured in the presence of FGF10 to achieve budding and engraftment in injured lacrimal glands (Gromova et al., 2017). In theory, engraftment of such cells taken directly from cancer patients before radiotherapy could in the future serve as a source of tissue regeneration. In general, knowledge of the molecular cascades functioning during physiological development provides a base for regenerative approaches where FGF10 or its downstream targets can be provided to cultured tissues to be used for engraftment. In the future, perhaps FGF10 could be directly supplied *in situ*, which could help patients with tissue damage or patients with congenital diseases caused by aberrant FGF10 function.

AUTHOR CONTRIBUTIONS

MP and OK took the lead in writing the manuscript. MP, JP, and PM produced the samples and characterized them by micro-CT analysis. All authors provided critical feedback and revised the manuscript.

FUNDING

Work in the authors' laboratories was funded by NIDCR R35-DE026602 (OK and PM), and Academy of Sciences of the Czech Republic (RVO 68378050), MEYS (LM2015040), and MEYS and ERDF (CZ.02.1.01/0.0/0.0/16_013/0001789; CZ.1.05/2.1.00/19.0395; and CZ.1.05/1.1.00/02.0109) (MP and JP).

ACKNOWLEDGMENTS

We are grateful to Dr. Adriane Joo for helpful suggestions, and to the reviewers for their constructive and thoughtful feedback.

SUPPLEMENTARY MATERIAL

The Supplementary Material for this article can be found online at: https://www.frontiersin.org/articles/10.3389/fgene.2018.00542/full#supplementary-material

REFERENCES

Alappat, S. R., Zhang, Z., Suzuki, K., Zhang, X., Liu, H., Jiang, R., et al. (2005). The cellular and molecular etiology of the cleft secondary palate in Fgf10 mutant mice. *Dev. Biol.* 277, 102–113. doi: 10.1016/j.ydbio.2004.09.010

Alvarez, Y., Alonso, M. T., Vendrell, V., Zelarayan, L. C., Chamero, P., Theil, T., et al. (2003). Requirements for FGF3 and FGF10 during inner ear formation. *Development* 130, 6329–6338. doi: 10.1242/dev.00881

Anderson, J., Burns, H. D., Enriquez-Harris, P., Wilkie, A. O., and Heath, J. K. (1998). Apert syndrome mutations in fibroblast growth factor receptor 2 exhibit increased affinity for FGF ligand. *Hum. Mol. Genet.* 7, 1475–1483. doi: 10.1093/hmg/7.9.1475

Basson, M. A., Echevarria, D., Petersen Ahn, C., Sudarov, A., Joyner, A. L., Mason, I. J., et al. (2008). Specific regions within the embryonic midbrain and cerebellum require different levels of FGF signaling during development. *Development* 135, 889–898. doi: 10.1242/dev.011569

Bochukova, E. G., Roscioli, T., Hedges, D. J., Taylor, I. B., Johnson, D., David, D. J., et al. (2009). Rare mutations of FGFR2 causing apert syndrome: identification of the first partial gene deletion, and an Alu element insertion from a new subfamily. *Hum. Mutat.* 30, 204–211. doi: 10.1002/humu.20825

Chatzeli, L., Gaete, M., and Tucker, A. S. (2017). Fgf10 and Sox9 are essential for the establishment of distal progenitor cells during mouse salivary gland development. *Development* 144, 2294–2305. doi: 10.1242/dev.146019

Cruz, C. V., Mattos, C. T., Maia, J. C., Granjeiro, J. M., Reis, M. F., Mucha, J. N., et al. (2017). Genetic polymorphisms underlying the skeletal Class III phenotype. *Am. J. Orthod. Dentofacial Orthop.* 151, 700–707. doi: 10.1016/j.ajodo.2016.09.013

Domínguez-Frutos, E., Vendrell, V., Alvarez, Y., Zelarayan, L. C., López-Hernández, I., Ros, M., et al. (2009). Tissue-specific requirements for FGF8 during early inner ear development. *Mech. Dev.* 126, 873–881. doi: 10.1016/j.mod.2009.07.004

El Agha, E., Al Alam, D., Carraro, G., MacKenzie, B., Goth, K., De Langhe, S. P., et al. (2012). Characterization of a novel fibroblast growth factor 10 (fgf10) knock-in mouse line to target mesenchymal progenitors during embryonic development. Königshoff M, editor. *PLoS One* 7:e38452. doi: 10.1371/journal.pone.0038452

Emmerson, E., May, A. J., Berthoin, L., Cruz-Pacheco, N., Nathan, S., Mattingly, A. J., et al. (2018). Salivary glands regenerate after radiation injury through SOX2-mediated secretory cell replacement. *EMBO Mol. Med.* 10, e8051. doi: 10.15252/emmm.201708051

Entesarian, M., Dahlqvist, J., Shashi, V., Stanley, C. S., Falahat, B., Reardon, W., et al. (2007). FGF10 missense mutations in aplasia of lacrimal and salivary glands (ALSG). *Eur. J. Hum. Genet.* 15, 379–382. doi: 10.1038/sj.ejhg.5201762

Eswarakumar, V. P., Monsonego-Ornan, E., Pines, M., Antonopoulou, I., Morriss-Kay, G. M., and Lonai, P. (2002). The IIIc alternative of Fgfr2 is a positive regulator of bone formation. *Development* 129, 3783–3793.

Garg, A., and Zhang, X. (2017). Lacrimal gland development: from signaling interactions to regenerative medicine: lacrimal gland development and regeneration. *Dev. Dyn.* 246, 970–980. doi: 10.1002/dvdy.24551

Govindarajan, V., Ito, M., Makarenkova, H. P., Lang, R. A., and Overbeek, P. A. (2000). Endogenous and ectopic gland induction by FGF-10. *Dev. Biol.* 225, 188–200. doi: 10.1006/dbio.2000.9812

Gromova, A., Voronov, D. A., Yoshida, M., Thotakura, S., Meech, R., Dartt, D. A., et al. (2017). Lacrimal Gland repair using progenitor cells: lacrimal gland repair with progenitor cells. *Stem Cells Transl. Med.* 6, 88–98. doi: 10.5966/sctm.2016-0191

Hajihosseini, M. K., Duarte, R., Pegrum, J., Donjacour, A., Lana-Elola, E., Rice, D. P., et al. (2009). Evidence that Fgf10 contributes to the skeletal and visceral defects of an Apert syndrome mouse model. *Dev. Dyn. Off. Publ. Am. Assoc. Anat.* 238, 376–385. doi: 10.1002/dvdy.21648

Hajihosseini, M. K., Wilson, S., De Moerlooze, L., and Dickson, C. (2001). A splicing switch and gain-of-function mutation in FgfR2-IIIc hemizygotes causes Apert/Pfeiffer-syndrome-like phenotypes. *Proc. Natl. Acad. Sci. U.S.A.* 98, 3855–3860. doi: 10.1073/pnas.071586898

Harada, H., Kettunen, P., Jung, H. S., Mustonen, T., Wang, Y. A., and Thesleff, I. (1999). Localization of putative stem cells in dental epithelium and their association with Notch and FGF signaling. *J. Cell Biol.* 147, 105–120. doi: 10.1083/jcb.147.1.105

Harada, H., Toyono, T., Toyoshima, K., Yamasaki, M., Itoh, N., Kato, S., et al. (2002). FGF10 maintains stem cell compartment in developing mouse incisors. *Development* 129, 1533–1541.

Hibberd, C. E., Bowdin, S., Arudchelvan, Y., Forrest, C. R., Brakora, K. A., Marcucio, R. S., et al. (2016). FGFR-associated craniosynostosis syndromes and gastrointestinal defects. *Am. J. Med. Genet. A* 170, 3215–3221. doi: 10.1002/ajmg.a.37862

Hosokawa, R., Oka, K., Yamaza, T., Iwata, J., Urata, M., Xu, X., et al. (2010). TGF-beta mediated FGF10 signaling in cranial neural crest cells controls development of myogenic progenitor cells through tissue-tissue interactions during tongue morphogenesis. *Dev. Biol.* 341, 186–195. doi: 10.1016/j.ydbio.2010.02.030

Jaskoll, T., Abichaker, G., Witcher, D., Sala, F. G., Bellusci, S., Hajihosseini, M. K., et al. (2005). FGF10/FGFR2b signaling plays essential roles during in vivo embryonic submandibular salivary gland morphogenesis. *BMC Dev. Biol.* 5:11. doi: 10.1186/1471-213X-5-11

Jiang, R., Lan, Y., Chapman, H. D., Shawber, C., Norton, C. R., Serreze, D. V., et al. (1998). Defects in limb, craniofacial, and thymic development in Jagged2 mutant mice. *Genes Dev.* 12, 1046–1057. doi: 10.1101/gad.12.7.1046

Juriloff, D. M. (1982). Differences in frequency of cleft lip among the A strains of mice. *Teratology* 25, 361–368. doi: 10.1002/tera.1420250313

Juriloff, D. M., Harris, M. J., McMahon, A. P., Carroll, T. J., and Lidral, A. C. (2006). Wnt9b is the mutated gene involved in multifactorial nonsyndromic cleft lip with or without cleft palate in A/WySn mice, as confirmed by a genetic complementation test. *Birth Defects Res. A Clin. Mol. Teratol.* 76, 574–579. doi: 10.1002/bdra.20302

Kettunen, P., Laurikkala, J., Itäranta, P., Vainio, S., Itoh, N., and Thesleff, I. (2000). Associations of FGF-3 and FGF-10 with signaling networks regulating tooth morphogenesis. *Dev. Dyn. Off. Publ. Am. Assoc. Anat.* 219, 322–332.

Knosp, W. M., Knox, S. M., and Hoffman, M. P. (2012). Salivary gland organogenesis. *Wiley Interdiscip. Rev. Dev. Biol.* 1, 69–82. doi: 10.1002/wdev.4

Lemmerling, M. M., Vanzieleghem, B. D., Dhooge, I. J., Van Cauwenberge, P. B., and Kunnen, M. F. (1999). The Lacrimo-Auriculo-Dento-Digital (LADD) syndrome: temporal bone CT findings. *J. Comput. Assist. Tomogr.* 23, 362–364. doi: 10.1097/00004728-199905000-00007

Lewandoski, M., Sun, X., and Martin, G. R. (2000). Fgf8 signalling from the AER is essential for normal limb development. *Nat. Genet.* 26, 460–463. doi: 10.1038/82609

Lombaert, I., Knox, S., and Hoffman, M. (2011). Salivary gland progenitor cell biology provides a rationale for therapeutic salivary gland regeneration: salivary gland regeneration using progenitor cells. *Oral Dis.* 17, 445–449. doi: 10.1111/j.1601-0825.2010.01783.x

Makarenkova, H. P., Hoffman, M. P., Beenken, A., Eliseenkova, A. V., Meech, R., Tsau, C., et al. (2009). Differential interactions of FGFs with heparan sulfate control gradient formation and branching morphogenesis. *Sci. Signal.* 2:ra55. doi: 10.1126/scisignal.2000304

Makarenkova, H. P., Ito, M., Govindarajan, V., Faber, S. C., Sun, L., McMahon, G., et al. (2000). FGF10 is an inducer and Pax6 a competence factor for lacrimal gland development. *Development* 127, 2563–2572.

May, A. J., Chatzeli, L., Proctor, G. B., and Tucker, A. S. (2015). Salivary gland dysplasia in Fgf10 heterozygous mice: a new mouse model of xerostomia. *Curr. Mol. Med.* 15, 674–682. doi: 10.2174/1566524015666150831141307

May, A. J., Headon, D., Rice, D. P., Noble, A., and Tucker, A. S. (2016). FGF and EDA pathways control initiation and branching of distinct subsets of developing nasal glands. *Dev. Biol.* 419, 348–356. doi: 10.1016/j.ydbio.2016.08.030

Milunsky, J. M., Zhao, G., Maher, T. A., Colby, R., and Everman, D. B. (2006). LADD syndrome is caused by FGF10 mutations. *Clin. Genet.* 69, 349–354. doi: 10.1111/j.1399-0004.2006.00597.x

Nakao, Y., Mitsuyasu, T., Kawano, S., Nakamura, N., Kanda, S., and Nakamura, S. (2013). Fibroblast growth factors 7 and 10 are involved in ameloblastoma proliferation via the mitogen-activated protein kinase pathway. *Int. J. Oncol.* 43, 1377–1384. doi: 10.3892/ijo.2013.2081

Oginuma, M., Moncuquet, P., Xiong, F., Karoly, E., Chal, J., Guevorkian, K., et al. (2017). A gradient of glycolytic activity coordinates FGF and Wnt signaling during elongation of the body axis in amniote embryos. *Dev. Cell* 40, 342.e10–353.e10. doi: 10.1016/j.devcel.2017.02.001

Ohuchi, H., Hori, Y., Yamasaki, M., Harada, H., Sekine, K., Kato, S., et al. (2000). FGF10 acts as a major ligand for FGF receptor 2 IIIb in mouse multi-organ development. *Biochem. Biophys. Res. Commun.* 277, 643–649. doi: 10.1006/bbrc.2000.3721

Ornitz, D. M., and Itoh, N. (2001). Fibroblast growth factors. *Genome Biol.* 2:reviews3005. doi: 10.1186/gb-2001-2-3-reviews3005

Ornitz, D. M., and Itoh, N. (2015). The fibroblast growth factor signaling pathway. *Wiley Interdiscip. Rev. Dev. Biol.* 4, 215–266. doi: 10.1002/wdev.176

Patel, V. N., Knox, S. M., Likar, K. M., Lathrop, C. A., Hossain, R., Eftekhari, S., et al. (2007). Heparanase cleavage of perlecan heparan sulfate modulates FGF10 activity during ex vivo submandibular gland branching morphogenesis. *Development* 134, 4177–4186. doi: 10.1242/dev.011171

Pauley, S., Wright, T. J., Pirvola, U., Ornitz, D., Beisel, K., and Fritzsch, B. (2003). Expression and function of FGF10 in mammalian inner ear development. *Dev. Dyn. Off. Publ. Am. Assoc. Anat.* 227, 203–215. doi: 10.1002/dvdy.10297

Petersen, C. I., Jheon, A. H., Mostowfi, P., Charles, C., Ching, S., Thirumangalathu, S., et al. (2011). FGF signaling regulates the number of posterior taste papillae by controlling progenitor field size. *PLoS Genet.* 7:e1002098. doi: 10.1371/journal.pgen.1002098

Pirvola, U., Spencer-Dene, B., Xing-Qun, L., Kettunen, P., Thesleff, I., Fritzsch, B., et al. (2000). FGF/FGFR-2(IIIb) signaling is essential for inner ear morphogenesis. *J. Neurosci.* 20, 6125–6134. doi: 10.1523/JNEUROSCI.20-16-06125.2000

Prochazka, J., Prochazkova, M., Du, W., Spoutil, F., Tureckova, J., Hoch, R., et al. (2015). Migration of founder epithelial cells drives proper molar tooth positioning and morphogenesis. *Dev. Cell.* 35, 713–724. doi: 10.1016/j.devcel.2015.11.025

Prochazkova, M., Häkkinen, T. J., Prochazka, J., Spoutil, F., Jheon, A. H., Ahn, Y., et al. (2017). FGF signaling refines Wnt gradients to regulate the patterning of taste papillae. *Development* 144, 2212–2221. doi: 10.1242/dev.148080

Qu, X., Carbe, C., Tao, C., Powers, A., Lawrence, R., van Kuppevelt, T. H., et al. (2011). Lacrimal gland development and Fgf10-Fgfr2b signaling are controlled by 2-O- and 6-O-sulfated heparan sulfate. *J. Biol. Chem.* 286, 14435–14444. doi: 10.1074/jbc.M111.225003

Rebustini, I. T., and Hoffman, M. P. (2009). ECM and FGF-dependent assay of embryonic SMG epithelial morphogenesis: investigating growth factor/matrix regulation of gene expression during submandibular gland development. *Methods Mol. Biol. Clifton N. J.* 522, 319–330. doi: 10.1007/978-1-59745-413-1_21

Rice, R., Spencer-Dene, B., Connor, E. C., Gritli-Linde, A., McMahon, A. P., Dickson, C., et al. (2004). Disruption of Fgf10/Fgfr2b-coordinated epithelial-mesenchymal interactions causes cleft palate. *J. Clin. Invest.* 113, 1692–1700. doi: 10.1172/JCI20384

Rohmann, E., Brunner, H. G., Kayserili, H., Uyguner, O., Nürnberg, G., Lew, E. D., et al. (2006). Mutations in different components of FGF signaling in LADD syndrome. *Nat. Genet.* 38, 414–417. doi: 10.1038/ng1757

Rosenquist, T. A., and Martin, G. R. (1996). Fibroblast growth factor signalling in the hair growth cycle: expression of the fibroblast growth factor receptor and ligand genes in the murine hair follicle. *Dev. Dyn. Off. Publ. Am. Assoc. Anat.* 205, 379–386. doi: 10.1002/(SICI)1097-0177(199604)205:4<379::AID-AJA2>3.0.CO;2-F

Rothova, M., Thompson, H., Lickert, H., and Tucker, A. S. (2012). Lineage tracing of the endoderm during oral development. *Dev. Dyn. Off. Publ. Am. Assoc. Anat.* 241, 1183–1191. doi: 10.1002/dvdy.23804

Scheckenbach, K., Balz, V., Wagenmann, M., and Hoffmann, T. K. (2008). An intronic alteration of the fibroblast growth factor 10 gene causing ALSG-(aplasia of lacrimal and salivary glands) syndrome. *BMC Med. Genet.* 9:114. doi: 10.1186/1471-2350-9-114

Schell, U., Hehr, A., Feldman, G. J., Robin, N. H., Zackai, E. H., de Die-Smulders, C., et al. (1995). Mutations in FGFR1 and FGFR2 cause familial and sporadic Pfeiffer syndrome. *Hum. Mol. Genet.* 4, 323–328. doi: 10.1093/hmg/4.3.323

Seymen, F., Koruyucu, M., Toptanci, I. R., Balsak, S., Dedeoglu, S., Celepkolu, T., et al. (2017). Novel FGF10 mutation in autosomal dominant aplasia of lacrimal and salivary glands. *Clin. Oral Investig.* 21, 167–172. doi: 10.1007/s00784-016-1771-x

Shams, I., Rohmann, E., Eswarakumar, V. P., Lew, E. D., Yuzawa, S., Wollnik, B., et al. (2007). Lacrimo-auriculo-dento-digital syndrome is caused by reduced activity of the fibroblast growth factor 10 (FGF10)-FGF receptor 2 signaling pathway. *Mol. Cell Biol.* 27, 6903–6912. doi: 10.1128/MCB.00544-07

Shi, M., Mostowska, A., Jugessur, A., Johnson, M. K., Mansilla, M. A., Christensen, K., et al. (2009). Identification of microdeletions in candidate genes for cleft lip and/or palate. *Birth Defects Res. A Clin. Mol. Teratol.* 85, 42–51. doi: 10.1002/bdra.20571

Song, Z., Liu, C., Iwata, J., Gu, S., Suzuki, A., Sun, C., et al. (2013). Mice with Tak1 deficiency in neural crest lineage exhibit cleft palate associated with abnormal tongue development. *J. Biol. Chem.* 288, 10440–10450. doi: 10.1074/jbc.M112.432286

Sugii, H., Grimaldi, A., Li, J., Parada, C., Vu-Ho, T., Feng, J., et al. (2017). The Dlx5-FGF10 signaling cascade controls cranial neural crest and myoblast

interaction during oropharyngeal patterning and development. *Development* 144, 4037–4045. doi: 10.1242/dev.155176

Tao, H., Shimizu, M., Kusumoto, R., Ono, K., Noji, S., and Ohuchi, H. (2005). A dual role of FGF10 in proliferation and coordinated migration of epithelial leading edge cells during mouse eyelid development. *Development* 132, 3217–3230. doi: 10.1242/dev.01892

Terao, F., Takahashi, I., Mitani, H., Haruyama, N., Sasano, Y., Suzuki, O., et al. (2011). Fibroblast growth factor 10 regulates Meckel's cartilage formation during early mandibular morphogenesis in rats. *Dev. Biol.* 350, 337–347. doi: 10.1016/j.ydbio.2010.11.029

Teshima, T. H. N., Lourenco, S. V., and Tucker, A. S. (2016). Multiple cranial organ defects after conditionally knocking out Fgf10 in the neural crest. *Front. Physiol.* 7:488. doi: 10.3389/fphys.2016.00488

Urness, L. D., Wang, X., Shibata, S., Ohyama, T., and Mansour, S. L. (2015). Fgf10 is required for specification of non-sensory regions of the cochlear epithelium. *Dev. Biol.* 400, 59–71. doi: 10.1016/j.ydbio.2015.01.015

Veistinen, L., Aberg, T., and Rice, D. P. C. (2009). Convergent signalling through Fgfr2 regulates divergent craniofacial morphogenesis. *J. Exp. Zool. B Mol. Dev. Evol.* 312B, 351–360. doi: 10.1002/jez.b.21276

Walker, K. A., Sims-Lucas, S., and Bates, C. M. (2016). Fibroblast growth factor receptor signaling in kidney and lower urinary tract development. *Pediatr. Nephrol.* 31, 885–895. doi: 10.1007/s00467-015-3151-1

Wright, T. J. (2003). Fgf3 and Fgf10 are required for mouse otic placode induction. *Development* 130, 3379–3390. doi: 10.1242/dev.00555

Xu, X., Weinstein, M., Li, C., Naski, M., Cohen, R. I., Ornitz, D. M., et al. (1998). Fibroblast growth factor receptor 2 (FGFR2)-mediated reciprocal regulation loop between FGF8 and FGF10 is essential for limb induction. *Development* 125, 753–765.

Yokohama-Tamaki, T., Ohshima, H., Fujiwara, N., Takada, Y., Ichimori, Y., Wakisaka, S., et al. (2006). Cessation of Fgf10 signaling, resulting in a defective dental epithelial stem cell compartment, leads to the transition from crown to root formation. *Development* 133, 1359–1366. doi: 10.1242/dev.02307

Young, N. M., Wat, S., Diewert, V. M., Browder, L. W., and Hallgrímsson, B. (2007). Comparative morphometrics of embryonic facial morphogenesis: implications for cleft-lip etiology. *Anat. Rec. Adv. Integr. Anat. Evol. Biol.* 290, 123–139. doi: 10.1002/ar.20415

Yu, Y., Zuo, X., He, M., Gao, J., Fu, Y., Qin, C., et al. (2017). Genome-wide analyses of non-syndromic cleft lip with palate identify 14 novel loci and genetic heterogeneity. *Nat. Commun.* 8:14364. doi: 10.1038/ncomms14364

Zhang, X., Ibrahimi, O. A., Olsen, S. K., Umemori, H., Mohammadi, M., and Ornitz, D. M. (2006). Receptor specificity of the fibroblast growth factor family. The complete mammalian FGF family. *J. Biol. Chem.* 281, 15694–15700. doi: 10.1074/jbc.M601252200

Conflict of Interest Statement: The authors declare that the research was conducted in the absence of any commercial or financial relationships that could be construed as a potential conflict of interest.

Copyright © 2018 Prochazkova, Prochazka, Marangoni and Klein. This is an open-access article distributed under the terms of the Creative Commons Attribution License (CC BY). The use, distribution or reproduction in other forums is permitted, provided the original author(s) and the copyright owner(s) are credited and that the original publication in this journal is cited, in accordance with accepted academic practice. No use, distribution or reproduction is permitted which does not comply with these terms.

frontiers in Genetics

ORIGINAL RESEARCH
published: 23 November 2018
doi: 10.3389/fgene.2018.00556

FGF10 Protects Against Renal Ischemia/Reperfusion Injury by Regulating Autophagy and Inflammatory Signaling

Xiaohua Tan[1,2], Hongmei Zhu[1], Qianyu Tao[1], Lisha Guo[1], Tianfang Jiang[3], Le Xu[3], Ruo Yang[1], Xiayu Wei[4], Jin Wu[4], Xiaokun Li[1,4] and Jin-San Zhang[1,3,4]**

[1] School of Pharmaceutical Sciences, Wenzhou Medical University, Wenzhou, China, [2] Qingdao University Medical College, Qingdao, China, [3] The First Affiliated Hospital, Wenzhou Medical University, Wenzhou, China, [4] Institute of Life Sciences, Wenzhou University, Wenzhou, China

Ischemia-reperfusion (I/R) is a common cause of acute kidney injury (AKI), which is associated with high mortality and poor outcomes. Autophagy plays important roles in the homeostasis of renal tubular cells (RTCs) and is implicated in the pathogenesis of AKI, although its role in the process is complex and controversial. Fibroblast growth factor 10 (FGF10), a multifunctional FGF family member, was reported to exert protective effect against cerebral ischemia injury and myocardial damage. Whether FGF10 has similar beneficial effect, and if so whether autophagy is associated with the potential protective activity against AKI has not been investigated. Herein, we report that FGF10 treatment improved renal function and histological integrity in a rat model of renal I/R injury. We observed that FGF10 efficiently reduced I/R-induced elevation in blood urea nitrogen, serum creatinine as well as apoptosis induction of RTCs. Interestingly, autophagy activation following I/R was suppressed by FGF10 treatment based on the immunohistochemistry staining and immunoblot analyses of LC3, Beclin-1 and SQSTM1/p62. Moreover, combined treatment of FGF10 with Rapamycin partially reversed the renoprotective effect of FGF10 suggesting the involvement of mTOR pathway in the process. Interestingly, FGF10 also inhibited the release of HMGB1 from the nucleus to the extracellular domain and regulated the expression of inflammatory cytokines such as TNF-α, IL-1β and IL-6. Together, these results indicate that FGF10 could alleviate kidney I/R injury by suppressing excessive autophagy and inhibiting inflammatory response and may therefore have the potential to be used for the prevention and perhaps treatment of I/R-associated AKI.

Keywords: FGF10, ischemia-reperfusion, acute kidney injury, autophagy, inflammation, HMGB1

OPEN ACCESS

Edited by:
Saverio Bellusci, Justus-Liebig-Universität Gießen, Germany

Reviewed by:
Hector A. Cabrera-Fuentes, Justus-Liebig-Universität Gießen, Germany
Fen Wang, Texas A&M University, United States

****Correspondence:***
Xiaokun Li
profxiaokunli@163.com
Jin-San Zhang
zhang_jinsan@163.com

Specialty section:
This article was submitted to Stem Cell Research, a section of the journal Frontiers in Genetics

Received: *28 September 2018*
Accepted: *31 October 2018*
Published: *23 November 2018*

Citation:
Tan X, Zhu H, Tao Q, Guo L, Jiang T, Xu L, Yang R, Wei X, Wu J, Li X and Zhang J-S (2018) FGF10 Protects Against Renal Ischemia/Reperfusion Injury by Regulating Autophagy and Inflammatory Signaling. Front. Genet. 9:556. doi: 10.3389/fgene.2018.00556

Abbreviations: AKI, acute kidney injury; ANOVA, analysis of variance; BUN, blood urea nitrogen; CKD, chronic kidney disease; DAMP, damage-associated molecular pattern; ELISA, enzyme-linked immunosorbent assay; ER, endoplasmic reticulum; FGF10, fibroblast growth factor 10; GFR, glomerular filtration rate; H&E, hematoxylin and eosin; HMGB1, high-mobility group box 1; I/R, ischemia-reperfusion; mTOR, mammalian target of rapamycin; PVDF, polyvinylidene fluoride; ROS, reactive oxygen species; RTCs, renal tubular epithelial cells; SCr, serum creatinine; SDS-PAGE, sodium dodecyl sulfate–polyacrylamide gel electrophoresis; TLRs, Toll-like receptors; TUNEL, terminal deoxynucleotidyl transferase dUTP nick end labeling; UPR, unfolded protein response.

INTRODUCTION

Acute kidney injury is a global health concern. AKI is mainly caused by renal I/R injury, sepsis, and nephrotoxicant (such as cisplatin, cyclosporine and aristolochic acid) (Paller et al., 1984; Thadhani et al., 1996; Zuk and Bonventre, 2016). The primary characteristic of AKI is the rapid decline in kidney function as measured by detection of GFR (Bonventre and Yang, 2011; Havasi and Borkan, 2011). Despite advances in therapeutic strategies and nursing measures, including dialysis and kidney transplantation, the mortality of patients after AKI remains very high (Ueda et al., 2000; Chertow et al., 2005). In the past decades, AKI has been extensively studied both in clinic and experimental animal settings. The disease mechanisms underlying the etiology and pathogenesis of AKI are complex and include mitochondrial dysfunction, ROS, ER stress, autophagy, inflammation, apoptosis and necrosis (Basile et al., 2012; Tan et al., 2013, 2017; He et al., 2014; Kaushal and Shah, 2016; Xu et al., 2016). To date, there are no satisfying strategies or drugs for the therapy of patients with AKI.

A number of recent studies have demonstrated the crucial role of autophagy in animal models of AKI induced by I/R injury and nephrotoxic agents (Mizushima and Komatsu, 2011; Basile et al., 2012; Jiang et al., 2012; He et al., 2014; Guan et al., 2015; De Rechter et al., 2016; Lenoir et al., 2016). Autophagy is a highly conserved eukaryotic cellular recycling process by which cytoplasmic components are engulfed and degraded in the lysosome (Mizushima and Komatsu, 2011). Generally, autophagy is thought to be highly inducible under stress conditions such as ischemia, hypoxia, nutrient deprivation, genotoxic stress, infection, UPR, and other insults, all of which participate in the pathogenesis of AKI (Mizushima and Komatsu, 2011; Basile et al., 2012; He et al., 2014; De Rechter et al., 2016; Kaushal and Shah, 2016; Zuk and Bonventre, 2016). Whether autophagy is protective or damaging in AKI remains controversial. Renoprotective effects of autophagy in AKI have been reported in several studies (Pallet et al., 2008; Jiang et al., 2012). However, excessive activation of autophagy results in widespread cell death predominantly in RTCs due to extensive degradation of essential materials and organelles (Chien et al., 2007; Suzuki et al., 2008; Inoue et al., 2010). Therefore, activation of autophagy has dual roles in regulating cell survival or cell death in AKI.

Inflammatory response is another important component in the initiation and exacerbation of AKI. Although inflammation is an essential element of the body's defense system, excessive activation of inflammatory cells and cytokine secretion impose severe damage to renal parenchyma cells (Jang and Rabb, 2009; Shibutani et al., 2015). High-mobility group box 1 is a member of the high-mobility group (HMG) protein family and one of the highly conserved and abundantly expressed proteins in almost all types of eukaryotic cells (Lotze and Tracey, 2005; Kang et al., 2014). Recently, the pathophysiological role of HMGB1 in human diseases has been extensively studied. In healthy circumstances, HMGB1 is localized in the nuclei of cells and participates in multiple cellular processes including DNA repair, transcription, and cell differentiation. However, HMGB1 can be released into the extracellular space and function as a signaling molecule in various biological processes such as inflammatory response (Tang et al., 2010a; Xu et al., 2014; Ouyang et al., 2016). Circulating HMBG1 is capable of engaging with toll-like receptors (TLRs), particularly TLR2 and TLR4, to activate the expression of multiple pro-inflammatory cytokines such as TNF-α, IL-1β and IL-6. Studies demonstrate that HMGB1 plays an important role in the interaction of autophagy and apoptosis/necrosis in various disorders including AKI (Nikoletopoulou et al., 2013; Kim et al., 2014; Chen et al., 2016).

Fibroblast growth factor 10, also known as Keratinocyte growth factor 2, is a typical paracrine FGF family member and signals through interactions with its high affinity receptor FGFR2-IIIb splicing isoform. FGF10 is a multifunctional growth factor playing crucial roles in the development of many organs and tissues including the kidney (Beenken and Mohammadi, 2009; Itoh, 2015). Deletion of either *Fgf10* or its receptor *Fgfr2-IIIb* in mice led to kidney dysgenesis characterized by fewer collecting ducts and nephrons (Bates, 2007). Overexpression of a dominant negative receptor isoform in transgenic mice has revealed more striking defects including renal aplasia or severe dysplasia (Bates, 2007). Recent studies have reported the protective effect of FGF10 on spinal cord injury, cerebral ischemia injury and acute lung injury via inhibiting inflammation, activating PI3K/AKT signaling pathway or mobilization of stem cells (Li et al., 2016; Tong et al., 2016; Chen et al., 2017). Currently, there are no published reports regarding whether exogenous FGF10 can promote the recovery of AKI. In the present work, we tested the hypothesis that FGF10 administration might protect renal cells exposed to I/R injury through regulating autophagy and inflammation.

MATERIALS AND METHODS

Reagents and Antibodies

Recombinant human FGF10 was acquired from Zhejiang Grost Biotechnology (Wenzhou). Antibodies against mTOR, LC3, SQSTM1, Beclin-1 and GAPDH were purchased from Santa Cruz Biotechnology (Santa Cruz, CA, United States). Antibodies against cleaved Caspase-3, HMGB1, phospho-FGFR, TNF-α and Caspase-9 were bought from Cell Signaling Technology (Beverly, MA, United States). TGF-β antibody was purchased from Abcam (Cambridge, MA, United States). The autophagy inhibitor chloroquine, autophagy activator rapamycin and 4′, 6-diamidino-2-phenylindole (DAPI) were purchased from Sigma-Aldrich (St Louis, MO, United States) and Invitrogen (Carlsbad, CA, United States), respectively.

Animals

Adult male Sprague Dawley (SD) rats (8–12 weeks old) were supplied by Shanghai SLAC Laboratory Animal Co., Ltd., and housed in SPF facility of Wenzhou Medical University. The protocols for all animal experiments were approved by the institutional Animal Care and Use committee. Rats were anesthetized with intra-peritoneal injection of 4% pentobarbital sodium (50 mg/kg, Merck, Germany) and underwent right

nephrectomy followed by ischemia for 60 min with renal artery clamping. SD rats were randomly divided into four groups: (I) Sham group: the left kidney was exposed with an unrestricted renal artery; (II) I/R group: the left kidneys were subjected to 60 min of ischemia by renal artery clamping followed by reperfusion (Kalogeris et al., 2012; Tan et al., 2017); (III) I/R-FGF10 group: a single dose of FGF10 (0.5 mg/kg) was injected into the abdominal cavity 30 min before the 60 min exposure to ischemia; (IV) RAPA group: a single dose of rapamycin (10 mg/kg, intramuscular injection, i.m) was injected followed by the injection of FGF10 same with I/R-FGF10 group, and then the left kidneys were subjected to 60 min of ischemia. For combined treatment with chloroquine (I/R-CL group): a single dose of chloroquine (60 mg/kg) was injected into the abdominal cavity 30 min before the 60 min exposure to ischemia. Animals were sacrificed at indicated time points after reperfusion upon surgical operation and kidneys were harvested for further experiment.

Renal Function and Histopathology

Serum creatinine and BUN were used to assess changes of renal function after AKI. The levels of SCr and BUN were determined by the Creatine and the Urease colorimetry methods, respectively, which were performed at the Medical Laboratory Center of the First Affiliated Hospital, Wenzhou Medical University. For renal histology analysis, Kidneys were dissected and fixed with 10% formaldehyde for 48 h, then embedded in paraffin. To access the severity of renal injury after AKI, sections (5 μm) were stained with H&E to observe the changes of the renal morphology.

Immunohistochemistry and Immunofluorescent Staining

The slides were incubated with antibodies against cleaved-Capase-3, p-FGFR, SQSTM1 and TNF-α at 4°C overnight and stained with Diaminobenzidine (DAB) and counterstained with hematoxylin. The slides were then subjected to gradient ethanol dehydration, dimethyl benzene transparent, and mounted with Neutral resin cover slides. Images were captured using a Nikon ECLPSE 80i. For immunofluorescent staining, 5 μm sections were incubated at 4°C overnight with primary antibody against LC3, Beclin-1 and HMGB1, respectively. The slides were then incubated with donkey anti-rabbit secondary antibodies (Abcam, MA, United States) or donkey anti-mouse IgG-PE secondary antibodies (Santa Cruz, CA, United States) for 1 h at room temperature. The images were captured using a laser confocal microscope (Nikon, Ti-E&A1 plus).

Apoptosis Assay

To measure the apoptosis rates after I/R injury, DNA fragmentation *in vivo* was detected using a one-step TUNEL Apoptosis Assay KIT (Roche, Mannheim, Germany) as previously described (Tan et al., 2017). The images were captured with a Nikon ECLPSE Ti microscope (Nikon, Japan).

Western Blot Analysis

Tissue protein samples were prepared with protein extraction reagents from renal tissues. Protein concentrations were measured with a Pierce BCA Protein Assay Kit (Thermo Fisher Scientific). Samples with equal amount of proteins were separated with SDS-PAGE and then transferred onto a PVDF membrane for Western blot analysis with specified antibodies. The ChemiDic TM XRS+ imaging system (Bio-Rad Laboratories, Hercules, United States) was used to analyze the signals and the band densities were quantified with Multi Gauge software of science Lab 2010 (FUJIFILM Corporation, Tokyo, Japan).

Real-Time Quantitative RT-PCR

Total RNA from kidney tissues was extracted using RNeasy column (QIAGEN), and reverse transcription was performed using Prime Script TM RT reagent Kit (TaKaRa) according to the manufacturer's instructions. Real-time RT-PCR was performed using the SYBR Green gene expression assays (TaKaRa) to access mRNA expression. The target values were normalized to GAPDH (Tan et al., 2017). The PCR primers used for mRNA expression analysis of *Tlr2, Tlr4, Il-Iβ, Il-6*, and *Gapdh* are summarized in **Table 1**.

Statistical Analysis

Data is expressed as the mean ± SEM of independent experiments ($n \geq 5$). Statistical significance was determined using Student's *t*-test when there were two experimental groups. When more than two groups were compared, statistical evaluation of the data was performed using one-way analysis of variance (ANOVA). $^{*}P < 0.05$, $^{**}P < 0.01$, $^{***}P < 0.001$, *P*-values < 0.05 was regarded as statistically significant.

RESULTS

FGF10 Ameliorates I/R-Induced Renal Dysfunction and Histological Damage

We employed an I/R injury rat model to investigate the potential effect of FGF10 on AKI at 24, 48, and 72 h, respectively. Renal histological changes were assessed by H&E staining, no apparent damage was observed in the kidney of sham group, whereas

TABLE 1 | Primer sequences used to amplify rat cDNAs.

Gene	GenBank	Primer sequences
GAPDH	NM_012675	5′- GACATGCCGCCTGGAGAAAC-3′ 5′-AGCCCAGGATGCCCTTTAGT-3′
IL-1β	NM_031512	5′-TGCAGGCTTCGAGATGAAC-3′ 5′-GGGATTTTGTCGTTGCTTGTC-3′
IL-6	NM_012589	5′-AAGCCAGAGTCATTCAGAGC-3′ 5′-GTCCTTAGCCACTCCTTCTG-3′
TLR2	NM_198769	5′-ATGAACACTAAGACATACCTGGAG-3′ 5′-CAAGACAGAAACAGGGTGGAG-3′
TLR4	NM_019178	5′-CATGACATCCCTTATTCAACCAAG-3′ 5′-GCCATGCCTTGTCTTCAATTG-3′
TNFα	NM_012675	5′-CTTCTCATTCCTGCTCGTGG-3′ 5′-TGATCTGAGTGTGAGGGTCTG-3′

GAPDH: Glyceraldehyde 3-phosphate dehydrogenase; IL-1β: interleukin-1β; IL-6: interleukin-6; TLR2: Toll-like receptor-2; TLR4: Toll-like receptor-4; TNFα: tumor necrosis factor-α.

the rats in I/R group and RAPA group showed swelling of RTCs, intraluminal necrotic cellular debris, interstitial congestion and luminal narrowing characteristic of I/R-induced tubular epithelial injury at each time point after reperfusion (**Figure 1A**). Significantly, Pre-administration of FGF10 markedly attenuated the degree of renal damages and largely preserved the normal tissue architecture and integrity. Renal function was assessed by measuring SCr and BUN at 48 h after reperfusion. As expected, the levels of SCr and BUN were both increased significantly in I/R rats compared to Sham group (**Figures 1C,D**). Notably, the levels of SCr and BUN in I/R-FGF10 group were significantly lower compared to that of I/R group ($P < 0.001$), whereas Rapamycin largely abolished the protective effect of FGF10 against I/R injury. To investigate the association between FGF10/FGFR signaling pathway and I/R injury, we detected the activation of FGFR by immunohistochemistry (IHC) staining with p-FGFR antibody. As shown in **Figure 1B**, few p-FGFR positive cells were detected in kidneys of sham group, whereas the number of p-FGFR

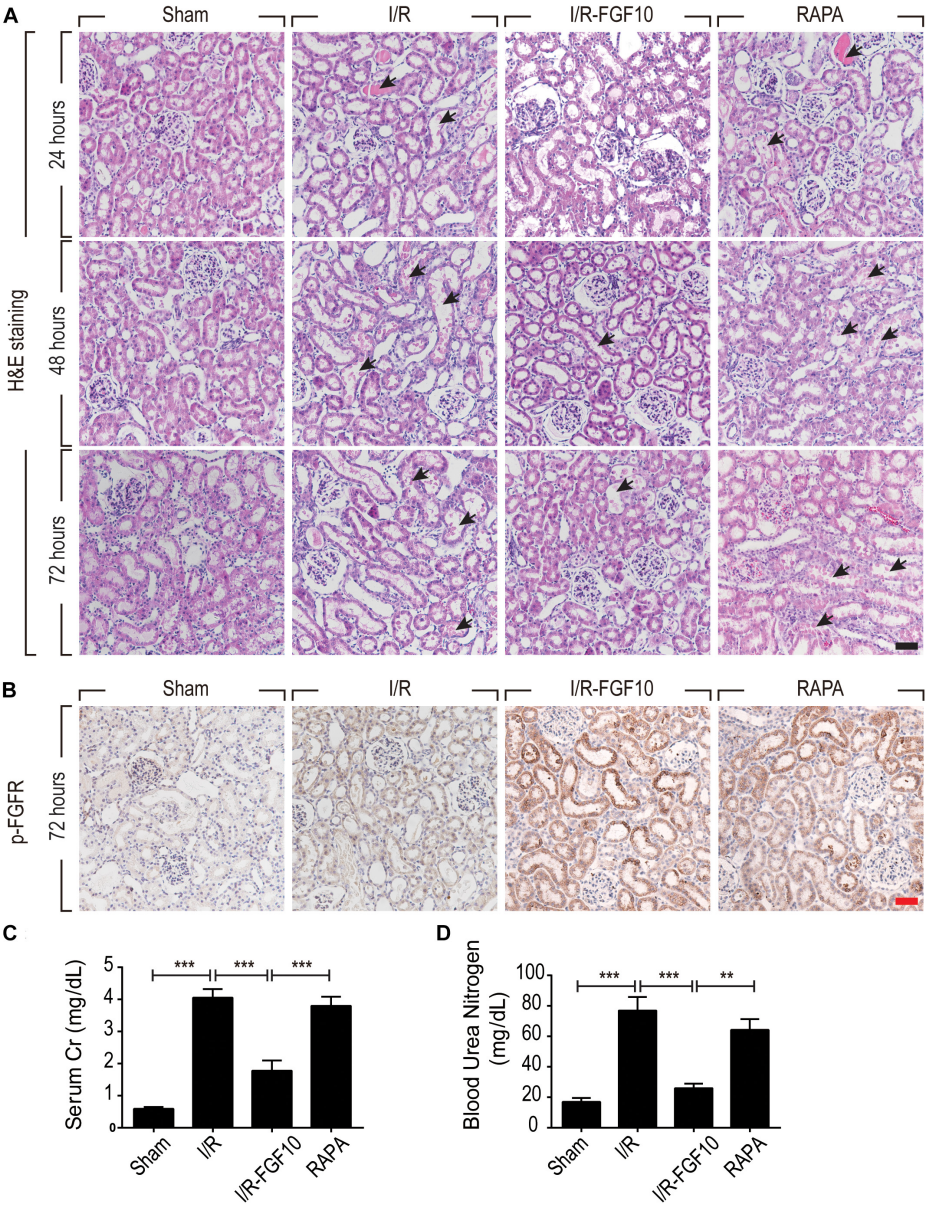

FIGURE 1 | FGF10 protects against renal histological and function damage after I/R injury. **(A)** Histological changes of kidneys detected by H&E staining at 24, 48, and 72 h, respectively, after reperfusion. Animals were randomly assigned into 4 groups: namely, Sham group, I/R group, I/R-FGF10 group and RAPA group. The details of operations and treatment animals received were described in the materials and methods. Arrows show intraluminal necrotic cells. Scale bars = 50 μm. **(B)** IHC staining for p-FGFR in renal tissue sections of indicated groups. Scale bars = 50 μm. **(C,D)** Determination of SCr and BUN levels in the above grouped rats at 2 days after reperfusion (mean ± SEM; $n = 5$). $^{**}P < 0.01$, $^{***}P < 0.001$.

positive cells was increased in I/R group at 48 h after reperfusion. However, both the number of p-FGFR positive renal tubular cells (RTCs) and the staining intensity were noticeably increased in kidneys of I/R-FGF10 group or RAPA group compared to I/R group.

FGF10 Reduced Apoptosis of RTCs via Regulation of Pro-apoptotic Proteins

TUNEL staining was carried out to assess the apoptosis in RTCs. As shown in **Figure 2A**, compared to the sham group, the number of TUNEL-positive cells in I/R rats was dramatically increased ($P < 0.001$). Significantly, the proportion of TUNEL-positive cells was much lower in I/R-FGF10 group ($P < 0.001$). However, this apparent effect of FGF10 against I/R-induced apoptosis was mostly antagonized by rapamycin treatment (**Figure 2A**). The number of TUNEL-positive cells was strikingly increased in RAPA group compared to the IR-FGF10 group. Quantification analysis of TUNEL staining revealed that the average percentage of apoptotic cells were 2.40% (24 h), 2.64% (48 h) and 1.92% (72 h) in sham group; 11.8% (24 h), 40.34% (48 h), 32.8% (72 h) in I/R group; 8.14% (24 h), 13.22% (48 h), 12.38% (72 h) in I/R-FGF10 group and 13.2% (24 h), 32.9% (48 h), 34.28% (72 h) in RAPA group, respectively (**Figure 2B**). The results indicated that FGF10 treatment protected RTCs from I/R-induced apoptosis based on TUNEL staining. However, the protective role of FGF10 against apoptosis was diminished by rapamycin.

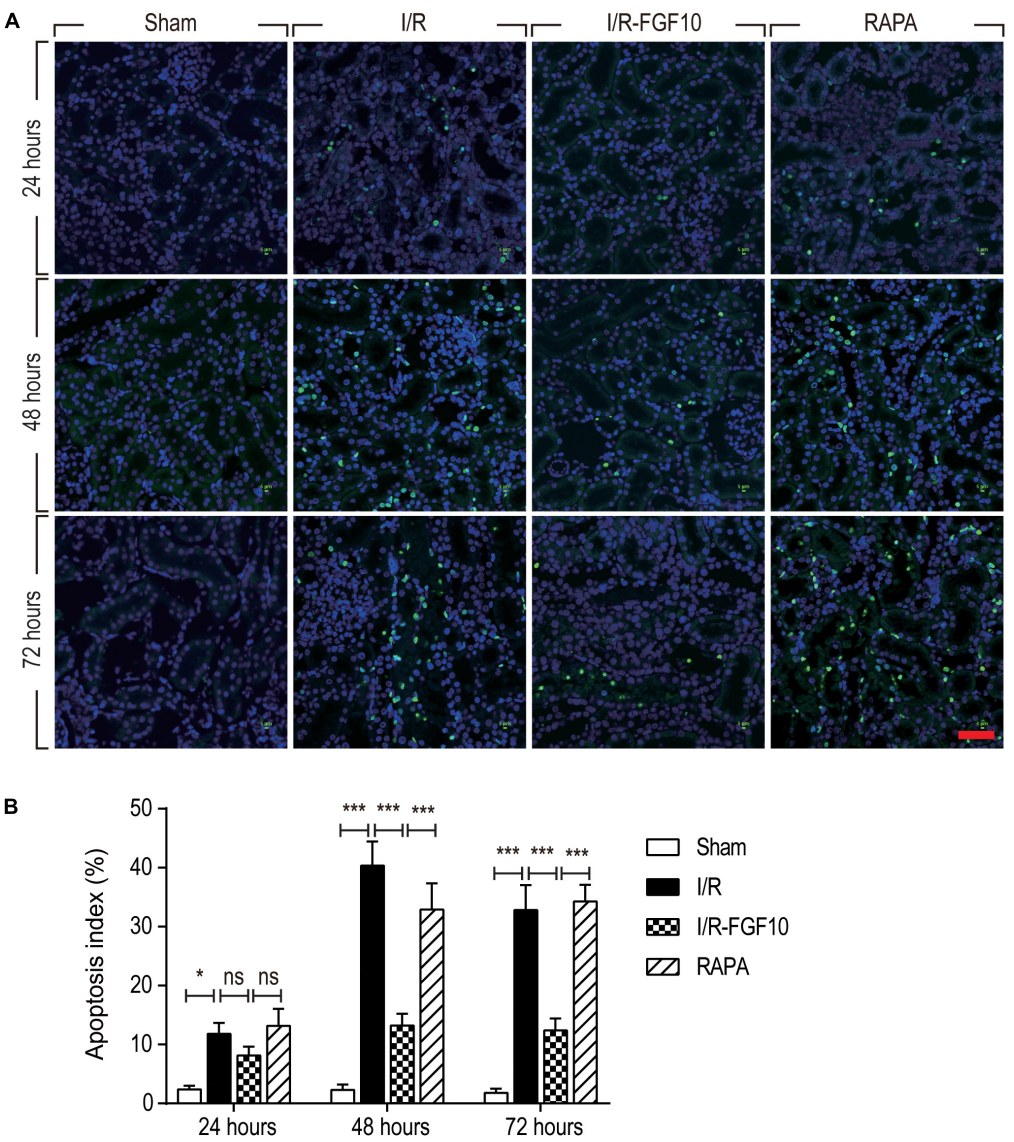

FIGURE 2 | FGF10 protects against I/R induced apoptosis in RTCs. **(A)** Representative sections of nuclear DNA fragmentation staining were performed using TUNEL in different groups at 24, 48, and 72 h, respectively, after reperfusion. Scale bars = 50 μM. **(B)** Quantitative analysis of the number of TUNEL-positive RTCs. Data are presented as the mean ± SD ($n = 5$). $^{*}P < 0.05$, $^{***}P < 0.001$. The percentage of positive cells was analyzed with 5 individual magnification × 400 fields per group.

To understand the protective mechanism of FGF10 against I/R-induced RTC apoptosis, we examined the expression of pro-apoptotic proteins involved in regulation of cell apoptosis (BCL-2, BAX) and cleaved-Caspase-3 by IHC staining (**Figure 3A**) and western blot (**Figures 3B–E**), respectively. The expression of BAX and cleaved-Caspase-3 were significantly increased upon I/R injury, whereas BCL2 expression was decreased. Significantly, FGF10 treatment inhibited the pro-apoptotic expression/activation of Bax/BCL2 and cleaved-Caspase-3, respectively. Consistent with the results of apoptosis, the effect of FGF10 was largely inhibited by co-treatment with rapamycin. Together, the results suggest that FGF10 protects RTCs from I/R-induced apoptosis via regulation of pro-apoptotic proteins. However, rapamycin inhibited the role of FGF10 and thus the expression of pro-apoptotic proteins was increased.

The Protective Effect of FGF10 Is Related to the Regulation of Autophagy via mTOR Pathway

Autophagy is known to play a crucial role in the etiology of AKI caused by renal I/R injury. The fact that rapamycin, a well-established allosteric mTOR kinase inhibitor and agonist of autophagy, mostly reduced the protective effect of FGF10 against I/R-induced renal damage apoptosis of RTCs prompted us to further examine the involvement of autophagy in mediating protective effect of FGF10.

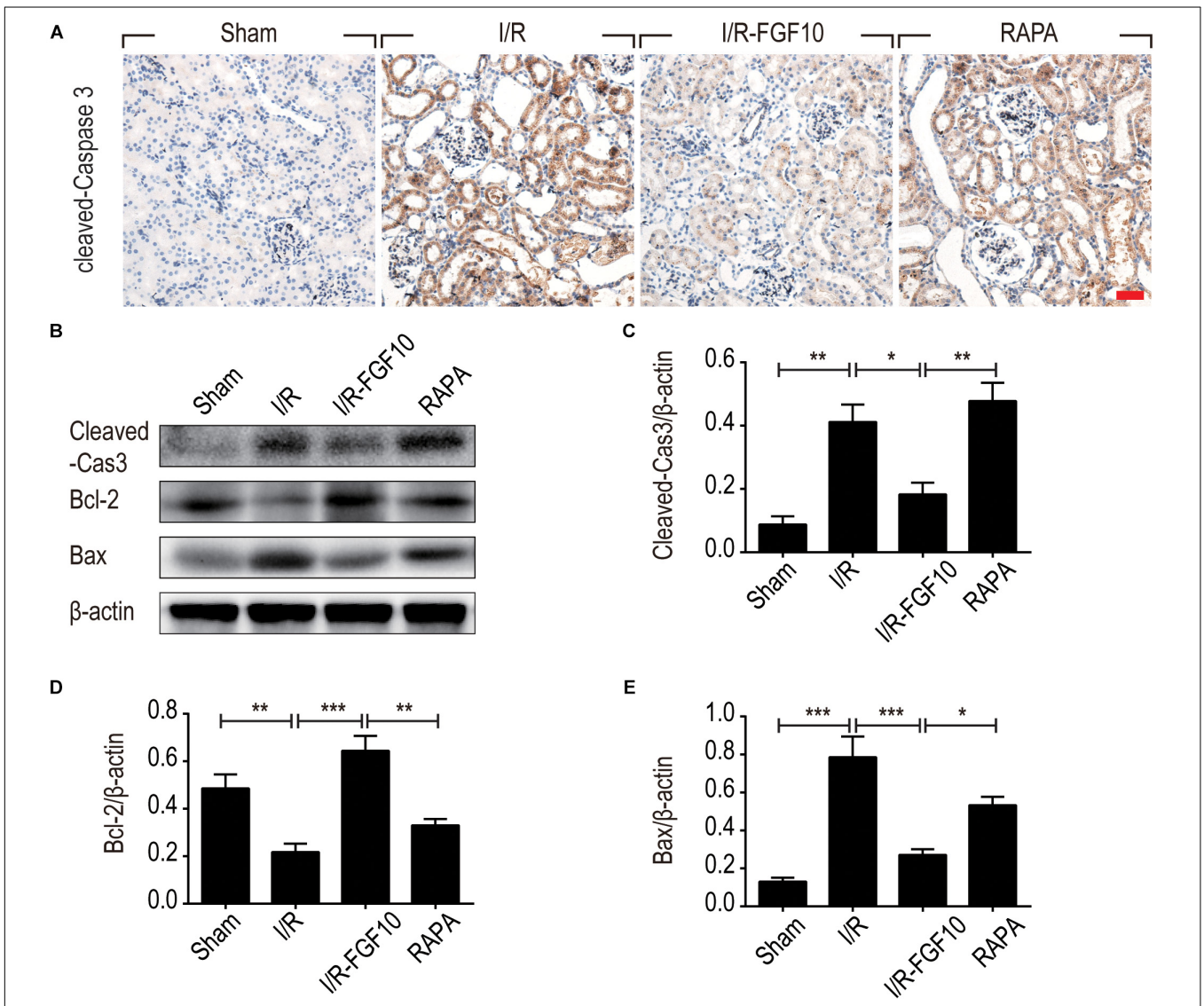

FIGURE 3 | FGF10 reduces the expression of pro-apoptotic proteins IHC staining and Western blot analyses were performed at 2 days after reperfusion. **(A)** IHC staining for cleaved caspase-3 in kidneys of indicated groups. Scale bars = 50 μm. **(B)** The expression of cleaved Caspase-3, Bcl-2 and Bax were detected by Western blot with β-actin as loading control. **(C–E)** The optical density analysis of cleaved Caspase-3, Bcl-2 and Bax (mean ± SEM; $n = 5$). $^{*}P < 0.05$, $^{**}P < 0.01$, $^{***}P < 0.001$.

Detection of LC3I to LC3II conversion and expression of Beclin-1 and SQSTM1/p62 (SQSTM1 is used hereafter) remains the most reliable methods to gauge autophagic activity. We therefore examined the expression of LC3, Beclin-1 and SQSTM1 at tissue and protein levels by immunofluorescence staining and immunoblot, respectively. The confocal imaging in **Figure 4A** shows that the number of LC3 positive dots (autophagosomes) were dramatically increased in the I/R group compared to sham group, but greatly reduced by FGF10. Rapamycin treatment effectively abolished the effect of FGF10 in this setting. However, chloroquine, as a specific autophagy inhibitor, markedly reduced the number of autophagosomes in RTCs caused by I/R injury. The statistical analysis about the number of autophagosomes in each group was shown in **Figure 4B**. This result is confirmed with immunoblot analysis showing that I/R induced LC3II was partially prevented by FGF10 treatment (**Figure 4C**, and quantification result in **Figure 4D**). Co-detection of Beclin-1 and LC3 by immunofluorescence staining also revealed that increased expression of Beclin-1 in I/R tissues was largely prevented by FGF10, an effect also reversed by treatment with rapamycin (**Figure 5A**). Western blot detection and quantification analysis on Beclin-1 expression (shown in **Figures 5B,C**) revealed a similar trend of alteration to LC3II (**Figures 4C,D**), and was consistent with confocal image analysis (**Figures 4A**, **5A**).

Besides LC3II and Beclin-1, we also examined the expression of SQSTM1, a selective autophagic receptor and substrate. As shown in **Figure 6A**, SQSTM1 was expressed in the cytoplasm of RTCs, which was significantly decreased in I/R group. It was evident that FGF10 not only reversed I/R-induced decrease of SQSTM1, but further increased its expression above the one observed for the sham control (**Figures 6B,C**), this effect again was abolished by rapamycin. To determine whether the

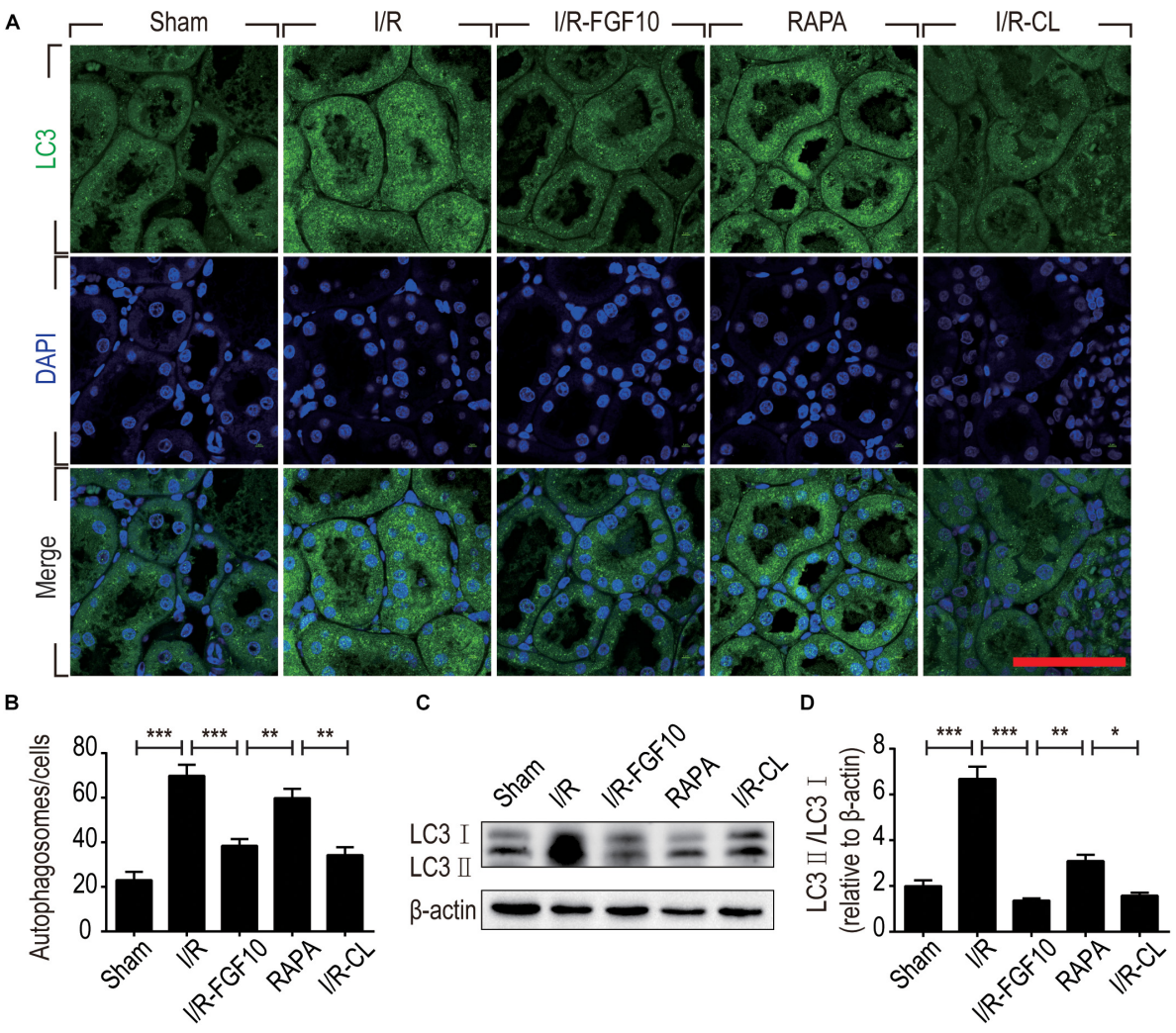

FIGURE 4 | FGF10 reduces the formation of autophagosome and the expression of LC3II. **(A)** Immunofluorescence staining of LC3 (green) was performed at 48 h after reperfusion. Nuclei were labeled with DAPI (blue). Scale bars = 50 μm. **(B)** Statistic analysis of the number of autophagosomes in RTCs with 5 randomly selected images in each group. **(C)** The protein expression of LC3II/LC3I in renal tissue was determined by Western blot and the optical densities were quantified **(D)**. Data are presented as the mean ± SEM ($n = 5$). $^{*}P < 0.05$, $^{**}P < 0.01$, $^{***}P < 0.001$.

mTOR pathway is subjected to FGF10 regulation, we examined the phosphorylation of mTOR by immunoblot. As shown in **Figure 6B**, the changes in phosphorylation of mTOR highly resembled that of SQSTM1, which was decreased in I/R group, but became markedly increased in FGF10 treated group, an effect mostly inhibited by co-treatment with rapamycin (**Figure 6D**).

FGF10 Inhibited the Release of HMGB1 in Response to Renal I/R Injury

HMGB1 is a major DAMP protein, which can be activated by renal I/R and participates in inflammatory response (Wu et al., 2010). We therefore examined the expression and localization of HMGB1 by Immunofluorescence staining and confocal imaging analyses. As expected, HMGB1 was predominantly localized in the nuclei of RTCs in sham control. Following I/R injury, the level of HMGB1 appeared to be decreased in nuclei, but increased in the cytoplasmic domain. Strikingly, FGF10 almost completely prevented the decrease of nuclear HMGB1 and concomitant increase in the cytoplasm, an effect abolished by rapamycin treatment (**Figure 7A**). To confirm the nucleus to cytoplasm shuttling and extracellular release of HMGB1, we further examined the levels of nuclear as well as serum HMGB1 by western blot and ELISA, respectively (**Figures 7B–D**). The expression of HMGB1 in the nuclear fraction was significantly decreased, whereas the serum HMGB1 was significantly increased in I/R group compared with sham group. FGF10 treatment

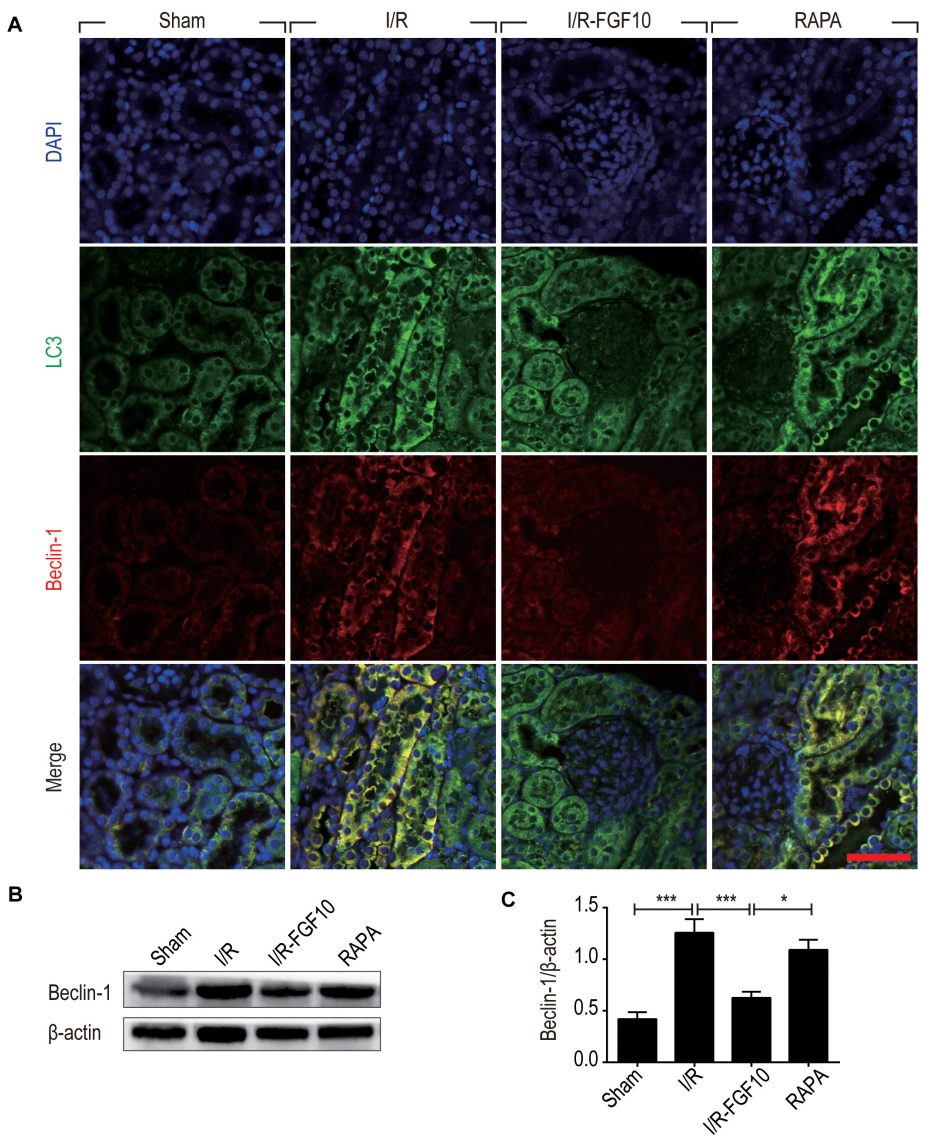

FIGURE 5 | FGF10 reduces the expression of Beclin-1. **(A)** Immunofluorescence staining and confocal images for LC3 (Green) and Beclin-1 (red) at 2 days after reperfusion. Nuclei were labeled with DAPI (blue). Scale bars = 50 μm. **(B)** Representative western blotting result for Beclin-1 expression. **(C)** Optical density analysis of protein bands. Data are presented as the mean ± SEM ($n = 5$). $^{*}P < 0.05$, $^{***}P < 0.001$.

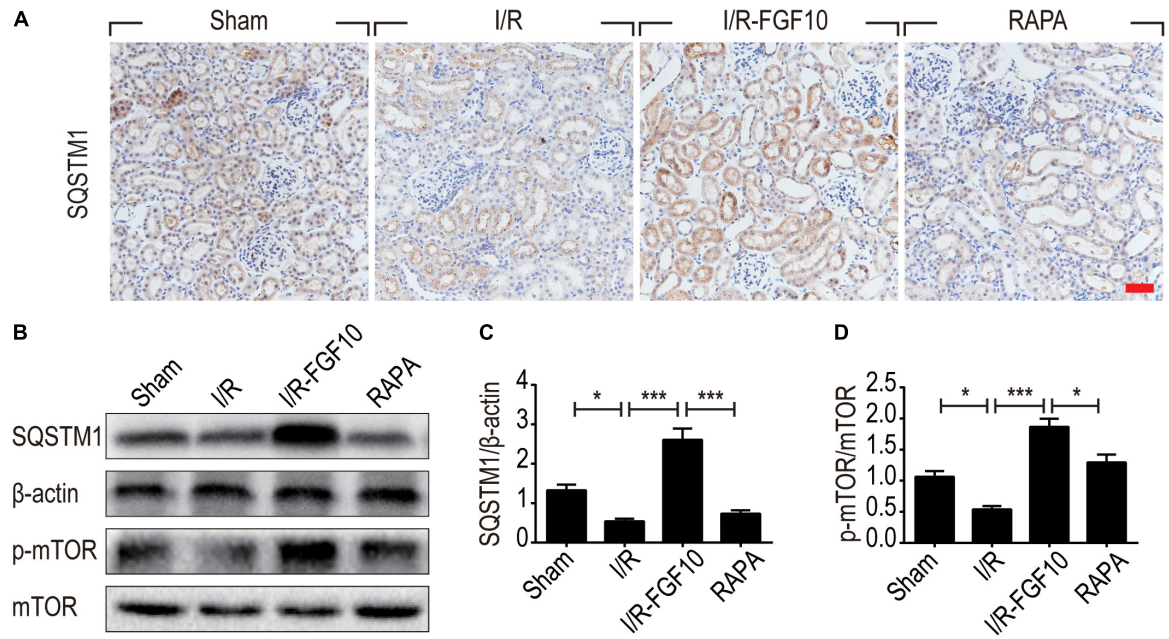

FIGURE 6 | FGF10 increases the expression of SQSTM1 and p-mTOR in I/R rats. **(A)** IHC staining was performed at 2 days after reperfusion for SQSTM1 in kidney tissues from indicated animal groups. Scale bars = 50 μm. **(B)** The expression of SQSTM1, p-mTOR and mTOR were detected by western blotting (mean ± SEM; $n = 5$). β-actin was used as control. $^{*}P < 0.05$, $^{***}P < 0.001$. **(C,D)** Optical density analysis for SQSTM1 and p-mTOR, which were normalized to β-actin and mTOR, respectively.

completely prevented the I/R-induced decrease of nuclear HMGB1 (**Figures 7B,C**), and largely abolished the increase in serum HMGB1 (**Figure 7D**). Extracellular HMGB1 is known to signal through TLRs, particularly TLR2 and TLR4, to activate pro-inflammatory response. Indeed, we found that the level of *Tlr2* mRNA expression was increased nearly threefold against sham-operated rats (**Figure 7E**). Importantly, FGF10 treatment mostly obliterated I/R-induced *Tlr2* expression, an effect partially reversed by rapamycin treatment. The effect of FGF10 on the mRNA expression of *Tlr4* was similar to that of *Tlr2* (**Figure 7F**). These results provide evidence that FGF10 could inhibit the release of HMGB1 from the nucleus to the extracellular matrix thereby preventing the HMGB1-mediated inflammatory response via the TLR2/TLR4 signaling pathway.

FGF10 Inhibited the Expression of Inflammatory Cytokines After I/R Injury

The ability of FGF10 to prevent I/R induced HMGB1 nuclear to cytoplasmic shuttling and releases, as well as TLR2 induction in response to I/R injury suggests that FGF10 may inhibit the expression of pro-inflammatory cytokines such as TNF-α. We therefore examined the expression of TNF-α in kidneys by IHC staining (**Figure 8A**) and western blot (**Figures 8B,C**). The serum TNF-α was also examined by ELISA (**Figure 8D**). I/R-induced TNF-α expression was mostly prevented by FGF10, but such effect, was largely obliterated by rapamycin treatment. We next performed RT-qPCR to determine the mRNA expression of two other inflammatory cytokines *Il-1*β and *Il-6* in renal tissues. These results also demonstrated that I/R-induced expression of these cytokines could be effectively inhibited by FGF10, but not in the presence of rapamycin (**Figures 8E,F**).

DISCUSSION

FGF10, a multifunctional growth factor, is crucial in transmitting mesenchymal to epithelial signaling in organ development and regenerative medicine (Itoh, 2016). The role of FGF10 in cerebral ischemia injury, pulmonary fibrosis and wound healing, has been extensively researched (Li et al., 2016; Tong et al., 2016; Chao et al., 2017; Chen et al., 2017; El Agha et al., 2017). As a typical paracrine growth factor, FGF10 and its predominant receptor FGFR2-IIIb plays crucial roles in the development of kidney. However, the potential effect of FGF10 on AKI has not been reported so far. We herein used a well-established renal I/R model to investigate the potential protection effect of FGF10 against I/R injury. We confirmed that I/R rats were associated with increased SCr and BUN indicating a decline in the GFR. The current work provided experimental evidence that FGF10 administration effectively alleviated I/R-induced functional impairment as well as histological damage of the kidney. Mechanistically, besides curbing apoptosis induction in RTCs, administration of FGF10 effectively alleviated the excessive autophagy, a common phenotype in RTCs exposed to I/R injury. HMGB1 is a damage-associated molecule that is rapidly released from nucleus to extracellular matrix and acts as a crucial molecule in the mediation of apoptosis and inflammation. We here demonstrated that FGF10 can inhibit the translocation of

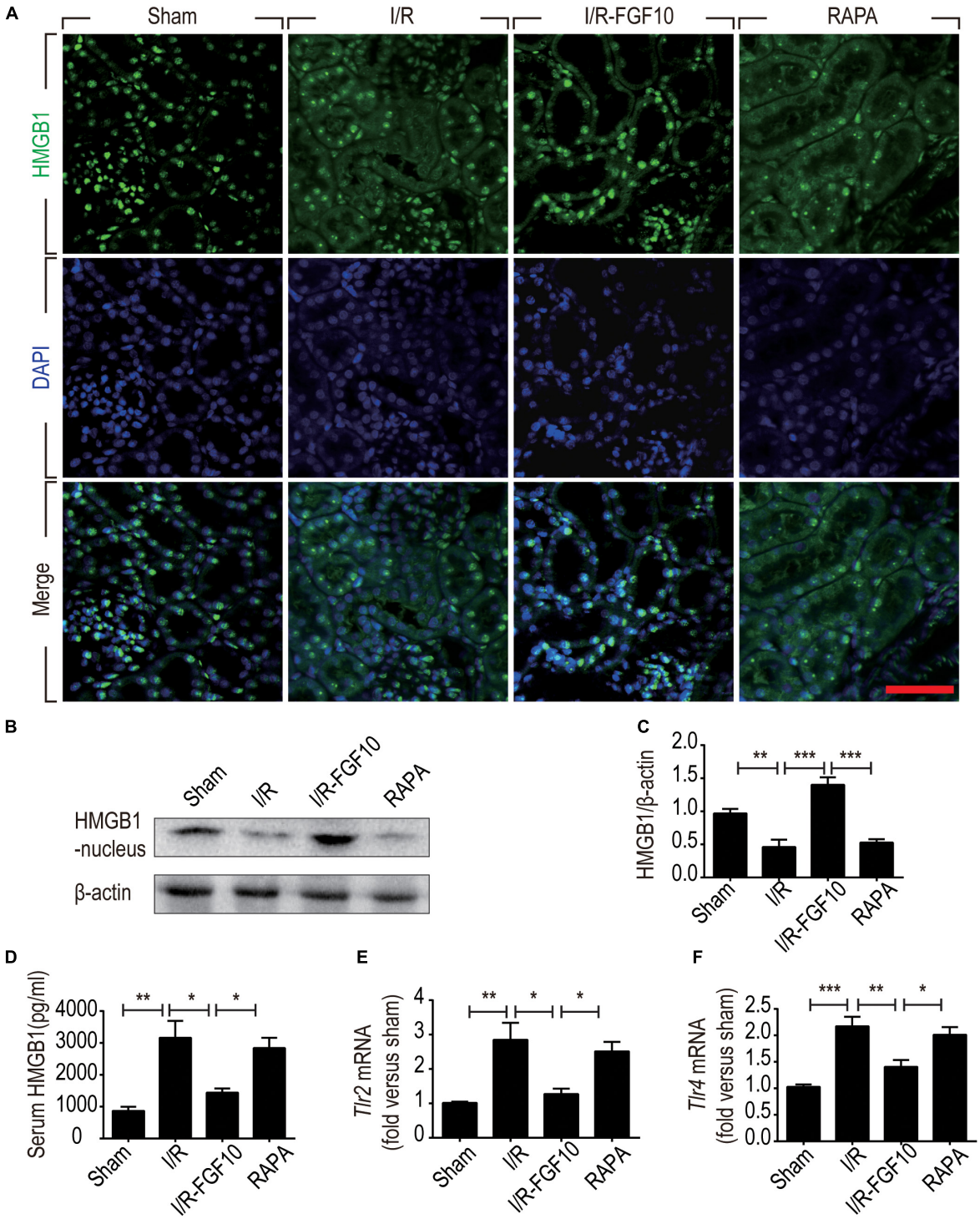

FIGURE 7 | FGF10 inhibits the release of nuclear HMGB1 to the serum and regulates the TLR mRNA expression. **(A)** Immunofluorescence staining of HMGB1 at 2 days after reperfusion. Nuclei were labeled with DAPI (blue). Scale bars = 50 μm. **(B,C)** Protein expression of HMGB1 in the nuclear fraction of renal tissues by Western blot and optical density analysis with β-actin as loading control (mean ± SEM; $n = 5$). $^{**}P < 0.01$, $^{***}P < 0.001$. **(D)** Level of serum HMGB1 was determined by ELISA (mean ± SEM; $n = 5$). $^{*}P < 0.05$, $^{**}P < 0.01$. **(E,F)** Expression of Tlr2 and Tlr4 mRNA in the kidney were examined by RT-qPCR and normalized to Gapdh. $^{*}P < 0.05$, $^{**}P < 0.01$, $^{***}P < 0.001$.

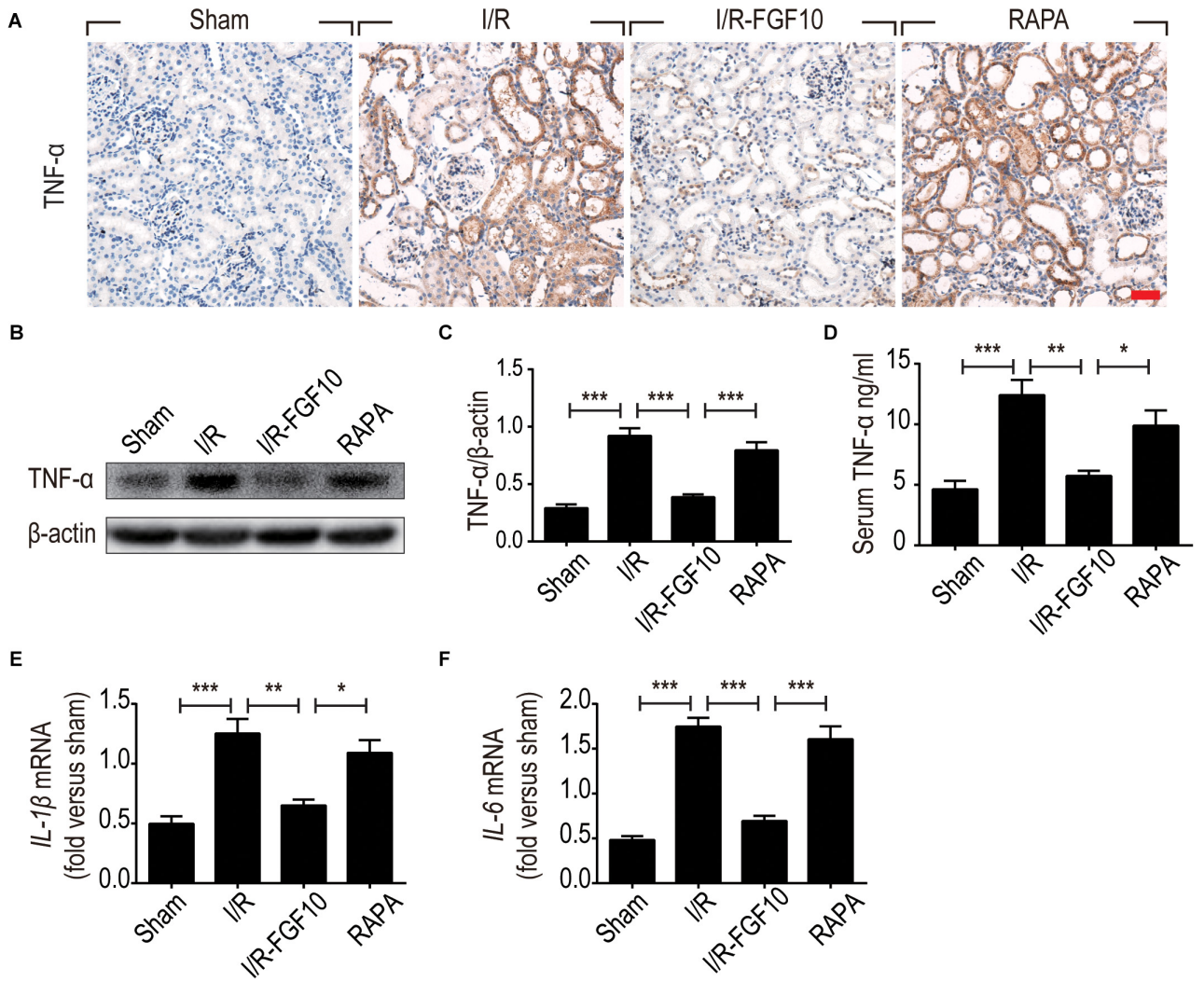

FIGURE 8 | FGF10 regulates the expression of inflammatory cytokines. **(A)** IHC staining for TNF-α in kidney tissues from indicated groups. Scale bars = 50 μm. **(B,C)** The expression of TNF-α was detected by western blot using TNF-α specific antibody. Optical density analyses (mean ± SEM; $n = 5$) with β-actin as control. **(D)** Levels of serum TNF-α were determined by ELISA (mean ± SEM; $n = 5$). $^{*}P < 0.05$, $^{**}P < 0.01$, $^{***}P < 0.001$. **(E,F)** The mRNA expression of Il-1β and Il-6 in the kidney was examined by RT-qPCR and normalized to Gapdh. $^{*}P < 0.05$, $^{**}P < 0.01$, $^{***}P < 0.001$.

HMGB1 and thus attenuates RTC apoptosis upon I/R injury. Therefore, FGF10 treatment appears to protect kidneys from AKI via the regulation of autophagy and HMGB1 mediated inflammatory signaling pathways.

Extensive research has demonstrated that death of renal parenchyma cells, including apoptosis and necrosis, is the major mechanism underlying the pathogenesis of the AKI, as well as inflammation (Oberbauer et al., 2001). The RTCs detached from basement membrane, along with other cellular debris, enter and obstruct the tubular lumen, thereby decrease GFR. Upon examining multiple parameters of cell death including TUNEL assays which detects both apoptosis and necrosis, as well as crucial mitochondrial regulators, we conclude that FGF10 treatment ameliorates the pro-apoptotic alteration of Bax/Bcl-2 as well Caspase-3, therefore RTC apoptosis following I/R injury. The results are in line with our previous studies showing that FGF2, another FGF family member, protects against renal I/R injury through attenuating mitochondrial damage (Tan et al., 2017). Two recent studies suggested that neuron and microglia or macrophage-derived FGF10 participates in activation of PI3K/AKT/mTOR, which contributes to either ameliorate cerebral ischemia injury or improve functional recovery after spinal cord injury (Li et al., 2016; Chen et al., 2017). Further studies will be required to delineate the molecular mechanisms underlying FGF10 mediated protection against renal I/R injury.

A number of reports have established the involvement of autophagy in I/R-induced AKI in various animal models. In a myocardial I/R model, FGF2 is shown to improve heart function recovery and survival of cardiomyocytes through inhibition

of excessive autophagy and increased ubiquitinated protein clearance via the activation of PI3K/AKT/mTOR signaling (Wang et al., 2015). Under normal physiological conditions, basal autophagy is required to maintain homeostasis in both visceral epithelial cells (podocytes) and RTCs. So far, both the beneficial and detrimental effects of autophagy have been reported after renal I/R injury in animal experiments (Decuypere et al., 2015; Kaushal and Shah, 2016; Lenoir et al., 2016). Autophagy has been reported to have a protective role in cell survival by degrading misfolded/unfolded proteins, damaged organelles and generate necessary nutrient substance during AKI in some reports (Kimura et al., 2011; Guan et al., 2015; Xie et al., 2018), whereas in others, it also causes apoptosis through excessive degradation of essential proteins and digestion of organelles (Shintani and Klionsky, 2004; Thorburn, 2008). Therefore, the role of autophagy in the pathogenesis and resolution of AKI injuries remains controversial, and is likely affected by the cellular context and also the extent of injury (Huber et al., 2012).

Given that rapamycin, an mTOR inhibitor and agonist of autophagy, impaired the protective effect of FGF10 on renal function, we therefore further examined several well-established autophagy parameters by immunoblot, immunofluorescence staining and associated autophagic phenotypes. LC3 is a crucial cytoplasmic protein required for the formation and elongation of autophagosome. LC3 positive punctate formation and the conversation of LC3I to LC3II are often used to examine the induction of autophagy. Our immunofluorescent analysis of LC3 indicated that FGF10 treatment could prevent I/R-induced conversion of LC3I to LC3II and inhibited the formation of autophagic vacuoles and autophagosome. More strikingly, the effect of FGF10 on I/R-induced autophagy was nearly completely antagonized by rapamycin therefore establishing a role of autophagy in the protective effect of FGF10 again I/R injury. Consistent results were observed with the expression of Beclin-1, a marker of autophagosome as well as SQSTM1, an ubiquitously expressed protein which directly interacts with LC3 and subsequently degraded in autophagosome (Johansen and Lamark, 2011; Weidberg et al., 2011). The decreased expression of SQSTM1 upon I/R injury was partially restored by FGF10 treatment. The data collectively suggest that FGF10 treatment could reduce autophagosome formation and inhibit excessive autophagy in RTCs after I/R injury via mTOR pathway.

Although both apoptosis and autophagy are rapidly induced in RTCs during AKI, but the role of autophagy in AKI is not as clear as apoptosis, and the interaction between apoptosis and autophagy in response to stimuli is complex and poorly defined. It is generally accepted that moderate autophagy may enhance the cellular ability to cope with stress response and thus promotes cell survival. Several studies have reported the renoprotective effect of autophagy in AKI caused by 25–40 min of renal ischemia-reperfusion (Kimura et al., 2011; Jiang et al., 2012; Xie et al., 2018). Once the autophagy is exacerbated due to severe injury, the program of apoptosis would be activated and eliminate the irreversibly damaged cells. Our results clearly indicate that FGF10 treatment could alleviate the excessive autophagy induced by 60 min of I/R exposure and thus protects RTCs from apoptosis. Therefore the extent of renal injury may render autophagy to either alleviate or augment the I/R injury. However, no study has shown a definite demarcation point to distinguish the dual roles of autophagy on damaged cells. The regulatory mechanism between autophagy and apoptosis in response to I/R injury should be a focus of future studies.

The innate immune response is another integral pathological mechanism with AKI and the subsequent CKD. Emerging evidence suggests that the relationship between autophagy and inflammation is far more complicated than previously appreciated (Leventhal et al., 2014). Both autophagy and immune response play crucial roles in the pathogenesis of AKI. Immune responses can affect the activation and perpetuation of autophagy in RTCs after reperfusion. Autophagy is identified a modulator that can both regulate and be regulated by immune responses in many diseases (Kaushal and Shah, 2016; Kimura et al., 2017). Further research is needed to clarify the precise effects of autophagy on inflammation.

Many studies reported the multiple roles of HMGB1 in the pathogenesis of various diseases. However, the crosstalk between HMGB1 and apoptosis is complicated and requires further elucidation. HMGB1 shows dual roles in the regulation of apoptosis. Intracellular HMGB1 is generally an anti-apoptosis molecule, whereas overexpression of extracellular HMGB1 promotes apoptosis (Kang et al., 2014). The two-way interaction between HMGB1 and autophagy has been wildly studied. Autophagy participates in various physiological and pathological processes including the release and degradation of HMGB1 (Thorburn et al., 2009; Dupont et al., 2011). Autophagy is regulated by HMGB1 which involves many molecules such as heat shock protein β-1 (HSPB1), Bcl-2 and Beclin-1 (Tang et al., 2010b; Zhao et al., 2011). Studies with HMGB1 knockout mice suggest that loss of HMGB1 leads to autophagy deficiency, whereas increased extracellular HMGB1 promotes autophagy through binding to Receptor for advanced glycation end products (RAGE), a negative regulator of apoptosis (Tang et al., 2010a; Yanai et al., 2013). HMGB1 participates in the formation of renal fibrosis in the development of CKD through binding to TLR2 and RAGE. Therefore, future studies are warranted to explore the effect of FGF10 on CKD.

In summary, the present study demonstrates for the first time that exogenously administered recombinant FGF10 protects against I/R-induced functional and tissue damage to the kidney. The potent protective effect is attributed to its ability to attenuate several I/R-induced pro-apoptotic alteration of BCL2/BAX expression and Caspase-3 activation, therefor apoptotic cell death of renal parenchyma cells. The present work also indicates that protective effect of FGF10 against I/R injury is related to its down-regulation of excessive autophagy as well as release of HMGB1, Which in turn regulates pro-inflammatory immune response via TLR2/TLR4 signaling pathway. Apoptosis and autophagy are both rapidly activated upon renal I/R injury, which may interact with each other to govern the pathological and recovery processes of AKI. Our study suggests that FGF10 may provide a potential therapeutic option for treating AKI.

AUTHOR CONTRIBUTIONS

XT and J-SZ conceived and designed the experiments. XT performed the animal operations and acquired the confocal images. HZ performed apoptosis assay, immunoblot, immunohistochemistry, and immunofluorescent staining. QT, LG, TJ, LX, XW, JW, and RY assisted in animal housing effort and acquisition of some of the experimental data related to RT-PCR, and ELISA. XT and HZ analyzed the data and prepared the figures. XT and J-SZ wrote and revised the manuscript. J-SZ and XL supervised and funded the study.

FUNDING

This study was partially supported by National Natural Science Foundation of China (81472601 and 81500519).

REFERENCES

Basile, D. P., Anderson, M. D., and Sutton, T. A. (2012). Pathophysiology of acute kidney injury. *Compr. Physiol.* 2, 1303–1353. doi: 10.1002/cphy.c110041

Bates, C. M. (2007). Role of fibroblast growth factor receptor signaling in kidney development. *Pediatr. Nephrol.* 22, 343–349. doi: 10.1007/s00467-006-0239-7

Beenken, A., and Mohammadi, M. (2009). The FGF family: biology, pathophysiology and therapy. *Nat. Rev. Drug Discov.* 8, 235–253. doi: 10.1038/nrd2792

Bonventre, J. V., and Yang, L. (2011). Cellular pathophysiology of ischemic acute kidney injury. *J. Clin. Invest.* 121, 4210–4221. doi: 10.1172/JCI45161

Chao, C. M., Yahya, F., Moiseenko, A., Tiozzo, C., Shrestha, A., Ahmadvand, N., et al. (2017). Fgf10 deficiency is causative for lethality in a mouse model of bronchopulmonary dysplasia. *J. Pathol.* 241, 91–103. doi: 10.1002/path.4834

Chen, J., Wang, Z., Zheng, Z., Chen, Y., Khor, S., Shi, K., et al. (2017). Neuron and microglia/macrophage-derived FGF10 activate neuronal FGFR2/PI3K/Akt signaling and inhibit microglia/macrophages TLR4/NF-kappaB-dependent neuroinflammation to improve functional recovery after spinal cord injury. *Cell Death Dis.* 8:e3090. doi: 10.1038/cddis.2017.490

Chen, Q., Guan, X., Zuo, X., Wang, J., and Yin, W. (2016). The role of high mobility group box 1 (HMGB1) in the pathogenesis of kidney diseases. *Acta Pharm. Sin. B* 6, 183–188. doi: 10.1016/j.apsb.2016.02.004

Chertow, G. M., Burdick, E., Honour, M., Bonventre, J. V., and Bates, D. W. (2005). Acute kidney injury, mortality, length of stay, and costs in hospitalized patients. *J. Am. Soc. Nephrol.* 16, 3365–3370. doi: 10.1681/ASN.2004090740

Chien, C. T., Shyue, S. K., and Lai, M. K. (2007). Bcl-xL augmentation potentially reduces ischemia/reperfusion induced proximal and distal tubular apoptosis and autophagy. *Transplantation* 84, 1183–1190. doi: 10.1097/01.tp.0000287334.38933.e3

De Rechter, S., Decuypere, J. P., Ivanova, E., Van Den Heuvel, L. P., De Smedt, H., Levtchenko, E., et al. (2016). Autophagy in renal diseases. *Pediatr. Nephrol.* 31, 737–752. doi: 10.1007/s00467-015-3134-2

Decuypere, J. P., Ceulemans, L. J., Agostinis, P., Monbaliu, D., Naesens, M., Pirenne, J., et al. (2015). Autophagy and the kidney: implications for ischemia-reperfusion injury and therapy. *Am. J. Kidney Dis.* 66, 699–709. doi: 10.1053/j.ajkd.2015.05.021

Dupont, N., Jiang, S., Pilli, M., Ornatowski, W., Bhattacharya, D., and Deretic, V. (2011). Autophagy-based unconventional secretory pathway for extracellular delivery of IL-1beta. *EMBO J.* 30, 4701–4711. doi: 10.1038/emboj.2011.398

El Agha, E., Moiseenko, A., Kheirollahi, V., De Langhe, S., Crnkovic, S., Kwapiszewska, G., et al. (2017). Two-way conversion between lipogenic and myogenic fibroblastic phenotypes marks the progression and resolution of lung fibrosis. *Cell Stem Cell* 20, 571. doi: 10.1016/j.stem.2017.03.011

Guan, X., Qian, Y., Shen, Y., Zhang, L., Du, Y., Dai, H., et al. (2015). Autophagy protects renal tubular cells against ischemia / reperfusion injury in a time-dependent manner. *Cell Physiol. Biochem.* 36, 285–298. doi: 10.1159/000374071

Havasi, A., and Borkan, S. C. (2011). Apoptosis and acute kidney injury. *Kidney Int.* 80, 29–40. doi: 10.1038/ki.2011.120

He, L., Livingston, M. J., and Dong, Z. (2014). Autophagy in acute kidney injury and repair. *Nephron Clin. Pract.* 127, 56–60. doi: 10.1159/000363677

Huber, T. B., Edelstein, C. L., Hartleben, B., Inoki, K., Jiang, M., Koya, D., et al. (2012). Emerging role of autophagy in kidney function, diseases and aging. *Autophagy* 8, 1009–1031. doi: 10.4161/auto.19821

Inoue, K., Kuwana, H., Shimamura, Y., Ogata, K., Taniguchi, Y., Kagawa, T., et al. (2010). Cisplatin-induced macroautophagy occurs prior to apoptosis in proximal tubules in vivo. *Clin. Exp. Nephrol.* 14, 112–122. doi: 10.1007/s10157-009-0254-7

Itoh, N. (2015). FGF10: a multifunctional mesenchymal-epithelial signaling growth factor in development, health, and disease. *Cytokine Growth Factor Rev.* 28, 63–69. doi: 10.1016/j.cytogfr.2015.10.001

Itoh, N. (2016). FGF10: a multifunctional mesenchymal-epithelial signaling growth factor in development, health, and disease. *Cytokine Growth Factor Rev.* 28, 63–69. doi: 10.1016/j.cytogfr.2015.10.001

Jang, H. R., and Rabb, H. (2009). The innate immune response in ischemic acute kidney injury. *Clin. Immunol.* 130, 41–50. doi: 10.1016/j.clim.2008.08.016

Jiang, M., Wei, Q., Dong, G., Komatsu, M., Su, Y., and Dong, Z. (2012). Autophagy in proximal tubules protects against acute kidney injury. *Kidney Int.* 82, 1271–1283. doi: 10.1038/ki.2012.261

Johansen, T., and Lamark, T. (2011). Selective autophagy mediated by autophagic adapter proteins. *Autophagy* 7, 279–296. doi: 10.4161/auto.7.3.14487

Kalogeris, T., Baines, C. P., Krenz, M., and Korthuis, R. J. (2012). Cell biology of ischemia/reperfusion injury. *Int. Rev. Cell Mol. Biol.* 298, 229–317. doi: 10.1016/B978-0-12-394309-5.00006-7

Kang, R., Chen, R., Zhang, Q., Hou, W., Wu, S., Cao, L., et al. (2014). HMGB1 in health and disease. *Mol. Aspects Med.* 40, 1–116. doi: 10.1016/j.mam.2014.05.001

Kaushal, G. P., and Shah, S. V. (2016). Autophagy in acute kidney injury. *Kidney Int.* 89, 779–791. doi: 10.1016/j.kint.2015.11.021

Kim, H. J., Park, S. J., Koo, S., Cha, H. J., Lee, J. S., Kwon, B., et al. (2014). Inhibition of kidney ischemia-reperfusion injury through local infusion of a TLR2 blocker. *J. Immunol. Methods* 407, 146–150. doi: 10.1016/j.jim.2014.03.014

Kimura, T., Isaka, Y., and Yoshimori, T. (2017). Autophagy and kidney inflammation. *Autophagy* 13, 997–1003. doi: 10.1080/15548627.2017.1309485

Kimura, T., Takabatake, Y., Takahashi, A., Kaimori, J., Matsui, I., Namba, T., et al. (2011). Autophagy protects the proximal tubule from degeneration and acute ischemic injury. *J. Am. Soc. Nephrol.* 22, 902–913. doi: 10.1681/ASN.2010070705

Lenoir, O., Tharaux, P. L., and Huber, T. B. (2016). Autophagy in kidney disease and aging: lessons from rodent models. *Kidney Int.* 90, 950–964. doi: 10.1016/j.kint.2016.04.014

Leventhal, J. S., He, J. C., and Ross, M. J. (2014). Autophagy and immune response in kidneys. *Semin. Nephrol.* 34, 53–61. doi: 10.1016/j.semnephrol.2013.11.008

Li, Y. H., Fu, H. L., Tian, M. L., Wang, Y. Q., Chen, W., Cai, L. L., et al. (2016). Neuron-derived FGF10 ameliorates cerebral ischemia injury via inhibiting NF-kappa B-dependent neuroinflammation and activating PI3K/Akt survival signaling pathway in mice. *Sci. Rep.* 6:19869. doi: 10.1038/srep19869

Lotze, M. T., and Tracey, K. J. (2005). High-mobility group box 1 protein (HMGB1): nuclear weapon in the immune arsenal. *Nat. Rev. Immunol.* 5, 331–342. doi: 10.1038/nri1594

Mizushima, N., and Komatsu, M. (2011). Autophagy: renovation of cells and tissues. *Cell* 147, 728–741. doi: 10.1016/j.cell.2011.10.026

Nikoletopoulou, V., Markaki, M., Palikaras, K., and Tavernarakis, N. (2013). Crosstalk between apoptosis, necrosis and autophagy. *Biochim. Biophys. Acta Mol. Cell Res.* 1833, 3448–3459. doi: 10.1016/j.bbamcr.2013.06.001

Oberbauer, R., Schwarz, C., Regele, H. M., Hansmann, C., Meyer, T. W., and Mayer, G. (2001). Regulation of renal tubular cell apoptosis and proliferation after ischemic injury to a solitary kidney. *J. Lab. Clin. Med.* 138, 343–351. doi: 10.1067/mlc.2001.118926

Ouyang, F., Huang, H., Zhang, M. Y., Chen, M. X., Huang, H. B., Huang, F., et al. (2016). HMGB1 induces apoptosis and EMT in association with increased autophagy following H/R injury in cardiomyocytes. *Int. J. Mol. Med.* 37, 679–689. doi: 10.3892/ijmm.2016.2474

Paller, M. S., Hoidal, J. R., and Ferris, T. F. (1984). Oxygen free radicals in ischemic acute renal failure in the rat. *J. Clin. Invest.* 74, 1156–1164. doi: 10.1172/JCI111524

Pallet, N., Bouvier, N., Legendre, C., Gilleron, J., Codogno, P., Beaune, P., et al. (2008). Autophagy protects renal tubular cells against cyclosporine toxicity. *Autophagy* 4, 783–791. doi: 10.4161/auto.6477

Shibutani, S. T., Saitoh, T., Nowag, H., Munz, C., and Yoshimori, T. (2015). Autophagy and autophagy-related proteins in the immune system. *Nat. Immunol.* 16, 1014–1024. doi: 10.1038/ni.3273

Shintani, T., and Klionsky, D. J. (2004). Autophagy in health and disease: a double-edged sword. *Science* 306, 990–995. doi: 10.1126/science.1099993

Suzuki, C., Isaka, Y., Takabatake, Y., Tanaka, H., Koike, M., Shibata, M., et al. (2008). Participation of autophagy in renal ischemia/reperfusion injury. *Biochem. Biophys. Res. Commun.* 368, 100–106. doi: 10.1016/j.bbrc.2008.01.059

Tan, X., Zhang, L., Jiang, Y., Yang, Y., Zhang, W., Li, Y., et al. (2013). Postconditioning ameliorates mitochondrial DNA damage and deletion after renal ischemic injury. *Nephrol. Dial. Transplant.* 28, 2754–2765. doi: 10.1093/ndt/gft278

Tan, X. H., Zheng, X. M., Yu, L. X., He, J., Zhu, H. M., Ge, X. P., et al. (2017). Fibroblast growth factor 2 protects against renal ischaemia/reperfusion injury by attenuating mitochondrial damage and proinflammatory signalling. *J. Cell Mol. Med.* 21, 2909–2925. doi: 10.1111/jcmm.13203

Tang, D., Kang, R., Livesey, K. M., Cheh, C. W., Farkas, A., Loughran, P., et al. (2010a). Endogenous HMGB1 regulates autophagy. *J. Cell Biol.* 190, 881–892. doi: 10.1083/jcb.200911078

Tang, D., Loze, M. T., Zeh, H. J., and Kang, R. (2010b). The redox protein HMGB1 regulates cell death and survival in cancer treatment. *Autophagy* 6, 1181–1183. doi: 10.4161/auto.6.8.13367

Thadhani, R., Pascual, M., and Bonventre, J. V. (1996). Acute renal failure. *N. Engl. J. Med.* 334, 1448–1460. doi: 10.1056/NEJM199605303342207

Thorburn, A. (2008). Apoptosis and autophagy: regulatory connections between two supposedly different processes. *Apoptosis* 13, 1–9. doi: 10.1007/s10495-007-0154-9

Thorburn, J., Frankel, A. E., and Thorburn, A. (2009). Regulation of HMGB1 release by autophagy. *Autophagy* 5, 247–249. doi: 10.4161/auto.5.2.7552

Tong, L., Zhou, J., Rong, L., Seeley, E. J., Pan, J., Zhu, X., et al. (2016). Fibroblast growth factor-10 (FGF-10) mobilizes lung-resident mesenchymal stem cells and protects against acute lung injury. *Sci. Rep.* 6:21642. doi: 10.1038/srep21642

Ueda, N., Kaushal, G. P., and Shah, S. V. (2000). Apoptotic mechanisms in acute renal failure. *Am. J. Med.* 108, 403–415. doi: 10.1016/S0002-9343(00)00311-9

Wang, Z. G., Wang, Y., Ye, J. M., Lu, X. H., Cheng, Y., Xiang, L. J., et al. (2015). bFGF attenuates endoplasmic reticulum stress and mitochondrial injury on myocardial ischaemia/reperfusion via activation of PI3K/Akt/ERK1/2 pathway. *J. Cell Mol. Med.* 19, 595–607. doi: 10.1111/jcmm.12346

Weidberg, H., Shvets, E., and Elazar, Z. (2011). Biogenesis and cargo selectivity of autophagosomes. *Annu. Rev. Biochem.* 80, 125–156. doi: 10.1146/annurev-biochem-052709-094552

Wu, H., Ma, J., Wang, P., Corpuz, T. M., Panchapakesan, U., Wyburn, K. R., et al. (2010). HMGB1 contributes to kidney ischemia reperfusion injury. *J. Am. Soc. Nephrol.* 21, 1878–1890. doi: 10.1681/ASN.2009101048

Xie, Y., Xiao, J., Fu, C. S., Zhang, Z. X., Ye, Z. B., and Zhang, X. L. (2018). Ischemic preconditioning promotes autophagy and alleviates renal ischemia/reperfusion injury. *Biomed. Res. Int.* 2018:8353987. doi: 10.1155/2018/8353987

Xu, W., Jiang, H., Hu, X., and Fu, W. (2014). Effects of high-mobility group box 1 on the expression of Beclin-1 and LC3 proteins following hypoxia and reoxygenation injury in rat cardiomyocytes. *Int. J. Clin. Exp. Med.* 7, 5353–5357.

Xu, Y., Guo, M., Jiang, W., Dong, H., Han, Y. F., An, X. F., et al. (2016). Endoplasmic reticulum stress and its effects on renal tubular cells apoptosis in ischemic acute kidney injury. *Renal Fail.* 38, 831–837. doi: 10.3109/0886022X.2016.1160724

Yanai, H., Matsuda, A., An, J., Koshiba, R., Nishio, J., Negishi, H., et al. (2013). Conditional ablation of HMGB1 in mice reveals its protective function against endotoxemia and bacterial infection. *Proc. Natl. Acad. Sci. U.S.A.* 110, 20699–20704. doi: 10.1073/pnas.1320808110

Zhao, M., Yang, M., Yang, L., Yu, Y., Xie, M., Zhu, S., et al. (2011). HMGB1 regulates autophagy through increasing transcriptional activities of JNK and ERK in human myeloid leukemia cells. *BMB Rep.* 44, 601–606. doi: 10.5483/BMBRep.2011.44.9.601

Zuk, A., and Bonventre, J. V. (2016). Acute Kidney Injury. *Annu. Rev. Med.* 67, 293–307. doi: 10.1146/annurev-med-050214-013407

Conflict of Interest Statement: The authors declare that the research was conducted in the absence of any commercial or financial relationships that could be construed as a potential conflict of interest.

Copyright © 2018 Tan, Zhu, Tao, Guo, Jiang, Xu, Yang, Wei, Wu, Li and Zhang. This is an open-access article distributed under the terms of the Creative Commons Attribution License (CC BY). The use, distribution or reproduction in other forums is permitted, provided the original author(s) and the copyright owner(s) are credited and that the original publication in this journal is cited, in accordance with accepted academic practice. No use, distribution or reproduction is permitted which does not comply with these terms.

frontiers in Genetics

CORRECTION
published: 12 November 2021
doi: 10.3389/fgene.2021.731406

Corrigendum: FGF10 Protects Against Renal Ischemia/Reperfusion Injury by Regulating Autophagy and Inflammatory Signaling

Xiaohua Tan[1,2], Hongmei Zhu[1], Qianyu Tao[1], Lisha Guo[1], Tianfang Jiang[3], Le Xu[3], Ruo Yang[1], Xiayu Wei[4], Jin Wu[4], Xiaokun Li[1,4] and Jin-San Zhang[1,3,4]**

[1]School of Pharmaceutical Sciences, Wenzhou Medical University, Wenzhou, China, [2]Qingdao University Medical College, Qingdao, China, [3]The First Affiliated Hospital, Wenzhou Medical University, Wenzhou, China, [4]Institute of Life Sciences, Wenzhou University, Wenzhou, China

Keywords: FGF10, ischemia-reperfusion (I/R), acute kidney injury, autophagy, inflammation, HMGB1

OPEN ACCESS

Edited and reviewed by:
Saverio Bellusci,
University of Giessen, Germany

****Correspondence:***
Xiaokun Li
profxiaokunli@163.com
Jin-San Zhang
Zhang_jinsan@163.com

Specialty section:
This article was submitted to Stem Cell Research, a section of the journal Frontiers in Genetics

Received: *27 June 2021*
Accepted: *20 October 2021*
Published: *12 November 2021*

Citation:
Tan X, Zhu H, Tao Q, Guo L, Jiang T, Xu L, Yang R, Wei X, Wu J, Li X and Zhang J-S (2021) Corrigendum: FGF10 Protects Against Renal Ischemia/Reperfusion Injury by Regulating Autophagy and Inflammatory Signaling. Front. Genet. 12:731406. doi: 10.3389/fgene.2021.731406

A Corrigendum on

FGF10 Protects Against Renal Ischemia/Reperfusion Injury by Regulating Autophagy and Inflammatory Signaling

by Tan, X., Zhu, H., Tao, Q., Guo, L., Jiang, T., Xu, L., Yang, R., Wei, X., Wu, J., Li, X., and Zhang, J. S. (2018). Front. Genet. 9:556. doi: 10.3389/fgene.2018.00556

In the original article, there were mistakes in **Figure 2A**, **Figure 6A**, and **Figure 7A** as published. The immunofluorescence and immunohistochemistry images in the Sham group (**Figure 2A**) and RAPA groups in **Figure 6A** and **Figure 7A**, respectively, were erroneously used. The corrected Figures appear below.

The authors deeply apologize for these errors and state that these corrections do not change the scientific conclusions of the article in any way. The original article has been updated.

Publisher's Note: All claims expressed in this article are solely those of the authors and do not necessarily represent those of their affiliated organizations, or those of the publisher, the editors and the reviewers. Any product that may be evaluated in this article, or claim that may be made by its manufacturer, is not guaranteed or endorsed by the publisher.

Copyright © 2021 Tan, Zhu, Tao, Guo, Jiang, Xu, Yang, Wei, Wu, Li and Zhang. This is an open-access article distributed under the terms of the Creative Commons Attribution License (CC BY). The use, distribution or reproduction in other forums is permitted, provided the original author(s) and the copyright owner(s) are credited and that the original publication in this journal is cited, in accordance with accepted academic practice. No use, distribution or reproduction is permitted which does not comply with these terms.

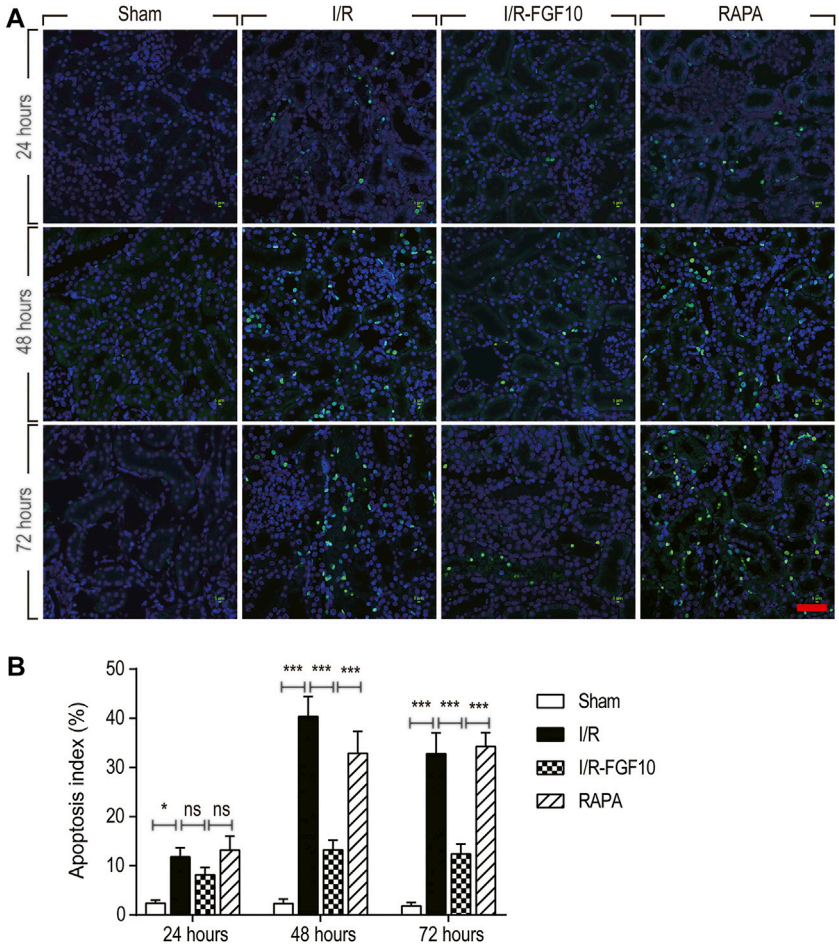

FIGURE 2 | FGF10 protects against I/R induced apoptosis in RTCs. **(A)** Representative sections of nuclear DNA fragmentation staining were performed using TUNEL in different groups at 24, 48, and 72 h, respectively, after reperfusion. Scale bars = 50 μM. **(B)** Quantitative analysis of the number of TUNEL-positive RTCs. Data are presented as the mean ± SD (n = 5). $^{*}p < 0.05$, $^{***}p < 0.001$. The percentage of positive cells was analyzed with 5 individual magnification × 400 fields per group.

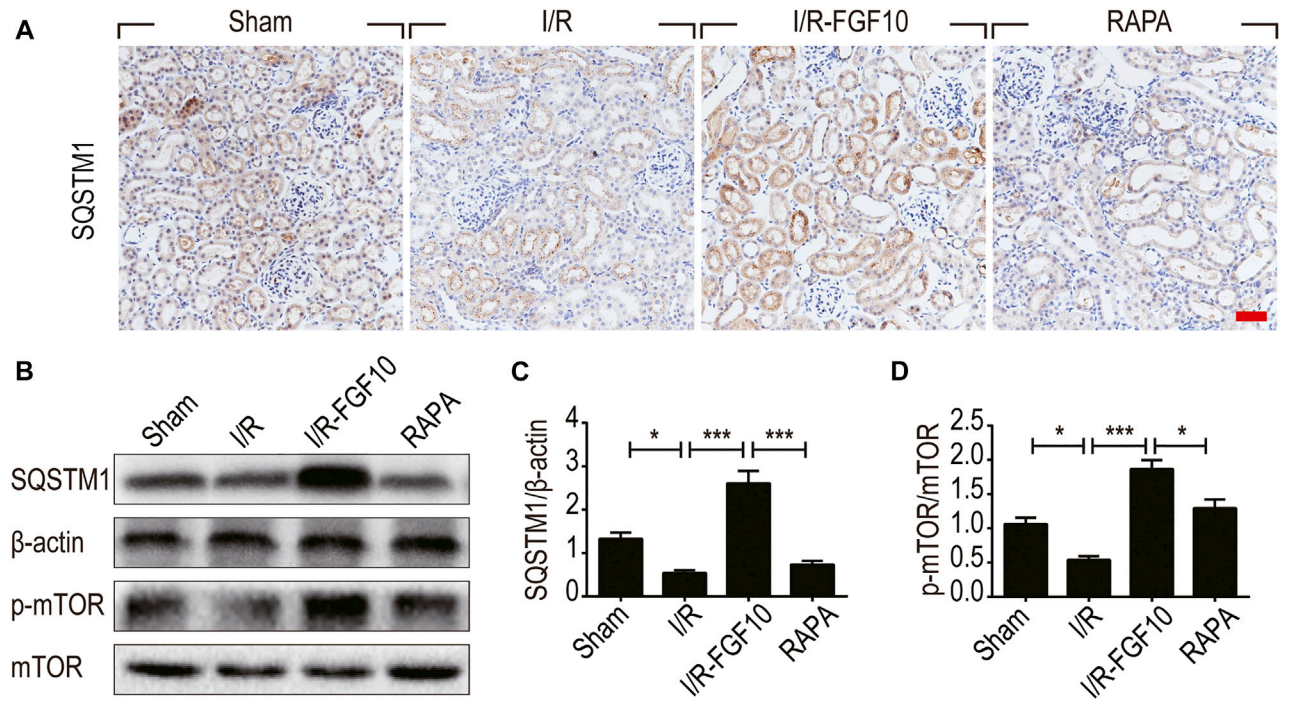

FIGURE 6 | FGF10 increases the expression of SQSTM1 and p-mTOR in I/R rats. **(A)** IHC staining was performed at 2 days after reperfusion for SQSTM1 in kidney tissues from indicated animal groups. Scale bars = 50 μm. **(B)** The expression of SQSTM1, p-mTOR and mTOR were detected by western blotting (mean ± SEM; $n = 5$). β-actin was used as control. $^{*}p < 0.05$, $^{***}p < 0.001$. **(C,D)** Optical density analysis for SQSTM1 and p-mTOR, which were normalized to β-actin and mTOR, respectively.

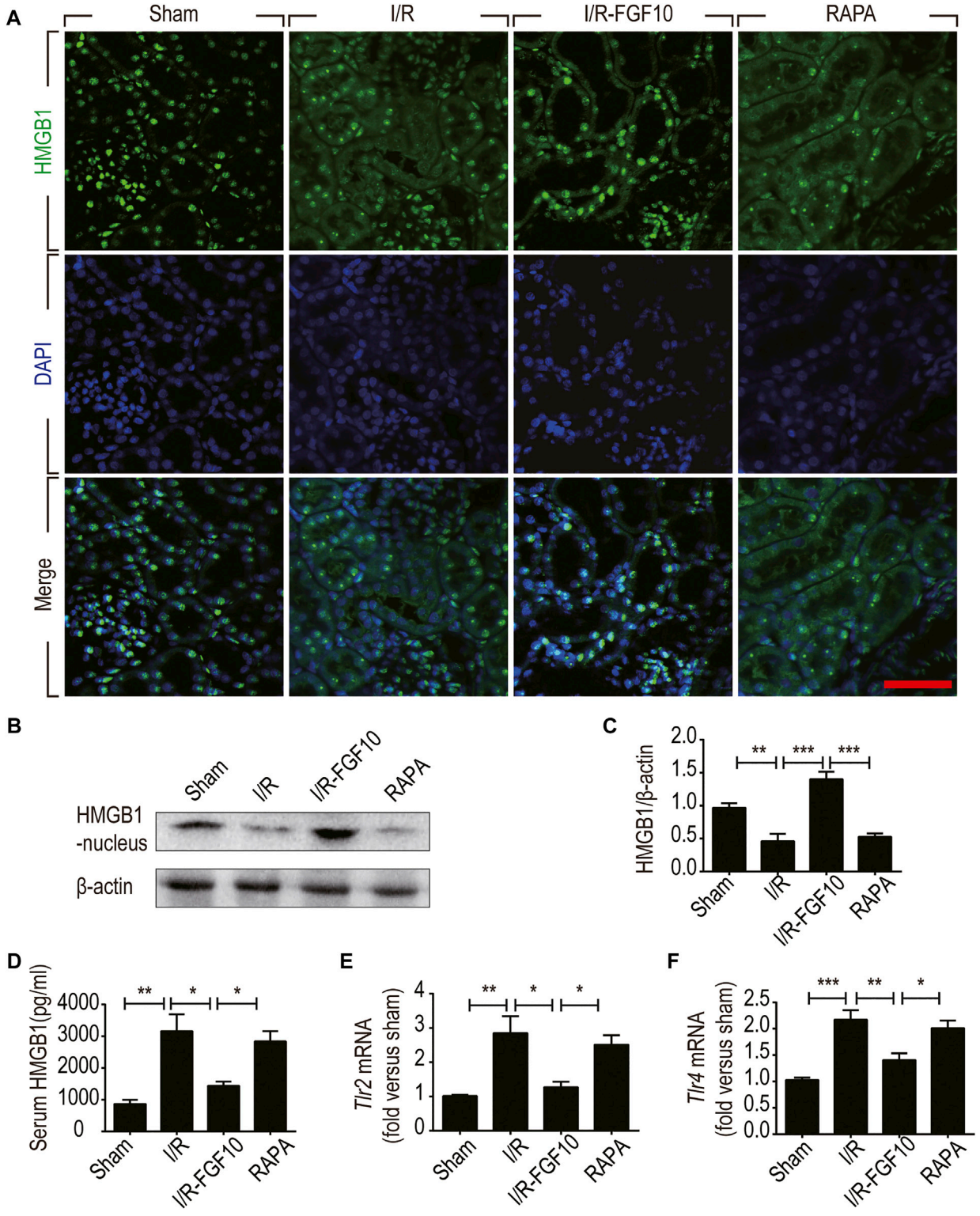

FIGURE 7 | FGF10 inhibits the release of nuclear HMGB1 to the serum and regulates the TLR mRNA expression. **(A)** Immunofluorescence staining of HMGB1 at 2 days after reperfusion. Nuclei were labeled with DAPI (blue). Scale bars = 50 m. **(B,C)** Protein expression of HMGB1 in the nuclear fraction of renal tissues by Western blot and optical density analysis with β-actin as loading control (mean ± SEM; $n = 5$). $^{**}p < 0.01$, $^{***}p < 0.001$. **(D)** Level of serum HMGB1 was determined by ELISA (mean ± SEM; $n = 5$). $^{*}p < 0.05$, $^{**}p < 0.01$. **(E,F)** Expression of Tlr2 and Tlr4 mRNA in the kidney were examined by RT-qPCR and normalized to Gapdh. $*p < 0.05$, $**p < 0.01$, $***p < 0.001$.

frontiers in Genetics

MINI REVIEW
published: 28 November 2018
doi: 10.3389/fgene.2018.00599

FGF10 Signaling in Heart Development, Homeostasis, Disease and Repair

*Fabien Hubert, Sandy M. Payan and Francesca Rochais**

Aix-Marseille Univ, INSERM, MMG, U1251, Marseille, France

Essential muscular organ that provides the whole body with oxygen and nutrients, the heart is the first organ to function during embryonic development. Cardiovascular diseases, including acquired and congenital heart defects, are the leading cause of mortality in industrialized countries. Fibroblast Growth Factors (FGFs) are involved in a variety of cellular responses including proliferation, differentiation, and migration. Among the 22 human/mouse FGFs, the secreted FGF10 ligand through the binding of its specific receptors (FGFR1b and FGFR2b) and subsequent activation of downstream signaling is known to play essential role in cardiac development, homeostasis and disease. FGF10 is one of the major marker of the early cardiac progenitor cells and a crucial regulator of differentiated cardiomyocyte proliferation in the developing embryo. Increasing evidence support the hypothesis that a detailed understanding of developmental processes is essential to identify targets for cardiac repair and regeneration. Indeed the activation of resident cardiomyocyte proliferation together with the injection of cardiac progenitors represent the most promising therapeutical strategies for cardiac regenerative medicine. The recent findings showing that FGF10 promotes adult cardiomyocyte cell cycle reentry and directs stem cell differentiation and cell reprogramming toward the cardiogenic lineage provide new insights into therapeutical strategies for cardiac regeneration and repair.

Keywords: FGF10, FGFR1/2, heart development, cardiomyocyte, cardiac regeneration

OPEN ACCESS

Edited by:
Saverio Bellusci,
Justus-Liebig-Universität Gießen, Germany

Reviewed by:
Ching-Ling Lien,
Children's Hospital Los Angeles, United States
Stefan Hadzic,
Justus-Liebig-Universität Gießen, Germany

***Correspondence:**
Francesca Rochais
francesca.rochais@univ-amu.fr

Specialty section:
This article was submitted to Stem Cell Research, a section of the journal Frontiers in Genetics

Received: *27 September 2018*
Accepted: *15 November 2018*
Published: *28 November 2018*

Citation:
Hubert F, Payan SM and Rochais F (2018) FGF10 Signaling in Heart Development, Homeostasis, Disease and Repair. Front. Genet. 9:599. doi: 10.3389/fgene.2018.00599

INTRODUCTION

The heart is an essential muscular organ that pumps blood and provides the whole body with oxygen and nutrients. During embryonic development, the heart is the first organ to form and cardiac morphogenesis is a tightly regulated process. Cardiovascular diseases including congenital and acquired heart diseases are the leading cause of mortality in industrialized countries (Writing Group Members et al., 2016).

By mediating a variety of cellular responses, Fibroblast Growth Factors (FGFs) are known to play an essential role in cardiac development, homeostasis and disease. The human/mouse FGF family comprises 22 members including secreted and intracellular FGFs. Secreted FGFs bind and activate cell surface tyrosine kinase receptors (FGF receptors; FGFRs) encoded by four genes (FGFR1-4). The alternate splicing of FGFR genes results in the generation of seven different receptors, each of them displaying distinct ligand-binding properties (Zhang et al., 2006). In contrast to secreted FGFs, intracellular FGFs serve as cofactors for voltage gated sodium channels and other

molecules (Ornitz and Itoh, 2015). Interaction between secreted FGFs and their specific receptors is tightly regulated by extracellular binding proteins including heparan sulfates and the Klotho family proteins that serve as cofactors and confer unique ligand-receptor binding properties. Activated tyrosine kinase FGF receptors mediate diverse intracellular signaling cascades including the RAS-MAPK, PI3K-AKT, PLCγ, and STAT signaling pathways (Ornitz and Itoh, 2015). Phylogenetic analysis suggest that secreted FGFs can be grouped into five subfamilies of paracrine FGFs and one subfamily of endocrine FGFs. The current consensus suggests that FGF10 belongs to a subfamily that comprises FGF3, FGF7, FGF10, and FGF22. Receptor-ligand specificities are well described. Indeed, FGF3, 7, 10, and 22 have been shown to activate preferentially the IIIb splice variant of FGFR2. In addition FGF3 and FGF10 also activate the IIIb splice variant of FGFR1 (Zhang et al., 2006). Nevertheless, ablation studies together with overlapping expression patterns strongly suggest potential functional redundancy between FGF family members in the developing and adult heart. Finally, the existence of heterodimer formation between FGFs and FGFRs may further increase receptor-ligand interaction possibilities (Sun et al., 2002) and thus the diversity of FGF signaling.

Here we will review a detailed understanding of FGF signaling in cardiovascular development, homeostasis, disease and repair, focusing on the particular role of the FGF10/FGFR1/FGFR2 pathway.

DEVELOPMENTAL ROLE OF THE FGF10 SIGNALING

Heart development is an extremely complex process that can be divided in two major growth phases distinguished by a shift in the major site of proliferation from an extracardiac progenitor cell population to fetal cardiomyocytes. The early embryonic phase relies on the extensive proliferation of cardiac progenitor cells termed the second heart field (SHF) and their progressive addition to the developing heart tube. Precise spatiotemporal control of SHF progenitor cell proliferation-differentiation balance is required for normal heart tube elongation. Cardiac neural crest (CNC) cells, a second extracardiac cell population, play a critical role in early heart development (Hutson and Kirby, 2007). Concomitant with SHF cell addition to the outflow tract (OFT) of the heart, CNC migrate from the dorsal neural tube into the OFT. Interactions between CNC cells and SHF progenitors are critical determinants for the correct addition of SHF cells to the heart tube. In contrast to early heart tube development, fetal heart growth is achieved through the proliferation of differentiated cardiomyocytes which tight control is essential for the correct morphogenesis of the heart. Indeed, perturbations in the regulation of fetal cardiomyocyte proliferation lead to congenital heart defects.

During the early embryonic phase of heart morphogenesis, proper communication between cardiac progenitor cells is a prerequisite for correct heart tube elongation, looping, and arterial pole alignment. FGFs are among the critical signals required for proper early cardiac morphogenesis (Kelly, 2012). By ensuring communication within and between developing heart progenitors, FGF signaling leads to their tight regulation of proliferation and specification. Indeed, transgenic mouse models with conditional inactivation of *Fgfr1/2*, conditional overexpression of *Sprouty2* (*Spry2*, which encodes an FGF signaling antagonist) or conditional ablation of *Frs2* (encoding a MAPK/PI3K signaling adaptor protein) within the SHF progenitor cell population revealed that interrupting autocrine FGF signaling in SHF mesoderm, by compromising SHF progenitor cell proliferation and by indirectly reducing cardiac neural crest cell recruitment into the outflow tract cushions, causes outflow tract misalignment and subsequently impaired cardiac morphogenesis (Park et al., 2008; Zhang et al., 2008). While FGFR-dependent regulation of SHF proliferation seems to depend on the PI3K/AKT pathway (Luo et al., 2015), the Ras/Erk downstream signaling seems to be required in the regulation of myocardial specification (Rochais et al., 2009; Hutson et al., 2010). All these studies thus strongly reveal iterative roles for FGF signaling in OFT development.

Multiple FGF ligands have been described to be expressed in cardiac progenitors and surrounding tissues (**Figures 1A–C**). FGF10 was identified as a specific endogenous marker of the SHF (Kelly et al., 2001). While *Fgf10* expression is restricted to SHF progenitors (Kelly et al., 2001), *Fgf8* is also expressed in the adjacent pharyngeal ectoderm and endoderm (Ilagan et al., 2006; Mesbah et al., 2012). *Fgf15* expression has been detected in the pharyngeal endoderm (Vincentz et al., 2005) and *Fgf3* is expressed in the pharyngeal endoderm and ectoderm (Urness et al., 2011).

The Wnt/β-catenin signaling pathway a key regulator of SHF development transcriptionally controls *Fgf10* expression within SHF progenitors (Cohen et al., 2007). Crucial transcription factors of SHF cardiac progenitor cell deployment are also known to control *Fgf10* expression. ISL1 and NKX2-5 control the expression of *Fgf10* in the SHF, through competitive binding to common regulatory elements in an intronic cardiac enhancer, thus, respectively, activating expression in progenitor cells and repressing transcription in differentiated myocytes (Watanabe et al., 2012). TBX1 also activates *Fgf10* through T-box binding sites in the same enhancer element (Watanabe et al., 2012).

Fgf10-null embryos, which die at birth due to lung aplasia, display altered heart morphology. In addition to the absence of pulmonary arteries and veins, *Fgf10* knockout embryos display an abnormal positioning of the ventricular apex in the thoracic cavity (Marguerie et al., 2006; Rochais et al., 2014). Nevertheless, early SHF deployment and subsequent heart tube elongation are not affected by *Fgf10* deletion. In contrast, deletion of the main FGF10 receptor, *Fgfr2b*, leads to major congenital heart defects including ventricular septal defects, OFT alignment defects, and thin and poorly trabeculated ventricles (Marguerie et al., 2006) strongly suggesting the existence of functional redundancy between FGF10 and other FGFR2b ligands during the early steps of heart development. FGF8 appears to be the major ligand regulating cardiac progenitor cell deployment. A series of conditional loss of function experiments has revealed that *Fgf8*, through a cell-autonomous mechanism, is required for SHF expansion and thus OFT elongation, septation, and

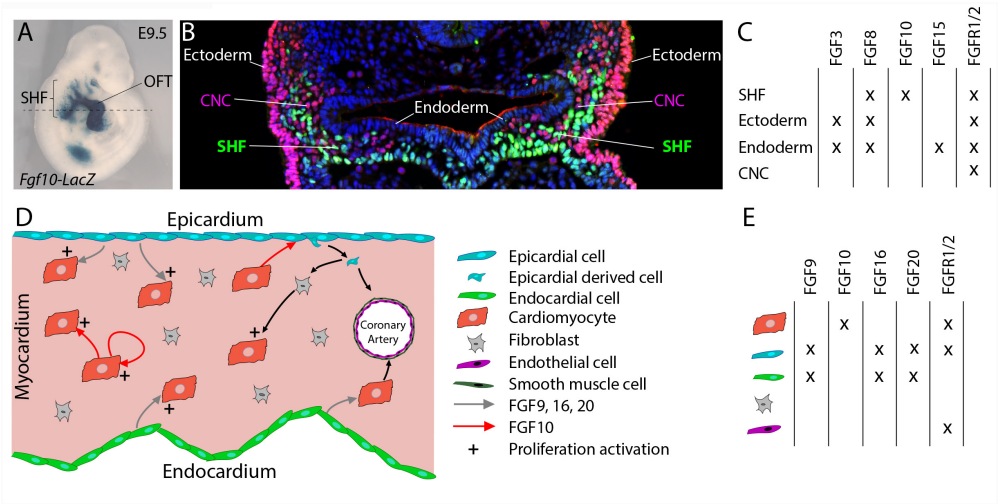

FIGURE 1 | FGF10 signaling in the developing heart. **(A)** Lateral whole-mount view and **(B)** transverse section of an embryo carrying an *Fgf10-LacZ* transgene (Kelly et al., 2001) at embryonic day E9.5. *Fgf10* transgene expression is observed in second heart field (SHF) progenitor cells, which are located in pharyngeal mesoderm adjacent to pharyngeal endoderm, and in the outflow tract (OFT). **(B)** Immunofluorescence on transverse section of an E9.5 embryo carrying an *Fgf10-LacZ* transgene, at the level of the dotted line in **(A)**. The anti-AP-2α (pink) antibody was used to detect cardiac neural crest (CNC) cells and ectodermal cells and the anti-β galactosidase (green) antibody to visualize SHF cells. **(C)** Table showing the overlapping expression patterns of key FGF ligands and receptors at E9.5 in the SHF and surrounding tissues. **(D)** FGF signaling role in fetal heart development. **(E)** Table showing the overlapping expression patterns of key FGF ligands and receptors in the fetal heart.

subsequent ventriculoarterial alignment (Ilagan et al., 2006; Park et al., 2008). Interestingly, the fact that heterozygous deletion of *Fgf10* in combination with homozygous loss of mesodermal *Fgf8* expression results in more severely altered anterior heart development (Watanabe et al., 2010) strongly supports mesodermal FGF8 and FGF10 functional redundancy. In addition, FGF3 and FGF10 have been also shown to play redundant and dosage sensitive requirement during heart tube elongation (Urness et al., 2011). All these studies highlight that critical FGF dosage, including FGF10, is crucial for SHF proliferation and deployment and thus for normal cardiac morphogenesis.

During the second phase of heart development (after embryonic day E10.5), subsequent growth and remodeling of the myocardium occur without significant further addition of cardiac progenitor cells to the heart. Instead, regulated proliferation of cardiac myocytes drives growth of the atrial and ventricular chambers. Tight spatio-temporal regulation of fetal cardiomyocyte proliferation thus appears to be required for proper heart formation and impairment of cardiomyocyte proliferation during fetal stages also results in congenital heart defects (Ahuja et al., 2007). FGF signals, through cell-autonomous or paracrine mechanisms, have been described as crucial regulators of fetal cardiomyocyte proliferation (**Figures 1D,E**; Smith and Bader, 2007). FGF ligands originating from the endocardium and the epicardium, including FGF9, FGF16, and FGF20, have been shown to regulate cardiomyocyte proliferation (Lavine et al., 2005; Hotta et al., 2008; Lu et al., 2008). Recent reports revealed the implication of FGF10 in the regulation of fetal cardiomyocyte proliferation. *Fgf10* mutant heart analysis demonstrates that FGF10 signaling, through a cell-type autonomous mechanism, specifically controls fetal right ventricular cardiomyocyte proliferation. In fact, at fetal stages, FGF10/FGFR2b signaling promotes cardiomyocyte proliferation through the phosphorylation of the FOXO3 transcription factor and subsequent downregulation of the cyclin dependent kinase inhibitor $p27^{kip1}$ expression (Rochais et al., 2014). In addition, myocardial FGF10 signaling, through the paracrine activation of FGFR1 and FGFR2 in the epicardium, has been suggested to promote epicardial-derived cell migration into the compact myocardial layer (Vega-Hernandez et al., 2011). In this study, the impairment in cardiac fibroblast numbers observed in *Fgf10*-mutant hearts, results indirectly in reduced fetal cardiomyocyte proliferation.

Despite cardiomyocyte proliferation, FGF signals, through redundant function of FGFR1 and FGFR2, originating from the epicardium and the endocardium, play pivotal role in coronary vasculature development (**Figure 1D**). In fact, in embryonic mouse heart, myocardial FGFR1/2 signaling by triggering Hedgehog signaling activation, *Vegf* and *Angiopoietin-2* expression, indirectly participate to the coronary vascular plexus formation and thus coronary vessel deployment (Lavine et al., 2006). Here the precise requirement of the FGF10 ligand has not been explored.

Several members of the FGF family are expressed in the vascular network (Presta et al., 2005; Beenken and Mohammadi, 2009). While the most studied FGF member, FGF2, is a potent inducer of angiogenesis, other FGFs (FGF 1, 2, 5, 7, 8, 16, and 18), but not FGF10, are expressed in endothelial and vascular smooth muscle cells (Antoine et al., 2005). Despite predominant FGFR1 and FGFR2 expression endothelial cells (Presta et al., 2005), mouse specific deletion of *Fgfr1* and *Fgfr2* in both endothelial

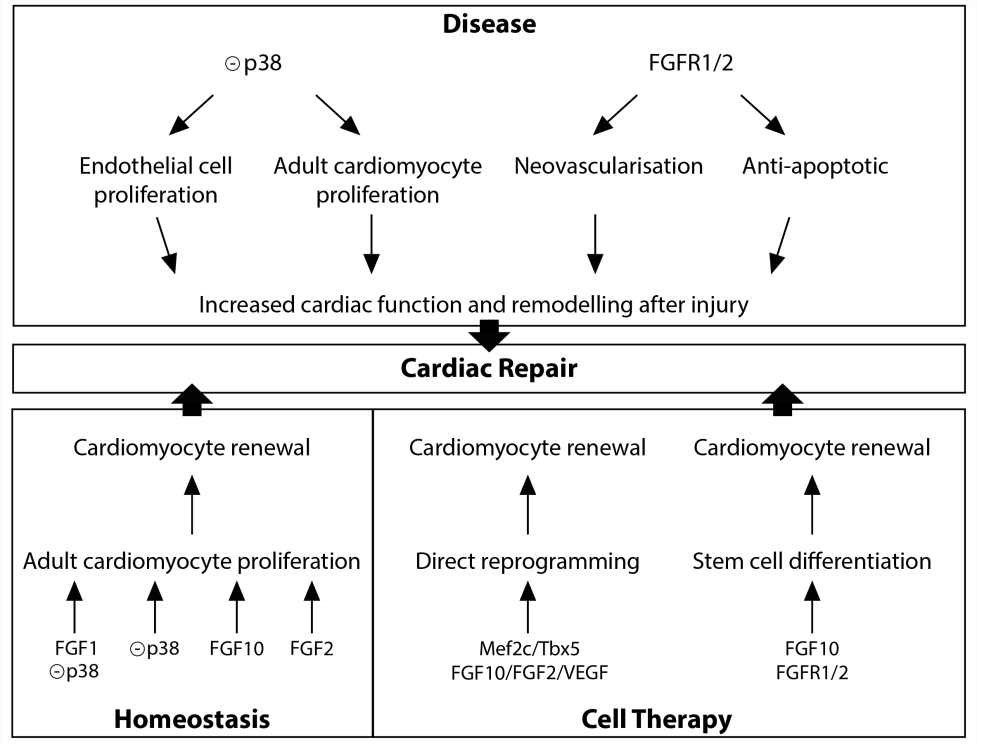

FIGURE 2 | FGF10 signaling in cardiac homeostasis, disease and repair.

and hematopoietic cell lineages has no impact on normal vascular development (Oladipupo et al., 2014; House et al., 2016). In contrast, in zebrafish, global FGFR signaling inhibition using allosteric inhibitor or a dominant negative form of the receptor revealed the critical requirement for FGF signaling in the maintenance vascular function and integrity (Murakami et al., 2008; De Smet et al., 2014). This strongly suggests, in mammals, the existence of functional redundancy between FGFR1, FGFR2, and FGFR3 that also expressed in endothelial cells.

FGF10 SIGNALING IN CARDIAC HOMEOSTASIS

Soon after birth, the ability of cardiomyocytes to proliferate is strongly reduced, and cardiac growth transitions from hyperplastic to hypertrophic (Pasumarthi and Field, 2002). For nearly a century, the adult heart has been considered to be a post-mitotic organ; however, recent studies have highlighted the importance of the homeostasis of the adult heart in physiological conditions. Indeed extensive studies on adult mammalian hearts including the human heart have led to a consensus that new cardiomyocytes are indeed generated throughout life (Soonpaa and Field, 1998; Bergmann et al., 2009, 2015). In the healthy adult murine and human heart, cardiomyocyte renewal is currently estimated at 0.5–2% per year (Eschenhagen et al., 2017).

Diverse FGFs and downstream signals, including FGF1, FGF2, FGF10, and p38 MAP kinase have been shown to be involved in the regulation of adult cardiomyocyte renewal (**Figure 2**). *In vitro* studies initially described FGF2 as a potent positive regulator of cardiomyocyte proliferation (Pasumarthi and Field, 2002). *In vitro* and *in vivo* experiments indicate that p38 MAP kinase inhibition alone (Jopling et al., 2012b) or in combination with FGF1 treatment (Engel et al., 2005, 2006), leads to partial cardiomyocyte dedifferentiation and cell-cycle progression. Furthermore, in the adult zebrafish, epicardial cells addition to the ventricle has been shown to support cardiac homeostasis in an FGF-dependent fashion (Wills et al., 2008). Finally, in the adult mouse heart, FGF10 has been described to be a potent regulator of cardiomyocyte proliferation. Indeed, temporal *Fgf10* overexpression rapidly enhanced adult cardiomyocyte cell cycle re-entry leading to increased ventricular wall thickness. While FGF10 regulation of fetal cardiomyocyte proliferation seems to occur through the FGFR2b, FGF10 may activate predominantly the FGFR1b to promote adult cardiomyocyte proliferation (Rochais et al., 2014).

IMPLICATION OF FGF10 SIGNALING IN CARDIOVASCULAR DISEASES AND REPAIR

Cardiovascular diseases are the leading cause of mortality in industrialized countries (Writing Group Members et al., 2016). Characterized by any molecular, cellular and physiological change in the myocardium, coronary vessels or valves, cardiac

diseases result in cardiomyocyte loss and impaired cardiac function that ultimately lead to congestive heart failure. Multiple FGFs including FGF10 signaling have been described to play pathophysiological roles in the cardiovascular system (Itoh et al., 2016).

Diverse studies highlighted a role for the FGFR1/2 signaling in the neovascularization after injury (**Figure 2**). In the zebrafish injured heart, epicardial *Fgfr2* expression is upregulated and FGFR signaling blockade leads to a failure in coronary neovascularization, resulting in severely impaired cardiac regeneration (Lepilina et al., 2006). In addition, neovascularization and vascular remodeling in response to injury is severely impaired in endothelial specific FGFR1/2 deficient mice (Oladipupo et al., 2014; House et al., 2016). Finally, endothelium-targeted overexpression of constitutively active FGFR2 post-myocardial infarction results in anti-apoptotic action with enhanced angiogenesis (Matsunaga et al., 2009).

While zebrafish adult heart fully regenerates after injury (Poss et al., 2002), damaged adult mammalian myocardium is replaced by fibrotic scar tissue. The MAPK pathway plays a crucial role in adult zebrafish heart regeneration (**Figure 2**). Indeed, the induction of p38 MAPK activity prevents cardiomyocyte proliferation and subsequent heart regeneration (Jopling et al., 2012a). In the adult mouse heart, p38 inhibitor injection, after acute myocardial injury, enhances cardiomyocyte and endothelial cell proliferation and preserves cardiac remodeling and function (Engel et al., 2006) strongly revealing that downstream FGF signaling may be beneficial to improve the limited innate regenerative capacities of the adult mammalian heart. In contrast to the adult heart, neonatal mammalian heart, including mouse, pig and human, possesses extensive regenerative capacities (Porrello et al., 2011; Haubner et al., 2016; Zhu et al., 2018). Nevertheless, the rapid and dramatic decrease in cardiomyocyte proliferation rate during the first week of postnatal life (Pasumarthi and Field, 2002) results in severely limited regenerative capacities in adult, strongly supporting the hypothesis that a detailed understanding of the regulation of fetal cardiomyocyte proliferation is essential to identify targets for cardiac regeneration. As described above, FGF10 has been identified as a crucial regulator of fetal cardiomyocyte proliferation (Rochais et al., 2014). The fact that decreased myocardial *Fgf10* expression has been observed in mouse postnatal heart during the time window where cardiomyocytes exit from the cell cycle (Rochais et al., 2014), coinciding with the loss of regenerative capacities, suggests that FGF10 signaling may play a role in cardiac regeneration. However, *Fgf10* overexpression in the neonatal mouse heart does not promote beneficial effects on post-natal cardiac regeneration (Rubin et al., 2013). Nevertheless, the ability for FGF10 to specifically induce adult cardiomyocyte cell-cycle reentry in physiological conditions suggests that FGF10 might be able to promote cardiomyocyte renewal in the adult injured heart (Rochais et al., 2014).

Together with the stimulation of existing cardiomyocyte renewal, cell therapy using the injection or tissue-based implantation of cardiac progenitor cells and direct reprogramming represent relevant therapeutic options for cardiac regenerative medicine (Tzahor and Poss, 2017). Several studies revealed the requirement of FGF10 signaling during stem cell specification into the cardiogenic lineage (**Figure 2**). Indeed, FGF10 signaling has been shown to play an important role in promoting cardiomyocyte differentiation in both embryonic and induced pluripotent stem cells (Chan et al., 2010). Furthermore, in addition to improve the quality of cardiac reprogramming in mouse fibroblasts, and in combination with FGF2 and the vascular endothelial growth factor (VEGF), FGF10, through the RAS-MAPK and PI3K/AKT pathways, is able to convert partially reprogrammed cells into functional cardiomyocyte-like cells (Yamakawa et al., 2015).

CONCLUSION

All the studies described in this review highlighted the crucial role for the FGF10 ligand and the related FGFR1/2 signaling in heart development, homeostasis and disease. The recent findings revealing a crucial role for FGF10 in controlling both adult cardiomyocyte cell cycle reentry and stem cell differentiation and cell reprogramming toward the cardiogenic lineage provide potential therapeutic strategies for cardiovascular diseases.

AUTHOR CONTRIBUTIONS

FH, SP, and FR wrote the manuscript.

FUNDING

This study was supported by the Agence Nationale de la Recherche grant ANR-14-CE12-12-02, the Fédération Française de Cardiologie, and the AFM-Téléthon grant n°20777 awarded by FR.

REFERENCES

Ahuja, P., Sdek, P., and MacLellan, W. R. (2007). Cardiac myocyte cell cycle control in development, disease, and regeneration. *Physiol. Rev.* 87, 521–544. doi: 10.1152/physrev.00032.2006

Antoine, M., Wirz, W., Tag, C. G., Mavituna, M., Emans, N., Korff, T., et al. (2005). Expression pattern of fibroblast growth factors (FGFs), their receptors and antagonists in primary endothelial cells and vascular smooth muscle cells. *Growth Factors* 23, 87–95. doi: 10.1080/08977190500096004

Beenken, A., and Mohammadi, M. (2009). The FGF family: biology, pathophysiology and therapy. *Nat. Rev. Drug Discov.* 8, 235–253. doi: 10.1038/nrd2792

Bergmann, O., Bhardwaj, R. D., Bernard, S., Zdunek, S., Barnabe-Heider, F., Walsh, S., et al. (2009). Evidence for cardiomyocyte renewal in humans. *Science* 324, 98–102. doi: 10.1126/science.1164680

Bergmann, O., Zdunek, S., Felker, A., Salehpour, M., Alkass, K., Bernard, S., et al. (2015). Dynamics of cell generation and turnover in the human heart. *Cell* 161, 1566–1575. doi: 10.1016/j.cell.2015.05.026

Chan, S. S., Li, H. J., Hsueh, Y. C., Lee, D. S., Chen, J. H., Hwang, S. M., et al. (2010). Fibroblast growth factor-10 promotes cardiomyocyte differentiation from embryonic and induced pluripotent stem cells. *PLoS One* 5:e14414. doi: 10.1371/journal.pone.0014414

Cohen, E. D., Wang, Z., Lepore, J. J., Lu, M. M., Taketo, M. M., Epstein, D. J., et al. (2007). Wnt/beta-catenin signaling promotes expansion of Isl-1-positive cardiac progenitor cells through regulation of FGF signaling. *J. Clin. Invest.* 117, 1794–1804. doi: 10.1172/JCI31731

De Smet, F., Tembuyser, B., Lenard, A., Claes, F., Zhang, J., Michielsen, C., et al. (2014). Fibroblast growth factor signaling affects vascular outgrowth and is required for the maintenance of blood vessel integrity. *Chem. Biol.* 21, 1310–1317. doi: 10.1016/j.chembiol.2014.07.018

Engel, F. B., Hsieh, P. C., Lee, R. T., and Keating, M. T. (2006). FGF1/p38 MAP kinase inhibitor therapy induces cardiomyocyte mitosis, reduces scarring, and rescues function after myocardial infarction. *Proc. Natl. Acad. Sci. U.S.A.* 103, 15546–15551. doi: 10.1073/pnas.0607382103

Engel, F. B., Schebesta, M., Duong, M. T., Lu, G., Ren, S., Madwed, J. B., et al. (2005). p38 MAP kinase inhibition enables proliferation of adult mammalian cardiomyocytes. *Genes Dev.* 19, 1175–1187. doi: 10.1101/gad.1306705

Eschenhagen, T., Bolli, R., Braun, T., Field, L. J., Fleischmann, B. K., Frisen, J., et al. (2017). Cardiomyocyte regeneration: a consensus statement. *Circulation* 136, 680–686. doi: 10.1161/CIRCULATIONAHA.117.029343

Haubner, B. J., Schneider, J., Schweigmann, U., Schuetz, T., Dichtl, W., Velik-Salchner, C., et al. (2016). Functional recovery of a human neonatal heart after severe myocardial infarction. *Circ. Res.* 118, 216–221. doi: 10.1161/CIRCRESAHA.115.307017

Hotta, Y., Sasaki, S., Konishi, M., Kinoshita, H., Kuwahara, K., Nakao, K., et al. (2008). Fgf16 is required for cardiomyocyte proliferation in the mouse embryonic heart. *Dev. Dyn.* 237, 2947–2954. doi: 10.1002/dvdy.21726

House, S. L., Castro, A. M., Lupu, T. S., Weinheimer, C., Smith, C., Kovacs, A., et al. (2016). Endothelial fibroblast growth factor receptor signaling is required for vascular remodeling following cardiac ischemia-reperfusion injury. *Am. J. Physiol. Heart Circ. Physiol.* 310, H559–H571. doi: 10.1152/ajpheart.00758.2015

Hutson, M. R., and Kirby, M. L. (2007). Model systems for the study of heart development and disease. Cardiac neural crest and conotruncal malformations. *Semin. Cell Dev. Biol.* 18, 101–110. doi: 10.1016/j.semcdb.2006.12.004

Hutson, M. R., Zeng, X. L., Kim, A. J., Antoon, E., Harward, S., and Kirby, M. L. (2010). Arterial pole progenitors interpret opposing FGF/BMP signals to proliferate or differentiate. *Development* 137, 3001–3011. doi: 10.1242/dev.051565

Ilagan, R., Abu-Issa, R., Brown, D., Yang, Y. P., Jiao, K., Schwartz, R. J., et al. (2006). Fgf8 is required for anterior heart field development. *Development* 133, 2435–2445. doi: 10.1242/dev.02408

Itoh, N., Ohta, H., Nakayama, Y., and Konishi, M. (2016). Roles of FGF signals in heart development, health, and disease. *Front. Cell Dev. Biol.* 4:110. doi: 10.3389/fcell.2016.00110

Jopling, C., Sune, G., Faucherre, A., Fabregat, C., and Izpisua Belmonte, J. C. (2012a). Hypoxia induces myocardial regeneration in zebrafish. *Circulation* 126, 3017–3027. doi: 10.1161/CIRCULATIONAHA.112.107888

Jopling, C., Sune, G., Morera, C., and Izpisua Belmonte, J. C. (2012b). p38alpha MAPK regulates myocardial regeneration in zebrafish. *Cell Cycle* 11, 1195–1201. doi: 10.4161/cc.11.6.19637

Kelly, R. G. (2012). The second heart field. *Curr. Top. Dev. Biol.* 100, 33–65. doi: 10.1016/B978-0-12-387786-4.00002-6

Kelly, R. G., Brown, N. A., and Buckingham, M. E. (2001). The arterial pole of the mouse heart forms from Fgf10-expressing cells in pharyngeal mesoderm. *Dev. Cell* 1, 435–440. doi: 10.1016/S1534-5807(01)00040-5

Lavine, K. J., White, A. C., Park, C., Smith, C. S., Choi, K., Long, F., et al. (2006). Fibroblast growth factor signals regulate a wave of Hedgehog activation that is essential for coronary vascular development. *Genes Dev.* 20, 1651–1666. doi: 10.1101/gad.1411406

Lavine, K. J., Yu, K., White, A. C., Zhang, X., Smith, C., Partanen, J., et al. (2005). Endocardial and epicardial derived FGF signals regulate myocardial proliferation and differentiation in vivo. *Dev. Cell* 8, 85–95. doi: 10.1016/j.devcel.2004.12.002

Lepilina, A., Coon, A. N., Kikuchi, K., Holdway, J. E., Roberts, R. W., Burns, C. G., et al. (2006). A dynamic epicardial injury response supports progenitor cell activity during zebrafish heart regeneration. *Cell* 127, 607–619. doi: 10.1016/j.cell.2006.08.052

Lu, S. Y., Sheikh, F., Sheppard, P. C., Fresnoza, A., Duckworth, M. L., Detillieux, K. A., et al. (2008). FGF-16 is required for embryonic heart development. *Biochem. Biophys. Res. Commun.* 373, 270–274. doi: 10.1016/j.bbrc.2008.06.029

Luo, W., Zhao, X., Jin, H., Tao, L., Zhu, J., Wang, H., et al. (2015). Akt1 signaling coordinates BMP signaling and beta-catenin activity to regulate second heart field progenitor development. *Development* 142, 732–742. doi: 10.1242/dev.119016

Marguerie, A., Bajolle, F., Zaffran, S., Brown, N. A., Dickson, C., Buckingham, M. E., et al. (2006). Congenital heart defects in Fgfr2-IIIb and Fgf10 mutant mice. *Cardiovasc. Res.* 71, 50–60. doi: 10.1016/j.cardiores.2006.03.021

Matsunaga, S., Okigaki, M., Takeda, M., Matsui, A., Honsho, S., Katsume, A., et al. (2009). Endothelium-targeted overexpression of constitutively active FGF receptor induces cardioprotection in mice myocardial infarction. *J. Mol. Cell Cardiol.* 46, 663–673. doi: 10.1016/j.yjmcc.2009.01.015

Mesbah, K., Rana, M. S., Francou, A., van Duijvenboden, K., Papaioannou, V. E., Moorman, A. F., et al. (2012). Identification of a Tbx1/Tbx2/Tbx3 genetic pathway governing pharyngeal and arterial pole morphogenesis. *Hum. Mol. Genet.* 21, 1217–1229. doi: 10.1093/hmg/ddr553

Murakami, M., Nguyen, L. T., Zhuang, Z. W., Moodie, K. L., Carmeliet, P., Stan, R. V., et al. (2008). The FGF system has a key role in regulating vascular integrity. *J. Clin. Invest.* 118, 3355–3366. doi: 10.1172/JCI35298

Oladipupo, S. S., Smith, C., Santeford, A., Park, C., Sene, A., Wiley, L. A., et al. (2014). Endothelial cell FGF signaling is required for injury response but not for vascular homeostasis. *Proc. Natl. Acad. Sci. U.S.A.* 111, 13379–13384. doi: 10.1073/pnas.1324235111

Ornitz, D. M., and Itoh, N. (2015). The fibroblast growth factor signaling pathway. *Wiley Interdiscip. Rev. Dev. Biol.* 4, 215–266. doi: 10.1002/wdev.176

Park, E. J., Watanabe, Y., Smyth, G., Miyagawa-Tomita, S., Meyers, E., Klingensmith, J., et al. (2008). An FGF autocrine loop initiated in second heart field mesoderm regulates morphogenesis at the arterial pole of the heart. *Development* 135, 3599–3610. doi: 10.1242/dev.025437

Pasumarthi, K. B., and Field, L. J. (2002). Cardiomyocyte cell cycle regulation. *Circ. Res.* 90, 1044–1054. doi: 10.1161/01.RES.0000020201.44772.67

Porrello, E. R., Mahmoud, A. I., Simpson, E., Hill, J. A., Richardson, J. A., Olson, E. N., et al. (2011). Transient regenerative potential of the neonatal mouse heart. *Science* 331, 1078–1080. doi: 10.1126/science.1200708

Poss, K. D., Wilson, L. G., and Keating, M. T. (2002). Heart regeneration in zebrafish. *Science* 298, 2188–2190. doi: 10.1126/science.1077857

Presta, M., Dell'Era, P., Mitola, S., Moroni, E., Ronca, R., and Rusnati, M. (2005). Fibroblast growth factor/fibroblast growth factor receptor system in angiogenesis. *Cytokine Growth Factor Rev.* 16, 159–178. doi: 10.1016/j.cytogfr.2005.01.004

Rochais, F., Mesbah, K., and Kelly, R. G. (2009). Signaling pathways controlling second heart field development. *Circ. Res.* 104, 933–942. doi: 10.1161/CIRCRESAHA.109.194464

Rochais, F., Sturny, R., Chao, C. M., Mesbah, K., Bennett, M., Mohun, T. J., et al. (2014). FGF10 promotes regional foetal cardiomyocyte proliferation and adult cardiomyocyte cell-cycle re-entry. *Cardiovasc. Res.* 104, 432–442. doi: 10.1093/cvr/cvu232

Rubin, N., Darehzereshki, A., Bellusci, S., Kaartinen, V., and Ling Lien, C. (2013). FGF10 signaling enhances epicardial cell expansion during neonatal mouse heart repair. *J. Cardiovasc. Dis. Diagn.* 1:101.

Smith, T. K., and Bader, D. M. (2007). Signals from both sides: control of cardiac development by the endocardium and epicardium. *Semin. Cell Dev. Biol.* 18, 84–89. doi: 10.1016/j.semcdb.2006.12.013

Soonpaa, M. H., and Field, L. J. (1998). Survey of studies examining mammalian cardiomyocyte DNA synthesis. *Circ. Res.* 83, 15–26. doi: 10.1161/01.RES.83.1.15

Sun, S., Albright, C. F., Fish, B. H., George, H. J., Selling, B. H., Hollis, G. F., et al. (2002). Expression, purification, and kinetic characterization of full-length human fibroblast activation protein. *Protein Expr. Purif.* 24, 274–281. doi: 10.1006/prep.2001.1572

Tzahor, E., and Poss, K. D. (2017). Cardiac regeneration strategies: staying young at heart. *Science* 356, 1035–1039. doi: 10.1126/science.aam5894

Urness, L. D., Bleyl, S. B., Wright, T. J., Moon, A. M., and Mansour, S. L. (2011). Redundant and dosage sensitive requirements for Fgf3 and Fgf10 in

cardiovascular development. *Dev. Biol.* 356, 383–397. doi: 10.1016/j.ydbio.2011.05.671

Vega-Hernandez, M., Kovacs, A., De Langhe, S., and Ornitz, D. M. (2011). FGF10/FGFR2b signaling is essential for cardiac fibroblast development and growth of the myocardium. *Development* 138, 3331–3340. doi: 10.1242/dev.064410

Vincentz, J. W., McWhirter, J. R., Murre, C., Baldini, A., and Furuta, Y. (2005). Fgf15 is required for proper morphogenesis of the mouse cardiac outflow tract. *Genesis* 41, 192–201. doi: 10.1002/gene.20114

Watanabe, Y., Miyagawa-Tomita, S., Vincent, S. D., Kelly, R. G., Moon, A. M., and Buckingham, M. E. (2010). Role of mesodermal FGF8 and FGF10 overlaps in the development of the arterial pole of the heart and pharyngeal arch arteries. *Circ. Res.* 106, 495–503. doi: 10.1161/CIRCRESAHA.109.201665

Watanabe, Y., Zaffran, S., Kuroiwa, A., Higuchi, H., Ogura, T., Harvey, R. P., et al. (2012). Fibroblast growth factor 10 gene regulation in the second heart field by Tbx1, Nkx2-5, and Islet1 reveals a genetic switch for down-regulation in the myocardium. *Proc. Natl. Acad. Sci. U.S.A.* 109, 18273–18280. doi: 10.1073/pnas.1215360109

Wills, A. A., Holdway, J. E., Major, R. J., and Poss, K. D. (2008). Regulated addition of new myocardial and epicardial cells fosters homeostatic cardiac growth and maintenance in adult zebrafish. *Development* 135, 183–192. doi: 10.1242/dev.010363

Writing Group Members, Mozaffarian, D., Benjamin, E. J., Go, A. S., Arnett, D. K., Blaha, M. J., et al. (2016). Executive summary: heart disease and stroke statistics–2016 update: a report from the american heart association. *Circulation* 133, 447–454. doi: 10.1161/CIR.0000000000000366

Yamakawa, H., Muraoka, N., Miyamoto, K., Sadahiro, T., Isomi, M., Haginiwa, S., et al. (2015). Fibroblast growth factors and vascular endothelial growth factor promote cardiac reprogramming under defined conditions. *Stem Cell Rep.* 5, 1128–1142. doi: 10.1016/j.stemcr.2015.10.019

Zhang, J., Lin, Y., Zhang, Y., Lan, Y., Lin, C., Moon, A. M., et al. (2008). Frs2alpha-deficiency in cardiac progenitors disrupts a subset of FGF signals required for outflow tract morphogenesis. *Development* 135, 3611–3622. doi: 10.1242/dev.025361

Zhang, X., Ibrahimi, O. A., Olsen, S. K., Umemori, H., Mohammadi, M., and Ornitz, D. M. (2006). Receptor specificity of the fibroblast growth factor family. The complete mammalian FGF family. *J. Biol. Chem.* 281, 15694–15700. doi: 10.1074/jbc.M601252200

Zhu, W., Zhang, E., Zhao, M., Chong, Z., Fan, C., Tang, Y., et al. (2018). Regenerative potential of neonatal porcine hearts. *Circulation* doi: 10.1161/CIRCULATIONAHA.118.034886 [Epub ahead of print].

Conflict of Interest Statement: The authors declare that the research was conducted in the absence of any commercial or financial relationships that could be construed as a potential conflict of interest.

Copyright © 2018 Hubert, Payan and Rochais. This is an open-access article distributed under the terms of the Creative Commons Attribution License (CC BY). The use, distribution or reproduction in other forums is permitted, provided the original author(s) and the copyright owner(s) are credited and that the original publication in this journal is cited, in accordance with accepted academic practice. No use, distribution or reproduction is permitted which does not comply with these terms.

frontiers in Genetics

MINI REVIEW
published: 21 December 2018
doi: 10.3389/fgene.2018.00673

Mathematical Approaches of Branching Morphogenesis

*Christine Lang†, Lisa Conrad† and Odyssé Michos**

Department of Biosystems Science and Engineering, ETH Zürich, Basel, Switzerland

Many organs require a high surface to volume ratio to properly function. Lungs and kidneys, for example, achieve this by creating highly branched tubular structures during a developmental process called branching morphogenesis. The genes that control lung and kidney branching share a similar network structure that is based on ligand-receptor reciprocal signalling interactions between the epithelium and the surrounding mesenchyme. Nevertheless, the temporal and spatial development of the branched epithelial trees differs, resulting in organs of distinct shape and size. In the embryonic lung, branching morphogenesis highly depends on FGF10 signalling, whereas GDNF is the driving morphogen in the kidney. Knockout of *Fgf10* and *Gdnf* leads to lung and kidney agenesis, respectively. However, FGF10 plays a significant role during kidney branching and both the FGF10 and GDNF pathway converge on the transcription factors ETV4/5. Although the involved signalling proteins have been defined, the underlying mechanism that controls lung and kidney branching morphogenesis is still elusive. A wide range of modelling approaches exists that differ not only in the mathematical framework (e.g., stochastic or deterministic) but also in the spatial scale (e.g., cell or tissue level). Due to advancing imaging techniques, image-based modelling approaches have proven to be a valuable method for investigating the control of branching events with respect to organ-specific properties. Here, we review several mathematical models on lung and kidney branching morphogenesis and suggest that a ligand-receptor-based Turing model represents a potential candidate for a general but also adaptive mechanism to control branching morphogenesis during development.

Keywords: branching morphogenesis, mathematical modelling, FGF10, lung, kidney

OPEN ACCESS

Edited by:
Mohammad K. Hajihosseini, University of East Anglia, United Kingdom

Reviewed by:
Poongodi Geetha-Loganathan, SUNY Oswego, United States
Eumorphia Remboutsika, National and Kapodistrian University of Athens, Greece

***Correspondence:**
Odyssé Michos
odysse.michos@mac.com

†These authors have contributed equally to this work

Specialty section:
This article was submitted to Stem Cell Research, a section of the journal Frontiers in Genetics

Received: *30 September 2018*
Accepted: *04 December 2018*
Published: *21 December 2018*

Citation:
Lang C, Conrad L and Michos O (2018) Mathematical Approaches of Branching Morphogenesis. Front. Genet. 9:673. doi: 10.3389/fgene.2018.00673

INTRODUCTION

Branching morphogenesis is a common developmental process by which arborized structures with a high surface-to-volume ratio are created. In vertebrate organ development, branching morphogenesis describes how an epithelial organ bud branches into its surrounding mesenchyme. Epithelial-mesenchymal interactions via ligand-receptor signalling are well-established regulators of developmental processes such as growth and patterning (Clément et al., 2012a; Perrimon et al., 2012). Yet, it remains poorly understood how morphogen signalling guides branching morphogenesis in a reproducible fashion, while also allowing for adaptation to environmental changes and how the use of common developmental principles results in organs of different shape, size and function.

Even though the signalling networks relevant to organogenesis have been defined and gene functions and interactions have been studied intensively, it remains unclear how macroscopic features of branched organs, including size, network topology and spatial patterning are encoded. Mathematical modelling has proven to be a valuable method for examining the impact of signalling interactions in developmental processes, such as branching morphogenesis. Consequently, a wide range of modelling approaches have been established that can differ not only in the mathematical framework but also in the spatial scale (Peters et al., 2018).

In the following, we will focus on the role of fibroblast growth factor (FGF) 10 during branching morphogenesis of the vertebrate kidney and the lung and discuss to which extent mathematical models can help our understanding of branching morphogenesis. Lung and kidney branching has been studied in model organisms other than the mouse and the rat and orthologs of the genes described here have similar roles in other species, but are not further discussed in the context of this mini-review (Böttcher and Niehrs, 2005; Moura et al., 2011; Sakiyama, 2003; Shifley et al., 2012).

MESENCHYMAL-EPITHELIAL INTERACTIONS VIA MORPHOGEN SIGNALLING AND THEIR RECEPTORS

FGF10 is a morphogen belonging to the fibroblast growth factor family and plays important roles in both kidney and lung development. FGF10 signalling is essential for lung development and guides directional bud outgrowth, sustains progenitor cell fate and affects expression of genes involved in a variety of developmental processes (Bellusci et al., 1997; Min et al., 1998; Lü et al., 2005; El Agha et al., 2014, 2017). In mesenchyme-free cultures of lung buds, only FGF10 and FGF1 are sufficient to induce branching of the epithelium (Nogawa and Ito, 1995; Bellusci et al., 1997). *Fgf10*$^{-/-}$ mice display kidney dysgenesis with impaired ureteric bud (UB) development and medullary dysplasia (Ohuchi et al., 2000; Michos et al., 2010).

Glial cell line-derived neurotrophic factor (GDNF), a morphogen related to the TGF-beta growth factor family, is critical for kidney organogenesis. The absence of GDNF as well as of its receptor tyrosine kinase RET and co-receptor GFRα1 lead to kidney agenesis or severe hypodysplasia (Schuchardt et al., 1994, 1996; Moore et al., 1996; Pichel et al., 1996; Sánchez et al., 1996; Cacalano et al., 1998). Interestingly, both morphogens induce ERK signalling and converge on the transcription factors ETV4/5 to induce and promote branching (Lu et al., 2009; Michos et al., 2010). FGF10 rescues the *Gdnf*$^{-/-}$ phenotype in the absence of *Sprouty1,* an inhibitor of ERK signalling induced by FGF10 and GDNF, suggesting that FGF10 is an important regulator of branching during kidney development, which functions at least partly redundant to GDNF (**Figure 1A**) (Michos et al., 2010).

Fgf10, Gdnf and their receptors have distinct expression patterns during organogenesis (**Figure 1B**). In the lung, *Fgf10* is expressed in the submesothelial mesenchyme, so that FGF10

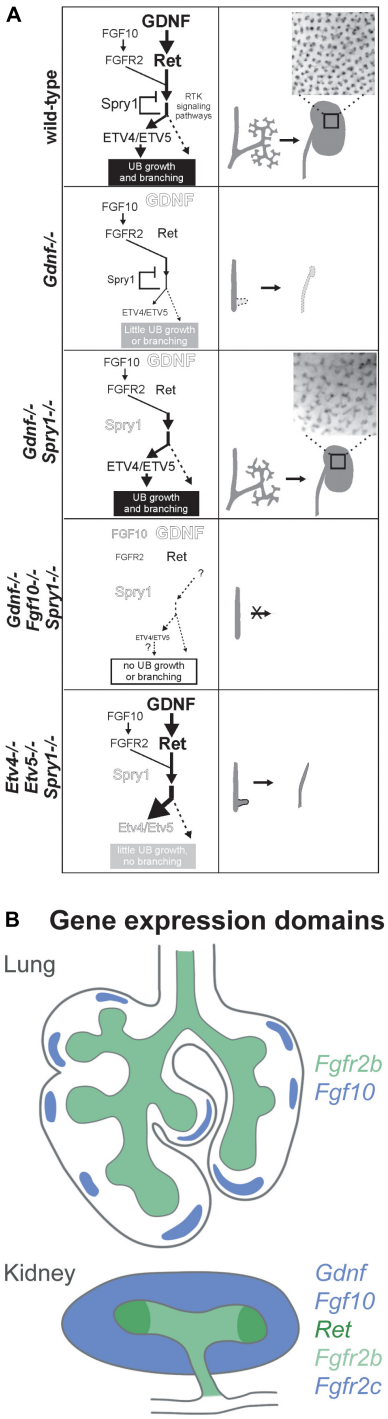

FIGURE 1 | (A) Ureteric bud branching morphogenesis is cooperatively regulated by FGF10 and GDNF via *Etv4* and *Etv5*, whereas Sprouty1 acts as a negative regulator of FGF10 and GDNF signalling downstream of FGFR2 and RET. (1) Regulation of UB branching in the wild type: GDNF is the main promoting factor for UB outgrowth and branching, while FGF10 plays a minor role. Sprouty1 counteracts ligand-receptor signalling, resulting in the development of a normal kidney. (2) The absence of GDNF abrogates UB branching and UB outgrowth, resulting in kidney agenesis or severe hypodysplasia. (3) If both the negative regulator Sprouty1 and GDNF are

(Continued)

FIGURE 1 | Continued
absent FGF10 signalling is sufficient to drive *Etv4/Etv5* expression, allowing for UB branching and kidney development. The branching pattern differs from the wild type, which points to a GDNF specific regulation of UB morphogenesis. (4) In the triple knockout, there is not enough ligand-receptor signalling to drive UB outgrowth and branching, even though Sprouty1 is absent as well. (5) Increased receptor tyrosine kinase signalling resulting from the absence of Sprouty1 does not rescue the renal agenesis phenotype of *Etv4 -/- Etv5 -/-* mice. In this triple knockout, the UB grows out, but fails to undergo branching and only ureters develop, suggesting that branching morphogenesis is dependent on *Etv4* and *Etv5*. The insets in 1 and 3 show the pattern of UB tips on the surface of P0 wild type and double mutant kidneys. Reproduced with permission from Michos et al. (2010). **(B)** Gene expression domains of *Fgf10* and *Gdnf* and their receptors in the developing lung and kidney at E11.5. In the lung, *Fgf10* is expressed in the submesothelial mesenchyme in a spotty fashion opposed to growing buds. *Fgfr2b* is expressed in the lung epithelium. In the kidney, *Fgf10* and *Gdnf* are expressed in the metanephric mesenchyme. *Fgfr2* is expressed both in the mesenchyme and the epithelium, whereas *Ret* is restricted to the branch tips (ampulla). Expression domains are colour coded as indicated.

diffuses toward the epithelium to meet its receptor FGFR2b, which is expressed along the distal lung epithelium. Additionally, whole-mount *in situ* hybridisation of embryonic lungs has shown that *Fgf10* is expressed in spots "in front of" terminal end buds (Bellusci et al., 1997). Interestingly, both FGF10 and FGF7 bind FGFR2b, whereas only signalling via FGF10 results in receptor recycling and trafficking to the cell membrane, thereby increasing the amount of available FGFR2b (Francavilla et al., 2013). Besides the signalling function between mesenchymal and epithelial cells, a cell autonomous mode of function has been recently identified for FGF10 that is based on nuclear translocation within FGF10-producing cells (Mikolajczak et al., 2016).

During kidney development, *Fgf10* and *Gdnf* are expressed throughout the metanephric mesenchyme (MM) (Towers et al., 1998; Michos et al., 2010). *Ret* is expressed by tip cells that form the ampulla, a swelling of the terminal end buds of the UB epithelium. Cells that do not express or lose *Ret* expression are excluded from the ampulla (Shakya et al., 2005; Chi et al., 2009; Riccio et al., 2016). *Fgfr2* is expressed throughout the UB (Zhao et al., 2004; Sanna-Cherchi et al., 2013).

The expression patterns of ligands and receptors suggest that their spatial organisation plays an important role in guiding branching morphogenesis. However, studies in the lung have shown that uniform expression of *Fgf10* does not abolish branching and in the $Gdnf^{-/-}$; $Sprouty1^{-/-}$ mutants UB branching occurs albeit both *Fgf10* and *Fgfr2* being expressed uniformly in the MM and the UB, respectively (Michos et al., 2010; Volckaert et al., 2013).

EFFECT ON THE EPITHELIAL BRANCHING PATTERN

Comparison of the branched epithelial trees of different organs could aid in understanding how organs of different shape and size are formed. Advancements in imaging techniques and analysis software are providing the opportunity to quantitatively study the morphometric differences between organs and to study the effect of mutations and drugs. To date, branching morphogenesis has been studied *ex vivo* using organ culture techniques that permit imaging of branching events over time or by reconstructing slices of fixed and stained organs or more recently by directly imaging dissected and fixed organs in 3D at different developmental time points (Michos, 2012).

The branching pattern of the lung has been well characterised. During the early stages of development, lateral branching dominates. From around E13.0 on, planar bifurcations subside as the main mode of branching and finally, orthogonal bifurcations are employed to efficiently fill all available space (Metzger et al., 2008). The same study reports lung branching to be extremely stereotyped, with only minor differences between mice of the same genetic background. Other publications have challenged this view, showing that branching varies after an initial, stereotypic establishment of the first branches and suggest that the epithelium can react to regional growth of the mesenchyme to efficiently fill the available space (Blanc et al., 2012; Short et al., 2013).

Kidney branching mainly employs terminal bifurcations and, more rarely, terminal trifurcations and lateral branching (Watanabe and Costantini, 2004; Short et al., 2014). *In vivo*, kidney branching does not follow stereotypic branching regimes on the organ-level, however, sub-trees that encompass daughter branches of the whole tree established by E12.5 seem to develop in a highly stereotypic manner (Short et al., 2014; Sampogna et al., 2015).

Absence of FGF10 or GDNF results in lung agenesis and kidney agenesis or severe hypodysplasia, respectively. Here, we focus on how the branching pattern is modified in response to changes in ligand-receptor signalling. FGF10 hypomorphic lungs exhibit reduced epithelial branching, resulting in lung hypoplasia (Ramasamy et al., 2007). This qualitative comparison of the branching pattern leaves open the question of whether branching is only temporarily delayed, or whether the morphology of the branched tree is changed as well. Elevated *Fgf10* expression in the pulmonary epithelium causes increased epithelial cell proliferation and progenitor state arrest, which leads to hyperplasia of the epithelium with large, empty lumens and larger interlobular distance (Nyeng et al., 2008).

The branching pattern of the developing kidney is modulated by the interplay between FGF10/GDNF signalling and negative regulation via SPRY1. Specific deletion of *Fgfr2* from the UB results in fewer UB tips with longer, thinner trunk segments (Zhao et al., 2004; Sims-Lucas et al., 2009). The absence of *Spry1* results in increased branching of the UB and the induction of supernumerary UBs, whereas $Gdnf^{+/-}$ kidneys show reduced branching (Basson et al., 2006). $Gdnf^{-/-}$;$Spry1^{-/-}$ and $Ret^{-/-}$;$Spry1^{-/-}$ kidneys show abnormal branching with irregular UB tip size, shape and branch angle (Michos et al., 2010).

Interestingly, gain-of-function mutations in *Fgfr2* cause major secondary branching defects in both lung and kidney that can be partly rescued by the genetic knockdown of Fgf10 expression (Hajihosseini et al., 2001, 2009).

IMPACT OF THE MESENCHYME ON BRANCHING

Mesenchyme-free cultures of isolated lung buds and UBs have shown the ability of the epithelium to branch in the presence of the correct growth factors, which *in vivo* are expressed in the mesenchyme, showing an intrinsic capability of the epithelium to branch that does not depend on cell contacts of epithelium and mesenchyme (Nogawa and Ito, 1995; Bellusci et al., 1997; Qiao et al., 1999). These branched epithelial structures, however, lack the directionality and shape of the branched trees that result from branching morphogenesis of intact organs *in vivo* and in organ culture experiments, suggesting an important role of the mesenchyme in shaping the growing organ and in specifying the identity of epithelial cells.

As exemplified by FGF10 and GDNF in the context of lung and kidney, the growth factors expressed by the mesenchyme differ in their composition and spatiotemporal expression, suggesting that ligand-receptor signalling modulates the branching pattern. But differences in mechanical properties of the tissues and the extracellular matrix (ECM) could also have an impact. Tissue recombination experiments have been used to study epithelial-mesenchymal interactions and how the mesenchyme influences branching morphogenesis and cell fate specification of a branching epithelium (Grobstein, 1953, 1955; Saxen et al., 1976; Kispert et al., 1996; Iwai et al., 1998; Shannon et al., 1998; Ohtsuka et al., 2001; Lin et al., 2003).

Recombination of UB epithelium with lung mesenchyme at E11.5 results in a branching pattern more similar to that of an early lung (Lin et al., 2001). The lung mesenchyme also induces expression of surfactant protein C and changes the collagen pattern of the ECM to that of an embryonic lung, however, the epithelium continues to express UB-specific genes such as *Wnt11, Ret* and *Pax-2* (Kispert et al., 1996; Sainio et al., 1997; Lin et al., 2001).

MODELLING BRANCHING EVENTS AS STOCHASTIC PROCESSES

There is a general distinction between approaches that model branching morphogenesis as a deterministic stereotypic programme of genetically encoded events and approaches that describe branching morphogenesis as a stochastic process based on generic rules (Miura, 2008; Wang et al., 2017).

Recently proposed stochastic models for kidney branching morphogenesis are based on rules regarding the ratio between epithelial growth speed and cell mobility (Hirashima et al., 2009a, 2017), the ratio between ureteric tip and mesenchymal tip cells (Zubkov et al., 2015), locally operative mechanism like inter tip-suppression (Lefevre et al., 2017), or a growth-factor dependent growth switch (Lambert et al., 2018). Although the models may explain why the structure of a branched tree evolves during development, these models are basically not addressing the underlying molecular regulatory processes of branching morphogenesis that would answer how the branching pattern forms.

Moreover, Hannezo et al. (2017) presented 'A unifying theory of branching morphogenesis' describing kidney branching as a self-organised process that is based on a simple set of statistical rules, including stochastic tip branching, random exploration of space and tip termination in high-density regions. However, a recent study is strongly challenging the stochastic nature of kidney branching morphogenesis and in particular the hypothesis that nephron differentiation leads to termination of tip branching (Short et al., 2018). Live imaging of cultured embryonic kidneys did not show any evidence for the influence of nephron formation on ureteric branching. Finally, Short et al. (2018) propose that kidney morphogenesis rather resembles stereotypic lung branching than stochastic mammary gland branching.

SIGNALLING MODELS BASED ON DIFFUSION-LIMITED GROWTH AND DISTANCE-BASED PATTERNING

The signalling pathways controlling branching morphogenesis have been extensively studied and appear to play a key role in the regulation and formation of branched epithelial structures. Since the key signalling factors in lung and kidney branching morphogenesis are diffusible proteins and interact with their corresponding receptors, several deterministic reaction-diffusion models have been proposed to describe the branching behaviour. For lung branching morphogenesis, most of these models are based on diffusion-limited growth (Miura and Shiota, 2002; Hartmann and Miura, 2006, 2007), gradient-sensing mechanisms (Clément et al., 2012a,b), or distance-based patterning (Hirashima et al., 2009b), and have been already reviewed in detail (Miura, 2008; Iber and Menshykau, 2013). By using idealised 2D shapes of lung buds, these models describe the diffusion of FGF10 from the sub-mesothelial mesenchyme to the epithelium and propose a relationship between the distance of these two tissue layers and the branching modes. While a large distance leads to high FGF10 concentration at the tip, a thin mesenchyme will lead to a split FGF10 localization at the sides of the tip. Assuming that FGF10 triggers outgrowth, these FGF10 concentration profiles will result in bud elongation or bifurcation, respectively. The main limitation of these models is that they are not in agreement with the experimental observations that branching is still occurring under homogeneous *Fgf10* expression or in the absence of mesenchyme with FGF10 added to the medium (Nogawa and Ito, 1995; Volckaert et al., 2013).

GEOMETRY EFFECT AND IMAGE-BASED MODELLING

Information about the developmental process of morphogenesis is naturally image-based and branching patterns emerge on growing domains. Therefore, modelling morphogenesis is implicitly related to deforming shapes and domains and

the question arises whether the geometry itself has an effect on patterning. It was computationally shown that the expression of ligands and receptors in different tissue layers gives rise to a diffusion-driven geometry effect (Nelson et al., 2006; Gleghorn et al., 2012). While this domain-specific ligand expression is able to create split branching patterns on static domains, it does not reproduce the actual outgrowth of buds on a growing domain because it is unstable under deforming curvature conditions (Menshykau et al., 2014).

George and Lubkin examined the effect of geometry on branch mode selection during lung development. Although the model identifies proximity and aspect ratios of the internal and external tissue surfaces as important geometric factors to determine branching modes like planar and orthogonal bifurcation, it is not able to explain lateral branching (George and Lubkin, 2018).

Considering the geometry effect, it is essential to perform model simulations on physiological growing domains in order to achieve biologically relevant predictions (Iber et al., 2015). The validity of most models was limited by the lack of high-resolution biological data both on the cellular and also on the whole-organ scale. Due to advancing imaging techniques, image-based modelling approaches have proven to be a valuable method for investigating the control of branching events with respect to organ-specific properties.

Consequently, a pipeline has been established that allows to test models on physiological geometries from cultured embryonic kidney and lung explants (Adivarahan et al., 2013; Menshykau and Iber, 2013; Iber et al., 2015, 2016; Gómez et al., 2017). The obtained 2D time-lapse movies are segmented to obtain the epithelial boundary for each time frame and to calculate the growth fields between consecutive time frames. In order to solve models on these geometries, the extracted domains need to be meshed. The simulated signalling fields can then be compared to the calculated growth fields. Similarly, this pipeline has been applied to 3D reconstructions of lung explants of different embryonic stages (Menshykau et al., 2014).

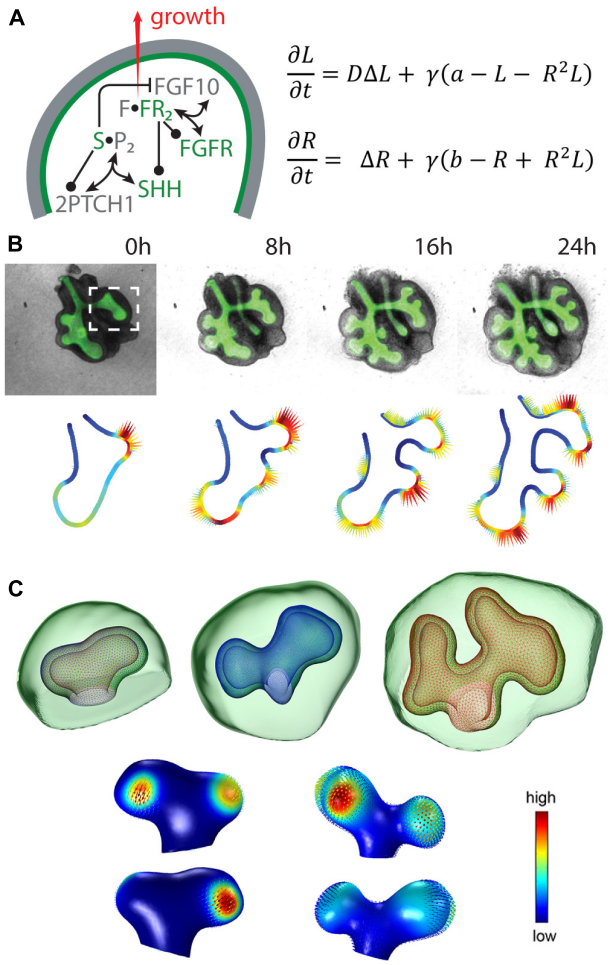

FIGURE 2 | The ligand-receptor based Turing model reproduces lung bud outgrowth in 2D and 3D. (**A**, left) Signalling network in lung branching morphogenesis includes the interactions between FGF10, SHH and the corresponding receptors in the epithelium (green) and the mesenchyme (grey). Reproduced with permission from Iber and Menshykau (2013). (**A**, right) The diffusion-reaction equations for ligand (L) and receptor (R) consider the diffusion coefficient ratio D, a scaling factor γ, production rates a and b, linear decay as well as cooperative binding. (**B**, top) 2D time-lapse data of an embryonic mouse lung showing the EGFP-expressing epithelium (green) and the mesenchyme (grey). Reproduced with permission from Menshykau et al. (2014). (**C**, top) 3D sequence of a mouse lung bud with epithelium (wireframe) and mesenchyme (green). Reproduced with permission from Menshykau et al. (2014). (**B,C**, bottom) The predicted signalling strength (solid colour) matches the experimentally observed growth fields (vector fields) in 2D and 3D, respectively. Reproduced with permission from Menshykau et al. (2014).

LIGAND-RECEPTOR-BASED TURING MECHANISM

The Turing mechanism has been suggested for many biological pattern phenomena, including morphogenesis (Miura and Maini, 2004; Kondo and Miura, 2010; Guo et al., 2014a,b; Xu et al., 2017), and is based on a diffusion-driven instability which leads to the self-organised emergence of many different kind of patterns (Turing, 1952; Gierer and Meinhardt, 1972). The underlying network structure includes at least two factors with substantially different diffusion rates that interact in a cooperative way leading to the upregulation of one of the factors. These requirements are typically true for many ligand-receptor systems.

For lung branching morphogenesis, a reaction-diffusion model has been proposed that includes FGF10 and sonic hedgehog (SHH) as key signalling factors (**Figure 2A**) (Celliere et al., 2012; Menshykau et al., 2012). In order to examine whether the Turing mechanism can be extended to other branched organs, the ligand-receptor Turing model has been applied to kidney branching morphogenesis by considering the regulatory interactions between GDNF and WNT11 (Adivarahan et al., 2013; Menshykau and Iber, 2013; Menshykau et al., unpublished).

Solving the model on static idealised 2D and 3D domains shows that the described interactions give rise to Turing

patterns that correspond to FGF10 or GDNF signalling patterns, respectively, representing the branching modes of lateral branching, bifurcations and trifurcations (Menshykau et al., 2012, 2014; Menshykau and Iber, 2013). As reported for embryonic kidney development, in this model bifurcations and trifurcations dominate over bud elongation and lateral branching, while trifurcations do not appear for the lung. Moreover, the model reproduces not only wild type but also mutant data (Menshykau et al., 2012).

Taking into account the dynamical processes during branching morphogenesis, 2D time-lapse movies of cultured lung and kidney explants and a 3D sequence of lung buds have been used to test alternative models and showed that only the ligand-receptor Turing model reproduces the areas of outgrowth for these physiological geometries (**Figures 2B,C**) (Menshykau et al., 2014; Menshykau et al., unpublished). Solving the model on 3D growing domains confirmed that the predicted signalling patterns support actual outgrowth (Menshykau et al., 2014).

The emerging Turing pattern is typically very dependent on the initial conditions. Combining tissue-specific expression of the considered signalling factors with the ligand-receptor based Turing model allowed for robust outgrowth behaviour despite noisy initial conditions due to the impact of the geometry (Menshykau et al., 2014; Menshykau et al., unpublished).

Therefore, the ligand-receptor based Turing mechanism potentially constitutes a common mechanism for regulating branching morphogenesis in both lungs and kidneys. However, Turing patterns only explain the branch point selection but not the regulation of branch lengths, widths or angles. In the lung, the length and width of branches seems to be controlled by a bias in cell division (Tang et al., 2011). Moreover, the Turing mechanism is highly sensitive to the included interactions and choice of parameter values and can only be applied in a qualitative but not in a quantitative manner (Combes, 2015).

CONCLUDING REMARKS

In this review, we focused on the signalling interactions during lung and kidney morphogenesis and discussed several modelling approaches. Based on the robustness and flexible applicability to different branched organs, we conclude that the ligand-receptor based Turing mechanism represents a potential candidate for a general regulatory mechanism for branching morphogenesis. However, several studies exist confirming that mechanical stresses influence branching morphogenesis (Lubkin and Murray, 1995; Lubkin, 2008; Unbekandt et al., 2008; Wan et al., 2008; Gjorevski and Nelson, 2010, 2012; Nelson and Gleghorn, 2012; Kim et al., 2013; Varner and Nelson, 2014). Since there is a close interaction between signalling factors and mechanical tissue properties, modelling approaches should also take into account the mechanics behind branching morphogenesis (Tanaka, 2015; Peters and Iber, 2017).

Although mathematical models have advanced our understanding of branching morphogenesis, none have yet proven to fulfil all criteria to explain the branching behaviour on a holistic level. This may be attributed to a lack of biological methods to obtain quantitative information on relevant modelling parameters and computational limitations regarding analysis of large imaging data. The latter is also relevant for solving complex mathematical models, which requires tremendous computational resources. However, combining the constant improvements in all domains will improve the conclusions that can be drawn from modelling approaches. We are hopeful that data based modelling will continue to improve our understanding of branching morphogenesis.

AUTHOR CONTRIBUTIONS

All authors listed have made a substantial, direct and intellectual contribution to the work, and approved it for publication.

REFERENCES

Adivarahan, S., Menshykau, D., Michos, O., and Iber, D. (2013). "Dynamic image-based modelling of kidney branching morphogenesis," in *Computational Methods in Systems Biology*, eds A. Gupta and T. A. Henzinger (Berlin: Springer), 106–119.

Basson, M. A., Watson-Johnson, J., Shakya, R., Akbulut, S., Hyink, D., Costantini, F. D., et al. (2006). Branching morphogenesis of the ureteric epithelium during kidney development is coordinated by the opposing functions of GDNF and Sprouty1. *Dev. Biol.* 299, 466–477. doi: 10.1016/j.ydbio.2006.08.051

Bellusci, S., Grindley, J., Emoto, H., Itoh, N., and Hogan, B. L. (1997). Fibroblast growth factor 10 (FGF10) and branching morphogenesis in the embryonic mouse lung. *Development* 124, 4867–4878.

Blanc, P., Coste, K., Pouchin, P., Azaïs, J.-M., Blanchon, L., Gallot, D., et al. (2012). A role for mesenchyme dynamics in mouse lung branching morphogenesis. *PLoS One* 7:e41643. doi: 10.1371/journal.pone.0041643

Böttcher, R. T., and Niehrs, C. (2005). Fibroblast growth factor signaling during early vertebrate development. *Endocr. Rev.* 26, 63–77. doi: 10.1210/er.2003-0040

Cacalano, G., Fariñas, I., Wang, L.-C., Hagler, K., Forgie, A., Moore, M., et al. (1998). GFRα1 is an essential receptor component for GDNF in the developing nervous system and kidney. *Neuron* 21, 53–62. doi: 10.1016/S0896-6273(00)80514-0

Celliere, G., Menshykau, D., and Iber, D. (2012). Simulations demonstrate a simple network to be sufficient to control branch point selection, smooth muscle and vasculature formation during lung branching morphogenesis. *Biol. Open* 1, 775–788. doi: 10.1242/bio.20121339

Chi, X., Michos, O., Shakya, R., Riccio, P., Enomoto, H., Licht, J. D., et al. (2009). Ret-dependent cell rearrangements in the wolffian duct epithelium initiate ureteric bud morphogenesis. *Dev. Cell* 17, 199–209. doi: 10.1016/j.devcel.2009.07.013

Clément, R., Blanc, P., Mauroy, B., Sapin, V., and Douady, S. (2012a). Shape self-regulation in early lung morphogenesis. *PLoS One* 7:e36925. doi: 10.1371/journal.pone.0036925

Clément, R., Douady, S., and Mauroy, B. (2012b). Branching geometry induced by lung self-regulated growth. *Phys. Biol.* 9:066006. doi: 10.1088/1478-3975/9/6/066006

Combes, A. N. (2015). Towards a quantitative model of kidney morphogenesis: kidney morphogenesis. *Nephrology* 20, 312–314. doi: 10.1111/nep.12407

El Agha, E., Herold, S., Alam, D. A., Quantius, J., MacKenzie, B., Carraro, G., et al. (2014). Fgf10-positive cells represent a progenitor cell population during lung development and postnatally. *Development* 141, 296–306. doi: 10.1242/dev.099747

El Agha, E., Kheirollahi, V., Moiseenko, A., Seeger, W., and Bellusci, S. (2017). Ex vivo analysis of the contribution of FGF10 + cells to airway smooth muscle cell formation during early lung development: FGF10 + cells during early lung development. *Dev. Dyn.* 246, 531–538. doi: 10.1002/dvdy.24504

Francavilla, C., Rigbolt, K. T. G., Emdal, K. B., Carraro, G., Vernet, E., Bekker-Jensen, D. B., et al. (2013). Functional proteomics defines the molecular switch underlying FGF receptor trafficking and cellular outputs. *Mol. Cell* 51, 707–722. doi: 10.1016/j.molcel.2013.08.002

George, U. Z., and Lubkin, S. R. (2018). Tissue geometry may govern lung branching mode selection. *J. Theor. Biol.* 442, 22–30. doi: 10.1016/j.jtbi.2017.12.031

Gierer, A., and Meinhardt, H. (1972). A theory of biological pattern formation. *Kybernetik* 12, 30–39. doi: 10.1007/BF00289234

Gjorevski, N., and Nelson, C. M. (2010). Endogenous patterns of mechanical stress are required for branching morphogenesis. *Integr. Biol.* 2, 424–434. doi: 10.1039/c0ib00040j

Gjorevski, N., and Nelson, C. M. (2012). Mapping of mechanical strains and stresses around quiescent engineered three-dimensional epithelial tissues. *Biophys. J.* 103, 152–162. doi: 10.1016/j.bpj.2012.05.048

Gleghorn, J. P., Kwak, J., Pavlovich, A. L., and Nelson, C. M. (2012). Inhibitory morphogens and monopodial branching of the embryonic chicken lung. *Dev. Dyn.* 241, 852–862. doi: 10.1002/dvdy.23771

Gómez, H. F., Georgieva, L., Michos, O., and Iber, D. (2017). "Image-based *in silico* models of organogenesis," in *Systems Biology*, eds J. Nielsen and S. Hohmann (Weinheim: Wiley-VCH), 319–340.

Grobstein, C. (1953). Inductive epithelio-mesenchymal interaction in cultured organ rudiments of the mouse. *Science* 118, 52–55. doi: 10.1126/science.118.3054.52

Grobstein, C. (1955). Inductive interaction in the development of the mouse metanephros. *J. Exp. Zool.* 130, 319–339. doi: 10.1007/s11626-009-9254-x

Guo, Y., Chen, T.-H., Zeng, X., Warburton, D., Boström, K. I., Ho, C.-M., et al. (2014a). Branching patterns emerge in a mathematical model of the dynamics of lung development: branching dynamics in a model of lung development. *J. Physiol.* 592, 313–324. doi: 10.1113/jphysiol.2013.261099

Guo, Y., Sun, M., Garfinkel, A., and Zhao, X. (2014b). Mechanisms of side branching and tip splitting in a model of branching morphogenesis. *PLoS One* 9:e102718. doi: 10.1371/journal.pone.0102718

Hajihosseini, M. K., Duarte, R., Pegrum, J., Donjacour, A., Lana-Elola, E., Rice, D. P., et al. (2009). Evidence that Fgf10 contributes to the skeletal and visceral defects of an apert syndrome mouse model. *Dev. Dyn.* 238, 376–385. doi: 10.1002/dvdy.21648

Hajihosseini, M. K., Wilson, S., De Moerlooze, L., and Dickson, C. (2001). A splicing switch and gain-of-function mutation in FgfR2-IIIc hemizygotes causes Apert/Pfeiffer-syndrome-like phenotypes. *Proc. Natl. Acad. Sci. U.S.A.* 98, 3855–3860. doi: 10.1073/pnas.071586898

Hannezo, E., Scheele, C. L. G. J., Moad, M., Drogo, N., Heer, R., Sampogna, R. V., et al. (2017). A unifying theory of branching morphogenesis. *Cell* 171, 242–255.e7. doi: 10.1016/j.cell.2017.08.026

Hartmann, D., and Miura, T. (2006). Modelling in vitro lung branching morphogenesis during development. *J. Theor. Biol.* 242, 862–872. doi: 10.1016/j.jtbi.2006.05.009

Hartmann, D., and Miura, T. (2007). Mathematical analysis of a free-boundary model for lung branching morphogenesis. *Math. Med. Biol.* 24, 209–224. doi: 10.1093/imammb/dql029

Hirashima, T., Iwasa, Y., and Morishita, Y. (2009a). Dynamic modeling of branching morphogenesis of ureteric bud in early kidney development. *J. Theor. Biol.* 259, 58–66. doi: 10.1016/j.jtbi.2009.03.017

Hirashima, T., Iwasa, Y., and Morishita, Y. (2009b). Mechanisms for split localization of *Fgf10* expression in early lung development. *Dev. Dyn.* 238, 2813–2822. doi: 10.1002/dvdy.22108

Hirashima, T., Rens, E. G., and Merks, R. M. H. (2017). Cellular Potts modeling of complex multicellular behaviors in tissue morphogenesis. *Dev. Growth Differ.* 59, 329–339. doi: 10.1111/dgd.12358

Iber, D., Karimaddini, Z., and Ünal, E. (2016). Image-based modelling of organogenesis. *Brief. Bioinform.* 17, 616–627. doi: 10.1093/bib/bbv093

Iber, D., and Menshykau, D. (2013). The control of branching morphogenesis. *Open Biol.* 3, 130088–130088. doi: 10.1098/rsob.130088

Iber, D., Tanaka, S., Fried, P., Germann, P., and Menshykau, D. (2015). "Simulating tissue morphogenesis and signaling," in *Tissue Morphogenesis*, ed. C. M. Nelson (New York, NY: Springer), 323–338. doi: 10.1007/978-1-4939-1164-6-21

Iwai, K., Hieda, Y., and Nakanishi, Y. (1998). Effects of mesenchyme on epithelial tissue architecture revealed by tissue recombination experiments between the submandibular gland and lung of embryonic mice. *Dev. Growth Differ.* 40, 327–334. doi: 10.1046/j.1440-169X.1998.t01-1-00008.x

Kim, H. Y., Varner, V. D., and Nelson, C. M. (2013). Apical constriction initiates new bud formation during monopodial branching of the embryonic chicken lung. *Development* 140, 3146–3155. doi: 10.1242/dev.093682

Kispert, A., Vainio, S., Shen, L., Rowitch, D. H., and McMahon, A. P. (1996). Proteoglycans are required for maintenance of WNT-11 expression in the ureter tips. *Development* 122, 3627–3637.

Kondo, S., and Miura, T. (2010). Reaction-diffusion model as a framework for understanding biological pattern formation. *Science* 329, 1616–1620. doi: 10.1126/science.1179047

Lambert, B., MacLean, A. L., Fletcher, A. G., Combes, A. N., Little, M. H., and Byrne, H. M. (2018). Bayesian inference of agent-based models: a tool for studying kidney branching morphogenesis. *J. Math. Biol.* 76, 1673–1697. doi: 10.1007/s00285-018-1208-z

Lefevre, J. G., Short, K. M., Lamberton, T. O., Michos, O., Graf, D., Smyth, I. M., et al. (2017). Branching morphogenesis in the developing kidney is governed by rules that pattern the ureteric tree. *Development* 144, 4377–4385. doi: 10.1242/dev.153874

Lin, Y., Zhang, S., Rehn, M., Itäranta, P., Tuukkanen, J., Heljäsvaara, R., et al. (2001). Induced repatterning of type XVIII collagen expression in ureter bud from kidney to lung type: association with sonic hedgehog and ectopic surfactant protein C. *Development* 128, 1573–1585.

Lin, Y., Zhang, S., Tuukkanen, J., Peltoketo, H., Pihlajaniemi, T., and Vainio, S. (2003). Patterning parameters associated with the branching of the ureteric bud regulated by epithelial-mesenchymal interactions. *Int. J. Dev. Biol.* 47, 3–13.

Lu, B. C., Cebrian, C., Chi, X., Kuure, S., Kuo, R., Bates, C. M., et al. (2009). Etv4 and Etv5 are required downstream of GDNF and Ret for kidney branching morphogenesis. *Nat. Genet.* 41, 1295–1302. doi: 10.1038/ng.476

Lü, J., Izvolsky, K. I., Qian, J., and Cardoso, W. V. (2005). Identification of FGF10 targets in the embryonic lung epithelium during bud morphogenesis. *J. Biol. Chem.* 280, 4834–4841. doi: 10.1074/jbc.M410714200

Lubkin, S. R. (2008). Branched organs: mechanics of morphogenesis by multiple mechanisms. *Curr. Top. Dev. Biol.* 81, 249–268. doi: 10.1016/S0070-2153(07)81008-8

Lubkin, S. R., and Murray, J. D. (1995). A mechanism for early branching in lung morphogenesis. *J. Math. Biol.* 34, 77–94. doi: 10.1007/BF00180137

Menshykau, D., Blanc, P., Unal, E., Sapin, V., and Iber, D. (2014). An interplay of geometry and signaling enables robust lung branching morphogenesis. *Development* 141, 4526–4536. doi: 10.1242/dev.116202

Menshykau, D., and Iber, D. (2013). Kidney branching morphogenesis under the control of a ligand–receptor-based Turing mechanism. *Phys. Biol.* 10:046003. doi: 10.1088/1478-3975/10/4/046003

Menshykau, D., Kraemer, C., and Iber, D. (2012). Branch Mode selection during early lung development. *PLoS Comput. Biol.* 8:e1002377. doi: 10.1371/journal.pcbi.1002377

Metzger, R. J., Klein, O. D., Martin, G. R., and Krasnow, M. A. (2008). The branching programme of mouse lung development. *Nature* 453, 745–750. doi: 10.1038/nature07005

Michos, O. (2012). *Kidney Development*. Totowa, NJ: Humana Press. doi: 10.1007/978-1-61779-851-1

Michos, O., Cebrian, C., Hyink, D., Grieshammer, U., Williams, L., D'Agati, V., et al. (2010). Kidney development in the absence of Gdnf and Spry1 requires Fgf10. *PLoS Genet.* 6:e1000809. doi: 10.1371/journal.pgen.1000809

Mikolajczak, M., Goodman, T., and Hajihosseini, M. K. (2016). Interrogation of a lacrimo-auriculo-dento-digital syndrome protein reveals novel modes of fibroblast growth factor 10 (FGF10) function. *Biochem. J.* 473, 4593–4607. doi: 10.1042/BCJ20160441

Min, H., Danilenko, D. M., Scully, S. A., Bolon, B., Ring, B. D., Tarpley, J. E., et al. (1998). Fgf-10 is required for both limb and lung development and exhibits striking functional similarity to *Drosophila branchless*. *Genes Dev.* 12, 3156–3161. doi: 10.1101/gad.12.20.3156

Miura, T. (2008). Modeling lung branching morphogenesis. *Curr. Top. Dev. Biol.* 81, 291–310. doi: 10.1016/S0070-2153(07)81010-6

Miura, T., and Maini, P. K. (2004). Periodic pattern formation in reaction-diffusion systems: an introduction for numerical simulation. *Anat. Sci. Int.* 79, 112–123. doi: 10.1111/j.1447-073x.2004.00079.x

Miura, T., and Shiota, K. (2002). Depletion of FGF acts as a lateral inhibitory factor in lung branching morphogenesis in vitro. *Mech. Dev.* 116, 29–38. doi: 10.1016/S0925-4773(02)00132-6

Moore, M. W., Klein, R. D., Fariñas, I., Sauer, H., Armanini, M., Phillips, H., et al. (1996). Renal and neuronal abnormalities in mice lacking GDNF. *Nature* 382, 76–79. doi: 10.1038/382076a0

Moura, R. S., Coutinho-Borges, J. P., Pacheco, A. P., daMota, P. O., and Correia-Pinto, J. (2011). FGF signaling pathway in the developing chick lung: expression and inhibition studies. *PLoS One* 6:e17660. doi: 10.1371/journal.pone.0017660

Nelson, C. M., and Gleghorn, J. P. (2012). Sculpting organs: mechanical regulation of tissue development. *Annu. Rev. Biomed. Eng.* 14, 129–154. doi: 10.1146/annurev-bioeng-071811-150043

Nelson, C. M., VanDuijn, M. M., Inman, J. L., Fletcher, D. A., and Bissell, M. J. (2006). Tissue geometry determines sites of mammary branching morphogenesis in organotypic cultures. *Science* 314, 298–300. doi: 10.1126/science.1131000

Nogawa, H., and Ito, T. (1995). Branching morphogenesis of embryonic mouse lung epithelium in mesenchyme-free culture. *Development* 121, 1015–1022.

Nyeng, P., Norgaard, G. A., Kobberup, S., and Jensen, J. (2008). FGF10 maintains distal lung bud epithelium and excessive signaling leads to progenitor state arrest, distalization, and goblet cell metaplasia. *BMC Dev. Biol.* 8:2. doi: 10.1186/1471-213X-8-2

Ohtsuka, N., Urase, K., Momoi, T., and Nogawa, H. (2001). Induction of bud formation of embryonic mouse tracheal epithelium by fibroblast growth factor plus transferrin in mesenchyme-free culture. *Dev. Dyn.* 222, 263–272. doi: 10.1002/dvdy.1206

Ohuchi, H., Hori, Y., Yamasaki, M., Harada, H., Sekine, K., Kato, S., et al. (2000). FGF10 acts as a major ligand for FGF receptor 2 IIIb in mouse multi-organ development. *Biochem. Biophys. Res. Commun.* 277, 643–649. doi: 10.1006/bbrc.2000.3721

Perrimon, N., Pitsouli, C., and Shilo, B.-Z. (2012). Signaling mechanisms controlling cell fate and embryonic patterning. *Cold Spring Harb. Perspect. Biol.* 4:a005975. doi: 10.1101/cshperspect.a005975

Peters, M. D., and Iber, D. (2017). Simulating organogenesis in COMSOL: tissue mechanics. *arXiv* [Preprint]. arXiv:1710.00553

Peters, M. D., Wittwer, L. D., Stopka, A., Barac, D., Lang, C., and Iber, D. (2018). Simulation of morphogen and tissue dynamics. *arXiv* [Preprint]. arXiv:1806.04138

Pichel, J. G., Shen, L., Sheng, H. Z., Granholm, A.-C., Drago, J., Grinberg, A., et al. (1996). Defects in enteric innervation and kidney development in mice lacking GDNF. *Nature* 382, 73–76. doi: 10.1038/382073a0

Qiao, J., Sakurai, H., and Nigam, S. K. (1999). Branching morphogenesis independent of mesenchymal-epithelial contact in the developing kidney. *Proc. Natl. Acad. Sci. U.S.A.* 96, 7330–7335. doi: 10.1073/pnas.96.13.7330

Ramasamy, S. K., Mailleux, A. A., Gupte, V. V., Mata, F., Sala, F. G., Veltmaat, J. M., et al. (2007). Fgf10 dosage is critical for the amplification of epithelial cell progenitors and for the formation of multiple mesenchymal lineages during lung development. *Dev. Biol.* 307, 237–247. doi: 10.1016/j.ydbio.2007.04.033

Riccio, P., Cebrian, C., Zong, H., Hippenmeyer, S., and Costantini, F. (2016). Ret and Etv4 promote directed movements of progenitor cells during renal branching morphogenesis. *PLoS Biol.* 14:e1002382. doi: 10.1371/journal.pbio.1002382

Sainio, K., Suvanto, P., Davies, J., Wartiovaara, J., Wartiovaara, K., Saarma, M., et al. (1997). Glial-cell-line-derived neurotrophic factor is required for bud initiation from ureteric epithelium. *Development* 124, 4077–4087.

Sakiyama, J.-I. (2003). Tbx4-Fgf10 system controls lung bud formation during chicken embryonic development. *Development* 130, 1225–1234. doi: 10.1242/dev.00345

Sampogna, R. V., Schneider, L., and Al-Awqati, Q. (2015). Developmental programming of branching morphogenesis in the kidney. *J. Am. Soc. Nephrol.* 26, 2414–2422. doi: 10.1681/ASN.2014090886

Sánchez, M. P., Silos-Santiago, I., Frisén, J., He, B., Lira, S. A., and Barbacid, M. (1996). Renal agenesis and the absence of enteric neurons in mice lacking GDNF. *Nature* 382, 70–73. doi: 10.1038/382070a0

Sanna-Cherchi, S., Sampogna, R. V., Papeta, N., Burgess, K. E., Nees, S. N., Perry, B. J., et al. (2013). Mutations in *DSTYK* and dominant urinary tract malformations. *N. Engl. J. Med.* 369, 621–629. doi: 10.1056/NEJMoa1214479

Saxen, L., Lehtonen, E., Karkinen-JääSkeläInen, M., Nordling, S., and Wartiovaara, J. (1976). Are morphogenetic tissue interactions mediated by transmissible signal substances or through cell contacts? *Nature* 259, 662–663. doi: 10.1038/259662a0

Schuchardt, A., D'Agati, V., Larsson-Blomberg, L., Costantini, F., and Pachnis, V. (1994). Defects in the kidney and enteric nervous system of mice lacking the tyrosine kinase receptor Ret. *Nature* 367, 380–383. doi: 10.1038/367380a0

Schuchardt, A., D'Agati, V., Pachnis, V., and Costantini, F. (1996). Renal agenesis and hypodysplasia in ret-k- mutant mice result from defects in ureteric bud development. *Development* 122, 1919–1929.

Shakya, R., Watanabe, T., and Costantini, F. (2005). The role of GDNF/ret signaling in ureteric bud cell fate and branching morphogenesis. *Dev. Cell* 8, 65–74. doi: 10.1016/j.devcel.2004.11.008

Shannon, J. M., Nielsen, L. D., Gebb, S. A., and Randell, S. H. (1998). Mesenchyme specifies epithelial differentiation in reciprocal recombinants of embryonic lung and trachea. *Dev. Dyn.* 212, 482–494. doi: 10.1002/(SICI)1097-0177(199808)212:4<482::AID-AJA2>3.0.CO;2-D

Shifley, E. T., Kenny, A. P., Rankin, S. A., and Zorn, A. M. (2012). Prolonged FGF signaling is necessary for lung and liver induction in *Xenopus*. *BMC Dev. Biol.* 12:27. doi: 10.1186/1471-213X-12-27

Short, K., Hodson, M., and Smyth, I. (2013). Spatial mapping and quantification of developmental branching morphogenesis. *Development* 140, 471–478. doi: 10.1242/dev.088500

Short, K. M., Combes, A., Lisnyak, V., Lefevre, J., Jones, L., Little, M. H., et al. (2018). Branching morphogenesis in the developing kidney is not impacted by nephron formation or integration. *eLife* 7:e38992. doi: 10.7554/eLife.38992

Short, K. M., Combes, A. N., Lefevre, J., Ju, A. L., Georgas, K. M., Lamberton, T., et al. (2014). Global quantification of tissue dynamics in the developing mouse kidney. *Dev. Cell* 29, 188–202. doi: 10.1016/j.devcel.2014.02.017

Sims-Lucas, S., Argyropoulos, C., Kish, K., McHugh, K., Bertram, J. F., Quigley, R., et al. (2009). Three-dimensional imaging reveals ureteric and mesenchymal defects in Fgfr2-mutant kidneys. *J. Am. Soc. Nephrol.* 20, 2525–2533. doi: 10.1681/ASN.2009050532

Tanaka, S. (2015). Simulation frameworks for morphogenetic problems. *Computation* 3, 197–221. doi: 10.3390/computation3020197

Tang, N., Marshall, W. F., McMahon, M., Metzger, R. J., and Martin, G. R. (2011). Control of mitotic spindle angle by the RAS-regulated ERK1/2 pathway determines lung tube shape. *Science* 333, 342–345. doi: 10.1126/science.1204831

Towers, P. R., Woolf, A. S., and Hardman, P. (1998). Glial cell line-derived neurotrophic factor stimulates ureteric bud outgrowth and enhances survival of ureteric bud cells in vitro. *Exp. Nephrol.* 6, 337–351. doi: 10.1159/000020541

Turing, A. M. (1952). The chemical basis of morphogenesis. *Philos. Transa. R. Soc. B Biol. Sci.* 237, 37–72. doi: 10.1098/rstb.1952.0012

Unbekandt, M., del Moral, P.-M., Sala, F. G., Bellusci, S., Warburton, D., and Fleury, V. (2008). Tracheal occlusion increases the rate of epithelial branching of embryonic mouse lung via the FGF10-FGFR2b-Sprouty2 pathway. *Mech. Dev.* 125, 314–324. doi: 10.1016/j.mod.2007.10.013

Varner, V. D., and Nelson, C. M. (2014). Cellular and physical mechanisms of branching morphogenesis. *Development* 141, 2750–2759. doi: 10.1242/dev.104794

Volckaert, T., Campbell, A., Dill, E., Li, C., Minoo, P., and De Langhe, S. (2013). Localized Fgf10 expression is not required for lung branching morphogenesis but prevents differentiation of epithelial progenitors. *Development* 140, 3731–3742. doi: 10.1242/dev.096560

Wan, X., Li, Z., and Lubkin, S. R. (2008). Mechanics of mesenchymal contribution to clefting force in branching morphogenesis. *Biomech. Model. Mechanobiol.* 7, 417–426. doi: 10.1007/s10237-007-0105-y

Wang, S., Sekiguchi, R., Daley, W. P., and Yamada, K. M. (2017). Patterned cell and matrix dynamics in branching morphogenesis. *J. Cell Biol.* 216, 559–570. doi: 10.1083/jcb.201610048

Watanabe, T., and Costantini, F. (2004). Real-time analysis of ureteric bud branching morphogenesis in vitro. *Dev. Biol.* 271, 98–108. doi: 10.1016/j.ydbio.2004.03.025

Xu, H., Sun, M., and Zhao, X. (2017). Turing mechanism underlying a branching model for lung morphogenesis. *PLoS One* 12:e0174946. doi: 10.1371/journal.pone.0174946

Zhao, H., Kegg, H., Grady, S., Truong, H.-T., Robinson, M. L., Baum, M., et al. (2004). Role of fibroblast growth factor receptors 1 and 2 in the ureteric bud. *Dev. Biol.* 276, 403–415. doi: 10.1016/j.ydbio.2004.09.002

Zubkov, V. S., Combes, A. N., Short, K. M., Lefevre, J., Hamilton, N. A., Smyth, I. M., et al. (2015). A spatially-averaged mathematical model of kidney branching morphogenesis. *J. Theor. Biol.* 379, 24–37. doi: 10.1016/j.jtbi.2015.04.015

Conflict of Interest Statement: The authors declare that the research was conducted in the absence of any commercial or financial relationships that could be construed as a potential conflict of interest.

Copyright © 2018 Lang, Conrad and Michos. This is an open-access article distributed under the terms of the Creative Commons Attribution License (CC BY). The use, distribution or reproduction in other forums is permitted, provided the original author(s) and the copyright owner(s) are credited and that the original publication in this journal is cited, in accordance with accepted academic practice. No use, distribution or reproduction is permitted which does not comply with these terms.

frontiers in Genetics

MINI REVIEW
published: 07 January 2019
doi: 10.3389/fgene.2018.00705

Fibroblast Growth Factor 10 and Vertebrate Limb Development

Libo Jin[1], *Jin Wu*[1], *Saverio Bellusci*[1,2,3]* *and Jin-San Zhang*[1,2,4]*

[1] *Institute of Life Sciences, Wenzhou University-Wenzhou Medical University Collaborative Innovation Center for Biomedicine, Wenzhou, China,* [2] *Department of Pulmonary and Critical Care Medicine, The First Affiliated Hospital of Wenzhou Medical University, Wenzhou, China,* [3] *Excellence Cluster Cardio-Pulmonary System, Universities of Giessen and Marburg Lung Center, member of the German Center for Lung Research, Justus-Liebig-University Giessen, Giessen, Germany,* [4] *School of Pharmaceutical Sciences, Wenzhou Medical University, Wenzhou, China*

Early limb development requires fibroblast growth factor (Fgf)-mediated coordination between growth and patterning to ensure the proper formation of a functional organ. The apical ectodermal ridge (AER) is a domain of thickened epithelium located at the distal edge of the limb bud that coordinates outgrowth along the proximodistal axis. Considerable amount of work has been done to elucidate the cellular and molecular mechanisms underlying induction, maintenance and regression of the AER. Fgf10, a paracrine Fgf that elicits its biological responses by activating the fibroblast growth factor receptor 2b (Fgfr2b), is crucial for governing proximal distal outgrowth as well as patterning and acts upstream of the known AER marker Fgf8. A transgenic mouse line allowing doxycycline-based inducible and ubiquitous expression of a soluble form of Fgfr2b has been extensively used to identify the role of Fgfr2b ligands at different time points during development. Overexpression of soluble Fgfr2b (sFgfr2b) post-AER induction leads to irreversible loss of cellular β-catenin organization and decreased Fgf8 expression in the AER. A similar approach has been carried out pre-AER induction. The observed limb phenotype is similar to the severe proximal truncations observed in human babies exposed to thalidomide, which has been proposed to block the Fgf10-AER-Fgf8 feedback loop. Novel insights on the role of Fgf10 signaling in limb formation pre- and post-AER induction are summarized in this review and will be integrated with possible future investigations on the role of Fgf10 throughout limb development.

Keywords: Fgf10, Limb, AER, β-catenin, Fgfr2b

OPEN ACCESS

Edited by:
Katiucia Batista Silva Paiva, University of São Paulo, Brazil

Reviewed by:
Steffen Scholpp, University of Exeter, United Kingdom
Takaaki Matsui, Nara Institute of Science and Technology (NAIST), Japan

***Correspondence:**
Saverio Bellusci
saverio.bellusci@innere.med.uni-giessen.de
Jin-San Zhang
zhang_jinsan@163.com

Specialty section:
This article was submitted to Stem Cell Research, a section of the journal Frontiers in Genetics

Received: *04 August 2018*
Accepted: *14 December 2018*
Published: *07 January 2019*

Citation:
Jin L, Wu J, Bellusci S and Zhang J-S (2019) Fibroblast Growth Factor 10 and Vertebrate Limb Development. Front. Genet. 9:705. doi: 10.3389/fgene.2018.00705

INTRODUCTION

Fibroblast Growth Factor 10 (Fgf10) is an evolutionary conserved secreted growth factor mediating mostly mesenchymal to epithelial signaling. Fgf10 belongs to the Fgf7 subfamily and shares similar biochemical and amino acid sequences with its constituent members (Fgf3, Fgf7 and Fgf22) (Min et al., 1998; Itoh and Ornitz, 2008).

The Fgf10 signaling cascade is initiated by its binding to epithelial Fgf receptors (Fgfrs) and heparin/heparan sulfate cofactor-proteoglycans (HS). Fgf10 mediates key intracellular signaling pathways in several cell types leading to the modulation of branching morphogenesis during development, wound healing and tissue repair (Itoh and Ohta, 2014). There are four known classical *Fgfr* genes (*Fgfr1-4*), these are alternatively spliced into "b" and "c" isoforms with exception to the *Fgfr4* gene. Alternative splicing confers tissue- plus cell- specific expression of these

receptor isoforms and different affinities for ligands (Ornitz et al., 1996; Plotnikov et al., 2000). Fgf10 has been shown to bind with high affinity Fgfr1b and Fgfr2b compared to the other Fgf receptors (Ornitz et al., 1996; Ohuchi et al., 2000; Zhang et al., 2006). The Fgf10-Fgfr1b/Fgfr2b-HS signaling complex is essential for activating downstream signal transduction pathways, which include activation of Phosphoinositid-phospholipase C gamma (Plcγ), mitogen-activated protein kinases (Mapk), Protein kinase B (Akt) and signal transducer and activator of transcription proteins (Stat) cascades (Goetz and Mohammadi, 2013). For more information on this topic, please refer to a separate review published in this special issue on Fgf10 (Watson and Francavilla, 2018).

The developing vertebrate limb is a well-studied model to uncover the reciprocal cellular and molecular bases of harmonious organ growth and patterning (Allard and Tabin, 2009; Zeller, 2010). In mouse, limb development begins first with the induction of the forelimb buds at embryonic day 9.5 (E9.5) followed by the formation of the hindlimb buds at E10 on both flanks of the embryo (marking the future forelimbs and hindlimbs respectively) (Lu et al., 2008; Danopoulos et al., 2013). The early limb buds are composed of mesenchymal cells derived from the lateral plate mesoderm. The mesoderm induces the formation of a pseudostratified epithelium at the tip bud (Kieny, 1968; Saunders and Reuss, 1974), the so-called Apical ectodermal ridge (AER) (Todt and Fallon, 1984; Fernandez-Teran and Ros, 2008). It has also been shown that the skeletal and muscle elements of the forelimbs and the hindlimbs originate from the lateral plate mesoderm (Sun et al., 2002).

The developing limb has three command centers: the AER, the zone of polarizing activity (ZPA) and the progress zone (PZ) (**Figure 1A**). Reciprocal interactions between the PZ and AER control the growth of the limb along the proximal-distal axis (Hara et al., 1998). After induction of the AER in the prospective limb field and outgrowth of the corresponding bud, the limb contains three distinct domains: the stylopod (humerus/femur), the zygopod (radius/tibia and ulna/fibula) and the autopod (carpal/tarsal, metacarpal/metatarsal, phalanges) (Saiz-Lopez et al., 2015). Genetic ablation of *Fgf10* in early mouse development results in death at birth and is associated with impressive developmental defects in multiple organs and tissues including the lung and the limb (Min et al., 1998; Sekine et al., 1999). In *Fgf10* knock out (KO) mice, limb bud formation is initiated but no further limb outgrowth is discernible, resulting in acute limb truncation with only rudimentary scapulae and pelvis remaining. In addition, skeletal staining at E17.5 in *Fgf10* KO fetuses confirms the absence of proximal limb elements such as the humerus (Min et al., 1998; Sekine et al., 1999). Notably, *Fgf10* KO mice display similar phenotypes to *Fgfr2b* KO mice in organogenesis (De Moerlooze et al., 2000) suggesting that, *in vivo*, Fgf10 acts mostly through Fgfr2b to control organogenesis. This review aims to provide an overview on the role and mechanism of Fgf10 signaling in limb development with a focus on the genetic data gathered from murine studies.

Abbreviations: AER, Apical ectodermal ridge; PZ, Progress zone; ZPA, Zone of polarizing activity; Fgf10, Fbiroblast growth factor; Fgfr2b, Fibroblast growth factor receptor 2b; Tbx, T-box; Hox, Homebox; Etv, E26 transformation-specific translocation variant.

FGF10 SIGNALING CONTROLS LIMB DEVELOPMENT

It has been previously described through tissue graft experiments that secreted factors from the limb mesenchyme are capable of initiating vertebrate limb bud formation (Saunders and Reuss, 1974). Fgf-soaked beads as well as cell aggregates expressing Fgf implanted in the flank of chick embryos led to the formation of ectopic limbs. Several Fgfs, including Fgf1, 2, 4, 8 and 10 were successfully tested (Cohn et al., 1995; Ohuchi et al., 1995, 1997; Crossley et al., 1996; Vogel et al., 1996). Interestingly, Fgf8 and Fgf10 are the only Fgfs expressed in the limb at the time of AER formation (Crossley et al., 1996; Vogel et al., 1996; Ohuchi et al., 1997). Both Fgf8 and Fgf10 are expressed before AER induction in the intermediate mesoderm and the lateral plate mesoderm within the limb field of the chick embryos respectively. Fgf8 and Fgf10 are also found in the AER and the PZ respectively (Crossley et al., 1996; Vogel et al., 1996). Similar expression pattern for *Fgf8* and *Fgf10* were observed in mouse limb buds at the time of AER induction (Min et al., 1998; Sekine et al., 1999). The precise expression of these Fgfs in regards to limb development before AER induction in mouse is still unclear. However, the study of Gros and Tabin (2014) using mouse limbs from *Fgf10* null embryos clearly shows that Fgf10 participates in the regulation of epithelial mesenchymal transition of the somatopleure (see An "untold story" is emerging for Fgf10 signaling in the pre-AER phase).

During early development, the position of the forelimb and hindlimb along the cranial-caudal axis is controlled by *Hox* genes (Pineault and Wellik, 2014). Disruption of *HoxA* and *HoxD* genes results in seriously reduced limb size, which was initially associated with sonic hedhehog (Shh) downregulation (**Figure 1C**) (Crossley et al., 1996). Early-activated homeobox gene A (*HoxA*) and homeobox gene D (*HoxD*) stimulate expression of *Fgf10* and result in considerable expression of *Fgf8* in the AER. *Hox* also regulate expression of *gremlin1* (*Grem1*) and Shh and hence maintain the cross-talk among Shh, Gli3, HoxA and HoxD (Zakany et al., 2007). Hox also induce *T-box 5* (*Tbx5*) in the forelimb and *T-box 4* (*Tbx4*) in the hindlimb (Pineault and Wellik, 2014) (**Figure 1B**). The differential expression of the two paralogous transcription factors Tbx4 and Tbx5 serve as molecular evidence for determining early limb identity (Gibson-Brown et al., 1996; Minguillon et al., 2009). In human, *TBX5* mutation causes Holt–Oram syndrome (HOS) which is associaited with upper limb abnormalities (Basson et al., 1997; Bongers et al., 2004), while *TBX4* mutation results in small patella syndrome, which is characterized by foot dysplasia (Bongers et al., 2004) (**Figure 1C**). Inactivation of *Tbx4* or *Tbx5* in mice leads to lack of *Fgf10* expression in the lateral plate mesoderm where the forelimb or hindlimb would normally form, respectively (Rodriguez-Esteban et al., 1999). During limb bud formation in mouse, both transcription factors trigger *Fgf10* expression in the limb mesenchyme (Saunders and Reuss, 1974;

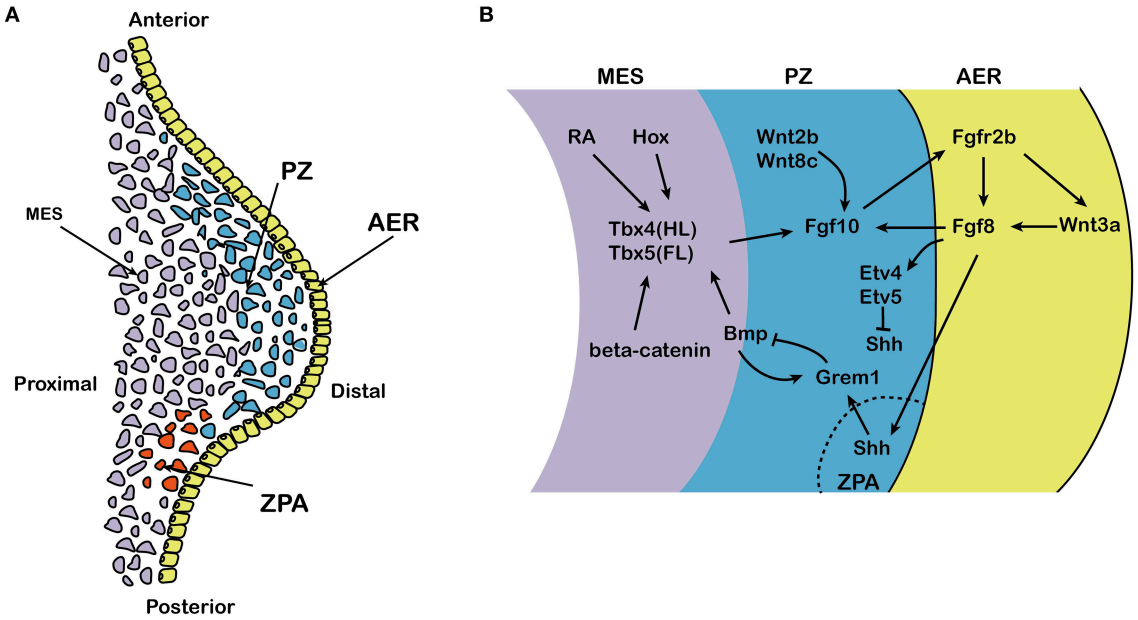

C

Genes	Associated Targets	Phenotype upon gene inactivation
HoxA&HoxD	Fgf10,Grem1,Shh,Tbx4&5	Reduced limb size
Tbx4&5	Hox, Fgf10	Small Patella Syndrome& Holt-Oram Syndrome
Gas1	Fgf10	Delayed digit formation&Attenuated cell programmed death
Etv4&5	Shh	Preaxial polydactyly
Sprouty	RTK, Fgf8, Fgf10	Polysyndactyly

FIGURE 1 | Effects of Fgf10 and its crosstalk network in early limb development. **(A)** Structure of early developing limb bud, from proximal to distal, there are three command centers: ZPA (controlling the anterior-posterior axis/digit identity), the AER and the PZ. Fgf10 expresses in the mesenchyme while Fgf8 expresses in the AER. **(B)** Hox/RA/β-catenin cooperatively triggers the activation of Tbx4/5 in the hindlimb and forelimb respectively. This leads to the up-regulation of Fgf10. Fgf10 activates Fgf8 in the overlying AER and they initiate a positive feedback loop that is essential for sustained limb growth. Shh, produced in the ZPA, acts to regulate correct anterior-posterior patterning during limb development. The Shh/Grem1/Fgf regulatory loop coordinates Shh signaling by the ZPA with Fgf signaling by the AER. **(C)** Specific genes correlated with Fgf10-AER-Fgf8 feedback loop and the targets as well as the effects of ectopic expression in limb development. MES, mesenchyme; PZ, progress zone; ZPA, zone of polarizing activity; AER, apical ectodermal ridge; HL, hindlimb; FL, forelimb.

Vogel et al., 1996; Naiche and Papaioannou, 2003; Minguillon et al., 2005). Fgf10 signaling then triggers Fgf8 expression. Furthermore, genetic ablation of either *Tbx4* and *Tbx5* results in outgrowth limb bud defects (Saunders and Reuss, 1974; Vogel et al., 1996; Ng et al., 2002; Naiche and Papaioannou, 2003; Duboc and Logan, 2011).

The AER, which is histologically characterized by a local thickening of the ectoderm, is the earliest signaling domain to be induced during limb bud formation. It is initiated from the lateral plate mesoderm and is the result of mesenchymal-Fgf10/AER-Fgfr2b signaling (Sekine et al., 1999; De Moerlooze et al., 2000). Using chick and zebrafish embryos, it was shown that Fgf10 expression in the proliferating cells of the PZ is stabilized by Wnt2b and Wnt8c in the forelimb and hindlimb, respectively (Kawakami et al., 2001; Ng et al., 2002), and induces the expression of *Wnt3a* and *Fgf8* in the AER (**Figure 1B**). *Fgf8* expression, which is stabilized by Wnt3a (Kengaku et al., 1998; Kawakami et al., 2001), in turn acts on the underlying mesenchymal cells located in the PZ to maintain *Fgf10* expression and triggers the amplification of the different skeletal progenitors of the limb (Mariani et al., 2008) [for review see (Fernandez-Teran and Ros, 2008)] (**Figure 1B**). Therefore, Fgf10 and Fgf8 display completementary roles in the AER, and interact in a feed-forward regulation loop (Ohuchi et al., 1997; Kawakami

et al., 2001). The Fgf10-AER-Fgf8 feed-forward loop is integrated with other signaling pathways, thereby constituting an elaborated network of interactions to govern limb formation.

Ets variant 1 (Etv1), a member of the E26 transformation-specific (Ets) transcription factors and transcriptional co-activator Ewings sarcoma RNA binding protein 1 (Ewsr1) (Munchberg and Steinbeisser, 1999; Park et al., 2013), acts downstream of AER-Fgfs to maintain a high level of *Fgf10* expression in the AER mesenchyme by stimulating the *Fgf10* promoter in a collaborative way (Yamamoto-Shiraishi et al., 2014). In addition, growth arrest specific gene 1 (*Gas1*) expression in the mesenchyme preserves Fgf10 expression at high level while Fgf10 is of vital importance in maintaining the expression of Fgf8 in AER. *Gas1* KO mice display delayed digit formation, reduced cell proliferation in AER and distal mesenchyme as well as attenuated cell programmed death in interdigital cells (Liu et al., 2002). The *Twist* gene encoding a basic helix–loop–helix (bHlh) transcription factor (Simpson, 1983; Jurgens et al., 1984) is expressed in the lateral plate mesoderm before limb bud formation (Stoetzel et al., 1995). *Twist* KO embryos display reduced expression of *Fgf10* in the limb bud mesenchyme, and is associated with decreased bud growth from its initiation onward (O'Rourke et al., 2002). Etv4 and Etv5 are two additional members of the Ets family of transcription factors working downstream of Fgf signaling and are both expressed in the limb mesenchyme (O'Rourke et al., 2002). In mice, *Etv4/Etv5* double KO embryos display ectopic expression of *Shh*, which in turn leads to preaxial polydactyly. Therefore, Etv4 and Etv5, working downstream of AER-Fgf, function to repress *Shh* expression outside of the ZPA (Zhang et al., 2009).

The AER activity is also mediated by other Fgfs emanating from the AER and acting on the underlying mesenchyme. Fgf8 expression in the AER is detected before the other Fgfs and spans the entire AER. Deletion of *Fgf8* in mice leads to decreased amplification of the mesenchymal progenitors resulting in impaired limb development (Lewandoski et al., 2000). Concomitant overexpression of *Fgf4* in AER cells where *Fgf8* has been deleted allows the rescue of limb development demonstrating that Fgf4 can functionally replace Fgf8 and that the *Fgf8* KO limb phenotype is likely the consequence of the unique timing of *Fgf8* expression vs. the other Fgfs (Lu et al., 2006).

The role of Sprouty (Spry) proteins, which were first explored in drosophila, have also been implicated in the negative regulation of Fgf10 signaling in other organs such as the lung (Minowada et al., 1999). Spry proteins are negative regulators of receptor tyrosine kinase (Rtk)-mediated Map kinase signaling (Hacohen et al., 1998). In a transcriptome analysis of early proximo-distal patterning of the Xenopus laevis limb bud, correlations of early gene expression patterns between Spry1, 2 and 4 and the expected range of Fgf8 and Fgf10 signaling in the developing limb bud has prompted a role for Spry in regulating Fgf signaling in normal limb development. It has been proposed that Spry2 acts as a negative regulator of AER-Fgf8 [(Lewandoski et al., 2000; Impagnatiello et al., 2001); **Figure 1C**]. Although the corresponding Spry roles in mammals are still scarce, *Spry4* KO mice displayed polysyndactyly, which is delineated by fusion and duplication of digits at the forelimbs. A large mutagenesis screening has identified the *Spry4* gene as a candidate regulator of normal limb formation (Taniguchi et al., 2007).

FGFR2B SIGNALING IN POST-AER INDUCTION

As stated above, Fgf10 shows high affinity to Fgfr2b. Fgfr2b has also been independently investigated for its role in limb genesis. Inactivation of *Fgfr2b* in the embryo leads to limb agenesis (De Moerlooze et al., 2000). RNA interference combined with Cre-LoxP system was carried out to attenuate *Fgfr2b* expression in the PZ of the limb and caused dysmorphia of digits (Bellusci et al., 1997). More recently, conditional inactivation of *Fgfr2* in the AER was carried out using the *Msx2-Cre* driver line to target the limb ectoderm (Lu et al., 2008; Yu and Ornitz, 2008). Consequently, $Fgfr2^{Msx2-Cre}$ embryos displayed complete hindlimb agenesis. The forelimb had normal stylopod (humerus/femur) and zygopod (radius/tibia and ulna/fibula) but absent autopod (carpal/tarsal, metacarpal/metatarsal, phalanges) (Yu and Ornitz, 2008). This demonstrated that inactivation of *Fgfr2* in the epithelium of the limb post-AER induction leads to the genetic ablation of the AER. In addition, the loss of autopod is consistent with AER inhibition in the forelimb (illustrated by decreased AER-Fgf8 expression). These results have been validated using a double transgenic system allowing the ubiquitous and robust expression of a secreted form of Fgfr2b capable of sequestering the endogenous Fgfr2b ligands at different time points during or post-AER induction (Danopoulos et al., 2013).

FGFR2B LIGANDS AND CANONICAL β-CATENIN SIGNALING

One of the major mechanistic insight into Fgfr2b signaling is the rapid inhibition of canonical Wnt signaling following Fgfr2b ligand inhibition. Using the Topgal reporter allele, a complete decrease in Wnt signaling was reported 1 h after doxycycline-intraperitoneal injection (Dox-IP). Such a decrease was validated by detecting the nuclear phosphorylated form of β-catenin (Danopoulos et al., 2013). How Fgfr2b signaling impacts β-catenin signaling is still unclear. *In vivo*, some of the genes were down-regulated upon inhibition of Fgfr2b ligands (6 h post Dox-IP at E11.5) activity including Wnt ligands (*Wnt3a, Wnt3, Wnt7a, Wnt7b, Wnt16*), Wnt receptors (*Fzd4, Fzd8, Fzd9*) and secreted Wnt inhibitor (*Wif1*) as well as Wnt1-induced secreted protein 1 (*Wilsp1*) (Danopoulos et al., 2013). Genes up-regulated include *Frzb*, a gene encoding a Wnt binding protein acting as a competitor for the Wnt receptor *Frzd* as well as *Pitx2*, encoding a transcription factor interacting with β-catenin and *Dkk1*, a gene encoding a secreted Wnt ligand inhibitor (Danopoulos et al., 2013). The collective regulation of these genes is likely to impact canonical Wnt signaling.

Immunofluorescence staining for β-catenin in the AER of experimental and control E11.5 limb 1 h after Dox-IP revealed reduced expression level and cellular disorganization of β-catenin

upon Fgfr2b ligand inhibition (Danopoulos et al., 2013). With less β-catenin available, this could be sufficient to lead to decreased Wnt signaling. In zebrafish, somitic mesoderm-derived retinoic acid (RA) signaling resulted in activation of *Wnt2b* expression in the mid-mesoderm, that signals to trigger *Tbx5* expression, In turn, Tbx5 is required for Fgf signaling in the limb bud and then brings about the activation of PR domain containing 1 (*Prdm1*), which then stimulates *Fgf10* expression (Mercader et al., 2006). The same series of events are likely occuring in the developing mammalian limbs since *Prdm1* expression is conserved between zebrafish and tetrapods. More studies will have to be done in the future to elucidate mechanistically the impact of Fgf signaling on β-catenin expression level and localization.

In order to elucidate the impact of transient inhibition of Fgfr2b signaling in limb development, the *Rosa26*^{rtTA} mice were crossed with *Tg(tet(O)solubleFgfr2b (Tg)* transgenic mice to generate double transgenic mice [*Rosa26*$^{rtTA/+}$;*Tg*/+], called hereafter DTG mice. These DTG mice were crossed together to generate experimental DTG and control single transgenic (STG) [*Rosa26*$^{rtTA/+}$; +/+] embryos. Allelic series for DTG embryos (with one or two copies of *Rosa26*^{rtTA} and one or two copies of *Tg*) were generated. This allowed analyzing the impact of different levels of soluble Fgfr2b on limb development. Pregnant mice carrying both control STG and experimental DTG embryos were injected intraperitoneally with a single dose of doxycline at E7.5, E8.5, E9.5 or E10 (Parsa et al., 2008, 2010). The resulting impact on the formation of the cartilage and bone in the limb was analyzed at E18.5 following alcian blue/alizarin red staining. Dox-IP at E7.5, 2 days before AER induction, indicated no phenotypic differences in the limbs of STG and DTG embryos. Dox-IP at E9.5, at the time of forelimb AER induction and 12 h before hindlimb AER induction led to complete forelimb and hindlimb agenesis supporting the previously reported *Fgfr2b* and *Fgf10* KO phenotypes. The difference in phenotype between E9.5 (limb agenesis) and E7.5 (no limb defects) demonstrated that sFgfr2b expression in our model is indeed reversible following Dox-IP injection (Danopoulos et al., 2013). The phenotype resulting from a single Dox-IP at E8.5 is described in the paragraph below.

A POTENTIAL CONNECTION BETWEEN THALIDOMIDE AND FGF10 SIGNALING

It has been proposed that the mesenchymal progenitors for the three skeletal domains (mostly for the stylopod) are being already amplified in a Fgfr2b ligand-dependent fashion during pre-bud formation from E8.5-E9.5 (Danopoulos et al., 2013; Gros and Tabin, 2014). E18.5 DTG heterozygous embryos ([*R26*$^{rtTA/+}$;*Tg*/+]) resulting from Dox-IP at E8.5 (corresponding to 1–1.5 days before forelimb and hindlimb induction, respectively) showed shorter forelimbs and almost normal hindlimbs. Bone/cartilage staining indicated normal scapula but reduced humerus as well as radius and ulna. A phenotypic difference between the right and left limbs was also observed. The right limbs were more severely affected, with a near absence of humerus and shortened femur, and the complete absence of ulna and fibula. Furthermore, while digits had formed in both forelimbs and hindimbs, these digits were fewer on the right side limbs. In addition, DTG homozygous embryos [*R26*$^{rtTA/rtTA}$;*Tg*/*Tg*] display forelimb agenesis and had severely reduced hindlimbs. Bone/cartilage staining revealed a shorter femur and no elements beyond a rudimentary tibia. Once again, the right hindlimbs appeared more severely affected than the left hindlimbs. The reason for this difference is still unclear and will deserve further investigation (Danopoulos et al., 2013).

The limb phenotype displayed upon inhibition of Fgfr2b signaling at E8.5 is similar to the severe proximal truncations observed in human babies exposed to thalidomide, a drug which became popular in the late 1950s (Cohen, 1962). It was initially prescribed for its effect on insomnia, anxiety, gastritis, tension and against nausea to alleviate morning sickness in pregnant women. Thalidomide adminstration to pregnant woman has been shown to cause phocomelia, a condition that involves malformations of the arms and legs. Short arm bones, fused fingers and missing thumbs as well as absent pelvic bones often occur (Kim and Scialli, 2011). The expression of nuclear factor k-B (Nf-κB), an important factor in mediating limb development, is drastically weakened upon thalidomide treatment, which in turn blocks limb cells to express Fgf10 and Twist in the PZ mesenchyme, followed with attenuated expression of Fgf8 in the AER. This process destroys the Fgf10/Fgf8 feedback loop between the PZ and AER and consequently prevents limb initiation (Crossley et al., 1996; Bushdid et al., 2001). It has been proposed that thalidomide limb teratogenicity is linked to oxidative stress damage, DNA intercalation and inhibition of angiogenesis. Cereblon has been identified as primary target of thalidomide and forms a E3 ubiquitin ligase complex with damaged DNA binding protein 1 and Cullin4a (Groisman et al., 2003; Ohtake et al., 2007). Damaged DNA binding protein 1 (*Dbb1*) and cullin 4a (*Cul4a*) regulate the expression of Fgf8 and limb development. Inactivation of cereblon (*Crbn*) in zebrafish leads to defective fin and otic vesicle development (Ito et al., 2010). It is likely that the mechanisms mentioned above can operate in parallel to impair limb formation. It will be important to better define the mechanisms of action of thalidomide on Fgfr2b signaling during this early phase of limb development in future studies.

AN "UNTOLD STORY" IS EMERGING FOR FGF10 SIGNALING IN THE PRE-AER PHASE

Gros and Tabin reported a new function for Fgf10 during pre-AER induction, namely, the induction of epithelial to mesenchymal transition (EMT) from the somatopleural epithelium to form the early mesenchymal limb progenitors, the building blocks of the future limbs (Gros and Tabin, 2014). It has been described in chick model that at stage 13–14 (**Figure 2A**), the somateuploral lateral plate mesoderm of the limb field which starts out as an epithelial-like structure will ultimately

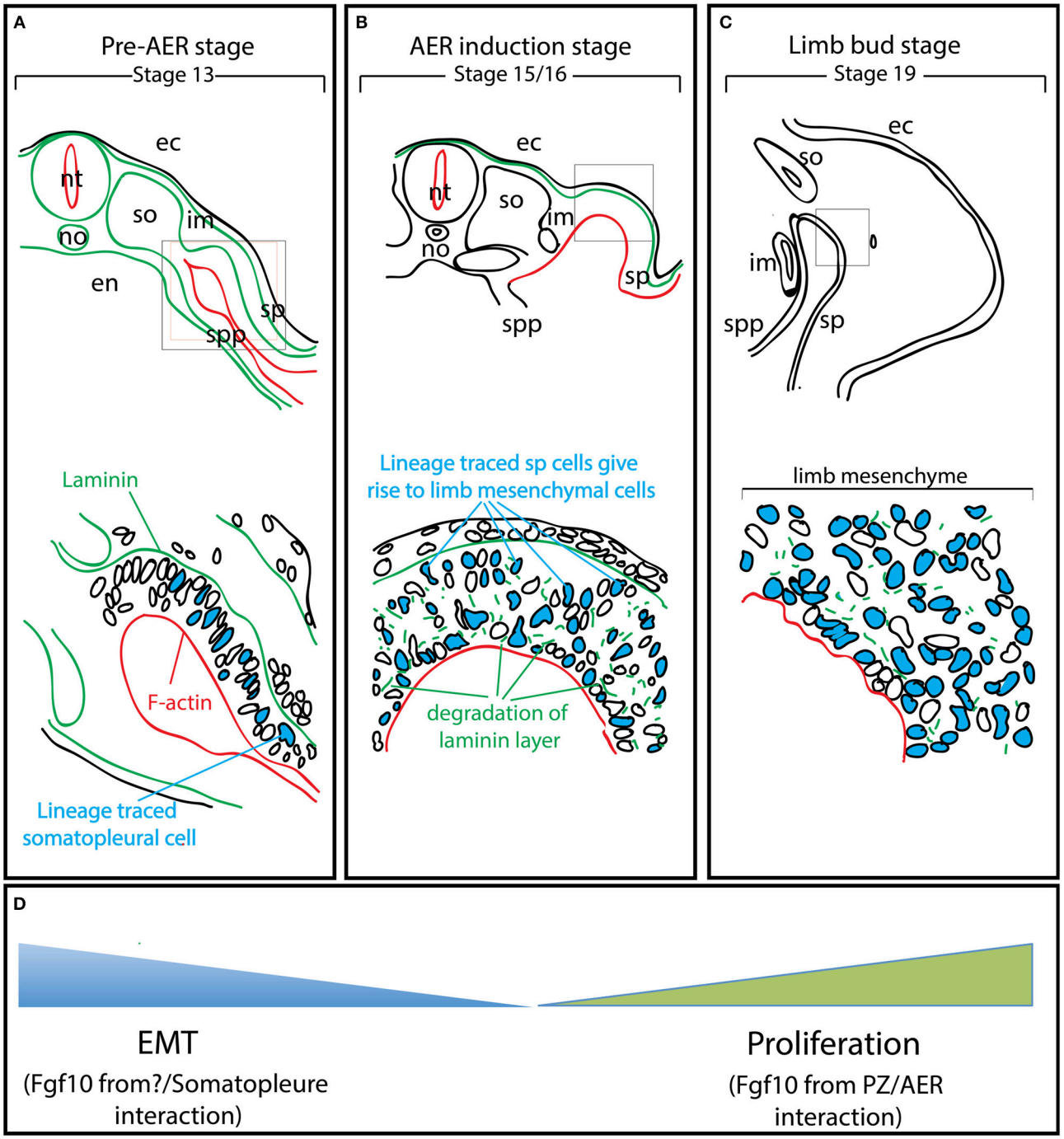

FIGURE 2 | EMT from the somatopleure epithelium is at the heart of limb induction. Adapted from Gros and Tabin's paper (Gros and Tabin, 2014). **(A)** Lineage labeling of the cells in the somatopleure. Note that the cells express laminin on their basal side and F-actin on their apical side. **(B)** The labeled cells undergo EMT. Note that this EMT is associated with the degradation of the laminin layer on the basal side. **(C)** Most of the mesenchymal cells in the rudimentary limb bud post-AER induction (Stage 19) arise from EMT. **(D)** The mesenchymal limb progenitors are first formed through EMT up to the AER induction stage and then amplified post-AER induction through the interaction of the Progress zone (Fgf10-positive) and the Apical Ectodermal ridge (AER). ec, ectoderm; en, endoderm; im, intermediate mesoderm; no, notochord; nt, neural tube; so, somites; sp, somatopleure; spp, splanchnopleure.

generate the progenitors for the limb bud mesenchyme through a process ressembling the EMT (**Figure 2D**). However, this is not likely a classical EMT as the characteristic transcription factors, *Snail* and *Slug* are not expressed. In addition, the somatopleural "epithelium," which is mesoderm-derived is unlikely to be a true epithelium. The role of Fgf10 on the somatopleural "epithelium" is therefore far from being clear and deserves further investigations. Lineage tracing using a GFP reporter in the somatopleure of stage 13-14 chick embryos demonstrated that most, if not all, mesenchymal cells of the early limb bud (stage 15-16, time of AER induction for the forelimb) (**Figure 2B**) originate from the "epithelial" somatopleure. Later on, induction of several Fgfs at the level of the prospective AER will allow the establishment of a feedback loop that will amplify the mesodermal progenitors and allow the formation of the different limb segments along the proximal-distal axis. It has also been reported that ectopic gain of function of Fgf10 (up to stage 17) induces limb bud formation (**Figure 2C**). Gros et al. show that this occurs through EMT from the epithelial trunk somatopleural cells but not from the amplification/proliferation of mesenchymal cells of the same rostrocaudal level (Gros and Tabin, 2014). In addition, failure of ectopic Fgf10 signaling (beyond stage 17) to induce limb formation was thought to be due to the trunk mesenchyme which became determined and was no longer capable to be redirected to a limb fate: this fundamental hypothesis, almost a dogma in the lung field, is no longer valid.

FGF10 SIGNALING IN MESENCHYMAL PROGENITOR FORMATION

The proposed molecular mechanism taking place during the pre-AER phase, based on the work from the Tabin's group, is that Fgf10 acts on the epithelial somatopleure to induce EMT (Gros and Tabin, 2014). This allows the formation of the early mesenchymal limb progenitors that will proliferate and differentiate during the post-AER phase to form the different limb segments. It also has been demonstrated that Fgfr2b ligand(s) signaling are critical in pre-AER induction (E8.5-E9.5) stage to allow the formation of the early mesenchymal progenitors for the limb. Future experiments should be designed to answer the following questions: Where and when is Fgf10 signaling active in the limb field before the induction of the AER (E8.5-E9.5)? Whether EMT is a direct effect of Fgf10 on the somatopleure epithelium should also be evaluated as well as the consequences of different Fgf10 mediated-pre-AER mesenchymal progenitor pool sizes on limb development. Finally, what are the different lineages that Fgf10-positive cells in the pre-AER pool contribute to?

AUTHOR CONTRIBUTIONS

SB and J-SZ conceived this paper. LJ and JW wrote the manuscript. SB, J-SZ and JW designed and drew the figures. LJ, J-SZ, and SB edited the manuscript. SB and J-SZ supervised the study and provided the funding. All authors approve it for publication.

ACKNOWLEDGMENTS

J-SZ was supported by the National Natural Science Foundation of China (grant number 81472601) as well as start up packages from Whenzhou University and Wenzhou Medical University; SB was supported by grants from the Deutsche Forschungsgemeinschaft (DFG; BE4443/6-1, KFO309 P7 and SFB1213-projects A02 and A04) and DZL. We apologize to those colleagues whose work has not been cited due to space restrictions on this interesting and diverse field.

REFERENCES

Allard, P., and Tabin, C. J. (2009). Achieving bilateral symmetry during vertebrate limb development. *Semin. Cell. Dev. Biol.* 20, 479–484. doi: 10.1016/j.semcdb.2008.10.011

Basson, C. T., Bachinsky, D. R., Lin, R. C., Levi, T., Elkins, J. A., Soults, J., et al. (1997). Mutations in human TBX5 [corrected] cause limb and cardiac malformation in Holt-Oram syndrome. *Nat. Genet.* 15, 30–35. doi: 10.1038/ng0197-30

Bellusci, S., Grindley, J., Emoto, H., Itoh, N., and Hogan, B. L. (1997). Fibroblast growth factor 10 (FGF10) and branching morphogenesis in the embryonic mouse lung. *Development* 124, 4867–4878.

Bongers, E. M., Duijf, P. H., van Beersum, S. E., Schoots, J., Van Kampen, A., Burckhardt, A., et al. (2004). Mutations in the human TBX4 gene cause small patella syndrome. *Am. J. Hum. Genet.* 74, 1239–1248. doi: 10.1086/421331

Bushdid, P. B., Chen, C. L., Brantley, D. M., Yull, F., Raghow, R., Kerr, L. D., et al. (2001). NF-kappaB mediates FGF signal regulation of msx-1 expression. *Dev. Biol.* 237, 107–115. doi: 10.1006/dbio.2001.0356

Cohen, S. (1962). Thalidomide polyneuropathy. *N. Engl. J. Med.* 266:1268. doi: 10.1056/NEJM196206142662409

Cohn, M. J., Izpisua-Belmonte, J. C., Abud, H., Heath, J. K., and Tickle, C. (1995). Fibroblast growth factors induce additional limb development from the flank of chick embryos. *Cell* 80, 739–746. doi: 10.1016/0092-8674(95)90352-6

Crossley, P. H., Minowada, G., MacArthur, C. A., and Martin, G. R. (1996). Roles for FGF8 in the induction, initiation, and maintenance of chick limb development. *Cell* 84, 127–136. doi: 10.1016/S0092-8674(00)80999-X

Danopoulos, S., Parsa, S., Al Alam, D., Tabatabai, R., Baptista, S., Tiozzo, C., et al. (2013). Transient Inhibition of FGFR2b-ligands signaling leads to irreversible loss of cellular beta-catenin organization and signaling in AER during mouse limb development. *PLoS ONE* 8:e76248. doi: 10.1371/journal.pone.0076248

De Moerlooze, L., Spencer-Dene, B., Revest, J. M., Hajihosseini, M., Rosewell, I., and Dickson, C. (2000). An important role for the IIIb isoform of fibroblast growth factor receptor 2 (FGFR2) in mesenchymal-epithelial signalling during mouse organogenesis. *Development* 127, 483–492. doi: 10.1042/cs099005P

Duboc, V., and Logan, M. P. (2011). Regulation of limb bud initiation and limb-type morphology. *Dev Dyn.* 240, 1017–1027. doi: 10.1002/dvdy.22582

Fernandez-Teran, M., and Ros, M. A. (2008). The apical ectodermal ridge: morphological aspects and signaling pathways. *Int. J. Dev. Biol.* 52, 857–871. doi: 10.1387/ijdb.072416mf

Gibson-Brown, J. J., Agulnik, S. I., Chapman, D. L., Alexiou, M., Garvey, N., Silver, L. M., et al. (1996). Evidence of a role for T-box genes in the evolution of limb

morphogenesis and the specification of forelimb/hindlimb identity. *Mech. Dev.* 56, 93–101. doi: 10.1016/0925-4773(96)00514-X

Goetz, R., and Mohammadi, M. (2013). Exploring mechanisms of FGF signalling through the lens of structural biology. *Nat. Rev. Mol. Cell Biol.* 14, 166–180. doi: 10.1038/nrm3528

Groisman, R., Polanowska, J., Kuraoka, I., Sawada, J., Saijo, M., Drapkin, R., et al. (2003). The ubiquitin ligase activity in the DDB2 and CSA complexes is differentially regulated by the COP9 signalosome in response to DNA damage. *Cell* 113, 357–367. doi: 10.1016/S0092-8674(03)00316-7

Gros, J., and Tabin, C. J. (2014). Vertebrate limb bud formation is initiated by localized epithelial-to-mesenchymal transition. *Science* 343, 1253–1256. doi: 10.1126/science.1248228

Hacohen, N., Kramer, S., Sutherland, D., Hiromi, Y., and Krasnow, M. A. (1998). Sprouty encodes a novel antagonist of FGF signaling that patterns apical branching of the *Drosophila* airways. *Cell* 92, 253–263. doi: 10.1016/S0092-8674(00)80919-8

Hara, K., Kimura, J., and Ide, H. (1998). Effects of FGFs on the morphogenic potency and AER-maintenance activity of cultured progress zone cells of chick limb bud. *Int. J. Dev. Biol.* 42, 591–599.

Impagnatiello, M. A., Weitzer, S., Gannon, G., Compagni, A., Cotten, M., and Christofori, G. (2001). Mammalian sprouty-1 and−2 are membrane-anchored phosphoprotein inhibitors of growth factor signaling in endothelial cells. *J. Cell Biol.* 152, 1087–1098. doi: 10.1083/jcb.152.5.1087

Ito, T., Ando, H., Suzuki, T., Ogura, T., Hotta, K., Imamura, Y., et al. (2010). Identification of a primary target of thalidomide teratogenicity. *Science* 327, 1345–1350. doi: 10.1126/science.1177319

Itoh, N., and Ohta, H. (2014). Fgf10: a paracrine-signaling molecule in development, disease, and regenerative medicine. *Curr. Mol. Med.* 14, 504–509. doi: 10.2174/1566524014666140414204829

Itoh, N., and Ornitz, D. M. (2008). Functional evolutionary history of the mouse Fgf gene family. *Dev. Dyn.* 237, 18–27. doi: 10.1002/dvdy.21388

Jurgens, G., Wieschaus, E., Nusslein-Volhard, C., and Kluding, H. (1984). Mutations affecting the pattern of the larval cuticle in*Drosophila* melanogaster: II. Zygotic loci on the third chromosome. *Wilehm Roux. Arch. Dev. Biol.* 193, 283–295. doi: 10.1007/BF00848157

Kawakami, Y., Capdevila, J., Buscher, D., Itoh, T., Rodriguez Esteban, C., and Izpisua Belmonte, J. C. (2001). WNT signals control FGF-dependent limb initiation and AER induction in the chick embryo. *Cell* 104, 891–900. doi: 10.1016/S0092-8674(01)00285-9

Kengaku, M., Capdevila, J., Rodriguez-Esteban, C., De La Pena, J., Johnson, R. L., Izpisua Belmonte, J. C., et al. (1998). Distinct WNT pathways regulating AER formation and dorsoventral polarity in the chick limb bud. *Science* 280, 1274–1277. doi: 10.1126/science.280.5367.1274

Kieny, M. (1968). [Variation in the inductive capacity of mesoderm and the competence of ectoderm during primary induction in the chick embryo limb bud]. *Arch. Anat. Microsc. Morphol. Exp.* 57, 401–418.

Kim, J. H., and Scialli, A. R. (2011). Thalidomide: the tragedy of birth defects and the effective treatment of disease. *Toxicol. Sci.* 122, 1–6. doi: 10.1093/toxsci/kfr088

Lewandoski, M., Sun, X., and Martin, G. R. (2000). Fgf8 signalling from the AER is essential for normal limb development. *Nat. Genet.* 26, 460–463. doi: 10.1038/82609

Liu, Y., Liu, C., Yamada, Y., and Fan, C. M. (2002). Growth arrest specific gene 1 acts as a region-specific mediator of the Fgf10/Fgf8 regulatory loop in the limb. *Development* 129, 5289–5300.

Lu, P., Minowada, G., and Martin, G. R. (2006). Increasing Fgf4 expression in the mouse limb bud causes polysyndactyly and rescues the skeletal defects that result from loss of Fgf8 function. *Development* 133, 33–42. doi: 10.1242/dev.02172

Lu, P., Yu, Y., Perdue, Y., and Werb, Z. (2008). The apical ectodermal ridge is a timer for generating distal limb progenitors. *Development* 135, 1395–1405. doi: 10.1242/dev.018945

Mariani, F. V., Ahn, C. P., and Martin, G. R. (2008). Genetic evidence that FGFs have an instructive role in limb proximal-distal patterning. *Nature* 453, 401–405. doi: 10.1038/nature06876

Mercader, N., Fischer, S., and Neumann, C. J. (2006). Prdm1 acts downstream of a sequential RA, Wnt and Fgf signaling cascade during zebrafish forelimb induction. *Development* 133, 2805–2815. doi: 10.1242/dev.02455

Min, H., Danilenko, D. M., Scully, S. A., Bolon, B., Ring, B. D., Tarpley, J. E., et al. (1998). Fgf-10 is required for both limb and lung development and exhibits striking functional similarity to *Drosophila* branchless. *Genes Dev.* 12, 3156–3161. doi: 10.1101/gad.12.20.3156

Minguillon, C., Del Buono, J., and Logan, M. P. (2005). Tbx5 and Tbx4 are not sufficient to determine limb-specific morphologies but have common roles in initiating limb outgrowth. *Dev. Cell* 8, 75–84. doi: 10.1016/j.devcel.2004.11.013

Minguillon, C., Gibson-Brown, J. J., and Logan, M. P. (2009). Tbx4/5 gene duplication and the origin of vertebrate paired appendages. *Proc. Natl. Acad. Sci. U.S.A.* 106, 21726–21730. doi: 10.1073/pnas.0910153106

Minowada, G., Jarvis, L. A., Chi, C. L., Neubuser, A., Sun, X., Hacohen, N., et al. (1999). Vertebrate Sprouty genes are induced by FGF signaling and can cause chondrodysplasia when overexpressed. *Development* 126, 4465–4475.

Munchberg, S. R., and Steinbeisser, H. (1999). The *Xenopus* Ets transcription factor XER81 is a target of the FGF signaling pathway. *Mech. Dev.* 80, 53–65. doi: 10.1016/S0925-4773(98)00193-2

Naiche, L. A., and Papaioannou, V. E. (2003). Loss of Tbx4 blocks hindlimb development and affects vascularization and fusion of the allantois. *Development* 130, 2681–2693. doi: 10.1242/dev.00504

Ng, J. K., Kawakami, Y., Buscher, D., Raya, A., Itoh, T., Koth, C. M., et al. (2002). The limb identity gene Tbx5 promotes limb initiation by interacting with Wnt2b and Fgf10. *Development* 129, 5161–5170.

Ohtake, F., Baba, A., Takada, I., Okada, M., Iwasaki, K., Miki, H., et al. (2007). Dioxin receptor is a ligand-dependent E3 ubiquitin ligase. *Nature* 446, 562–566. doi: 10.1038/nature05683

Ohuchi, H., Hori, Y., Yamasaki, M., Harada, H., Sekine, K., Kato, S., et al. (2000). FGF10 acts as a major ligand for FGF receptor 2 IIIb in mouse multi-organ development. *Biochem. Biophys. Res. Commun.* 277, 643–649. doi: 10.1006/bbrc.2000.3721

Ohuchi, H., Nakagawa, T., Yamamoto, A., Araga, A., Ohata, T., Ishimaru, Y., et al. (1997). The mesenchymal factor, FGF10, initiates and maintains the outgrowth of the chick limb bud through interaction with FGF8, an apical ectodermal factor. *Development* 124, 2235–2244.

Ohuchi, H., Nakagawa, T., Yamauchi, M., Ohata, T., Yoshioka, H., Kuwana, T., et al. (1995). An additional limb can be induced from the flank of the chick embryo by FGF4. *Biochem. Biophys. Res. Commun.* 209, 809–816. doi: 10.1006/bbrc.1995.1572

Ornitz, D. M., Xu, J., Colvin, J. S., McEwen, D. G., MacArthur, C. A., Coulier, F., et al. (1996). Receptor specificity of the fibroblast growth factor family. *J. Biol. Chem.* 271, 15292–15297. doi: 10.1074/jbc.271.25.15292

O'Rourke, M. P., Soo, K., Behringer, R. R., Hui, C. C., and Tam, P. P. (2002). Twist plays an essential role in FGF and SHH signal transduction during mouse limb development. *Dev. Biol.* 248, 143–156. doi: 10.1006/dbio.2002.0730

Park, J. H., Kang, H. J., Kang, S. I., Lee, J. E., Hur, J., Ge, K., et al. (2013). A multifunctional protein, EWS, is essential for early brown fat lineage determination. *Dev. Cell* 26, 393–404. doi: 10.1016/j.devcel.2013.07.002

Parsa, S., Kuremoto, K., Seidel, K., Tabatabai, R., Mackenzie, B., Yamaza, T., et al. (2010). Signaling by FGFR2b controls the regenerative capacity of adult mouse incisors. *Development* 137, 3743–3752. doi: 10.1242/dev.051672

Parsa, S., Ramasamy, S. K., De Langhe, S., Gupte, V. V., Haigh, J. J., Medina, D., et al. (2008). Terminal end bud maintenance in mammary gland is dependent upon FGFR2b signaling. *Dev. Biol.* 317, 121–131. doi: 10.1016/j.ydbio.2008.02.014

Pineault, K. M., and Wellik, D. M. (2014). Hox genes and limb musculoskeletal development. *Curr. Osteoporos. Rep.* 12, 420–427. doi: 10.1007/s11914-014-0241-0

Plotnikov, A. N., Hubbard, S. R., Schlessinger, J., and Mohammadi, M. (2000). Crystal structures of two FGF-FGFR complexes reveal the determinants of ligand-receptor specificity. *Cell* 101, 413–424. doi: 10.1016/S0092-8674(00)80851-X

Rodriguez-Esteban, C., Tsukui, T., Yonei, S., Magallon, J., Tamura, K., and Izpisua Belmonte, J. C. (1999). The T-box genes Tbx4 and Tbx5 regulate limb outgrowth and identity. *Nature* 398, 814–818. doi: 10.1038/19769

Saiz-Lopez, P., Chinnaiya, K., Campa, V. M., Delgado, I., Ros, M. A., and Towers, M. (2015). An intrinsic timer specifies distal structures of the vertebrate limb. *Nat. Commun.* 6:8108. doi: 10.1038/ncomms9108

Saunders, J. W. Jr., and Reuss, C. (1974). Inductive and axial properties of prospective wing-bud mesoderm in the chick embryo. *Dev. Biol.* 38, 41–50. doi: 10.1016/0012-1606(74)90257-7

Sekine, K., Ohuchi, H., Fujiwara, M., Yamasaki, M., Yoshizawa, T., Sato, T., et al. (1999). Fgf10 is essential for limb and lung formation. *Nat. Genet.* 21, 138–141. doi: 10.1038/5096

Simpson, P. (1983). Maternal-zygotic gene interactions during formation of the dorsoventral pattern in *Drosophila* embryos. *Genetics* 105, 615–632.

Stoetzel, C., Weber, B., Bourgeois, P., Bolcato-Bellemin, A. L., and Perrin-Schmitt, F. (1995). Dorso-ventral and rostro-caudal sequential expression of M-twist in the postimplantation murine embryo. *Mech. Dev.* 51, 251–263. doi: 10.1016/0925-4773(95)00369-X

Sun, X., Mariani, F. V., and Martin, G. R. (2002). Functions of FGF signalling from the apical ectodermal ridge in limb development. *Nature* 418, 501–508. doi: 10.1038/nature00902

Taniguchi, K., Ayada, T., Ichiyama, K., Kohno, R., Yonemitsu, Y., Minami, Y., et al. (2007). Sprouty2 and Sprouty4 are essential for embryonic morphogenesis and regulation of FGF signaling. *Biochem. Biophys. Res. Commun.* 352, 896–902. doi: 10.1016/j.bbrc.2006.11.107

Todt, W. L., and Fallon, J. F. (1984). Development of the apical ectodermal ridge in the chick wing bud. *J. Embryol. Exp. Morphol.* 80, 21–41.

Vogel, A., Rodriguez, C., and Izpisua-Belmonte, J. C. (1996). Involvement of FGF-8 in initiation, outgrowth and patterning of the vertebrate limb. *Development* 122, 1737–1750.

Watson, J., and Francavilla, C. (2018). Regulation of FGF10 signaling in development and disease. *Front. Genet.* 9:500. doi: 10.3389/fgene.2018.00500

Yamamoto-Shiraishi, Y., Higuchi, H., Yamamoto, S., Hirano, M., and Kuroiwa, A. (2014). Etv1 and Ewsr1 cooperatively regulate limb mesenchymal Fgf10 expression in response to apical ectodermal ridge-derived fibroblast growth factor signal. *Dev. Biol.* 394, 181–190. doi: 10.1016/j.ydbio.2014.07.022

Yu, K., and Ornitz, D. M. (2008). FGF signaling regulates mesenchymal differentiation and skeletal patterning along the limb bud proximodistal axis. *Development* 135, 483–491. doi: 10.1242/dev.013268

Zakany, J., Zacchetti, G., and Duboule, D. (2007). Interactions between HOXD and Gli3 genes control the limb apical ectodermal ridge via Fgf10. *Dev. Biol.* 306, 883–893. doi: 10.1016/j.ydbio.2007.03.517

Zeller, R. (2010). The temporal dynamics of vertebrate limb development, teratogenesis and evolution. *Curr. Opin. Genet. Dev.* 20, 384–390. doi: 10.1016/j.gde.2010.04.014

Zhang, X., Ibrahimi, O. A., Olsen, S. K., Umemori, H., Mohammadi, M., and Ornitz, D. M. (2006). Receptor specificity of the fibroblast growth factor family. The complete mammalian FGF family. *J. Biol. Chem.* 281, 15694–15700. doi: 10.1074/jbc.M601252200

Zhang, Z., Verheyden, J. M., Hassell, J. A., and Sun, X. (2009). FGF-regulated Etv genes are essential for repressing Shh expression in mouse limb buds. *Dev. Cell* 16, 607–613. doi: 10.1016/j.devcel.2009.02.008

Conflict of Interest Statement: The authors declare that the research was conducted in the absence of any commercial or financial relationships that could be construed as a potential conflict of interest.

Copyright © 2019 Jin, Wu, Bellusci and Zhang. This is an open-access article distributed under the terms of the Creative Commons Attribution License (CC BY). The use, distribution or reproduction in other forums is permitted, provided the original author(s) and the copyright owner(s) are credited and that the original publication in this journal is cited, in accordance with accepted academic practice. No use, distribution or reproduction is permitted which does not comply with these terms.

frontiers in Genetics

ORIGINAL RESEARCH
published: 23 January 2019
doi: 10.3389/fgene.2018.00746

A Comprehensive Analysis of Fibroblast Growth Factor Receptor 2b Signaling on Epithelial Tip Progenitor Cells During Early Mouse Lung Branching Morphogenesis

Matthew R. Jones[1,2†], Salma Dilai[2†], Arun Lingampally[2], Cho-Ming Chao[1,2], Soula Danopoulos[3], Gianni Carraro[4], Regina Mukhametshina[5], Jochen Wilhelm[2], Eveline Baumgart-Vogt[2], Denise Al Alam[3], Chengshui Chen[1], Parviz Minoo[6], Jin San Zhang[1,7,8] and Saverio Bellusci[1,2,3,7,8*]*

[1] Department of Pulmonary and Critical Care Medicine, The First Affiliated Hospital of Wenzhou Medical University, Wenzhou, Zhejiang, China, [2] Department of Internal Medicine II, Member of the German Lung Center, Excellence Cluster Cardio-Pulmonary Systems, University of Giessen Lung Center, Giessen, Germany, [3] Developmental Biology and Regenerative Medicine Program, Saban Research Institute of Children's Hospital Los Angeles and University of Southern California, Los Angeles, CA, United States, [4] Department of Medicine, Cedars-Sinai Medical Center, Lung and Regenerative Medicine Institutes, Los Angeles, CA, United States, [5] Institute of Fundamental Medicine and Biology, Kazan Federal University, Kazan, Russia, [6] Division of Newborn Medicine, Department of Pediatrics, Children's Hospital Los Angeles, University of Southern California, Los Angeles, CA, United States, [7] Institute of Life Sciences, Wenzhou University, Zhejiang, China, [8] International Collaborative Research Center on Growth Factors, Wenzhou Medical University, Zhejiang, China

OPEN ACCESS

Edited by:
Maria Caterina Mione, University of Trento, Italy

Reviewed by:
Poongodi Geetha-Loganathan, SUNY Oswego, United States
Liping Xiao, UCONN Health, United States

***Correspondence:**
Jin San Zhang
zhang.jinsan@mayo.edu
Saverio Bellusci
Saverio.Bellusci@innere.med.uni-giessen.de

[†]These authors have contributed equally to this work

Specialty section:
This article was submitted to Stem Cell Research, a section of the journal Frontiers in Genetics

Received: *26 October 2018*
Accepted: *27 December 2018*
Published: *23 January 2019*

Citation:
Jones MR, Dilai S, Lingampally A, Chao C-M, Danopoulos S, Carraro G, Mukhametshina R, Wilhelm J, Baumgart-Vogt E, Al Alam D, Chen C, Minoo P, Zhang JS and Bellusci S (2019) A Comprehensive Analysis of Fibroblast Growth Factor Receptor 2b Signaling on Epithelial Tip Progenitor Cells During Early Mouse Lung Branching Morphogenesis. Front. Genet. 9:746. doi: 10.3389/fgene.2018.00746

This study demonstrates that FGF10/FGFR2b signaling on distal epithelial progenitor cells, via ß-catenin/EP300, controls, through a comprehensive set of developmental genes, morphogenesis, and differentiation. Fibroblast growth factor (FGF) 10 signaling through FGF receptor 2b (FGFR2b) is mandatory during early lung development as the deletion of either the ligand or the receptor leads to lung agenesis. However, this drastic phenotype previously hampered characterization of the primary biological activities, immediate downstream targets and mechanisms of action. Through the use of a dominant negative transgenic mouse model (*Rosa26rtTA; tet(o)sFgfr2b*), we conditionally inhibited FGF10 signaling *in vivo* in E12.5 embryonic lungs via doxycycline IP injection to pregnant females, and *in vitro* by culturing control and experimental lungs with doxycycline. The impact on branching morphogenesis 9 h after doxycycline administration was analyzed by morphometry, fluorescence and electron microscopy. Gene arrays at 6 and 9 h following doxycycline administration were carried out. The relationship between FGF10 and ß-catenin signaling was also analyzed through *in vitro* experiments using IQ1, a pharmacological inhibitor of ß-catenin/EP300 transcriptional activity. Loss of FGF10 signaling did not impact proliferation or survival, but affected both adherens junctions (up-regulation of E-cadherin), and basement membrane organization (increased laminin). Gene arrays identified multiple direct targets of FGF10, including main transcription factors. Immunofluorescence showed a down-regulation of the distal epithelial marker SOX9 and mis-expression distally of the proximal marker SOX2. Staining for the transcriptionally-active form of ß-catenin showed a reduction in experimental vs.

control lungs. *In vitro* experiments using IQ1 phenocopied the impacts of blocking FGF10. This study demonstrates that FGF10/FGFR2b signaling on distal epithelial progenitor cells via ß-catenin/EP300 controls, through a comprehensive set of developmental genes, cell adhesion, and differentiation.

Keywords: FGF10, FGFR2b, lung, branching morphogenesis, differentiation, ß-catenin

INTRODUCTION

In mice, the first morphological evidence of lung development is seen at embryonic day (E) 9.5 with the budding of the ventral foregut endoderm, forming the tracheal primordium ventrally and the esophagus dorsally. Concomitantly, distal to the tracheal primordium, two primary lung buds form, initiating the early stages of pseudoglandular development (E9.5-E12.5) [for reviews on early lung development, see (Warburton et al., 2008, 2010; El Agha and Bellusci, 2014)]. During this early stage, the lung epithelium undergoes branching morphogenesis, a semi-stereotypical, and reiterative budding process whereby a tree-like structure, the scaffold of the future conducting airway network, is formed. At the tip of each bud reside multipotent epithelial progenitor cells, which are positive for the transcription factors SOX9 and ID2. These cells either self-renew, if they remain distally, or give rise to bronchial progenitors when they exit the tip domain, subsequently acquiring SOX2 expression (Rawlins, 2008).

Branching morphogenesis and epithelial differentiation depend on poorly understood cross-talk among a number of signaling pathways, involving fibroblast growth factors (FGF), sonic hedgehog (SHH), bone morphogenic proteins (BMP), and wingless/integrase 1 (WNT) ligands (El Agha and Bellusci, 2014). For example, fibroblast growth factor 10 (FGF10), signaling via its epithelial receptor FGFR2b, is sufficient to induce branching morphogenesis of isolated lung endoderm grown in Matrigel (Bellusci et al., 1997b). Additionally, demonstrating that FGF10 signaling is necessary to control branching morphogenesis, both *Fgf10*- and *Fgfr2b*-null embryos display lung agenesis (Sekine et al., 1999; De Moerlooze et al., 2000), while *Fgf10* hypomorphic lungs display decreased ramifications (Ramasamy et al., 2007). Less is known about the regulation of distal tip multipotent epithelial stem cell maintenance and differentiation. Interestingly, *Fgf10* gain-of-function experiments prevent the differentiation of epithelial tip cells toward the bronchial progenitor lineage (Volckaert et al., 2013).

Almost twenty years after the discovery of FGF10 as a key growth factor regulating branching morphogenesis, the primary targets and biological activities controlled by FGF10 are still unclear (El Agha and Bellusci, 2014). Addressing this issue has been difficult, since loss of *Fgf10* leads to lung agenesis, therefore leaving little tissue to study; and while conditional deletions are possible, the lapse of time separating either constitutive or inducible Cre activity (in the case of a CreERT2 system) from complete gene inactivation is usually 24 to 48 h, it is difficult to distinguish between primary and secondary effects (Abler et al., 2009). Furthermore, genetic deletion of *Fgf10* does not necessarily mean simultaneous loss of corresponding functional protein. The stability of the protein depends, for example, on the degradation rate of FGF10 present in the extracellular matrix and bound to heparin sulfate proteoglycans (Makarenkova et al., 2009; Patel et al., 2017), and it might take hours or days before a complete loss of function is achieved.

Genetically modified mouse strains, based on the reverse tetracycline transactivator (rtTA) system, do exist to conditionally inhibit FGF ligand activity at the protein level, and employ a dominant negative soluble form of FGFR2b. Soluble FGFR2b is a hybrid protein, where the extracellular part of the receptor, responsible for binding FGF ligands, is fused to the heavy chain of mouse immunoglobulin (Celli et al., 1998). This hybrid protein, once secreted, sequesters all FGFR2b ligands in the extracellular matrix.

Little research has explicitly used soluble FGFR2b to study the role of FGF signaling on early lung development, while the papers that do exist only touch on the question tangentially. For example, Hokuto et al. (2003) induced soluble FGFR2b at various pre- and postnatal stages to elicit the role played by FGF signaling in alveologenesis. While the authors reported a clear phenotype in early lungs (for example, branching defects) associated with FGF inhibition, detailed analyses of these defects were missing. Therefore, in this paper, we focused our study at E12.5, a stage where FGF10 is the only FGFR2b ligand significantly expressed. We performed both *in vitro* and *in vivo* experiments to analyze the impact of blocking FGF10 activity at the protein level. We used the developing lung as a model system to decipher the primary role of FGF10 in branching morphogenesis. Through the use of a previously validated dominant negative transgenic mouse model (*Rosa26rtTA; tet(o)sFgfr2b*; Parsa et al., 2008, 2010; Volckaert et al., 2011, 2017) we conditionally inhibited FGF10 signaling *in vivo* in E12.5 embryonic lungs via doxycycline IP injection to pregnant females, and *in vitro* by culturing lungs with doxycycline. The impact on branching morphogenesis 9 h after doxycycline administration was analyzed by morphometry, fluorescence, and electron microscopy. Gene arrays at 6 and 9 h following doxycycline administration were performed. The relationship between FGF10 and ß-catenin signaling was also analyzed using IQ1, a pharmacological inhibitor of ß-catenin/EP300 transcriptional activity.

This study demonstrates that FGF10/FGFR2b signaling on distal epithelial progenitor cells via ß-catenin/EP300 controls, through a comprehensive set of developmental genes, cell adhesion, and differentiation. Altogether, our results clarify

the role of FGF10 on tip epithelial progenitor cells during development. Our transcriptomic approach has also provided a valuable dataset for future mechanistic studies aiming to characterize the role of newly found players in FGF10 signaling. Such knowledge will be instrumental to better understanding the role of FGF10 signaling at later stages of lung development, as well as during the repair process after injury.

RESULTS

Expression of *Fgf* Genes Encoding the Main FGFR2b Ligands During Early Lung Development and Validation of the Transgenic Approach to Inactivate FGFR2b Ligands

First, at different stages during embryonic lung development, we monitored by qPCR the expression of *Fgf* genes encoding ligands of FGFR2b, of which only *Fgf1*, *7,* and *10* were detected ($n = 3$; **Figure 1A**). At E12.5, *Fgf10* was the predominantly expressed *Fgf* gene, while the expressions of *Fgf1* and *7* progressively increased during development, as previously described (Bellusci et al., 1997b). Next, we validated the double transgenic approach to block the activity of all FGFR2b ligands via the inducible expression of soluble FGFR2b using the *Rosa26*$^{rtTA/rtTA}$*; tet(o)sFgfr2b/+* transgenic mouse line (**Figure 1B**). The ubiquitous expression of soluble FGFR2b is achieved upon exposure to doxycycline (Dox), delivered via food, water, or intraperitoneal (IP) injection. Efficient inhibition of FGF10 activity occurs shortly after the soluble receptor is produced (usually within minutes after exposure to Dox; Danopoulos et al., 2013). **Figure S1A** shows the *in vivo* validation of this approach on lung development. Our results indicate severely impaired branching of the lung, with long, non-ramified epithelial tubes reminiscent of the primary bronchi. As expected, the earliest time points of treatment were the ones leading to the more severe phenotype. Dox-food exposure from E9.5 onwards led to complete lung agenesis (data not shown), similar to the genetic loss of *Fgf10* or *Fgfr2b* (Sekine et al., 1999; De Moerlooze et al., 2000). **Figure S1B** shows the *in vitro* validation of our transgenic approach. While control lungs underwent significant branching over time (**Figure S1Ba,c,e,g**), experimental lungs failed to branch, but instead formed long tubular extensions (**Figure S1Bb,d,f,h**) similar to that observed *in vivo*.

Therefore, our results indicate that *Fgf10* is the predominantly expressed FGFR2b ligand at E12.5 and that we have a validated transgenic system allowing the inducible blockade at the protein level of FGFR2b ligands. Due to our choice of E12.5 to run our experiments, we therefore conclude that inhibiting FGFR2b ligands at this stage is functionally equivalent to inhibiting FGF10 activity. In addition, supporting our choice to focus this study on FGF10, *Fgf1* and *Fgf7* knock out mice are viable and do not display any respiratory defects (Guo et al., 1996; Miller et al., 2000).

Impact of FGF10 Inhibition on Branching Morphogenesis

We performed *in vitro* live imaging experiments for up to 24 h on control and experimental E12.5 lungs cultured with Dox ($n = 3$). This enabled us to characterize the changes occurring in the branching of the epithelium. We focused on the left lobe over this 24-h period (**Figure 1C**). While the number of distal buds in control lungs increased (from 12.0 ± 1.2 to 17 ± 1.5), no new buds were observed in experimental lungs (**Figure 1Da**). We also measured the total epithelial surface vs. the total surface of the left lobes (**Figure 1Db**). Our results indicate a phase of retraction of the epithelial surface in experimental lungs (−12.0% ± 4.0 at 3 h, −15.0% ± 4.2 at 6 h, −16.6% ± 5.7 at 9 h, and −9.8% ± 5.7 at 24 h). At the same time-points, the epithelial surface ratio increased in the control lungs (+4.0% ± 0.7 at 3 h, +13.0% ± 3.3 at 6 h, +12.7% ± 0.9 at 9 h, and + 24.0% ± 3.5 at 24 h). Next, we measured the distance between the epithelium at the tip of the buds and the adjacent mesothelium (see white arrows **Figures 1C, Dc**). We observed a progressive increase in the space between the tip epithelium and the mesothelium in experimental lungs over time (+18.0% ± 12.4 at 3 h, +24.0% ± 15.7 at 6 h, 29.5% ± 16.0 at 9 h, and 31.0% ± 17.0 at 24 h), while this distance decreased in control lungs (−8.7% ± 3.7 at 3 h, −10.5% ± 4.5 at 6 h, −16% ± 3.9 at 9 h, and −36.6% ± 1.2 at 24 h). Finally, we quantified the lengths of the different epithelial domain branches over time (**Figure 1Dd–i**). These domain branches were named according to the previously described nomenclature (Metzger et al., 2008b). In both control and experimental lungs, L1, L2, L3, L4, D1, and D2 were clearly visible. Note that the experimental lung shown in **Figure 1Cf** was slightly delayed in terms of branching, compared to the lung shown in **Figure 1Ca**, as is often the case between lungs within a given litter. Consequently, in the control lung, L1 and L2 were already ramified, while only L1 was in the experimental lung. In both control and experimental lungs, L3, L4, D1, and D2 were not ramified. Our results indicate that the temporal increase in length of D1 and D2 was less in experimental lungs, compared to controls (**Figure 1Dh,i**). Furthermore, when comparing branches that were already ramified (such as L1 in control and experimental), there was no difference between experimental and control lungs during the time period considered (**Figure 1Dd**). However, caution should be exercised when comparing ramified branches with non-ramified branches (such as L2 in the control and experimental lungs shown), as there tended to be an increase in the rate of lengthening of the initially non-ramified branch, compared to the initially ramified branch. This could explain why the average L2 branch length in the experimental lungs showed a greater increase over time compared to the control branch (**Figure 1De**).

In conclusion, our detailed analysis reveals that subtle branching defects were already apparent 3 h after exposure to Dox. The major impact of inhibiting FGF10 activity was on the epithelium, where a complete arrest in budding, and a transient retraction of the epithelium (which correlated with an increase in the distance between the mesothelium and the distal tip epithelium), was observed.

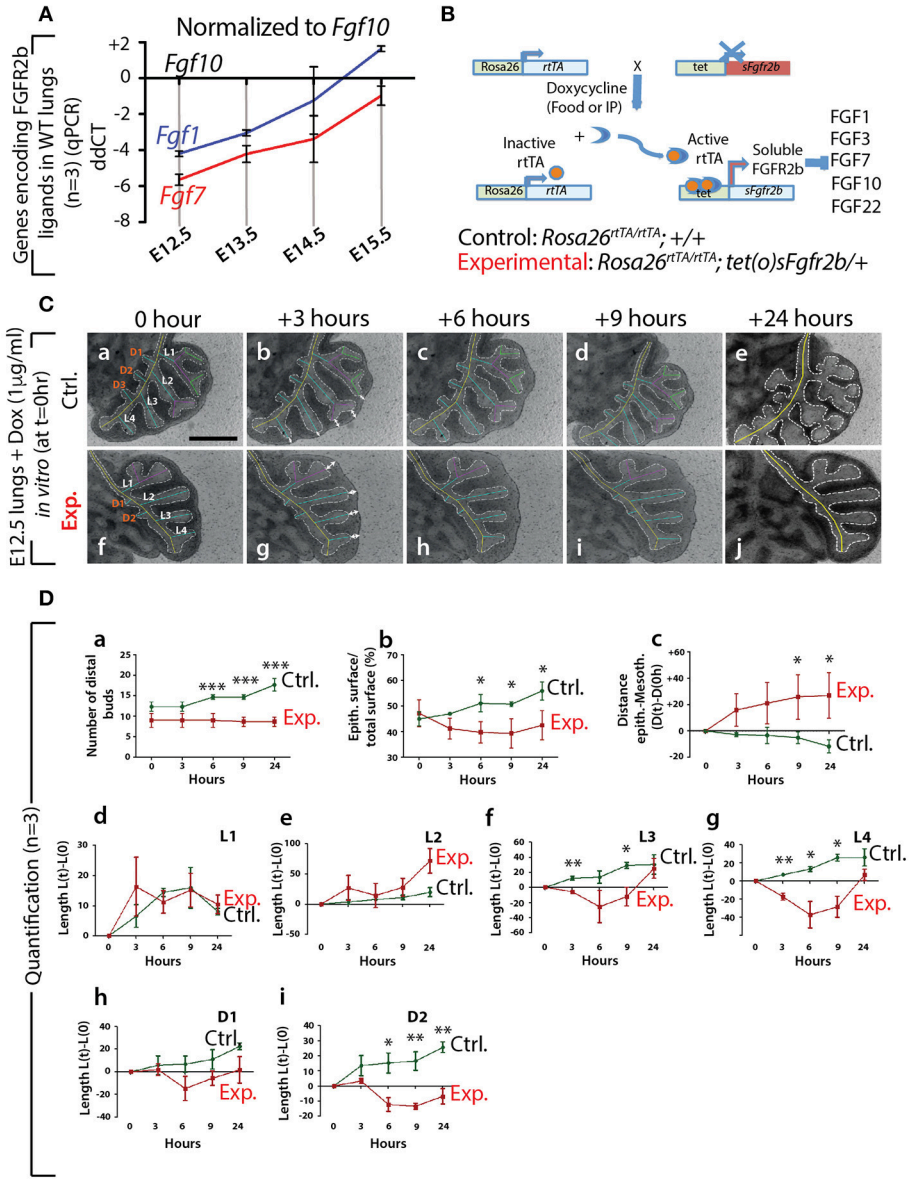

FIGURE 1 | Expression of genes encoding the main FGFR2b ligands during early lung development and impact of FGFR2b ligand inactivation on branching morphogenesis **(A)** qPCR for *Fgf1*, *7*, and *10* in mouse embryonic lungs at E12.5, E13.5, E14.5, and E15.5. *Fgf10* is the main ligand expressed at E12.5 ($n = 3$). **(B)** *Rosa26*$^{rtTA/rtTA}$*; tet(O)sFgfr2b/+* double transgenic system inducing, upon doxycycline exposure (via food, water, or IP), the expression of a soluble form of FGFR2b acting as a dominant negative receptor. **(C)** Impact of FGFR2b ligand inactivation on the branching process. Branches (a and f) are labeled according to established domain branching nomenclature (L,lateral branch; D,dorsal branch). Arrows (b and g) indicate the distance between distal tip epithelium and the adjacent mesothelium. *Scale bar:* 400 µm. **(D)** Quantification of the branching defects. (Data are presented as mean ± SEM; significance determined by unpaired two-tailed Student's *t*-test; $n = 3$; **p*-value < 0.05, ***p*-value < 0.01, ****p*-value < 0.001).

Inhibition of FGF10 Activity Leads to Reduction of Epithelial Bud Lumen Area Associated With Cell Rearrangements

Next, we analyzed the branching defects at the cellular level using 3D-reconstructions of serial confocal images of distal epithelial buds in control and experimental lungs. These lungs were isolated 9 h following a Dox-IP to pregnant females carrying E12.5 embryos, and were whole-mount stained with CDH1 (E-cadherin) antibody. **Figure 2A** shows a longitudinal section, cross section, and 3D projection of control (a, c, e) and experimental (b, d, f) buds (see corresponding movies in **Supplementary Materials**). Quantification of the relative lumen area at different positions within the bud shows a clear reduction in this ratio in experimental buds, compared to controls ($n = 3$; **Figure 2B**). In addition, the average epithelial thickness was larger in experimental buds, compared to controls (**Figure 2B**).

This increased thickness was likely a consequence of epithelial cells piling atop one another, and failing to form an ordered monolayer, as seen in control buds. Altogether, inhibition of FGF10 activity led to the collapse of the lumen within the bud, and to increased epithelial thickness, which we think are the consequences of cell rearrangements within the epithelial layer. This conclusion is supported by the fact that extensive analysis of cell proliferation and cell death in the epithelium and mesenchyme, at this time point, did not indicate any difference between control and experimental lungs ($n = 3$; **Figure 3**).

We also analyzed the appearance of epithelial tip cells in control and experimental lungs by transmission electron microscopy (TEM; **Figure 2C**). Our results reveal numerous interesting impacts of blocking FGF10 signaling in experimental vs. control epithelial tip cells, including altered Golgi morphology, decreased microvilli size and number, and opened tight junctions (see **Figure S2**). In terms of impacts on cell rearrangement, in experimental lungs, the thickness of the basement membrane was consistently greater than that of control lungs (see dashed line in **Figure 2Cb,d**). This increase in basement membrane thickness was confirmed by immunofluorescence for laminin (LAMA1; **Figure 2De–h**). Second, epithelial cell-cell adhesion was affected in experimental lungs, compared to controls. This is evidenced by the many large gaps between adjacent epithelial cells in experimental lungs (see the asterisks in **Figure 2Cc,d**), whereas adjacent epithelial cells in control samples formed tight associations with few gaps. Impacts on adhesion are further demonstrated by looking at the adherens junctions, where a darker staining was observed in experimental lungs, compared to controls (**Figure 2Ce–h**). This darker staining suggests an accumulation of adherens junction associated protein, most likely CDH1. Indeed, immunofluorescent staining revealed drastically increased CDH1 expression in the distal epithelium of experimental lungs vs. controls (**Figure 2Da–d**).

Our results demonstrate that inhibition of FGF10 signaling leads to impaired distal bud morphology, including collapsed bud lumens and thicker epithelial layers. It is likely that this phenotype is primarily a result of epithelial disorganization caused by adhesion and rearrangement defects.

Identification of Early FGF10 Target Genes by Gene Array

Based on the previous results, we selected E12.5 as the ideal time point to determine the specific transcriptomic targets of FGF10 *in vivo* using our transgenic system. Since a single Dox-IP is sufficient to quickly induce soluble FGFR2b expression at E12.5 (Danopoulos et al., 2013), we administered single Dox-IPs to pregnant females and isolated embryos 6 or 9 h later (**Figure 4A**). Compared to control lungs (**Figure 4Ba,b**), the experimental lungs showed branching simplification and an increased distance between the distal epithelium and the mesothelium at 6 h (**Figure 4Bc,d**), a phenotype which was more pronounced at 9 h (**Figure 4Be,f**). RNA isolated from single experimental lungs at 6 and at 9 h was used for whole transcriptome analysis by gene array. As the difference in terms of size and branching between control lungs at 6 and 9 h was minimal, we chose two controls at 6 h and one control at 9 h for the gene array. **Figure 4C** shows the corresponding volcano plots, demonstrating significant sets of genes being either up- or down-regulated between experimental and control lungs at these two time points. **Figure 4D** shows the heatmap of the top 100 regulated genes (selected according to p-value; $n = 3$) between experimental and control lungs at 6 h, as well as the corresponding expression levels for those genes at 9 h. **Figure 4F** shows the heatmap of the top 100 regulated genes (selected according to p-value; $n = 3$) between experimental and control lungs at 9 h, as well as the corresponding expression levels for those genes at 6 h. At both the 6 and 9 h reference points, four gene clusters can be identified based on similar expression patterns (**Figures 4E,G**). Of great interest are the genes contained in the Early 4 and Late 4 clusters. These genes showed early down-regulation upon attenuation of FGF10 signaling, and their expression continued to decrease over time. These genes, therefore, are likely primary targets of FGF10. The heatmaps for the other gene clusters, as well as their regions of expression in the embryonic lung using the genepaint database, are shown in supplementary data (**Figures S3–S10**).

Figure 4H displays the list of genes found in the Early 4 and Late 4 clusters (representing the "FGF10 gene signature"), as well as Late 3 and Late 1 (presented as a validation for the array). Interestingly, Early 4 (6 h) contains only 14 genes while Late 4 (9 h) contains 43 genes (10 of which overlap with the Early 4 genes), suggesting progressive transcriptional-level changes with time. As expected, Early 4 contains genes linked to multipotent epithelial cell differentiation, such as *Sftpc* and *Id2*. The transcription factor *Etv5*, an accepted bona fide target of FGF signaling, was also among the first genes to be down-regulated. The Early 4 cluster also contains genes linked to cell adhesion (e.g., *Tspan8* and *Lin7a*), signaling and transcriptional regulation (e.g., *Gprc5a* and *Sp5*), neuronal processes (e.g., *Gprin3, Enc1,* and *Sema4f*), apoptosis and cell cycle (e.g., *Bid* and *Rai14*), and transport (e.g., *Arrdc1* and *Slco2a1*).

The Late 4 cluster displays supplementary genes linked to epithelial differentiation, such as *Sftpa1*, *Sftpb*, and *Hopx*. *Etv5* was also found among these top-regulated genes. *Etv4,* a related transcription factor working redundantly with *Etv5* (Herriges et al., 2015), was also down-regulated, albeit at a lower level (data not show). Furthermore, the Late 4 cluster includes many additional genes regulating the biological processes described for the Early 4 cluster (e.g., cell adhesion genes *Lama3*, *Lamc2*, and *Ctnnd2*; signaling and transcriptional regulation genes *Kiss1*, *Akap5*, *Cytl1, Apcdd1*, and *Shh*; and apoptosis and cell cycle genes *Bex4*, *Dhx33*, *Klf16*, and *Aen*). **Figure 4J** shows KEGG pathway analyses for the 6 and 9 h time points, highlighting the cellular and signaling processes significantly regulated in experimental vs. control lungs. Significant changes in cytokine-cytokine receptor interactions, calcium signaling, WNT signaling, and Hedgehog signaling were observed at 6 h. In addition to these changes, at 9 h, we also observed significant alterations in the ECM-receptor interaction and cell adhesion molecules, reflecting the morphological alterations observed in **Figure 2**.

In order to gain more insight into the genes identified in each of the four groups, we made use of the online expression-profiling

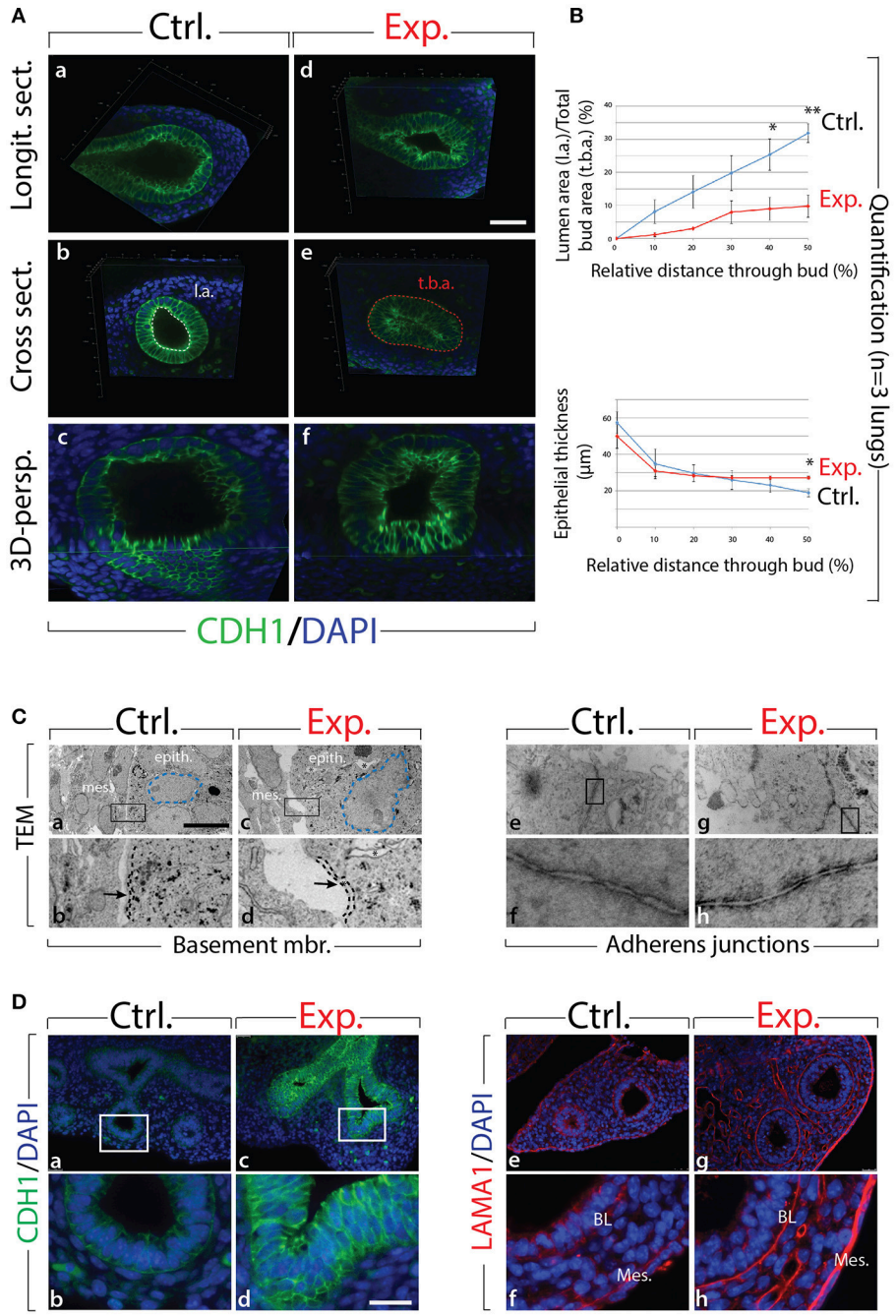

FIGURE 2 | Inhibition of FGF10 activity for 9 h in E12.5 lungs leads to collapse of the epithelial bud associated with cell rearrangements and altered cell-cell adhesion **(A)** whole-mount confocal images of distal lung buds. Control buds show open lumens and an ordered epithelial monolayer (a–c), while experimental lung buds show collapsed lumens associated with multi-layered epithelium (d–f). Please note that due to our fluorescence acquisition requirements, the intensity of the signal cannot be compared between control and experimental samples. l.a. = lumen area; t.b.a. = total bud area. *Scale bar:* (a,b,d,e) 40 µm; (c,f) 16 µm. **(B)** Quantification of relative lumen area (l.a./t.b.a.) and epithelial thickness. (Data are presented as mean ± SEM; significance determined by unpaired two-tailed Student's *t*-test; $n = 3$; **p*-value < 0.05, ***p*-value < 0.01). **(C)** TEM of distal lung buds highlighting the thickened basement membrane (black dashed line and arrows; a–d) and the darker staining around the adherens junctions (arrows; e–h) in experimental vs. control lungs. Note also the enlarged and irregularly shaped nuclei (blue dashed line; a,c) and the gaps between adjacent epithelial cells (asterisk; c,d) in experimental vs. control lungs. mes. = mesenchyme; epith. = epithelium. *Magnification:* (a,c) 7,750x; (e,g) 27800x; (b,d) 38,750x; (f,h) 139,000x. **(D)** Immunofluorescent staining for E-cadherin (CDH1) and laminin (LAMA1). E-cadherin shows increased expression in experimental lungs (c,d) compared to controls (a,b). Laminin deposition is increased in the basal lamina (BL) and mesothelium (Meso.) in experimental (g,h) vs. control lungs (e,f). *Scale bar:* (a,c) 75 µm; (b,d) 19 µm.

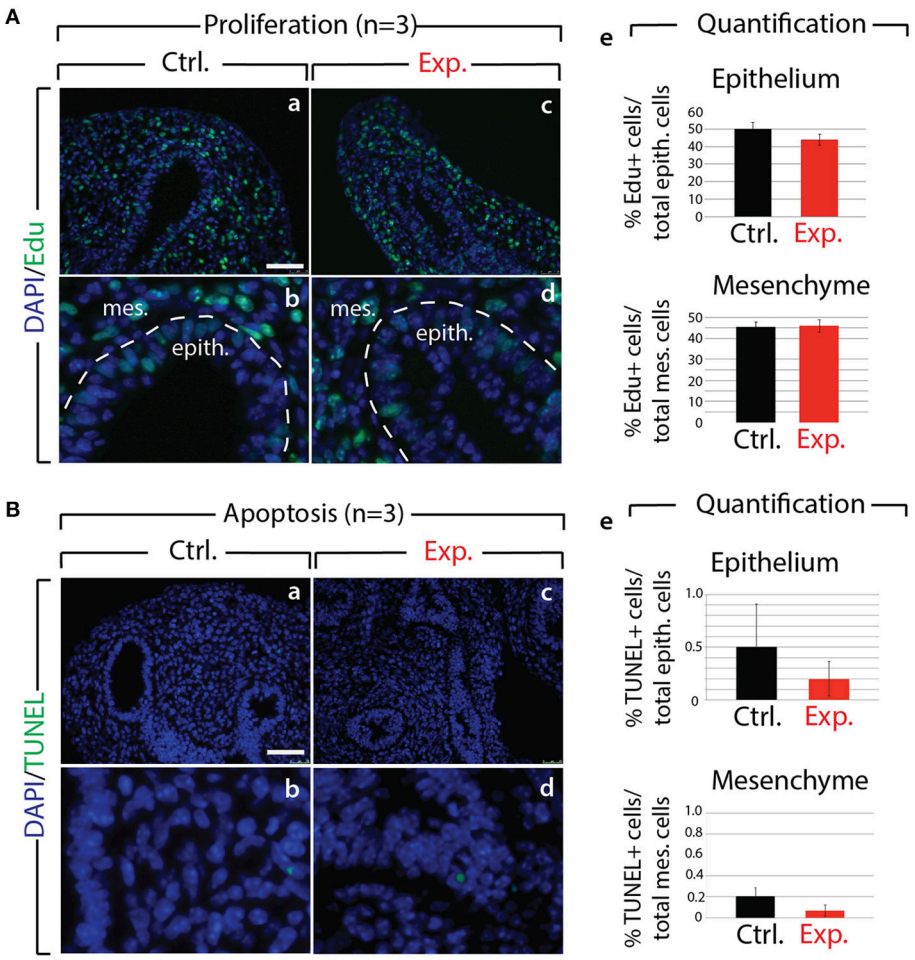

FIGURE 3 | Analysis of proliferation and cell death in control and experimental lungs **(A)** Proliferation analysis following Edu injection to pregnant females in control (a,b) and experimental (c,d) E12.5 lungs. Quantification of Edu signal indicates no major difference in the number of proliferating cells in control vs. experimental lungs (e). ($n = 3$) *Scale bar:* (a,c) 50 μm; (b,d) 17 μm. **(B)** Apoptosis analysis by TUNEL showing no major difference (e) in the number of apoptotic cells in control (a,b) vs. experimental (c,d) lungs. ($n = 3$) *Scale bar:* (a,c) 50 μm; (b,d) 17 μm.

database "Genepaint.org" to identify the expression domain of the genes found in the different groups (**Figures S3–S10**). In addition, we carried out a gene array between isolated distal tip epithelial and mesenchymal cells of E12.5 wild type lungs ($n = 3$). Our results allowed us to determine the genes differentially expressed between the two compartments (see **Figure S11A** for details). With this data, we reanalysed the genes in the Early 4, Late 4, Late 3, and Late 1 clusters according to their relative expression in the epithelium or mesenchyme. All the genes present in the Early 4 group were more highly expressed in the epithelium, supporting the idea that at this early time point, and for this group, our global transcriptomic approach was able to identify mainly epithelial specific changes.

We then compared the differential expression of the Early 4 and Late 4 genes (FGF10 signature genes), determined from the epithelium vs. mesenchyme gene array, with their expression after FGF10 inhibition (**Figures S11C,D**). Genes which are expressed at high or medial levels in the epithelium, and which are highly or moderately regulated following inhibition of FGF10 activity, should be prioritized for further investigation. Promising candidates include *Lin7a*, *Sp5*, *Tspan8*, *Cytl1*, *Pthlh*, *Sftpa1*, *Sftpc*, and *Bspry* (**Figure S11G**).

A similar analysis was performed for the Late 3 and Late 1 groups (**Figures S11E,F**), which likely contain late acting, or secondary FGF10 targets. Particularly interesting from the Late 3 group is *Wnt7b*, as we have previously demonstrated that an FGF10/WNT7b loop regulates repair in conducting airways following naphthalene injury (Volckaert et al., 2011, 2017). Equally interesting in this group is the down-regulation of genes expressed preferentially in the mesenchyme and involved in Hedgehog signaling (*Foxl1*, *Foxf1*, *Gli1*, and *Ptch2*), which suggests our array captures one of the best-known epithelial-mesenchymal interactions: the FGF10-SHH interaction (reviewed in Warburton et al., 2008, 2010).

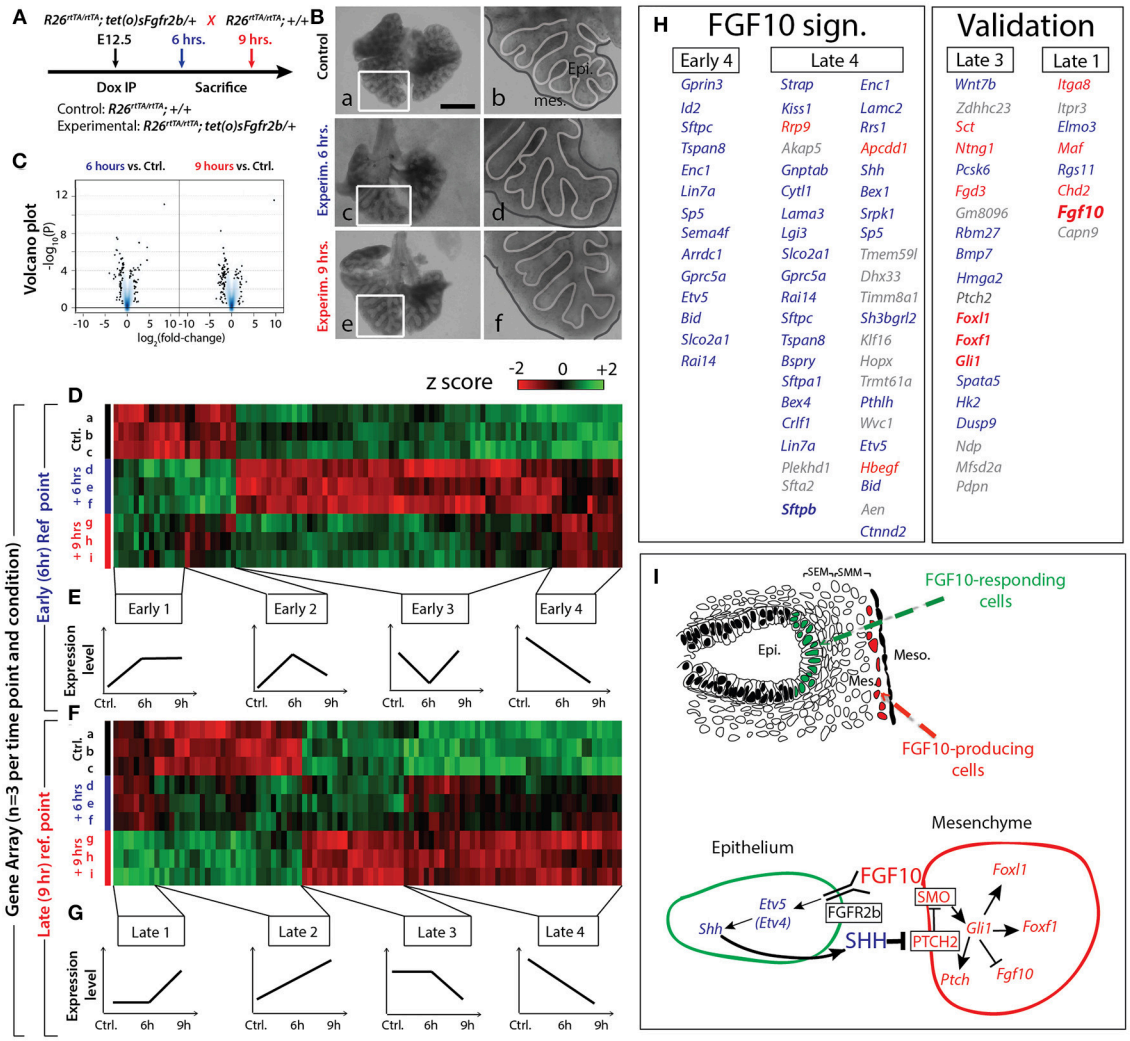

J KEGG analysis at E12.5 (DoxIP+6 hrs vs. control)

	KEGG name	n GenesInSet	n expr. genes	*p* value
Cellular processes	Peroxisome	80	62	0,00861
	Lysosome	123	106	0,02259
	Cell Cycle	124	110	0,03108
	P53 signaling pathway	68	55	0,03661
	Focal adhesion	201	154	0,05589
Environment. info. process.	Cytokine-cytokine receptor int.	179	88	0,00031
	Calcium signaling pathway	87	59	0,00787
	Wnt signaling pathway	146	71	0,00876
	Hedgehog signaling pathway	275	59	0,01179

KEGG analysis at E12.5 (DoxIP+9 hrs vs. control)

	KEGG name	n GenesInSet	n expr. genes	*p* value
Cellular processes	Focal adhesion	201	155	1.40E-05
	Lysosome	123	105	0,00028
	Endocytosis	217	169	0,00088
	Peroxisome	80	63	0,00105
	Cell cycle	124	110	0,02304
	Phagosome	170	101	0,02569
	Regulation of actin cytoskeleton	216	152	0,04386
Environment. info. process.	Calcium signaling pathway	179	88	1.17E-05
	ECM-receptor interaction	87	59	2.00E-05
	Cell adhesion molecules (CAMs)	146	71	5.61E-05
	Neuroactive ligand-receptor int.	275	59	0,00107
	ABC transporters	45	29	0,00450
	Cytokine-cytokine receptor int.	238	100	0,01277
	Hedgehog signaling pathway	55	38	0,02436
	MAPK signaling pathway	268	189	0,02677
	Wnt signaling pathway	153	121	0,04889

FIGURE 4 | Identification of early FGF10 target genes by a gene array approach **(A)** E12.5 littermate control and experimental lungs were collected 6 or 9 h after a single Dox-IP injection to pregnant females. **(B)** FGFR2b signaling attenuation leads to visible branching defects at Dox-IP+9 h (increased mesothelial-epithelial distance and branching inhibition). Meso.=Mesothelium; Epi.=Epithelium. *Scale bar:* (a,c,e) 500 μm; (b,d,f) 175 μm. **(C)** Volcano plots showing genes which are either down- or up-regulated at 6 or 9 h Dox-IP compared to the time-matched control lungs. **(D)** Heatmap of the top 100 genes differentially expressed between

(Continued)

FIGURE 4 | experimental and control lungs at 6 hrs (based on *p*-values). **(E)** Four classes of genes, grouped according to expression pattern (Early 1–4). **(F)** Heatmap of the top 100 genes differentially expressed between experimental and control lungs at 9 h (based on *p*-values). **(G)** Four classes of genes, grouped according to expression pattern (Late 1–4). **(H)** Genes identified in the Early 4 and Late 4 clusters are direct targets of FGF10 signaling and comprise the "FGF10 gene signature." Many genes in the Late 3 and Late 1 clusters are involved in the FGF10/SHH regulatory feedback loop (see **I**), validating the gene array approach (note the presence of *Fgf10* in the Late 1 cluster). Genes enriched in the epithelium or mesenchyme are color coded in blue or red, respectively. **(I)** Reconstitution of the FGF10-FGFR2b-ETV4/5-SHH-FGF10 signaling axis from the gene array. **(J)** KEGG results for 6 and 9 h Dox-IP vs. control. [**(D,F)** $n = 3$; see *Materials and Methods* for details on the statistical analysis of gene arrays].

Shh is an epithelial gene encoding a secreted growth factor, and was down-regulated in our array concomitantly with *Etv4* and *Etv5*, beginning 6 h after FGF10 inhibition (Late 4). The combined decrease of *Etv4* and *Etv5* was likely causative for the loss of *Shh* (Herriges et al., 2015; see Discussion). Following the decrease in *Shh* expression, the mesenchymal-specific Hedgehog signaling genes *Foxl1*, *Foxf1*, *Gli1,* and *Ptch2* all showed a delayed down-regulation (only between 6 and 9 h). Furthermore, as SHH is known to regulate *Fgf10* transcription in the mesenchyme (Bellusci et al., 1997a; Lebeche et al., 1999), we also determined if *Fgf10* expression was affected by *Shh* down-regulation. We found that the Late 1 cluster, containing genes up-regulated between experimental and control at 9 h, but not at 6 h, contained *Fgf10*. Taken together, this evidence functionally validates our gene array, and leads to the model proposed in **Figure 4I**.

Identification of Lung-Specific Transcription Factors Controlled by FGF10

Next, we evaluated the expression of the major transcription factors expressed in the lung at E12.5. A previous report indicated that out of 1100 transcription factors analyzed (covering 90% of all transcription factors encoded in the mouse genome), only 62 exhibited localized expression in the epithelium and/or mesenchyme of the developing lung (Herriges et al., 2012). Of these 62 genes, from our gene array, 17 were either induced or repressed with significance in experimental vs. control lungs at 6 or 9 h ($n = 3$; **Figure 5A**). From these 17, 11 were exclusively or predominantly expressed in the epithelium (**Figure 5B** shows the expression of some of these genes in the developing lung by *in situ* hybridization). Among the repressed genes in the epithelium, we found early regulation of genes such as *Etv4* and *Etv5* (belonging to the TF1 cluster), delayed regulation of *Sox9* (belonging to the TF2 cluster), as well as transiently regulated genes such as *Grhl2*, *Nkx2-1,* and *Id2* (from the TF3 cluster). These "repressed" genes are likely direct targets of FGF10, required to elicit the different facets of FGF10 activity. Among the induced genes in the epithelium, we found the early regulation of *Sox2* (forming the TF4 cluster), the transiently regulated genes *Nkx1–2* and *Pitx2* (from the TF5 cluster), and the late regulation of *Lmo1* and *Elf5* (from cluster TF6). These "induced" genes are likely repressed by FGF10 during early lung development.

FGF10/FGFR2b Signaling Is Required to Maintain the Differentiation Status of the Epithelial Multipotent Progenitors

Next, we examined the impact of attenuated FGFR2b signaling on the differentiation of the multipotent epithelial progenitor cells. **Figure 5C** confirms the reduced expression of SOX9 distally in experimental (d–f) vs. control (a–c) lungs at 9 h post Dox-IP. In control lungs, SOX2 expression in the proximal epithelium established a clear boundary between proximal and distal regions (**Figure 5Cg–i**). However, in experimental lungs, SOX2 expression in the proximal epithelium expanded more distally, showing a salt and pepper expression pattern with increased expression in the mesenchyme around the conducting airway (**Figure 5Cj–l**).

Until recently, the close examination of epithelial tip cell differentiation was limited, as only a few signature genes denoting differentiation status were known to be expressed in those cells. However, this limitation has been overcome after a paradigm-shifting paper published by Treutlein et al. (2014), which used single cell transcriptomic approaches to characterize the genetic signatures of lung distal epithelial cells at E14.5, at E16.5, and at E18.5. The authors proposed a list of specific markers for alveolar epithelial cell type I (AT1) and type II (AT2) cells, and showed that a common progenitor cell, called a bipotent progenitor, expressed markers of both cell types. Our gene array data shown in **Figure 4** indicate that some of these markers of differentiation (*Sftpc, Etv5, Sftpa1, Sftpb, Hopx, Pdpn*) are actually regulated by FGF10 in multipotent epithelial progenitors. In order to probe more extensively the status of these differentiation markers in the epithelial tip cells, we assessed the AT1 and AT2 signatures from our gene array (experimental vs. control) at the 9 h time point. **Figure 5D** shows a clear global reduction in the markers characteristic of the AT2 signature, with minimal change in the AT1 signature. Gene set analysis confirms a very significant difference in the AT2 signature in experimental vs. control lungs ($n = 3$; $p = 0.000004$). No significant change was observed in the AT1 signature. We therefore conclude that upon inhibition of FGF10, the tip epithelial cells, which include the progenitors for the bipotent cells, lose expression of the markers characteristic of the AT2 signature, and that globally the expression of these genes is under the control of FGF10.

Connecting FGF10 and ß-Catenin Signaling

Our KEGG analysis indicated that WNT signaling was also significantly regulated by FGF10 inhibition (**Figure 4J**), in particular, those genes involved in the canonical WNT pathway ($n = 3$; **Figure 6B**). Of note, *Wnt7b*, which codes for a growth factor secreted by the epithelium and acting on the mesenchyme, appears highly regulated by FGF10 (**Figure 6B**; see also **Figure S11E**). Downstream targets of WNT7b, such as the transcription factors *Lef1* and *Tcf7*, were also transcriptionally down-regulated. To confirm the down-regulation of WNT signaling in experimental lungs at the protein level, we examined

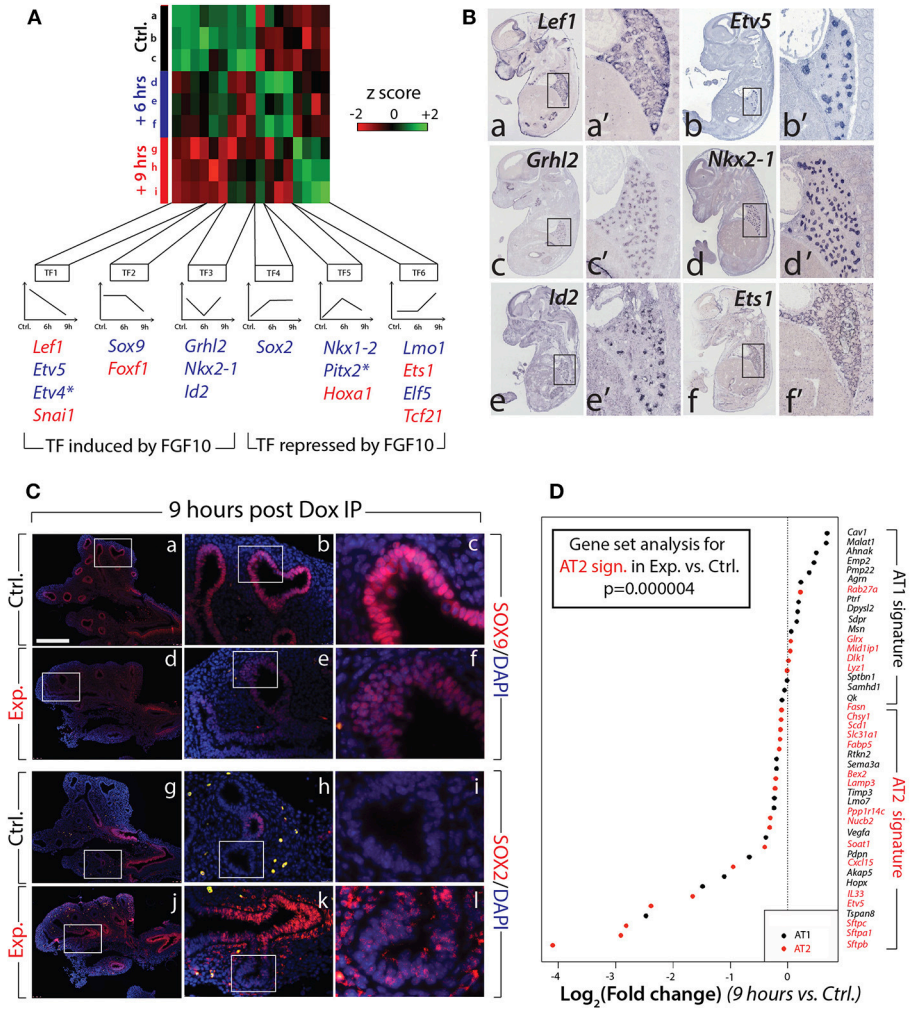

FIGURE 5 | Identification of the transcription factors regulated by FGF10 and impacts on epithelial differentiation **(A)** Heatmap of highly regulated transcription factors between control, Dox-IP+6 h and Dox-IP+9 h conditions. Six classes of transcription factors (TF1-6) were identified based on their expression profiles. Genes in blue and in red are preferentially expressed in the epithelium and mesenchyme, respectively (asterisks denote genes found in both compartments). **(B)** *In situ* hybridization on E14.5 lungs for *Lef1* (a,a'), *Etv5* (b,b'), *Grhl2* (c,c'), *Nkx2-1* (d,d'), *Id2* (e,e''), and *Ets1* (f,f''). **(C)** Validation by IF of changes in SOX9 (a–f) and SOX2 (g–l) expression in experimental vs. control lungs. *Scale bar:* (a,d,g,j) 300 μm; (b,e,h,k) 100 μm; (c,f,i,l) 33 μm. **(D)** Expression of AT1 and AT2 markers in 9 h vs. control lungs. Note the significant global reduction in the expression of the AT2 markers. ($n = 3$; see *Materials and Methods* for details on the statistical analysis of gene sets).

by immunofluorescence the levels of the transcriptionally active form of CTNNB1 (ß-catenin) and the transcription factor LEF1 (**Figure 6A**). A loss of expression of activated ß-catenin was observed in both the epithelium and mesenchyme of experimental lungs (**Figure 6Aa–d**). In addition, LEF1 was also lost in the mesenchyme, correlating with the decrease in *Wnt7b* expression (**Figure 6Ae–h**).

Given that WNT/ß-catenin signaling is vital for proper branching morphogenesis and cellular differentiation (for a review see De Langhe and Reynolds, 2008) and that we observed a drastic reduction in activated ß-catenin in our experimental lungs, we investigated the degree to which the effect of inhibiting FGF10 was mediated through WNT/ß-catenin signaling. We made use of a pharmacological inhibitor of ß-catenin transcriptional activity, called IQ1. This inhibitor decreases the interaction between ß-catenin and one of its transcriptional coactivators, EP300, and has been shown to disrupt branching morphogenesis, and proximalize the lung epithelium, during the pseudoglandular stage of lung development (Sasaki and Kahn, 2014).

Figures 6C–E shows the results of inhibiting, *in vitro*, the ß-catenin/EP300 interaction for 24 h in E12.5 lung explants. While control lung explants displayed continued branching over this time (**Figure 6Ca–d**), the experimental lungs failed to branch, forming instead long epithelial tubes (**Figure 6Ce–h**). The failure of experimental lungs to branch, as well as the relative area of the epithelial surface and the distance between the distal epithelium and mesothelium, is quantified in **Figure 6D** ($n =$ 3 for control

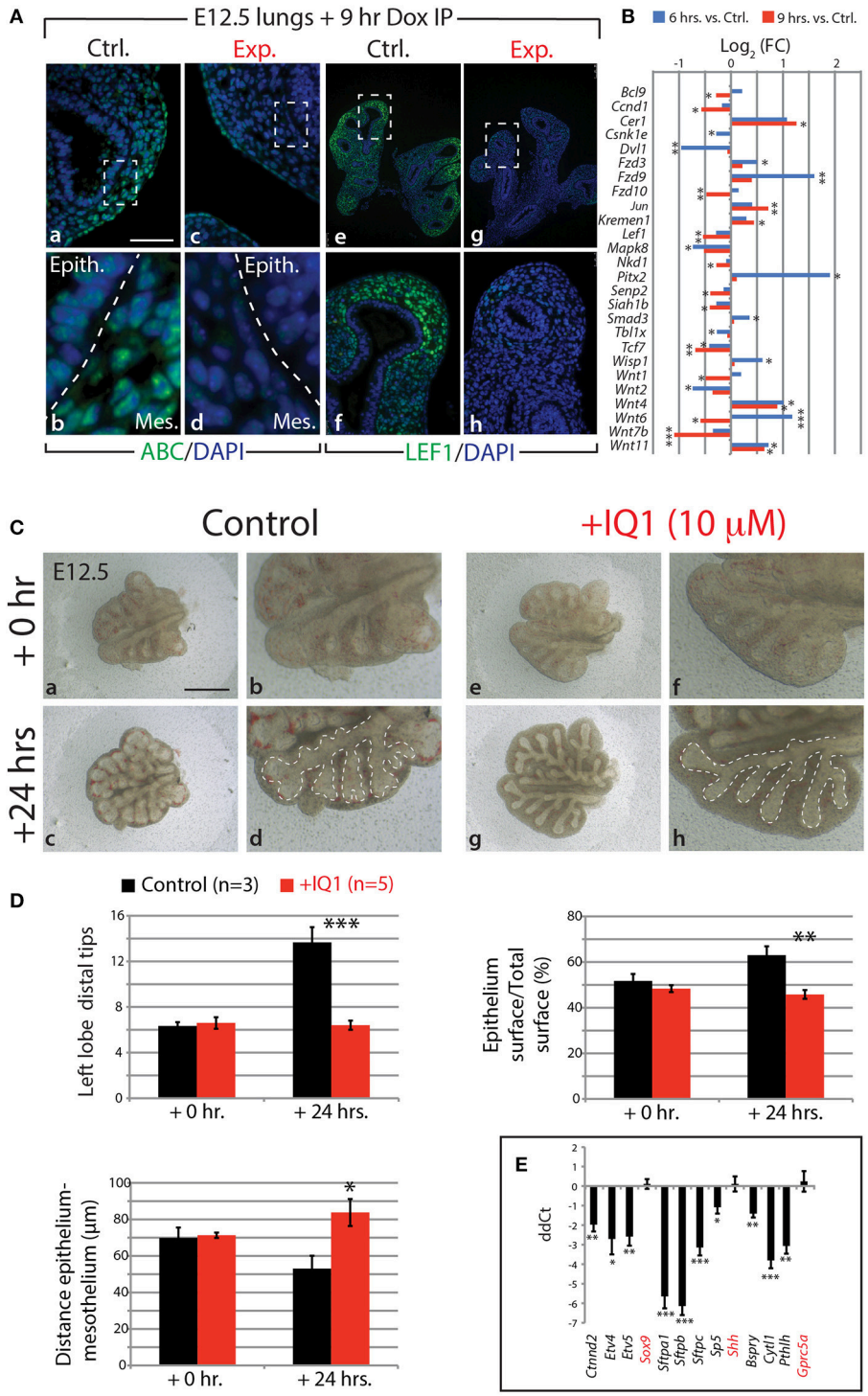

FIGURE 6 | FGF10 activity is primarily mediated through ß-catenin/EP300 **(A)** IF for transcriptionally active ß-catenin (ABC) and for LEF1 in control and experimental lungs. *Scale bar:* (a,c) 50 μm; (b,d) 15 μm; (e,g) 300 μm; (f,h) 75 μm. **(B)** Gene expression changes in the canonical WNT pathway at 6 and 9 h vs. controls. ($n = 3$; see *Materials and Methods* for details on the statistical analysis of gene arrays; **p*-value < 0.05, ***p*-value < 0.01, ****p*-value < 0.001). **(C)** E12.5 lungs cultured with (experimental) or without (control) IQ1 for 24 h. Note the similarity to FGF10 inhibition on the branching in experimental lungs. *Scale bar:* (a,c,e,g) 500 μm; (b,d,f,h) 250 μm. **(D)** Quantification of branching defects in experimental vs. control lungs. **(E)** qPCR analysis on a subset of the "FGF10 gene signature." Except for *Sox9*, *Shh*, and *Gprc5a*, inhibition of ß-catenin/EP300 produces a similar down-regulation of genes as in FGF10 inhibition. [**(D,E)** Data are presented as mean ± SEM; significance determined by unpaired two-tailed Student's *t*-test; $n = 3$ for control and $n = 5$ for experimental; **p*-value < 0.05, ***p*-value < 0.01, ****p*-value < 0.001].

and $n = 5$ for experimental). These phenotypic impacts are very similar to those seen by blocking FGF10 *in vitro* (see for comparison **Figure 1Dk–m**).

We also compared, by qPCR, the expression levels of a number of genes found in the "FGF10 gene signature" between experimental and control lung explants ($n = 3$ for control and $n = 5$ for experimental; **Figure 6E**). Ten of the 13 genes assessed showed drastic reductions in expression in IQ1 treated lung explants, similar to the down-regulation seen in our *in vivo* inhibition of FGF10. Interestingly, the transcription factor *Sox9*, as well as *Shh*, showed no change in expression between control and experimental lungs at this time point, indicating, perhaps, compensatory mechanisms.

In the attempt to produce results more comparable to the 9 h *in vivo* inhibition of FGF10, we also conducted a 9 h inhibition of the ß-catenin/EP300 interaction (**Figure 7**). While the branching defects, after this time point, were less pronounced than those seen in either the 24 h IQ1 treatment, or the 9 h *in vivo* FGF10 inhibition (**Figure 7Ae–h**), noticeable effects on the relative epithelial surface and the distance between distal epithelium and mesothelium could be observed ($n = 6$; **Figure 7B**). We also conducted a gene array on control vs. IQ1 treated lung explants after 9 h of inhibition ($n = 2$ for control and $n = 3$ for experimental). A gene set analysis using the "FGF10 gene signature" revealed that this set of genes was significantly down-regulated in IQ1 treated lung explants ($p < 0.001$; **Figure 7C**). Finally, immunofluorescent stains for SOX9 and SOX2 protein revealed a decrease in SOX9 expression (**Figure 7Dd–f**), and a concomitant advancement of SOX2 expression distally (**Figure 7Dj–l**), reminiscent of the proximalization of lung epithelium after 9 h of FGF10 inhibition (see **Figure 5C**).

In summary, our data suggest that a large proportion of the regulation by FGF10 signaling of epithelial branching morphogenesis and differentiation is mediated specifically through ß-catenin/EP300 transcriptional activity.

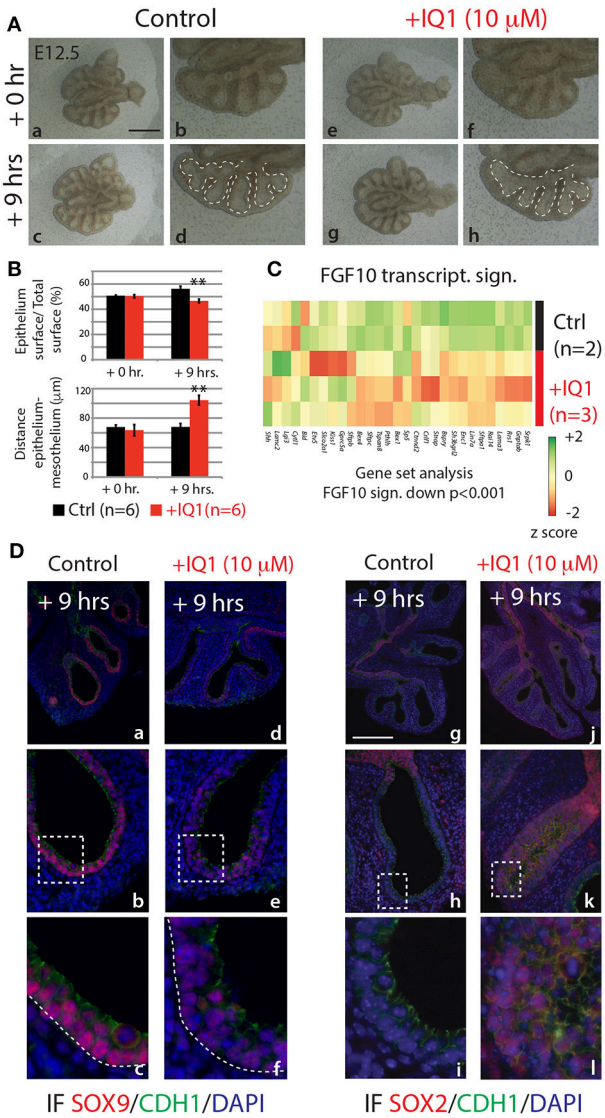

FIGURE 7 | IQ1 treatment for 9 h phenocopies 9 h FGF10 inhibition **(A)** E12.5 lungs cultured with (experimental) or without (control) IQ1 for 9 h. *Scale bar:* (a,c,e,g) 500 μm; (b,d,f,h) 250 μm. **(B)** Quantification of branching defects showing a decreased relative epithelial surface and a concomitant increase in the distance between the epithelium and mesothelium. (Data are presented as mean ± SEM; significance determined by unpaired two-tailed Student's *t*-test; $n = 6$; $^{**}p$-value < 0.01). **(C)** A heatmap of IQ1 lungs treated for 9 h vs. control showing the "FGF10 gene signature." A gene set analysis demonstrates the significant down-regulation of this group of genes ($n = 2$ for control and $n = 3$ for experimental; see *Materials and Methods* for details on the statistical analysis of gene sets). **(D)** IF for SOX9 (a–f) and for SOX2 (g–l). *Scale bar:* (a,d,g,j) 300 μm; (b,e,h,k) 75 μm; (c,f,i,j) 45 μm.

Discussion

In this paper, we report the impacts on the epithelial tip cells of E12.5 lungs by blocking FGFR2b ligands, primarily FGF10. Both *in vivo* and *in vitro* experiments inhibiting FGF10 resulted in arrested epithelial branching and collapsed distal bud lumens associated with abnormal cellular adhesion. Gene arrays at 6 and 9 h inhibition revealed the transcriptomic regulation of FGFR2b signaling. From these arrays, we identified an FGF10 gene signature primarily composed of genes enriched in the epithelium and positively regulated by FGF10. We also highlighted a set of lung-specific transcription factors significantly regulated by FGF10. Our data on SOX9 and SOX2 expression, as well as gene-set analyses on differentiation markers of AT2 cells, which are found to be expressed in multipotent epithelial progenitor cells, demonstrated the proximalization of the tip epithelium and a loss of distal differentiation markers 9 h after FGF10 inhibition. Finally, the effects of blocking FGF10 signaling on ß-catenin activity were assessed. *In vitro* experiments using IQ1, a pharmacological inhibitor of the ß-catenin/EP300 interaction, were able to phenocopy a large proportion of the impacts found by FGF10 inhibition, suggesting that FGF10 signaling on E12.5 distal tip progenitors is significantly mediated via ß-catenin/EP300. These findings are summarized in a model of FGF10 signaling during pseudoglandular lung development provided in **Figure 8**.

Validation, and Limitations, of *in vivo* Inhibition of FGF10 Signaling

One of the major limitations of our *in vivo* model to inhibit FGF10 signaling during pseudoglandular lung development (E12.5) is that the production of soluble FGFR2b is global, potentially inducing secondary effects. Furthermore, soluble FGFR2b is secreted into the mesenchyme, potentially inhibiting mesenchyme-specific FGF signaling. Indeed, we have recently reported that FGF10 can directly act on the rat lung mesenchyme during the late canalicular/early saccular stage (E19) to control the differentiation of lipofibroblast progenitors (Al Alam et al., 2015). Although we could not detect any significant increase in P-ERK on primary culture of lung mesenchyme isolated at the mid-pseudoglandular stage (E14.5; De Langhe et al., 2006), we cannot exclude that FGF10 is active on discrete mesenchymal subpopulations throughout the pseudoglandular stage.

To control for the potential secondary effects of our model, we validated the location of FGF10's primary targets by a gene array comparing expression of genes in the epithelium vs. mesenchyme of E12.5 wild type lungs (**Figure S11**), and also by the online expression-profiling database "genepaint.org" (**Figures S3–S10**). We are confident that our global *in vivo* approach does indeed detect the impacts of FGF10 signaling on epithelial-specific targets.

Furthermore, we assessed the well-established FGF10-SHH regulatory feedback loop during lung development as a means of validating our array (**Figures 4H,I**). Our array detects the down-regulation of *Shh* within 6 h of FGF10 inhibition, and also the delayed impacts on the downstream targets of SHH at 9 h, including the up-regulation of *Fgf10*. Additionally, our array supports the recently reported data showing that the inactivation of FGF-regulated *Etv4* and *Etv5* in the multipotent epithelial progenitor cells during lung development leads to the loss of *Shh* expression (Herriges et al., 2015). We therefore propose that FGF10 acts via FGFR2b, positively regulating the expression of ETV4/ETV5, and, subsequently, the SHH pathway.

FGF10 Primary Targets

From our gene array data, we identified an "FGF10 gene signature." These genes, primarily enriched in the epithelium, show decreased expression shortly after FGF10 inhibition, and continue to decrease during inhibition; therefore, these genes likely represent primary targets of FGF10, and are potential key mediators of FGF10/FGFR2b signaling.

We also found that FGF10 regulates many previously identified lung specific transcription factors (Herriges et al., 2012). Some of these transcription factors are established mediators of FGF10 signaling (e.g., *Etv4*, *Etv5*, *Sox9*), whereas little is known of the others in the context of FGF10 signaling. Knock-out and over-expression studies on many of these transcription factors show impacts very similar to the effects seen in our study. For example, Metzger et al. (2007, 2008a) found that *Elf5* (group TF6, **Figure 5**) is regulated by FGF10 and FGF7, and that over-expression of *Elf5* leads to branching defects and delayed AT2 differentiation; Quaggin et al. (1999) reported that *Tcf21* (group TF6) knock-out mice display reduced branching, smaller lungs, and a proximalization of lung epithelium at E14.5; finally, Varma et al. (2012) studied the transcription factor *Grhl2* (group TF 3, **Figure 5**) during lung development, and found that GRHL2 controls cell adhesion and migration, forms a positive feedback loop with NKX2-1 during branching morphogenesis, and is associated with proper AT2 differentiation.

We propose that the comprehensive set of target genes and transcription factors identified in our study is a valuable resource for future investigations on early lung branching morphogenesis and differentiation.

FGF10's Regulation of Tip Cell Differentiation and Morphology via SOX9

Sustained SOX9 expression in the tip epithelium of the developing lung has been associated with epithelial stem cell self-renewal. The current model predicts that individual tip cells, under the influence of FGF10, are prone to remain in the tip domain; as these cells divide, some of the daughter cells acquire bronchial progenitor characteristics associated with the exit from the tip domain.

The transcription factor SOX9 has been extensively studied during early lung development (Perl et al., 2005; Chang et al., 2013; Rockich et al., 2013). For example, Chang et al. (2013) found that knocking out *Sox9* before E12 leads to branching defects, an increase between the distal epithelium and mesothelium, and smaller lungs. Furthermore, it was found that FGFR2b signaling regulates *Sox9*, and that SOX9 suppresses the initiation of alveolar differentiation. Rockich et al. (2013) found similar findings, and also assessed the impacts on cell adhesion in *Sox9* loss-of-function E14.5 lungs. Using TEM, the authors found multiple cellular defects similar to what we found in our *in vivo* dominant negative model, including: irregularly shaped epithelial cells, gaps with protruding pseudopodia between adjacent cells, partial to complete loss of microvilli, and a disjointed basement membrane filled with gaps.

As SOX9 is lost in the distal epithelial cells of experimental lungs, the expression of SOX2 in these cells increases, further suggesting these cells are losing their multipotency, and are adopting a proximal fate. This idea is supported by the evidence, at this stage, of a loss of the AT2 signature in the multipotent progenitors upon FGF10 inhibition.

Taken together, our data suggest that the loss of SOX9, downstream of FGF10 signaling, affects the morphogenesis and multipotent potential of distal epithelial cells.

FGF10 Regulation of ß-Catenin Levels

The importance of ß-catenin signaling during pseudoglandular branching morphogenesis has been extensively studied (reviewed in De Langhe and Reynolds, 2008). In our dominant negative *in vivo* model, transcriptionally active ß-catenin was greatly reduced in experimental lungs after 9 h inhibition (**Figure 6**). Since *Ctnnb1* gene expression was unaltered in our gene array, the drastic decrease in activated ß-catenin was likely a result of post-translational modifications, such as altered phosphorylation and/or reduced cytoplasmic pools of available ß-catenin.

An intriguing possibility concerning available cytoplasmic ß-catenin is the relationship between ß-catenin and CTNND2,

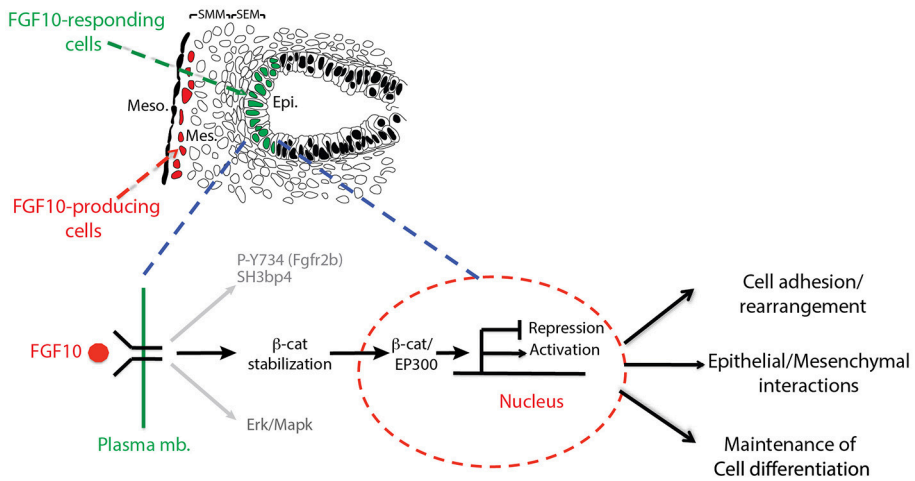

FIGURE 8 | Graphical summary: FGF10 signaling leads to phosphorylation of Y734 on FGFR2 associated with Sh3bp4 recruitment (Francavilla et al., 2013). FGF10 signaling also induces Erk/Mapk phosphorylation and stabilizes ß-catenin, promoting its translocation to the nucleus where it binds to EP300, acting as a transcriptional regulator. The resulting activated (FGF10 transcriptomic signature) and/or repressed genes in turn control cell adhesion/rearrangement, contribute to epithelial/mesenchymal interactions, and maintain distal tip differentiation.

which regulate E-cadherin stability at the adherens junction complex of epithelial cells. While ß-catenin stabilizes E-cadherin to promote cell adhesion, CTNND2 leads to E-cadherin destabilization, the release of ß-catenin to the cytoplasm, and cell motility (Lu et al., 1999; Kim et al., 2012). Indeed, high levels of stable E-cadherin have been shown to inhibit budding and branching morphogenesis in isolated embryonic lung epithelium (Liu et al., 2008). Once ß-catenin is released from E-cadherin, it contributes to the pool of transcriptionally active ß-catenin (Kam and Quaranta, 2009). With reduced CTNND2, levels of E-cadherin remain relatively high, and ß-catenin becomes sequestered at the adherens junction, being removed from the transcriptionally active pool. Thus, E-cadherin destabilization by CTNND2 regulates proper branching morphogenesis and the cytoplasmic availability of ß-catenin. Interestingly, loss of *CTNND2* in humans is associated with the "Cri du chat" syndrome (Medina et al., 2000), wherein affected babies may develop breathing problems at birth and require respiratory treatments. Additionally, a high rate of lung infection is also common during the first years of life. In the future, it will be important to delineate the impact of loss of CTNND2 on the formation and maturation of the lung epithelium in the context of homeostasis, as well as repair after injury.

Our data support the importance of the proposed CTNND2/CDH1/CTNNB1 regulatory axis. Contained in the FGF10 gene signature is the drastic reduction of *Ctnnd2* (group Late 4, **Figure 4H**), while E-cadherin is greatly increased in experimental lungs (**Figure 2D**), which could explain to an appreciable degree not only the morphological defects, but also the lack of activated ß-catenin seen in these samples.

FGF10 Regulation via ß-Catenin/EP300

In the nucleus, ß-catenin associates with a number of transcriptional co-activators to regulate gene expression via the TCF/LEF family of DNA-bound transcription factors (reviewed in Hoppler and Kavanagh, 2007). Two of these co-activators, CBP and EP300, are critical for balancing cellular differentiation and branching morphogenesis (Miyabayashi et al., 2007; Sasaki and Kahn, 2014). Through the use of a pharmacological inhibitor of the ß-catenin/EP300 interaction, IQ1, Sasaki and Kahn (2014) report numerous impacts on pseudoglandular stage lungs, including arrested branching and an increase between the distal epithelium and adjacent mesothelium, similar to what we found in our *in vivo* inhibition of FGF10 (compare **Figures 1C**, **6C**). Furthermore, Sasaki and Kahn (2014) show that inhibiting ß-catenin/EP300 leads to the proximalization of lung epithelium via a reduction in distal marker expression (*Bmp4* and *Fgf10*), and an increase in the proximal markers *Sox2* and *Scgb1a1*. In our 24 h IQ1 inhibition experiment, we likewise found a number of distal marker genes down regulated, including *Etv4*, *Etv5*, *Sftpa1*, *Sftpb*, and *Sftpc* (see **Figure 6E**). Interestingly, *Sox9* showed no change in expression between control and experimental lungs at this time point. In our 9 h IQ1 inhibition experiment, we were able to detect significant overall down regulation of the FGF10 gene signature, although some of the individual genes showed little regulation at this time point (see **Figure 7C**). This suggests that not all the genes regulated in our *in vivo* inhibition of FGF10 are similarly regulated by inhibiting ß-catenin/EP300. Furthermore, staining for SOX9 and SOX2 supports the idea that ß-catenin/EP300 sustains the multipotency of distal epithelial cells (see **Figure 7D**). This data is in line with a recent report showing that ß-catenin deletion in the SOX9-positive cells leads to ectopic expression of SOX2 (Ostrin et al., 2018).

In summary, the *in vitro* inhibition of ß-catenin/EP300 produces branching defects and the proximalization of epithelial cells as early as 9 h. Phenotypically, these impacts greatly overlap with the impacts of inhibiting FGF10 signaling. Many of the

direct targets of FGF10 signaling are similarly regulated by ß-catenin/EP300, suggesting that FGF10 regulation is significantly mediated through ß-catenin/EP300.

In conclusion, we have carried out a comprehensive analysis of FGF10/FGFR2b signaling on epithelial tip progenitor cells during E12.5 mouse lung development. This analysis revealed a new "FGF10 transcriptomic signature" which will be instrumental in designing new mechanistic studies concerning the role of FGF10 in alveolar epithelium formation during development, as well as maintenance during homeostasis and repair after injury.

MATERIALS AND METHODS

Contact for Reagent and Resource Sharing

Further information and requests for resources and reagents should be directed to, and will be fulfilled by, the corresponding author, Dr. Saverio Bellusci (saverio.bellusci@innere.med.uni-giessen.de).

Experimental Model and Subject Details

Ethical Statement and Husbandry

Animal experiments were performed at Children's Hospital Los Angeles under the research protocols (31–08 and 31–11) approved by the Animal Research Committee and in strict accordance with the recommendations in the Guide for the Care and Use of Laboratory Animals of the National Institutes of Health. The approval identification for Children's Hospital Los Angeles is AAALAC A3276-01. Harvesting organs and tissues from wild type and mutant mice following euthanasia using pentobarbital was approved at Justus Liebig University Giessen by the federal authorities for animal research of the Regierungspraesidium Giessen, Hessen, Germany (Approved Protocol GI 20/10 Nr. G 84/2016).

All mice used to generate experimental and control embryos were housed in a specific pathogen free (SPF) environment with free access to food and water. Up to five females were housed together, while males were housed singly. Females between 9 and 12 weeks of age were used to generate embryos.

In vivo Mouse Model to Inhibit FGFR2b Ligands

In vivo studies were conducted using an inducible dominant negative mouse model: *Rosa26*$^{rtTA/+}$; *tet(o)sFgfr2b/+* (B6-Cg-Gt(ROSA)26Sor$^{tm1.1(rtTA,EGFP)Nagy}$ Tg(tetO-Fgfr2b/lgh)1.3Jaw/sbel). This mouse model employs a reverse tetracycline transactivator (rtTA) under the transcriptional control of the ubiquitous *Rosa26* locus. Upon administration of doxycycline, the rtTA is able to bind to the tetracycline operator (tetO), inducing the transcription of a soluble dominant negative form of *Fgfr2b* (*sFgfr2b*). These mice were generated by crossing *Rosa26*$^{rtTA/+}$ (*Gt(ROSA)26Sor*$^{Tm1.1(rtTA,EGFP)Nagy}$) with *tet(o)sFgfr2b/+* mice (Tg(tetO-Fgfr2b/Igh)1.3Jaw, obtained from Dr. Jeffrey Whitsett, Cincinnati, USA). Experimental (*Rosa26*$^{rtTA/rtTA}$; *tet(o)sFgfr2b/+*) and littermate control (*Rosa26*$^{rtTA/rtTA}$; *+/+*) embryos were generated by crossing *Rosa26*$^{rtTA/rtTA}$; *tet(o)sFgfr2b/+* and *Rosa26*$^{rtTA/rtTA}$; *+/+* animals.

Timed-pregnant females were used to conduct *in vivo* experiments. Doxycycline was administered either through food (625 mg doxycycline/kg food pellets), or via an intraperitoneal injection (i.p.; Dosage: 0.0015 mg doxycycline/g mouse weight) at the desired embryonic time point (E), where E0.5 was assumed to be noon on the day a vaginal copulation plug was found. At a determined time post-doxycycline i.p., a lethal dose of pentobarbital sodium was administered to animals via i.p. (Dosage: 0.4 mg pentobarbital/g mouse weight). After breathing ceased and a lack of pupil response to light was observed, cervical dislocation was performed to ensure death. Embryos were then harvested and washed in PBS with gentle shaking for ∼2 min. Embryonic lungs were then dissected and prepared for subsequent analyses.

In vitro Lung Culture

Embryonic lungs used for *in vitro* experiments were obtained either from genetically modified embryos generated as described above, or from C57BL/6 wild-type embryos.

Embryonic lungs were dissected and cultured on 13 mm Whatman Track-Etch polycarbonate membranes, with 8.0 μm pores (Merck, Darmstadt, Germany) positioned atop DMEM culture medium in a 24-well culture dish [medium contained: Dulbecco's Modified Eagle Medium (1x DMEM), supplemented with D-Glucose, L-Glutamine, HEPES, Pyruvate, and Phenol red (Gibco, Paisley, UK), 10% fetal bovine serum (FBS), 1% penicillin (10,000 units/ml)-streptomycin (10 mg/ml)]. Lungs were incubated at 5% CO_2 and 37°C for ∼45 min to allow them to settle. At the beginning of the experiment ($t = 0$ h.), doxycycline dissolved in PBS (1 μg/ml) or IQ1 dissolved in DMSO (10 μM; Selleckchem, Munich, Germany) was added to the experimental lungs, while the vehicle (either PBS or DMSO) was added to control samples. Lungs were incubated at 5% CO_2 and 37°C for the duration of the experiment.

Method Details

Still and Live Image Acquisition

Brightfield images of lungs from *in vivo* and *in vitro* experiments were captured either on a Leica MZ 125 stereoscopic dissecting microscope using a Spot Insight 2.0 Mp Color Mosaic camera and Spot 4.5.9 imaging software, or were obtained from live imaging experiments using a Leica DM6000B inverted microscope, DFC 305FX camera, and Leica Application Suite Advanced Fluorescence imaging software.

Separation of Mesenchyme and Epithelium to Assess Relative Gene Expression in the Distal Tips Via Microarray

To assess the expression of genes in the epithelial and mesenchymal compartments of distal E12.5 lung tips, C57BL/6 wild type embryos were used. Embryonic lungs were isolated in culture medium, and the distal epithelial buds, along with the surrounding mesenchyme and mesothelium, were carefully dissected with fine-tipped pincers. The dissected tips were then immediately transferred to 500 μl undiluted dispase (Corning, Amsterdam, The Netherlands) where they were incubated for 20–30 min on ice. The dispase-digested samples were then

transferred to pure FBS, and incubated for 15 min on ice, thus blocking the enzymatic activity of dispase. Using tungsten microdissection needles, the epithelium was gently separated from the surrounding mesenchyme. Separated tissues were then prepared for total RNA extraction and microarray analysis.

Immunofluorescence

Freshly dissected E12.5 lungs were washed in sterile PBS (2 × 5 min), fixed in 4% PFA for 20 min on ice, and then washed again (3 × 5 min). Lungs were dehydrated by successive washes in a graded ethanol series (30, 50, 70, 100, 100%) for 5 min each, and stored in 100% ethanol at −20°C.

To embed the lungs in paraffin, they were first washed in Xylol (2 × 5 min, or until clear), incubated for 1 h at 60°C in a 1:1 Xylol/paraffin mixture, washed in pure paraffin (3 × 20 min) at 60°C, and then stored in pure paraffin overnight at 60°C. Lungs were then embedded in paraffin blocks and sectioned to a thickness of 4 or 5 μm. Sections were placed in a 40°C water bath for ∼30 min, and then placed on glass slides and incubated at 37°C overnight.

Before antibody staining, sections were first washed with gentle shaking in Xylol (3 × 10 min), and then in serial dilutions of ethanol (100, 70, 50, and 30%) for 3 min each, and finally in distilled water for 5 min. For each stain an antigen retrieval step was performed, which involved incubating the slides in 75–90°C citrate-based antigen unmasking solution (pH 6.0; Vector Laboratories, Peterborough, UK) for 15 min and then cooling on ice for ∼30 min. Sections were then washed with PBST (1x PBS + 0.1% TWEEN20; 3 × 5 min). Blocking solution (1x PBS + 3% BSA + 0.4% TritonX) was then added atop each section for 1 h at room temperature. Primary antibodies were added to incubation buffer (1x PBS + 1.5% BSA + 0.2% TritonX) and samples were incubated overnight at 4°C (anti-SOX2, anti-Phospho-ßCatenin (Ser552), and anti-LEF1 were added at 1:100 dilution; anti-CDH1, anti-LAMA1, and anti-SOX9 were added at 1:200 dilution; see **Table S1** for antibody details). Following primary antibody incubation, samples were washed in PBST (3 × 5 min) and secondary antibodies were added (all at a 1:500 dilution) for 1 h at room temperature, in the dark. Samples were washed in PBST (3 × 10 min) and PBS for 5 min, with gentle shaking. Finally, ProLong Gold antifade reagent with DAPI (Invitrogen, Schwerte, Germany) was added to each section and covered with a glass coverslip.

Sections were imaged on a Leica DM 5500B upright fluorescent microscope system, with a DFC 360FX camera, and Leica Application Suite Advanced Fluorescence imaging software. Signal intensity was optimized to either a control or experimental sample for an experiment, and the acquisition and intensity values were similarly applied to each sample in that experiment, thus ensuring valid comparisons.

Whole Mount Immunofluorescence and Confocal Microscopy

To assess the morphology of intact distal lung buds in control and experimental embryos, whole mount immunofluorescence followed by confocal imaging was performed.

E12.5 lungs were dissected and fixed in 4% PFA for 20 min on ice. Samples were washed in PBS + 1% TritonX (3 × 10 min), and incubated in blocking buffer (1x PBS + 1% TritonX + 10% FBS) for 1.5 h at room temperature, followed by two washes in blocking buffer. Samples were then incubated for 2 h with FITC-conjugated anti-CDH1 (Dilution: 1:200) diluted in 1/4 blocking buffer and PBS, at 4°C in the dark. Lungs were then washed in PBS (3 × 10 min), and transferred to custom made imaging dishes (composed of a 35,0/10 mm glass bottom cell culture dish (Greiner Bio-One, Frickenhausen, Germany) and a 10,0/1 mm rubber washer fixed to the middle of the dish with a suitable adhesive, thus creating an ideal well to mount and image the sample). ProLong Gold antifade reagent with DAPI was added to each well and covered with a glass coverslip.

Z-stacks of distal lung buds were obtained on a Leica TCS SP5 confocal microscopy system using Leica Application Suite X software. For each bud, the first optical section of the z-stack was acquired at the basal edge of the epithelium. Z-stack images were taken at 0.5 μm increments through the bud, until imaging was no longer possible due to complete loss of signal intensity. Compensation of intensity loss through the bud was obtained using the linear compensation by AOTF option. 3-D reconstructions and movies were created using Leica Application Suite X software.

Transmission Electron Microscopy

To identify the effects of FGFR2b ligand inhibition on the ultrastructure of distal epithelial and mesenchymal cells, control and experimental E12.5 lungs were prepared for transmission electron microscopy.

The chest cavities of freshly harvested E12.5 embryos were gently opened by incising from the lower abdomen, through the sternum, to just under the chin using a pair of fine dissection scissors. An incision was made along the diaphragm from the midline to the spine. The embryos were then immediately placed, ventral side up, in an immersion fixative solution containing 4% PFA + 2% sucrose + 0.05% calcium chloride + 1x PIPES buffer (0.1M, pH 7.4; Sigma-Aldrich, Taufkirchen, Germany) in a 50 ml Falcon tube, such that each sample was immersed in 5X the volume of fixative in its own tube. Tubes were placed on ice and gently shaken for 2 h, after which the fixative was removed and replaced by 4% PFA + 0.05% glutaraldehyde (GA; Sigma-Aldrich, Taufkirchen, Germany), 2% sucrose, 0.05% calcium chloride + 1X PIPES buffer (0.1 M, pH 7.4). Samples remained in this fixative overnight at 4°C.

The next morning, the samples were processed for routine transmission electron microscopy. Briefly, the fixed lungs were dissected and placed into molten agar, which was allowed to harden before the samples were cut longitudinally in half. Each half was fixed for 30 min in 1.5% GA fixative containing 2% sucrose + 0.05% calcium chloride + 1X PIPES buffer (0.1 M, pH 7.4). The fixative solution was then removed and samples were washed with 1X PIPES (3 × 5 min). Samples were then incubated for 1 h at room temperature in reduced osmium fixation solution containing 0.15% sodium hexacyanoferrate(II) and 2% reduced osmium, then washed very briefly with distilled water, and dehydrated via washes in a graded ethanol series (70, 80, 90, 100%), 3 times 10 min each step. Samples were then embedded by immersion in propylene oxide (3 × 5 min), in 1:1 propylene oxide:Agar 100 epoxy resin (1 × 30 min) following

the manufacturer's instructions to produce blocks of medium hardness (Agar Scientific, Essex, UK), and finally in pure Agar 100 epoxy resin in a desiccation chamber at room temperature overnight.

The Agar 100 resin-penetrated lungs were then flat embedded into fresh Agar 100 resin and polymerized at 60°C for at least 2 days, or until complete polymerization was achieved. Ultrathin sections were then prepared and micrographs were obtained using a Zeiss LEO 906 transmission electron microscope equipped with a TRS slow-scan 2K CCD camera and ImageSP software.

DNA Isolation and PCR

DNA was isolated from the tails and hind limbs of E12.5 embryos. Gene-specific primers were used to detect the presence of *Rosa26rtTA* (wild type and transgene specific forward primer 5′- GAG TTC TCT GCT GCC TCC TG; wild type specific reverse primer 5′- CGA GGC GGA TAC AAG CAA TA; transgene specific reverse primer 5′- AAG ACC GCG AAG AGT TTG TC; expected product size of ∼200 bp for the transgene and 322 bp for the wild type) and *tet(o)sFgfr2b* (transgene specific forward primer 5′- GAA GGA GAT CAC GGC TTC C; transgene specific reverse primer 5′- AGA CAG ATG ATA CTT CTG GGA CTG T; expected product size of 110 bp). The PCR reaction mix was calculated for 20 µl per reaction, and included 10 µl 2xTaq PCR Master Mix (Qiagen, Hilden, Germany), primers at a final concentration of 0.2 µM, RNase-free water, and up to 1 µg of genomic DNA. PCRs were performed in a C1000 Thermocycler (Bio-Rad). The cycling protocol to amplify *Rosa26rtTA* was as follows: initial denaturation at 94°C for 3 min; 35 cycles of denaturation at 94°C for 1 min, annealing at 63°C for 1 min, and extension at 72°C for 1.5 min; final extension at 72°C for 5 min; and hold at 4°C. The protocol to amplify *tet(o)sFgfr2b* was as follows: initial denaturation at 95°C for 2 min; 35 cycles of denaturation at 95°C for 5 seconds, annealing at 58°C for 5 s, and extension at 72°C for 20 s; final extension at 72°C for 2 min; and hold at 4°C. Capillary gel electrophoresis was performed using a QIAxcel Advanced capillary electrophoresis system (Qiagen).

RNA Isolation and RT-qPCR

Whole embryonic lungs or separated epithelium and mesenchyme used for total RNA isolation were first put in 700 µl QIAzol Lysis Reagent (Qiagen, Hilden, Germany). For tissue disruption and homogenization, the samples were transferred to gentleMACS M Tubes and homogenized in a gentleMACS Dissociator (Miltenyi Biotec) for 1 min. Total RNA was then isolated using the miRNeasy Mini Kit (Qiagen, Hilden, Germany), and eluted in 30 µl RNase-free water. RNA amount and purity was assessed with a NanoDrop 2000c (Thermo Scientific). Up to 1 µg of total RNA for each sample was then reverse transcribed using the QuantiTect Reverse Transcription Kit (Qiagen, Hilden, Germany).

Primers were designed to amplify specific mature mRNAs using NCBI's primer-BLAST option (https://www.ncbi.nlm.nih.gov/tools/primer-blast/; last accessed, 01–08–2018). Primers were further validated by PCR-based gel electrophoresis (see **Table S2** for primer sequences). qPCR reaction mixtures were set up using the PowerUp SYBR Green Master Mix (Thermo Fisher, Schwerte, Germany), with a final volume of 20 µl for each reaction. Reaction mixtures included the following components: 10 µl of 2X PowerUp SYBR Green Master Mix, between 300 and 800 nM of each primer, between 1 and 10 ng cDNA, and nuclease-free water. Samples were run with two or three technical replicates on a LightCycler 480II (Celli et al.) using the following protocol: UDG activation at 50°C for 2 min; DNA polymerase activation at 95°C for 2 min; and 40 cycles of denaturation at 95°C for 15 s, annealing at 60°C for 15 s, and extension at 72°C for 1 min. To validate amplification specificity, a dissociation step was also included for each sample. Threshold cycles (Ct) were calculated and used for relative expression analyses, using mouse *Hprt* as the reference gene.

Microarray Analysis

Differential gene expression was investigated using microarray analysis. Depending on the amount of RNA isolated per sample in an experiment, one of two possible microarray protocols was used. For RNA concentrations >50 ng/µl, the T7-protocol was followed. In this protocol, purified total RNA was amplified and Cy3-labeled using the LIRAK kit (Agilent Technologies, Waldbronn, Germany) following the kit instructions. Per reaction, 200 ng of total RNA was used. The Cy3-labeled aRNA was hybridized overnight to 8 × 60 K 60mer oligonucleotide spotted microarray slides (Agilent Technologies, design ID 028005).

For experiments where samples yielded <50 ng/µl of RNA, the SPIA-protocol was utilized. In this protocol, purified total RNA was amplified using the Ovation PicoSL WTA System V2 kit (NuGEN Technologies, Leek, The Netherlands). Per sample, 2 µg amplified cDNA was Cy-labeled using the SureTag DNA labeling kit (Agilent Technologies). The Cy3-labeled aRNA was hybridized overnight to 8 × 60 K 60mer oligonucleotide spotted microarray slides (Agilent Technologies, design ID 074809).

For each protocol, hybridization, and subsequent washing and drying of the slides were performed following the Agilent hybridization protocol. The dried slides were scanned at 2 µm/pixel resolution using the InnoScan is900 (Innopsys). Image analysis was performed with Mapix 6.5.0 software, and calculated values for all spots were saved as GenePix results files. Stored data were evaluated using the R software (version 3.3.2) and the limma package (version 3.30.13) from BioConductor. Gene annotation was supplemented by NCBI gene IDs via biomaRt (last accessed 08–03–2018).

Assessing Proliferation and Apoptosis

Proliferation in E12.5 lungs was assessed using the Click-iT EdU Imaging Kit (Invitrogen, Schwerte, Germany). 5-ethynyl-2′-deoxyuridine (EdU), a nucleoside analog of thymidine incorporated into DNA during DNA synthesis, was injected (i.p.) 2 h before pregnant females were sacrificed (Dosage: 0.005 mg EdU / g mouse weight). Embryonic lungs were harvested, paraffin embedded, sectioned and placed on glass slides. Sections were then deparaffinised and stained for EdU according to the manufacturer's protocol.

Apoptosis was assessed using the TdT-mediated dUTP Nick-End Labeling (TUNEL) assay. The assay was performed using the DeadEnd Fluorometric TUNEL System (Promega, Mannheim, Germany). E12.5 lungs were harvested, paraffin embedded, sectioned and placed on glass slides. The assay was performed according to the manufacturer's protocol.

Gene Expression Patterns

To assess the expression patterns of genes in early stage embryonic lungs (E14.5), the online database genepaint.org was used (last accessed 01–08–2018). Each of the genes significantly regulated in our *in vivo* studies was entered in genepaint. The whole embryo section displaying the clearest gene expression in the lung, along with a magnification of the lung itself, was chosen for the figures.

Quantification and Statistical Analysis

Morphometric Quantifications

Using still images of lungs, mesothelium and airways were traced in Adobe Illustrator CS6 (version 16.0.4) to create skeletal outlines. These outlines were exported and lengths and areas were quantified either using MetaMorph (version 1.5.0) or FIJI (version 2.0.0-rc-68/1.52g) software.

Significance was determined by unpaired two-tailed Student's *t*-tests. All data are presented as mean ± SEM. Values of $p < 0.05$ were considered significant. The number of independent samples (n) can be found in the figures.

Relative Gene Expression From qPCR Data

ΔCt and ΔΔCt values were calculated according to the following formulas:

$$\Delta Ct = Ct_{\text{Reference}} - Ct_{\text{gene of interest}} \quad (1)$$

Note, this equation accounts for the fact that Ct is proportional to the –log of gene expression. ΔCt is therefore positively related to the expression of the gene of interest.

$$\Delta\Delta Ct_{\text{Experimental}-\text{control}} = Mean\Delta Ct_{\text{Experimental}} - Mean\Delta Ct_{\text{Control}} \quad (2)$$

Unpaired two-tailed Student's *t*-tests were performed on the ΔCt values, which can be assumed to be normally distributed. Number of "n" and significance level is indicated either in the figures or in the figure legends.

Microarray Analyses

Mean spot signals were background corrected with an offset of 1 using the NormExp procedure on the negative control spots. The logarithms of the background-corrected values were quantile-normalized. The normalized values were then averaged for replicate spots per array. From different probes addressing the same NCBI gene ID, the probe showing the maximum average signal intensity over the samples was used in subsequent analyses. Genes were ranked for differential expression using an unpaired two-tailed Student's *t*-test on a moderated t-statistic, and heatmaps were generated displaying genes according to descending *p*-values. Gene set tests were done on the ranks of the *t*-values, using the function "geneSetTest" in the limma package from BioConductor. The number of independent samples (n) can be found in the figures. Gene sets were either user defined or, for pathway analyses, according to the KEGG database (last accessed 08–03–2018). The data from the microarray experiments have been deposited in the NCBI's gene expression omnibus (GEO accession GSE124157).

AUTHOR CONTRIBUTIONS

SB, MJ, JZ, PM, and CC: concept and design; MJ, SaD, AL, SoD, JW, GC, and RM: acquisition of data; SB, MJ, JW, EB-V, and DA: analysis and interpretation; MJ, SaD, SB, and JZ: drafting and editing of the manuscript. All authors read and approved the final manuscript.

FUNDING

SB was supported by grants from the Deutsche Forschungsgemeinschaft (DFG; BE4443/1-1, BE4443/4-1, BE4443/6-1, KFO309 P7 and SFB1213-projects A02 and A04), Landes-Offensive zur Entwicklung Wissenschaftlich-ökonomischer Exzellenz, the Universtätsklinikum Giessen Marburg, the University of Giessen Marburg Lung Center, the German Center for Lung Research (DZL) and COST (BM1201). SB was supported by the Deutsche Forschungsgemeinschaft (SFB1221, C05; SFB-TR84, B2; EXC147), the Universitätsklinikum Giessen & Marburg (UKGM, FOKOOPV), and the German Center for Lung Research (DZL). JZ was supported by the National Natural Science Foundation of China (81472601).

ACKNOWLEDGMENTS

We would like to thank Kerstin Goth and Jana Rostkovius for managing and genotyping the mice used for experiments. We also thank Dr. Elie El Agha for the critical reading of this manuscript.

SUPPLEMENTARY MATERIAL

The Supplementary Material for this article can be found online at: https://www.frontiersin.org/articles/10.3389/fgene.2018.00746/full#supplementary-material

Figure S1 | Experimental validation of the *Rosa26$^{rtTA/rtTA}$; tet(o)sFgfr2b/+* double transgenic mice **(A)** Pregnant females carrying control (*Rosa26$^{rtTA/rtTA}$; +/+)* and experimental *(Rosa26$^{rtTA/rtTA}$; tet(o)sFgfr2b/+)* embryos were fed with Dox food starting either at E10.5, E11.5, E13.5, or E14.5 and sacrificed at E18.5. The lungs were dissected and shown in c–f. *Scale bar:* (b–f) 500 μm. **(B)** Pregnant females carrying control (a,c,e,g and a',c',e',g') and experimental (b,d,f,g and b',d',f',h') embryos were sacrificed at E12.5. The lungs were dissected and cultured for 72 h in the presence of Dox added to the culture medium. *Scale bar:* (a–h) 500 μm; (a'–h') 125 μm.

Figure S2 | Transmission electron microscopy: Compared to controls, experimental lungs (DoxIP + 9 h) show reduced numbers and stunted microvilli (see black arrows, a–d), opened tight junctions (see black arrows in e and g; white asterisks in f and h), and flattened Golgi with increased staining (see black arrows, i–l). epith. =epithelium. *Magnification:* (a,c,e,g,i,k) 27,800x; (b,d,f,h,j,l) 139,000x.

Figure S3 | Genes and Expression pattern found in the Early 1 cluster **(A)** Graphical representation of changes in the level of gene expression over time. **(B)** Heat map. **(C)** Corresponding *in situ* hybridization results at E14.5 from genepaint.

Figure S4 | Genes and Expression pattern found in the Early 2 cluster **(A)** Graphical representation of changes in the level of gene expression over time. **(B)** Heat map. **(C)** Corresponding *in situ* hybridization results at E14.5 from genepaint.

Figure S5 | Genes and Expression pattern found in the Early 3 cluster **(A)** Graphical representation of changes in the level of gene expression over time. **(B)** Heat map. **(C)** Corresponding *in situ* hybridization results at E14.5 from genepaint.

Figure S6 | Genes and Expression pattern found in the Early 4 cluster **(A)** Graphical representation of changes in the level of gene expression over time. **(B)** Heat map. **(C)** Corresponding *in situ* hybridization results at E14.5 from genepaint.

Figure S7 | Genes and Expression pattern found in the Late 1 cluster **(A)** Graphical representation of changes in the level of gene expression over time. **(B)** Heat map. **(C)** Corresponding *in situ* hybridization results at E14.5 from genepaint.

Figure S8 | Genes and Expression pattern found in the Late 2 cluster **(A)** Graphical representation of changes in the level of gene expression over time. **(B)** Heat map. **(C)** Corresponding *in situ* hybridization results at E14.5 from genepaint.

Figure S9 | Genes and Expression pattern found in the Late 3 cluster **(A)** Graphical representation of changes in the level of gene expression over time. **(B)** Heat map. **(C)** Corresponding *in situ* hybridization results at E14.5 from genepaint.

Figure S10 | Genes and Expression pattern found in the Late 4 cluster **(A)** Graphical representation of changes in the level of gene expression over time. **(B)** Heat map. **(C)** Corresponding *in situ* hybridization results at E14.5 from genepaint.

Figure S11 | Relative level of expression of the genes of interest in epithelium and mesenchyme of WT E12.5 lungs and regulation of gene expression upon FGF10 inhibition **(A)** Determination of genes differentially expressed in the distal epithelium vs. mesenchyme of E12.5 wild type lungs by gene array ($n = 3$; see *Materials and Methods* for details on the statistical analysis of gene arrays). **(B)** Impact of *in vivo* FGF10 inhibition on lung branching at 6 and 9 h using our double transgenic system. Corresponding gene arrays allowed the identification of genes belonging to Early 4, Late 4, Late 3, and Late 1 groups. **(C)** Analysis of the genes found in the Early 4 cluster. The first LogFC (identified with "^{A}" after the gene) represents the differential expression of this gene in the epithelium vs. mesenchyme of WT E12.5 lungs. The second LogFC (identified with "^{B}" after the gene) represents the level of regulation upon FGF10 inhibition. Blue indicates genes enriched in the epithelium, and red indicates genes enriched in the mesenchyme. Genes in black were not found in our gene array in **(A)**. Note that all the genes in Early 4 are blue, and therefore enriched in the epithelium. Some of these genes were differentially expressed in the epithelium at a high level (Log_2FC more than 2; *Id2*, *Sftpc*, *Tspan8*, *Lin7a*, *Sp5*, *Sema4f*, *Arrdc1*, *Gprc5a*, and *Slco2a1*), a medial level (Log_2FC between 1 and 2; *Etv5* and *Rai14*), or a lower level (Log_2FC between 0 and 1; *Gprin3*, *Enc1*, and *Bid*). We found that some of these genes were highly regulated upon FGF10 inhibition (Log_2FC <-2; *Gprin3*), moderately regulated (Log_2FC between −1 and −2; *Id2*, *Sftpc*, *Tspan8*, *Lin7a*, *Sp5*, *Sema4f*, *Gprc5a*, *Etv5*, *Slco2a1*), or weakly regulated (Log_2FC between 0 and −1; *Enc1*, *Arrdc1*, *Bid*, *Rai14*). It is likely that genes which are expressed at high or medial levels in the epithelium, and which are highly or moderately regulated following inhibition of FGF10 activity, are involved in mediating FGF10 activity. One exception is *Gprin3*, which is only weakly enriched in the epithelium, but which nonetheless is highly regulated by FGF10. **(D)** Analysis of the genes found in the Late 4 cluster. Note again that most of the genes are blue, confirming the enrichment in the Late 4 cluster for epithelial genes. Out of 43 genes, 29 were preferentially expressed in the epithelium, two were preferentially expressed in the mesenchyme, while information on the 11 other genes was not available in the array. With the exception of *Gprin3*, *Id2*, *Arrdc1*, and *Sema4f*, all the other genes found in the Early 4 cluster are also found in the Late 4 group. Some of these genes were expressed at a high level in the epithelium (Log_2FC more than 2; *Cytl1*, *Lama3*, *Slco2a1*, *Gprc5a*, *Sftpc*, *Tspan8*, *Bspry*, *Sftpa1*, *Bex4*, *Crlf1*, *Lin7a*, *Shh*, *Bex1*, *Sp5*, *Ctnnd2*, and *Pthlh*), at a medial level (Log_2FC between 1 and 2; *Kiss1*, *Lgi3*, *Rai14*, *Sftpb*, *Sh3bgrl2*, and *Etv5*), or at a lower level (Log_2FC between 0 and 1; *Strap*, *Gnptab*, *Enc1*, *Lamc2*, *Rrs1*, *Srpk1*, and *Bid*). We also classified the genes in the Late 4 cluster according to their regulation following FGF10 inactivation: highly regulated (Log_2FC <-2; *Cytl1*, *Sftpc*, *Bspry*, *Sftpa1*, *Lin7a*, *Sftpb*, *Sp5*, *Pthlh*, and *Etv5*), moderately regulated (Log_2FC between −1 and −2; *Strap*, *Kiss1*, *Lgi3*, *Slco2a1*, *Gprc5a*, *Bex4*, *Enc1*, *Lamc2*, *Sh3bgrl2*, and *Ctnnd2*), or weakly regulated (Log_2FC between 0 and −1; *Rrp9*, *Gnptab*, *Lama3*, *Rai14*, *Crlf1*, *Rrs1*, *Shh*, *Bex1*, *Srpk1*, and *Bid*). As with the Early 4 analysis, it would be logical to prioritize genes for future studies based both on their expression in the epithelium and their level of regulation by FGF10. *Cytl1*, *Sftpc*, *Bspry*, *Sftpa1*, *Lin7a*, *Sp5,* and *Pthlh* fit these prioritization criteria. **(E)** Analysis of the genes found in the Late 3 cluster. Note the presence of genes belonging to the Hedgehog signaling pathway. This group contains 20 genes, eight of which were preferentially expressed in the epithelium, five preferentially expressed in the mesenchyme, and six other genes not identified in the epithelium vs. mesenchyme array. Of the genes contained in the Late 3 cluster, some were expressed at a high level in the epithelium (Log_2FC more than 2; *Wnt7b*, and P*csk6*), at a medial level (Log_2FC between 1 and 2; *Bmp7*, and *Dusp9*), or at a lower level (Log_2FC between 0 and 1; *Rbm27*, *Hmga2*, *Spata5*, and *Hk2*). We also classified the genes according to their level of regulation following FGF10 inactivation: highly regulated (Log_2FC <-2; no genes), moderately regulated (Log_2FC between −1 and −2; *Wnt7b*, *Pcsk6*, *Fgd3*, *Hmga2*, *Gli1*, *Hk2*, and *Dusp9*), or weakly regulated (Log_2FC between 0 and −1; *Sct*, *Ntng1*, *Rbm27*, *Bmp7*, *Foxf1*, and *Spata5*). **(F)** Analysis of the genes found in Late 1 cluster. Note the presence of *Fgf10* in this cluster. **(G)** Graphical representation of the FGF10 gene signature showing those genes both enriched in the epithelium (X-axis) and down-regulated after 9 hrs FGF10 inhibition (Y-axis).

Table S1 | Primary antibodies.

Table S2 | Primer sequences for qRT-PCR.

Movie S1 | Longitudinal section of control bud.

Movie S2 | Longitudinal section of experimental bud (9 h Dox-IP).

Movie S3 | Cross section of control bud.

Movie S4 | Cross section of experimental bud (9 h Dox-IP).

REFERENCES

Abler, L. L., Mansour, S. L., and Sun, X. (2009). Conditional gene inactivation reveals roles for Fgf10 and Fgfr2 in establishing a normal pattern of epithelial branching in the mouse lung. *Dev. Dyn.* 238, 1999–2013. doi: 10.1002/dvdy.22032

Al Alam, D., El Agha, E., Sakurai, R., Kheirollahi, V., Moiseenko, A., Danopoulos, S., et al. (2015). Evidence for the involvement of fibroblast growth factor 10 in lipofibroblast formation during embryonic lung development. *Development* 142, 4139–4150. doi: 10.1242/dev.109173

Bellusci, S., Furuta, Y., Rush, M. G., Henderson, R., Winnier, G., and Hogan, B. L. (1997a). Involvement of Sonic hedgehog (Shh) in mouse embryonic lung growth and morphogenesis. *Development* 124, 53–63.

Bellusci, S., Grindley, J., Emoto, H., Itoh, N., and Hogan, B. L. (1997b). Fibroblast growth factor 10 (FGF10) and branching morphogenesis in the embryonic mouse lung. *Development* 124, 4867–4878.

Celli, G., LaRochelle, W. J., Mackem, S., Sharp, R., and Merlino, G. (1998). Soluble dominant-negative receptor uncovers essential roles for fibroblast growth factors in multi-organ induction and patterning. *EMBO J.* 17, 1642–1655. doi: 10.1093/emboj/17.6.1642

Chang, D. R., Martinez Alanis, D., Miller, R. K., Ji, H., Akiyama, H., McCrea, P. D., et al. (2013). Lung epithelial branching program antagonizes alveolar differentiation. *Proc. Natl. Acad. Sci. U.S.A.* 110, 18042–18051. doi: 10.1073/pnas.1311760110

Danopoulos, S., Parsa, S., Al Alam, D., Tabatabai, R., Baptista, S., Tiozzo, C., et al. (2013). Transient Inhibition of FGFR2b-ligands signaling leads to irreversible loss of cellular beta-catenin organization and signaling in AER during mouse limb development. *PLoS ONE* 8:e76248. doi: 10.1371/journal.pone.0076248

De Langhe, S. P., Carraro, G., Warburton, D., Hajihosseini, M. K., and Bellusci, S. (2006). Levels of mesenchymal FGFR2 signaling modulate smooth muscle progenitor cell commitment in the lung. *Dev. Biol.* 299, 52–62. doi: 10.1016/j.ydbio.2006.07.001

De Langhe, S. P., and Reynolds, S. D. (2008). Wnt signaling in lung organogenesis. *Organogenesis* 4, 100–108. doi: 10.4161/org.4.2.5856

De Moerlooze, L., Spencer-Dene, B., Revest, J. M., Hajihosseini, M., Rosewell, I., and Dickson, C. (2000). An important role for the IIIb isoform of fibroblast

growth factor receptor 2 (FGFR2) in mesenchymal-epithelial signalling during mouse organogenesis. *Development* 127, 483–492.

El Agha, E., and Bellusci, S. (2014). Walking along the fibroblast growth factor 10 route: a key pathway to understand the control and regulation of epithelial and mesenchymal cell-lineage formation during lung development and repair after injury. *Scientifica* 2014:538379. doi: 10.1155/2014/538379

Francavilla, C., Rigbolt, K. T., Emdal K. B., Carraro, G., Vernet, E., Bekker-Jensen, D. B., et al. (2013). Functional proteomics defines the molecular switch underlying FGF receptor trafficking and cellular outputs. *Mol. Cell.* 51, 707–722. doi: 10.1016/j.molcel.2013.08.002

Guo, L., Degenstein, L., and Fuchs, E. (1996). Keratinocyte growth factor is required for hair development but not for wound healing. *Genes Dev.* 10, 165–175. doi: 10.1101/gad.10.2.165

Herriges, J. C., Verheyden, J. M., Zhang, Z., Sui, P., Zhang, Y., Anderson, M. J., et al. (2015). FGF-regulated ETV transcription factors control FGF-SHH feedback loop in lung branching. *Dev. Cell* 35, 322–332. doi: 10.1016/j.devcel.2015.10.006

Herriges, J. C., Yi, L., Hines, E. A., Harvey, J. F., Xu, G., Gray, P. A., et al. (2012). Genome-scale study of transcription factor expression in the branching mouse lung. *Dev. Dyn.* 241, 1432–1453. doi: 10.1002/dvdy.23823

Hokuto, I., Perl, A. K., and Whitsett, J. A. (2003). Prenatal, but not postnatal, inhibition of fibroblast growth factor receptor signaling causes emphysema. *J. Biol. Chem.* 278, 415–421. doi: 10.1074/jbc.M208328200

Hoppler, S., and Kavanagh, C. L. (2007). Wnt signalling: variety at the core. *J. Cell. Sci.* 120, 385–393. doi: 10.1242/jcs.03363

Kam, Y., and Quaranta, V. (2009). Cadherin-bound beta-catenin feeds into the Wnt pathway upon adherens junctions dissociation: evidence for an intersection between beta-catenin pools. *PLoS ONE* 4:e4580. doi: 10.1371/journal.pone.0004580

Kim, H., He, Y., Yang, I., Zeng, Y., Kim, Y., Seo, Y.-W., et al. (2012). δ-Catenin promotes E-cadherin processing and activates β-catenin-mediated signaling: implications on human prostate cancer progression. *Biochim. Biophys. Acta Mol. Basis Dis.* 1822, 509–521. doi: 10.1016/j.bbadis.2011.12.015

Lebeche, D., Malpel, S., and Cardoso, W. V. (1999). Fibroblast growth factor interactions in the developing lung. *Mech. Dev.* 86, 125–136. doi: 10.1016/S0925-4773(99)00124-0

Liu, Y., Martinez, L., Ebine, K., and Abe, M. K. (2008). Role for mitogen-activated protein kinase p38 alpha in lung epithelial branching morphogenesis. *Dev. Biol.* 314, 224–235. doi: 10.1016/j.ydbio.2007.12.003

Lu, Q., Paredes, M., Medina, M., Zhou, J., Cavallo, R., Peifer, M., et al. (1999). delta-catenin, an adhesive junction-associated protein which promotes cell scattering. *J. Cell. Biol.* 144, 519–532. doi: 10.1083/jcb.144.3.519

Makarenkova, H. P., Hoffman, M. P., Beenken, A., Eliseenkova, A. V., Meech, R., Tsau, C., et al. (2009). Differential interactions of FGFs with heparan sulfate control gradient formation and branching morphogenesis. *Sci. Signal.* 2:ra55. doi: 10.1126/scisignal.2000304

Medina, M., Marinescu, R. C., Overhauser, J., and Kosik, K. S. (2000). Hemizygosity of delta-catenin (CTNND2) is associated with severe mental retardation in cri-du-chat syndrome. *Genomics* 63, 157–164. doi: 10.1006/geno.1999.6090

Metzger, D. E., Stahlman, M. T., and Shannon, J. M. (2008a). Misexpression of ELF5 disrupts lung branching and inhibits epithelial differentiation. *Dev. Biol.* 320, 149–160. doi: 10.1016/j.ydbio.2008.04.038

Metzger, D. E., Xu, Y., and Shannon, J. M. (2007). Elf5 is an epithelium-specific, fibroblast growth factor-sensitive transcription factor in the embryonic lung. *Dev. Dyn.* 236, 1175–1192. doi: 10.1002/dvdy.21133

Metzger, R. J., Klein, O. D., Martin, G. R., and Krasnow, M. A. (2008b). The branching programme of mouse lung development. *Nature* 453, 745–750. doi: 10.1038/nature07005

Miller, D. L., Ortega, S., Bashayan, O., Basch, R., and Basilico, C. (2000). Compensation by fibroblast growth factor 1 (FGF1) does not account for the mild phenotypic defects observed in FGF2 null mice. *Mol. Cell. Biol.* 20, 2260–2268. doi: 10.1128/MCB.20.6.2260-2268.2000

Miyabayashi, T., Teo, J. L., Yamamoto, M., McMillan, M., Nguyen, C., and Kahn, M. (2007). Wnt/beta-catenin/CBP signaling maintains long-term murine embryonic stem cell pluripotency. *Proc. Natl. Acad. Sci. U.S.A.* 104, 5668–5673. doi: 10.1073/pnas.0701331104

Ostrin, E. J., Little, D. R., Gerner-Mauro, K. N., Sumner,. E. A., Rios-Corzo, R., Ambrosio, E., et al. (2018). Beta-Catenin maintains lug epithelial progenitors after lung specification. *Development* 145:5. doi: 10.1242/dev.160788

Parsa, S., Kuremoto, K., Seidel, K., Tabatabai, R., Mackenzie, B., Yamaza, T., et al. (2010). Signaling by FGFR2b controls the regenerative capacity of adult mouse incisors. *Development* 137, 3743–3752. doi: 10.1242/dev.051672

Parsa, S., Ramasamy, S. K., De Langhe, S., Gupte, V. V., Haigh, J. J., Medina, D., et al. (2008). Terminal end bud maintenance in mammary gland is dependent upon FGFR2b signaling. *Dev. Biol.* 317, 121–131. doi: 10.1016/j.ydbio.2008.02.014

Patel, V. N., Pineda, D. L., and Hoffman, M. P. (2017). The function of heparan sulfate during branching morphogenesis. *Matrix Biol.* 57–58, 311–323. doi: 10.1016/j.matbio.2016.09.004

Perl, A. K., Kist, R., Shan, Z., Scherer, G., and Whitsett, J. A. (2005). Normal lung development and function after Sox9 inactivation in the respiratory epithelium. *Genesis* 41, 23–32. doi: 10.1002/gene.20093

Quaggin, S. E., Schwartz, L., Cui, S., Igarashi, P., Deimling, J., Post, M., et al. (1999). The basic-helix-loop-helix protein pod1 is critically important for kidney and lung organogenesis. *Development* 126, 5771–5783.

Ramasamy, S. K., Mailleux, A. A., Gupte, V. V., Mata, F., Sala, F. G., Veltmaat, J. M., et al. (2007). Fgf10 dosage is critical for the amplification of epithelial cell progenitors and for the formation of multiple mesenchymal lineages during lung development. *Dev. Biol.* 307, 237–247. doi: 10.1016/j.ydbio.2007.04.033

Rawlins, E. L. (2008). Lung epithelial progenitor cells: lessons from development. *Proc. Am. Thorac. Soc.* 5, 675–681. doi: 10.1513/pats.200801-006AW

Rockich, B. E., Hrycaj, S. M., Shih, H. P., Nagy, M. S., Ferguson, M. A., Kopp, J. L., et al. (2013). Sox9 plays multiple roles in the lung epithelium during branching morphogenesis. *Proc. Natl. Acad. Sci. U.S.A.* 110, E4456–4464. doi: 10.1073/pnas.1311847110

Sasaki, T., and Kahn, M. (2014). Inhibition of beta-catenin/p300 interaction proximalizes mouse embryonic lung epithelium. *Transl. Respir. Med.* 2:8. doi: 10.1186/s40247-014-0008-1

Sekine, K., Ohuchi, H., Fujiwara, M., Yamasaki, M., Yoshizawa, T., Sato, T., et al. (1999). Fgf10 is essential for limb and lung formation. *Nat. Genet.* 21, 138–141. doi: 10.1038/5096

Treutlein, B., Brownfield, D. G., Wu, A. R., Neff, N. F., Mantalas, G. L., Espinoza, F. H., et al. (2014). Reconstructing lineage hierarchies of the distal lung epithelium using single-cell RNA-seq. *Nature* 509, 371–375. doi: 10.1038/nature13173

Varma, S., Cao, Y., Tagne, J. B., Lakshminarayanan, M., Li, J., Friedman, T. B., et al. (2012). The transcription factors Grainyhead-like 2 and NK2-homeobox 1 form a regulatory loop that coordinates lung epithelial cell morphogenesis and differentiation. *J. Biol. Chem.* 287, 37282–37295. doi: 10.1074/jbc.M112.408401

Volckaert, T., Campbell, A., Dill, E., Li, C., Minoo, P., and De Langhe, S. (2013). Localized Fgf10 expression is not required for lung branching morphogenesis but prevents differentiation of epithelial progenitors. *Development* 140, 3731–3742. doi: 10.1242/dev.096560

Volckaert, T., Dill, E., Campbell, A., Tiozzo, C., Majka, S., Bellusci, S., et al. (2011). Parabronchial smooth muscle constitutes an airway epithelial stem cell niche in the mouse lung after injury. *J. Clin. Invest.* 121, 4409–4419. doi: 10.1172/JCI58097

Volckaert, T., Yuan, T., Chao, C. M., Bell, H., Sitaula, A., Szimmtenings, L., et al. (2017). Fgf10-hippo epithelial-mesenchymal crosstalk maintains and recruits lung basal stem cells. *Dev. Cell* 43, 48–59 e45. doi: 10.1016/j.devcel.2017.09.003

Warburton, D., El-Hashash, A., Carraro, G., Tiozzo, C., Sala, F., Rogers, O., et al. (2010). Lung organogenesis, organogenesis in development. *Curr Top Dev Biol.* 90, 73–158. doi: 10.1016/S0070-2153(10)90003-3

Warburton, D., Perin, L., Defilippo, R., Bellusci, S., Shi, W., and Driscoll, B. (2008). Stem/progenitor cells in lung development, injury repair, and regeneration. *Proc. Am. Thorac. Soc.* 5, 703–706. doi: 10.1513/pats.200801-012AW

Conflict of Interest Statement: The authors declare that the research was conducted in the absence of any commercial or financial relationships that could be construed as a potential conflict of interest.

Copyright © 2019 Jones, Dilai, Lingampally, Chao, Danopoulos, Carraro, Mukhametshina, Wilhelm, Baumgart-Vogt, Al Alam, Chen, Minoo, Zhang and Bellusci. This is an open-access article distributed under the terms of the Creative Commons Attribution License (CC BY). The use, distribution or reproduction in other forums is permitted, provided the original author(s) and the copyright owner(s) are credited and that the original publication in this journal is cited, in accordance with accepted academic practice. No use, distribution or reproduction is permitted which does not comply with these terms.

frontiers in Genetics

REVIEW
published: 30 January 2019
doi: 10.3389/fgene.2019.00012

Intrinsic FGFR2 and Ectopic FGFR1 Signaling in the Prostate and Prostate Cancer

Cong Wang[1], Ziying Liu[1,2], Yuepeng Ke[2] and Fen Wang[2]**

[1] School of Pharmaceutical Sciences, Wenzhou Medical University, Wenzhou, China, [2] Institute of Biosciences and Technology, Texas A&M University, College Station, TX, United States

Advanced castrate-resistant prostate cancer (CRPC) is a poorly prognostic disease currently lacking effective cure. Understanding the molecular mechanism that underlies the initiation and progression of CRPC will provide new strategies for treating this deadly disease. One candidate target is the fibroblast growth factor (FGF) signaling axis. Loss of the intrinsic FGF7/FGF10-type 2 FGF receptor (FGFR2) pathway and gain of the ectopic type 1 FGF receptor (FGFR1) pathway are associated with the progression to malignancy in prostate cancer (PCa) and many other epithelial originating lesions. Although FGFR1 and FGFR2 share similar amino acid sequences and structural domains, the two transmembrane tyrosine kinases elicit distinctive, even sometime opposite signals in cells. Recent studies have revealed that the ectopic FGFR1 signaling pathway contributes to PCa progression via multiple mechanisms, including promoting tumor angiogenesis, reprogramming cancer cell metabolism, and potentiating inflammation in the tumor microenvironment. Thus, suppression of FGFR1 signaling can be an effective novel strategy to treat CRPC.

Keywords: growth factor, receptor tyrosine kinase, prostate, cancer progression, cell signaling

OPEN ACCESS

Edited by:
Saverio Bellusci,
University of Giessen, Germany

Reviewed by:
David Ornitz,
Washington University in St. Louis, United States
Richard Grose,
Queen Mary University of London, United Kingdom

****Correspondence:***
Cong Wang
cwang@wmu.edu.cn
Fen Wang
fwang@ibt.tamhsc.edu

Specialty section:
This article was submitted to Cancer Genetics, a section of the journal Frontiers in Genetics

Received: *21 November 2018*
Accepted: *11 January 2019*
Published: *30 January 2019*

Citation:
Wang C, Liu Z, Ke Y and Wang F (2019) Intrinsic FGFR2 and Ectopic FGFR1 Signaling in the Prostate and Prostate Cancer. Front. Genet. 10:12. doi: 10.3389/fgene.2019.00012

THE PROSTATE AND PROSTATE CANCER

The prostate is an accessory gland of the male reproductive system, which secretes many components of semen. In Western societies, prostate cancer (PCa) is the most frequently diagnosed cancer in males and the second leading cause of cancer death. The human prostate has three distinct zones: the peripheral zone, the transition zone, and the central zone, accounting for about 5, 10, and 85% of human PCa cases, respectively (Jemal et al., 2009). The progression of PCa is a slow and multiple-step process. PCa at early stages is organ-confined and androgen-responsive. Advanced PCas, however, are frequently metastatic and castration resistant (Denmeade and Isaacs, 2002). Although androgen-deprivation and surgery are common for treating PCa at early stages, there are no effective cure for advanced PCa so far. Understanding the mechanisms underlying the onset, progression to castration resistance, and metastasis of PCa is needed for developing new diagnostic, preventive, and therapeutic approaches for patients with PCa.

The prostate is composed of epithelial and stromal compartments, which are separated by basement membranes (Wang et al., 2013). The epithelium has three major cell types: luminal cells, basal cells, and neuroendocrine cells (NE) (Wang, 2011). The luminal cells express cytokeratins 8 and 18, the cell surface marker CD57, and the androgen receptor (AR). They are terminally differentiated cells that produce prostatic secretory proteins in an androgen-dependent manner.

Androgen withdrawal induces massive apoptosis in the luminal cells. Basal cells, which express cytokeratins 5 and 14, CD44, and P63, reside between the luminal cells and the basement membranes. Although some basal cells weakly express the AR, many of them are AR negative and are not androgen dependent. Neuroendocrine cells, which are a minor cell population in the epithelial compartment, express synaptophysin, chromogranin A, and synaptic vesicle protein 2 (Portela-Gomes et al., 2000). The prostate stroma is a fibromuscular tissue comprised of smooth muscle (SMC)-like cells expressing α-actin and fibroblast-like cells that do not express α-actin. Although the cells in the two compartments are separated by the basement membranes, they maintain active two-way regulatory communications mediated by paracrine growth factors. The fibroblast growth factor (FGF) signaling axis is a major regulatory mechanism in the prostate, required for the development, tissue homeostasis, and function of the prostate (**Figure 1**). Mutations, ablations, and abnormal activations of the FGF signaling axis components are pathological and contribute to cancer development and progression. Disruption of these homeostasis-promoting two-way regulatory communications is a common feature in PCa (Yan et al., 1992, 1993; Feng et al., 1997; Matsubara et al., 1998; McKeehan et al., 1998; Lu et al., 1999; Nakano et al., 1999).

THE FGF SIGNALING AXIS

The fibroblast growth factor family consists of 18 intrinsic tissue regulatory polypeptides, which controls a broad spectrum of cellular processes through binding and activating the transmembrane FGF receptor (FGFR) tyrosine kinase (**Figure 2A**). The FGFR is a glycosylated polypeptide that consists of an extracellular ligand-binding domain, a transmembrane domain, and an intracellular tyrosine kinase domain. Although only four genes (Fgfr1, Fgfr2, Fgfr3, and Fgfr4) encode FGFRs, the diversity of the FGFR family is substantially expanded through alternative splicing. These variants differ in their tissue distributions, binding activities and specificities for ligands and heparan sulfates, and functions. Generally, FGFR variations in the extracellular domain, particularly in the second half of Ig-like domain III, namely IIIb and IIIc, define the ligand-binding specificity, whereas in the intracellular domain, they define the signaling specificity (Li et al., 2016). In addition, heparan sulfate cofactors in the FGF-FGFR signaling complex determine not only the affinity, but also the specificity of the FGF-FGFR interaction.

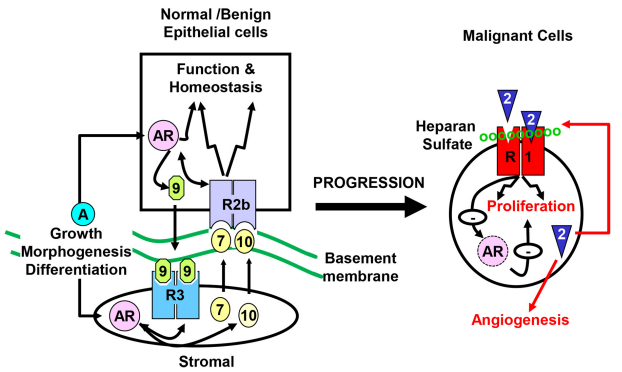

FIGURE 1 | Compartmentalization of the prostate. The prostate epithelial cells are separated from the stromal cells by basement membranes. Testosterone controls direction-specific FGF signaling between the stroma and the epithelium, which maintains prostate tissue homeostasis. The paracrine FGF loops between the stroma and the epithelium is abrogated in cancer cells, and are replaced with autocrine FGF loops that promote cell proliferation, migration, survival, and angiogenesis, which contributes to castration resistance. R1, FGFR1; R2b, FGFR2IIIb; R3, FGFR3; 2, 7, 9, and 10, FGF2, FGF7, FGF9, and FGF10, respectively; AR, androgen receptor.

Binding of the FGF to the FGFR changes the conformation of the HS-FGFR kinase complexes and leads to receptor autophosphorylation, which activates the kinase activity by altering the conformation of an auto inhibitory loop in the kinase domain. Although the four FGFRs share over 80% homology in their primary sequences, they elicit receptor- and cell-type specific activities in cells (Feng et al., 1997; Matsubara et al., 1998; Xian et al., 2007; Luo et al., 2009; Li et al., 2016; Molotkov et al., 2017). Alternative splicing of FGFR1 also contributes to signaling specificity (Brewer et al., 2015). Nevertheless, the mitogen-activated protein kinase (MAPK), phosphoinositide 3-kinase (PI3K), phospholipase Cγ (PLCγ), STAT3, P38, and JNK pathways are considered the downstream pathways in the FGFR1 signaling cascade (Brewer et al., 2016). Tyrosine phosphorylation of FGFR substrate 2α (FRS2α) by the FGFR kinase recruits the growth factor receptor-bound protein 2/son of sevenless homolog 1 (GRB2/SOS1) and SRC homology 2 domain containing phosphatase 2 (SHP2) to FGFR kinases for activation of the MAPK and PI3K/AKT signaling pathways (**Figure 2B**). In addition to these common pathways for FGFRs, emerging evidence demonstrates that FGFRs also have isoform-specific downstream targets, including those discussed in later sections, which, at least in part, account for FGFR signaling specificity. Future efforts are needed to identify these FGFR isoform-specific substrates or pathways.

THE INTRINSIC STROMA-TO-EPITHELIUM FGF7/10-FGFR2 SIGNALING AXIS IN THE PROSTATE CONTROLS PROSTATE DEVELOPMENT, FUNCTION, AND TISSUE HOMEOSTASIS

In the prostate, the epithelial and stromal compartments are separated by the basal membranes. Specific isoforms of FGF and FGFR are partitioned between the two compartments, forming directional communications between them, which regulate development, function, and tissue homeostasis of the prostate (Li et al., 2016). FGFR2 has two isoforms designated FGFR2IIIb and FGFR2IIIc as a result of highly regulated, cell type-specific, and mutually exclusive splicing of exon IIIb or exon IIIc, the two exons coding for the second half of Ig-loop 3. The expression of FGFR2IIIb and FGFR2IIIc isoforms is highly tissue specific.

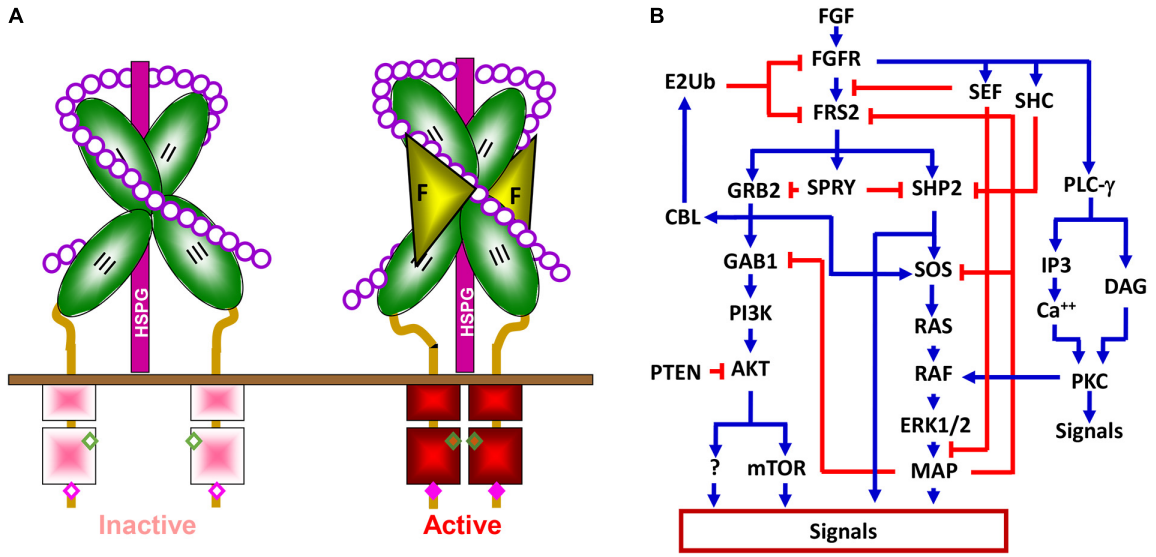

FIGURE 2 | The FGFR signaling pathway. **(A)** The FGFR signaling complex. Interaction with heparin sulfate chains restricts FGFR in an inactive conformation. Docking of FGF releases this negative restriction and changes the FGFR to an active conformation where adjacent kinases trans-phosphorylate each other. II, Ig-loop II; III, Ig-loop III; F, FGF; K, kinase domain; HSPG, heparan sulfate proteoglycan; circles, monosaccharides of heparan sulfate chains; and solid bar, plasma membrane. **(B)** Simplified signaling pathways by FGFR tyrosine kinase. Blue lines represent positive regulation, and red lines represent negative effects.

The exclusive expression of isoform FGFR2IIIb is a hallmark of epithelial cells in a variety of tissues that consist of multiple compartments.

Redundant FGF isoform expression governs appropriate FGF signaling in the prostate. The stromal-derived FGFs, such as FGF7 and FGF10, control epithelial cell resident FGFR2IIIb activities, promote net tissue homeostasis, and restraint tumor cells from progression to malignancy (Feng et al., 1997; Matsubara et al., 1998; Ricol et al., 1999). Interestingly, FGF10, but not FGF7, is required for prenatal, and adolescent prostate development. Ablation of the *Fgf10* alleles disrupts prenatal prostate development and the androgen-responsiveness of prostatic rudiments grafted to kidney capsules of wildtype mice (Donjacour et al., 2003).

Conditional ablation of *Fgfr2* in the prostate epithelium compromises prostate development (Lin et al., 2007). Unlike the normal prostate that composed of 4 pairs of anterior, dorsal, lateral, and ventral lobes, most *Fgfr2* null prostates only have 2 pairs of dorsal and lateral lobes with poorly formed intraluminal infoldings (Lin et al., 2007). Normal prostate undergoes significant atrophy within a few days after androgen-deprivation and fast regeneration after androgen replenishment. Intriguingly, the *Fgfr2* null prostate does not have a significant prostatic atrophy 2 weeks after castration, nor does it have significant cell proliferation after androgen replenishment to the castrated males. This indicates that the *Fgfr2* null prostate is not strictly androgen-dependent with respect to tissue homeostasis. However, similar to normal prostates, production of secretory proteins in the *Fgfr2* null prostate is strictly androgen dependent. Although the protein composition of the prostatic fluid is different between wildtype and *Fgfr2* null prostates, mice bearing *Fgfr2* null alleles are fertile, implying that ablation of *Fgfr2* in the prostate partially impairs prostate function (Lin et al., 2007). Whether other FGFR isoforms compensates the loss of FGFR2 in the prostate remains to be determined. Similarly, targeted expression of a truncated construct of FGFR2IIIb lacking the kinase domain and functions as a dominant negative FGFR2 (dnFGFR2b) in the prostatic epithelium leads to a smaller prostate in mice (Foster et al., 2002). Many epithelial prostatic ducts are disorganized and contain rounded cells that express cytokeratins and do not tightly associate with the basement membrane. The stroma compartment is also poorly organized. The smooth muscle-like cells do not form a tight layer surrounding the epithelial ducts. Together, these data demonstrate that disruption of FGFR2 signaling in the prostate epithelium compromises androgen dependency with respect to tissue homeostasis, as well as the secretory function. Therefore, it appears that the FGF7/FGF10-FGFR2 signaling axis only mediates a subset of AR signaling.

Similar to other tissues, the prostate has tissue stem cells, designated prostate stem cells (P-SCs) that are capable of giving rise to basal, luminal, and neuroendocrine cells, the three cell types in the prostate epithelium. Multiple techniques have been used to identify and characterize P-SCs, which include prostasphere or organoid cultures, renal capsule implantation, and cell lineage tracing with luminal and basal specific proteins (Bhatia-Gaur et al., 1999; Xin et al., 2007; Chua et al., 2014; Karthaus et al., 2014; Huang et al., 2015a). Both adult human and mouse prostate have two types of P-SCs: the basal cell compartment derived sphere-forming cells that express P63, designated basal P-SCs (P-bSCs), and luminal compartment derived cells that express luminal cytokeratins and NKX3.1, designated luminal P-SCs

(P-lSCs) or castrate-resistant Nkx3.1-expressing cells (CARNs) (Wang et al., 2009). Ablation of *Fgfr2* in $P63^+$ cells *in vitro* causes the loss of sphere-forming activity (Huang et al., 2015b). The results demonstrate that FGFR2 signaling is required for formation and maintenance of prostaspheres. Ablation of *Fgfr2* in the prostate epithelium reduces P63-expressing cells in the basal cell compartment, promotes a basal stem cell-to-luminal cell differentiation, and causes prostate developmental defects in the postnatal stage (Huang et al., 2015a,b).

Prostate cancer progression is associated with the loss of resident FGFR2b expression, which abrogates the stroma-epithelium signaling axis (Yan et al., 1993). The loss of epithelial FGFR2 and changes in HS cofactors, are often found associated with tumor progression in a variety of tissues (Wang, 2011; Wang et al., 2013; Yang et al., 2013; Li et al., 2016). In addition, expression of dnFGFR2 potentiates the development and progression of prostatic intraepithelial neoplasia (PIN) lesions induced by expression of ectopic FGFR1 kinase, demonstrating the cooperation between ablation of resident FGFR2 and expression of ectopic FGFR1 in promoting PCa progression (Jin et al., 2003; Wang et al., 2004). Restoration of FGFR2IIIb in human PC cells increases the sensitivity to chemotherapeutic reagents (Shoji et al., 2014) and in stromal cells derived from the DT3327 rat PCa model restores the interaction between PCa and prostate stromal cells (Feng et al., 1997).

ECTOPIC FGF SIGNALING AXIS PERTURBS TISSUE HOMEOSTASIS AND INDUCES TUMORIGENESIS IN THE PROSTATE

Aberrant activation of the FGF signaling axis due to ectopic expression of FGF, FGFR, and heparan sulfate proteoglycans (HSPG) is often associated with various cancers, including PCa. The loss of the homeostasis-promoting intrinsic FGFR2 signaling and concurrent gain of ectopic FGFR1 expression in epithelial tissues of a variety of organs are found associated with tumor progression (Li et al., 2016). Ectopic expression of FGFR1IIIc appears to elicit a new set of abnormal signals in epithelial cells. At the same time, the switch from FGFR2IIIb to FGFR2IIIc isoform cuts off epithelial cells from homeostasis-promoting stromal signals (FGF7/FGF10) that activate FGFR2IIIb (Yan et al., 1993; Feng et al., 1997). Loss of FGF7/FGF10 diminishes the homeostasis promoting function of FGFR2IIIb is also common during PCa progression (Yan et al., 1992; Lu et al., 1999; Wang, 2011; Wang et al., 2013; Li et al., 2016), which, together with gain of FGF2 that activates ectopic FGFR1IIIc, contributes to PCa progression (**Figure 1**). Changes in HSPG core protein expression and in the sulfation patterns of heparin sulfates, which alter the FGF-FGFR specificity, are associated with cancer progression (Li et al., 2016). Multiple transgenic mouse models show that overexpression of FGF2, FGF3, FGF7, or FGF8 in prostate epithelial cells lead to prostatic lesions, ranging from low grade PIN, high-grade PIN to PCa (Chua et al., 2002; Foster et al., 2002; Song et al., 2002; Konno-Takahashi et al., 2004). Furthermore, overexpression of FGF8 promotes PCa development in Pten haploid-insufficient mice, whereas the lesions in mice carrying either the FGF8 transgene or one Pten null allele generally progress only up to PIN (Zhong et al., 2006).

FGF9 has been reported to promote PCa metastasis to bone, the major organ site of PCa metastasis. Previous studies have shown that AR-negative human PCa cells induced bone metastasis is mediated by FGF9 (Li et al., 2008) and that patients with PCa overexpressing FGF9 have a higher risk of a biochemical recurrence (Teishima et al., 2012). Overexpression of FGF9 in mouse prostate epithelial cells leads to development of prostate lesions in an expression level- and age-dependent manner (Huang et al., 2015c). Furthermore, overexpression of FGF9 in the TRAMP (transgenic adenocarcinoma of the mouse prostate) PCa model accelerates the development of advanced PCa. Interestingly, overexpression of FGF9 causes significant changes in the tumor microenvironment, which includes hyper cellularity and hyper proliferation in the stromal compartment. TGFβ1, a key signaling molecule overexpressed in reactive stroma, is expressed at a higher level in FGF9 transgenic and FGF9/TRAMP bi-genic prostates than those that do not carry the FGF9 transgene. *In vivo, in vitro,* and *in silico* analyses of currently available data bases all demonstrate that FGF9 promotes TGFβ1 expression (Huang et al., 2015c). Therefore, FGF9 overexpression in PCa cells augments the formation of reactive stroma in the tumor microenvironment and promotes PCa initiation and progression.

Emerging evidence shows that acquisition of ectopic FGFR1 expression in epithelial cells often accompanies with PCa progression (Wang et al., 2013). Overexpression of FGFR1 in prostate epithelial cells derived from benign, androgen-responsive Dunning 3327PAP tumors increases the malignancy of the cells in a time-dependent manner (Feng et al., 1997; Wang et al., 2002). Expression of the constitutively active FGFR1 (caFGFR1) construct in prostate epithelial cells disrupts tissue homeostasis and induces progressive PIN lesions in a time and expression level-dependent manner in transgenic mice (Jin et al., 2003; Wang et al., 2004). JOCK1, a transgenic mouse model for PCa, highly expresses the membrane-anchored FGFR1 kinase domain fused in frame with a FK506 binding protein (FKBP12) at the C-terminus (Freeman et al., 2003). Sustained activation of this FGFR kinase construct in mice by chemical induced dimerization of FK506 leads to development of low grade PIN by 12 weeks, high grade PIN by 6 months, and adenocarcinoma at later stages (Freeman et al., 2003; Acevedo et al., 2007). Androgen-deprivation to treat metastatic PCa often leads to tumors that bypass the requirement of a functional AR. These PCas are notable for increased MAPK activity. Blocking the FGFR or MAPK pathways with pharmacological inhibitors compromises the growth of these PCas both *in vitro* and *in vivo*, indicating that FGFR/MAPK contributes to escaping from the AR regulation and that the FGFR/MAPK blockade can be a new strategy to treat metastatic PCa with an AR-null phenotype (Bluemn et al., 2017).

ECTOPIC FGFR1 SIGNALING IN PCa CELLS REPROGRAMS CELL METABOLISM AND PROMOTES TUMOR GROWTH

Unlike resident FGFR2 that promotes tissue homeostasis, ectopic FGFR1 promotes tumorigenicity by stimulating proliferation and migration, as well as by preventing cell death (Li et al., 2016). We recently also reported that FGFR1 in PCa cells reprograms cellular energy metabolism by changing the expression profile of lactate dehydrogenase (LDH) isozymes (Liu et al., 2018). Metabolic reprograming from oxidative phosphorylation to aerobic glycolysis, designated the Warburg effect, is a common event in cancer progression. Compared with oxidative phosphorylation, aerobic glycolysis is less efficient with respect to generating ATP. However, it provides metabolites as building blocks for cancer cells to meet the anabolic demands of rapidly growing cells. Reduction of pyruvate to lactate is the last step of glycolysis. LDH is an enzyme catalyzing the reversible conversion between pyruvate and lactate. It is a tetramer composed of two types of subunits, LDHA, and LDHB. The LDHB subunit favors the conversion of lactate to pyruvate, and therefore, oxidative phosphorylation. The LDHA subunit, however, favors the conversion of pyruvate to lactate, and therefore, aerobic glycolysis (Fritz, 1965). FGFR1 tyrosine phosphorylates LDHA, which prevents its degradation, and therefore, increases LDHA activity in the cells. In addition, FGFR1 reduces LDHB expression by promoting CpG island methylation of the LDHB promoter (Liu et al., 2018). Through this mechanism, FGFR1 reprograms PCa cell metabolism from oxidative phosphorylation to aerobic glycolysis (**Figure 3**). Experiments with PCa xenografts show that LDHA depletion compromises the tumor growth, while LDHB depletion promotes tumor growth. Systematic analyses of a tissue microarray derived from PCa patients with 15 year follow-up reveal that FGFR1 overexpression is associated with high LDHA/low LDHB expression, as well as with short overall survival and biochemical recurrence times of the patients (Liu et al., 2018). The results indicate that ectopic FGFR1 expression together with LDH isoform profiles can serve as a biomarker for PCa diagnosis and prognosis.

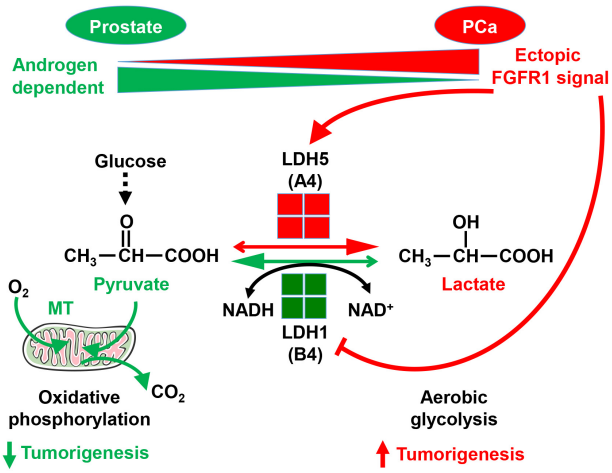

FIGURE 3 | Ectopic FGFR1 signaling in reprograming cell metabolism and promoting tumorigenesis. FGFR1 reprograms cell metabolism by controlling LDH isoform expression a. A, LDHA; B, LDHB; MT, mitochondria. This figure was originally published in Liu et al. (2018).

ECTOPIC FGFR1 SIGNALING IN PCa CELLS PROMOTES INFLAMMATION IN THE TUMOR MICROENVIRONMENT

Inflammation in the tumor microenvironment is one of the hallmark in cancer progression (Hanahan and Weinberg, 2011). Cancer cells produce multiple inflammation-promoting chemokines and cytokines that attract lymphocytes to infiltrate into the tumor microenvironment. Among them is the NF-κB signaling axis. We recently discovered that FGF promotes NF-κB signaling in PCa cells (Wang et al., 2018). Interestingly, the three common signaling pathways downstream of FGFR1 kinase, ERK1/2, PI3K/AKT, and PLCγ, are not required for FGFR1 to augment NF-κB signaling. Instead, FGFR1 phosphorylates transforming growth factor β–activating kinase 1 (TAK1), an adaptor protein in the TNFα/NF-κB pathway. This phosphorylation reduces ubiquitination-dependent TAK1 degradation, and therefore, promotes NF-κB signaling (**Figure 4**). Ablation of *Fgfr1* alleles in the prostate epithelium reduces inflammation in the TRAMP tumors. Consistently, activation of the FGFR1 kinase increases inflammation in the JOCK1 mouse model (Wang et al., 2018). It has been well documented that inflammation is important for PCa initiation and progression. Therefore, promoting inflammation in the tumor microenvironment is one of the mechanisms underlying the tumor promoting activity of FGFR1.

INACTIVATING ECTOPIC FGF SIGNALING SUPPRESSES PROSTATE TUMORIGENESIS

The involvement of ectopic FGF signaling pathways in PCa initiation and progression suggests that blockading these pathways can be used to treat patients with PCa. Multiple small molecule inhibitors for the FGFR tyrosine kinases have been developed and are currently used in clinical trials for a variety of cancers, including CRPCs (Corn et al., 2013).

FGF2, which is frequently overexpressed in human PCa, promotes cell proliferation, prevents cell death, and increases tumor angiogenesis (Giri et al., 1999). Ablation of *Fgf2* alleles in TRAMP mice significantly inhibits the progression to poorly differentiated prostatic tumors, decreases metastasis to other organs, and increases the lifespan of the mice. Furthermore, ablation of only one *Fgf2* allele also affects

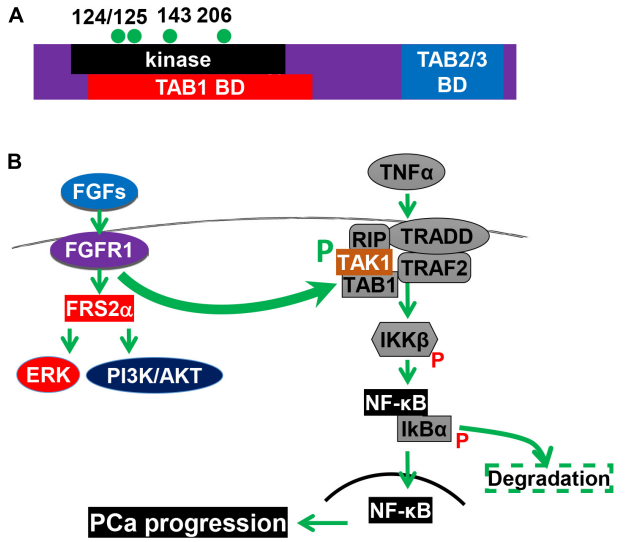

FIGURE 4 | The FGFR1 pathway promotes NF-κB signaling. **(A)** Structural domains and tyrosine phosphorylation sites of TAK1. **(B)** FGFR1 phosphorylates TAK1 and augments the NF-κB pathways. 124, 125, 143, and 206, four tyrosine phosphorylation sites; BD, binding domain; CD, C-terminal binding domain; KD, kinase domain; and P, phosphorylation. This figure was originally published in Wang et al. (2018).

TRAMP tumorigenesis, indicating that FGF2 has a gene dosage-dependent effect on PCa progression (Polnaszek et al., 2003). These data underscore the role of FGF2 in PCa progression as illustrated in **Figure 1**. TRAMP mice with *Fgfr1* ablation in prostate epithelial cells developed smaller tumors with characteristic early, well-differentiated lesions and phyllodes-type tumors. *Fgfr1* null TRAMP mice survived significantly longer than control TRAMP mice. All metastases in TRAMP/*Fgfr1* null mice were primarily those that escape *Fgfr1* disruption and highly expressed FGFR1, or neuroendocrine tumors regardless of FGFR1 status. Together, the results indicate that ectopic FGFR1 plays a critical role in the initiation, progression, and particularly metastasis of PCa (Yang et al., 2013).

FRS2 is an adaptor protein in the FGFR tyrosine kinase signaling cascade (Wang et al., 2016). It is extensively tyrosine phosphorylated by the activated FGFR kinase. The phosphorylation creates binding sites for GRB2 (Y196, Y306, Y349, Y392) that mainly link to PI3K activation, and SHP2 (Y436 and Y471) that mainly links the FGFR kinase to the MAP kinase pathway (Li et al., 2016; Wang et al., 2016). *Frs2α* is expressed almost ubiquitously in both fetal and adult tissues (McDougall et al., 2001). A rearrangement in the human Frs2α gene located in 12q15 is common in a range of tumors, suggesting that aberrant expression of FRS2α is involved in tumorigenesis. Disruption of *Frs2α* alleles in the prostate epithelium compromises the branching morphogenesis of the mouse prostate. Unlike *Fgfr2* ablation that weakens androgen dependency, ablation of *Frs2α* does not affect androgen dependency with respect to the production of secretory proteins and tissue homeostasis (Zhang et al., 2008). In the adult prostate, *Frs2α* is not expressed in luminal epithelial cells. However, it is highly expressed in TRAMP tumor epithelial cells. Conditional ablation of *Frs2α* alleles in prostate epithelial cells represses PCa initiation and progression, as evidenced by fewer and lower grade of PIN lesion foci at early stages, less advanced tumors at mid stages, and a longer lifespan of *Frs2α* conditional null TRAMP than that of parental TRAMP mice (Zhang et al., 2008).

Furthermore, analyses of a PCa tissue microarray consisting of 225 PCa samples reveals that over activation of FRS2α, cJUN, and hypoxia-inducible factor α (HIF1α) is positively correlated with blood vessel density and malignancy of human PCa (Liu et al., 2015). Ablation of *Frs2α* in mouse prostate epithelial cells reduces vascular endothelial growth factor A (VEGF-A) expression in a cJUN and HIF1α dependent manner. Depletion of FRS2α expression in human PCa cells and in MDA PCa 118b, a human PCa-derived xenograft, also suppresses tumor angiogenesis, as well as decreases bone metastasis of the tumor. Together, the result indicates that acquisition of FRS2α-mediated signaling in epithelial cells is involved in PCa initiation and progression. It also indicates that overexpressed FRS2α has the potential to serve as a biomarker for PCa diagnosis and prognosis.

REMARKS

Although the four FGFR kinases are highly homologous in their primary sequences and share similar structural domains and tyrosine phosphorylation sites, their signaling specificities are different and sometimes function in opposite directions. Although the four FGFRs share multiple common downstream pathways, they have isoform-specific downstream targets that contributes to isoform-specific signaling. Aberrant expression, activation, or inactivation of the FGF signaling pathways have been identified as culprits for diverse developmental disorders and diseases, including PCa. No clinical benefits have been reported in the five clinical trials using a broad tyrosine kinase inhibitor for multiple growth factor receptors, including FGFR1, to treat CRPC. In addition, simply treating PCa cells with pan-FGFR kinase inhibitors promotes neuroendocrine differentiation. Therefore, developing new FGFR isoform-specific inhibitors are urgently needed for treating cancers with ectopic FGFR isoform expression. Understanding the detailed molecular basis for the cell type- and receptor isoform-specific activities of the four FGFRs is essential for developing strategies to target FGFR isoform-specific signaling. Furthermore, suppression of ectopic FGFR1 signaling reduces inflammation in the tumor microenvironment and reverses metabolic reprogramming of cancer cells, both of which have profound effects on anti-cancer chemotherapies and anti-checkpoint treatment. Therefore, combination of blocking FGFR1 signals with other anti-cancer drugs shall be a promising novel strategy for treating CRPC and other cancers with ectopic FGFR1 expression.

AUTHOR CONTRIBUTIONS

All authors participated in reference gathering, reviewing, manuscript writing, and proofreading.

FUNDING

This work was supported by in part by TAMU1400302 and CPRIT 110555 to FW, a gift from Agilent Technologies, and the National Natural Science Foundation of China 81101712, 31371470, and 81270761, Natural Science Foundation of Zhejiang Province of China LY16H140004 to CW.

ACKNOWLEDGMENTS

We thank Dr. Stefan Siwko for critical reading of this manuscript.

REFERENCES

Acevedo, V. D., Gangula, R. D., Freeman, K. W., Li, R., Zhang, Y., Wang, F., et al. (2007). Inducible FGFR-1 activation leads to irreversible prostate adenocarcinoma and an epithelial-to-mesenchymal transition. *Cancer Cell* 12, 559–571. doi: 10.1016/j.ccr.2007.11.004

Bhatia-Gaur, R., Donjacour, A. A., Sciavolino, P. J., Kim, M., Desai, N., Young, P., et al. (1999). Roles for Nkx3.1 in prostate development and cancer. *Genes Dev.* 13, 966–977. doi: 10.1101/gad.13.8.966

Bluemn, E. G., Coleman, I. M., Lucas, J. M., Coleman, R. T., Hernandez-Lopez, S., Tharakan, R., et al. (2017). Androgen receptor pathway-independent prostate cancer is sustained through FGF signaling. *Cancer Cell* 32, 474.e6–489.e6. doi: 10.1016/j.ccell.2017.09.003

Brewer, J. R., Mazot, P., and Soriano, P. (2016). Genetic insights into the mechanisms of Fgf signaling. *Genes Dev.* 30, 751–771. doi: 10.1101/gad.277137.115

Brewer, J. R., Molotkov, A., Mazot, P., Hoch, R. V., and Soriano, P. (2015). Fgfr1 regulates development through the combinatorial use of signaling proteins. *Genes Dev.* 29, 1863–1874. doi: 10.1101/gad.264994.115

Chua, C. W., Shibata, M., Lei, M., Toivanen, R., Barlow, L. J., Bergren, S. K., et al. (2014). Single luminal epithelial progenitors can generate prostate organoids in culture. *Nat. Cell Biol.* 16, 951–961. doi: 10.1038/ncb3047

Chua, S. S., Ma, Z. Q., Gong, L., Lin, S. H., DeMayo, F. J., and Tsai, S. Y. (2002). Ectopic expression of FGF-3 results in abnormal prostate and Wolffian duct development. *Oncogene* 21, 1899–1908. doi: 10.1038/sj.onc.1205096

Corn, P. G., Wang, F., McKeehan, W. L., and Navone, N. (2013). Targeting fibroblast growth factor pathways in prostate cancer. *Clin. Cancer Res.* 19, 5856–5866. doi: 10.1158/1078-0432.CCR-13-1550

Denmeade, S. R., and Isaacs, J. T. (2002). A history of prostate cancer treatment. *Nat. Rev. Cancer* 2, 389–396. doi: 10.1038/nrc801

Donjacour, A. A., Thomson, A. A., and Cunha, G. R. (2003). FGF-10 plays an essential role in the growth of the fetal prostate. *Dev. Biol.* 261, 39–54. doi: 10.1016/S0012-1606(03)00250-1

Feng, S., Wang, F., Matsubara, A., Kan, M., and McKeehan, W. L. (1997). Fibroblast growth factor receptor 2 limits and receptor 1 accelerates tumorigenicity of prostate epithelial cells. *Cancer Res.* 57, 5369–5378.

Foster, B. A., Evangelou, A., Gingrich, J. R., Kaplan, P. J., DeMayo, F., and Greenberg, N. M. (2002). Enforced expression of FGF-7 promotes epithelial hyperplasia whereas a dominant negative FGFR2iiib promotes the emergence of neuroendocrine phenotype in prostate glands of transgenic mice. *Differentiation* 70, 624–632. doi: 10.1046/j.1432-0436.2002.700915.x

Freeman, K. W., Welm, B. E., Gangula, R. D., Rosen, J. M., Ittmann, M., Greenberg, N. M., et al. (2003). Inducible prostate intraepithelial neoplasia with reversible hyperplasia in conditional FGFR1-expressing mice. *Cancer Res.* 63, 8256–8263.

Fritz, P. J. (1965). Rabbit muscle lactate dehydrogenase 5; a regulatory enzyme. *Science* 150, 364–366. doi: 10.1126/science.150.3694.364

Giri, D., Ropiquet, F., and Ittmann, M. (1999). Alterations in expression of basic fibroblast growth factor (FGF) 2 and its receptor FGFR-1 in human prostate cancer. *Clin. Cancer Res.* 5, 1063–1071.

Hanahan, D., and Weinberg, R. A. (2011). Hallmarks of cancer: the next generation. *Cell* 144, 646–674. doi: 10.1016/j.cell.2011.02.013

Huang, Y., Hamana, T., Liu, J., Wang, C., An, L., You, P., et al. (2015a). Prostate sphere-forming stem cells are derived from the P63-expressing basal compartment. *J. Biol. Chem.* 290, 17745–17752. doi: 10.1074/jbc.M115.661033

Huang, Y., Hamana, T., Liu, J., Wang, C., An, L., You, P., et al. (2015b). Type 2 fibroblast growth factor receptor signaling preserves stemness and prevents differentiation of prostate stem cells from the basal compartment. *J. Biol. Chem.* 290, 17753–17761. doi: 10.1074/jbc.M115.661066

Huang, Y., Jin, C., Hamana, T., Liu, J., Wang, C., An, L., et al. (2015c). Overexpression of FGF9 in prostate epithelial cells augments reactive stroma formation and promotes prostate cancer progression. *Int. J. Biol. Sci.* 11, 948–960. doi: 10.7150/ijbs.12468

Jemal, A., Siegel, R., Ward, E., Hao, Y., Xu, J., and Thun, M. J. (2009). Cancer statistics, 2009. *CA Cancer J. Clin.* 59, 225–249. doi: 10.3322/caac.20006

Jin, C., McKeehan, K., Guo, W., Jauma, S., Ittmann, M. M., Foster, B., et al. (2003). Cooperation between ectopic FGFR1 and depression of FGFR2 in induction of prostatic intraepithelial neoplasia in the mouse prostate. *Cancer Res.* 63, 8784–8790.

Karthaus, W. R., Iaquinta, P. J., Drost, J., Gracanin, A., van Boxtel, R., Wongvipat, J., et al. (2014). Identification of multipotent luminal progenitor cells in human prostate organoid cultures. *Cell* 159, 163–175. doi: 10.1016/j.cell.2014.08.017

Konno-Takahashi, N., Takeuchi, T., Nishimatsu, H., Kamijo, T., Tomita, K., Schalken, J. A., et al. (2004). Engineered FGF-2 expression induces glandular epithelial hyperplasia in the murine prostatic dorsal lobe. *Eur. Urol.* 46, 126–132. doi: 10.1016/j.eururo.2004.02.004

Li, X., Wang, C., Xiao, J., McKeehan, W. L., and Wang, F. (2016). Fibroblast growth factors, old kids on the new block. *Semin. Cell Dev. Biol.* 53, 155–167. doi: 10.1016/j.semcdb.2015.12.014

Li, Z. G., Mathew, P., Yang, J., Starbuck, M. W., Zurita, A. J., Liu, J., et al. (2008). Androgen receptor-negative human prostate cancer cells induce osteogenesis in mice through FGF9-mediated mechanisms. *J. Clin. Invest.* 118, 2697–2710. doi: 10.1172/JCI33093

Lin, Y., Liu, G., Zhang, Y., Hu, Y. P., Yu, K., Lin, C., et al. (2007). Fibroblast growth factor receptor 2 tyrosine kinase is required for prostatic morphogenesis and the acquisition of strict androgen dependency for adult tissue homeostasis. *Development* 134, 723–734. doi: 10.1242/dev.02765

Liu, J., Chen, G., Liu, Z., Liu, S., Cai, Z., You, P., et al. (2018). Aberrant FGFR tyrosine kinase signaling enhances the warburg effect by reprogramming LDH isoform expression and activity in prostate cancer. *Cancer Res.* 78, 4459–4470. doi: 10.1158/0008-5472.CAN-17-3226

Liu, J., You, P., Chen, G., Fu, X., Zeng, X., Wang, C., et al. (2015). Hyperactivated FRS2alpha-mediated signaling in prostate cancer cells promotes tumor angiogenesis and predicts poor clinical outcome of patients. *Oncogene* 35, 1750–1759. doi: 10.1038/onc.2015.239

Lu, W., Luo, Y., Kan, M., and McKeehan, W. L. (1999). Fibroblast growth factor-10. A second candidate stromal to epithelial cell andromedin in prostate. *J. Biol. Chem.* 274, 12827–12834. doi: 10.1074/jbc.274.18.12827

Luo, Y., Yang, C., Jin, C., Xie, R., Wang, F., and McKeehan, W. L. (2009). Novel phosphotyrosine targets of FGFR2IIIb signaling. *Cell. Signal.* 21, 1370–1378. doi: 10.1016/j.cellsig.2009.04.004

Matsubara, A., Kan, M., Feng, S., and McKeehan, W. L. (1998). Inhibition of growth of malignant rat prostate tumor cells by restoration of fibroblast growth factor receptor 2. *Cancer Res.* 58, 1509–1514.

McDougall, K., Kubu, C., Verdi, J. M., and Meakin, S. O. (2001). Developmental expression patterns of the signaling adapters FRS-2 and FRS-3 during early embryogenesis. *Mech. Dev.* 103, 145–148. doi: 10.1016/S0925-4773(01)00337-9

McKeehan, W. L., Wang, F., and Kan, M. (1998). The heparan sulfate-fibroblast growth factor family: diversity of structure and function. *Prog. Nucleic Acid Res. Mol. Biol.* 59, 135–176. doi: 10.1016/S0079-6603(08)61031-4

Molotkov, A., Mazot, P., Brewer, J. R., Cinalli, R. M., and Soriano, P. (2017). Distinct requirements for FGFR1 and FGFR2 in primitive endoderm development and exit from pluripotency. *Dev. Cell* 41, 511–526e4. doi: 10.1016/j.devcel.2017.05.004

Nakano, K., Fukabori, Y., Itoh, N., Lu, W., Kan, M., McKeehan, W. L., et al. (1999). Androgen-stimulated human prostate epithelial growth mediated by stromal-derived fibroblast growth factor-10. *Endocr. J.* 46, 405–413. doi: 10.1507/endocrj.46.405

Polnaszek, N., Kwabi-Addo, B., Peterson, L. E., Ozen, M., Greenberg, N. M., Ortega, S., et al. (2003). Fibroblast growth factor 2 promotes tumor progression in an autochthonous mouse model of prostate cancer. *Cancer Res.* 63, 5754–5760.

Portela-Gomes, G. M., Lukinius, A., and Grimelius, L. (2000). Synaptic vesicle protein 2, A new neuroendocrine cell marker. *Am. J. Pathol.* 157, 1299–1309. doi: 10.1016/S0002-9440(10)64645-7

Ricol, D., Cappellen, D., El Marjou, A., Gil-Diez-de-Medina, S., Girault, J. M., Yoshida, T., et al. (1999). Tumour suppressive properties of fibroblast growth factor receptor 2- IIIb in human bladder cancer. *Oncogene* 18, 7234–7243. doi: 10.1038/sj.onc.1203186

Shoji, K., Teishima, J., Hayashi, T., Ohara, S., McKeehan, W. L., and Matsubara, A. (2014). Restoration of fibroblast growth factor receptor 2IIIb enhances the chemosensitivity of human prostate cancer cells. *Oncol. Rep.* 32, 65–70. doi: 10.3892/or.2014.3200

Song, Z., Wu, X., Powell, W. C., Cardiff, R. D., Cohen, M. B., Tin, R. T., et al. (2002). Growth factor 8 isoform b overexpression in prostate epithelium: a new mouse model for prostatic intraepithelial neoplasia. *Cancer Res.* 62, 5096–5105.

Teishima, J., Shoji, K., Hayashi, T., Miyamoto, K., Ohara, S., and Matsubara, A. (2012). Relationship between the localization of fibroblast growth factor 9 in prostate cancer cells and postoperative recurrence. *Prostate Cancer Prostatic Dis.* 15, 8–14. doi: 10.1038/pcan.2011.48

Wang, C., Ke, Y., Liu, S., Pan, S., Liu, Z., Zhang, H., et al. (2018). Ectopic fibroblast growth factor receptor 1 promotes inflammation by promoting nuclear factor-kappaB signaling in prostate cancer cells. *J. Biol. Chem.* 293, 14839–14849. doi: 10.1074/jbc.RA118.002907

Wang, C., McKeehan, W. L., and Wang, F. (2016). "FRS2α, at the center of FGF signaling," in *Fibroblast Growth Factors*, ed. M. Simons (NJ, New Jersey: World Scientific).

Wang, F. (2011). Modeling human prostate cancer in genetically engineered mice. *Prog. Mol. Biol. Transl. Sci.* 100, 1–49. doi: 10.1016/B978-0-12-384878-9.00001-7

Wang, F., Luo, Y., and McKeehan, W. (2013). "The FGF signaling axis in prostate tumorigenesis," in *Molecular Oncology: Causes of Cancer and Targets for Treatment*, eds E. P. Gelmann, C. L. Sawyers, and F. J. III Rauscher (London: University Press). doi: 10.1017/CBO9781139046947.017

Wang, F., McKeehan, K., Yu, C., Ittmann, M., and McKeehan, W. L. (2004). Chronic activity of ectopic type 1 fibroblast growth factor receptor tyrosine kinase in prostate epithelium results in hyperplasia accompanied by intraepithelial neoplasia. *Prostate* 58, 1–12. doi: 10.1002/pros.10311

Wang, F., McKeehan, K., Yu, C., and McKeehan, W. L. (2002). Fibroblast growth factor receptor 1 phosphotyrosine 766: molecular target for prevention of progression of prostate tumors to malignancy. *Cancer Res.* 62, 1898–1903.

Wang, X., Kruithof-de Julio, M., Economides, K. D., Walker, D., Yu, H., Halili, M. V., et al. (2009). A luminal epithelial stem cell that is a cell of origin for prostate cancer. *Nature* 461, 495–500. doi: 10.1038/nature08361

Xian, W., Schwertfeger, K. L., and Rosen, J. M. (2007). Distinct roles of fibroblast growth factor receptor 1 and 2 in regulating cell survival and epithelial-mesenchymal transition. *Mol. Endocrinol.* 21, 987–1000. doi: 10.1210/me.2006-0518

Xin, L., Lukacs, R. U., Lawson, D. A., Cheng, D., and Witte, O. N. (2007). Self-renewal and multilineage differentiation in vitro from murine prostate stem cells. *Stem Cells* 25, 2760–2769. doi: 10.1634/stemcells.2007-0355

Yan, G., Fukabori, Y., McBride, G., Nikolaropolous, S., and McKeehan, W. L. (1993). Exon switching and activation of stromal and embryonic fibroblast growth factor (FGF)-FGF receptor genes in prostate epithelial cells accompany stromal independence and malignancy. *Mol. Cell. Biol.* 13, 4513–4522. doi: 10.1128/MCB.13.8.4513

Yan, G., Fukabori, Y., Nikolaropoulos, S., Wang, F., and McKeehan, W. L. (1992). Heparin-binding keratinocyte growth factor is a candidate stromal-to-epithelial-cell andromedin. *Mol. Endocrinol.* 6, 2123–2128.

Yang, F., Zhang, Y., Ressler, S. J., Ittmann, M. M., Ayala, G. E., Dang, T. D., et al. (2013). FGFR1 is essential for prostate cancer progression and metastasis. *Cancer Res.* 73, 3716–3724. doi: 10.1158/0008-5472.CAN-12-3274

Zhang, Y., Zhang, J., Lin, Y., Lan, Y., Lin, C., Xuan, J. W., et al. (2008). Role of epithelial cell fibroblast growth factor receptor substrate 2{alpha} in prostate development, regeneration and tumorigenesis. *Development* 135, 775–784. doi: 10.1242/dev.009910

Zhong, C., Saribekyan, G., Liao, C. P., Cohen, M. B., and Roy-Burman, P. (2006). Cooperation between FGF8b overexpression and PTEN deficiency in prostate tumorigenesis. *Cancer Res.* 66, 2188–2194. doi: 10.1158/0008-5472.CAN-05-3440

Conflict of Interest Statement: The authors declare that the research was conducted in the absence of any commercial or financial relationships that could be construed as a potential conflict of interest.

Copyright © 2019 Wang, Liu, Ke and Wang. This is an open-access article distributed under the terms of the Creative Commons Attribution License (CC BY). The use, distribution or reproduction in other forums is permitted, provided the original author(s) and the copyright owner(s) are credited and that the original publication in this journal is cited, in accordance with accepted academic practice. No use, distribution or reproduction is permitted which does not comply with these terms.

frontiers in Genetics

MINI REVIEW
published: 12 February 2019
doi: 10.3389/fgene.2019.00102

Structural Biology of the FGF7 Subfamily

*Allen Zinkle and Moosa Mohammadi**

Department of Biochemistry and Molecular Pharmacology, New York University Langone Medical Center, New York, NY, United States

Mammalian fibroblast growth factor (FGF) signaling is intricately regulated via selective binding interactions between 18 FGF ligands and four FGF receptors (FGFR1–4), three of which (FGFR1–3) are expressed as either epithelial ("b") or mesenchymal ("c") splice isoforms. The FGF7 subfamily, consisting of FGF3, FGF7, FGF10, and FGF22, is unique among FGFs in that its members are secreted exclusively by the mesenchyme, and specifically activate the "b" isoforms of FGFR1 (FGFR1b) and FGFR2 (FGFR2b) present in the overlying epithelium. This unidirectional mesenchyme-to-epithelium signaling contributes to the development of essentially all organs, glands, and limbs. Structural analysis has shown that members of the FGF7 subfamily achieve their restricted specificity for FGFR1b/FGFR2b by engaging in specific contacts with two alternatively spliced loop regions in the immunoglobulin-like domain 3 (D3) of these receptors. Weak basal receptor-binding affinity further constrains the FGF7 subfamily's specificity for FGFR1b/2b. In this review, we elaborate on the structural determinants of FGF7 subfamily receptor-binding specificity, and discuss how affinity differences among the four members for the heparin sulfate (HS) co-receptor contribute to their disparate biological activities.

Keywords: FGF7, FGF10, signaling specificity, crystal structure, threshold model

OPEN ACCESS

Edited by:
Mohammad K. Hajihosseini, University of East Anglia, United Kingdom

Reviewed by:
Lin Chen, Daping Hospital, China
Chunying Li, Georgia State University, United States

***Correspondence:**
Moosa Mohammadi
moosa.mohammadi@nyumc.org

Specialty section:
This article was submitted to Stem Cell Research, a section of the journal Frontiers in Genetics

Received: *04 December 2018*
Accepted: *29 January 2019*
Published: *12 February 2019*

Citation:
Zinkle A and Mohammadi M (2019) Structural Biology of the FGF7 Subfamily. Front. Genet. 10:102. doi: 10.3389/fgene.2019.00102

INTRODUCTION

The fibroblast growth factor (FGF) 7 subfamily is comprised of FGF3, FGF7 (the founding member), FGF10, and FGF22, and constitutes one of five paracrine-acting FGF subfamilies (Itoh and Ornitz, 2004). Members of the FGF7 subfamily are essential for organogenesis and tissue patterning in the embryo, and mediate wound healing and tissue homeostasis in adult mammals (Beenken and Mohammadi, 2009). Specifically, FGF3 is required for inner ear development (Tekin et al., 2007, 2008), FGF7 for the development of the kidney, thymus, and hippocampus (Qiao et al., 1999; Alpdogan et al., 2006; Terauchi et al., 2010; Lee et al., 2012), FGF10 for limb, lung, thyroid, pituitary, lacrimal, and salivary gland (LG and SMG, respectively) development (Bellusci et al., 1997; Min et al., 1998; Xu et al., 1998; Sekine et al., 1999; De Moerlooze et al., 2000; Makarenkova et al., 2000; Hoffman et al., 2002; Izvolsky et al., 2003), and FGF22 for presynaptic neural differentiation (Umemori et al., 2004). Reflecting this functional pleiotropy, aberrant signaling by FGF7 subfamily ligands is responsible for a variety of heritable and acquired human diseases, including congenital deafness (LAMM syndrome) (Tekin et al., 2007, 2008),

lacrimo-auriculo-dento-digital (LADD) syndrome (Milunsky et al., 2006), inflammatory bowel disease (Finch et al., 1996), Apert syndrome (AS) (Wilkie et al., 1995; Anderson et al., 1998; Ibrahimi et al., 2001), and prostate cancer (Memarzadeh et al., 2007), among others (Itoh and Ornitz, 2011; Belov and Mohammadi, 2013).

Paracrine FGFs share a core homology region of about 120 amino acids (Beenken and Mohammadi, 2009) that adopt a β-trefoil fold comprised of 12 β-strands (β1 through β12) (Eriksson et al., 1991; Zhu et al., 1991; Osslund et al., 1998; Bellosta et al., 2001; Plotnikov et al., 2001) flanked by N- and C-terminal extensions of variable length and sequence (Mohammadi et al., 2005). These ligands mediate their activities by binding to, dimerizing, and consequently activating cell surface FGF receptors (FGFRs), a family within the single-pass transmembrane receptor tyrosine kinase superfamily. Mammals have four FGFR genes (*FGFR1–4*), each encoding an extracellular portion composed of three Ig-like domains (termed D1–D3) connected by flexible linkers, and an intracellular segment containing a tyrosine kinase domain bounded by flexible N-terminal juxtamembrane and C-terminal tail regions (Mohammadi et al., 2005). Ligand binding requires the D2, D3, and D2–D3 linker regions, whereas the D1 and D1–D2 linker are implicated in receptor autoinhibition (Plotnikov et al., 1999, 2000; Schlessinger et al., 2000; Stauber et al., 2000; Yeh et al., 2003; Olsen et al., 2004, 2006; Liu et al., 2017; Chen et al., 2018). Alternative splicing in the D3 domains of FGFR1–3 generates epithelium- and mesenchyme-specific "b" and "c" isoforms, respectively, with each isoform harboring primary sequence differences in the ligand-binding region in the second half of D3, thus expanding the number of principal FGFRs from four to seven (Orr-Urtreger et al., 1993; Mohammadi et al., 2005).

Paracrine FGFs interact with HS glycosaminoglycans (HSGAG), a mandatory co-receptor/factor in paracrine FGF signaling. HS is a heterogeneously sulfated linear glycan chain of HS proteoglycans, which are ubiquitously expressed either on the cell surface or as soluble components deposited in the extracellular matrix (ECM) (Rapraeger et al., 1991; Yayon et al., 1991; Ornitz et al., 1992; Liu et al., 1996; Perrimon and Bernfield, 2000; Esko and Selleck, 2002). The HS binding site (HBS) of FGFs, housed within the FGF core, is formed by residues from the loop between the β1 and β2 strands as well as the stretch between the β10 and β12 strands (Beenken and Mohammadi, 2009). The HBS regions are rich in basic amino acid residues that engage with sulfate and carboxylate moieties of HS, resulting in avid interaction with HS and sequestration of paracrine FGFs in the ECM. Amino acid variations within the HBS account for the different HS-binding affinities of FGFs across and within paracrine FGF subfamilies. Despite their primary sequence differences, the HBS region between the β10 and β12 strands adopts a common conformation among paracrine FGFs. Nevertheless, in contrast to that of other paracrine FGFs, the conformation of the β10–β11 strand pair HBS region in the FGF7 subfamily is loosely supported by only a single hydrogen bond between the two strands (Yeh et al., 2003).

Heparin sulfate promotes paracrine FGF signaling by orchestrating the formation of a symmetric 2:2 FGF:FGFR dimer on the cell surface. This juxtaposes the intracellular kinase domains in a proximity/orientation necessary for activation loop (A-loop) transphosphorylation, a prerequisite for kinase activation (Plotnikov et al., 1999; Schlessinger et al., 2000; Mohammadi et al., 2005). Following this reaction, additional tyrosine transphosphorylation occurs in the kinase C-terminal tail and juxtamembrane (JM) regions, enabling the activated FGFR to recruit and phosphorylate intracellular signaling molecules (Plotnikov et al., 1999; Mohammadi et al., 2005). In the dimer, FGFRs are located centrally and are bound by both FGFs at the periphery. The dimer interface is mediated by reciprocal contacts between D2 and the FGF ligand from one 1:1 protomer with D2 in the adjoining 1:1 FGF–FGFR protomer. Each HS molecule simultaneously engages the HBS of one FGF and that of the two FGFRs (located in the D2 domain) from both 1:1 protomers (Schlessinger et al., 2000). In doing so, HS enhances the contacts between the FGF and FGFR within each 1:1 protomer in addition to those at the dimer interface, thereby stabilizing the 1:1 complex and buttressing the 2:2 dimer.

FGF–FGFR binding specificity is a key regulator of FGF signaling (Ornitz et al., 1996; Zhang et al., 2006), and is determined by differences in the primary sequences among FGFs and FGFRs, as well as differences in their spatiotemporal expression patterns and HS sulfation motifs. Notably, FGF–FGFR binding specificity establishes bidirectional communication between the epithelium and mesenchyme during development. The FGF7 subfamily is the sole subfamily expressed exclusively in the mesenchyme, and interacts primarily with the "b" isoforms of FGFR2 (FGFR2b) and, to a lesser extent, FGFR1 (FGFR1b) (Mason et al., 1994; Zhang et al., 2006). The remaining four paracrine-acting subfamilies are secreted by epithelial tissues and bind almost exclusively to mesenchyme-specific "c" FGFR isoforms (Ornitz et al., 1996; Zhang et al., 2006; Beenken and Mohammadi, 2009). Because of its tight receptor-binding specificity, the FGF7 subfamily serves as an ideal model for studying the structural determinants of FGF–FGFR binding specificity and function. Indeed, the FGF10-FGFR2b structure – the only FGF7 subfamily FGF–FGFR complex whose atomic structure is currently known – in combination with sequence alignment of the remaining three FGF7 subfamily ligands, has provided major insight into the molecular basis for the entire FGF7 subfamily's restricted receptor-binding specificity. Furthermore, structural analysis has also shed light on differences among FGF7 subfamily members that explain their non-redundant functions. Specifically, differences in HS-binding affinity suggest that the biological activity of each subfamily member may be governed by distinct thresholds of FGFR dimerization strength, as previously demonstrated in FGF1 (Huang et al., 2017).

STRUCTURAL DETERMINANTS OF FGF7 SUBFAMILY'S SPECIFICITY

Based on the 1:1 FGF10:FGFR2b crystal structure (Yeh et al., 2003), the exquisite specificity of the FGF7 subfamily for "b" splice isoform FGFRs is dictated primarily by contacts between

ligand and the alternatively spliced regions in the receptor D3 domain. However, the structure also reveals an additional determinant of FGF7 subfamily receptor-binding specificity – namely, a weakened affinity for the D2 domain – which accentuates the subfamily's reliance on specific contacts with the alternatively spliced D3.

Specific Contacts With the Alternatively Spliced Regionsin D3

The FGF10-FGFR2b crystal structure shows that most of the FGF10-D3 contacts involve a wide cleft in the membrane-distal end of the D3 domain (Yeh et al., 2003). This cleft is formed between the βB′ strand and the βB′-βC loop located in the constant region (first half of D3) and the βC′-βE loop from the alternatively spliced second half of D3 (**Figure 1A**). Interactions between Ile-317 on the βC′-βE loop of the receptor and a cluster of hydrophobic residues in FGF10, including Val-116 in the β4 strand, Tyr-131 in the β6 strand, and Phe-146 on the β7-β8 loop, support the formation of the D3 cleft. In doing so, these hydrophobic contacts facilitate hydrogen-bonding interactions between residues from the N-terminus, β1, and β4 strands of FGF10 with residues from both the constant and spliced portions in the D3 cleft (**Figure 1A**). Most importantly, Asp-76 – conserved in FGF7 and FGF22 – forms two highly specific hydrogen bonds with Ser-315 in the alternatively spliced βC′-βE loop of the receptor. Ser-315 is conserved in FGFR1b, but is replaced by tryptophan and alanine in FGFR3b and FGFR4, respectively, thus explaining the FGF7 subfamily's particular preference for the "b" isoforms of FGFR1 and FGFR2. Another notable specific receptor-binding residue of FGF10 is Thr-114 on the β4 strand, which engages the alternatively spliced βC′-βE loop of the D3 cleft through both direct and water-mediated hydrogen bonds (**Figure 1A**). Additionally, Arg-78 in the β1 strand, proceeding Asp-76, makes numerous contacts with the constant βB′-βC loop within the D3 cleft, including three hydrogen bonds with Ser-282 and Asp-283. Crucially, Arg-78 also forms three intramolecular hydrogen bonds with His-72 and Gly-75. These contacts facilitate the overall conformation of the FGF10 N-terminus and indirectly buttress the Asp-76–Ser-315 hydrogen bonds (**Figure 1A**). FGF10 core residues also augment FGF10-FGFR2b binding specificity by engaging in specific contacts with the alternatively spliced βF-βG loop outside of the D3 cleft. Specifically, Arg-155 and Ile-156 (each in the β8 strand of FGF10) engage in hydrophobic contacts and hydrogen bonding with Tyr-345 in the alternatively spliced βF-βG loop (**Figure 1B**). Tyr-345 is conserved only in FGFR1b. In FGFR3b, this position is occupied by a phenylalanine, whereas in FGFR1c-3c and FGFR4, the corresponding residue is a serine. These substitutions further limit the specificity of FGF10 for FGFR1b and FGFR2b.

The crystallographically deduced mode of FGF10-FGFR2b specificity has been validated by mutagenesis experiments in FGF10 (Yeh et al., 2003; Wang et al., 2010) and FGF7 (Bottaro et al., 1993; Ron et al., 1993; Gray et al., 1995; Reich-Slotky et al., 1995; Wang et al., 1995; Osslund et al., 1998; Sher et al., 2000, 2003). Specifically, alanine substitutions of Asp-76 or Arg-78 each significantly reduce the biological activity of the respective FGF10 mutants compared to wild-type FGF10, using DNA synthesis as an index of cell proliferation (Yeh et al., 2003). Moreover, replacement of Thr-114 with alanine or arginine decreases FGF10-FGFR2b binding affinity and the mitogenic activity of FGF10 in tracheal epithelial cells (Wang et al., 2010). Conversely, substitutions of His-314 and Ser-315 in the βC′-βE loop in FGFR2b to the corresponding residues in FGFR2c (threonine and alanine, respectively) completely eliminates FGF7 binding (Wang et al., 1995). Also in FGF7, N-terminal truncation at sites upstream of Asp-63 (Asp-76 in FGF10) and Arg-65 (Arg-78 in FGF10), respectively, results in a complete loss of FGF7-induced mitogenic activity in Balb/MK cells (Ron et al., 1993). Additionally, mutations of Asp-63 and Arg-65 to alanine each reduce the binding affinity of FGF7 for FGFR2b, with the latter mutation lowering the mitogenic response of FGF7 in Balb/MK cells by 200-fold (Sher et al., 2003). Replacement of the FGF7 subfamily-conserved Val-103 in the β4 strand of FGF7 (Val-116 in FGF10) (one of the constituents of the aforementioned hydrophobic patch) with glutamic acid also significantly reduces FGF7-FGFR2b binding affinity (Sher et al., 2000). The significance of the Arg-155 (Leu-142 in FGF7)–Tyr-345 interaction has been experimentally validated by data showing that mutating Tyr-345 to serine in FGFR2b significantly reduces receptor activation by FGF7 (Gray et al., 1995), and that replacing Arg-155 with alanine diminishes the ability of FGF10 to promote Balb/MK cell proliferation (Yeh et al., 2003). In FGF7, replacing Leu-142 with alanine results in a three-fold reduction in binding affinity to FGFR2b, as well as a significant loss of mitogenic activity in Balb/MK cells (Sher et al., 2003). Biochemical analysis of a pathogenic mutation in FGF10 lends further support to the importance of these interactions in promoting FGF10-FGFR2/1b signaling. Specifically, mutation of Ile-156 to arginine (I156R) is causative of LADD (Milunsky et al., 2006), a rare genetic disorder characterized by defects in the lacrimal and salivary glands as well as abnormalities in the teeth and distal limbs. Modeling studies show that the I156R mutation introduces steric clashes with residues in the ligand-binding pocket, including Tyr-345 in the alternatively spliced βF-βG loop (**Figure 1B**), thus explaining the loss-of-function phenotype of this mutation.

Weak Contacts With Receptor D2 Further Constrain Specificity

FGF7 subfamily receptor-binding specificity is further restricted by its members' low basal FGFR-binding affinities. Notably, in FGF7, FGF10, and FGF22, a phenylalanine (Phe-83 in FGF10) replaces a highly conserved tyrosine residue in the β1 strand found in all other FGFs (Tyr-29 in FGF1) (**Figure 1C**). This tyrosine – located at the center of the primarily hydrophobic and largely conserved FGF-D2 interface – makes hydrophobic contacts with residues in the βA′ strand in addition to forming two hydrogen bonds with the FGFR-invariant residues Leu-166 and Ala-168. This conserved pattern of hydrogen bonds fixes the D2 orientation relative to the FGF ligand, accounting for the common D2 disposition among all FGF–FGFR complexes.

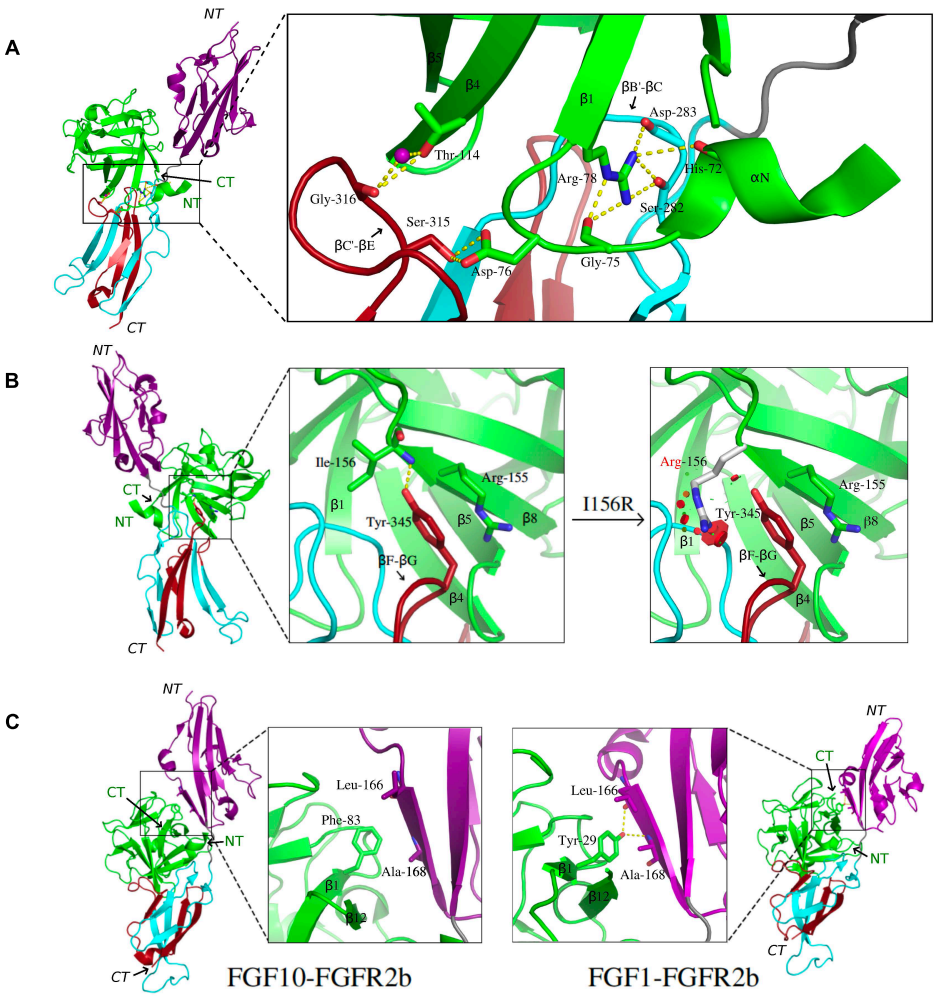

D

```
                                                αN        β1        β2        β3        β4
FGF10  38  QALGQDMVSPEATNSSSSSFSSPSSAGRHVRSYNHLQ-GDVRWRKLFSFTKYFLKIEKNGKVSGTKKENCPYSILETNSVEIGVVA  122
FGF3   18              AAGPGARLRRD..GRGGV.E.G-.AP.R...YCA...H.QLHPS.R.N.SL-..SA.....A..V.I..   87
FGF7   32          CNDMTPEQMATNVNC..PE..T...DYMEG..I.V.R..CR.QWY.R.D.R...K..QEMKNN.N.M..RT.AV.I..  109
FGF22  23                      TP..S.GP...P..E-.....R..S.HF..RVDPG.R.Q..RWRHGQD....R..HV...V   85

                                 β5        β6        β7        β8        β9                  β10       β11
FGF10  123 VKAINSNYHLAMNKKGKLYGSKEFNNDCKLKERIEENGYNTYASFNWQHN----------GRQMYVALNGKGAPRRGQKTRRKN  196
FGF3    88 IRGLF.GR.....R.R..A.EHYSAE.EFV...H.L.......RLYRTVSSTPGARRQPSAE.LW..SV....R....F....TQ  173
FGF7   109 I.GVE.EF.....E....AK..C.E..NF..L.L..H.....AK.T..----------.GE.F....Q..I.V..K..KKEQ  183
FGF22   85 I..VS.GF.V...RR.R....RLYTV..RFR.....H.....QR.RRR----------.QP.FL..DRR.G..P.GR...YH  159

                                 β12
FGF10  197 TSAHFLPMVVHS                                                                        208
FGF3   174 K.SL...R.LDHRDHEMVRQLQSGLPRPPGKGVQPRRRRQKQSPDNLEPSHVQASRLGSQLEASAH                 239
FGF7   184 KT.....AIT                                                                         194
FGF22  160 L.....VL.S                                                                         170
```

FIGURE 1 | Structural basis for FGF7 subfamily specificity toward "b" isoform FGFRs. **(A)** Left: cartoon representation of the overall structure of the FGF10-FGFR2b complex, with FGF10 in green, D2 of FGFR2b in purple, the constant region of D3 in cyan, the alternatively spliced D3 in red, hydrogen bonds shown as yellow dashes, and the region of interest boxed. N-and C-termini of ligand (in green) and receptor (italics) are labeled NT and CT, respectively. Right: expanded view of FGF10 N-terminal interactions with the FGFR2b D3 domain. Arg-78 of the β1 strand forms three intramolecular hydrogen bonds with Gly-75 and His-72 in the N-terminus, stabilizing it and enabling Asp-76 to form two highly specific hydrogen bonds with Ser-315 in the alternatively spliced βC′-βE loop of D3. Thr-114 of the β4 strand also interacts with the βC′-βE loop via both water-mediated and direct hydrogen bonds with Gly-316. **(B)** Left: overall view of the FGF10-FGFR2b structure, with boxed region of interest shown in expanded forms at right. The first of these (left) shows Arg-155 and Ile-156 of the β8 strand interacting with Tyr-345 on the "b" splice isoform-specific βF-βG loop; the second (right) highlights the LADD mutation (Ile-156 to Arg), which introduces steric clashes with Tyr-345 on the βF-βG loop. Relevant residues and hydrogen bonds are depicted as in **(A)**, with steric clashes illustrated by red circles. **(C)** Comparison of the ligand-D2 interface between FGF10-FGFR2b (left) and FGF1-FGFR2b (right), with each FGF–FGFR complex depicted as a cartoon with the same color scheme as in **(A)**; boxed regions on each complex are expanded to show the ligand β1 strand interacting with D2 of the receptor. Note that in FGF10, a conserved β1 Tyr is replaced with Phe, resulting in a loss of two hydrogen bonds. In **(A–C)**, relevant residues and hydrogen bonds are shown as sticks and yellow dashes, respectively; water molecules

(Continued)

FIGURE 1 | Continued
appear as purple spheres; oxygen atoms are in red, nitrogen in blue, and carbon in the same color as the molecules to which they belong. FGF10-FGFR2b (PDB ID: 1NUN) (Yeh et al., 2003) and FGF1-FGFR2b (PDB ID: 3OJ2) (Beenken et al., 2012) structures were edited using PyMol (The PyMOL Molecular Graphics System, Version 2.0 Schrödinger, LLC). **(D)** Structure-based sequence alignment of human FGF10, FGF3, FGF7, and FGF22. Dots denote homology with FGF10; dashes denote gaps introduced to optimize sequence alignment. Residues are highlighted according to the FGFR region with which they interact: D2 (purple), D2–D3 linker (gray), constant D3 (cyan), and alternatively spliced D3 (red). Residues which interact with both spliced and non-spliced regions of D3 are highlighted in yellow; those which interact with both the D2 and D2–D3 linker are highlighted in dark blue. Above the sequence, red lines indicate residues comprising secondary structures.

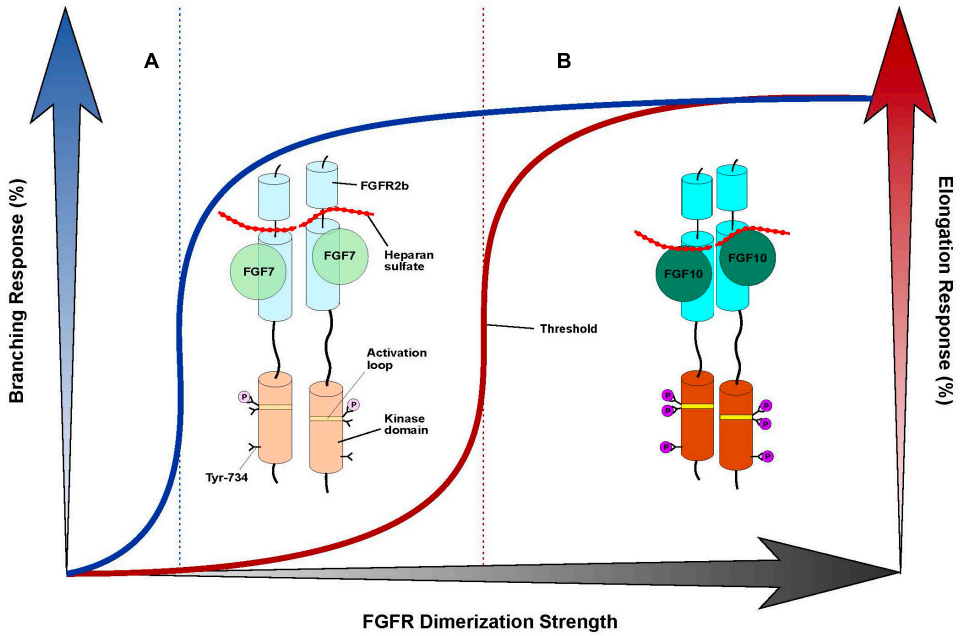

FIGURE 2 | "Threshold model" accounts for differences in branching morphogenesis and FGFR2b tyrosine transphosphorylation between FGF7 and FGF10. Cartoon representation of a "threshold model," with the FGF7-FGFR2b complex at left **(A)** and the FGF10-FGFR2b complex at right **(B)**. FGF ligands are depicted as different shades of green circles; the FGFR2b ectodomain and kinase domains are shown as cylinders of different shades of cyan and orange, respectively; HS is depicted as a dotted red line; the A-loop region within the kinase domain is shown as a stripe in different shades of yellow; phosphorylated tyrosines are represented as circles colored in different shades of purple. The extent of shading/transparency denotes the strength of ligand-induced FGFR2b dimerization and activation. **(A)** Because of its weak affinity for HS, FGF7 induces comparably weak/transient FGFR dimerization which causes quantitatively less A-loop transphosphorylation/kinase activation such that Tyr-734 is left unphosphorylated; this complex is sufficient to induce branching, but not elongation. **(B)** Owing to its higher affinity for HS, FGF10 forms a more stable FGFR2b dimer that enables greater A-loop tyrosine transphosphorylation and FGFRb activation. Consequently, FGF10 can induce Tyr-734 transphosphorylation and elicit an elongation response. Note that the threshold of FGFR dimerization strength necessary for inducing elongation (depicted as a vertical, red dashed line to the left) is higher than that mediating the branching response (indicated by a vertical, blue dashed line in the center). On the x-axis, a shaded black arrow represents the increasing value of FGF-induced FGFR dimerization strength. On the y-axis, on left, a shaded blue arrow denotes the increasing rate of the branching response, which is correlated with a blue line; on right, a shaded red arrow indicates the increasing rate of the elongation response, which is correlated with a red line.

Replacement of this tyrosine with phenylalanine therefore significantly reduces general FGFR-binding affinity and also causes a ∼20–25° rotation in D2 orientation relative to other FGF–FGFR complexes.

The importance of weak basal FGF–FGFR binding affinity in restricting FGF7 subfamily receptor-binding specificity is underscored by two pathological *FGFR2* mutations, S252W and P253R, each affecting the D2–D3 linker region and causative of AS, a severe form of craniosynostosis (Wilkie et al., 1995; Anderson et al., 1998; Ibrahimi et al., 2001). These gain-of-function mutations create additional non-specific FGF–FGFR contacts that increase basal FGF–FGFR affinity, thereby enabling pathological binding of FGF10 and/or FGF7 to FGFR2c as well as binding of epithelial-expressed ligands such as FGF2, FGF6, and/or FGF9 to FGFR2b (Yu et al., 2000; Ibrahimi et al., 2001). Genetic ablation of *FGF10* in mice harboring AS-causing *FGFR2* mutations reverses some of the skeletal, visceral, and tracheal abnormalities stemming from AS (Hajihosseini et al., 2009; Tiozzo et al., 2009), implying that aberrant FGF10-FGFR2c signaling plays a significant role in AS etiology.

MOLECULAR RATIONALE BEHIND THE NON-REDUNDANT FUNCTIONS OF FGF7 SUBFAMILY MEMBERS

Gene-knockout studies in mice have shown that despite their shared, restricted specificity for FGFR1b/2b, FGF7 subfamily

members have non-overlapping biological functions. For example, while *FGF7*-knockout mice present only subtle developmental abnormalities affecting the kidney, thymus, and hippocampus (Qiao et al., 1999; Alpdogan et al., 2006; Terauchi et al., 2010; Lee et al., 2012), *FGF10*-knockout mice die at birth due to a failure of lung and limb development (Min et al., 1998; Sekine et al., 1999). Structurally, this functional dichotomy between FGF10 and FGF7 can be attributed to the lower HS-binding affinity of FGF7 relative to FGF10 (Igarashi et al., 1998; Luo et al., 2006; Asada et al., 2009). HS-binding affinity differences could impact FGF signaling in one, or both, of the following ways: (1) by changing the extent of ligand diffusion and creating distinct morphogenetic gradients, or (2) by generating distinct thresholds of receptor dimerization and eliciting qualitatively/quantitatively distinct intracellular signals.

A potential role for HS-binding affinity in differentiating the morphogenetic activities of FGF7 and FGF10 can be inferred by data from *ex vivo* epithelial branching model systems in cultured LG and SMG explants (Steinberg et al., 2005; Makarenkova et al., 2009). Due to its relatively low affinity for HS, we postulated that FGF7 would diffuse more readily than FGF10 in an HS-containing matrix (used as surrogate for the ECM) (Makarenkova et al., 2009), thus acting on both the distal and proximal parts of the developing epithelial bud to stimulate branching. On the other hand, the higher HS-binding affinity of FGF10 would limit its range of diffusion such that it can reach only the tip of the epithelial buds, thereby inducing their elongation. To test that these distinct responses are indeed due to different diffusion gradients rather than ligand identity *per se*, we selectively mutated residues at the HBS of FGF10 to the corresponding ones in FGF7, and identified one mutation – Arg-187 in the β11 strand to valine (R187V) – which imparted upon FGF10 a similar range of diffusion as FGF7 (Makarenkova et al., 2009). We then showed that the R187V FGF10 mutant could functionally mimic FGF7 by inducing branching rather than elongation of epithelial buds. It is tempting to speculate that comparable HS-binding affinity differences exist between FGF3 and FGF22 which lead to the generation of FGF7 subfamily ligand-specific diffusion gradients in the ECM, in turn conferring distinct biological activities. However, as the affinity of FGF–HS interactions also dictates the longevity/stability of paracrine FGF–FGFR dimers (Schlessinger et al., 2000), it is plausible that quantitative differences in HS-dependent receptor dimerization may also contribute to the different morphogenetic responses between FGF10 and FGF7. Indeed, the R187V FGF10 mutant is reminiscent of an engineered HS-binding deficient FGF1 mutant which we used to show that the FGF1 mitogenic response could be uncoupled from its metabolic response by reducing FGFR dimer stability (Huang et al., 2017). These data pointed to the existence of a distinct threshold of FGF1-induced receptor dimerization strength required for transitioning from an exclusively metabolic response to a combined metabolic/mitogenic response. Thus, the potential role of HS-dependent FGFR dimerization strength in defining the non-redundancy of the FGF7 subfamily members merits further exploration.

CONCLUSION AND FUTURE DIRECTIONS

The FGF7 subfamily is unique among FGFs in that its members exclusively activate and signal through FGFR2b and, to a lesser extent, FGFR1b. The molecular rationale behind this stringent level of receptor-binding specificity stems primarily from specific contacts made between FGF7 subfamily members and the alternatively spliced βC′-βE and βF-βG loop regions in D3, and is further reinforced by weaker D2 interactions (**Figures 1C,D**). FGF7 subfamily members elicit non-redundant functions, the structural basis of which can be partially attributed to different HS-binding affinities. These affinity differences in turn raise the possibility that the unique functions of each of the FGF7 subfamily ligands may be determined by distinct diffusion gradients through the ECM and/or a "threshold model" of FGFR1b/2b dimerization strength. In this model, different thresholds in FGFR dimer strength/stability translate into quantitatively and qualitatively distinct levels of FGFR activation (that is, tyrosine transphosphorylation). This in turn manifests in different magnitudes of intracellular signals and the recruitment of distinct substrates, culminating in unique cell fates (Zinkle and Mohammadi, 2018). Indeed, previous work has already shown that FGF10 – which binds more tightly than FGF7 to HS – stimulates the recruitment of distinct intracellular substrates due to its unique ability to induce transphosphorylation of a single FGFR2b tyrosine residue, Tyr-734 (Francavilla et al., 2013). Because FGF7-binding cannot induce transphosphorylation of Tyr-734, there may be a certain threshold of FGFR2b dimerization strength that FGF10 (but not FGF7) can reach to induce Tyr-734 phosphorylation (**Figure 2**). Future studies should try to address the veracity of the threshold model, especially as it relates to the FGF7 subfamily. If validated, this model should prove a reliable guide for functionally converting one FGF7 subfamily member to another, thereby enabling novel tools/strategies for dissecting the roles of individual members of the subfamily during development and in disease pathogenesis.

AUTHOR CONTRIBUTIONS

MM contributed to the conception, writing, and revising the manuscript and approved the submitted version. AZ prepared the first draft of the manuscript including the figures and contributed to manuscript revision.

FUNDING

The authors acknowledge support provided by National Institutes of Health grant R01 DE13686 (to MM).

ACKNOWLEDGMENTS

The authors thank Nick Cowan for critically reading and editing the manuscript.

REFERENCES

Alpdogan, O., Hubbard, V. M., Smith, O. M., Patel, N., Lu, S., Goldberg, G. L., et al. (2006). Keratinocyte growth factor (KGF) is required for postnatal thymic regeneration. *Blood* 107, 2453–2460. doi: 10.1182/blood-2005-07-2831

Anderson, J., Burns, H. D., Enriquez-Harris, P., Wilkie, A. O., and Heath, J. K. (1998). Apert syndrome mutations in fibroblast growth factor receptor 2 exhibit increased affinity for FGF ligand. *Hum. Mol. Genet.* 7, 1475–1483. doi: 10.1093/hmg/7.9.1475

Asada, M., Shinomiya, M., Suzuki, M., Honda, E., Sugimoto, R., Ikekita, M., et al. (2009). Glycosaminoglycan affinity of the complete fibroblast growth factor family. *Biochim. Biophys. Acta* 1790, 40–48. doi: 10.1016/j.bbagen.2008.09.001

Beenken, A., Eliseenkova, A. V., Ibrahimi, O. A., Olsen, S. K., and Mohammadi, M. (2012). Plasticity in interactions of fibroblast growth factor 1 (FGF1) N-terminus with FGF receptors underlies promiscuity of FGF1. *J. Biol. Chem.* 287, 3067–3078. doi: 10.1074/jbc.M111.275891

Beenken, A., and Mohammadi, M. (2009). The FGF family: biology, pathophysiology and therapy. *Nat. Rev. Drug Discov.* 8, 235–253. doi: 10.1038/nrd2792

Bellosta, P., Iwahori, A., Plotnikov, A. N., Eliseenkova, A. V., Basilico, C., and Mohammadi, M. (2001). Identification of receptor and heparin binding sites in fibroblast growth factor 4 by structure-based mutagenesis. *Mol. Cell. Biol.* 21, 5946–5957. doi: 10.1128/MCB.21.17.5946-5957.2001

Bellusci, S., Grindley, J., Emoto, H., Itoh, N., and Hogan, B. L. (1997). Fibroblast growth factor 10 (FGF10) and branching morphogenesis in the embryonic mouse lung. *Development* 124, 4867–4878.

Belov, A. A., and Mohammadi, M. (2013). Molecular mechanisms of fibroblast growth factor signaling in physiology and pathology. *Cold Spring Harb. Perspect. Biol.* 5:a015958. doi: 10.1101/cshperspect.a015958

Bottaro, D. P., Fortney, E., Rubin, J. S., and Aaronson, S. A. (1993). A keratinocyte growth factor receptor-derived peptide antagonist identifies part of the ligand binding site. *J. Biol. Chem.* 268, 9180–9183.

Chen, G., Liu, Y., Goetz, R., Fu, L., Jayaraman, S., Hu, M. C., et al. (2018). alpha-Klotho is a non-enzymatic molecular scaffold for FGF23 hormone signalling. *Nature* 553, 461–466. doi: 10.1038/nature25451

De Moerlooze, L., Spencer-Dene, B., Revest, J. M., Hajihosseini, M., Rosewell, I., and Dickson, C. (2000). An important role for the IIIb isoform of fibroblast growth factor receptor 2 (FGFR2) in mesenchymal-epithelial signalling during mouse organogenesis. *Development* 127, 483–492.

Eriksson, A. E., Cousens, L. S., Weaver, L. H., and Matthews, B. W. (1991). Three-dimensional structure of human basic fibroblast growth factor. *Proc. Natl. Acad. Sci. U.S.A.* 88, 3441–3445. doi: 10.1073/pnas.88.8.3441

Esko, J. D., and Selleck, S. B. (2002). Order out of chaos: assembly of ligand binding sites in heparan sulfate. *Annu. Rev. Biochem.* 71, 435–471. doi: 10.1146/annurev.biochem.71.110601.135458

Finch, P. W., Pricolo, V., Wu, A., and Finkelstein, S. D. (1996). Increased expression of keratinocyte growth factor messenger RNA associated with inflammatory bowel disease. *Gastroenterology* 110, 441–451. doi: 10.1053/gast.1996.v110.pm8566591

Francavilla, C., Rigbolt, K. T., Emdal, K. B., Carraro, G., Vernet, E., Bekker-Jensen, D. B., et al. (2013). Functional proteomics defines the molecular switch underlying FGF receptor trafficking and cellular outputs. *Mol. Cell.* 51, 707–722. doi: 10.1016/j.molcel.2013.08.002

Gray, T. E., Eisenstein, M., Shimon, T., Givol, D., and Yayon, A. (1995). Molecular modeling based mutagenesis defines ligand binding and specificity determining regions of fibroblast growth factor receptors. *Biochemistry* 34, 10325–10333. doi: 10.1021/bi00033a002

Hajihosseini, M. K., Duarte, R., Pegrum, J., Donjacour, A., Lana-Elola, E., Rice, D. P., et al. (2009). Evidence that Fgf10 contributes to the skeletal and visceral defects of an Apert syndrome mouse model. *Dev. Dyn.* 238, 376–385. doi: 10.1002/dvdy.21648

Hoffman, M. P., Kidder, B. L., Steinberg, Z. L., Lakhani, S., Ho, S., Kleinman, H. K., et al. (2002). Gene expression profiles of mouse submandibular gland development: FGFR1 regulates branching morphogenesis in vitro through BMP- and FGF-dependent mechanisms. *Development* 129, 5767–5778. doi: 10.1242/dev.00172

Huang, Z., Tan, Y., Gu, J., Liu, Y., Song, L., Niu, J., et al. (2017). Uncoupling the Mitogenic and Metabolic Functions of FGF1 by Tuning FGF1-FGF Receptor Dimer Stability. *Cell Rep.* 20, 1717–1728. doi: 10.1016/j.celrep.2017.06.063

Ibrahimi, O. A., Eliseenkova, A. V., Plotnikov, A. N., Yu, K., Ornitz, D. M., and Mohammadi, M. (2001). Structural basis for fibroblast growth factor receptor 2 activation in Apert syndrome. *Proc. Natl. Acad. Sci. U.S.A.* 98, 7182–7187. doi: 10.1073/pnas.121183798

Igarashi, M., Finch, P. W., and Aaronson, S. A. (1998). Characterization of recombinant human fibroblast growth factor (FGF)-10 reveals functional similarities with keratinocyte growth factor (FGF-7). *J. Biol. Chem.* 273, 13230–13235. doi: 10.1074/jbc.273.21.13230

Itoh, N., and Ornitz, D. M. (2004). Evolution of the Fgf and Fgfr gene families. *Trends Genet.* 20, 563–569. doi: 10.1016/j.tig.2004.08.007

Itoh, N., and Ornitz, D. M. (2011). Fibroblast growth factors: from molecular evolution to roles in development, metabolism and disease. *J. Biochem.* 149, 121–130. doi: 10.1093/jb/mvq121

Izvolsky, K. I., Shoykhet, D., Yang, Y., Yu, Q., Nugent, M. A., and Cardoso, W. V. (2003). Heparan sulfate-FGF10 interactions during lung morphogenesis. *Dev. Biol.* 258, 185–200. doi: 10.1016/S0012-1606(03)00114-3

Lee, C. H., Javed, D., Althaus, A. L., Parent, J. M., and Umemori, H. (2012). Neurogenesis is enhanced and mossy fiber sprouting arises in FGF7-deficient mice during development. *Mol. Cell. Neurosci.* 51, 61–67. doi: 10.1016/j.mcn.2012.07.010

Liu, J., Shworak, N. W., Fritze, L. M., Edelberg, J. M., and Rosenberg, R. D. (1996). Purification of heparan sulfate D-glucosaminyl 3-O-sulfotransferase. *J. Biol. Chem.* 271, 27072–27082. doi: 10.1074/jbc.271.43.27072

Liu, Y., Ma, J., Beenken, A., Srinivasan, L., Eliseenkova, A. V., and Mohammadi, M. (2017). Regulation of receptor binding specificity of FGF9 by an autoinhibitory homodimerization. *Structure* 25, 1325–1336.e3. doi: 10.1016/j.str.2017.06.016

Luo, Y., Ye, S., Kan, M., and McKeehan, W. L. (2006). Structural specificity in a FGF7-affinity purified heparin octasaccharide required for formation of a complex with FGF7 and FGFR2IIIb. *J. Cell. Biochem.* 97, 1241–1258. doi: 10.1002/jcb.20724

Makarenkova, H. P., Hoffman, M. P., Beenken, A., Eliseenkova, A. V., Meech, R., Tsau, C., et al. (2009). Differential interactions of FGFs with heparan sulfate control gradient formation and branching morphogenesis. *Sci. Signal.* 2:ra55. doi: 10.1126/scisignal.2000304

Makarenkova, H. P., Ito, M., Govindarajan, V., Faber, S. C., Sun, L., McMahon, G., et al. (2000). FGF10 is an inducer and Pax6 a competence factor for lacrimal gland development. *Development* 127, 2563–2572.

Mason, I. J., Fuller-Pace, F., Smith, R., and Dickson, C. (1994). FGF-7 (keratinocyte growth factor) expression during mouse development suggests roles in myogenesis, forebrain regionalisation and epithelial-mesenchymal interactions. *Mech. Dev.* 45, 15–30. doi: 10.1016/0925-4773(94)90050-7

Memarzadeh, S., Xin, L., Mulholland, D. J., Mansukhani, A., Wu, H., Teitell, M. A., et al. (2007). Enhanced paracrine FGF10 expression promotes formation of multifocal prostate adenocarcinoma and an increase in epithelial androgen receptor. *Cancer Cell* 12, 572–585. doi: 10.1016/j.ccr.2007.11.002

Milunsky, J. M., Zhao, G., Maher, T. A., Colby, R., and Everman, D. B. (2006). LADD syndrome is caused by FGF10 mutations. *Clin. Genet.* 69, 349–354. doi: 10.1111/j.1399-0004.2006.00597.x

Min, H., Danilenko, D. M., Scully, S. A., Bolon, B., Ring, B. D., Tarpley, J. E., et al. (1998). Fgf-10 is required for both limb and lung development and exhibits striking functional similarity to Drosophila branchless. *Genes Dev.* 12, 3156–3161. doi: 10.1101/gad.12.20.3156

Mohammadi, M., Olsen, S. K., and Ibrahimi, O. A. (2005). Structural basis for fibroblast growth factor receptor activation. *Cytokine Growth. Factor. Rev.* 16, 107–137. doi: 10.1016/j.cytogfr.2005.01.008

Olsen, S. K., Ibrahimi, O. A., Raucci, A., Zhang, F., Eliseenkova, A. V., Yayon, A., et al. (2004). Insights into the molecular basis for fibroblast growth factor receptor autoinhibition and ligand-binding promiscuity. *Proc. Natl. Acad. Sci. U.S.A.* 101, 935–940. doi: 10.1073/pnas.0307287101

Olsen, S. K., Li, J. Y., Bromleigh, C., Eliseenkova, A. V., Ibrahimi, O. A., Lao, Z., et al. (2006). Structural basis by which alternative splicing modulates the organizer activity of FGF8 in the brain. *Genes Dev.* 20, 185–198. doi: 10.1101/gad.1365406

Ornitz, D. M., Xu, J., Colvin, J. S., McEwen, D. G., MacArthur, C. A., Coulier, F., et al. (1996). Receptor specificity of the fibroblast growth factor family. *J. Biol. Chem.* 271, 15292–15297. doi: 10.1074/jbc.271.25.15292

Ornitz, D. M., Yayon, A., Flanagan, J. G., Svahn, C. M., Levi, E., and Leder, P. (1992). Heparin is required for cell-free binding of basic fibroblast growth factor to a soluble receptor and for mitogenesis in whole cells. *Mol. Cell. Biol.* 12, 240–247. doi: 10.1128/MCB.12.1.240

Orr-Urtreger, A., Bedford, M. T., Burakova, T., Arman, E., Zimmer, Y., Yayon, A., et al. (1993). Developmental localization of the splicing alternatives of fibroblast growth factor receptor-2 (FGFR2). *Dev. Biol.* 158, 475–486. doi: 10.1006/dbio.1993.1205

Osslund, T. D., Syed, R., Singer, E., Hsu, E. W., Nybo, R., Chen, B. L., et al. (1998). Correlation between the 1.6 A crystal structure and mutational analysis of keratinocyte growth factor. *Protein Sci.* 7, 1681–1690. doi: 10.1002/pro.5560070803

Perrimon, N., and Bernfield, M. (2000). Specificities of heparan sulphate proteoglycans in developmental processes. *Nature* 404, 725–728. doi: 10.1038/35008000

Plotnikov, A. N., Eliseenkova, A. V., Ibrahimi, O. A., Shriver, Z., Sasisekharan, R., Lemmon, M. A., et al. (2001). Crystal structure of fibroblast growth factor 9 reveals regions implicated in dimerization and autoinhibition. *J. Biol. Chem.* 276, 4322–4329. doi: 10.1074/jbc.M006502200

Plotnikov, A. N., Hubbard, S. R., Schlessinger, J., and Mohammadi, M. (2000). Crystal structures of two FGF-FGFR complexes reveal the determinants of ligand-receptor specificity. *Cell* 101, 413–424. doi: 10.1016/S0092-8674(00)80851-X

Plotnikov, A. N., Schlessinger, J., Hubbard, S. R., and Mohammadi, M. (1999). Structural basis for FGF receptor dimerization and activation. *Cell* 98, 641–650. doi: 10.1016/S0092-8674(00)80051-3

Qiao, J., Uzzo, R., Obara-Ishihara, T., Degenstein, L., Fuchs, E., and Herzlinger, D. (1999). FGF-7 modulates ureteric bud growth and nephron number in the developing kidney. *Development* 126, 547–554.

Rapraeger, A. C., Krufka, A., and Olwin, B. B. (1991). Requirement of heparan sulfate for bFGF-mediated fibroblast growth and myoblast differentiation. *Science* 252, 1705–1708. doi: 10.1126/science.1646484

Reich-Slotky, R., Shaoul, E., Berman, B., Graziani, G., and Ron, D. (1995). Chimeric molecules between keratinocyte growth factor and basic fibroblast growth factor define domains that confer receptor binding specificities. *J. Biol. Chem.* 270, 29813–29818. doi: 10.1074/jbc.270.50.29813

Ron, D., Bottaro, D. P., Finch, P. W., Morris, D., Rubin, J. S., and Aaronson, S. A. (1993). Expression of biologically active recombinant keratinocyte growth factor. Structure/function analysis of amino-terminal truncation mutants. *J. Biol. Chem.* 268, 2984–2988.

Schlessinger, J., Plotnikov, A. N., Ibrahimi, O. A., Eliseenkova, A. V., Yeh, B. K., Yayon, A., et al. (2000). Crystal structure of a ternary FGF-FGFR-heparin complex reveals a dual role for heparin in FGFR binding and dimerization. *Mol. Cell.* 6, 743–750. doi: 10.1016/S1097-2765(00)00073-3

Sekine, K., Ohuchi, H., Fujiwara, M., Yamasaki, M., Yoshizawa, T., Sato, T., et al. (1999). Fgf10 is essential for limb and lung formation. *Nat. Genet.* 21, 138–141. doi: 10.1038/5096

Sher, I., Lang, T., Lubinsky-Mink, S., Kuhn, J., Adir, N., Chatterjee, S., et al. (2000). Identification of residues important both for primary receptor binding and specificity in fibroblast growth factor-7. *J. Biol. Chem.* 275, 34881–34886. doi: 10.1074/jbc.M003293200

Sher, I., Yeh, B. K., Mohammadi, M., Adir, N., and Ron, D. (2003). Structure-based mutational analyses in FGF7 identify new residues involved in specific interaction with FGFR2IIIb. *FEBS Lett.* 552, 150–154. doi: 10.1016/S0014-5793(03)00909-8

Stauber, D. J., DiGabriele, A. D., and Hendrickson, W. A. (2000). Structural interactions of fibroblast growth factor receptor with its ligands. *Proc. Natl. Acad. Sci. U.S.A.* 97, 49–54. doi: 10.1073/pnas.97.1.49

Steinberg, Z., Myers, C., Heim, V. M., Lathrop, C. A., Rebustini, I. T., Stewart, J. S., et al. (2005). FGFR2b signaling regulates ex vivo submandibular gland epithelial cell proliferation and branching morphogenesis. *Development* 132, 1223–1234. doi: 10.1242/dev.01690

Tekin, M., Hismi, B. O., Fitoz, S., Ozdag, H., Cengiz, F. B., Sirmaci, A., et al. (2007). Homozygous mutations in fibroblast growth factor 3 are associated with a new form of syndromic deafness characterized by inner ear agenesis, microtia, and microdontia. *Am. J. Hum. Genet.* 80, 338–344. doi: 10.1086/510920

Tekin, M., Ozturkmen Akay, H., Fitoz, S., Birnbaum, S., Cengiz, F. B., Sennaroglu, L., et al. (2008). Homozygous FGF3 mutations result in congenital deafness with inner ear agenesis, microtia, and microdontia. *Clin. Genet.* 73, 554–565. doi: 10.1111/j.1399-0004.2008.01004.x

Terauchi, A., Johnson-Venkatesh, E. M., Toth, A. B., Javed, D., Sutton, M. A., and Umemori, H. (2010). Distinct FGFs promote differentiation of excitatory and inhibitory synapses. *Nature* 465, 783–787. doi: 10.1038/nature09041

Tiozzo, C., De Langhe, S., Carraro, G., Alam, D. A., Nagy, A., Wigfall, C., et al. (2009). Fibroblast growth factor 10 plays a causative role in the tracheal cartilage defects in a mouse model of Apert syndrome. *Pediatr. Res.* 66, 386–390. doi: 10.1203/PDR.0b013e3181b45580

Umemori, H., Linhoff, M. W., Ornitz, D. M., and Sanes, J. R. (2004). FGF22 and its close relatives are presynaptic organizing molecules in the mammalian brain. *Cell* 118, 257–270. doi: 10.1016/j.cell.2004.06.025

Wang, F., Kan, M., Xu, J., Yan, G., and McKeehan, W. L. (1995). Ligand-specific structural domains in the fibroblast growth factor receptor. *J. Biol. Chem.* 270, 10222–10230. doi: 10.1074/jbc.270.17.10222

Wang, J. F., Cai, X., Zou, M. J., Wang, Y. Y., Wang, J. X., and Xu, D. G. (2010). Thr-114 is an important functional residue of fibroblast growth factor 10 identified by structure-based mutational analysis. *Cytokine* 49, 338–343. doi: 10.1016/j.cyto.2009.11.023

Wilkie, A. O., Slaney, S. F., Oldridge, M., Poole, M. D., Ashworth, G. J., Hockley, A. D., et al. (1995). Apert syndrome results from localized mutations of FGFR2 and is allelic with Crouzon syndrome. *Nat. Genet.* 9, 165–172. doi: 10.1038/ng0295-165

Xu, X., Weinstein, M., Li, C., Naski, M., Cohen, R. I., Ornitz, D. M., et al. (1998). Fibroblast growth factor receptor 2 (FGFR2)-mediated reciprocal regulation loop between FGF8 and FGF10 is essential for limb induction. *Development* 125, 753–765.

Yayon, A., Klagsbrun, M., Esko, J. D., Leder, P., and Ornitz, D. M. (1991). Cell surface, heparin-like molecules are required for binding of basic fibroblast growth factor to its high affinity receptor. *Cell* 64, 841–848. doi: 10.1016/0092-8674(91)90512-W

Yeh, B. K., Igarashi, M., Eliseenkova, A. V., Plotnikov, A. N., Sher, I., Ron, D., et al. (2003). Structural basis by which alternative splicing confers specificity in fibroblast growth factor receptors. *Proc. Natl. Acad. Sci. U.S.A.* 100, 2266–2271. doi: 10.1073/pnas.0436500100

Yu, K., Herr, A. B., Waksman, G., and Ornitz, D. M. (2000). Loss of fibroblast growth factor receptor 2 ligand-binding specificity in apert syndrome. *Proc. Natl. Acad. Sci. U.S.A.* 97, 14536–14541. doi: 10.1073/pnas.97.26.14536

Zhang, X., Ibrahimi, O. A., Olsen, S. K., Umemori, H., Mohammadi, M., and Ornitz, D. M. (2006). Receptor specificity of the fibroblast growth factor family. The complete mammalian FGF family. *J. Biol. Chem.* 281, 15694–15700. doi: 10.1074/jbc.M601252200

Zhu, X., Komiya, H., Chirino, A., Faham, S., Fox, G. M., Arakawa, T., et al. (1991). Three-dimensional structures of acidic and basic fibroblast growth factors. *Science* 251, 90–93. doi: 10.1126/science.1702556

Zinkle, A., and Mohammadi, M. (2018). A threshold model for receptor tyrosine kinase signaling specificity and cell fate determination. *F1000Res* 7:F1000 Faculty Rev-872. doi: 10.12688/f1000research.14143.1

Conflict of Interest Statement: The authors declare that the research was conducted in the absence of any commercial or financial relationships that could be construed as a potential conflict of interest.

Copyright © 2019 Zinkle and Mohammadi. This is an open-access article distributed under the terms of the Creative Commons Attribution License (CC BY). The use, distribution or reproduction in other forums is permitted, provided the original author(s) and the copyright owner(s) are credited and that the original publication in this journal is cited, in accordance with accepted academic practice. No use, distribution or reproduction is permitted which does not comply with these terms.

frontiers in Genetics

MINI REVIEW
published: 12 March 2019
doi: 10.3389/fgene.2019.00170

FGF Signaling in Lung Development and Disease: Human Versus Mouse

*Soula Danopoulos, Jessica Shiosaki and Denise Al Alam**

Saban Research Institute, Children's Hospital Los Angeles, Los Angeles, CA, United States

Fibroblast growth factor 10 (FGF10) plays an important role in mouse lung development, injury, and repair. It is considered the main morphogen driving lung branching morphogenesis in rodents. While many studies have found FGF10 SNPs associated with COPD and branch variants in COPD smokers, there is no evidence of a causative role for FGF10 or these SNPs in human lung development and pediatric lung diseases. We and others have shown divergent roles for FGF10 in mouse lung development and early human lung development. Herein, we only review the existing literature on FGF signaling in human lung development and pediatric human lung diseases, comparing what is known in mouse lung to that in human lung.

Keywords: FGF10, human lung, development, disease, FGF signaling

OPEN ACCESS

Edited by:
Saverio Bellusci,
University of Giessen, Germany

Reviewed by:
Stijn De Langhe,
University of Alabama at Birmingham, United States
Robbert J. Rottier,
Erasmus University Rotterdam, Netherlands

***Correspondence:**
Denise Al Alam
dalalam@chla.usc.edu

Specialty section:
This article was submitted to Stem Cell Research, a section of the journal Frontiers in Genetics

Received: *21 December 2018*
Accepted: *15 February 2019*
Published: *12 March 2019*

Citation:
Danopoulos S, Shiosaki J and Al Alam D (2019) FGF Signaling in Lung Development and Disease: Human Versus Mouse. Front. Genet. 10:170. doi: 10.3389/fgene.2019.00170

INTRODUCTION

The mammalian lung is derived from invagination of the foregut endoderm that ultimately forms the primitive lung buds. These buds undergo a series of branching, proliferation, and differentiation to eventually become a fully functioning air exchange organ. Stages of lung development are thought to be comparable among mammalian species, primarily between humans and rodents, thus making rodents a very widely used model to study lung development and disease. The knowledge gained from rodent studies has been crucial in advancing our understanding of basic biological processes in the lung. However, in light of the low success rate in clinical trials [14% reported in 2018 (Wong et al., 2018)], the necessity to better understand human lung biology has become increasingly important.

Although there are numerous similarities between the mouse and human lung, many differences have also been noted at the structural, cellular, and molecular levels. Grossly, the structure, size, and scale of the lung are notably different between the two species. Although they are both five lobed units, the mouse lung comprises a single large left lobe and four right lobes (cranial lobe, middle lobe, caudal lobe, and accessory lobe), whereas the human lung has two left lobes (superior lobe of left lung and inferior lobe of left lung) and three right lobes (superior lobe of right lung, middle lobe of right lung, and inferior lobe of right lung). Embedded in these lobes is the highly structured, arborized, epithelial tree. Starting from the trachea as generation 0 and moving down to the bronchioles, the human lung contains a total of 17–21 branch generations, whereas in mouse, there are only 13–17 branch generations (Irvin and Bates, 2003). This also reflects differences in total lung capacity, alveolar numbers and volume. The total lung capacity is 6×10^3 ml in adult humans compared to 1 ml in adult mouse (Irvin and Bates, 2003). The volume of one alveolus is 4.2×10^6 μm^3 in humans compared to 2.2×10^4 μm^3 in mouse (Wansleeben et al., 2013), and the estimated average number of alveoli is 4.8×10^8 in humans compared to 2.31×10^6 in mouse (Ochs et al., 2004; Knust et al., 2009). In addition to the very apparent differences in

size and structure, there have also been multiple cellular and molecular differences that have been described during development and adulthood. For instance, cartilaginous rings are restricted to the trachea and main bronchi in mouse, whereas in humans, these extend into the bronchioles (**Figure 1**). Similarly, submucosal glands are only present in the upper part of the mouse trachea, whereas in humans, they extend further down into the respiratory bronchioles. Differences in epithelial structure and cell type distribution are further detailed in **Figure 1**. These changes in cellular composition result in different molecular interactions and expression patterns.

For years, it was well-established that the progenitor cell population of the proximal epithelium in the developing mouse lung is Sox2+, whereas that of the distal epithelium is solely Sox9+. We and others have demonstrated that during the pseudoglandular stage of human lung development, the distal epithelial cells express a double positive SOX2/SOX9 progenitor cell population that is no longer present during the canalicular stage of development, suggesting its importance to human lung branching morphogenesis (**Figure 2**) (Nikolic et al., 2017; Miller et al., 2018; Danopoulos et al., 2018a). This difference of progenitor cell populations is accompanied by a change in smooth muscle cell expression. In mouse, ACTA2+ cells are primarily localized in the proximal region of the epithelium, surrounding the Sox2+ cells, whereas in humans, we showed that the ACTA2+ cells extend to the most distal region of the developing lung, surrounding the SOX2+ cells of the proximal epithelium, as well as being located between the clefts of branch points, yet not extending into the region of the SOX2/SOX9 population (**Figure 2**) (Danopoulos et al., 2018a). Nikolic et al. performed transcriptomic analyses of these SOX2/SOX9 positive cells as well as SOX2 stalk cells and compared them to available transcriptomic data from mouse lung epithelial tips. The authors showed that the transcriptomic profile of these SOX2/SOX9 epithelial tips shares similarities with mouse epithelial tips, but more importantly, they showed that some genes were unique to mouse and others were unique to humans, claiming about 348 total unique genes in human lung tips (Nikolic et al., 2017). These analyses were performed only in epithelial lung tip cells, excluding the many other cell types in the lung. Similar comparison and observations were also made by Miller et al. (2018). Many of these molecular and cellular differences between mouse and human lung development are of great significance and may pertain to lung branching morphogenesis such as the SOX2/SOX9 double positive population shown to be required for proper lung branching (Danopoulos et al., 2018a).

Recent advances in human lung development and the *in vitro* models used for these studies have been recently reviewed by Nikolic et al. (2018). Other reviews by Prince and Yuan et al. have also extensively reviewed the role of FGF10 in lung development, homeostasis, and disease, across the life span and in animal models (Prince, 2018; Yuan et al., 2018). In the present concise review, we mainly focus on FGF signaling during human lung development and congenital/pediatric human lung diseases.

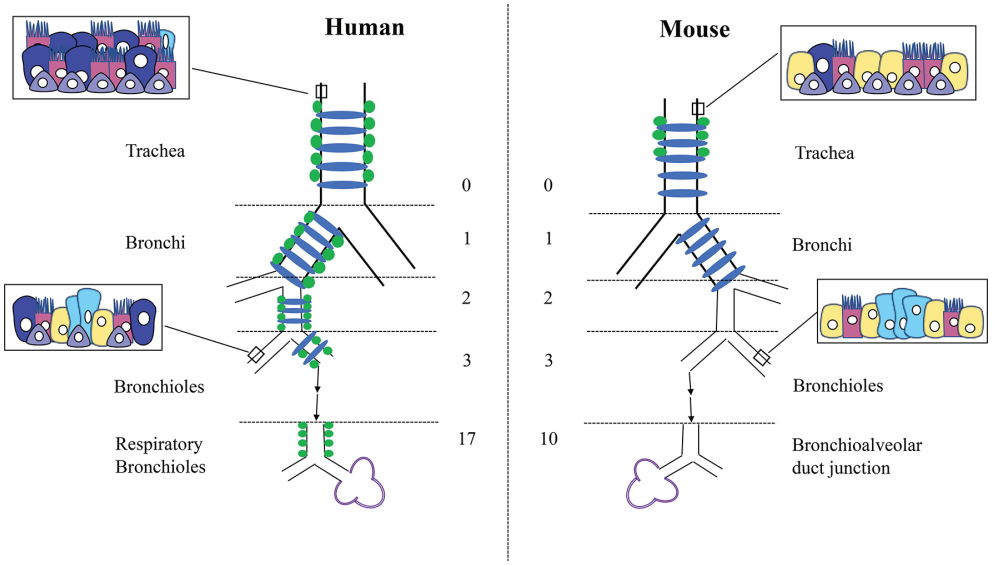

FIGURE 1 | Differences in structure and cellular composition between human and mouse lungs. Cartilage rings (blue) extend into the bronchioles in human lungs but are present only in the trachea and bronchi in mouse. Submucosal glands (green) are limited to the trachea in mouse but are present into the smaller respiratory bronchioles in humans. In mouse, only the trachea and main stem bronchi are lined with pseudostratified epithelium, whereas in humans, all the conducting airways from the trachea to the bronchioles are lined with pseudostratified epithelium. Basal cells (purple) are found deeper into the bronchioles only in humans. The human lung consists of more goblet cells (dark blue) in the proximal epithelium, with Club cells (yellow) mostly restricted to the smaller airways. Conversely, the mouse lung contains more Club cells (yellow) through the trachea and bronchi, with less goblet cells throughout. Neuroendocrine cells (light blue) are present within the bronchioles in clusters in the mouse and isolated or in much smaller clusters throughout the entire epithelial tree in human. Club cells = yellow, Ciliated cells = pink, Basal cells = purple, Goblet cells = dark blue, Neuroendocrine cells = light blue.

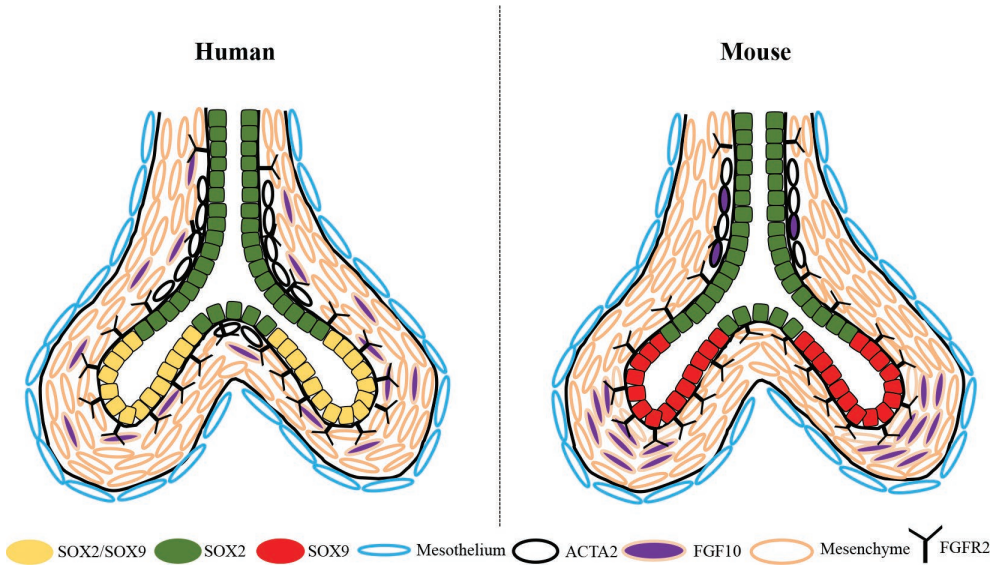

FIGURE 2 | Schematic depiction of the differential expression of SOX2, SOX9, ACTA2, and FGF10 between the developing human and mouse lung during the pseudoglandular stage. SOX2/SOX9 double positive progenitor cells are present in the distal epithelial tips of the human lung, whereas only SOX9+ cells are present in the distal tips of the mouse. ACTA2+ smooth muscle cells are found in both human and mouse surrounding the proximal airway, but extend more distally into the human lung and are closely associated with SOX2+ cells only, they are also in human at the bifurcation of the branch tips. In mouse lung, *Fgf10* is highly expressed in the mesenchyme adjacent to the epithelial tips and in the smooth muscle cells surrounding the airways; whereas in humans *FGF10*+ cells are found dispersed throughout the mesenchyme with little expression in the smooth muscle cells.

FGF FAMILY

Fibroblast growth factors are a family of growth factors described in many multicellular species such as xenopus, drosophila, zebrafish, rodents, and humans and are known to be involved in a wide range of biological processes, including organogenesis, homeostasis, repair, and metabolism. There are 22 known FGFs in both human and mouse that have been divided into seven different subfamilies (FGF1, FGF4, FGF7, FGF8, FGF9, FGF11, and FGF15/19), which are categorized according to similarities in biochemical function, sequence, and evolutionary relationships (Ornitz and Itoh, 2015). The FGF1, FGF4, FGF7, FGF8, and FGF9 subfamilies are known as the canonical FGFs, suggesting that they function in a paracrine/autocrine manner, binding to one of the FGFRs (FGFR1-FGFR4, with FGFR1-FGFR3 having a IIIb or IIIc splice variant), with heparin or heparan sulfate as a cofactor (Ornitz and Itoh, 2015). This in turn activates phosphorylation of a specific tyrosine residue on the FGFR, resulting in the initiation of downstream intracellular signaling pathway: RAS-MAPK, PI3K-AKT, PLCγ, or STAT. FGF10 is a canonical FGF and belongs to the FGF7 family (Furdui et al., 2006; Ornitz and Itoh, 2015). The FGF11 subfamily, consisting of FGF11, FGF12, FGF13, and FGF14, is categorized as the intracellular/intracrine FGFs, which as a result do not bind to any of the FGFRs (Olsen et al., 2003). The members of this subfamily are associated with voltage-gated sodium channels and the regulation of neuron activity. The FGFs associated in the final subfamily (FGF15/19, FGF21, and FGF23), the FGF15/19, are also known as the endocrine FGFs. This is where human and mouse differ in terms of FGF expression. In humans, there is no Fgf15, whereas in rodents (mice and rats), there is no expression of FGF19. Therefore, it is believed that Fgf15 and FGF19 are orthologous genes (Wright et al., 2004). The endocrine FGFs do bind to FGFRs; however, in order to increase the affinity to the receptor, it is necessary to have the presence of an additional single pass transmembrane protein known as Klotho (alpha or beta) to act as a cofactor and ensure binding efficiency (Hu et al., 2013). With the presence of 22 different ligands and 4 receptors, not including the different isoforms, it is quite evident that FGF signaling is very complex.

FGFS AND FGFRS MUTATIONS ARE ASSOCIATED WITH HUMAN LUNG DISEASES

Although there is a clear association between *Fgf10* mutations and lung malformation in mouse, such is not evident in humans. The two most familiar conditions associated with human *FGF10* mutations are autosomal dominant aplasia of lacrimal and salivary glands (ALSG) (Entesarian et al., 2005; Seymen et al., 2017) and lacrimo-auriculo-dento-digital syndrome (LADD) (Milunsky et al., 2006; Rohmann et al., 2006), with both conditions lacking a primary lung complication. LADD patients also harbor mutations in the *FGFR2* and *FGFR3* genes (Rohmann et al., 2006), suggesting that additional FGFs may be contributing

factors to the syndrome. Although one study demonstrated that ALSG patients displayed lower lung function (reduced FEV1) and irreversible airway obstruction consistent with chronic obstructive pulmonary disease (COPD) (Klar et al., 2011), 6 of the 12 patients studied had asthma and another four had other allergies. Therefore, it is unclear whether lung function changes were a direct cause of *FGF10* mutations or other unrelated factors. Furthermore, none of these patients were diagnosed with lung malformation (Klar et al., 2011). Another study suggested that single nucleotide polymorphisms (SNPs) in the *FGF10* gene may be associated with COPD (Ren et al., 2013). Interestingly, it has also been shown that *FGF10* SNPs are associated with airway branch variants, where the right medial basal segmental airway was absent in smoker COPD patients but remained unaffected in nonsmoker COPD patients (Smith et al., 2018). In addition, significant associations between lung function and SNPs in the FGF10 gene have been found (Jackson et al., 2018). However, combined, these studies still do not establish a direct causative role for *FGF10* mutations/SNPs in human congenital lung malformations, specifically in branching defects. Importantly, the effect of these SNPs on *FGF10* gene expression is unclear. A recent study by Karolak et al. demonstrated the presence of rare FGF10 and TBX4 mutations in lethal pulmonary acinar dyslasia and alveolar dysplasia (Karolak et al., 2019). They showed that FGF10 mutations or SNPs are mostly associated with alveolar dysplasia occurring past the pseudoglandular stage of development. However, the study suggested that these mutations alone are not sufficient to cause these severe lung phenotypes but rather support complex compound inheritance of additional noncoding variants or a genetic modifiers other places in the genome (Karolak et al., 2019). Finally, one cannot exclude that homozygous mutations in FGF10 might cause yet undocumented lethality in early fetal life.

Alternatively, FGF receptors have been associated with lung or airway anomalies. Activating mutations of FGFR2 cause Crouzon, Apert, and Pfeiffer syndromes (Robertson et al., 1998). While these syndromes are primarily characterized by craniofacial and skeletal defects, defects in tracheal cartilaginous ring formation resulting in mortality due to respiratory distress have also been reported (Devine et al., 1984; Cinalli et al., 1995; Gonzales et al., 2005). In these patients, the only lung associated deficiency witnessed is a cartilaginous sleeve that surrounds the trachea with no visible cartilage rings. In contrast, homozygous FGFR2 loss of function mutation (p.R255Q) results in ectrodactyly and pulmonary acinar dysplasia, a rare congenital lung malformation characterized by in utero arrest of lung development at the pseudoglandular stage (Barnett et al., 2016). This suggests that *FGFR2* signaling plays a key role in the progression of lung development from the pseudoglandular stage onwards. However, it is unclear which *FGFR2* ligands are responsible for this effect.

Moreover, SNPs in the *FGFR4* gene were shown to be associated with bronchopulmonary dysplasia (BPD) and respiratory distress syndrome (RDS), whereas SNPs in the *FGFR2* gene had no association with neither BPD nor RDS (Rezvani et al., 2013). SNPs in *FGF3* and *FGF7* but not *FGF2*, *FGF4*, or *FGF18* showed associations with RDS only but not BPD (Rezvani et al., 2013). These findings suggest *FGFR4, FGF3*, *and FGF7* play an important role in human distal lung growth.

FGF10 IN HUMAN LUNG DEVELOPMENT

Several FGF ligands and receptors have been shown to play important roles in organogenesis of multiple organ systems including the lung. In particular, *Fgf10* has been shown to be the main morphogen driving lung branching morphogenesis in mouse. Absence of *Fgf10* or its receptor *Fgfr2b* results in complete lung agenesis in mouse (Sekine et al., 1999; De Moerlooze et al., 2000). Until recently, the temporal and spatial expression of *FGF10* and its receptors in the developing human lung were unknown. We showed that *FGF10* is expressed throughout human lung development from 10 weeks of gestation up to 21 weeks of gestation (Al Alam et al., 2015; Danopoulos et al., 2018b). Unlike mouse where *Fgf10* expression increases during the pseudoglandular stage, in humans, *FGF10* expression was stable in the pseudoglandular stage and increased significantly in the canalicular stage (Al Alam et al., 2015; Danopoulos et al., 2018b). Fluorescent *in situ* hybridization allowed us to assess the spatial distribution of *FGF10* in the developing human lung and we showed that *FGF10* is expressed throughout the lung parenchyma with some expression in the airway and vascular smooth muscle cells (Danopoulos et al., 2018b). This expression was different than what has been described in mouse where *Fgf10* is abundantly expressed in the distal mesenchyme adjacent to epithelial buds (Bellusci et al., 1997). FGF10 receptors, *FGFR1* and *FGFR2*, are expressed in both epithelium and mesenchyme of the human developing lung between 11–18 weeks of gestation (Danopoulos et al., 2018b) with a stronger expression of *FGFR2* in the distal epithelium as compared to proximal epithelium, comparable to what is observed in mouse. The importance of FGF10 localization for directed branching has been reported in several mouse studies (Bellusci et al., 1997; Hirashima et al., 2009; Makarenkova et al., 2009) though others suggest that this localization is not important for the branching process (Volckaert et al., 2013).

The role of FGF10 in human lung development was unexplored until recently, and it remains incompletely understood. A report by Graeff et al. in 1999 showed that FGF7 and FGF10 both induced liquid secretion and enlargement in distal tips in human fetal lung explants cultured *in vitro* (Graeff et al., 1999). In mouse lung explants in vitro, FGF10 induces branch formation and allows the maintenance of the proximal-distal patterning characterized by SOX2 expression proximally and SOX9 expression distally (Volckaert et al., 2013). We performed more in depth analyses of the effect of FGF10, but also FGF7 and FGF9 on human lung explants cultured in vitro. We demonstrated, similar to the previous work, that FGF10 induces distal bud cysting and inhibits branching in human lung explants in vitro (Danopoulos et al., 2018b). Moreover, FGF10 does not modulate proliferation of either the epithelium or the mesenchyme following 48 hours culture in vitro (Danopoulos et al., 2018b); though an increase in p-ERK was

seen, demonstrating that FGF10 successfully binds to its receptor(s) and induces downstream signaling activation in our culture conditions. Other groups have used in vitro organoid cultures from 12 weeks post conception human fetal lung distal epithelial tips to assess the role of growth factors on growth, branching, and self-renewal (Nikolic et al., 2017; Miller et al., 2018). Miller et al. initially showed that these organoids grow and expand up to 6 weeks in presence of FGF7, CHIR99021 (GSK3 inhibitor), retinoic acid (RA), and FGF10. However, removal of FGF10 alone from the media did not affect the growth or expression of the distal tip markers SOX2 and SOX9, suggesting that FGF10 is dispensable for the maintenance and growth of these human bud tips. Similar results were obtained on organoids derived from human pluripotent stem cells (hPSCs) (Miller et al., 2018). Nikolic et al. grew 5–9 weeks postconception human fetal lung tips with a combination of 7 factors (EGF, FGF7, FGF10, NOGGIN, RSPO1, CHIR99021, and the TGFβ inhibitor SB431542) (Nikolic et al., 2017). They showed that removal of FGF10 from the culture media at day 13 (during the branching period) did not affect the initial establishment of the organoid. Following passaging of the organoids, withdrawal of FGF10 only at day 6 of culture (when organoids are spherical) for 3 days did not alter organoid morphology or RNA expression of *SOX2* and *SOX9*, whereas a decrease in SOX2/SOX9 double positive cells was seen by IF. Taken together, these studies suggest that FGF10 is not required for the initial establishment of SOX2/SOX9 double positive progenitors and for human lung branching, while FGF signaling is important in this process. However, both of these studies used a GSK3 inhibitor CHIR99021 that could possibly compensate for the removal of FGF10, as FGF10 is a major activator of ß-catenin signaling. Interestingly, a more recent study showed that treatment of foregut spheroids with 1% serum and high concentrations of FGF10 was sufficient to the generation of lung organoids containing airway like structures, mesenchymal cells, and cells expressing alveolar epithelial cells type I and type II markers (Miller et al., 2019). But, FGF10 alone was not sufficient to give rise to the bud tip progenitor population co-expressing SOX2 and SOX9. Together, this suggests an important role for FGF10 signaling in later stages of human lung development, more specifically the establishment of the distal fate past the pseudoglandular into canalicular stage and alveolar formation, as well as during the differentiation of airway epithelial cells. Furthermore, it is still unclear whether another FGF ligand or a combination of ligands plays the role in human lung branching that FGF10 plays in mouse lung branching.

FGF10 IN PEDIATRIC HUMAN LUNG DISEASES

Whereas FGF10 mutations alone may not be sufficient to cause severe human lung malformations or congenital lung disease, alterations in *FGF10* expression have been described in bronchopulmonary dysplasia (BPD). The number of mesenchymal cells staining positive for FGF10 was decreased in the lung of BPD patients as compared to controls (Benjamin et al., 2007). In contrast, two independent GWAS studies found no association between BPD and FGF10 SNPs and no change in *FGF10* gene expression between BPD and controls (Bhattacharya et al., 2012; Li et al., 2015; Hamvas et al., 2018). Additionally, in congenital cystic adenomatoid malformation (CCAM), *FGF10, FGF7*, and *FGFR2* gene levels are unchanged in the lung mesenchyme (Cass et al., 1998; Jancelewicz et al., 2008), whereas epithelial *FGF9* expression is increased 4-fold in the CCAM samples compared to controls (Jancelewicz et al., 2008). Furthermore, there is no evidence of altered *FGF10* expression or signaling in human congenital small lung or lung hypoplasia, although its expression is different in mouse and rat experimental models of hypoplasia (Teramoto et al., 2003; Wang et al., 2018). However, a decrease in *FGF18* expression has been described in hypoplastic lungs from patients with congenital diaphragmatic hernia (Boucherat et al., 2007). In cystic fibrosis, fluid secretion and transport defects play an important role in the pathogenesis of the disease. While there is no clear evidence in human data sets of a role for FGF10 and/or FGF10 signaling in cystic fibrosis, studies in pig models showed that FGF10 treatment induced fluid secretion in non-CF fetal lung explants but was unable to do so in CF fetal lung explants (Meyerholz et al., 2018), suggesting that FGF10 signaling may play an important role in the pathogenesis of the disease.

CONCLUSION

The role of FGF10 signaling in human lung development and disease remains poorly understood. Despite the limitations associated with the use and manipulation of human tissues, studies in human development and disease are necessary to better understand the role of FGF10 and other pathways that have been shown to be important in mouse, e.g., FGF, Wnt, and Hippo pathways. The disappointingly high failure rate of clinical trials has made studying human tissues critical, along with the necessity to accelerate the development of therapies for pediatric lung diseases. FGF10, under the drug name Repifermin, failed to prove efficacy in clinical trials for wound healing, mucositis, and ulcerative colitis (Freytes et al., 2004), though it had highly protective and therapeutic effects in animal models. Understanding the role of FGF signaling in human lung development and disease will help tailor its possible therapeutic effects and targets, if any, to the appropriate site of action and patient population.

AUTHOR CONTRIBUTIONS

SD, JS and DA reviewed the literature, wrote the review, edited and approved the final version.

FUNDING

We acknowledge support of NIH/NHLBI HL to DA and Hastings Fellowship to SD.

REFERENCES

Al Alam, D., El Agha, E., Sakurai, R., Kheirollahi, V., Moiseenko, A., Danopoulos, S., et al. (2015). Evidence for the involvement of fibroblast growth factor 10 in lipofibroblast formation during embryonic lung development. *Development* 142, 4139–4150. doi: 10.1242/dev.109173

Barnett, C. P., Nataren, N. J., Klingler-Hoffmann, M., Schwarz, Q., Chong, C. E., Lee, Y. K., et al. (2016). Ectrodactyly and lethal pulmonary acinar dysplasia associated with homozygous FGFR2 mutations identified by exome sequencing. *Hum. Mutat.* 37, 955–963. doi: 10.1002/humu.23032

Bellusci, S., Grindley, J., Emoto, H., Itoh, N., and Hogan, B. L. (1997). Fibroblast growth factor 10 (FGF10) and branching morphogenesis in the embryonic mouse lung. *Development* 124, 4867–4878.

Benjamin, J. T., Smith, R. J., Halloran, B. A., Day, T. J., Kelly, D. R., and Prince, L. S. (2007). FGF-10 is decreased in bronchopulmonary dysplasia and suppressed by Toll-like receptor activation. *Am. J. Phys. Lung Cell. Mol. Phys.* 292, L550–L558. doi: 10.1152/ajplung.00329.2006

Bhattacharya, S., Go, D., Krenitsky, D. L., Huyck, H. L., Solleti, S. K., Lunger, V. A., et al. (2012). Genome-wide transcriptional profiling reveals connective tissue mast cell accumulation in bronchopulmonary dysplasia. *Am. J. Respir. Crit. Care Med.* 186, 349–358. doi: 10.1164/rccm.201203-0406OC

Boucherat, O., Benachi, A., Barlier-Mur, A. M., Franco-Montoya, M. L., Martinovic, J., Thebaud, B., et al. (2007). Decreased lung fibroblast growth factor 18 and elastin in human congenital diaphragmatic hernia and animal models. *Am. J. Respir. Crit. Care Med.* 175, 1066–1077. doi: 10.1164/rccm.200601-050OC

Cass, D. L., Quinn, T. M., Yang, E. Y., Liechty, K. W., Crombleholme, T. M., Flake, A. W., et al. (1998). Increased cell proliferation and decreased apoptosis characterize congenital cystic adenomatoid malformation of the lung. *J. Pediatr. Surg.* 33, 1043–1046. discussion 1047. doi: 10.1016/S0022-3468(98)90528-0

Cinalli, G., Renier, D., Sebag, G., Sainte-Rose, C., Arnaud, E., and Pierre-Kahn, A. (1995). Chronic tonsillar herniation in Crouzon's and Apert's syndromes: the role of premature synostosis of the lambdoid suture. *J. Neurosurg.* 83, 575–582. doi: 10.3171/jns.1995.83.4.0575

Danopoulos, S., Alonso, I., Thornton, M. E., Grubbs, B. H., Bellusci, S., Warburton, D., et al. (2018a). Human lung branching morphogenesis is orchestrated by the spatiotemporal distribution of ACTA2, SOX2, and SOX9. *Am. J. Phys. Lung Cell. Mol. Phys.* 314, L144–L149. doi: 10.1152/ajplung.00379.2017

Danopoulos, S., Thornton, M. E., Grubbs, B. H., Frey, M. R., Warburton, D., Bellusci, S., et al. (2018b). Discordant roles for FGF ligands in lung branching morphogenesis between human and mouse. *J. Pathol.* 247, 254–265. doi: 10.1002/path.5188

De Moerlooze, L., Spencer-Dene, B., Revest, J. M., Hajihosseini, M., Rosewell, I., and Dickson, C. (2000). An important role for the IIIb isoform of fibroblast growth factor receptor 2 (FGFR2) in mesenchymal-epithelial signalling during mouse organogenesis. *Development* 127, 483–492.

Devine, P., Bhan, I., Feingold, M., Leonidas, J. C., and Wolpert, S. M. (1984). Completely cartilaginous trachea in a child with Crouzon syndrome. *Am. J. Dis. Child.* 138, 40–43. doi: 10.1001/archpedi.1984.02140390032010

Entesarian, M., Matsson, H., Klar, J., Bergendal, B., Olson, L., Arakaki, R., et al. (2005). Mutations in the gene encoding fibroblast growth factor 10 are associated with aplasia of lacrimal and salivary glands. *Nat. Genet.* 37, 125–127. doi: 10.1038/ng1507

Freytes, C. O., Ratanatharathorn, V., Taylor, C., Abboud, C., Chesser, N., Restrepo, A., et al. (2004). Phase I/II randomized trial evaluating the safety and clinical effects of repifermin administered to reduce mucositis in patients undergoing autologous hematopoietic stem cell transplantation. *Clin. Cancer Res.* 10, 8318–8324. doi: 10.1158/1078-0432.CCR-04-1118

Furdui, C. M., Lew, E. D., Schlessinger, J., and Anderson, K. S. (2006). Autophosphorylation of FGFR1 kinase is mediated by a sequential and precisely ordered reaction. *Mol. Cell* 21, 711–717. doi: 10.1016/j.molcel.2006.01.022

Gonzales, M., Heuertz, S., Martinovic, J., Delahaye, S., Bazin, A., Loget, P., et al. (2005). Vertebral anomalies and cartilaginous tracheal sleeve in three patients with Pfeiffer syndrome carrying the S351C FGFR2 mutation. *Clin. Genet.* 68, 179–181. doi: 10.1111/j.1399-0004.2005.00477.x

Graeff, R. W., Wang, G., and McCray, P. B. Jr. (1999). KGF and FGF-10 stimulate liquid secretion in human fetal lung. *Pediatr. Res.* 46, 523–529. doi: 10.1203/00006450-199911000-00006

Hamvas, A., Feng, R., Bi, Y., Wang, F., Bhattacharya, S., Mereness, J., et al. (2018). Exome sequencing identifies gene variants and networks associated with extreme respiratory outcomes following preterm birth. *BMC Genet.* 19:94. doi: 10.1186/s12863-018-0679-7

Hirashima, T., Iwasa, Y., and Morishita, Y. (2009). Mechanisms for split localization of Fgf10 expression in early lung development. *Dev. Dyn.* 238, 2813–2822. doi: 10.1002/dvdy.22108

Hu, M. C., Shiizaki, K., Kuro-o, M., and Moe, O. W. (2013). Fibroblast growth factor 23 and Klotho: physiology and pathophysiology of an endocrine network of mineral metabolism. *Annu. Rev. Physiol.* 75, 503–533. doi: 10.1146/annurev-physiol-030212-183727

Irvin, C. G., and Bates, J. H. (2003). Measuring the lung function in the mouse: the challenge of size. *Respir. Res.* 4:4. doi: 10.1186/rr199

Jackson, V. E., Latourelle, J. C., Wain, L. V., Smith, A. V., Grove, M. L., Bartz, T. M., et al. (2018). Meta-analysis of exome array data identifies six novel genetic loci for lung function. *Wellcome Open Res.* 3:4. doi: 10.12688/wellcomeopenres.12583.3

Jancelewicz, T., Nobuhara, K., and Hawgood, S. (2008). Laser microdissection allows detection of abnormal gene expression in cystic adenomatoid malformation of the lung. *J. Pediatr. Surg.* 43, 1044–1051. doi: 10.1016/j.jpedsurg.2008.02.027

Karolak, J. A., Vincent, M., Deutsch, G., Gambin, T., Cogne, B., Pichon, O., et al. (2019). Complex compound inheritance of lethal lung developmental disorders due to disruption of the TBX-FGF pathway. *Am. J. Hum. Genet.* 104, 213–228. doi: 10.1016/j.ajhg.2018.12.010

Klar, J., Blomstrand, P., Brunmark, C., Badhai, J., Hakansson, H. F., Brange, C. S., et al. (2011). Fibroblast growth factor 10 haploinsufficiency causes chronic obstructive pulmonary disease. *J. Med. Genet.* 48, 705–709. doi: 10.1136/jmedgenet-2011-100166

Knust, J., Ochs, M., Gundersen, H. J., and Nyengaard, J. R. (2009). Stereological estimates of alveolar number and size and capillary length and surface area in mice lungs. *Anat. Rec.* 292, 113–122. doi: 10.1002/ar.20747

Li, J., Yu, K. H., Oehlert, J., Jeliffe-Pawlowski, L. L., Gould, J. B., Stevenson, D. K., et al. (2015). Exome sequencing of neonatal blood spots and the identification of genes implicated in bronchopulmonary dysplasia. *Am. J. Respir. Crit. Care Med.* 192, 589–596. doi: 10.1164/rccm.201501-0168OC

Makarenkova, H. P., Hoffman, M. P., Beenken, A., Eliseenkova, A. V., Meech, R., Tsau, C., et al. (2009). Differential interactions of FGFs with heparan sulfate control gradient formation and branching morphogenesis. *Sci. Signal.* 2:ra55. doi: 10.1126/scisignal.2000304

Meyerholz, D. K., Stoltz, D. A., Gansemer, N. D., Ernst, S. E., Cook, D. P., Strub, M. D., et al. (2018). Lack of cystic fibrosis transmembrane conductance regulator disrupts fetal airway development in pigs. *Lab. Investig.* 98, 825–838. doi: 10.1038/s41374-018-0026-7

Miller, A. J., Dye, B. R., Ferrer-Torres, D., Hill, D. R., Overeem, A. W., Shea, L. D., et al. (2019). Generation of lung organoids from human pluripotent stem cells in vitro. *Nat. Protoc.* 14, 518–540. doi: 10.1038/s41596-018-0104-8

Miller, A. J., Hill, D. R., Nagy, M. S., Aoki, Y., Dye, B. R., Chin, A. M., et al. (2018). In vitro induction and in vivo engraftment of lung bud tip progenitor cells derived from human pluripotent stem cells. *Stem Cell Reports* 10, 101–119. doi: 10.1016/j.stemcr.2017.11.012

Milunsky, J. M., Zhao, G., Maher, T. A., Colby, R., and Everman, D. B. (2006). LADD syndrome is caused by FGF10 mutations. *Clin. Genet.* 69, 349–354. doi: 10.1111/j.1399-0004.2006.00597.x

Nikolic, M. Z., Caritg, O., Jeng, Q., Johnson, J. A., Sun, D., Howell, K. J., et al. (2017). Human embryonic lung epithelial tips are multipotent progenitors that can be expanded in vitro as long-term self-renewing organoids. *elife* 6. doi: 10.7554/eLife.26575

Nikolic, M. Z., Sun, D., and Rawlins, E. L. (2018). Human lung development: recent progress and new challenges. *Development* 145. doi: 10.1242/dev.163485

Ochs, M., Nyengaard, J. R., Jung, A., Knudsen, L., Voigt, M., Wahlers, T., et al. (2004). The number of alveoli in the human lung. *Am. J. Respir. Crit. Care Med.* 169, 120–124. doi: 10.1164/rccm.200308-1107OC

Olsen, S. K., Garbi, M., Zampieri, N., Eliseenkova, A. V., Ornitz, D. M., Goldfarb, M., et al. (2003). Fibroblast growth factor (FGF) homologous factors share structural but not functional homology with FGFs. *J. Biol. Chem.* 278, 34226–34236. doi: 10.1074/jbc.M303183200

Ornitz, D. M., and Itoh, N. (2015). The Fibroblast Growth Factor signaling pathway. *Wiley Interdiscip. Rev. Dev. Biol.* 4, 215–266. doi: 10.1002/wdev.176

Prince, L. S. (2018). FGF10 and human lung disease across the life spectrum. *Front. Genet.* 9:517. doi: 10.3389/fgene.2018.00517

Ren, J. T., Feng, K., Wang, P., Peng, W. H., Jia, H. Y., Liu, K., et al. (2013). Relationship between the gene polymorphism in fibroblast growth factor-10 and susceptibility to chronic obstructive pulmonary disease 220 cases. *Zhonghua Jie He He Hu Xi Za Zhi* 36, 935–939.

Rezvani, M., Wilde, J., Vitt, P., Mailaparambil, B., Grychtol, R., Krueger, M., et al. (2013). Association of a FGFR-4 gene polymorphism with bronchopulmonary dysplasia and neonatal respiratory distress. *Dis. Markers* 35, 633–640. doi: 10.1155/2013/932356

Robertson, S. C., Meyer, A. N., Hart, K. C., Galvin, B. D., Webster, M. K., and Donoghue, D. J. (1998). Activating mutations in the extracellular domain of the fibroblast growth factor receptor 2 function by disruption of the disulfide bond in the third immunoglobulin-like domain. *Proc. Natl. Acad. Sci. U. S. A.* 95, 4567–4572.

Rohmann, E., Brunner, H. G., Kayserili, H., Uyguner, O., Nurnberg, G., Lew, E. D., et al. (2006). Mutations in different components of FGF signaling in LADD syndrome. *Nat. Genet.* 38, 414–417. doi: 10.1038/ng1757

Sekine, K., Ohuchi, H., Fujiwara, M., Yamasaki, M., Yoshizawa, T., Sato, T., et al. (1999). Fgf10 is essential for limb and lung formation. *Nat. Genet.* 21, 138–141. doi: 10.1038/5096

Seymen, F., Koruyucu, M., Toptanci, I. R., Balsak, S., Dedeoglu, S., Celepkolu, T., et al. (2017). Novel FGF10 mutation in autosomal dominant aplasia of lacrimal and salivary glands. *Clin. Oral Investig.* 21, 167–172. doi: 10.1007/s00784-016-1771-x

Smith, B. M., Traboulsi, H., Austin, J. H. M., Manichaikul, A., Hoffman, E. A., Bleecker, E. R., et al. (2018). Human airway branch variation and chronic obstructive pulmonary disease. *Proc. Natl. Acad. Sci. U. S. A.* 115, E974–E981. doi: 10.1073/pnas.1715564115

Teramoto, H., Yoneda, A., and Puri, P. (2003). Gene expression of fibroblast growth factors 10 and 7 is downregulated in the lung of nitrofen-induced diaphragmatic hernia in rats. *J. Pediatr. Surg.* 38, 1021–1024. doi: 10.1016/S0022-3468(03)00183-0

Volckaert, T., Campbell, A., Dill, E., Li, C., Minoo, P., and De Langhe, S. (2013). Localized Fgf10 expression is not required for lung branching morphogenesis but prevents differentiation of epithelial progenitors. *Development* 140, 3731–3742. doi: 10.1242/dev.096560

Wang, J., Liu, H., Gao, L., and Liu, X. (2018). Impaired FGF10 signaling and epithelial development in experimental lung hypoplasia with esophageal atresia. *Front. Pediatr.* 6:109. doi: 10.3389/fped.2018.00109

Wansleeben, C., Barkauskas, C. E., Rock, J. R., and Hogan, B. L. (2013). Stem cells of the adult lung: their development and role in homeostasis, regeneration, and disease. *Wiley Interdiscip. Rev. Dev. Biol.* 2, 131–148. doi: 10.1002/wdev.58

Wong, C. H., Siah, K. W., and Lo, A. W. (2018). Estimation of clinical trial success rates and related parameters. *Biostatistics* doi: 10.1093/biostatistics/kxx069

Wright, T. J., Ladher, R., McWhirter, J., Murre, C., Schoenwolf, G. C., and Mansour, S. L. (2004). Mouse FGF15 is the ortholog of human and chick FGF19, but is not uniquely required for otic induction. *Dev. Biol.* 269, 264–275. doi: 10.1016/j.ydbio.2004.02.003

Yuan, T., Volckaert, T., Chanda, D., Thannickal, V. J., and De Langhe, S. P. (2018). Fgf10 signaling in lung development, homeostasis, disease, and repair after injury. *Front. Genet.* 9:418. doi: 10.3389/fgene.2018.00418

Conflict of Interest Statement: The authors declare that the research was conducted in the absence of any commercial or financial relationships that could be construed as a potential conflict of interest.

Copyright © 2019 Danopoulos, Shiosaki and Al Alam. This is an open-access article distributed under the terms of the Creative Commons Attribution License (CC BY). The use, distribution or reproduction in other forums is permitted, provided the original author(s) and the copyright owner(s) are credited and that the original publication in this journal is cited, in accordance with accepted academic practice. No use, distribution or reproduction is permitted which does not comply with these terms.

frontiers in Genetics

ORIGINAL RESEARCH
published: 14 March 2019
doi: 10.3389/fgene.2019.00178

Characterization of *Tg(Etv4-GFP)* and *Etv5^{RFP}* Reporter Lines in the Context of Fibroblast Growth Factor 10 Signaling During Mouse Embryonic Lung Development

Matthew R. Jones[1,2†], Arun Lingampally[2†], Salma Dilai[2], Amit Shrestha[2], Barry Stripp[3], Francoise Helmbacher[4], Chengshui Chen[1], Cho-Ming Chao[2,5,6] and Saverio Bellusci[1,2,6*]*

[1] Department of Pulmonary and Critical Care Medicine, The First Affiliated Hospital of Wenzhou Medical University, Wenzhou, China, [2] Department of Internal Medicine II, Member of the German Lung Center, Cardio-Pulmonary Institute, University of Giessen Lung Center, Giessen, Germany, [3] Department of Medicine, Cedars-Sinai Medical Center, Lung and Regenerative Medicine Institutes, Los Angeles, CA, United States, [4] Aix Marseille University, CNRS, IBDM, UMR7288, Marseille, France, [5] Department of General Pediatrics and Neonatology, University Children's Hospital Gießen, Justus-Liebig-University, Gießen, Germany, [6] International Collaborative Center on Growth Factor Research, Life Science Institute, Wenzhou University-Wenzhou Medical University, Wenzhou, China

Members of the PEA3 transcription factors are emerging as bone fide targets for fibroblast growth factor (FGF) signaling. Among them, ETV4 and ETV5 appear to mediate FGF10 signaling during early embryonic lung development. In this paper, recently obtained *Tg(Etv4-GFP)* and *Etv5$^{CreERT2-RFP}$* fluorescent reporter lines were generally characterized during early embryonic development and in the context of FGF10 signaling, in particular. We found that both *Tg(Etv4-GFP)* and *Etv5$^{CreERT2-RFP}$* were primarily expressed in the epithelium of the lung during embryonic development. However, the expression of *Etv5$^{CreERT2-RFP}$* was much higher than that of *Tg(Etv4-GFP)*, and continued to increase during development, whereas *Tg(Etv4-GFP)* decreased. The expression patterns of the surrogate fluorescent protein GFP and RFP for ETV4 and ETV5, respectively, agreed with known regions of FGF10 signaling in various developing organs, including the lung, where ETV4-GFP was seen primarily in the distal epithelium and to a lesser extent in the surrounding mesenchyme. As expected, ETV5-RFP was restricted to the lung epithelium, showing a decreasing expression pattern from distal buds to proximal conducting airways. FGF10 inhibition experiments confirmed that both *Etv4* and *Etv5* are downstream of FGF10 signaling. Finally, we also validated that both fluorescent reporters responded to FGF10 inhibition *in vitro*. In conclusion, these two reporter lines appear to be promising tools to monitor FGF10/FGFR2b signaling in early lung development. These tools will have to be further validated at later stages and in other organs of interest.

Keywords: ETV4, ETV5, FGF10, lung development, branching morphogenesis

OPEN ACCESS

Edited by:
Emmanuel S. Tzanakakis, Tufts University, United States

Reviewed by:
Laszlo Farkas, Virginia Commonwealth University, United States
Jincheng Wu, Novartis Institutes for BioMedical Research, United States

***Correspondence:**
Cho-Ming Chao
Cho-Ming.Chao@paediat.med.uni-giessen.de
Saverio Bellusci
saverio.bellusci@innere.med.uni-giessen.de

†These authors have contributed equally to this work

Specialty section:
This article was submitted to Stem Cell Research, a section of the journal Frontiers in Genetics

Received: *28 September 2018*
Accepted: *18 February 2019*
Published: *14 March 2019*

Citation:
Jones MR, Lingampally A, Dilai S, Shrestha A, Stripp B, Helmbacher F, Chen C, Chao C-M and Bellusci S (2019) Characterization of Tg(Etv4-GFP) and Etv5^{RFP} Reporter Lines in the Context of Fibroblast Growth Factor 10 Signaling During Mouse Embryonic Lung Development. Front. Genet. 10:178. doi: 10.3389/fgene.2019.00178

INTRODUCTION

PEA3 transcription factors are a subfamily of the E26 transformation-specific (ETS) transcription factor family consisting of three members: ETV1 (also known as Er81), ETV4 (also known as PEA3), and ETV5 (also known as ERM) (reviewed by Sharrocks et al., 1997). Evidence from multiple studies has demonstrated that ETV4 and ETV5 are primary mediators of fibroblast growth factor (FGF) signaling via fibroblast growth factor receptor 2b (FGFR2b), and play overlapping roles in the patterning, morphogenesis, differentiation, and homeostasis of multiple organs and structures. For example, ETV4 and ETV5 have been shown to repress *Shh* expression in mouse limb buds, thus promoting bud outgrowth and proper anterior-posterior patterning (Mao et al., 2009; Zhang et al., 2009); studies in the mouse lung have shown that ETV4- and ETV5-mediated induction of *Shh* appear to regulate branching morphogenesis (Herriges et al., 2015); furthermore, ETV5 was shown to maintain alveolar type 2 (AT2) cell identity during mouse lung homeostasis and repair after injury, and has been implicated in lung tumorigenesis (Zhang et al., 2017); during development of the lacrimal gland in mice, it was demonstrated that PEA3 transcription factors control epithelial cell fate determination (Garg et al., 2018); in the kidney as well, research has shown that ETV4 and ETV5 play a wide range of functions within multiple signaling pathways, including FGF signaling, to regulate Wolffian duct and ureteric bud morphogenesis (Kuure et al., 2010); finally, a study in zebrafish has found that knocking down *Etv4* and *Etv5* resulted in embryonic abnormalities similar to a loss of FGF signaling, including cardiac, and left/right patterning defects (Znosko et al., 2010).

Lung organogenesis is a complex process involving a number of signaling pathways, and is divided into distinct stages comprising embryonic (E) and postnatal (P) development. In the mouse, these stages include the pseudoglandular stage (E9.5–16.5), the canalicular stage (E16.5–17.5), the saccular stage (E17.5–P5), and the alveolar stage (P5–P30) (reviewed in Chao et al., 2015). During each of the embryonic and postnatal stages, FGF signaling plays critical roles. For instance, during the pseudoglandular stage of lung development, the majority of the lung architecture is established via branching morphogenesis, and also most of the epithelial and mesenchymal cell types are formed (reviewed in El Agha and Bellusci, 2014). Disruption of FGFR2b signaling during this stage leads to morphological and differentiation defects (Bellusci et al., 1997b), while either *Fgf10*- or *Fgfr2b*-null embryos display complete lung agenesis (Sekine et al., 1999; De Moerlooze et al., 2000).

Another critical signaling pathway during pseudoglandular lung development is the sonic hedgehog (SHH) pathway. SHH is a negative regulator of *Fgf10* expression in the distal mesenchyme, and serves to limit the action of FGF10/FGFR2b signaling (Bellusci et al., 1997a). Recent studies propose that FGF10 acts on SHH via ETV4 and ETV5, creating an FGF10/ETV4/ETV5/SHH axis required for orchestrating proper branching morphogenesis (Herriges et al., 2015). It is unclear, however, how FGF10 acts on ETV4 and ETV5; whether it acts directly to regulate the expression of these transcription factors, for example, or whether these are regulated indirectly via another pathway.

To aid the study of the role of ETV4 and ETV5 during organogenesis, two transgenic reporter mice have recently been developed, *Tg(Etv4-GFP)* (Lamballe et al., 2011) and *Etv5*$^{CreERT2-RFP}$ (also referred to as *Etv5*^{RFP}). These lines report, via green and red fluorescent markers, the expression of *Etv4* and *Etv5*, respectively. Furthermore, *Etv5*$^{CreERT2-RFP}$ can be used to drive inducible genetic recombination in *Etv5* positive cells, upon administration of tamoxifen. These lines can, therefore, potentially be used as invaluable research tools to study the role of ETV4 and ETV5 during the development of multiple organs, especially in the context of FGF signaling.

In this paper, we characterize these two reporter mouse lines during early embryogenesis (up to E16.5). We report the areas and organs of expression of ETV4-GFP and ETV5-RFP in the mouse embryo. We then focus on the expression of *Etv4* and *Etv5* in isolated embryonic lung mesenchyme and epithelium as well as the dynamic expression of the ETV4-GFP and ETV5-RFP protein during pseudoglandular development. Finally, various FGF10 inhibition experiments were carried out *in vitro* to determine the impact on the expression of ETV4-GFP and ETV5-RFP activity.

MATERIALS AND METHODS

Animal Husbandry and Experimental Embryos

All animals were housed in a specific-pathogen-free (SPF) facility in accordance with local, state, and national laws. Timed pregnancies were set-up to obtain experimental embryos for analysis at the desired embryonic stage (from E9.5 to E18.5). Noon on the day of the vaginal plug was considered E0.5.

To obtain experimental and littermate control embryos, mice heterozygous for *Etv5*$^{CreERT2-RFP}$ (*B6.Cg-Etv5<tm1(cre/ERT2)Brst>*), or hemizygous for *Tg(Etv4-GFP)* (*B6-Tg(Etv4/EGFP)4Fhel*) (Lamballe et al., 2011), were crossed with wild type mice. Embryos were harvested at the desired embryonic stage. Briefly, pregnant females were sacrificed with an overdose of pentobarbital sodium (dosage: 0.4 mg pentobarbital / g mouse weight), embryos removed, and washed in PBS for ∼2 min. Organs were dissected under a stereoscope and positioned for imaging.

DNA was extracted from tails and limbs following basic lab procedures and prepared for PCR-based genotyping. The *Tg(Etv4-GFP)* gene was detected using the following primer sequences: Forward−5′-GGA ATC TTG GGC CTT GAG AAC AGC-3′; reverse−5′-CGC TGA ACT TGT GGC CGT TTA CG-3′. The cycling protocol was as follows: denaturation at 94°C for 3 min; 40 cycles of denaturation at 94°C for 15 s, annealing at 60°C for 30 s, and extension at 72°C for 1 min; finish with a final extension at 72°C for 5 min. The *Etv5*$^{CreERT2-RFP}$ gene as well as the wild type *Etv5*, was detected using the following primer sequences: *Etv5*$^{CreERT2-RFP}$ forward−5′-TCG ATG CAA CGA GTG ATG AG-3′; *Etv5*$^{CreERT2-RFP}$ reverse−5′-TTC GGC TAT ACG TAA CAG GGT-3′; *Etv5* forward−5′-AAA GAG

GAA CGC GGT CTG AG-3′; *Etv5* reverse−5′-CCA GCT GAG TCT CGT GTG AT-3′. The cycling protocol was as follows: denaturation at 95°C for 3 min; 30 cycles of denaturation at 94°C for 30 s, annealing at 60°C for 30 s, and elongation at 72°C for 80 s. Product bands were detected by capillary gel electrophoresis.

FACS-based Isolation of Epithelial and Mesenchymal Cells

Lungs from embryonic mice were dissected at desired time points (E14.5, E16.5, and E18.5), and transferred to ice-cold Hank's Balanced Salt Solution (HBSS). Lungs were finely chopped with a sterile razor blade on a glass plate. The tissue was then added to a falcon tube and digested in 0.5% collagenase at 37°C for 45 min, with constant mixing. Single cell suspensions were made by successively flushing the samples through 18, 20, and 24 g grade needles and then filtering the samples through 70 and 40 μm nylon strainers (BD Biosciences). The cell suspensions were diluted with 5 ml HBSS and centrifuged at 12,000 rpm for 5 min. and the supernatant was discarded. The pellet was resuspended in 10 μl blocking buffer and the following antibodies were added: 488-CD31 (1:50); FITC-CD45 (1:50); and Apc Cy7 EpCam (Epithelial cell adhesion molecule) (1:50) (Biolegend), for 20 min at 4°C. The samples were washed 2x with 100 μl FACS buffer and centrifuged at 12,000 rpm for 5 min at 4°C. The supernatant was discarded. The pellet was resuspended in 100 μl FACS buffer.

Cell sorting and isolation was performed using the FACSAria^{TM} III (BD Biosciences) cell sorter. Alveolar epithelial cells were identified as CD45^{-ve}/CD31^{-ve}/ Epcam^{+ve} and mesenchymal cells as CD45^{-ve}/CD31^{-ve}/ Epcam^{-ve}. Cells were sorted through a flow chamber with a 100-μm nozzle tip under 25 psi sheath fluid pressure. Isolated cells were used for RNA isolation. As a main criterion for gating, we used the settings allowing to capture 98% of the cells in the isotype control and then we applied these gating conditions to the stained cells.

RT-qPCR

Either FACS-isolated cells, or embryonic lungs were lysed in Qiazol lysis reagent, and total RNA isolated using a miRNeasy mini RNA extraction kit according to the manufacturer's instructions (Qiagen). Please note that from cell dissociation to RNA isolation, the process takes 3–4 h. Our results indicate that there is very little variability between samples from the same time point and same group (epithelium or mesenchyme).

Up to 1 μg RNA was reverse-transcribed using the QuantiTect reverse transcription kit (Qiagen). cDNA was used to specifically amplify the desired DNA sequence by quantitative PCR (qPCR). Primers were designed to amplify specific mature mRNAs using NCBI's primer-BLAST option (https://www.ncbi.nlm.nih.gov/tools/primer-blast/) (last accessed, 01-08-2018). Primers were further validated by PCR-based gel electrophoresis. The following primer sequences were used: *Etv4* (FWD-5′-CAGACTTCGCCTAC GACTCA-3′; REV-5′- GCCATAACCCATCACTCCAT-3′); *Etv5* (FWD-5′-GTGGCCGCTCAGGAGTA-3′; REV-5′-GTGCTTC CTTCCAAAGTCTCCG CT-3′); *RFP* (FWD-5′-GCGTGATG AACTTCGAGGAC-3′; REV-5′-TTCACCTTG TAGATC AGCGTG-3′); *Hprt* (FWD-5′-CCTAAGATGAGCGCAAGTT GAA-3′; REV-5′-CCACAGGACTAGAACACCTGCTAA-3′).

qPCR reaction mixtures were set up using the PowerUp SYBR Green Master Mix kit following the manufacturer's instructions (Thermo Fisher). Samples were run with three technical replicates on a LightCycler 480II (Roche) using the following protocol: UDG activation at 50°C for 2 min; DNA polymerase activation at 95°C for 2 min; and 40 cycles of denaturation at 95°C for 15 s, annealing at 60°C for 15 s, and extension at 72°C for 1 min. To validate amplification specificity, a dissociation step was also included for each sample. Threshold cycles (Ct) were calculated and used for relative expression analyses, using mouse *Hprt* as the reference gene.

ΔCt and ΔΔCt values were calculated according to the following formulas:

$$\Delta Ct = Ct_{Reference} - Ct_{geneof\ interest}$$

Note, this equation accounts for the fact that Ct is proportional to the –log of gene expression. ΔCt is therefore positively related to the expression of the gene of interest.

Expression relative to *Hprt* $= 2^{\Delta Ct}$

$$\Delta\Delta Ct_{Experimental-control} = Mean\Delta Ct_{Experimental} - Mean\Delta Ct_{Control}$$

Unpaired two-tailed Student's *t*-tests were performed on the ΔCt values, which can be assumed to be normally distributed. Number of "n" form of graphical representation, and significance level is indicated either in the figures or in the figure legends.

Lung Explant Culture for *in vitro* Experiments

Embryonic lungs used for *in vitro* experiments were obtained either from genetically modified embryos generated as described above, or from C57BL/6 wild-type embryos.

Embryonic lungs were dissected and cultured on 13 mm Whitman Track-Etch polycarbonate membranes, with 8.0 μm pores (Merck) positioned atop DMEM culture medium in a 24-well culture dish [medium contained: Dulbecco's Modified Eagle Medium (1x DMEM), supplemented with D-Glucose, L-Glutamine, HEPES, Pyruvate, and Phenol red (Gibco), 10% fetal bovine serum (FBS), 1% penicillin (10,000 units/ml)-streptomycin (10 mg/ml)]. Lungs were incubated at 5% CO_2 and 37°C for ∼45 min to allow them to settle. At the desired time, recombinant FGF7 (50 ng/ml), FGF10 (250 ng/ml), soluble FGFR2b (5 μg/ml) (R and D Systems), or anti-FGF10 blocking antibody (20 μg/ml) (Santa Cruz Biotechnology) was added to the experimental lungs (as described in Sakaue et al., 2002), while the vehicle was added to control samples. Lungs were incubated at 5% CO_2 and 37°C for the duration of the experiment.

In vivo Model to Inhibit FGFR2b Signaling

In vivo studies were conducted using an inducible dominant negative mouse model: *Rosa26*$^{rtTA/+}$; *Tg(tetO-Fgfr2b)/+* (*B6-Cg-Gt(ROSA)26Sor*$^{tm1.1(rtTA,EGFP)Nagy}$ *Tg(tetO-Fgfr2b/lgh)1.3Jaw/sbel*). Doxycycline was administered via

intraperitoneal injection to timed-pregnant females, as previously described (Danopoulos et al., 2013).

Imaging Acquisition and Measurements

Brightfield images of lungs from *in vivo* and *in vitro* experiments were captured either on a Leica MZ 125 stereoscopic dissecting microscope using a Spot Insight 2.0 Mp Color Mosaic camera and Spot 4.5.9 imaging software, or were obtained from live imaging experiments using a Leica DM6000B inverted microscope, DFC 305FX camera, and Leica Application Suite Advanced Fluorescence imaging software. Fluorescence intensities were quantified using FIJI software (version 2.0.0-rc-68/1.52 g).

Branching was quantified by counting and averaging the distal tips of the left lobe of control and experimental samples at 0 and 24 h. These groups were analyzed using a two-factorial quasi-Poisson model, with the dispersion parameter estimated as 0.317. Differences were considered statistically significant at $p < 0.05$.

Gene Expression Patterns

To assess the expression patterns of genes in early stage embryonic lungs (E14.5), the online database genepaint.org was used (last accessed 01-08-2018). Each of the genes significantly regulated in our *in vivo* studies was entered in genepaint. The whole embryo section displaying the clearest gene expression in the lung, along with a magnification of the lung itself, was chosen for the figures.

RESULTS AND DISCUSSION

Tg(Etv4-GFP) Expression During Early Embryonic Development

The *Tg(Etv4-GFP)* mouse line was created by Lamballe et al. (2011). These researchers used a bacterial artificial chromosome containing the *Etv4* gene fused with a green fluorescent protein gene (*GFP*) in frame with exon 9, to generate the *Tg(Etv4-GFP)* transgenic mouse line (**Figure 1A**). In the process, exons 10–12 of the *Etv4* construct were deleted. Thus, the randomly inserted *Tg(Etv4-GFP)* transgene is non-functional, and does not interfere with endogenous *Etv4* activity.

To characterize *Tg(Etv4-GFP)* expression in various organs during development, embryos were generated at different stages (E9.5, E11.5, E12.5, and E13.5). *Tg(Etv4-GFP)* was crossed with wild type mice to generate controls ($Etv4^{+/+}$) and transgenic embryos (*Tg(Etv4-GFP)/+*) at different developmental stages. **Figure 1B** shows the PCR-based strategy designed to detect the band corresponding to the presence of the transgene (see sequence of the primers in materials and methods). **Figure 1C** shows embryos negative for GFP (**Figures 1Ca,g,n,u**) and positive for GFP (**Figures 1Cb,r,h,v**) at different developmental stages. At E9.5, GFP was detected in the nasal placode, the mandibullary and maxillary processes, and at the mid-brain/hindbrain junction (**Figures 1Cc**), the anterior limb bud and the mammary line (**Figures 1Ce**), the otic placode (**Figures 1Cd**), and the tail bud (**Figures 1Cf**). Similar expression sites were found at E11.5 (**Figures 1Ch–l**). Close examination of the lung indicated that GFP was expressed specifically at the tips in the epithelium and mesenchyme (**Figures 1Cm**). This expression overlaps with the previously reported endogenous *Etv4* expression in the E12.5 lung (Yin et al., 2011). At E12.5, the external expression of GFP did not appear as specific. However, upon dissection of internal organs, GFP was enriched in the posterior (glandular) stomach (**Figures 1Co**), the developing kidneys (**Figures 1Cq**), the epithelium of the cecum (**Figures 1Cs**), and the lung epithelium and mesenchyme (**Figures 1Ct**, see also insert in **figure 1t**). At E13.5, GFP was found in similar places (**Figures 1Cw,y,z**). In addition, GFP was located at the tip of the forming digits (**Figures 1Cx**).

$Etv5^{CreERT2-RFP/+}$ Expression During Early Embryonic Development

The $Etv5^{CreERT2-RFP/+}$ mouse line was recently generated by Barry Stripp (Cedars-Sinai Medical Center, Los Angeles, USA). In this line, a knock-in of *CreERT2/RFP* in the 3′ untranslated region of the *Etv5* gene was carried in embryonic stem cells (**Figure 1D**). Recombinant clones were used to generate $Etv5^{CreERT2-RFP/+}$ knock-in mice. **Figure 1E** shows the PCR based strategy to detect the presence of the $Etv5^{RFP}$ knock in allele in heterozygous or homozygous embryos (see sequence of the primers in materials and methods). We performed a similar characterization on this line as we did on the *Tg(Etv4-GFP)* mouse line.

$Etv5^{CreERT2-RFP/+}$ mice were crossed with wild type mice to generate controls ($Etv5^{+/+}$) and heterozygous embryos ($Etv5^{CreERT2-RFP/+}$) at different developmental stages. During the E9.5 and E11.5 stages, RFP expression was general throughout the embryo (**Figures 1Fa,g**). At E9.5, expression was seen in the heart (**Figures 1Fb**), otic placode (**Figures 1Fd**), and nasal placode (**Figures 1Fc**). Expression in the tail was seen at E9.5 and E11.5 (**Figures 1Ff,k**), and in limb buds, limbs and the tips of forming digits in all stages (**Figures 1Ff,h,q,w**). Expression was seen in whisker regions (**Figures 1Fn,t**). After dissection, RFP was found to be enriched in the anterior stomach (**Figures 1Fp**), kidneys (**Figures 1Frx**), and epithelium of the cecum (**Figures 1Fj,v**). The expression of RFP in the lung at E11.5 did not appear enriched in the epithelium (**Figures 1Fl**). However, in later stages, RFP expression did appear enriched in the epithelium (**Figures 1Fo,s,u**), not only distally, but throughout the epithelium, with the expression disappearing in the main bronchi and trachea (e.g., **Figures 1Fo,s**, see also **Figures 4**, **6**).

Expression of *Etv4* and *Etv5* During Embryonic Lung Development

To assess the relative expression of *Etv4* and *Etv5* during embryonic lung development, epithelial and mesenchymal cells from embryonic wild type mouse lungs were separated using FACS at different stages (E14.5, E16.5, and E18.5). Please note that while our protocol allows excluding the CD31-positive endothelium and CD45-positive hematopoietic cells, the isolated mesenchyme (negative for the surface marker Epcam, an epithelial cell adhesion molecule used to isolate epithelial cells) was a mixture of nerve cells, smooth muscle cells, mesothelial cells and resident mesenchymal cells. RNA

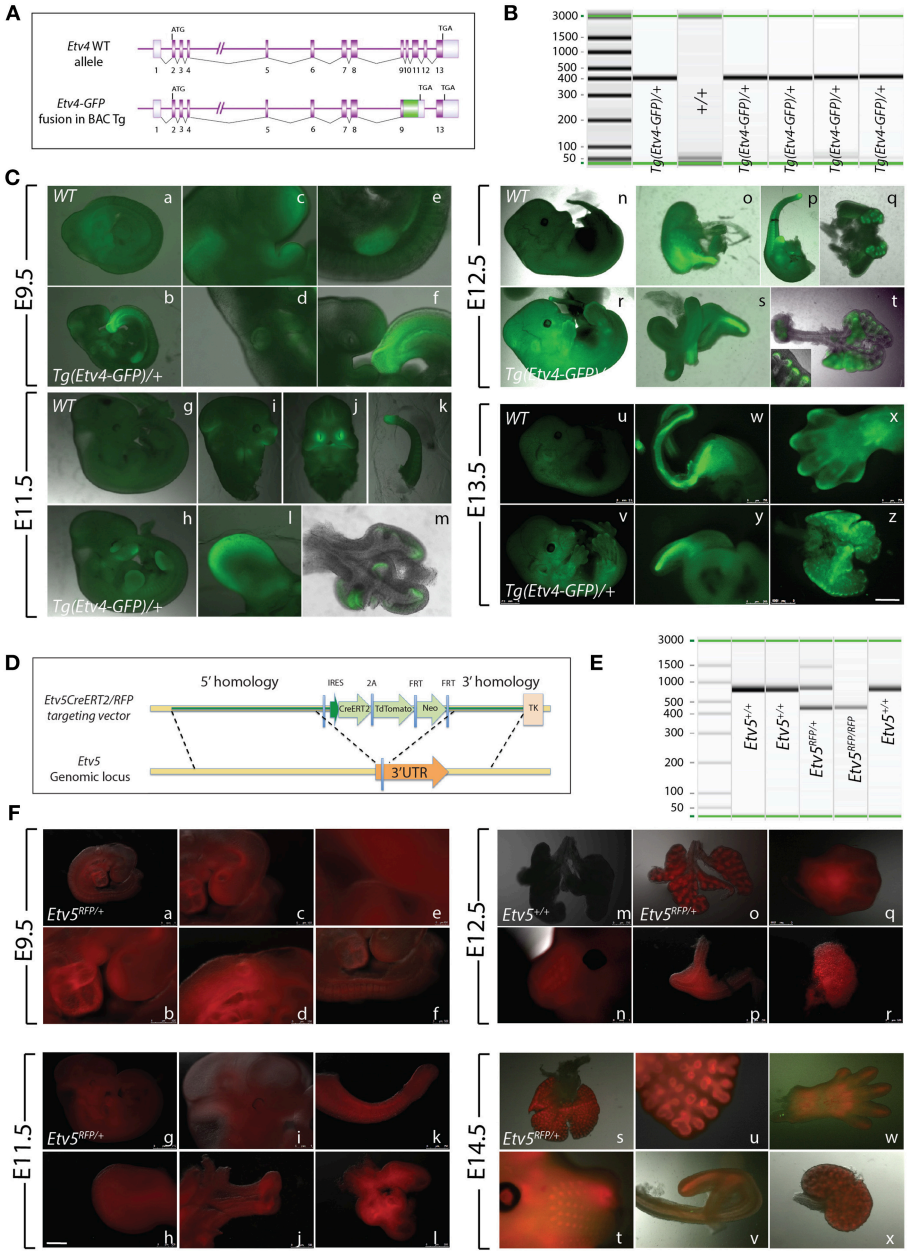

FIGURE 1 | Early embryonic expression of ETV4-GFP and ETV5-RFP **(A)** *Tg(Etv4-GFP)* genetic construct. **(B)** Genotype detecting the *Tg(Etv4-GFP)* transgene at ∼400 bp. **(C)** ETV4-GFP expression pattern in various embryonic organs at E9.5 (a–f), E11.5 (g–m), E12.5 (n–t), and E13.5 (u–z). See text for details. Note the increased expression of ETV4-GFP in the distal tips of the lung (see inset in "t," and "z"). Scale bar: (a,b,g,h,n,r,u,v) 2.5 mm; (c–f,i–l,o–q,s,y) 500 μm; (w,x) 750 μm; (t,m,z) 1,000 μm. **(D)** *Etv5*^{RFP} genetic construct. **(E)** Genotype detecting the *Etv5*^{RFP} transgene at ∼450 bp and the wild type *Etv5* at ∼827 bp. **(F)** ETV5-RFP expression pattern in various embryonic organs at E9.5 (a–f), E11.5 (g–l), E12.5 (o–r), and E14.5 (s–x). Please note that the *Etv5*$^{+/+}$ lungs do not show any autofluorescence (**Figure 1Fm**). See text for details. Note the differential expression level of ETV5-RFP in the distal lung epithelium vs. the proximal conducting airways (see "o" and "s"). Scale bar: (a,i,n,t) 1 mm; (b) 250 μm; (c,d,f,h,j,l,m,o,q-s,u,w,x) 500 μm; (e) 100 μm; (g) 2.5 mm; (k,p,v) 750 μm.

was extracted from the Epcam-positive (epithelial) and Epcam-negative (mesenchymal) cells and qPCR analysis was performed (**Figure 2A**). *Etv4* expression was seen in both the mesenchyme and epithelium during embryonic development. At E14.5, *Etv4* was more highly expressed in the epithelium than in the mesenchyme. However, at later stages (E16.5 and E18.5), *Etv4* expression decreased in the epithelium while remaining relatively constant in the mesenchyme (**Figure 2B**).

Etv5 was likewise expressed in both the mesenchymal and epithelial compartments throughout embryonic development. However, its expression in the epithelium was much higher than in the mesenchyme (around 10 times higher at E14.5,

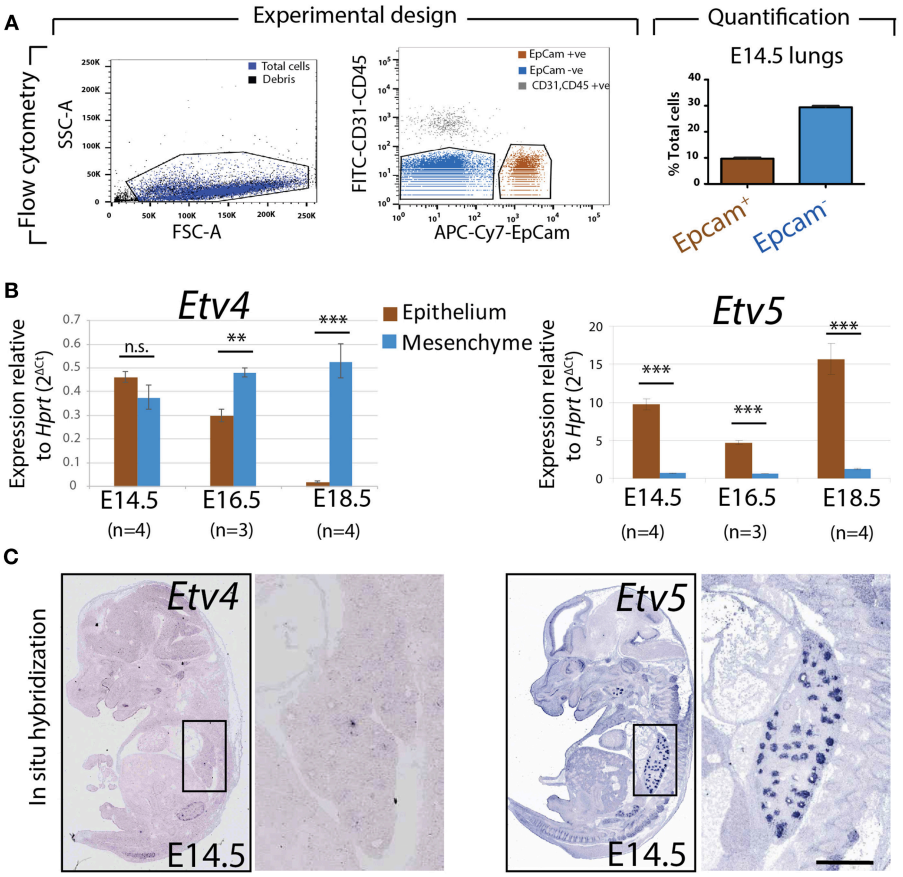

FIGURE 2 | Expression of *Etv4* and *Etv5* in isolated embryonic lung epithelium and mesenchyme **(A)** Experimental design for the FACS-based isolation of embryonic lung epithelial and mesenchymal cells at E14.5 ($n = 4$; 44.88 ± 17.54 ng/μl RNA from epithelial cells, 64.70 ± 18.10 ng/μl RNA from mesenchymal cells), E16.5 ($n = 3$; 16.38 ± 5.69 ng/μl RNA from epithelial cells, 75.18 ± 13.79 ng/μl RNA from mesenchymal cells), and E18.5 ($n = 4$; 28.77 ± 3.06 ng/μl RNA from epithelial cells, 44.89 ± 15.30 ng/μl RNA from mesenchymal cells). Approximately 10 and 30% of the cells in E14.5 lungs were epithelial and mesenchymal, respectively. **(B)** RT-qPCR for *Etv4* and *Etv5* in isolated epithelial and mesenchymal cells. Note the different scales of the y-axis between *Etv4* and *Etv5* graphs. (Data are presented as geometric mean ± SE; n.s. = not significant, $^{**}p < 0.01$, $^{***}p < 0.001$). **(C)** *In situ* hybridization from the genepaint database showing the expression of *Etv4* and *Etv5* in E14.5 embryos.

and 15 times higher at E18.5). *Etv5* epithelial expression decreased at E16.5 before greatly increasing at E18.5, compared to E14.5 (**Figure 2B**).

The expression of *Etv4* and *Etv5* was also validated using the publicly available genepaint.org data base. While *Etv4* expression was diffusely seen in the lung epithelium and surrounding mesenchyme, *Etv5* showed very strong expression restricted to the epithelium (compare insets in **Figure 2C**).

Dynamic GFP Expression Reports FGF10 Signaling

To monitor the expression of *Tg(Etv4-GFP)* in the epithelial buds of pseudoglandular stage lungs in the context of FGF10 signaling, E12.5 *Tg(Etv4-GFP)* lungs were cultured and live imaged for 24 h, after which FGF10 signaling was blocked using an anti-FGF10 antibody for an additional 24 h (**Figure 3A**). During the first 24 h, ETV4-GFP was dynamically expressed, showing greater expression at the distal tips of growing buds, in likely regions of active FGF10 signaling (see **Figures 3Ba–c** and **Supplementary Movie 1**). During the FGF10 inhibition, ETV4-GFP expression was greatly reduced. Still images from multiple time points during the live imaging from three independent lungs were used to quantify these global changes in fluorescence intensity (**Figure 3C**). We also confirmed that the loss of GFP expression of the E12.5 lungs after 24 h in culture was neither due to bleaching, nor to a normal decrease in ETV4-GFP expression. **Supplementary Figure 1** shows that the expression of ETV4-GFP in E12.5 transgenic lungs was maintained in culture for at least 38 h. Furthermore, still images of individual buds were used to quantify the dynamic expression of ETV4-GFP in three regions of the bud during a branching event (**Figures 3D,E**). Intensity was measured during new branch formation at the tip (regions 4 and 6), stalk (regions 1–3; 7–9) and cleft (region 5). Tip ETV4-GFP fluorescence intensity initially increased before stabilizing (**Figures 3Ea**), whereas stalk

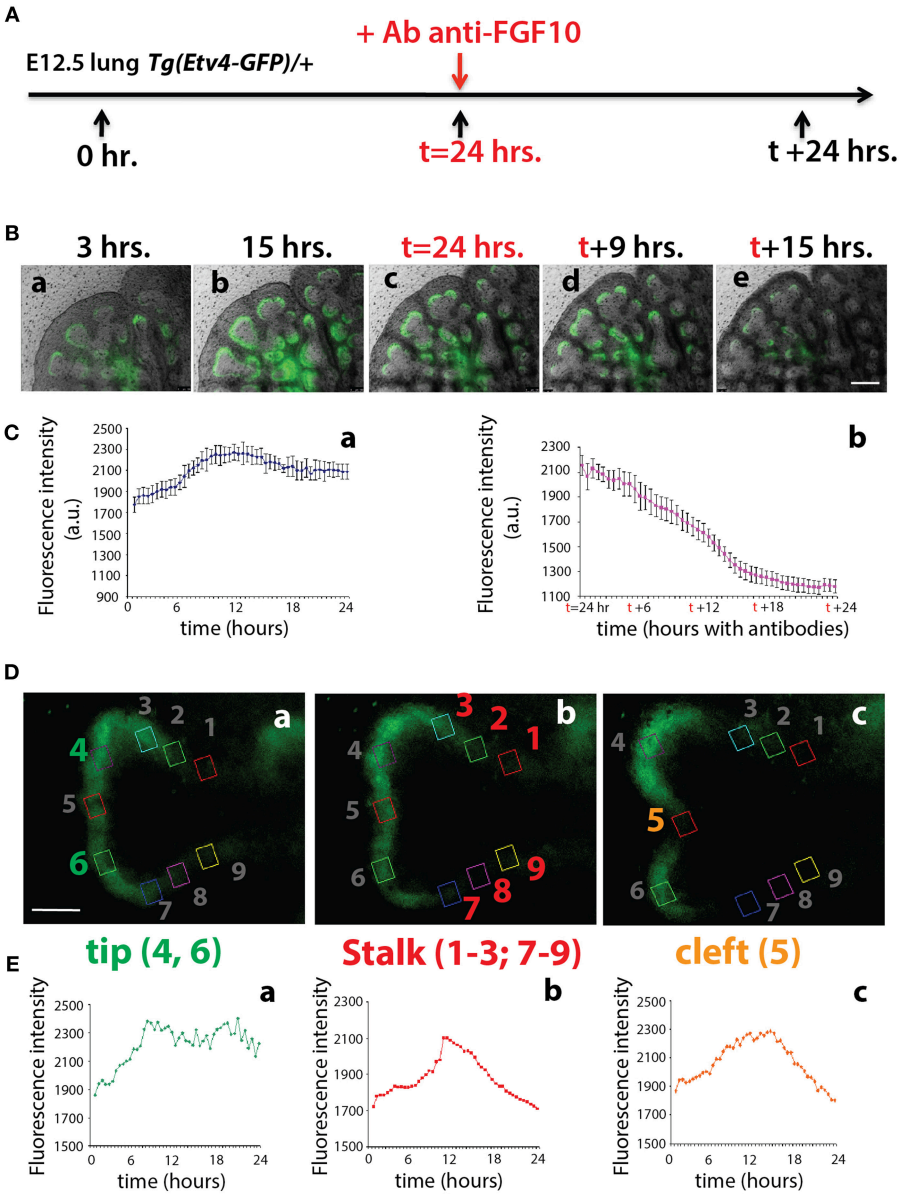

FIGURE 3 | ETV4-GFP is dynamically expressed in regions of active FGF10 signaling during early lung development **(A)** Experimental design: E12.5 *Tg(Etv4-GFP)* lungs were isolated, cultured and live imaged for 48 h. After 24 h anti-FGF10 antibody was added to inhibit FGF10 activity. **(B)** Still images from different time points during the live imaging experiment. Note how ETV4-GFP expression increases before leveling off within the first 24 h (a–c), and, once the antibody is added, the expression decreases to almost zero by the end of the experiment (c–e). Scale bar: 125 μm. **(C)** Global ETV4-GFP fluorescence intensity measured at various time points before (a) and after (b) adding the FGF10 blocking antibody. ($n = 3$; data are presented as average fluorescence intensity in arbitrary units (a.u.) ± standard deviation). **(D)** Example images of a branching tip at three successive time points (a–c), highlighting three regions of dynamic ETV4-GFP expression: the tip (4 and 6), the stalk (1–3, and 7–9), and the cleft (5). See text for details. Scale bar: 30 μm. **(E)** Representative plot of ETV4-GFP expression in three independent regions [(a) tip, (b) stalk, and (c) cleft] of a single bud over a period of 24 h ($n = 1$; a.u. = arbitrary units).

and cleft fluorescence intensity increased before decreasing to initial levels (**Figures 3Eb,c**). The expression patterns of the stalk and cleft reflected the initial single bud branching into two buds.

These results suggest that the *Tg(Etv4-GFP)* mouse line can be used as a valid tool to report FGF10 signaling in the distal tips of lungs during pseudoglandular development. This conclusion is supported by the previously described dynamic expression pattern of *Sprouty2* during the branching process (Mailleux et al., 2001). *Sprouty2* is a well-accepted target of FGF10 signaling in the lung, and displays a remarkably similar expression pattern to what we found for *Tg(Etv4-GFP)*.

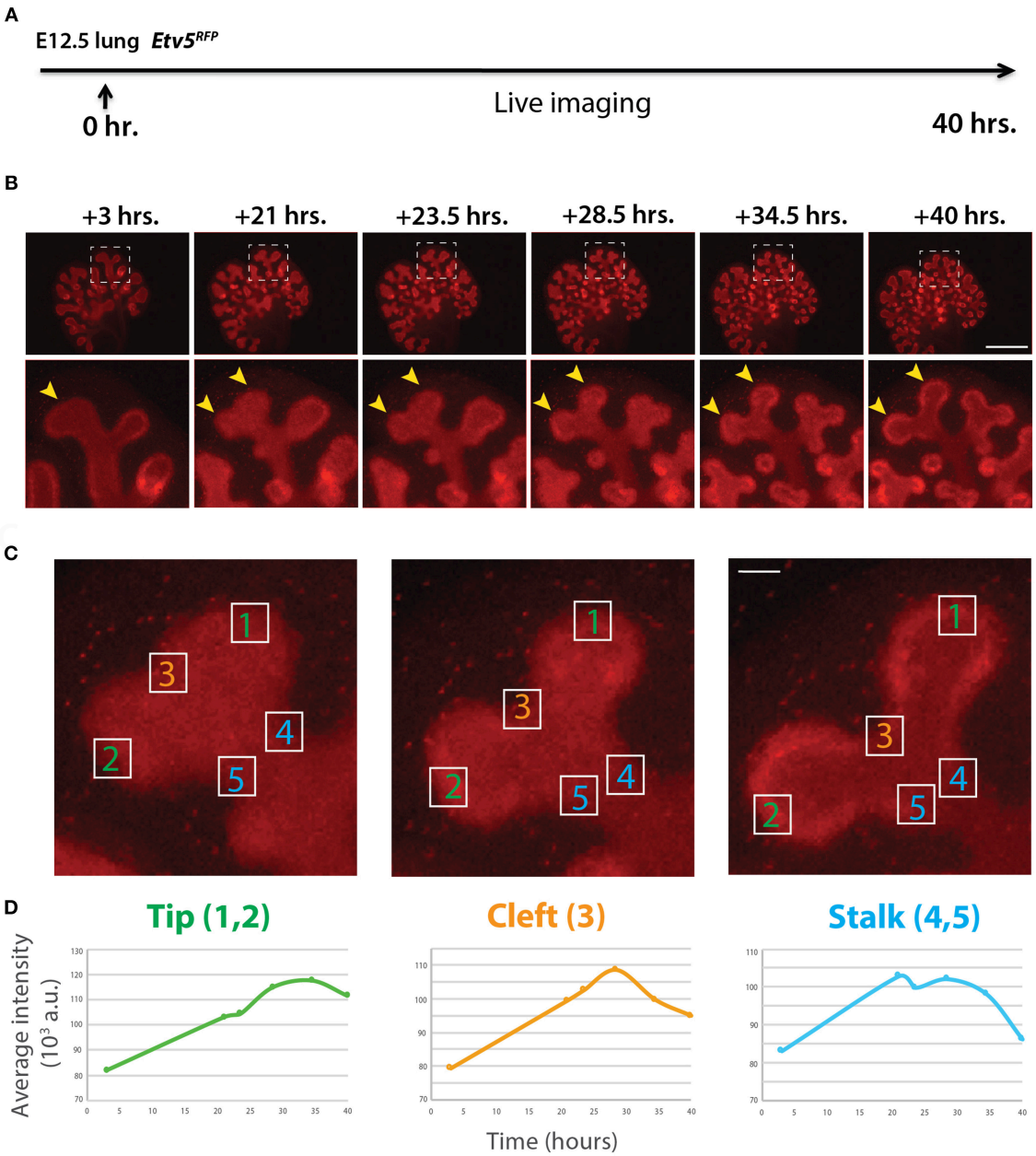

FIGURE 4 | Expression pattern of ETV5-RFP in distal lung epithelium during early development **(A)** Experimental design: E12.5 *Etv5*^{RFP} lung explants were cultured for 40 h and live imaged. **(B)** Still images showing representative ETV5-RFP expression both globally and in the distal tips (boxes). Arrows indicate increased expression in the tips over time. Scale bar: (Top row) 500 μm; (Bottom row) 125 μm. **(C)** Example images of a branching tip at three successive time points (a–c), highlighting three regions of dynamic ETV5-RFP expression: the tip (1 and 2), the cleft (3), and the stalk (4 and 5). See text for details. Scale bar: 37 μm. **(D)** Representative plot of ETV5-RFP expression in three independent regions [(a) tip, (b) stalk and (c) cleft] of a single bud over a period of 40 h ($n = 1$; a.u. = arbitrary units).

Quantification of Dynamic ETV5-RFP Fluorescence

Similar to the analysis of ETV4-GFP expression in early lung development, the expression of ETV5-RFP in branching epithelial buds was assessed. E12.5 *Etv5*$^{CreERT2-RFP/+}$ lungs were cultured and live imaged for 40 h (**Figure 4A**). During this time ETV5-RFP was expressed throughout the epithelial tree at the exception of the primary bronchi and trachea. This was in contrast with the expression of ETV4-GFP, which was only at the tip. Interestingly, the more proximal regions of ETV5-RFP expression were not localized to known areas of FGF10 signaling. Close-up examination of ETV5-RFP indicated higher expression in distal tips compared to more proximal regions (see arrows in **Figure 4B** and

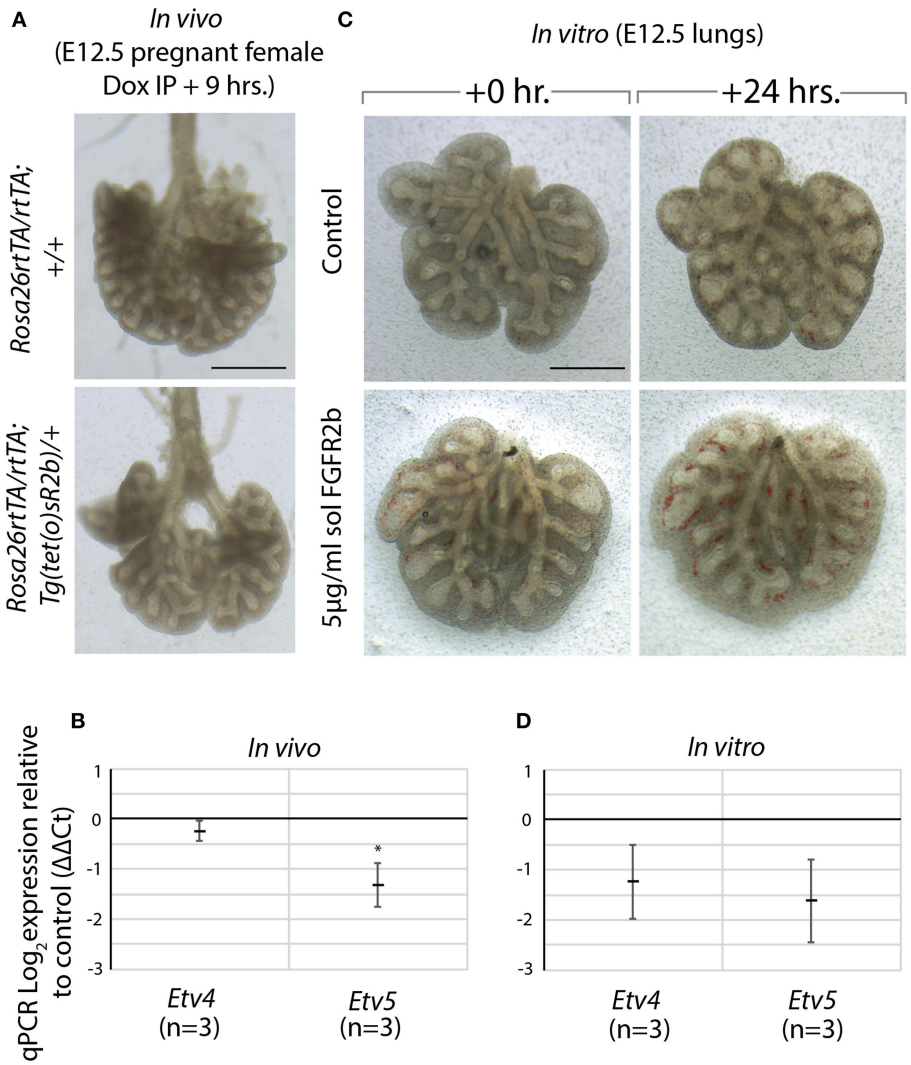

FIGURE 5 | Model to inhibit FGF10 *in vivo* and *in vitro* demonstrates *Etv4* and *Etv5* are downstream of FGF10/FGFR2b signaling **(A)** *In vivo* model to inhibit FGF10/FGFR2b signaling: pregnant females carrying experimental (*Rosa26*$^{rtTA/rtTA}$; *Tg*$^{Tet(o)sR2b/+}$) and littermate control (*Rosa26*$^{rtTA/rtTA}$; *Tg*$^{+/+}$) embryos were injected with doxycycline. Embryonic lungs were isolated 9 h later. *Scale bar:* 500 µm. **(B)** Corresponding RT-qPCR analysis showing *Etv4* and *Etv5* expression in experimental vs. control lungs. **(C)** *In vitro* model to inhibit FGF10/FGFR2b signaling: E12.5 lung explants were cultured for 24 h with (experimental) or without (control) 5 µg/ml recombinant (soluble) FGFR2b. Scale bar: 500 µm. **(D)** Corresponding RT-qPCR analysis showing *Etv4* and *Etv5* expression in experimental vs. control lungs. (Data are presented as mean ± SEM; *$p < 0.05$).

Supplementary Movie 2). Finally, we quantified the fluorescence intensity of bud regions during a branching event using still images at multiple time points (**Figures 4Ca–c**). Fluorescence intensity at the tip (regions 1 and 2) increased before leveling off around 30 h, and then decreased slightly (**Figures 4Da**), whereas intensity at the cleft and stalk regions (regions 3 and 4–5, respectively) initially increased before decreasing to original levels (**Figures 4Db,c**). This temporal expression pattern was similar to what was found for *Tg(Etv4-GFP)* lungs, and is likely a consequence of the initial bud branching into two buds.

Model to Inhibit FGF10 Confirms *Etv4* and *Etv5* Are Downstream of FGF10/FGFR2b Signaling

We made use of a model to inhibit all FGFR2b ligands *in vivo* via inducible expression of a dominant negative form of the FGFR2b receptor, called soluble FGFR2b (*Rosa26*$^{rtTA/rtTA}$; *Tg(tet(o)sR2b)/+*) (Parsa et al., 2008, 2010). Upon administration of doxycycline, soluble FGFR2b is produced and secreted from cells, functionally inhibiting all FGFR2b ligands from properly signaling. We have previously shown that at E12.5, FGF10 is the predominant FGF ligand signaling in the lung (Bellusci et al.,

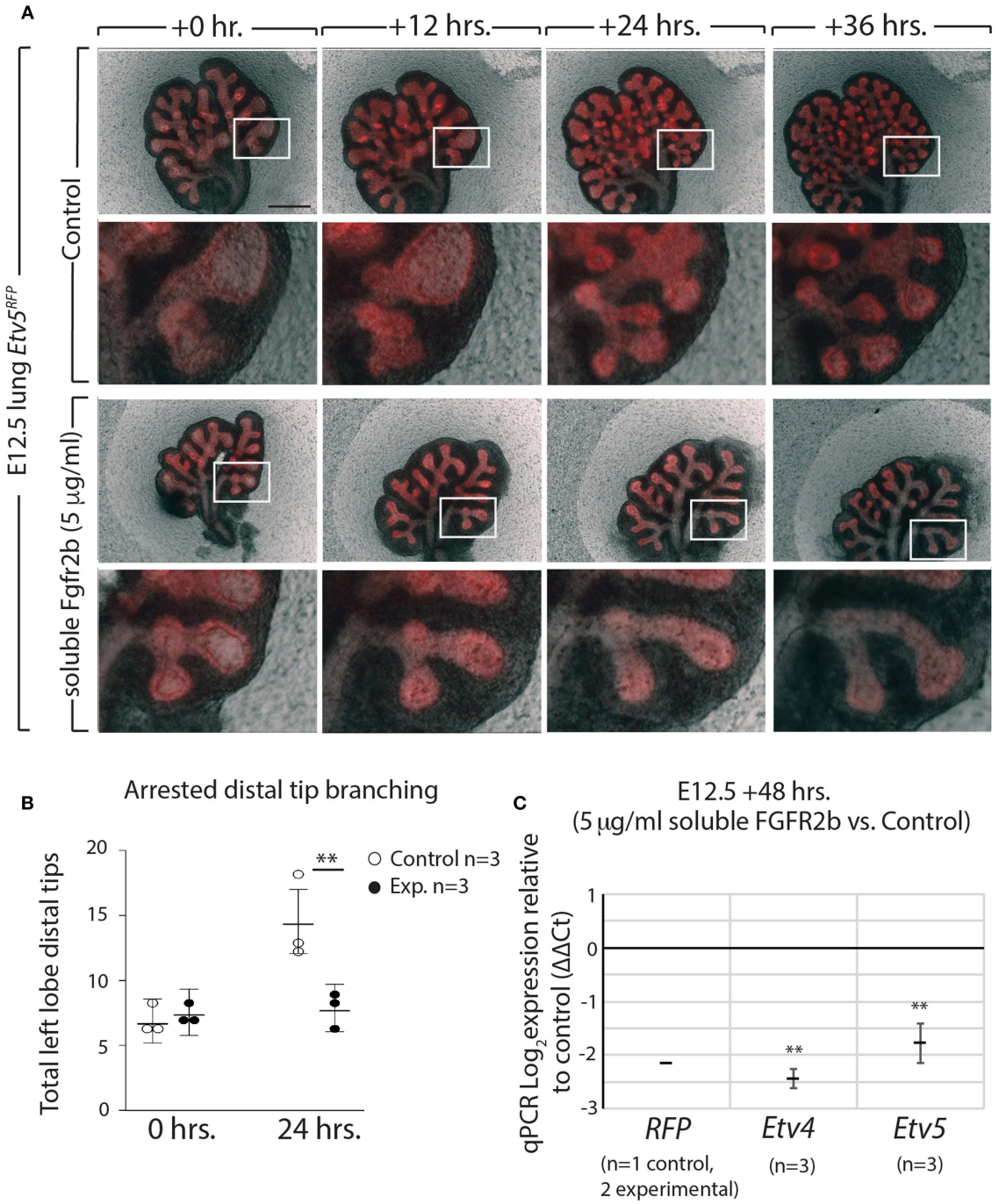

FIGURE 6 | ETV5-RFP reports FGF10/FGFR2b signaling *in vitro* **(A)** E12.5 *Etv5*^{RFP} lungs were harvested and cultured with (experimental) or without (control) 5 μg/ml recombinant (soluble) FGFR2b for 48 h. *Scale bar:* (Top rows) 500 μm; (Boxes) 125 μm. **(B)** Left lobe distal tips show arrested branching in experimental lungs after 24 h. FGF10/FGFR2b inhibition, compared to control lungs. While both control lungs and experimental lungs had a similar number of average tips at 0 h, only control lungs showed an increase in branching over time (Data are presented as mean with 95% CI; $^{**}p < 0.01$). **(C)** RT-qPCR analysis of the lungs showing downregulation of *RFP*, *Etv4*, and *Etv5*, in experimental lungs, demonstrating the usefulness of the *Etv5*^{RFP} line to report FGF10/FGFR2b signaling. Note, we only had one control *Etv5*^{RFP} lung and two experimental *Etv5*^{RFP} lungs, thus statistical analysis was not possible (Data are presented as mean ± SEM; $^{**}p < 0.01$).

1997b). Therefore, induction of soluble FGFR2b at this time point inhibits FGF10 signaling. As **Figure 5A** shows, after only 9 h of FGF10 inhibition, experimental lungs were smaller, displayed simplified branching, and had fewer distal buds. Furthermore, the expressions of *Etv4* and *Etv5*, as evaluated by RT-qPCR, were reduced (**Figure 5B**).

A similar approach to inhibiting FGFR2b signaling was conducted *in vitro*. In this experiment, wild type E12.5 lungs were harvested and cultured with (experimental) or without (control) recombinant FGFR2b added to the culture medium for 24 h (**Figure 5C**). A similar phenotype to that seen *in vivo* was produced in experimental lungs, while the downregulation of *Etv4* and *Etv5* mRNA was even more pronounced (**Figure 5D**).

Taken together, these results suggest that FGF10 signaling can be inhibited both *in vitro* and *in vivo*, and that *Etv4* and *Etv5* are regulated by FGF10.

ETV5-RFP Expression Reports FGF10 Signaling *in vitro*

Using our *in vitro* approach to inhibit FGF10/FGFR2b signaling in pseudoglandular stage lungs, we investigated whether the *Etv5*$^{CreERT2-RFP}$line could be used as a tool to report FGF10/FGFR2b signaling. E12.5 *Etv5*$^{CreERT2-RFP}$ lungs were cultured and live imaged for 48 h with (experimental) or without (control) recombinant soluble FGFR2b (**Figure 6A**). As can be seen in the still images, the soluble FGFR2b treated lungs showed arrest in branching over time, compared to the control (**Figure 6B**). This phenotype is a hallmark of inhibited FGF10 signaling. Furthermore, demonstrating the usefulness of this line to report FGF10/FGFR2b signaling, the fluorescence intensity of the ETV5-RFP decreased over time in experimental lungs, while that of the controls remained constant. This finding is supported by RT-qPCR results after 48 h, which show a decrease in the expression of *RFP, Etv4,* and *Etv5* in experimental lungs compared to controls (**Figure 6C**).

These results not only confirm that soluble FGFR2b can be used to inhibit FGF10 signaling in *Etv5*$^{CreERT2-RFP}$ lung explants, but they also suggest that the *Etv5*$^{CreERT2-RFP}$ line responds to FGF10/FGFR2b signaling in the developing lung.

CONCLUSION

In conclusion, the *Tg(Etv4-GFP)* and *Etv5*^{RFP} reporter mouse lines appear to be promising tools to monitor FGF10/FGFR2b signaling in early lung development. These tools will have to be further validated at later stages and in other organs of interest.

ETHICS STATEMENT

Animal experiments, harvesting organs and tissues from wild type and mutant mice following euthanasia using pentobarbital was approved at Justus Liebig University Giessen by the federal authorities for animal research of the Regierungspraesidium Giessen, Hessen, Germany (Approved Protocol GI 20/10 Nr. G 84/2016).

AUTHOR CONTRIBUTIONS

SB, CC, C-MC, BS, and FH concept and design. MJ, AL, SD, and AS acquisition of data. MJ, SB, C-MC, and SD analysis and interpretation. MJ and SB drafting and editing of the manuscript. All authors read and approved the final manuscript.

FUNDING

SB was supported by grants from the Deutsche Forschungsgemeinschaft [DFG; BE4443/1-1, BE4443/4-1, BE4443/6-1, KFO309 P7 and SFB1213-projects A02 and A04, EXC2026 (Project ID 390649896)], Landes-Offensive zur Entwicklung Wissenschaftlich-Ökonomischer Exzellenz (LOEWE), UKGM, Universities of Giessen and Marburg Lung Center (UGMLC), DZL, and COST (BM1201). C–MC also acknowledges the support of the University Hospital Giessen and Marburg (UKGM) and the German Center for Lung Research (DZL). CC acknowledges the support of The National Nature Science Foundation of China (81570075, 81770074, 31471269, 81600062), Zhejiang Provincial Natural Science Foundation (LZ15H010001, LY18H010006), Zhejiang Provincial Science Technology Department Foundation (2015103253, 2018264229), the National Key Research and Development Program of China (2016YFC1304000), Wenzhou public welfare science and technology project (Y20180125), Scientific research incubation project of the First Affiliated Hospital of Wenzhou Medical University (FHY2015037).

ACKNOWLEDGMENTS

We acknowledge the precious help provided by Kerstin Goth and Jana Rostkovius in managing the mouse colonies and for the genotyping of the mice. We thank Dr. Jochen Wilhelm for the statistical interpretation of the generated data.

SUPPLEMENTARY MATERIAL

The Supplementary Material for this article can be found online at: https://www.frontiersin.org/articles/10.3389/fgene.2019.00178/full#supplementary-material

Supplementary Movie 1 | ETV4-GFP in the E12.5 developing lung for 24 h.

Supplementary Movie 2 | ETV5-RFP in the E12.5 developing lung for 24 h.

Supplementary Figure 1 | ETV4-GFP expression is stable for at least 38 h *in vitro* To monitor the expression pattern of ETV4-GFP in E12.5 lungs *in vitro*, lungs were cultured and live imaged in control medium **(a–d)**, with additional recombinant FGF7 **(e–h)**, or additional recombinant FGF10 **(i–l)** for 38 h. Scale bar: 125 μm.

REFERENCES

Bellusci, S., Furuta, Y., Rush, M. G., Henderson, R., Winnier, G., and Hogan, B. L. (1997a). Involvement of Sonic hedgehog (Shh) in mouse embryonic lung growth and morphogenesis. *Development* 124, 53–63.

Bellusci, S., Grindley, J., Emoto, H., Itoh, N., and Hogan, B. L. (1997b). Fibroblast growth factor 10 (FGF10) and branching morphogenesis in the embryonic mouse lung. *Development* 124, 4867–4878.

Chao, C. M., El Agha, E., Tiozzo, C., Minoo, P., and Bellusci, S. (2015). A breath of fresh air on the mesenchyme: impact of impaired mesenchymal

development on the pathogenesis of bronchopulmonary dysplasia. *Front. Med.* 2:27. doi: 10.3389/fmed.2015.00027

Danopoulos, S., Parsa, S., Al Alam, D., Tabatabai, R., Baptista, S., Tiozzo, C., et al. (2013). Transient Inhibition of FGFR2b-ligands signaling leads to irreversible loss of cellular beta-catenin organization and signaling in AER during mouse limb development. *PLoS ONE* 8:e76248. doi: 10.1371/journal.pone.0076248

De Moerlooze, L., Spencer-Dene, B., Revest, J. M., Hajihosseini, M., Rosewell, I., and Dickson, C. (2000). An important role for the IIIb isoform of fibroblast growth factor receptor 2 (FGFR2) in mesenchymal-epithelial signalling during mouse organogenesis. *Development* 127, 483–492. doi: 10.1042/cs099005P

El Agha, E., and Bellusci, S. (2014). Walking along the Fibroblast growth factor 10 route: a key pathway to understand the control and regulation of epithelial and mesenchymal cell-lineage formation during lung development and repair after injury. *Scientifica* 2014:538379. doi: 10.1155/2014/538379

Garg, A., Hannan, A., Wang, Q., Collins, T., Teng, S., Bansal, M., et al. (2018). FGF-induced Pea3 transcription factors program the genetic landscape for cell fate determination. *PLoS Genet.* 14:e1007660. doi: 10.1371/journal.pgen.1007660

Herriges, J. C., Verheyden, J. M., Zhang, Z., Sui, P., Zhang, Y., Anderson, M. J., et al. (2015). FGF-regulated ETV transcription factors control FGF-SHH feedback loop in lung branching. *Dev. Cell* 35, 322–332. doi: 10.1016/j.devcel.2015.10.006

Kuure, S., Chi, X., Lu, B., and Costantini, F. (2010). The transcription factors Etv4 and Etv5 mediate formation of the ureteric bud tip domain during kidney development. *Development* 137, 1975–1979. doi: 10.1242/dev.051656

Lamballe, F., Genestine, M., Caruso, N., Arce, V., Richelme, S., Helmbacher, F., et al. (2011). Pool-specific regulation of motor neuron survival by neurotrophic support. *J. Neurosci.* 31, 11144–11158. doi: 10.1523/JNEUROSCI.2198-11.2011

Mailleux, A. A., Tefft, D., Ndiaye, D., Itoh, N., Thiery, J. P., Warburton, D., et al. (2001). Evidence that SPROUTY2 functions as an inhibitor of mouse embryonic lung growth and morphogenesis. *Mech. Dev.* 102, 81–94. doi: 10.1016/S0925-4773(01)00286-6

Mao, J., McGlinn, E., Huang, P., Tabin, C. J., and McMahon, A. P. (2009). Fgf-dependent Etv4/5 activity is required for posterior restriction of Sonic Hedgehog and promoting outgrowth of the vertebrate limb. *Dev. Cell* 16, 600–606. doi: 10.1016/j.devcel.2009.02.005

Parsa, S., Kuremoto, K., Seidel, K., Tabatabai, R., Mackenzie, B., Yamaza, T., et al. (2010). Signaling by FGFR2b controls the regenerative capacity of adult mouse incisors. *Development* 137, 3743–3752. doi: 10.1242/dev.051672

Parsa, S., Ramasamy, S. K., De Langhe, S., Gupte, V. V., Haigh, J. J., Medina, D., et al. (2008). Terminal end bud maintenance in mammary gland is dependent upon FGFR2b signaling. *Dev. Biol.* 317, 121–131. doi: 10.1016/j.ydbio.2008.02.014

Sakaue, H., Konishi, M., Ogawa, W., Asaki, T., Mori, T., Yamasaki, M., et al. (2002). Requirement of fibroblast growth factor 10 in development of white adipose tissue. *Genes Dev.* 16, 908–912. doi: 10.1101/gad.983202

Sekine, K., Ohuchi, H., Fujiwara, M., Yamasaki, M., Yoshizawa, T., Sato, T., et al. (1999). Fgf10 is essential for limb and lung formation. *Nat. Genet.* 21, 138–141. doi: 10.1038/5096

Sharrocks, A. D., Brown, A. L., Ling, Y., and Yates, P. R. (1997). The ETS-domain transcription factor family. *Int. J. Biochem. Cell Biol.* 29, 1371–1387. doi: 10.1016/S1357-2725(97)00086-1

Yin, Y., Wang, F., and Ornitz, D. M. (2011). Mesothelial- and epithelial-derived FGF9 have distinct functions in the regulation of lung development. *Development* 138, 3169–3177. doi: 10.1242/dev.065110

Zhang, Z., Newton, K., Kummerfeld, S. K., Webster, J., Kirkpatrick, D. S., Phu, L., et al. (2017). Transcription factor Etv5 is essential for the maintenance of alveolar type II cells. *Proc. Natl. Acad. Sci. U.S.A.* 114, 3903–3908. doi: 10.1073/pnas.1621177114

Zhang, Z., Verheyden, J. M., Hassell, J. A., and Sun, X. (2009). FGF-regulated Etv genes are essential for repressing Shh expression in mouse limb buds. *Dev. Cell* 16, 607–613. doi: 10.1016/j.devcel.2009.02.008

Znosko, W. A., Yu, S., Thomas, K., Molina, G. A., Li, C., Tsang, W., et al. (2010). Overlapping functions of Pea3 ETS transcription factors in FGF signaling during zebrafish development. *Dev. Biol.* 342, 11–25. doi: 10.1016/j.ydbio.2010.03.011

Conflict of Interest Statement: The authors declare that the research was conducted in the absence of any commercial or financial relationships that could be construed as a potential conflict of interest.

Copyright © 2019 Jones, Lingampally, Dilai, Shrestha, Stripp, Helmbacher, Chen, Chao and Bellusci. This is an open-access article distributed under the terms of the Creative Commons Attribution License (CC BY). The use, distribution or reproduction in other forums is permitted, provided the original author(s) and the copyright owner(s) are credited and that the original publication in this journal is cited, in accordance with accepted academic practice. No use, distribution or reproduction is permitted which does not comply with these terms.

frontiers in Genetics

ORIGINAL RESEARCH
published: 28 May 2019
doi: 10.3389/fgene.2019.00362

FGF Gradient Controls Boundary Position Between Proliferating and Differentiating Cells and Regulates Lacrimal Gland Growth Dynamics

*Suharika Thotakura, Liana Basova and Helen P. Makarenkova**

Department of Molecular Medicine, The Scripps Research Institute, San Diego, CA, United States

Fibroblast growth factor (FGF) signaling plays an important role in controlling cell proliferation, survival, and cell movements during branching morphogenesis of many organs. In mammals branching morphogenesis is primarily regulated by members of the FGF7-subfamily (FGF7 and FGF10), which are expressed in the mesenchyme, and signal to the epithelial cells through the "b" isoform of fibroblast growth factor receptor-2 (FGFR2). Our previous work demonstrated that FGF7 and FGF10 form different gradients in the extracellular matrix (ECM) and induce distinct cellular responses and gene expression profiles in the lacrimal and submandibular glands. The last finding was the most surprising since both FGF7 and FGF10 bind signal most strongly through the same fibroblast growth factor receptor-2b isoform (FGFR2b). Here we revisit this question to gain an explanation of how the different FGFs regulate gene expression. For this purpose, we employed our *ex vivo* epithelial explant migration assay in which isolated epithelial explants are grown near the FGF loaded beads. We demonstrate that the graded distribution of FGF induces activation of ERK1/2 MAP kinases that define the position of the boundary between proliferating "bud" and differentiating "stalk" cells of growing lacrimal gland epithelium. Moreover, we showed that gene expression profiles of the epithelial explants exposed to distinct FGFs strictly depend on the ratio between "bud" and "stalk" area. Our data also suggests that differentiation of "stalk" and "bud" regions within the epithelial explants is necessary for directional and persistent epithelial migration. Gaining a better understanding of FGF functions is important for development of new approaches to enhance tissue regeneration.

Keywords: FGF gradient, lacrimal gland, lung, ERK1/2, boundary position

OPEN ACCESS

Edited by:
Mohammad K. Hajihosseini, University of East Anglia, United Kingdom

Reviewed by:
Denise Al Alam, University of Southern California, United States
Lawrence S. Prince, University of California, San Diego, United States

***Correspondence:**
Helen P. Makarenkova
hmakarenkl@scripps.edu

Specialty section:
This article was submitted to Stem Cell Research, a section of the journal Frontiers in Genetics

Received: *13 November 2018*
Accepted: *04 April 2019*
Published: *28 May 2019*

Citation:
Thotakura S, Basova L and Makarenkova HP (2019) FGF Gradient Controls Boundary Position Between Proliferating and Differentiating Cells and Regulates Lacrimal Gland Growth Dynamics. Front. Genet. 10:362. doi: 10.3389/fgene.2019.00362

INTRODUCTION

The lacrimal glands (LGs), salivary glands (SGs), and lungs are classic examples of organs that develop through branching morphogenesis, an important mechanism employed during formation of many organs. Branching morphogenesis is primarily regulated by members of the fibroblast growth factor-7 subfamily (FGF7-subfamily) FGF10 and FGF7, which are expressed in the

mesenchyme and bind the "b" isoform of fibroblast growth factor receptor-2 (FGFR2), located in the epithelial cells. In particular FGF10 was found necessary for lacrimal and Harderian gland development (Govindarajan et al., 2000; Makarenkova et al., 2000), branching of the submandibular gland (SMG) (Jaskoll et al., 2005; Steinberg et al., 2005), lungs (Wang et al., 2018), and development of other organs (Ohuchi et al., 2000; Zhang et al., 2006; Parsa et al., 2008). Moreover, several studies have identified mutations in FGF10 in people with aplasia of the lacrimal and salivary glands (ALSG) and in lacrimo-auriculo-dento-digital (LADD) syndrome (Milunsky et al., 2006; Rohmann et al., 2006; Shams et al., 2007). These studies support an idea that FGF10 signaling through FGFR2b is a common mechanism that regulate branching morphogenesis in the mouse and man.

Although FGF7 and 10 bind to FGFR2b with a similar high affinity (Igarashi et al., 1998), they elicit a distinct impact on branching morphogenesis (Steinberg et al., 2005; Makarenkova et al., 2009). Moreover, *Fgf10-null* mice die at birth and show a lack of limbs, lungs, LG, mammary and salivary gland development, whereas *Fgf7-null* mice are viable, and have a relatively normal development within all branched organs. FGF signaling also requires binding of the growth factor to heparin sulfate HS (Forsberg and Kjellen, 2001). It has been shown that FGF10-mediated induction and outgrowth of the lacrimal gland bud happens through localized activation of the *Ndst-Fgfr-Shp2* signaling cascade and requires specific modification of heparan sulfate proteoglycan (HSPG) by Ndst genes (Pan et al., 2008; Qu et al., 2011).

Our previous work suggests that differences in the binding of FGF7 and FGF10 to HSPG within the extracellular matrix (ECM) result in the formation of different gradients that dictate distinct functional activities of these FGFs during branching morphogenesis (Makarenkova et al., 2009). Whereas FGF7 forms a shallow gradient and induces branching of epithelial buds, FGF10 forms a much sharper gradient, and induces bud elongation. Replacement of a single residue in the heparin sulfate-binding site of FGF10 with the corresponding residue of FGF7 resulted in a mutant FGF10 that acted as a functional mimic of FGF7 with respect to gradient formation and regulation of cellular responses (Makarenkova et al., 2009). This study connects the structural differences of FGFs with their biological function in LG and SMG morphogenesis. We also demonstrated that monomeric FGF ligands exhibit reduced HSPG binding ability, resulting in their increased HSPG-dependent diffusion, and demonstrating that homodimerization not only changes FGF/receptor binding but also regulates FGF concentration gradients in the ECM (Kalinina et al., 2009). In addition, distinct FGF signaling may induce expression of specific signaling molecules that can also cooperate with or hinder FGF signaling, thus adding an additional level of precision to FGF-mediated morphogenesis. Stimulation of epithelial explants expressing the same FGFR2b with distinct FGF ligands generated not only specific cellular responses but also distinct gene expression. This phenomenon could not be explained by different levels of FGFRb activation and remains still largely unknown.

In this study, we demonstrate that differentiation of stalk and bud regions is necessary for directional and persistent explant migration. We also show that the graded distribution of FGFs within the heparin sulfate rich ECM defines the position of the boundary between proliferating and differentiating cells within the explant. Thus, the distal "bud" region (area close to FGF signals) shows mitogen activated protein kinase (MAPK) ERK1/2 activation, has high level of cell proliferation and expresses genes specific for undifferentiated and proliferating cells, whereas the proximal "stalk" region (area further away from FGF signals) has low level or no ERK1/2 activation, low numbers of proliferating cells, and expresses genes specific for cell differentiation. Thus, differential gene expression in the LG or SMG explants after exposure to different FGFs could be explained by relative contribution ratio of "bud" or "stalk" regions within the explant.

MATERIALS AND METHODS

Mice

All experiments described herein were performed in accordance with the Association for Research in Vision and Ophthalmology (ARVO) statement for the Use of Animals in Ophthalmic and Vision Research and were approved by the Scripps Research Institute Animal Care and Use Committee. Wild-type C57BL/6 timed-pregnant females were euthanized and embryos were harvested between E12 and E15.5.

Lung Explant Cultures

Embryos have been harvested at E12.5 from timed-pregnant C57BL/6 wild-type mice. Isolated lung primordia were cut into lobes using tungsten needles. Lobes of approximately similar size were collected and each lobe was placed on a 0.8-μm Millipore membrane (Millipore, Billerica, MA, United States), supported by a metal grid, and cultured in an air-fluid interface in defined medium. The defined medium was prepared, as follows: Fitton-Jackson modified BGJb medium was supplemented with 0.1% Albumax I (11020-021: Thermo Fisher Scientific), insulin-transferrin-selenium (1300-044: Thermo Fisher scientific), human transferrin (4 mg/10 ml) (10652202001: Sigma-Aldrich), non-essential amino acids (11140050: Thermo Fisher Scientific), Glutamax (35050061: Thermo Fisher Scientific), L-Ascorbic (0.5 mM, 72132: StemCell Technologies), and antibiotic-antimycotic (15240062: Thermo Fisher Scientific). Lungs were cultured in an air-fluid interface. The cultures were maintained in 100% humidity, with an atmosphere of 95% air and 5% CO_2 for 2–4 days. The medium was changed daily.

To prepare FGF-loaded beads, heparin acrylic beads (Makarenkova et al., 2009) were washed in PBS and incubated with 4 nM of FGF protein or BSA (control) for 4 h. Incubated beads were washed 3X in PBS, and each bead was implanted into the center area of lung explant. After 30 h of incubation, explants were photographed using a SPOT digital camera and a Leica microscope. The images were imported into Canvas

X (ACD Systems, British Columbia, Canada). The dilated area within each explant was outlined and measured using ImageJ software (Image Processing and Analysis in Java). All experiments were repeated four times. The measurements of the dilated areas induced by FGF were averaged and data was processed for statistical analysis using the Student's *t* test. Results were determined to be significant if P was <0.05.

Epithelial Explant Cultures and an *in vitro* Epithelial Bud Extension Essay

Lacrimal gland and lung epithelium was isolated and an *in vitro* epithelial bud extension assay was performed as previously described (Makarenkova et al., 2000; Weaver et al., 2000). Briefly, single lacrimal (E15.5) and lung (E12.0–E12.5) epithelial buds were separated from the surrounding mesenchyme and placed inside of a drop of BD Matrix Growth Factor Reduced Matrigel (356230: BD Biosciences). Heparin acrylic beads were loaded with equimolar concentration (1.5 nM) of recombinant human FGF3 (1206-F3-025/CF: R&D), FGF7 (251-KG/CF: R&D), or FGF10 (345-FG/CF: R&D) and the bead was placed at approximately 100 μm from the distal tip of the epithelial bud.

The bud migration was monitored at each time point by measuring the distance between the bud tips and the FGF-loaded beads. To study gene expression specifically in "bud" and "stalk" regions of the explant, explants were grown in matrigel near FGF10-loaded beads for 30 h. The matrigel was removed using BD Cell Recovery Solution (354253: BD Bioscience) and "bud" (approximately 1/4–1/3 of distal part of explant close to the bead) and "stalk" (the proximal 2/3 of explant) areas were separated mechanically using tungsten needles. "Buds" and "stalks" were collected into separate Eppendorf tubes and processed for qRT PCR as described previously (Makarenkova et al., 2009).

Real-Time RT-PCR Array

RNA from separated "buds" and "stalks" was prepared using TRizol and the Ambion DNA-free kit (AM1906, Thermo Fisher Scientific) and reverse transcribed with RT2 First Strand Kit (Qiagen) and processed for qRT PCR as described previously (Basova et al., 2017). Primers to *Map2k6* (NM_011943, PPM03568C), *Col1a1* (NM_007742, PPM03845F), *Mef2c* (QT02520560), *Egfr* (NM_007912, PPM03714F), *Mapk11* (NM_011161, PPM04540B), *Ccnd1* (NM_007631, PPM02903F), *Myc* (NM_001177352, PPM02924F), *Ccnb1* (NM_172301, PPM02894F), and *Cdk2* (NM_016756, PPM02902F) as well as RT^2 SYBR Green qPCR Mastermix were purchased from Qiagen. Amplification of target genes was performed in triplicate with an ABI 7300 real-time PCR system (Life Technologies, Grand Island, NY, United States). Results of the triplicate experiments were averaged. Data analysis was based on the dCt method (Yuan et al., 2008) and normalized to ubiquitin-like 4 housekeeping gene (*Ubl4*) (NM_145405, PPM25042A), using online normalization and analysis tools (provided in the public domain[1]).

[1]https://www.qiagen.com/us/shop/genes-and-pathways/data-analysis-center-overview-page/?akamai-feo=off

BrdU Labeling and Detection

Labeling and detection of LG proliferating cells was performed with a BrdU Labeling and Detection Kit (11444611001: Sigma-Aldrich) combined with a Mouse on Mouse (M.O.M.^{TM}) Blocking Reagent according to manufacturer protocol (Makarenkova et al., 2009). Explants were cultured for 24 h and incubated with 10 μM BrdU for 1.5 h. Cultures were then washed with warm medium and PBS then fixed in 50 mM glycine pH 2.0 in 70% ethanol, for 15–20 min at −20°C. Explants were stained with anti-BrdU antibody for 2 h and the secondary antibody for 1 h at 37°C.

Quantification of BrdU labeled cells was performed manually under the Leica microscope equipped with a calibrated scale. Quantification of proliferating cells was performed in three regions, "bud" (adjacent to bead), "distal stalk" (stalk region adjacent to the bud), and "proximal stalk" regions (the most proximal area of stalk). The number of proliferating cells were normalized per number of nuclei (number of cells/100 nuclei).

Alternatively, an anti-mouse-Rhodamine red secondary antibody was used to detect proliferating cells, images were obtained using a Zeiss LSM 780 confocal laser scanning microscope. Quantification of labeled cells was performed using ImageJ software.

Cell Culture

The human salivary epithelial A253 cell line was maintained in DMEM, containing 5% serum and Glutamax in six well dishes. Two days prior the FGF treatment cells, grown to 60% confluence, were washed with PBS and the medium was gradually replaced with DMEM containing 1,5, 0.5, 0.1, and 0.05% serum within 12 h. One hour prior to experimentation the culture medium containing 0.05% of serum was replaced with a serum-free medium. FGFs were applied for 5 min in serum free medium and medium containing FGF was replaced with a fresh serum free medium. Cellular extracts were prepared 5, 10, 15, 30, 60, and 120 min after FGF treatment using standard procedures.

Western Blotting

For Western blotting, 10 g of total protein was used per lane. Lysates were loaded onto 4–12% SDS-polyacrylamide gel and electrophoresis was performed according to the procedure of Laemmli (1970). After electrophoresis, the separated proteins were transferred to a nitrocellulose membrane and the membrane was blocked with 5-powdered milk in TBST (tris–buffered saline pH 7.4 and 0.05% Tween-20). Primary rabbit monoclonal antibody against phospho-ERK1/2 at the Thr202/Tyr204 positions (137F5, Cell Signaling) was used to detect MAPK activation. Total ERK1/2 antibody (M5670: Sigma-Aldrich) was blotted for loading controls. The appropriate secondary horseradish peroxidase-conjugated antibodies (Jackson Immuno Research Lab) were used for immunodetection. Detection of peroxidase was performed using the ECL-detection system and radiographic film. After film development, quantification of signal intensities of the bands in the Western blots was carried out using ImageJ software.

Western Blot Analysis in Separated Buds and Stalks

Lacrimal gland explants were isolated from two litters of embryos and grown near the FGF10-loaded beads for 30–36 h. At the end of this period "buds" and "stalks" were separated with tungsten needles and collected into separate 500 μl Eppendorf LoBind microcentrifuge tubes (022431064 : Eppendorff). Tissue was then homogenized in an appropriate volume of 1× NuPAGE LDS Sample Buffer (NP0007; Thermo Fisher Scientific) supplemented with proteases and phosphatase inhibitors. Lysates were heat-denatured for 5 min at 90°C and loaded on a 10% Bis-Tris polyacrylamide gel (Bio-Rad). After electrophoresis proteins were transferred to an Immun-Blot PVDF Membrane (1620177: Bio-Rad). Membranes were blocked for 1 h in 5% non-fat dry milk (BioRad) dissolved in TBST. After blocking, membranes were probed overnight at 4°C with the phospho-ERK1/2 antibody (see above) and the appropriate peroxidase-conjugated secondary antibodies (see above). After washing with TBST, antibody detection was performed with SuperSignal West Femto Maximum Sensitivity substrate (34095: Thermo Fisher Scientific). The same membrane was re-probed with total ERK1/2 antibody.

ERK1/2 Inhibition

The ERK inhibitor (FR180204) (Ohori et al., 2005) was purchased from Tocris (3706: Tocris), dissolved in dimethyl sulfoxide, and aliquots of the stock solution were stored at -80°C. FR180204 inhibitor was used at 10 μM, a concentration previously determined to provide optimal selective inhibition for ERK relative to off target kinases. Briefly, epithelial explants at the single bud stage (E15.5) were isolated from approximately 20–24 embryos and placed near the bead soaked with FGF10. Four hours later ERK1/2 inhibitor or DMSO (vehicle control) were added to the culture medium and explants were analyzed 30 h later.

Inhibition of Integrin-β1

Lacrimal gland epithelial explants isolated from the E15.5 mouse embryos were pre-treated with the function-blocking anti-mouse Integrin β1 (ITGB1) antibody [LEAF^{TM} purified anti-mouse CD29 Armenian hamster IgG (clone HMB1-1, Biolegend)] or control non-specific IgG for 15 min and were placed near the FGF3 soaked bead. Culture medium containing the ITGB1 antibody or control IgG at 10 μg/ml concentration was added to the explants and they were cultured for 48 h.

Statistical Analysis and Data Presentation

Statistical analyses were performed using Prism Software (GraphPad, San Diego, CA, United States). In bar graphs, data is presented as means ± SD of replicates from a representative experiment or of the normalized data from several experiments. In the latter case, mean fold changes were calculated by first determining the ratio of the test conditions over the appropriate control conditions for each individual measurement and then averaging these ratios. The Anderson-Darling normality test was performed prior to further data analyses. The unpaired two-tailed Student's *t*-test was used to determine significance ($P < 0.05$) in the differences between data sets.

RESULTS

FGF3, FGF7, and FGF10 Diffuse Differently in Embryonic Lung Organ Cultures

We previously demonstrated that labeled FGF7 and 10 differentially diffuse through the ECM and form distinct gradients: FGF10 forms a short and sharp gradient and FGF7 forms a long and shallow gradient (Makarenkova et al., 2009). To visualize the FGF gradient in the explant system *ex vivo*, we used an embryonic lung explant culture system. FGF application to the embryonic lung induced cyst-like enlargement of lung epithelium (lung airway dilation) (Park et al., 1998; Warburton et al., 2000; Jesudason et al., 2005; Kalinina et al., 2009). Heparin acrylic beads were loaded with the FGF3, 7 or 10, and each bead containing one of the FGFs or BSA (control) was implanted into the lung tissue (see section "Materials and Methods"). We compared the areas of dilation in the whole-lung explants after the implantation of heparin acrylic beads containing BSA (control), FGF3, 7, or 10 recombinant proteins (**Figures 1A,B**). As expected, the FGF3 and FGF10, that require the 6-O-Sulfation for their binding and promotion their mitogenic activity (Ye et al., 2001; Qu et al., 2011), were strongly bound to highly sulfated ECM and formed a "short and steep" gradient and therefore induced lung explant dilation only at a short distance from the bead. Whereas FGF7, which has highest affinity to undersulfated octasaccharides HS (Thacker et al., 2014) diffused at longer distances from the bead and induced dilation throughout the whole lung explant (**Figures 1A,B**). No lung dilation was observed around the BSA bead (**Figure 1A**).

FGF Gradient Determines the Position of Boundaries Between Proliferating and Differentiating Cells

First, we studied the effect of different FGFs on growth/migration of lung epithelial explants. Lung epithelial explants were isolated as it was described previously (Weaver et al., 2000) and placed near the FGF3, FGF10 or FGF7-loaded bead. Similar to the LG, lung explants exposed to FGF10 (Makarenkova et al., 2009), migrated towards the bead and had a distinct bud/stalk morphology (**Figure 1C**), FGF3 induced no bud formation, while explants exposed to FGF7 grow extensively and formed a single large bud (with no stalk formed) (**Figure 1C** and **Supplementary Figures S1A,B**).

The LG epithelial explants (distal part of the LG epithelial tissue) exposed to FGF3 formed very small buds or no buds at all (**Figure 1D**). As previously reported (Weaver et al., 2000; Dean et al., 2004; Steinberg et al., 2005), explants exposed to FGF10 developed a well-defined distal ("bud") and proximal ("stalk") morphology and migrated towards the FGF10-loaded beads (**Figure 1D**), whereas exposure

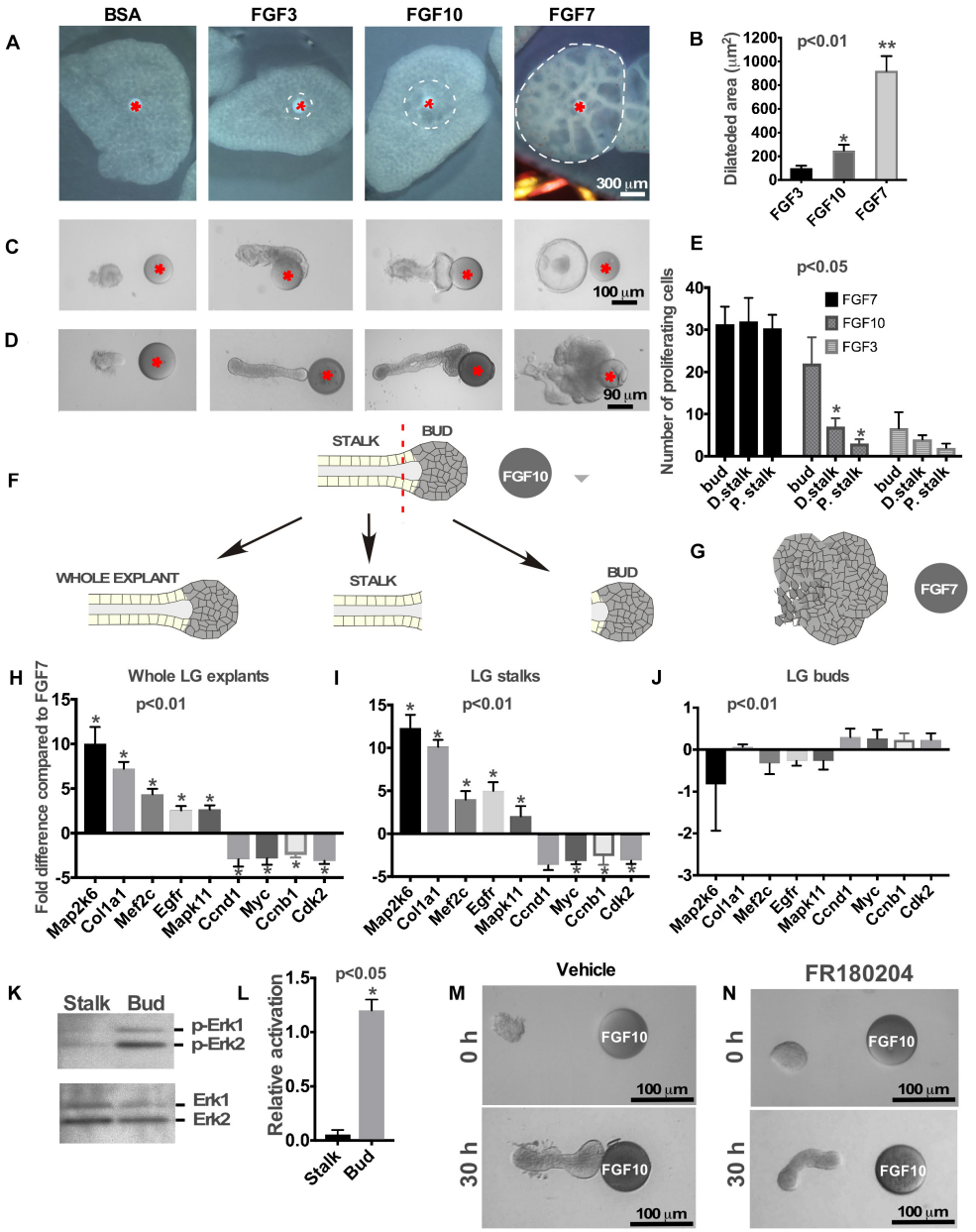

FIGURE 1 | Effects of FGFs on LG and lung explants. **(A)** Different FGFs induce different lung airway dilation. Heparin sulfate beads were loaded with different FGFs or BSA (control) and implanted into the central part of each lung explant (isolated from mouse embryos at E12.5). FGF3 forms a much sharper gradient than FGF10 and induces lung dilation at a shorter distance from the bead, while FGF7 diffuses more freely inducing dilation within a large lung area. **(B)** Graphical representation of lung dilation shown in **(A)** $p < 0.01$, $n = 10$. **(C,D)** Different FGFs induce different morphology of lung **(C)** and LG **(D)** epithelial explants. Lung and LG epithelial explants exposed to FGF10 migrate towards the bead and have defined "bud" and "stalk" morphology, while FGF3 have a well-formed "stalk" but almost no "bud." Both LG and lung explants exposed to FGF7 show extensive growth and formation of enlarged buds but not stalks (Beads are shown with red asterisk). **(E)** Quantification of BrdU labeling in different regions of the LG explants exposed to FGF3, 7, and 10 ligands. Explants exposed to FGF3 showed no significant increase in cell proliferation within the bud area, whereas explants exposed to FGF7 showed increase in cell proliferation throughout the whole explant. Application of the FGF10 induced cell proliferation only within the "bud" region. Quantification of proliferating cells was performed in four independent experiments (in 8–12 explants of each kind). "*" marks significant difference between "D. stalk," "P. stalk," and "bud" regions. **(F,G)** Schematic diagram of experimental design. LG explants were exposed to FGF10 **(F)** or FGF7 **(G)** for 30 h and processed for qRT PCR. "Buds" and "stalks" areas of some explants exposed to FGF10 were separated mechanically and processed for qRT PCR. **(H–J)** Gene expression levels were examined by real-time RT-PCR custom array focused on the proliferation and differentiation markers in whole LG explants **(H)**, stalks **(I)**, and buds **(J)** of explants exposed to FGF10 and the expression profiles of these groups of genes were compared to that of FGF7 [shown as a 0 (zero) line]. "*" marks significant difference in each gene expression compared to FGF7. **(K)** Extracellular signal-regulated kinases (ERK1/2) phosphorylation by FGF10 is significantly downregulated in "stalk" compared to "bud" areas of the LG epithelial explant. **(L)** Graphic representation of results ($n = 3$) shown in **(K)**. "*" marks significant difference in ERK1/2 phosphorylation between "stalk" and "bud" regions. **(M,N)** Selective inhibition of extracellular signal-regulated kinase ERK1/2 leads to lack of epithelial bud and decreased migration towards the FGF10 loaded bead.

to FGF7 induced extensive growth with almost no stalk region formed (**Figure 1D**). These experiments show that morphological changes induced by certain FGF are identical for lungs, LGs and SMGs.

We previously showed that distinct distal "bud" structure (the part of the explant close to the bead that is exposed to high concentration of FGF) correlates with high levels of cell proliferation (Makarenkova et al., 2009). We performed BrdU labeling on the explants exposed to different FGF (FGF3, FGF7, and FGF10) ligands and counted proliferating cells in three different locations along the explant: within the area close to the bead ("bud"), middle part of the explant ("distal stalk"), and proximal part of the explant ("proximal stalk"). Analysis of cell proliferation showed that FGF7 induced cell proliferation throughout the explant (**Figure 1E** and **Supplementary Figures S2A–D,I**) with no significant differences between "bud" and "distal stalk" and "proximal stalk" parts of the explant. FGF10 induced high level of cell proliferation only within the "bud" area (**Figure 1E** and **Supplementary Figures S2E–I**), in contrast, FGF3 exposed explants that have not formed distinguishable end buds demonstrated no significant differences in cell proliferation in designated regions (**Figure 1E**). Thus, differential HSPG affinity influences the shape of FGF3, FGF7, and FGF10 gradients to determine the areas of proliferating and differentiating cells. We previously reported that exposure of LG and SMG explants to FGF7 and FGF10 induces differential gene expression within the explant (Makarenkova et al., 2009). This was an unexpected finding since both FGF10 and FGF7 bind to the same receptor with the similar affinity. We hypothesized that difference in gene expression could be explained by differential access of FGF7 and FGF10 to the proximal and distal regions of the explant rather than by the induction of different signaling pathways. The more freely diffusing FGF7 signals to all parts of the epithelial explant (distal and proximal), while FGF10 signals can reach only distal (closest to the bead) parts of the explant. To test this hypothesis, we isolated LG epithelial explants from two litters of embryos at E15.5 and grew them for 30 h in near FGF7 or FGF10-loaded beads (**Figures 1F,G**). At the end of the culture period explants exposed to FGF10 were removed from the gel and the adjacent to bead "bud" area (approximately 1/4–1/3 of distal part of explant) and distal to bead "stalk" (the proximal part of explant) regions of the grown explant were separated mechanically using tungsten needles (**Figure 1F**). These separated "buds" and "stalks" were processed for RNA isolation and qRT PCR using markers of cell proliferation (*Ccnd1, Myc, Ccnb1,* and *Cdk2)* and differentiation (*Map2k6, Col1a1, Mef2c, Egfr,* and *Mapk11*) (Makarenkova et al., 2009). Expression of these genes in "buds" and "stalks" and whole explants exposed to FGF10 was compared to gene expression in whole LG explants exposed to FGF7 (**Figures 1H–J**). This data shows that the expression profile of genes in stalks and whole LG explants exposed to FGF10 was very similar to each other (**Figures 1H,I**). In contrast the expression profile of genes in "buds" was almost identical to the gene expression found in explants treated with FGF7 (**Figure 1J**).

ERK1/2 MAPK is the main mediator of FGF signaling in many biological processes (Brewer et al., 2016; Furusho et al., 2017; Sagomonyants et al., 2017; Chen et al., 2018). We studied whether the decrease of FGF-induced ERK1/2 activation is taking place after differentiation of stalk cells. Isolated epithelial explants were exposed to FGF10 loaded on the beads and the "buds" and "stalks" were separated and processed for western blotting using antibodies to phospho-ERK1/2 and total ERK1/2. As expected ERK1/2 was activated in the "bud" region whereas little or no activation was observed in the "stalk" region (**Figures 1K,L**). At the same time, total ERK1/2 was equally detected in both bud and stalk regions (**Figure 1K**). To test our hypothesis that FGF7 gradient induces ERK1/2 phosphorylation throughout the whole LG explant, we grew LG epithelial explants (obtained from 3 litters of mice at E15.5) near the FGF7 loaded bead for 30 h. At the end of the culture period explants were removed from the gel and were divided into three pieces by tungsten needles: distal (closest to the bead), middle (the part of explant between distal and proximal parts) and proximal the (the most distant from the bead part of explant) (**Supplementary Figure S3A**). Western blotting using phospho- and total ERK1/2 antibodies showed that exposure to FGF7 resulted in similar level of ERK1/2 phosphorylation in all parts of LG explant (**Supplementary Figure S3B**). However, we observed a slight decrease in ERK1/2 phosphorylation in the proximal part of the explant, suggesting that FGF7 can bind matrigel with low affinity, which decreases its diffusion toward the proximal parts of the explant.

This experiment suggests that, similar to other cells/tissues (Luongo et al., 2002; Chambard et al., 2007), downregulation of ERK1/2 phosphorylation is responsible for the initiation of cell differentiation within epithelial explants. Next, we checked whether ERK1/2 signaling is required for "bud" formation in the LG explants exposed to FGF10. In these experiments, epithelial explants were exposed to FGF10 loaded on the heparin acrylic beads, and treated with the ERK1/2 inhibitor or DMSO (vehicle control) added to the culture medium. We found that LG explants treated with vehicle formed well distinguished "bud" and "stalk" regions (**Figure 1M**) and reached the bead in 30 h. Whereas explants exposed to the ERK inhibitor elongated but did not have a distinguishable "bud" structure formed (**Figure 1N**). Moreover, growth of these explants ceased and they failed to reach the FGF10-loaded bead (**Figure 1N**). This suggests that ERK1/2 activation is necessary for bud formation and to sustain growth of the explant.

Taken together this data further suggests that graded distribution of FGFs within the ECM controls the position of the boundary between cell proliferation and differentiation.

LG Explants Exposed to Different FGFs Migrate With a Different Speed

We also monitored the speed of explant migration towards the FGF-loaded beads, measuring the distance between the tip of the explant and the bead at different time points (**Figure 2A**). We found that the LG explant exposed to an FGF3 migrates faster than the one exposed to FGF10 or FGF7. Thus, explants exposed to FGF3 reached the bead in less than 24 h, while explants exposed to FGF10 reached the bead in 30–36 h, whereas explants exposed to FGF7 just grew in size and reached the bead later than 48 h.

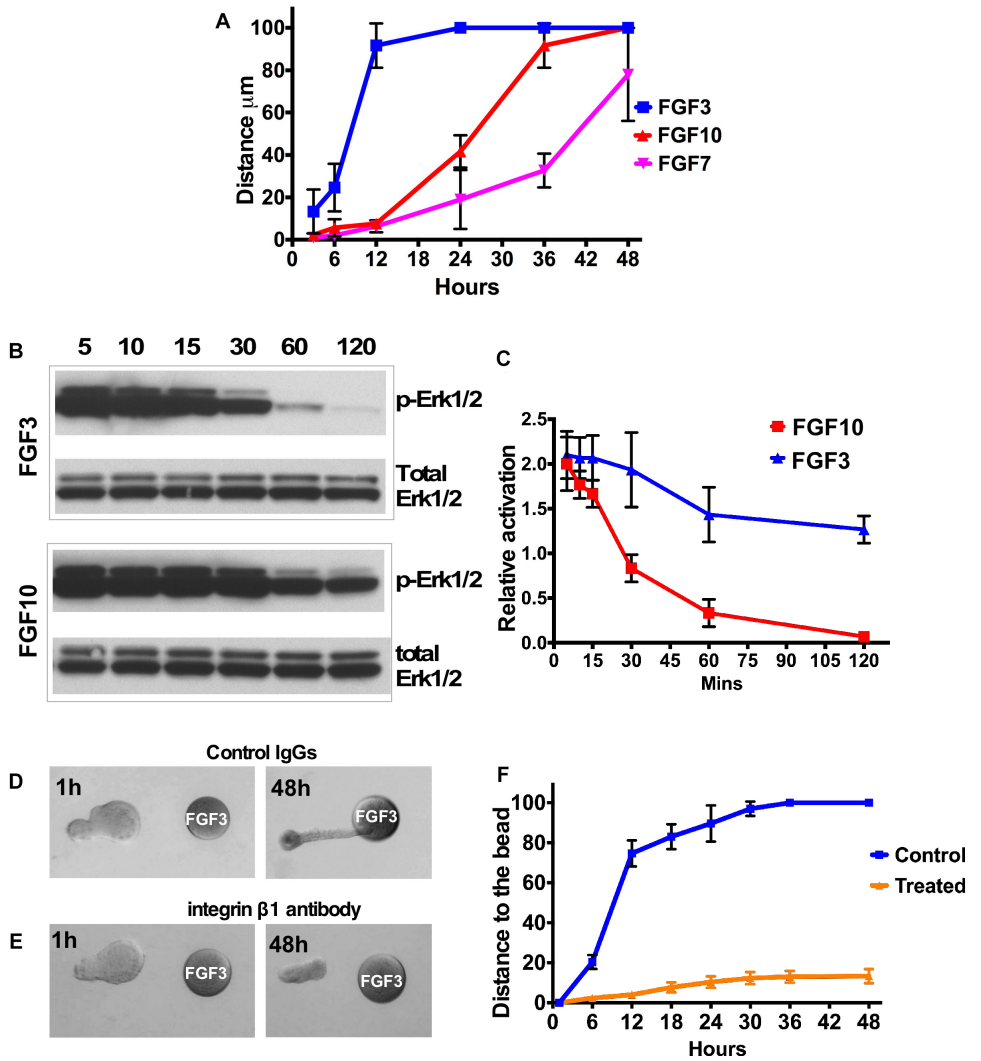

FIGURE 2 | FGF gradient controls explant migration and ERK1/2 activation. **(A)** Analysis of LG explant migration towards the FGF3, 7, and 10-soaked beads. Migration was estimated as the change of the distance between bead and the tip of the explant. **(B,C)** A253 cells were incubated with 1.5 nM FGF3 **(A)** or FGF10 **(B)**, and phospho-ERK1/2 was monitored by Western blots. Values were normalized to the amount of total protein (total ERK1/2). **(C)** The graphic representation of the result. $n = 3$; $P < 0.01$. FGF10 induces longer MAPK/ERK1/2 activation than FGF3 does. **(D–F)** Blocking integrin β1 decreases speed of epithelial explant migration toward the FGF3-loaded bead. LG epithelial explants grown near FGF3 beads were treated with Control IgG **(D)** or the blocking antibody against the integrin subunit β1 **(E)**. **(F)** Quantification of epithelial growth shown in **(D,E)**. Result represents 3 independent experiments (12 control and 13 treated buds), $p < 0.05$.

In addition, we grew epithelial explants for 96 h to test whether FGF gradient can maintain epithelial growth/migration. We found that distal parts of explants that reached the FGF3-loaded bead became slightly enlarged spreading onto the surface of the bead (**Supplementary Figures S4A,B**). At the same time the distal parts of epithelial explant that reached the bead loaded with FGF10 (**Supplementary Figures S4C,D**) or FGF7 (**Supplementary Figures S4E,F**) engulfed the bead. However, explants exposed to FGF7 were much larger and formed a cyst in the proximal part of the explant (**Supplementary Figures S4E,F**). The lack of complete bead engulfment by explants exposed to FGF3 could be possibly explained by the low number of cells that reach the bead or much faster degradation of FGF3 in culture medium.

FGF10 Induces Longer MAPK/ERK1/2 Activation Than FGF3

A key FGF downstream pathway is the RAS-MAPK/ERK1/2 cascade. Recent studies have demonstrated that not only the pathway but also the degree and duration of the activation of ERK1/2 may be critical (Walker et al., 1998; Bakin et al., 2003; Watson and Francavilla, 2018). Sustained ERK1/2 activation has been shown to be important for cell proliferation during branching morphogenesis (Gual et al., 2000; Omori et al., 2008),

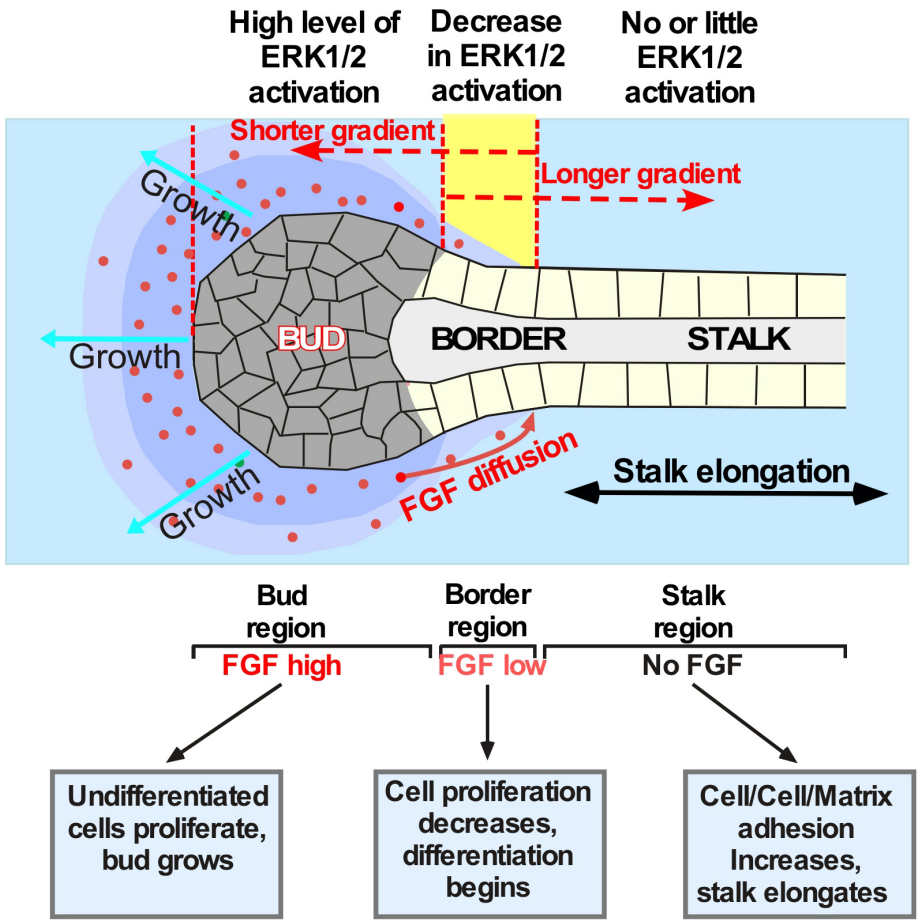

FIGURE 3 | Schematic showing establishment of the boundaries between proliferating and differentiating cells in the explants exposed to different FGF gradients. Application of different FGFs leads to establishment of different ratios between the "bud" and the "stalk" area size. For example, secreted FGF10 (red dots) diffuses through the ECM and binds to FGR2b expressed by epithelial cells. These events indices the ERK1/2 phosphorylation followed by a signaling cascade that keeps cells undifferentiated and proliferating. The undifferentiated proliferating cells form the "bud" structure. Bud cells express MMPs dissolving the ECM and helping the "bud" migration through the ECM. The boundary between proliferating and differentiating cells (shown in yellow) is formed within the area of lowest FGF concentration. Cells proximal to this region that are no longer exposed to FGF start to differentiate, become polarized and flattened, and anchor the ECM. This process induces "stalk" elongation that further promotes "bud" movement through the ECM towards the source of the FGF. If the FGF has low ECM binding and forms longer gradient (as the FGF7 does) no "stalk" region is formed and the migration of cells is largely non-directional. FGFs with a more restricted diffusion (as that of FGF10) induce formation of well-defined "bud" and "stalk" regions and induce directional migration of the epithelial cells. However, if FGF diffusion is highly restricted (as that of FGF3) the longer "stalk" and smaller "bud" regions are formed and faster migration through the ECM is observed.

while a high level of ERK1/2 activation is required for focal adhesion turnover and cell migration (Ishibe et al., 2003). We monitored ERK1/2 activation in A253 epithelial cells at different time points after FGF3 or FGF10 application (**Figures 2B,C**). We found that FGF3 induced a strong and fast activation of ERK1/2 that lasted for only 30 min while FGF10 induced sustained activation of ERK1/2, which was maintained for more than 2 h (**Figures 2B,C**).

Blocking Beta 1 Integrin Perturbs Epithelial Migration

Cell attachment to the ECM is known to influence a variety of cellular responses such as polarization, migration, and proliferation. Integrins, consisting of an α- and a β-subunit, are cell adhesion glycoprotein transmembrane receptors that play the central role in establishing the orientation of epithelial cell polarity and cell migration. We and others have demonstrated expression of several integrins (including integrin β-1) in the LG (Saarloos et al., 1999; Gierow et al., 2002; Andersson et al., 2006; Umazume et al., 2015). Moreover epithelial β1 integrin has important functions in branching morphogenesis and epithelial cell differentiation (Davies and Fisher, 2002; Zhang et al., 2009; Smeeton et al., 2010; Plosa et al., 2014; Yazlovitskaya et al., 2015). To test whether the ECM cell interactions are necessary for epithelial migration, isolated LG epithelial explants grown near FGF3 beads were treated with the blocking antibody against the integrin subunit β1 (see section "Materials and Methods") or control IgG. Explants treated with control IgG elongated and reached the bead in 24–30 h (**Figures 2D,F**), whereas explants

treated with blocking antibody elongated slightly but did not reach the bead (**Figures 2E,F**). These experiments demonstrated that function of integrin β1 is important for directional epithelial explant migration.

DISCUSSION

We have previously reported that FGF7 and FGF10 induce distinct morphology and gene expression in the LG and SMG epithelial explants. In this study, we demonstrate that FGFs induce phosphorylation of downstream mitogen-activated protein kinase (MAPK) ERK1 and 2 only within the range of FGF diffusion which induces cell proliferationłand restricts epithelial cells differentiation by keeping cells in an immature state.

The formation and maintenance of boundaries between neighboring zones within the growing LG bud is necessary for branching morphogenesis because cells within each zone have distinct functions (**Figure 3**). We showed that separated LG "stalk" and "bud" areas of the epithelial explant exposed to FGF10 have a distinct gene expression patterns and therefore different function in branching morphogenesis. Our data also establishes that the MAPK pathway is heterogeneously activated in "buds" and "stalks." Thus, the activation of ERK1/2 was observed only in the "bud" regions and not seen in the stalks in of explants exposed to FGF10. Profiling of mRNA expression for markers of proliferating or differentiating cells show that the "bud" area has a pattern of gene expression similar to that induced by FGF7 (with prevalent expression of proliferation markers), while in the "stalks" these markers were downregulated and differentiation markers were increased. Thus, FGF7 that diffuses to farther distances simply induces formation of larger buds than FGF10 and FGF3 that bind to the ECM more robustly. Our study suggests that different patterns of morphogenetic changes observed in the explants exposed to different FGFs is due to changes in the position of the boundary between proliferating and differentiating parts of the epithelial explant. The boundary position is determined by the decrease/loss of ERK1/2 activation between the "stalks" and "buds." Similar concept of boundaries between gene expression domains could be implied to different tissues and is central to many developmental processes (Cottrell et al., 2012; Caggiano et al., 2017; Neijts and Deschamps, 2017; Li et al., 2018). For example Sawada and coauthors (Sawada et al., 2001) showed that FGF/MAPK signaling is a crucial positional cue in somite boundary formation. They reported that the signaling gradient across the field is converted into gene expression domains by the concentration-specific response of target genes (Sawada et al., 2001). Thus, if signaling and gene expression boundaries change their positions or are defective, the downstream patterning event is correspondingly changed, or disrupted. This is in agreement with our previous work showing that changes in FGF10 gradient by any manipulation induces completely different morphogenetic events (Makarenkova et al., 2009).

Thus, LG epithelial cells exposed to FGF signals proliferate and form "buds" (**Figure 3**), that express MMPs (Tsau et al., 2011) dissolving ECM ahead of the "buds," whereas "stalk" cells that are not exposed to FGF signals differentiate and anchor to ECM, became polarized, and maintain stalk elongation and bud propagation. Our model (**Figure 3**) suggests that the FGF concentration gradient across the field is converted into specific gene expression pattern that regulate cellular responses. Moreover, the speed of explant migration/elongation is also controlled by the position of boundaries between proliferating and differentiating cells: the larger the bud the slower the explant migration.

Our study provides experimentally supported explanations on how FGFR stimulation with distinct ligands generates distinct gene expression and different cellular responses.

ETHICS STATEMENT

All experiments described herein were performed in accordance with the Association for Research in Vision and Ophthalmology (ARVO) Statement for the Use of Animals in Ophthalmic and Vision Research and were approved by the Scripps Research Institute Animal Care and Use Committee. Wild-type C57BL/6 timed-pregnant females were euthanized and embryos were harvested at E12 or E15.5.

AUTHOR CONTRIBUTIONS

HM conceived the project, prepared the study design and methodology, analyzed and interpreted the results, and wrote and finalized the manuscript. ST assisted in study design, performed the microsurgical tissue dissection and explant cultures preparation, performed gene and protein expressions and cell proliferation studies, analyzed and interpreted the results, and finalized the manuscript. LB assisted in study design, statistical analysis, interpretation of the results, and finalization of the manuscript.

FUNDING

This work was supported by National Institutes of Health, National Eye Institute Grants 1R01EY028983 and 1R01EY026202 (to HM).

SUPPLEMENTARY MATERIAL

The Supplementary Material for this article can be found online at: https://www.frontiersin.org/articles/10.3389/fgene.2019.00362/full#supplementary-material

FIGURE S1 | (A) Lung epithelial bud exposed to FGF7 for 30 h forms a dilated "bud," that increases its size several times after 72 h in culture. **(B)** This enlarged "bud" does not have a distinct stalk region. Bead are labeled with red asterisk.

FIGURE S2 | Cell proliferation in the epithelial explants treated with FGFs. Examples of cell proliferation pattern in the explants treated with FGF10 **(A–D)** and FGF7 **(E–H)**. Proliferation of cells only observed at the tip of the

bud in the explant exposed to FGF10 **(B)**, while proliferation of cells throughout whole explant is observed in the explant exposed to FGF7 **(F)**. Quantification of the proliferating cells exposed to different FGFs **(I)**. The scale bar is 50 μm. "*" labels significant changes in cell proliferation in "D. stalk" and "P. stalk" compared to "bud" region in the epithelial explant exposed to FGF10.

FIGURE S3 | ERK1/2 phosphorylation is induced by FGF7 throughout all areas of the LG epithelial explant. **(A)** Schematic representation of the experiment. Epithelial explants grown near the FGF7 bead for 30 h were divided into three pieces and processed for Western blotting using phospho ERK1/2 and total ERK1/2 antibodies. **(B)** Similar ERK1/2 phosphorylation is induced in all parts of epithelial explant exposed to FGF7.

FIGURE S4 | Effect of FGF gradient on explant migration after 96 h in culture. **(A,B)** The distal part of the explant exposed to FGF3 tends to spread out the bead surface after 96 h in culture, but never completely engulf the bead. **(C,D)** Examples of explants growth near the FGF10 loaded beads. FGF10 exposure induces complete engulfment of the FGF10-bead by the explant cells. **(E,F)** FGF7 forms shallow gradient and causes cyst formation but still induces distal explant tissue to engulf the FGF7 loaded bead.

REFERENCES

Andersson, S. V., Hamm-Alvarez, S. F., and Gierow, J. P. (2006). Integrin adhesion in regulation of lacrimal gland acinar cell secretion. *Exp. Eye Res.* 83, 543–553. doi: 10.1016/j.exer.2006.02.006

Bakin, R. E., Gioeli, D., Sikes, R. A., Bissonette, E. A., and Weber, M. J. (2003). Constitutive activation of the Ras/mitogen-activated protein kinase signaling pathway promotes androgen hypersensitivity in LNCaP prostate cancer cells. *Cancer Res.* 63, 1981–1989.

Basova, L. V., Tang, X., Umasume, T., Gromova, A., Zyrianova, T., Shmushkovich, T., et al. (2017). Manipulation of panx1 activity increases the engraftment of transplanted lacrimal gland epithelial progenitor cells. *Invest. Ophthalmol. Vis. Sci.* 58, 5654–5665. doi: 10.1167/iovs.17-22071

Brewer, J. R., Mazot, P., and Soriano, P. (2016). Genetic insights into the mechanisms of Fgf signaling. *Genes Dev.* 30, 751–771. doi: 10.1101/gad.277137.115

Caggiano, M. P., Yu, X., Bhatia, N., Larsson, A., Ram, H., Ohno, C. K., et al. (2017). Cell type boundaries organize plant development. *eLife* 6:e27421. doi: 10.7554/eLife.27421

Chambard, J. C., Lefloch, R., Pouyssegur, J., and Lenormand, P. (2007). ERK implication in cell cycle regulation. *Biochim. Biophys. Acta* 1773, 1299–1310. doi: 10.1016/j.bbamcr.2006.11.010

Chen, X. J., Chen, X., Wu, W. J., Zhou, Q., Gong, X. H., and Shi, B. M. (2018). Effects of FGF-23-mediated ERK/MAPK signaling pathway on parathyroid hormone secretion of parathyroid cells in rats with secondary hyperparathyroidism. *J. Cell Physiol.* 233, 7092–7102. doi: 10.1002/jcp.26525

Cottrell, D., Swain, P. S., and Tupper, P. F. (2012). Stochastic branching-diffusion models for gene expression. *Proc. Natl. Acad. Sci. U.S.A.* 109, 9699–9704. doi: 10.1073/pnas.1201103109

Davies, J. A., and Fisher, C. E. (2002). Genes and proteins in renal development. *Exp. Nephrol.* 10, 102–113. doi: 10.1159/000049905

Dean, C., Ito, M., Makarenkova, H. P., Faber, S. C., and Lang, R. A. (2004). Bmp7 regulates branching morphogenesis of the lacrimal gland by promoting mesenchymal proliferation and condensation. *Development* 131, 4155–4165. doi: 10.1242/dev.01285

Forsberg, E., and Kjellen, L. (2001). Heparan sulfate: lessons from knockout mice. *J. Clin. Invest.* 108, 175–180. doi: 10.1172/jci13561

Furusho, M., Ishii, A., and Bansal, R. (2017). Signaling by FGF receptor 2, not FGF receptor 1, regulates myelin thickness through activation of ERK1/2-MAPK, which promotes mTORC1 activity in an akt-independent manner. *J. Neurosci.* 37, 2931–2946. doi: 10.1523/JNEUROSCI.3316-16.2017

Gierow, J. P., Andersson, S., and Sjogren, E. C. (2002). Presence of alpha-and beta-integrin subunits in rabbit lacrimal gland acinar cells cultured on a laminin-rich matrix. *Adv. Exp. Med. Biol.* 506, 59–63. doi: 10.1007/978-1-4615-0717-8_7

Govindarajan, V., Ito, M., Makarenkova, H. P., Lang, R. A., and Overbeek, P. A. (2000). Endogenous and ectopic gland induction by FGF-10. *Dev. Biol.* 225, 188–200. doi: 10.1006/dbio.2000.9812

Gual, P., Giordano, S., Williams, T. A., Rocchi, S., Van Obberghen, E., and Comoglio, P. M. (2000). Sustained recruitment of phospholipase C-gamma to Gab1 is required for HGF-induced branching tubulogenesis. *Oncogene* 19, 1509–1518. doi: 10.1038/sj.onc.1203514

Igarashi, M., Finch, P. W., and Aaronson, S. A. (1998). Characterization of recombinant human fibroblast growth factor (FGF)-10 reveals functional similarities with keratinocyte growth factor (FGF-7). *J. Biol. Chem.* 273, 13230–13235. doi: 10.1074/jbc.273.21.13230

Ishibe, S., Joly, D., Zhu, X., and Cantley, L. G. (2003). Phosphorylation-dependent paxillin-ERK association mediates hepatocyte growth factor-stimulated epithelial morphogenesis. *Mol. Cell* 12, 1275–1285. doi: 10.1016/s1097-2765(03)00406-4

Jaskoll, T., Abichaker, G., Witcher, D., Sala, F. G., Bellusci, S., Hajihosseini, M. K., et al. (2005). FGF10/FGFR2b signaling plays essential roles during in vivo embryonic submandibular salivary gland morphogenesis. *BMC Dev. Biol.* 5:11.

Jesudason, E. C., Smith, N. P., Connell, M. G., Spiller, D. G., White, M. R., Fernig, D. G., et al. (2005). Developing rat lung has a sided pacemaker region for morphogenesis-related airway peristalsis. *Am. J. Respir. Cell Mol. Biol.* 32, 118–127. doi: 10.1165/rcmb.2004-0304oc

Kalinina, J., Byron, S. A., Makarenkova, H. P., Olsen, S. K., Eliseenkova, A. V., Larochelle, W. J., et al. (2009). Homodimerization controls the fibroblast growth factor 9 subfamily's receptor binding and heparan sulfate-dependent diffusion in the extracellular matrix. *Mol. Cell Biol.* 29, 4663–4678. doi: 10.1128/MCB.01780-08

Laemmli, U. K. (1970). Cleavage of structural proteins during the assembly of the head of bacteriophage T4. *Nature* 227, 680–685. doi: 10.1038/227680a0

Li, C., Zhang, L., and Nie, Q. (2018). Landscape reveals critical network structures for sharpening gene expression boundaries. *BMC Syst. Biol.* 12:67. doi: 10.1186/s12918-018-0595-5

Luongo, D., Mazzarella, G., Della, R. F., Maurano, F., and Rossi, M. (2002). Down-regulation of ERK1 and ERK2 activity during differentiation of the intestinal cell line HT-29. *Mol. Cell Biochem.* 231, 43–50.

Makarenkova, H. P., Hoffman, M. P., Beenken, A., Eliseenkova, A. V., Meech, R., Tsau, C., et al. (2009). Differential interactions of FGFs with heparan sulfate control gradient formation and branching morphogenesis. *Sci. Signal.* 2:ra55. doi: 10.1126/scisignal.2000304

Makarenkova, H. P., Ito, M., Govindarajan, V., Faber, S. C., Sun, L., Mcmahon, G., et al. (2000). FGF10 is an inducer and Pax6 a competence factor for lacrimal gland development. *Development* 127, 2563–2572.

Milunsky, J. M., Zhao, G., Maher, T. A., Colby, R., and Everman, D. B. (2006). LADD syndrome is caused by FGF10 mutations. *Clin. Genet.* 69, 349–354. doi: 10.1111/j.1399-0004.2006.00597.x

Neijts, R., and Deschamps, J. (2017). At the base of colinear Hox gene expression: cis-features and trans-factors orchestrating the initial phase of Hox cluster activation. *Dev. Biol.* 428, 293–299. doi: 10.1016/j.ydbio.2017.02.009

Ohori, M., Kinoshita, T., Okubo, M., Sato, K., Yamazaki, A., Arakawa, H., et al. (2005). Identification of a selective ERK inhibitor and structural determination of the inhibitor-ERK2 complex. *Biochem. Biophys. Res. Commun.* 336, 357–363. doi: 10.1016/j.bbrc.2005.08.082

Ohuchi, H., Hori, Y., Yamasaki, M., Harada, H., Sekine, K., Kato, S., et al. (2000). FGF10 acts as a major ligand for FGF receptor 2 IIIb in mouse multi-organ development. *Biochem. Biophys. Res. Commun.* 277, 643–649. doi: 10.1006/bbrc.2000.3721

Omori, S., Kitagawa, H., Koike, J., Fujita, H., Hida, M., Pringle, K. C., et al. (2008). Activated extracellular signal-regulated kinase correlates with cyst formation and transforming growth factor-beta expression in fetal obstructive uropathy. *Kidney Int.* 73, 1031–1037. doi: 10.1038/ki.2008.3

Pan, Y., Carbe, C., Powers, A., Zhang, E. E., Esko, J. D., Grobe, K., et al. (2008). Bud specific N-sulfation of heparan sulfate regulates Shp2-dependent FGF signaling during lacrimal gland induction. *Development* 135, 301–310. doi: 10.1242/dev.014829

Park, W. Y., Miranda, B., Lebeche, D., Hashimoto, G., and Cardoso, W. V. (1998). FGF-10 is a chemotactic factor for distal epithelial buds during lung development. *Dev. Biol.* 201, 125–134. doi: 10.1006/dbio.1998.8994

Parsa, S., Ramasamy, S. K., De Langhe, S., Gupte, V. V., Haigh, J. J., Medina, D., et al. (2008). Terminal end bud maintenance in mammary gland is dependent upon FGFR2b signaling. *Dev. Biol.* 317, 121–131. doi: 10.1016/j.ydbio.2008.02.014

Plosa, E. J., Young, L. R., Gulleman, P. M., Polosukhin, V. V., Zaynagetdinov, R., Benjamin, J. T., et al. (2014). Epithelial beta1 integrin is required for lung branching morphogenesis and alveolarization. *Development* 141, 4751–4762. doi: 10.1242/dev.117200

Qu, X., Carbe, C., Tao, C., Powers, A., Lawrence, R., Van Kuppevelt, T. H., et al. (2011). Lacrimal gland development and Fgf10-Fgfr2b signaling are controlled by 2-O- and 6-O-sulfated heparan sulfate. *J. Biol. Chem.* 286, 14435–14444. doi: 10.1074/jbc.M111.225003

Rohmann, E., Brunner, H. G., Kayserili, H., Uyguner, O., Nurnberg, G., Lew, E. D., et al. (2006). Mutations in different components of FGF signaling in LADD syndrome. *Nat. Genet.* 38, 414–417. doi: 10.1038/ng1757

Saarloos, M. N., Husa, M. R., Jackson, R. S. II, and Ubels, J. L. (1999). Intermediate filament, laminin and integrin expression in lacrimal gland acinar cells: comparison of an immortalized cell line to primary cells, and their response to retinoic acid. *Curr. Eye Res.* 19, 439–449. doi: 10.1076/ceyr.19.5.439.5287

Sagomonyants, K., Kalajzic, I., Maye, P., and Mina, M. (2017). FGF Signaling Prevents the Terminal Differentiation of Odontoblasts. *J. Dent. Res.* 96, 663–670. doi: 10.1177/0022034517691732

Sawada, A., Shinya, M., Jiang, Y. J., Kawakami, A., Kuroiwa, A., and Takeda, H. (2001). Fgf/MAPK signalling is a crucial positional cue in somite boundary formation. *Development* 128, 4873–4880.

Shams, I., Rohmann, E., Eswarakumar, V. P., Lew, E. D., Yuzawa, S., Wollnik, B., et al. (2007). Lacrimo-auriculo-dento-digital syndrome is caused by reduced activity of the fibroblast growth factor 10 (FGF10)-FGF receptor 2 signaling pathway. *Mol. Cell Biol.* 27, 6903–6912. doi: 10.1128/mcb.00544-07

Smeeton, J., Zhang, X., Bulus, N., Mernaugh, G., Lange, A., Karner, C. M., et al. (2010). Integrin-linked kinase regulates p38 MAPK-dependent cell cycle arrest in ureteric bud development. *Development* 137, 3233–3243. doi: 10.1242/dev.052845

Steinberg, Z., Myers, C., Heim, V. M., Lathrop, C. A., Rebustini, I. T., Stewart, J. S., et al. (2005). FGFR2b signaling regulates ex vivo submandibular gland epithelial cell proliferation and branching morphogenesis. *Development* 132, 1223–1234. doi: 10.1242/dev.01690

Thacker, B. E., Xu, D., Lawrence, R., and Esko, J. D. (2014). Heparan sulfate 3-O-sulfation: a rare modification in search of a function. *Matrix Biol.* 35, 60–72. doi: 10.1016/j.matbio.2013.12.001

Tsau, C., Ito, M., Gromova, A., Hoffman, M. P., Meech, R., and Makarenkova, H. P. (2011). Barx2 and Fgf10 regulate ocular glands branching morphogenesis by controlling extracellular matrix remodeling. *Development* 138, 3307–3317. doi: 10.1242/dev.066241

Umazume, T., Thomas, W. M., Campbell, S., Aluri, H., Thotakura, S., Zoukhri, D., et al. (2015). Lacrimal gland inflammation deregulates extracellular matrix remodeling and alters molecular signature of epithelial stem/progenitor cells. *Invest. Ophthalmol. Vis. Sci.* 56, 8392–8402. doi: 10.1167/iovs.15-17477

Walker, F., Kato, A., Gonez, L. J., Hibbs, M. L., Pouliot, N., Levitzki, A., et al. (1998). Activation of the Ras/mitogen-activated protein kinase pathway by kinase-defective epidermal growth factor receptors results in cell survival but not proliferation. *Mol. Cell Biol.* 18, 7192–7204. doi: 10.1128/mcb.18.12.7192

Wang, J., Liu, H., Gao, L., and Liu, X. (2018). Impaired FGF10 signaling and epithelial development in experimental lung hypoplasia with esophageal atresia. *Front. Pediatr.* 6:109. doi: 10.3389/fped.2018.00109

Warburton, D., Schwarz, M., Tefft, D., Flores-Delgado, G., Anderson, K. D., and Cardoso, W. V. (2000). The molecular basis of lung morphogenesis. *Mech. Dev.* 92, 55–81. doi: 10.1016/s0925-4773(99)00325-1

Watson, J., and Francavilla, C. (2018). Regulation of FGF10 signaling in development and disease. *Front. Genet.* 9:500. doi: 10.3389/fgene.2018.00500

Weaver, M., Dunn, N. R., and Hogan, B. L. (2000). Bmp4 and Fgf10 play opposing roles during lung bud morphogenesis. *Development* 127, 2695–2704.

Yazlovitskaya, E. M., Tseng, H. Y., Viquez, O., Tu, T., Mernaugh, G., Mckee, K. K., et al. (2015). Integrin alpha3beta1 regulates kidney collecting duct development via TRAF6-dependent K63-linked polyubiquitination of Akt. *Mol. Biol. Cell* 26, 1857–1874. doi: 10.1091/mbc.E14-07-1203

Ye, S., Luo, Y., Lu, W., Jones, R. B., Linhardt, R. J., Capila, I., et al. (2001). Structural basis for interaction of FGF-1, FGF-2, and FGF-7 with different heparan sulfate motifs. *Biochemistry* 40, 14429–14439. doi: 10.1021/bi011000u

Yuan, J. S., Wang, D., and Stewart, C. N. Jr. (2008). Statistical methods for efficiency adjusted real-time PCR quantification. *Biotechnol. J.* 3, 112–123. doi: 10.1002/biot.200700169

Zhang, X., Mernaugh, G., Yang, D. H., Gewin, L., Srichai, M. B., Harris, R. C., et al. (2009). beta1 integrin is necessary for ureteric bud branching morphogenesis and maintenance of collecting duct structural integrity. *Development* 136, 3357–3366. doi: 10.1242/dev.036269

Zhang, X., Stappenbeck, T. S., White, A. C., Lavine, K. J., Gordon, J. I., and Ornitz, D. M. (2006). Reciprocal epithelial-mesenchymal FGF signaling is required for cecal development. *Development* 133, 173–180. doi: 10.1242/dev.02175

Conflict of Interest Statement: The authors declare that the research was conducted in the absence of any commercial or financial relationships that could be construed as a potential conflict of interest.

Copyright © 2019 Thotakura, Basova and Makarenkova. This is an open-access article distributed under the terms of the Creative Commons Attribution License (CC BY). The use, distribution or reproduction in other forums is permitted, provided the original author(s) and the copyright owner(s) are credited and that the original publication in this journal is cited, in accordance with accepted academic practice. No use, distribution or reproduction is permitted which does not comply with these terms.

Advantages of publishing in Frontiers

OPEN ACCESS
Articles are free to read for greatest visibility and readership

FAST PUBLICATION
Around 90 days from submission to decision

HIGH QUALITY PEER-REVIEW
Rigorous, collaborative, and constructive peer-review

TRANSPARENT PEER-REVIEW
Editors and reviewers acknowledged by name on published articles

Frontiers
Avenue du Tribunal-Fédéral 34
1005 Lausanne | Switzerland

Visit us: www.frontiersin.org
Contact us: frontiersin.org/about/contact

REPRODUCIBILITY OF RESEARCH
Support open data and methods to enhance research reproducibility

DIGITAL PUBLISHING
Articles designed for optimal readership across devices

FOLLOW US
@frontiersin

IMPACT METRICS
Advanced article metrics track visibility across digital media

EXTENSIVE PROMOTION
Marketing and promotion of impactful research

LOOP RESEARCH NETWORK
Our network increases your article's readership